

Dissertation zur Erlangung des Doktorgrades
der Fakultät für Chemie und Pharmazie
der Ludwig-Maximilians-Universität München

Energetic Materials based on
Isocyanuric acid and 1,2,4-Oxadiazole
Derivatives
-
Synthesis and Characterization

Norbert Thorsten Mayr

aus

Dillingen an der Donau
(Deutschland)

2013

Erklärung

Diese Dissertation wurde im Sinne von § 7 der Promotionsordnung vom 28. November 2011 von Herrn Prof. Dr. Thomas M. Klapötke betreut.

Eidesstattliche Versicherung

Diese Dissertation wurde eigenständig und ohne unerlaubte Hilfe erarbeitet.

München 25. Februar 2013

Norbert Mayr

Dissertation eingereicht am

1. Gutachter	Prof. Dr. Thomas M. Klapötke
2. Gutachter	Prof. Dr. Konstantin Karaghiosoff
Mündliche Prüfung	21. März 2013

“If something comes to life in others because of you,
then you have made an approach to immortality. “

Norman Cousins (* 24. Juni 1915; † 30. November 1990)

Für meine Familie und alle lieben Menschen,
die den Weg mit mir bis hier gegangen sind.

Danksagung

Zuerst möchte ich mich bei meinem Doktorvater Prof. Dr. Thomas M. Klapötke bedanken, nicht nur für die Möglichkeit der Dissertation sondern vor allem für seine Unterstützung in dieser Zeit, für die Inspiration, das Vertrauen und die Offenheit gegenüber ungewöhnlichen Ansätzen.

Meinem Zweitgutachter Prof. Dr. Konstantin Karaghiosoff möchte ich für sein freundliche väterliche Unterstützung und die viele fruchtbare Diskussionen nicht nur über Chemie bedanken.

Bei Frau Irene Scheckenbach, die gute Seele des Arbeitskreises, bedanke ich mich für Ihre unendliche Unterstützung bei organisatorischen und bürokratischen Unwegbarkeiten an der LMU.

Bei Dr. Jörg Stierstorfer bedanke ich mich für seine schier grenzenlose Energie und viel Motivation.

Dr. Franz Martin und Dr. Marianne Rotter danke ich für ihre Ehrlichkeit, ihr Vertrauen und Ihre Freundschaft.

Meinen Laborkollegen Sebastian Rest, Richard Moll, Dr. Karina Tarantik und Dr. Xaver Steemann danke für viele Jahre voll Freude, chemischer Genialität, jede Menge schlechte Kalauer und endlosen Stunden Rock Antenne und Helge Schneider.

Ich könnte jetzt viele nennen die Ihren Weg mit mir begonnen und längst ihr Weg gemacht haben aber besonders stolz bin ich die folgenden Menschen kennengelernt haben zu dürfen: Dr. Richard Betz, Dr. Stefan Sproll, Dr. Hendrik Radies, Dr. Michael Göbel und Dr. Matthias Scherr.

Ohne die Arbeit vieler Forschungspraktikanten und Bacheloranden wäre diese Arbeit nicht möglich gewesen. Vielen Dank Harald Budde, Monika, Holzner, Dániel Izsák, Martin Kunzmann, Andreas Maier, Gergely Rozsák, Stefanie Seel und den vielen AC3-Praktikanten.

Vielen Dank auch an alle im Arbeitskreis, die für ein wunderbares, kreatives und ergebnisreiches Klima gesorgt und die Zeit der Doktorarbeit zu einer schönen Zeit gemacht haben.

Für den Rückhalt und die Liebe, die ich durch meinen besten Freund Alex und meine Partner Jerryl und Micha in der Zeit der Doktorarbeit erfahren habe, bedanke ich mich sehr.

Ebenso bedanke ich mich bei meinem Tanzpartner Thomas, der viele Launen ertragen musste in dieser Zeit.

Besonders bedanken möchte ich mich bei meiner Familie und allen Freunden, die immer da waren, wenn sie gebraucht wurden, mir zugehört und an mich geglaubt haben.

Die vorliegende Arbeit wurde in der Zeit von März 2006 bis März 2011 am Department für Chemie der Ludwig-Maximilians-Universität München unter Anleitung

von

Prof. Dr. Thomas M. Klapötke

angefertigt.

1 Table of Contents

PART I	INTRODUCTION	15
1	INTRODUCTION	16
1.1	<i>General</i>	16
1.2	<i>Pyrotechnics</i>	17
1.3	<i>Developments in Energetic Materials Research</i>	17
1.4	<i>Stability and Performance</i>	19
1.5	<i>Explosives and Environment</i>	19
2	OBJECTIVES OF THE RESEARCH IN THIS THESIS	20
3	PARTS AND CHAPTERS	21
4	INTRODUCTION OF USED METHODS	21
4.1	<i>Theory of explosion and explosion products</i>	22
4.1.1	Physical and chemical explosion	22
4.1.2	Burning, deflagration and detonation	22
4.1.3	Deflagration to Detonation transition	23
4.1.4	Brisance vs. Explosiveness	23
4.2	<i>Calculation of energetic properties using EPXLO5 code^[29]</i>	24
4.2.1	Shock wave propagation and Chapman-Jouguet velocity	24
4.2.2	Becker-Kistiakovsky-Wilson equation of state (BKW-EOS)	24
4.2.3	Explosion products - Kistiakovsky-Wilson and Springall-Roberts Rules ^[2a]	24
4.2.4	Input parameters: Oxygen balance, heat of formation and density	25
4.3	<i>Practical methods</i>	25
4.3.1	Sensitivity testing	25
4.3.2	Determination of density	27
4.3.3	Measuring the Heat of formation	28
5	REFERENCES	28
PART II	EXPLOSIVE UREA DERIVATIVES	31
CHAPTER I	A COMPREHENSIVE STUDY ON N,N'-BIS(TRIS(NITRATOMETHYL)METHYL)OXAMIDE	33
1	INTRODUCTION	34
2	RESULTS AND DISCUSSION	35
2.1	<i>Comparison of crystal structures</i>	35
2.2	<i>Vibrational and thermodynamical data and Calculations</i>	39
2.2.1	Thermodynamical calculation and experimental data	42
2.3	<i>Electrostatic potential (ESP) and Decomposition</i>	45
2.4	<i>Thermostability: DSC and RADEX measurements</i>	47
2.5	<i>Energetic properties</i>	48
2.5.1	Comparison of energetic properties of BTNMMoxamide to common explosives	48
2.5.2	Koenen (steel sleeves) test	49
3	CONCLUSIONS	50
4	EXPERIMENTAL	51
4.1	<i>Crystal structures</i>	51
4.2	<i>Properties</i>	51
4.3	<i>Spectroscopic data and elemental analysis</i>	51
4.4	<i>Preparation</i>	51
5	REFERENCES	52
CHAPTER II	ENERGETIC CYANURIC ACID DERIVATIVES	55
1	INTRODUCTION	56
1.1.1	Nitro urea compounds	57
2	DISCUSSION	59
2.1	<i>Synthesis</i>	59

2.2	<i>Vibrational spectroscopy</i>	59
2.2.1	N,N',N''-Tris-(nitroxymethyl)-isocyanuric acid (3)	59
2.3	<i>Thermostability</i>	61
2.3.1	N,N',N''-Tris-(nitroxymethyl)-isocyanuric acid (3)	61
2.4	<i>Crystal structure</i>	62
2.4.1	N,N',N''-Tris-(nitroxymethyl)-isocyanuric acid (3)	62
2.4.2	1,3,5-Tris(hydroxyethyl)cyanuric acid(2)	65
2.4.3	1,3,5-Tris(nitratoethyl)-cyanuric acid (4)	66
2.5	<i>Calculation of thermodynamic data and surface potential</i>	68
2.5.1	Electrostatic surface potential of N,N',N''-Tris-(nitroxymethyl)-isocyanuric acid(3)	68
2.5.2	Electrostatic surface potential of N,N',N''-Tris-(nitroxyethyl)- isocyanuric acid (4)	69
2.5.3	Calculation of the enthalpy of formation	69
2.1	<i>Energetic Properties</i>	71
2.1.1	Detonation Parameters	71
3	CONCLUSIONS	72
4	EXPERIMENTAL	73
4.1	<i>Crystal structures</i>	73
4.2	<i>Properties</i>	73
4.3	<i>Spectroscopic data and elemental analysis</i>	73
4.4	<i>Preparation</i>	73
5	REFERENCES	75
CHAPTER III N²,N⁴,N⁶-TRIS(TRIS(NITRATOMETHYL)METHYL)-1,3,5-TRIAZINO-2,4,6-TRICARBOXAMIDE (NOX-		
1) – BIG AND BANG		
1	INTRODUCTION	80
2	DISCUSSION	81
2.1	<i>Structure of triazine derivatives</i>	81
2.1.1	Description of the molecule structure and the monoclinic crystal structure in comparison to the reported hexagonal structure	83
2.2	<i>Synthesis</i>	88
2.3	<i>Thermodynamical and Spectroscopic Characterization</i>	89
2.4	<i>Crystal structure data</i>	91
2.5	<i>Energetic data</i>	93
3	CONCLUSIONS	93
4	EXPERIMENTAL PART	94
4.1	<i>Instrumental setups</i>	94
	PD-XRAY	94
	IR samples	94
	NMR-samples	94
	RAMAN samples	94
	DSC Measurements	94
	SC-XRAY data	94
	NCS-Elemental analysis	94
	Mass Spectrometry	94
	Friction and impact sensitivity	94
4.2	<i>Preparation</i>	94
4.2.1	[1,3,5]Triazine-2,4,6-tricarboxylic acid triethyl ester (2)	94
4.2.2	N ² ,N ⁴ ,N ⁶ -Tris(tris(hydroxymethyl)methyl)-1,3,5-triazino-2,4,6-tricarboxamide (TTHMM-TCA, 3)	95
4.2.3	N ² ,N ⁴ ,N ⁶ -Tris(tris(nitratomethyl)methyl)-1,3,5-triazino-2,4,6-tricarboxamide (TTNMM-TCA, NOX, 4)	95
5	REFERENCES	96
PART III ENERGETIC MATERIALS BASED ON 1,2,4-OXADIAZOLE DERIVATIVES		99

CHAPTER IV	3,3'-BIS-(1,2,4-OXADIAZOL-5-ONE) AND DERIVATIVES – A COMPREHENSIVE STUDY	101
1	COMPARISON OF 3,3'-BIS-1,2,4-OXADIAZOL-5-ONE AND 5,5'-BIS-1H-TETRAZOLE	102
1.1	Introduction	102
1.2	Discussion	102
1.3	Synthesis	106
1.4	Conclusions	107
1.5	Experimental	107
1.5.1	Crystal structures	107
1.5.2	Properties	107
1.5.3	Spectroscopic Data and elemental analysis	107
1.5.4	Preparation	107
1.6	References	108
2	INSENSITIVE EXPLOSIVES AND PROPELLANTS BASED 1,2,4-OXADIAZOL DERIVATIVES	110
2.1	Introduction	110
2.2	Syntheses	111
2.3	Crystal structures	112
2.3.1	Diammonium bis-(1,2,4-oxadiazol-5-onate)	112
2.3.2	Dihydrazinium bis-(1,2,4-oxadiazol-5-onate)	114
2.3.3	Diguanidinium bis-(1,2,4-oxadiazol-5-onate) (G ₂ OD, 6)	116
2.3.4	Bis-aminoguanidinium 3,3'-bis-(1,2,4-oxadiazol-5-onate) (AG ₂ OD, 7)	119
2.3.5	Di-triaminoguanidinium 3,3'-bis-(1,2,4-oxadiazol-5-onate) (TAG ₂ OD, 9)	121
2.4	Energetic properties	123
2.5	Conclusions	124
2.6	Experimental	125
2.6.1	Crystal structures	125
2.6.2	Properties	125
2.6.3	Spectroscopic Data and elemental analysis	125
2.6.4	Preparation	125
2.7	References	128
3	SMOKELESS PYROTECHNICAL COLORANTS BASED ON 3,3'-BIS-(1,2,4-OXADIAZOL-5-ONE SALTS	130
3.1	Introduction	130
3.2	Discussion	131
3.2.1	Syntheses	131
3.2.2	Crystal structures	132
	TETRAAQUA-3,3'-BIS(1,2,4-OXADIAZOL-5-ON)-ATO COPPER(II)	135
3.2.3	Thermostability	142
3.3	Conclusion	144
3.4	Experimental	144
3.4.1	Crystal structures	144
3.4.2	Properties	144
3.4.3	Spectroscopic Data and elemental analysis	144
3.4.4	Preparation	145
3.5	References	146
CHAPTER V	3,5-DIAMINO-1,2,4-OXADIAZOLE – A SUBSTITUTE FOR GUANYLUREA IN ENERGETIC MATERIALS	149
1	INTRODUCTION	150
2	RESULTS AND DISCUSSION	151
2.1	Synthesis and Characterization of 3,5-diamino-1,2,4-oxadiazole (DAOd, 1)	151
2.1.1	3,5-diamino- 1,2,4-Oxadiazole (1, DAOd)	151
2.2	Syntheses of 3,5-diamino-1,2,4(4H)-oxadiazolium salts	159
2.2.1	The 3,5-diamino-1,2,4(4H)-oxadiazolium cation	159
2.2.2	3,5-Diamino-1,2,4-oxadiazolium nitrate (2)	162
2.2.3	3,5-Diamino-1,2,4-oxadiazolium perchlorate (3)	163

2.2.4	3,5-Diamino-1,2,4-oxadiazolium picrate (4)	169
2.2.5	3,5-Diamino-1,2,4-oxadiazolium dinitramide (5)	172
2.2.6	2.3.6 3,5-Diamino-1,2,4-oxadiazolium-5-aminotetrazolate (6)	174
2.2.7	3,5-Diamino-1,2,4-oxadiazolium-5-nitrotetrazolat (IX)	175
2.2.8	3,5-Diamino-1,2,4-oxadiazolium-5,5'-azotetrazolate (X)	176
2.2.9	3,5-Diamino-4-methyl-1,2,4-oxadiazolium iodide (XI)	177
2.3	<i>Synthesis of complex bond 3,5-diamino-1,2,4-oxadiazole (7)</i>	177
2.4	<i>Diazotation reaction of 1 by sodium nitrite (i)</i>	178
2.5	<i>Oxidation and Nitration of 3,5-diamino-1,2,4-oxadiazole (1)</i>	179
2.5.1	Oxidation or nitration with HNO ₃ (100 %)	181
2.5.2	Oxidation or nitration with HNO ₃ (100 %) and H ₂ SO ₄ (conc.)	181
2.5.3	Oxidation or nitration by sodium nitrite (ii–iv)	181
2.5.4	Oxidation with H ₂ SO ₄ (conc.), H ₂ O ₂ (30 %) and (NH ₄) ₂ S ₂ O ₈ (v)	182
2.5.5	Oxidation by potassium permanganate (vi)	182
2.5.6	Oxidation by ammonium dichromate (vii)	183
2.5.7	Oxidation by bromine (viii)	183
2.5.8	Nitration with HNO ₃ (100%) and Ac ₂ O	184
2.6	<i>Energetic Data</i>	184
3	SUMMARY AND CONCLUSIONS	185
3.1	<i>Summary</i>	185
3.1.1	Energetic salts of DAOd	186
3.1.2	Oxidation, Nitration and Diazotation of DAOd.	186
3.2	<i>Conclusion and Outlook</i>	187
4	EXPERIMENTAL PART	187
4.1	<i>Common</i>	187
4.2	<i>Analytical apparatus</i>	187
4.3	<i>Calculations</i>	189
4.4	<i>Preparation of energetic DAOd (1) and salts thereof</i>	191
4.5	<i>Oxidation and Nitration products of DAOd(1)</i>	194
5	REFERENCES	197
CHAPTER VI	3-AMINO-1,2,4-OXADIAZOL-5-ONE – THE INSENSITIVE 5-AMINO-TETRAZOLE ? COMMONS AND DIFFERENCES	201
1	INTRODUCTION	202
2	RESULTS AND DISCUSSION	204
2.1	<i>Synthesis of aOD</i>	204
2.1.1	Overview	205
2.1.2	Synthetic Route A	206
2.1.3	Synthesis route B	209
2.1.4	One-Pot-Synthesis according to route B	219
2.1.5	Summary	220
2.2	<i>Solubility of aOD</i>	220
2.3	<i>Azo-coupling of aOD</i>	221
2.4	<i>Salts of aOD</i>	222
2.4.1	Copper aOD (9)	222
2.4.2	Silver aOD (10)	223
2.4.3	Strontium aOD (11) trihemihydrate	223
2.4.4	Barium aOD (12)	224
2.4.5	Aminoguanidinium aOD (13)	224
2.4.6	Sodium aOD (14) monohydrate	225
2.4.7	Summary	229
2.5	<i>Methylation of 3-amino-1,2,4(4H)-oxadiazol-5-one</i>	230
2.6	<i>Synthesis of salts with aODH⁺ as cation</i>	231
2.6.1	Summary	241

2.7	<i>Energetic data</i>	242
3	CONCLUSIONS	245
4	OUTLOOK	245
5	EXPERIMENTAL PART	246
5.1	<i>Chemicals and Methods</i>	246
5.2	<i>Preparation</i>	246
5.2.1	Dipotassium cyanodithioimidocarbonate (4)	246
5.2.2	Dimethylcyanodithioimidocarbonat (5)	247
5.2.3	Potassium S-methyl-N-cyanocarbamate (3)	247
5.2.4	3-Amino-1,2,4(4H)-oxadiazol-5-one (A) (1)	248
5.2.5	(Z)-amino[(ethoxycarbonyl)amino]-N-hydroxymethaniminium chloride /N-(ethoxycarbonyl)-N'-hydroxy-guanidinium chloride (8)	248
5.2.6	3-Amino-1,2,4(4H)-oxadiazol-5-one (B) (1)	249
5.2.1	One-pot-synthesis of amino-1,2,4(4H)-oxadiazol-5-one (B) (1)	250
5.2.1	Copper aOD 2 H ₂ O (9)	251
5.2.2	Silver aOD (10)	251
5.2.3	Strontium aOD·x 1.5 H ₂ O (11)	251
5.2.4	Barium aOD (12)	252
5.2.5	Aminoguanidinium aOD (13)	252
5.2.6	Sodium aOD (14)	253
5.3	<i>Solubility in different solvents</i>	253
5.4	<i>Further investigated reactions</i>	253
5.4.1	(Z)-amino[(methoxycarbonyl)amino] N-hydroxymethaniminium chloride (B I)	253
5.4.2	Alternative ring closure reaction for aOD (1) with diphosgen (B III, 6)	254
5.5	<i>Synthesis of aOD salts with aODH⁺ as cation:</i>	254
5.5.1	Synthesis of aODH ⁺ nitrate	254
5.5.2	Synthesis of aODH ⁺ perchlorate	255
5.5.3	Synthesis of aODH ⁺ picrate	256
5.6	<i>Azo-Coupling of aOD (15)</i>	256
5.7	<i>Methylation of aOD (16a, 16b)</i>	257
6	REFERENCES	258
CHAPTER VII	3-DINITROMETHYLENYL-1,2,4(4H)-OXADIAZOL-5-ONE AND DERIVATIVES – HIGH EXPLOSIVE, STABLE, INSENSITIVE	261
1	INTRODUCTION	262
2	SYNTHESIS	263
2.1	<i>By-product (6)</i>	264
2.2	<i>Salts of DNM-OD (7,9)</i>	265
3	DISCUSSION	266
3.1	<i>Spectroscopic Properties</i>	266
3.2	<i>Crystal structures</i>	267
3.2.1	2-Ethyl-3-amino-3-(hydroxyimin)-propanoate (2)	267
3.2.1	Ethyl (3Z)-3-amino-3-[(methoxycarbonyl)oxy]imino}propanoate (3a)	267
3.2.1	Dinitro-([1,2,4]oxadiazol-5-on-3-yl)-acetic acid ethyl ester (5)	268
3.2.1	Sodium (4-{2-[(ethoxycarbonyl)oxy]propan-2-yl}-5-oxo-4,5-dihydro-1,2,4-oxadiazol-3-yl)(dinitro)methanide monohydrate (rearrangement product) (6)	269
3.2.2	Di-Sodium DNM-OD dihydrate (7b)	271
3.2.3	Di-Ammonium DNM-OD (9b)	272
3.2.4	Bis-Guanidinium DNM-OD (9a)	274
3.3	<i>Calculations – thermodynamical properties</i>	275
3.4	<i>Structure Optimization of DNM-OD and DNM-OD²⁻</i>	275
3.5	<i>Energetic properties</i>	276
3.5.1	Pyrotechnical colorants	276
3.5.2	High-Nitrogen containing cations	276

4	CONCLUSIONS	277
5	OUTLOOK	278
6	EXPERTIMENTAL	278
6.1	<i>Common</i>	278
6.2	<i>Analytical apparatus</i>	278
6.3	<i>Preparation</i>	280
6.3.1	2-Ethyl-3-amino-3-(hydroxyimin)-propanoate (1)	280
6.3.1	Ethyl-2-(1,2,4-oxadiazol-5-on-3-yl) acetate - two step reaction (10)	280
6.3.2	Ethyl-(3Z)-3-amino-[[[(methoxycarbonyl)oxy]imino]-propanoat (9)	280
6.3.3	3-Ethyl (5-oxo-4,5-dihydro-1,2,4-oxadiazol-3-yl)-acetate (2)	281
6.3.4	Dinitro-([1,2,4]oxadiazol-5-on-3-yl)-acetic acid ethyl ester (3)	282
6.3.5	Sodium (4-[2-[(ethoxycarbonyl)oxy]propan-2-yl]-5-oxo-4,5-dihydro-1,2,4-oxadiazol-3-yl)(dinitro)methanide monohydrate (rearrangement product) (5)	282
6.4	<i>Alkaline and alkaline earth metal salts of DNM-OD (7)</i>	282
6.4.1	General procedure	282
6.4.2	Lithium DNM-OD	283
6.4.3	Sodium DNM-OD x 2 H ₂ O	283
6.4.4	Potassium DNM-OD	283
6.4.5	Barium DNM-OD x 3.5 H ₂ O	283
6.5	<i>Nitrogen rich salts of DNM-OD</i>	283
6.5.1	Bis-Guanidinium DNM-OD x H ₂ O (9a)	284
6.5.1	Di-Ammonium DNM-OD x H ₂ O (9b)	284
7	REFERENCES	284
PART IV	CONCLUSIONS AND OUTLOOK	287
1	PART II – UREA BASED DERIVATIVES	288
1.1	<i>Conclusions</i>	288
1.2	<i>Outlook</i>	288
2	PART III – 1,2,4- OXADIAZOLE AND 1,2,4- OXDIAZOL-5-ONE BASED COMPOUNDS	288
2.1	<i>Conclusions</i>	288
2.2	<i>Outlook</i>	289
PART V	APPENDIX	291
CHAPTER VIII	TABLES OF CRYSTAL STRUCTURES	293
1	COMPOUNDS- CHAPTER I	294
2	COMPOUNDS - CHAPTER II	295
3	COMPOUNDS - CHAPTER III	296
4	COMPOUNDS - CHAPTER IV	297
4.1	<i>Metal salts</i>	297
4.2	<i>Nitrogen rich salts</i>	298
5	COMPOUNDS – CHAPTER V	299
6	COMPOUNDS - CHAPTER VI	300
7	COMPOUNDS - CHAPTER VII	301
CHAPTER IX	INDEX OF ABBREVIATIONS	303
CHAPTER X	ABSTRACT AND SUMMARY	307
CHAPTER XI	CURRICULUM VITAE	309
PART VI	INDEX	313
CHAPTER XII	FIGURES	315
CHAPTER XIII	TABLES	323

Part I

INTRODUCTION

1 Introduction

By the invention of the black powder in China about 2200 years ago for the first time an explosive was discovered. In Europe at least in the 13th century established, it was the only known explosive for a long period. The research and development of new and better formulations was extremely accelerated by the many wars in the 19th and 20th century.

Nonetheless for the most reason the research in the field of new and more destructive energetic compositions have been driven by war. Especially the World War I and II have brought a wide arsenal of different types of explosives like the Royal Demolition Explosive (RDX) and the High Melting Explosive (HMX) both have set standard for over 100 years in price, availability and last but not least in performance for secondary explosives. The field of primary explosives, which is known for initializers has also been untouched for nearly 100 years and the lead azide claims it since.^[1]

1.1 General

The common term “explosion” describes a process which releases a high amount of energy and gas in a short period. It must be distinguished between nuclear, chemical and physical explosion. The condition for an explosion is the local accumulation of energy, which is released in a sudden and passed on in a certain way like shock wave or thermal and ionizing irradiation

The term of chemical explosion has to be differentiated between deflagration and detonation. *Deflagration* describes the energy transfer by heat with a propagation of the reaction front below the velocity of sound and a clearly visible and audible flame. Distinct from a usual burning pressure is built up. In contrast a *detonation* is the propagation of the reaction front with a velocity higher than the velocity of sound. If the reaction front - in the case of a deflagration - is breaking the sound barrier by sufficient external pressure, it turns into a detonation. That is called a *deflagration-to-detonation transition*.

Explosives consist of an oxidizing agent (oxidizer) and an oxidizable material (fuel). These can be combined in one molecule for example nitroglycerine (1,2,3-glycerine trinitrate or propane-1,2,3-triol nitrate) or composed of multiple components like in black powder (standard mixture: 75 % potassium nitrate, 15 % charcoal, 10 % sulfur).

There are a lot of possible ways to classify high energetic materials. The most common classification divides them into explosives, propellants and pyrotechnics. Explosives can be subdivided into primary or initial explosives and secondary explosives.^[2]

Primary explosives like lead azide are initiated easily by impact, friction, electrostatic discharge or heat. The detonation velocity is in the range of 3500- 5500 ms⁻¹, which is in many cases a fast deflagration-to-detonation transition.

Secondary explosives are significantly more stable than primaries. That is why they are detonating only on the behalf of a preceding heat or shock wave from an initial

explosive. During the detonation secondary explosives release more energy despite their higher stability. The class includes well known compounds like TNT (2,4,6-trinitro toluene), RDX (1,3,5- trinitrohexahydro-1,3,5-triazine, 1,3,5-trinitro-1,3,5-triazahexane) and PETN (pentaerythritole tetranitrate). The *oxidation agents* in these compounds are mostly nitrate esters (R-ONO₂), nitro (R-NO₂) or nitramine groups (N-NO₂) and a carbon skeleton as *fuel*. Usually the detonation velocities are greater than 7000 ms⁻¹.

1.2 Pyrotechnics

While *pyrotechnics* have the particular feature that they deflagrate after ignition, whereas the released pressure is used as a driving thrust to serve the production of various acoustic and visual effects, such as fireworks, smoke grenades, gas generators or signal flares.

The pyrotechnical compositions therefore are a group of energetic materials that was explored for many years. But not driven by any war or military use for the last 50 years but for leisure. Commercially pyrotechnics for private and public fireworks like in theme parks, movie special effects and for holiday tribute have become a very lucrative market.

1.3 Developments in Energetic Materials Research

The standards are still set by TNT and RDX, which detonation parameters are listed in table 1, as the compounds described in the following are measured with respect to this standard.

Table 1. Detonation parameter of TNT and RDX.^[2b]

	$\Delta_f U^\circ / \text{kJkg}^{-1}$	$\Omega / \%$	ρ / gcm^{-3}	Q_v / kJkg^{-1}	D / ms^{-1}	V_0 / Lkg^{-1}
TNT	-219.1	-73.9	1.64	-3612	6900	975
RDX	400.2	-21.6	1.82	-5277	8750	927

While the above-mentioned older explosives obtain their energy mainly from the oxidation of the carbon scaffold, an attempt is made in modern explosives, to build up additionally a highest possible ring or cage tension, which is then released again during the explosion. Representatives of this type are the melt-castable TNAZ^[3,4] (1,3,3-trinitroazetidine), ONC^[5] (1,2,3,4,5,6,7,8-octanitrocubane) or CL-20^[6] (2,4,6,8,10,12-Hexanitro hexaazaisowurtzitan-4,6,8,10,12). Compounds with very high nitrogen content are also an interesting approach, as they have due to many N-N and C-N bonds higher energies of formation, and mostly high densities and well-adjusted oxygen balances. Known are for example ionic compounds like the 5,5'-azotetrazolate anion (ZT; 85.36% nitrogen).

Furthermore, in the view of research are so-called insensitive munitions, for which at the expense of as little power as necessary sensitivity to external influences is reduced as much as possible. Industry standard in this class is the 120 years ago discovered TATB (1,3,5-triamino-2,4,6-trinitrobenzene), whose crystal structure was solved in 1965 by Cady and Larson.^[7] Due to the extreme insensitivity it is used including in the

detonators of the British nuclear weapons^[8], because it stands a plane crash unscathed. Still under development, promising compounds are modern FOX-7^[9] (1,1-diamino-2,2-dinitroethen) and NTO^[10] (3-nitro-1,2,4-triazole-5-one). The latter is already in use as gas generator for air bags, where it could eventually replace the toxic sodium azide.

A well-recognized overview articles on modern energetic materials and their synthesis are found in various literatures. ^[11,12]

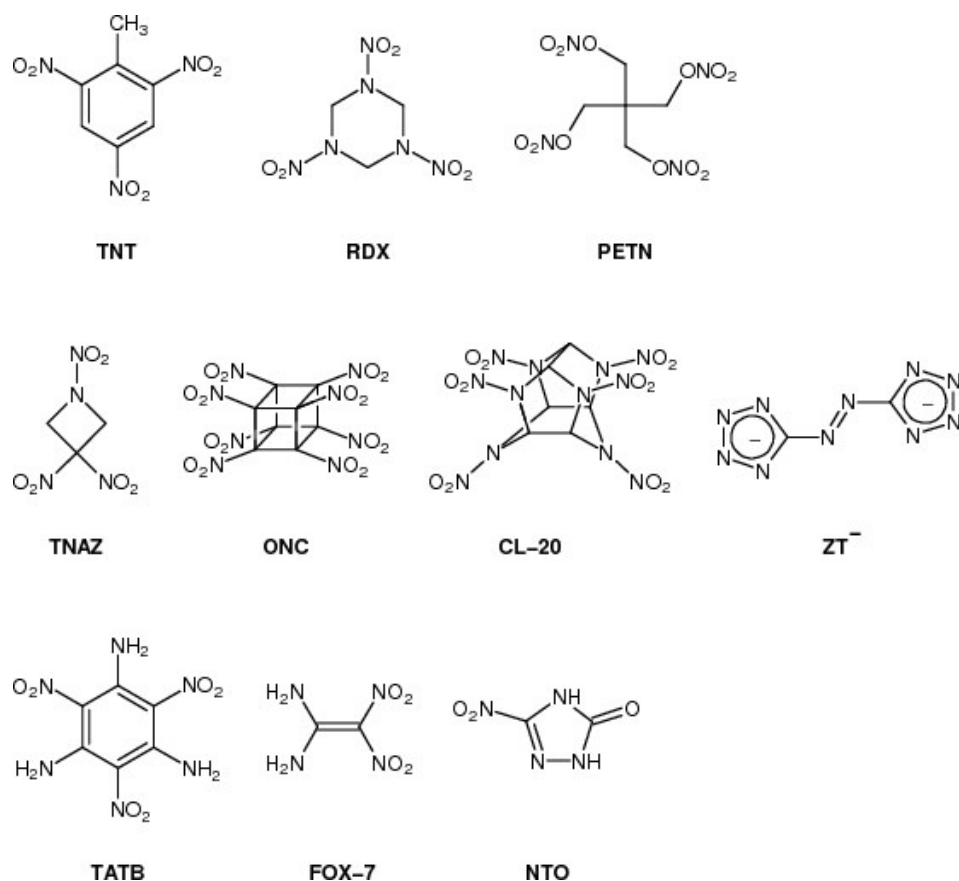


Figure 1. Molecular structure of secondary explosives

Trends in recent research regarding secondary explosives are summarized in three main categories:

- ✓ Increased performance
- ✓ Decreased sensitivity e.g. insensitive ammunition (IM)
- ✓ Decreased toxicity of explosives and the respective degradation and decomposition products

To increase the performance of secondary explosives the following criteria have to be investigated

- Heat of explosion Q in $[J \cdot kg^{-1}]$
- Detonation velocity D in $[m \cdot s^{-1}]$
- Detonation pressure p in $[kbar]$

In propellants the respective parameters are

- Temperature of explosion T in [K]
- Released gas volume V per kg explosive in [L·kg⁻¹].

1.4 Stability and Performance

Many concepts have been found during the last 60 years of continuing research in this field. But although much is known about the performance influencing chemical building blocks, like nitramines, nitro and nitrate groups, nitrogen-nitrogen single and double bonds and carbon-carbon triple bonds as precursors and hetero atom containing ring systems which form products with highly exothermic enthalpies of formation like nitrogen, carbon dioxide and water, there is little known about the sensitivity of energetic molecules.^[13]

Although research has been done in this area for years only for small neutral molecules in the gas phase, some claims can be done on stability at all. But no further determination of real sensitivity data could be done. The influence of grain size, crystal shape, morphology, solid state phase, cocrystallization with solvents, packing, hydrogen bridged bonding and many further material science values have only been examined for known and commercially available explosives. But no conclusions for theoretical determination have been drawn out of this yet for prediction of unknown or new developed energetic materials.^[14]

There are some trends found over the last years which have not been determined so far and hopefully will. The most influence in the sensitivity of materials seems to be found in molecule-molecule interactions like the van-der-Waals forces or the hydrogen bridging bonds, as obvious also dipole-dipole interactions like nitrogen oxygen contacts of nitro groups or carbonyl contacts are highly involved in those. They all are contributing to the bigger system the molecule packing in a crystal or solid state material.^[15]

Forming a homogeneous solid powder or crystal is not as much a chemical than more a physical aspect. That is why a lot of technical processes have been developed through the years considering the shape and size of solid energetic materials. Though to speak most spherical shape is found to be best at minimal grain size and nearly perfect crystals without inclusions or defects, as example could be mentioned the reduced sensitivity RDX (RS-RDX) which is produced since a couple of years exactly meeting this aspects.^[16]

1.5 Explosives and Environment

The environmental impact of modern explosives also plays an increasingly important role.^[17] The use of lead azide, for example, led to significant lead contamination in military or police training grounds.^[18] At the fireworks the colors red and green are predominantly produced by strontium and barium compounds. By the development of new compounds and compositions the use of these heavy metals should be avoided as completely as possible or at least substantially reduced.^[19] Explosives with high nitrogen content not only show, as already mentioned, better performance, but release

while exploding mostly N_2 as a gaseous explosion product, basically nothing more than hot air (N_2 content in the atmosphere: 78%).

The most environmentally friendly explosives would be thus of the type N_x . Although several compounds with a composition of N_6 and N_8 were calculated to be at least metastable, their synthesis has not been successful so far. [20,21] In fact recently a cubic high pressure modification of polymeric nitrogen was made, but this is only metastable at room temperature above 42 GPa. [22,23]

A polymeric nitrogen modification of a mixture of nitrogen and hydrogen, which was formed at 35 GPa, is stable down to a pressure of 6 GPa, however, below the pressure of 84 GPa no complete conversion of N_2 to N_x takes place. [24] Stable ionic polymeric nitrogen compounds are

besides the known azide anion (N_3^-) and the relatively new N_5^+ not existing so far. [25,26]

Further environmentally critical research are:

- Halogens like chlorine from the oxidizer perchlorate used in rocket propellants (e.g. Space Shuttle/ Ariane booster rockets) Perchlorate is known to affect the thyroid gland as it can substitute iodine in organisms. [27]
- Water solubility of explosives affects the intake into drinking water reservoirs, which disturbs microbiological systems and effects on aquatic animals are not well-known yet. [28]

Therefore energetic materials that only consist of carbon, hydrogen, oxygen and nitrogen which decompose to dinitrogen, dioxygen, carbon dioxide and water are desired and future proof.

High nitrogen moieties like azoles have been investigated for over ten years in the working group of Prof. Dr. T.M. Klapötke and found application as primary and secondary explosives as well as propellants and pyrotechnics.

2 Objectives of the Research in this Thesis

The overall topic of this thesis is to show and deepen the understanding of energetic materials from neutral small energetic molecules to combinatorial investigation of salts. The idea that has driven the research was starting with cheap and good available molecule classes like urea, oxamide and isocyanuric acid derivatives and convert those to energetic materials. This way was left after a certain and the main molecule class to investigate was chosen the 1,2,4-oxadiazole and its derivatives. This class combines a heterocyclic molecule which is not energetic at all, as basis for a research area. How is a stable molecule be brought to be energetic? This is not a simple task to do, as there are not known such energetic motifs. The furazanes or better 1,2,5-oxadiazoles are already in use for high performance energetic materials. So there has been chosen some other to investigate: The 1,2,4-oxadiazol-5-one motif which is compatible in structure and most of chemical issues with the tetrazole motif and the 3,5-diamino-1,2,4-oxadiazole

which compares to 3,5-diamino-1,2,4-triazole and also to the already investigated guanylurea molecule.

Both should prove to be good model systems to show how stability and performance could be influenced and tailored. The research goal to understand not only what makes an energetic molecule more or less energetic but also to design stability and sensitivity has to make this work an effort to take.

3 Parts and Chapters

This thesis compiles a few selected themes out of the area of energetic research and contains seven parts and seven enclosed chapters. The parts separate some literal manners like Introduction, Conclusions, Appendix and Index as well as they separate the two main investigation fields the Explosive Urea Derivatives and the Oxadiazole Derivatives

- First chapter will introduce a literature known molecule N,N'-bis-(trinitratomethyl)methyl oxamide which was reinvestigated by the matter of stability and performance.
- Second chapter tells about isocyanuric acid derivatives which were examined with special interest on performance and sensitivity increase and decrease regarding the energetic groups introduced.
- Third chapter shows the characteristics of N,N',N''-tris-(trinitratomethyl)methyl 1,3,5-triazine-2,4,6-carboxylamide which combines the same energetic motives as the aforementioned both structures.
- Fourth chapter introduces the 3,3'-bis-1,2,4(4*H*)-oxadiazol-5-one and compares the energetic properties to the properties of the 5,5'-bistetrazole. Also the structures and properties of some metal salts which were made for the use as pyrotechnical colorants and some nitrogen rich salts for the use as propellant additions are characterized.
- Fifth chapter's results are the combination of the 3,5-diamino-1,2,4-oxadiazolium-cation with a bunch of energetic anions. These salts are studied by calculation and experimentally analyzed regarding their performance and stability
- Sixth chapter introduces the 3-amino-1,2,4(4*H*)-oxadiazol-5-one and some salts to be compared with the very similar 5-amino-1*H*-tetrazole
- Seventh chapter shows the 3-(dinitromethyl)-1,2,4(4*H*)-oxadiazol-5-one and its derivatives. The energetic properties are shown as well as the synthesis from the scratch.

4 Introduction of Used Methods

The introduction to the methods used in this thesis summarizes and points out the most important working schemes. It also focuses mainly on the energetic investigations and the accompanying calculations. Therefore subtopics briefly summarize all necessary knowledge for the further understanding of the thesis' special approach. Also

this should avoid repeating introductions on the topics in each chapter which discuss the compounds and their properties.

4.1 Theory of explosion and explosion products

4.1.1 Physical and chemical explosion

To clarify the term explosion it is important to distinguish between implosion and explosion. Both start with sudden propagation of a wave which will be transferred by a medium. During an implosion the difference between a space without or filled less medium than the surrounding is introduced by the burst of the barrier and penetration of the surrounding medium in a fast way that effects the medium and leads to a hearable wave propagation. While a physical explosion works the other way round when an overpressure is suddenly released to the surrounding space and also propagates a wave through the medium. A physical explosion shows no light or heat.

A chemical explosion combines a physical explosion with light and heat exposure. This is a result of a chemical exothermic reaction of an instable or metastable material which could be initiated by heat, shock, friction or electric discharge. A chemical explosion is mostly followed by a shock wave which is driven by the released energy in the medium. A physical explosion contains only the energy regarding to the difference of medium density, while the chemical explosion gets most of its energy out of the formation enthalpy of the explosive substance and the reaction of this with the surrounding medium. This could lead to a two stage explosion when the first stage is the release of gas directly formed by the substance e.g. nitrogen direct from an azide and the second stage the reaction of oxygen with the carbon and hydrogen which will form the heat and light but will consume the whole oxygen content of the air at the same time.

So a good explosive will at the same time release the same amount of nitrogen or intramolecular formed carbon dioxide and water than it consumes oxygen from its surroundings so that there is no implosive effect while propagating a shock wave in the air. This leads to two kinds of impressive explosives those with an oxygen balance (calculation see below) of zero which means no external oxygen is needed or a good combination of instantaneously formed gas and oxygen consumption of the surrounding.

4.1.2 Burning, deflagration and detonation

For a proper explanation of burning, deflagration and detonation the term of burning rate has to be introduced. This describes velocity of an exothermic reaction of substance with oxygen showing a flame. The measurement is rather easy a certain amount is put in a line and with a stop watch the time from beginning to ending of the defined length of the line is measured.

If one is looking at the phenomena of a burning you will find a fire which is continuous exothermic reaction releasing heat and light. Deflagration adds to the heat and light a sound which is beneath the sonic barrier. A detonation shows a wave propagation of

energy through the medium which is over the sonic barrier and mostly you will not find a flame but a heat and light which is propagating with the wave front.

4.1.3 Deflagration to Detonation transition

If you put a deflagrating substance in a confined vessel or you compress such a substance to a certain level you will find a deflagration to detonation transition which is just a self-compression of the material by the pressure released of the exothermic reaction and leads to an acceleration of the shock wave from a non-sonic level to a level with over sonic propagation.

4.1.4 Brisance vs. Explosiveness

Brisance describes the possible performance or destructive effect of an explosive and is calculated from the load density, the specific energy and the detonation velocity according to

$$B = \rho \times F \times D$$

(ρ : load density, F : specific energy $F = p \times V$, D : detonation velocity)

While specific energy and detonation velocity are compound specific values, the load density can be influenced. The theoretical maximum density (crystal structure analysis) of a compound is the limit of the loading density.

Explosiveness or explosibility describes possibility of a material to be explosive and is found to be equal to the Berthelot-Roth-product. There for a mixture or single compound can be assigned a value which expresses the likeliness to be an explosive in comparison to the common explosives. Therefore it is calculated from the exhaust gas volume of an explosion the heat of explosion and the load density.

$$B_R = \rho^2 \times V_0 \times Q_V$$

(ρ load density, V_0 : exhaust gas volume, Q_V : heat of explosion)

The minimum value of 1193 (Oppauer Salt) reflects if a compound is explosible or not. Table 1 lists some values for comparison.

Table 2. Values for load density ρ_0 and the Berthelot-Roth product B_R of some selected explosives.^[2b]

Explosive	ρ_0 [kg·m ⁻³]	B_R [kJ·m ⁻³]
HMX	1.96	18707
NG	1.60	12448
TNT	1.65	9588
Schwarzpulver	1.87	2913
Hydrazin	1.00	3558
Oppauer-Salt (55 % NH ₄ NO ₃ + 45 % (NH ₄) ₂ SO ₄)	1.10	1193

The load density ρ contributes by square into the Berthelot-Roth product. The density must be considered as very important value to evaluate as well the explosiveness as the brisance.

4.2 Calculation of energetic properties using EPXLO5 code^[29]

4.2.1 Shock wave propagation and Chapman-Jouguet velocity

The shock wave is a model of a wave travelling through matter with a certain density. The difference to a normal wave like sinus wave which is an oscillating form of a transversal wave the shock wave has one high initiation point where in short period most assumed to one point in time the pressure on a matter rises from normal (ambient) pressure to a very high pressure. This is described best in form of a square curve. This pressure propagates due to the density of the medium with a velocity and collapses slowly at the transition from one medium to another. While the beginning of the reduction of velocity of the travelling occurs readily after the initiation, the overall pressure begins to decrease at the transition. ^[30]

The above described form of a shock wave is found for physical and chemical shock initiated waves. Therefore in explosive chemistry the shock wave is kept up by a following exothermic chemical reaction, which releases the necessary energy. The equilibrium of consumed energy for the detonation occurring and the exothermic reaction is called Chapman-Jouguet condition. The initiation point of the reaction when the chemical reaction starts, is the so called von-Neumann spike. There the equilibrium is not present and more energy is released and high pressure is applied as shock to build up the following shock wave from the scratch..^[31]

4.2.2 Becker-Kistiakovsky-Wilson equation of state (BKW-EOS)

The Becker Kistiakovsky-Wilson equation of state is used to calculate the explosion products.

$$\frac{p \cdot v}{RT} = 1 + X \cdot e^{\beta \cdot X} \text{ with } X = \frac{\kappa \sum x_i k_i}{v \cdot (T + \theta)^\alpha}$$

The EXPL05 code uses as constants $\alpha=0.5$, $\beta=0.176$, $\kappa=14.71$, $\theta=6620$. Those values are fitted by experimental data. The values for x_i and k_i are applied that the equation shows a minimum. The reciprocal density is equal to the specific volume, which results in a specific energy if it is multiplied with the pressure. The whole energy in the system is represented by the energy of formation. ^[32]

4.2.3 Explosion products - Kistiakovsky-Wilson and Springall-Roberts Rules^[2a]

The outcome of an explosion is besides the energy and shock wave a couple of gaseous products. Most of those are carbon monoxide, carbon dioxide, water and nitrogen. But at an increased oxygen balance over zero there are also nitrogen oxides formed. If the oxygen balance is lower than zero solids like carbon are in the output, too.

The Kistiakowsky-Wilson rules predict the explosion products and are nowadays nearly completely substituted by the more progressive Springall-Roberts Rules. To guess the explosion products by this rule.

First every carbon is converted to carbon monoxide, afterwards all hydrogens are converted with the oxygen to water. If there is not enough oxygen left than

carbonmonoxide is converted back to carbon. If there is oxygen left carbonmonoxide is further oxidized to carbon dioxide.

4.2.4 Input parameters: Oxygen balance, heat of formation and density

As input parameters for the calculation are necessary the density of the condensed phase (solid state) of an explosive compound or mixture, which is necessary for the calculation of the propagation of the detonation wave respectively the detonation velocity. The sum formula and as resulting out of it the oxygen balance which is essential for the right assumption of the products of the explosion and their thermodynamic output and pressure. Last but not least the heat of formation or better the energy of formation per kg explosive assumes the whole energy in the compound or mixture which could be used for the explosion. These three parameters are from the point of physics the only ones interesting for the process of explosion.

Oxygen balance	$C_aH_bN_cO_d$	$\Omega = \frac{(d - 2a - \frac{1}{2}b) \cdot 1600}{M}$	(M= molecular mass)
-----------------------	----------------	---	---------------------

Heat of formation	determined by bomb calorimetry or calculated by ab initio methods
--------------------------	---

Density	determined by pygrometer or crystal structure analysis
----------------	--

The influence on those three parameters from the view of a chemist is not easy, especially as there are demands like sensitivity and thermostability which also influence the application of an explosive.

So to speak the efforts on the demands of explosives are not simple to fulfill. The limitations are set by nature. It is possible to form energetic materials with high energy content and good density but a very lack of stability and great sensitivity like azido compounds of tetrazoles. On the other hand stability is found in interaction of nitro groups, hydrogen bonding etc. Those often decrease the performance inevitably.[33]

4.3 Practical methods

4.3.1 Sensitivity testing

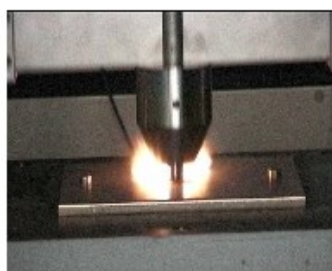
The sensitivity values of a compound or mixture are essential for working with dangerous substances. To determine the sensitivity data there are used different methods, the BAM drophammer for impact sensitivity, the friction tester for friction sensitivity and the ESD apparatus for measuring the sensitivity to electric discharge.

A compound is regarded sensitive or insensitive according to the STANAG and UN standards when it compares to the values listed in table 3.^[34]

Table 3. Classifications according to UN standards (*non-UN conform italic*).

E_{dr} / J	Impact sensitivity	E_{dr} / J	F_r / N	friction sensitivity
>40	not sensitive			
<40..5	slightly sensitive		360	slightly sensitive
35..>11	<i>little</i>			
11..>5	<i>modest</i>	<35..4	<360..>80	sensitive
5..>4	<i>increased</i>			
4..>3	<i>high</i>	3..0	80..>10	very sensitive
3..>1	<i>very high</i>		10..0	extreme sensitive

BAM DROPHAMMER



In the impact sensitivity test the used apparatus is the BAM drophammer, which is constructed according to the plans of the Bundesanstalt für Materialprüfung (BAM) in Berlin. Therefore a material that should be tested is filled to a small sleeve consisting of two stainless steel cylinders and a steel ring. This probe is set in the apparatus where a defined weight (0.5 to 10 kg) is dropped from a defined height (10 cm to 1 m) on the probe. This test is repeated until a reaction is observed (smoke, crack, detonation etc.) and at this height and with this weight five times confirmed to be not a random reaction. The determined value is the minimum impact energy for decomposition.

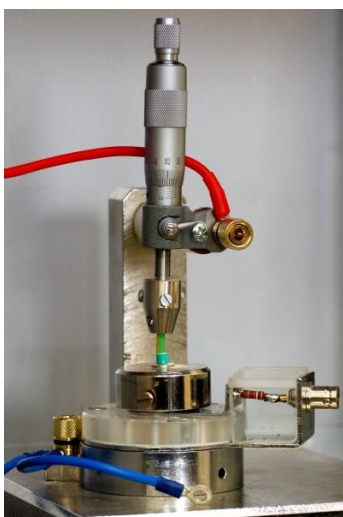
FRICTION TESTER



In the friction sensitivity test the used apparatus is the OZM friction tester. Therefore a material that should be tested is put on ceramic plate (2 cm x2 cm) and a ceramic cone is set with the cone end on the sample. Then a weight (0.2 kg to 36 kg) is applied to press the cone end on the probe. Now by a rotating motor the connecting rod moves the cone end over the substance. This test is repeated until a reaction is observed (color change, smoke, crack, detonation etc.) and

with this weight five times confirmed to be not a random reaction. The determined value is the minimum friction force for decomposition.

ESD APPARATUS



The sensitivity to electrostatic discharge is measured by using a small amount of a compound pressed in plastic cap. This is placed beneath a metal needle and on top of a conductive surface. According to the used electric energy which should be applied to the probe there is chosen a set of condensers and mounted at the apparatus. Afterwards the condensers are loaded and the whole electric energy is released in a sudden to the probe as high voltage spark/lightning out of the tip of the needle to the grounded surface through the probe. If the probe detonates or burns the compound either is extremely sensitive or the energy applied energy was too high. The minimum energy is determined at the point the compound does not show an obvious reactions but if the probe is examined after the treatment and there is found any change in color of the compound, the test is positive.

4.3.2 Determination of density

PYGNOMETER

The gas pynometer is designed to measure densities. The method includes a defined volume of container in which a sample of a compound is filled and the sample weight is determined. After closing the volume is evacuated and purged with helium. After another evacuation the helium of a certain volume is inserted in the probe. The last step is repeated with increasing volume of helium until it is near the volume of the container. By calculation of the volume filled by the sample substance and the mass of the sample, the density is easily determined.

X-RAY DIFFRACTION

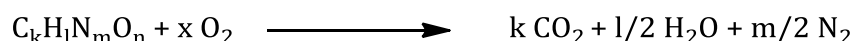
This short introduction will not describe the whole method of x-ray diffraction single crystal determination, but it is mentioned as method to gain the density of a material in

a simple way and what is more important - a theoretical maximum density (TMD). This is important especially for energetic materials. As those are compressed for use, the TMD is the value to which a compound could be pressed at maximum. While the experimental data by a pycnometer can have failure by inclusion of air and solvent during preparation although it may be pure substance there are porous, fluffy or very hard materials which do not let helium penetrate in the material or through it. Therefore a crystal by definition is the most efficient packing of molecules or atoms in a certain space or volume. There can also be included solvents which are found by solving the crystal structure.

4.3.3 Measuring the Heat of formation

BOMB CALORIMETRY

Under pressure of 10 atm oxygen in a stainless steel bomb the sample substance is burned together with benzoic acid as standard. The temperature difference of a defined amount of water before burning and after burning the probe is measured and the heat of the burning is gained. From this heat of burning the substance to the products water, carbon dioxide and nitrogen the heat of formation can be calculated by difference of the heats of formation of the products and the determined heat of burning (reaction energy). To calculate the enthalpy of formation the entropic change of the number of molecules before and after the reaction has to be taken in account.



5 References

- [1] J. Akhavan, *The Chemistry of Explosives*, 2nd edition, The Royal Society of Chemistry, Cambridge, **2004**.
- [2] a) T. M. Klapötke, *Chemie der hochenergetischen Materialien*, Walter de Gruyter, Berlin, New York, **2009**. b) Köhler J., Meyer R., Homburg A., *Explosivstoffe*, 10. Auflage, Wiley-VCH, Weinheim, **2008**
- [3] T. G. Archibald, R. Gilardi, K. Baum, C. George, *J. Org. Chem.* **1990**, 55, 2920.
- [4] M. D. Coburn, M. A. Hiskey, T. G. Archibald, *Waste Manage.* **1997**, 17, 143.
- [5] M. X. Zhang, P. E. Eaton, R. Gilardi, *Angew. Chem. Int. Ed.* **2000**, 39, 401.
- [6] A. T. Nielsen, A. P. Chafin, S. L. Christian, D. W. Moore, M. P. Nadler, R. A. Nissan, D. J. Vanderah, R. D. Gilardi, C. F. George, J. L. Flippen-Anderson, *Tetrahedron* **1998**, 54, 11793.
- [7] H. H. Cady, A. C. Larson, *Acta. Cryst.* **1965**, 18, 485.
- [8] [United Kingdom Parliament, »Memorandum from Prospect, 23 January 2006«, <http://www.parliament.uk>, (29.08.2009).
- [9] N. V. Latypov, J. Bergman, A. Langlet, U. Wellmar, U. Bemm, *Tetrahedron* **1998**, 54, 11525.
- [10] K.-Y. Lee, L. B. Chapman, M. O. Coburn, *J. Energ. Mater.* **1987**, 5, 27.

- [11] P. F. Pagoria, G. S. Lee, A. R. Mitchell, R. D. Schmidt, *Thermochim. Acta* **2002**, 384, 187.
- [12] A. K. Sikder, N. Sikder, *J. Hazard. Mater.* **2004**, 112, 1.
- [13] J. P. Agrawal, R. Hodgson, *Organic Chemistry of Explosives*, Wiley, Chichester, **2007**.
- [14] D. T. Cromer, H. L. Ammon, J. R. Holden, *A Procedure for Estimating the Crystal Densities of Organic Explosives*, Defense Technical Information Center, **1987**.
- [15] B. M. Rice, J. J. Hare, E. F. C. Byrd, Accurate Prediction of Crystal Densities Using Quantum Mechanical Molecular Volumes, *J. Phys. Chem. A* 111, **2007**, 10874.
- [16] J.P. Agrawal, *High Energy Material Materials*, Wiley-VCH, Weinheim, **2010**, pp 131.
- [17] T. M. Klapötke, G. Holl, *Green Chem.* **2001**, 3, G75.
- [18] M. E. Barsan, A. Miller, *Health Hazard Evaluation Report 91-0346-2572*, National Institute for Occupational Safety and Health (NIOSH), Cincinnati, OH, USA, **1996**
- [19] T. M. Klapötke, G. Steinhauser, *Angew. Chem.* **2008**, 120, 3376.
- [20] T. M. Klapötke in *Moderne Anorganische Chemie* (Hrsg. E. Riedel), 3. Auflage, Walter de Gruyter, Berlin, New York, **2007**.
- [21] H. Abou-Rachid, A. Hu, V. Timoshevskii, Y. Song, L.-S. Lussier, *Phys. Rev. Lett.* **2008**, 100, 196401-1.
- [22] M. I. Eremets, A. G. Gavriliuk, I. A. Trojan, D. A. Dzivenko, R. Boehler, *Nat. Mater.* **2004**, 3, 558.
- [23] M. I. Eremets, A. G. Gavriliuk, I. A. Trojan, *Appl. Phys. Lett.* **2007**, 90, 171904.
- [24] J. A. Ciezak, T. A. Jenkins, 26th Army Science Conference, Orlando, FL, USA, 1–4. Dezember, **2008**, GP-01.
- [25] K. O. Christe, W. W. Wilson, J. A. Sheehy, J. A. Boatz, *Angew. Chem. Int. Ed.* **2000**, 38, 2004.
- [26] A. Vij, W. W. Wilson, V. Vij, F. S. Tham, J. A. Sheehy, K. O. Christe, *J. Am. Chem. Soc.* **2001**, 123, 6308.
- [27] "Perchlorate: Health And Environmental Impacts Of Unregulated Exposure". *United States Congress*. Retrieved 15 April **2012**.
- [28] Yinon, Jehuda, Toxicity and metabolism of explosives. *CRC Press*. **1990**, pp. 176, ISBN 0-8493-5128-6.
- [29] M. Sućeska, *EXPLO5 5.04*, Zagreb, Hrvatska, **2009**.
- [30] P. O. K. Krehl, "Shock wave physics and detonation physics — a stimulus for the emergence of numerous new branches in science and engineering", *European Physical Journal H* **2011**, 36, 85.
- [31] D. L. Chapman, *Phil. Mag.* **1899**, 47, 390; b) J. C. E. Jouguet, *J. Maths Pure Appl.* **1905**, 7, 347.

- [32] a) C. L Mader, Numerical Modeling of Detonations, University of California Press, Los Angeles, USA, **1979**, p. 57, b) 2. C. L Mader, Numerical Modeling of Explosives and Propellants, CRC Press, New York, USA, **1998**, p. 33.
- [33] a) J. Stierstorfer, Dissertation, LMU München, **2009**. b) F. A. Martin, Dissertation, LMU München, **2010**. c) J. M. Welch, Dissertation, LMU München, **2008**.
- [34] a) M. Sućeska, Test Methods for Explosives, Springer, New York, **1995**. b) NATO Standardization Agreement 4489 (STANAG 4489), 17. September, **1999**. c) WIWEB-Standardarbeitsanweisung 4-5.1.02, 08. November, **2002**. d) NATO Standardization Agreement 4487 (STANAG 4487), 22. August, **2002**. e) WIWEB-Standardarbeitsanweisung 4-5.1.03, 08. November, **2002**. f) Recommendations on the Transport of Dangerous Goods, Manual of Tests and Criteria, 4th edition, United Nations, New York, Geneva, **1999**.
- [35] a) REICHEL & PARTNER GmbH, <http://reichel-partner.de/> b) Test methods according to the UN Recommendations on the Transport of Dangerous Goods, Manual of Test and Criteria, fourth revised edition, United Nations Publication, New York and Geneva, **2003**, ISBN 92-1-139087-7, Sales No. E.03.VIII.2; 13.4.2 Test 3(a)(ii) BAM Fallhammer.

Part II

EXPLOSIVE UREA DERIVATIVES

Chapter I

A COMPREHENSIVE STUDY ON N,N'-

BIS(TRIS(NITRATOMETHYL)METHYL)OXAMIDE

Abstract:

The explosive properties of N,N'-bis-(tris-(nitratomethyl)-methyl)-oxamide and the sensitivity is explained by consideration of the crystal structures and the calculated (DFT/B3LYP 6-31g(2d,p)) electrostatic surface potential (ESP). The calculated and experimental data for N,N'-bis-(tris-(nitratomethyl)-methyl)-oxamide shows strong similarity with PETN and thus a comparison in properties is discussed closely, although the anisotropic aspect of impact sensitivity of PETN is not found in the oxamide derivative. This makes N,N'-bis-(tris-(nitratomethyl)-methyl)-oxamide good alternative to PETN. In particular, powder samples of N,N'-bis-(tris-(nitratomethyl)-methyl)-oxamide show low sensitivity to impact and friction which is important for handling and processing.

Keywords: PETN, Tris-(hydroxymethyl)-aminomethane (TRIS), N,N'-Bis-(tris-(nitratomethyl) methyl)-oxamide, sensitivity, crystal structure, ESP, thermodynamic data, DFT, B3LYP, CBS-4M, enthalpy of formation, energetic data.

1 Introduction

In the search for new energetic materials for use as secondary explosives certain properties are particularly desirable. The ideal explosive should exhibit high density, combine fuel and oxidizer in one compound and show low sensitivity towards shock and friction. One common explosive showing nearly all of these properties is the pentaerythritol tetranitrate (PETN). Although PETN is cheap and shows a high performance, it is relatively sensitive and is therefore mostly used in mixtures with TNT, RDX or HMX e.g. SEMTEX.

But one other problem leads in pure PETN to an uncompleted combustion. The fact that impact sensitivity of PETN is highly depending on the direction the PETN crystal is compressed^[1]. Therefore an explosive that shows an impact sensitivity which is independent of the direction the external pressure is applied could overcome this problem and result in a better burn rate.

To disorder the high ordered tetragonal crystal structure of PETN it is necessary to introduce a rigid bridge that will not affect the explosive performance. This is achieved by the incorporation of an oxamide bridge which is oxygen and nitrogen rich, and stiffens the whole molecule by its delocalized electrons.

In addition, the investigation of the N,N'-bis-(tris-(nitratomethyl)-methyl)-oxamide is also of interest in order to elucidate further information of an energetic materials regarding the structure, stability and sensitivity. This is performed by comparison of the experimental determined solid state structure with the calculated electrostatic surface potential.

2 Results and Discussion

The structures of the N,N'-bis-(tris-(nitratomethyl)-methyl)-oxamide (BTNMM-oxamide) and PETN differ only in the presence of an oxamide bridge (NHCO)₂ instead of the CH₂ONO₂-group, which is present in PETN. The presence of the oxamide bridge is not expected to greatly affect the explosive properties, since the explosion products are mostly gases such as CO, CO₂, H₂O(g) and N₂ as well as various nitrogen oxides. However, the sensitivity should be very different. It is well known that a molecule wants to take the least room in space which means a sphere like geometry. Through the shortening of the distance between the energetic nitrate groups in the molecule (**II**), we would expect a much higher electrostatic surface potential (ESP), which is also known as a factor in the calculation of sensitivity data. The calculated ESP data is compared to the experimentally obtained data, such as crystal structures, friction and impact sensitivity data, the calculated explosive data and the calculated energies of formation.

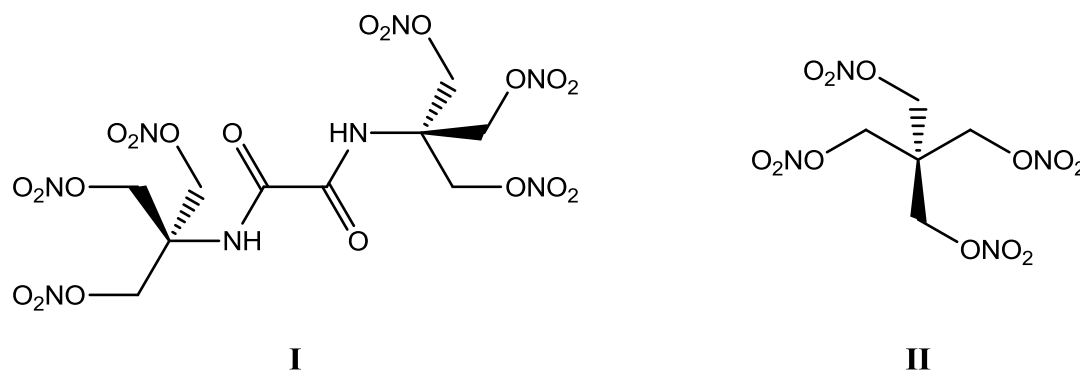


Figure 1. Structures of BTNMM-oxamide(I) and PETN (II).

The impact and friction sensitivities were measured using the standard BAM methods (drop hammer and friction test). The thermodynamic values were determined experimentally using differential scanning calorimetry and bomb calorimetry.

The PETN derivative BTNMM-oxamide was chosen because PETN is a standard model molecule which has been investigated for many years. Nearly all relevant data has been published about PETN including the sensitivity data^[2], ESP calculations^[3,4], crystal structure^[5] and decomposition mechanism^[6,7]. These properties of PETN will be compared with those determined in this work for BTNMM-oxamide, which has been thoroughly investigated for the first time in this work.

2.1 Comparison of crystal structures

The explosive character of N,N'-Bis-(tris-(nitratomethyl)-methyl)-oxamide (**I**) has been previously reported in the literature^[8] using a lead block test. However no further sensitivity data has been reported. BTNMM-oxamide is a very stable powder with a high melting point of 155°C and decomposes at 158°C. In the crystalline state no melting point was observed prior to decomposition at 157°C.

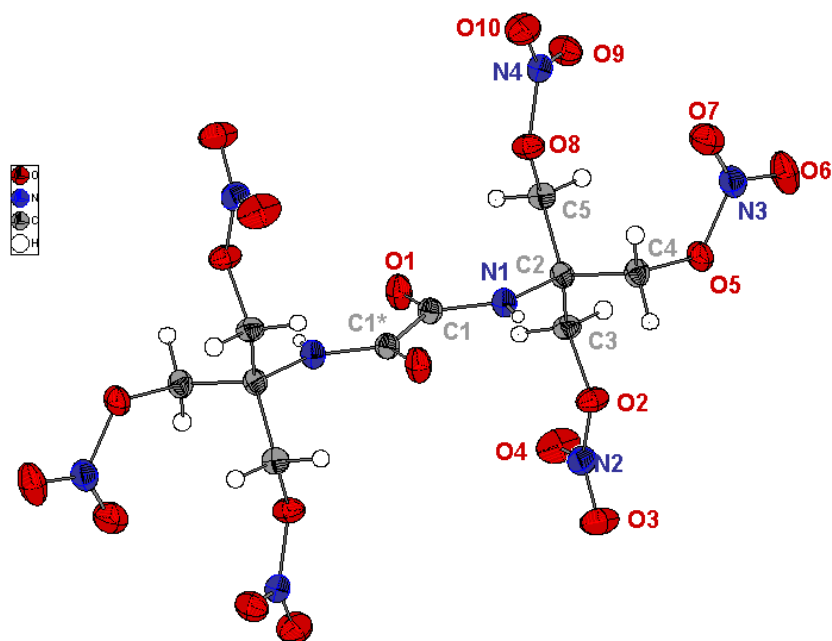


Figure 2. Molecular structure of BTNMM-oxamide in crystalline state determined by SC-XRD with thermal ellipsoids at 50% probability level; selected bond length [Å] and angles [°] C1–C1* 1.531(4); C1–N1 1.337(2), C1–O1 1.222(2), N1–C2 1.461(2), C2–C3 1.529(3), C3–O2 1.444(2), O2–N2 1.404(2), N2–O3 1.205(2), N2–O4 1.194(2), C1*–C1–O1 121.9(2), C1*–C1–N1 112.1(2), O1–C1–N1 126.0(2), C1–N1–C2 125.2(2).

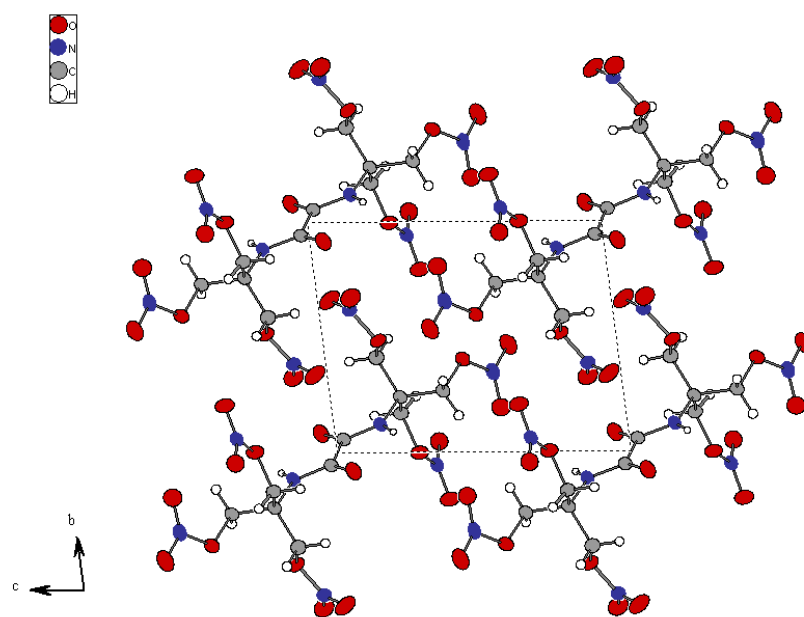


Figure 3. A view of the unit cell of BTNMM-oxamide along a-axes; determined by SC-XRD with thermal ellipsoids at 50% probability level; no shear planes available.

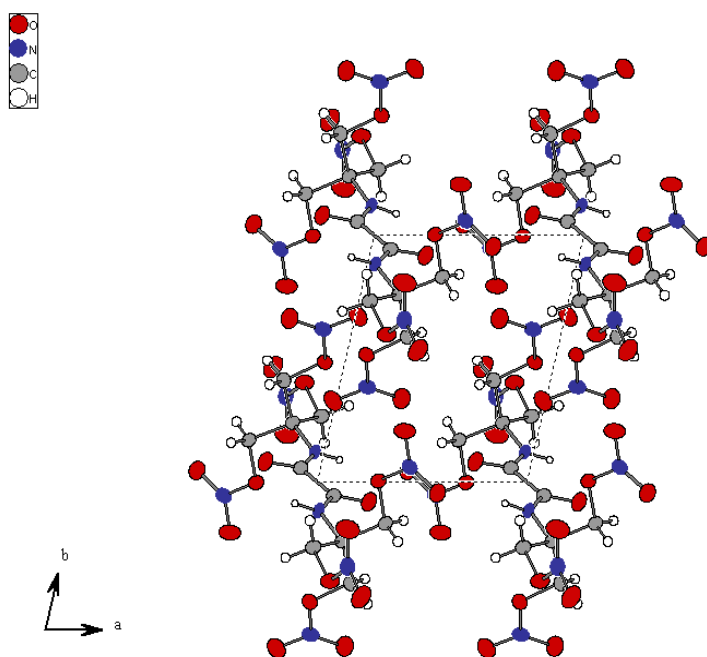


Figure 4. A view of the unit cell of BTNMM-oxamide along c-axes; determined by SC-XRD with thermal ellipsoids at 50% probability level; no shear planes available.

The oxamide building block is expected to be the place where the molecules would crack first into two parts. Such a crack leads to a high amount of activation energy which is able to start or accelerate the upcoming explosion. This means that the molecule is a good explosive although the sensitivity to impact or shock especially in a mono- or polycrystalline state will raise.

The shearing of the crystal lattice in one direction will turn the propeller like tris-(nitromethyl)-methane against the more rigid conjugated oxamide bridge. The sudden high tension in the molecule will happen to crack one of the carbon monoxide building blocks out of the molecule which comes up with a chain reaction through the whole crystal and leads to an explosion. These shear forces would imply a high friction sensitivity, but there is no sensitivity measurable. This does not mean that it is not existent but the device for measuring the friction sensitivity first crushes the crystals to the very insensitive powder. This is possible because the crystal is held together only by rather weak van-der-Waals interaction.

The explosion would not only happen if shear forces or pressure are applied to the crystal, but also if there is a high temperature. The molecule movement will also stress the predetermined breaking point between the both carbonyl carbon atoms (C1 and C*) respectively the bond between the nitrogen (N1) and branched carbon atom(C2).

The stable PETN I low temperature crystal structures is determined through its nearly tetrahedral molecular structure for a different crystal packing. The S4-center of symmetry is settled in the middle of central carbon atom. This leads to a higher symmetry in the crystal by default^[5].

The crystal structure of the BTNMM-oxamide is triclinic and has only one inversion center in between the two carbon atoms of the oxamide bridge. As there are no more interactions between the molecules the ordering will be according to the best space filling. In this case the repulsion of the electronegative flexible nitrato-groups will prearrange in the densest ordering of the molecules in the crystal.

As an opposed structure the BTHMM-oxamide can be mentioned which lacks the nitrato group and has in spite of that hydroxy functions which can stabilize a higher ordered orthorhombic space group. The intermolecular hydrogen bondings prearrange the molecules to very close packing^[9]. Comparing these three crystal structures it is shown that the very stable BTHMM-oxamide is forced by the nitration to the BTNMM-oxamide to overcome the hydrogen bonding and assemble only in a weaker bonded structure as so the PETN structure does. The effect of lower lattice energy should be found as a noticeable value in the explosive data where the PETN compared to the BTNMM-oxamide should perform better in all data because of the rather small molecule that are easily abstracted from the single crystal during combustion.

Table 4. Crystallographic data for the PETN, BTHMM-oxamide and BTNMM-oxamide.

name	BTHMM-oxamide ^[9]	BTNMM-oxamide	PETN I ^[5]
formula	C ₁₀ H ₂₀ N ₂ O ₈	C ₁₀ H ₁₄ N ₈ O ₂₀	C ₅ H ₈ N ₄ O ₁₂
mol. weight	296.28	566.3	316.14
crystal system	Orthorhombic, <i>Pna</i> 2 ₁	Triclinic, <i>P</i> -1	Tetragonal, <i>P</i> -42 ₁ c
a / Å	21.4097(3)	6.911(5)	9.38
b / Å	6.1559(6)	8.014(5)	9.38
c / Å	10.0605(13)	10.163(5)	6.71
α / °	90	79.262(5)	90
β / °	90	74.543(5)	90
γ / °	90	74.640(5)	90
V / Å³	1325.9(2)	519.1(6)	589.495
Z	4	1	2
crystal form	Colorless needle	Colorless block	-
crystal size [mm³]	0.30 x 0.10 x 0.10	0.18 x 0.14 x 0.08	-
ρ_{calc.} / g cm⁻³	1.48	1.81	1.78
radiation	Mo / K _a , 0.71	Mo / K _a , 0.71	-
T / K	150(2)	200(2)	283-303
θ / °	2.9 – 27.5	4.16 – 27.00	-
μ / mm⁻¹	0.13	0.18	-
refl. param.	9375	2927	-
independ. refl.	1573	2224	-
Refl.	1282	1252	-
R_{int}	0.101	0.04	-
Parameters	235	200	-
W_R2 (all data)	0.12	0.07	0.152
R1 (I > 2 σ (I))	0.05	0.04	-
S (GooF)	1.02	0.82	-

2.2 Vibrational and thermodynamical data and Calculations

The Raman spectrum shows intense signals at approx. 3000 cm⁻¹, which correspond to the methylene moiety, whereas the signals at about 1250 cm⁻¹ are typical for the nitro vibrations. Carbonyl group vibration around 1750 cm⁻¹ and the amide vibration at about 1470 cm⁻¹ are typical for oxamide moiety.

The spectra should complement according to the methods but as shown here the very characteristic signals like the methylene moiety, the nitrate as well as the carbonyl moiety are found in both spectra. Some vibrations are only observed in the IR spectrum like the N-H stretching vibration for the amide at 3300 cm⁻¹.

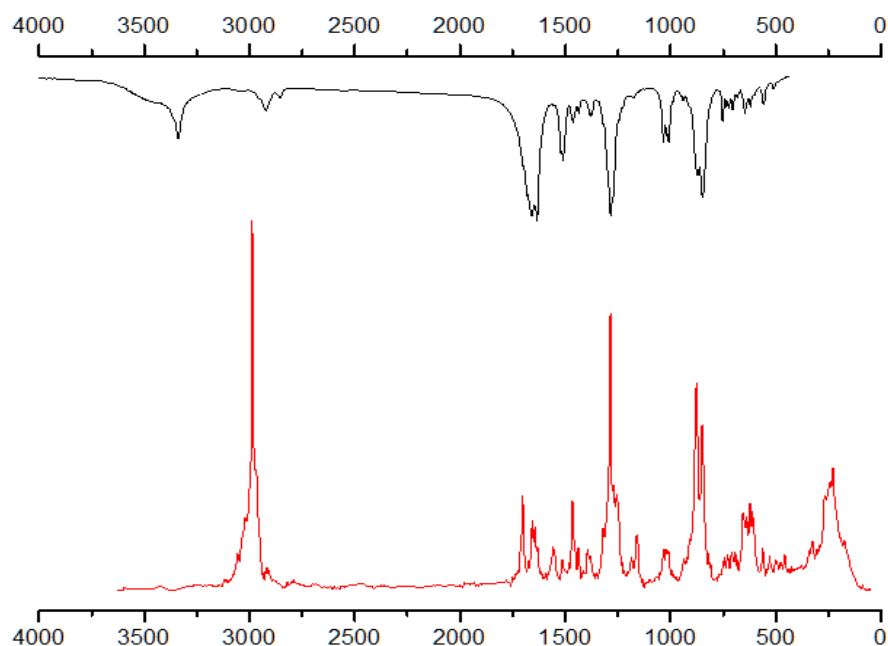


Figure 5. Experimental Raman (red) and IR (black) spectrum of BTNMM-oxamide plotted in one diagram; scales are given in wave numbers (cm^{-1}).

Not only the correlation between the two vibrational methods like Raman and IR have been done, but also a calculation of the vibrations with B3LYP method at 6-31G(2d,p) level of theory. This calculation was accomplished to assign the functional groups to the observed vibrational absorptions.

Table 5. IR-vibrations calculated with gaussian03 B3LYP/ 6-31g (2d,p), these vibrations are corrected by an fitting factor and compared to those of the experiment.

Calculated vibrations $/\text{cm}^{-1}$	Intensity $/\text{D}(10^{-40}\text{esu}^2\text{cm}^3)$	Corrected by factor 0.975 $/\text{cm}^{-1}$	measured $/\text{cm}^{-1}$
			751(m)
860	1060	838	846(m)
			871(m)(O-N)
			1008(m)
1060	112	1033	1033(s)(C-O)
1330	757	1296	1284(m)
1430	100		
1550	723	1511	1509(m) (C=N)
			1634(s) (N-O,NO ₂)
1770	1529	1725	1658(s)(C=O)
3052-3150	8 – 20	2975-3071	2922 (w)(C-H)
3552/3529	100	3463/3440	3338 (m,br)(N-H)

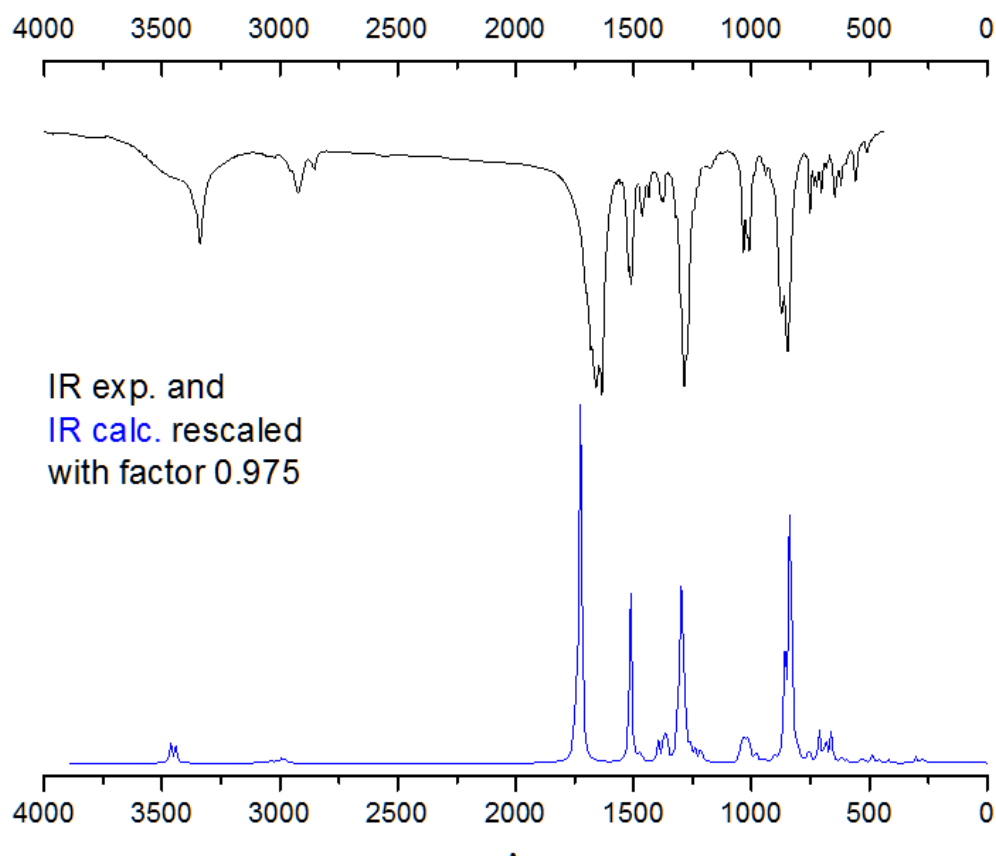


Figure 6. Calculated IR-spectra, gaussian03 B3LYP/ 6-31g (2d,p) (blue) and exp. values (black) visualisation of table 2; scales given in wave numbers (cm^{-1}).

After fitting the calculated results with a factor of 0.975 the data of the measured IR and the calculated spectra were in good accordance. This data was used to evaluate the peaks according to the vibrations of the functional groups. The peaks with relevant intensities were compared and found to be fitting very well. This does not only support the theory for which major vibrations are found as well in the solid phase (measured) as in the gas phase (calculation) but shows in a highly effective way which molecular vibrations are affected most by the differences in states. The C-H vibrations for example are higher in solid state as well as the C-O single bond vibrations about 1050 cm^{-1} . In gas phase they are found to have rotational degrees of freedom around while both are fixed to a certain position in solid state. Therefore similar directional adjustment seems to influence the intensities in IR spectroscopy more than expected especially when bond to rotating centers or atoms.

2.2.1 Thermodynamical calculation and experimental data

Table 6. Thermodynamical data of BTNMM-oxamide: calculation and experiment.

ΔH_f° (experimental)	– 329.3 kcal mol ⁻¹
ΔH_f° (calculated by Gaussian03 [13] B3LYP/6-31G(2d,p))	– 349.0 kcal mol ⁻¹
ΔH_f° (calculated by Gaussian03 [13] CBS-4M)	– 233.8 kcal mol ⁻¹
ΔH_f° (Joback estimation method)	– 274.3 kcal mol ⁻¹

The experimental heat of formation was determined by bomb calorimetry, while the calculated heat of formation was obtained by the Gaussian03 calculation of the energy of formation at *B3LYP/6-31G(2d,p)* level and following a more sophisticated method at *CBS-4M* level. Also the Gaussian based methods are very close to the experimental observed value a third theoretical method was applied. This was done due to the fact that it took very much computer performance and was very time consuming according to the precision of the *CBS-4M* which is the best method for calculating heat of formation by its implementation. The *Joback* method gives a rough estimation especially for big molecules with many degrees of freedom to get a fast and a not too bad result for estimating heat of formation. This will especially be useful during the third chapter concerning a molecule with a weight of more than 900 a.u.. Thermodynamical values for such a molecule are hard to calculate for many available programs at a reasonable time and performance scale.

CBS-4M METHOD

The CBS-4M method is a Gaussian program package implemented method which consists of a set of single calculations which are done subsequently to refine the result. Therefore stands the abbreviation Complete Basis Set (CBS) methods.

The first step is a structural optimization based on Hartree Fock methods. The second step is a frequency optimization with HF basis and refinement on MP2 level and the third step is a MP4SDQ (electron correlation energy 4th order perturbation) calculation. While the normal procedures only include the self consistent field energies (SCF) the CBS methods also include the electron correlation energy, which is not negligible in the correct description of the energy of state like the enthalpy of formation. [14a-h]

Table 7. Enthalpy of formation calculated values by Gaussian03 (values in Hartree/particle); experimental enthalpy of formation for the atoms from the database of the National Institute of Standards and Technology(US) Chemistry Webbook; (values in kcal/mol).

Compound	CBS-4M Enthalpy at 298K	Experimental ΔH_f° (NIST) [10]
BTNMM-oxamide	-2328.451869	-
H	-0.500991	52.103
C	-37.786156	171.29
N	-54.522462	112.97
O	-74.991202	59.56

The CBS-4M method is applied by atomization of the molecule and afterwards reformation which is compared between the calculated formation and the formation of the atomization enthalpy measured in experiments. These values will result in a theoretical value of the energy involved in the reaction. This is the enthalpy of formation as found for a certain molecule from this method in gas phase.

To get a value for the solid phase, there is calculated a phase transition which is estimated by the rule of Trouton by the melting point (T_m).

$$\text{Trouton's Rule} \quad \Delta H_{\text{sub.}} [\text{J mol}^{-1}] = 188 T_m [\text{K}]$$

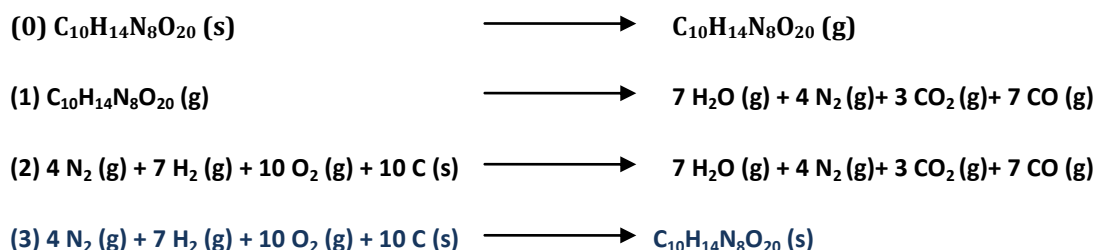
$$188 \text{ Jmol}^{-1}\text{K}^{-1} \times 428.2 \text{ K} = 80502 \text{ Jmol}^{-1} = 19240 \text{ cal mol}^{-1} \sim \mathbf{19.2 \text{ kcal mol}^{-1}}$$

B3LYP- METHOD

According to the following equations and the Hess's law the heat of formation was gained for the B3LYP method.

Table 8. Enthalpy of formation calculated values by Gaussian03 (values in Hartree/particle) ; experimental enthalpy of formation from the database of the National Institute of Standards and Technology (US) Chemistry Webbook; (values in kJ/mol).

Compound	B3LYP/6-31G(2d,p) Energy at 298K	Experimental ΔH_f° (NIST) [10]
BTNMM-oxamide	-2330.883267	
CO ₂ (g)	-188.577077	-393.52
CO (g)	-113.307668	-110.53
H ₂ O (g)	-76.399983	-241.83
H ₂ O (l)		-285.83
N ₂ (g)	-109.518238	0



$$\text{Hess's law} \quad \sum \Delta H_f^0 (\text{reaction}) = \sum \Delta H_f^0 (\text{products}) - \sum \Delta H_f^0 (\text{reactants})$$

The reaction equation 3 shows the important one for the heat of formation, as defined from the elements. Equation 1 is the one used for the calculated reaction the enthalpy thereof is combined with the experimental enthalpy for equation 2 gained from the NIST Webbook of Chemistry tables. Equation 0 is only a phase transition which is estimated by the rule of Trouton by the melting point (T_m)

JOBACK – METHOD – ESTIMATION

The Joback method for estimating the heat of formation uses fragments of a carbon, hydrogen, nitrogen and oxygen containing backbone and assigns to those specific values for heat of formation and heat of fusion. The following equation show how the fragment values are summed up. [14 a-e]

Heat of Formation (Ideal Gas, 298 K)

$$\Delta H_{\text{formation}} = 68.29 + \sum H_i$$

Heat of Fusion

$$\Delta H_{\text{fusion}} = -0.88 + \sum G_i$$

Table 9. Functional groups are assigned with values for heat of formation and heat of fusion given in kcal mol⁻¹.

Functional group	Heat of formation	Heat of fusion
-CH ₂ -	-20.640	2.590
>C<	82.230	-1.460
>C=O (nonring)	-133.220	4.189
-O- (nonring)	-132.220	1.188
-COO- (ester)	-337.920	6.959
>NH (non-ring)	53.470	5.099
-NO ₂	-66.570	9.679

Table 10. The values of table 6 are used with the stated equations to result in the following heat of formation of BTNMMoxamide in solid state.

ΔH_f^0 (gas)	-1243.33	kJ mol^{-1}	-297.15587	kcal mol^{-1}
ΔH_{fusion}	95.518	kJ mol^{-1}	22.828802	kcal mol^{-1}
ΔH_f^0 (solid)	estimated		-274.327068	kcal mol^{-1}

The rough estimation by this fragmental method is compared to the experimental value ($-329.3 \text{ kcal mol}^{-1}$) the closest with a value $-274.327068 \text{ kcal mol}^{-1}$.

Therefore it is found to be in good accordance with all the other methods applied to determine or calculate the enthalpy of formation. To have fast results and get an exceptional good estimation this method is used in further investigations as a first shot or a substitute for calculations which cannot be carried out by the other used methods properly.

2.3 Electrostatic potential (ESP) and Decomposition

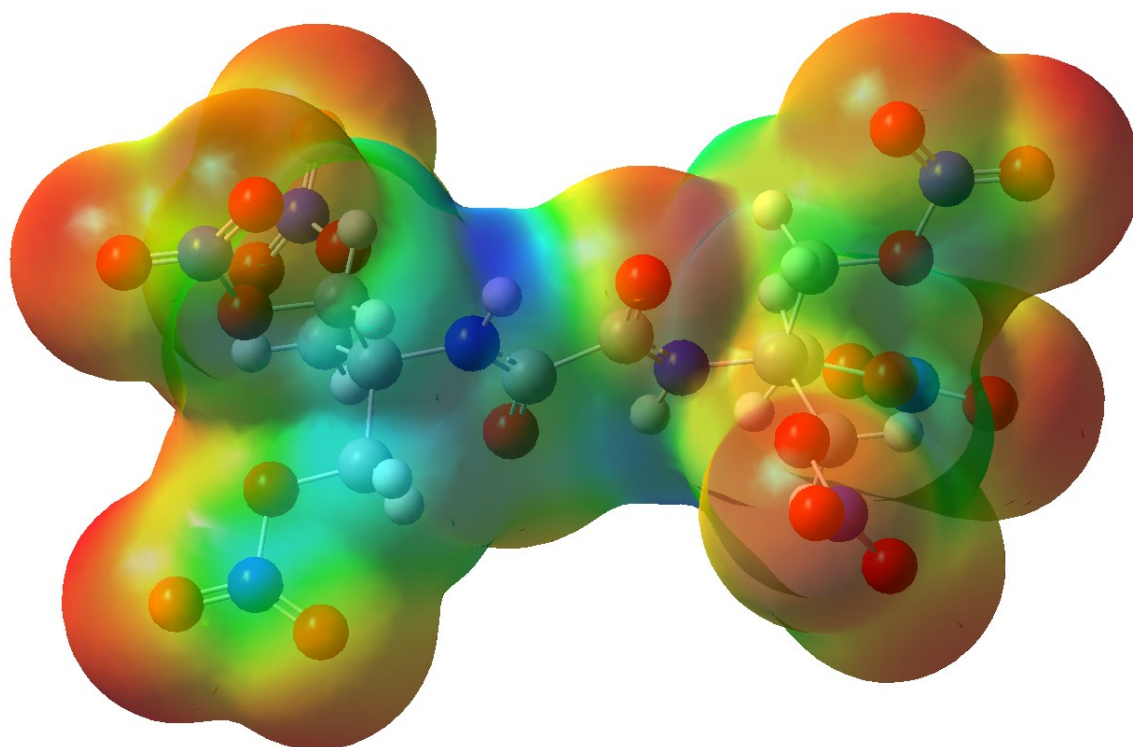


Figure 7. Electrostatic Surface Potential; calculation gaussian03 B3LYP/ 6-31G (2d,p) plot: GaussView^[13b] 0.001 e /bohr³, rendering from -0.023 (red) till 0.080 (blue).

The ESP calculation result in a negative potential at the outer rim, whilst in the inside the positive potential sums up (Fig 7). The ESP of the molecule is the nearly symmetrical distribution of the negative potential on the surface. This belt like potential may lead to an increased stability to impact, shock and friction. Although the difference between the positive (blue) and negative (red) regions of the molecule are common for explosives and they show an extreme high possibility to split of the negative groups like the nitro groups undergoing a spontaneous decomposition.

The initial decomposition of PETN has been shown to occur via the abstraction of an NO_2 -group by homolytic splitting of the $\text{O}-\text{NO}_2$ bond. The mechanism for this initial decomposition step has been well investigated [6,7]. By analogy a mechanism for cracking the bond between the oxamide-N1 and the C2 (Fig 5) can be proposed as an alternative initial decomposition to the splitting off of a NO_2 - group. Also it corroborates the thesis that the twisted molecule will decompose easier. The six membered ring in the transitional state of the mechanism can only form if the molecule is turned out of the optimized structure the calculation and the crystal structure show. That is possible by shearing the lattices in the crystal.

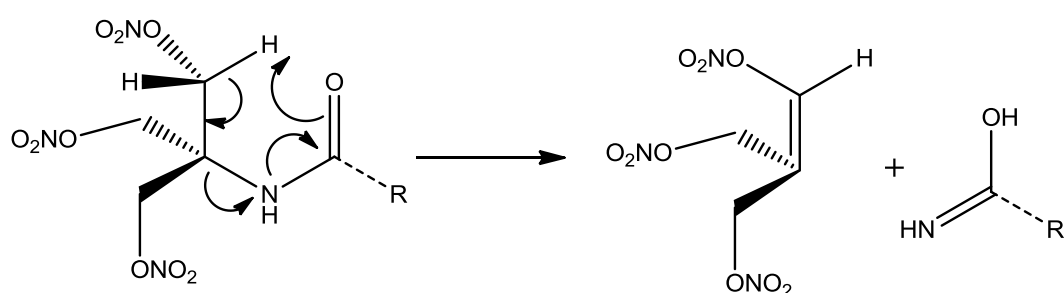


Figure 8. Analogous split-off of the oxamide from the to the propagated mechanism of Chambers et al. for the PETN molecule after loosing one NO_2 [7].

The ESP plotting also shows the electronegative parts are localized on the NO_2 -groups and on the oxamide bridge that gives the molecule a barbell like form with a waist at the oxamide bridge. Comparing this form with the near star-like tetrahedral ESP plotting of the PETN[3] there is no other possibility for PETN to start combustion, only the crack-off of NO_2 -group.

2.4 Thermostability: DSC and RADEX measurements

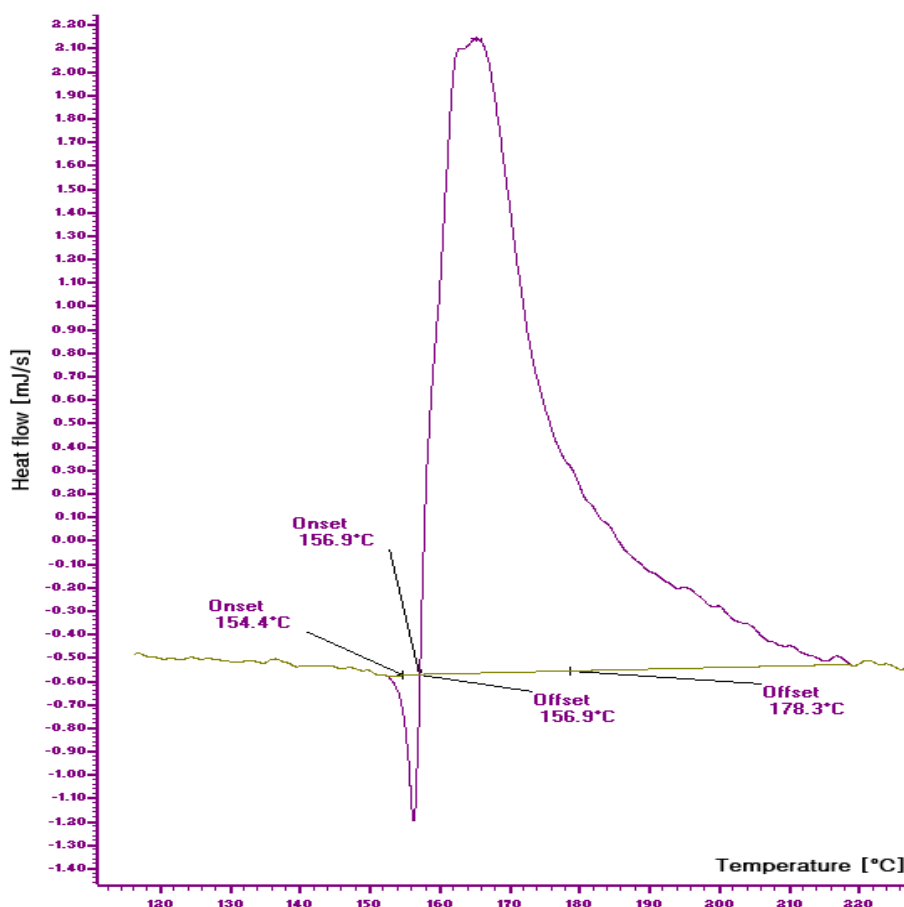


Figure 9. DSC measurement of BTNMM-oxamide: endothermic down and exothermic up, Onset point according to IUPAC standards.

Thermostability is measured in two ways, namely the stability to heating the substance and the long term stability at high temperatures. The first one is measured by DSC and found to be in a good range, except the fact that the material melts and decomposes right afterwards which makes it difficult to distinguish between the real decomposition point and the starting point of decomposition, as the last one may occur during the melting. Looking on the DSC graph these two effects are concurrent which means the endothermic melting phase transition is minimized by the exothermic decomposition and leads not to a right value to evaluate the enthalpies but for correctness of value: the melting point with 154 °C (onset) and 157 °C decomposition point (onset) where definitely more exothermic than endothermic effect is observed (Fig. 9).

The long term stability test is performed by TSC (Thermostability Calorimetry) or RADEX measurements. At a temperature 40°C below decomposition temperature the sample is heated for 24 to 48 hours. To get a positive result there must not be any difference between the sample substance before and after the measurement which means no obvious color change, no weight loss and no decomposition. This test is especially important for storage and use of explosives under extreme climate conditions like in deserts.

2.5 Energetic properties

2.5.1 Comparison of energetic properties of BTNMMoxamide to common explosives

The comparison of the energetic properties besides the sensitivity and decomposition shows some similarities of both BTNMM-oxamide and PETN. In contrast to the other common explosives like TNT and RDX, BTNMM-oxamide and PETN have a very exothermic energy of formation. Although they have nearly the same density they differ in the heat of explosion, the temperature of explosion and in the pressure. But the volume of gas and the velocity of explosion are very similar. So the BTNMM-oxamide is not as good as RDX but very close to the performance of PETN and better than TNT (Table 2).

Table 11. Comparison of the thermodynamical, sensitivity and explosion data (calculated by EXPLO 5^[11]) of BTNMM-oxamide (crystal A, powder) with TNT, RDX and PETN.

comp	TMD / g cm ⁻³	U _f / kJ kg ⁻¹	Ox. bal.	Q _v / kJ kg ⁻¹	V ₀ / L kg ⁻¹	T _{ex} / K	P / kbar	D / ms ⁻¹	imp / J	fric / N	mp / °C	T _{dec} / °C
TNT exptl	1.64 1.64	-184.9	-74	-5089	622	3741	202 210	7150 6950	15	>353	81	300
RDX exptl	1.80 1.80	+417	-21	-6034	769	4334	340 347	8882 8750	7.4	120	204	213
PETN ^[12] (EXPLO 5)	1.77	-1594	-10	-5975	769	4140 4398	331 318	8350 8599	3		141	163
BTNMM- oxamide (powder, crystal)	- 1.81	-2488	-20	-4729	730	3670	282	8181	>30 2	>360 (>360)	155 -	160 157

As the values for the ESP were calculated, the enthalpy of formation can also be calculated from the gained data. Comparing these values with the data of the bomb calorimeter test it is possible to say that the chosen calculation method leads to very good results (Table 3).

2.5.2 Koenen (steel sleeves) test

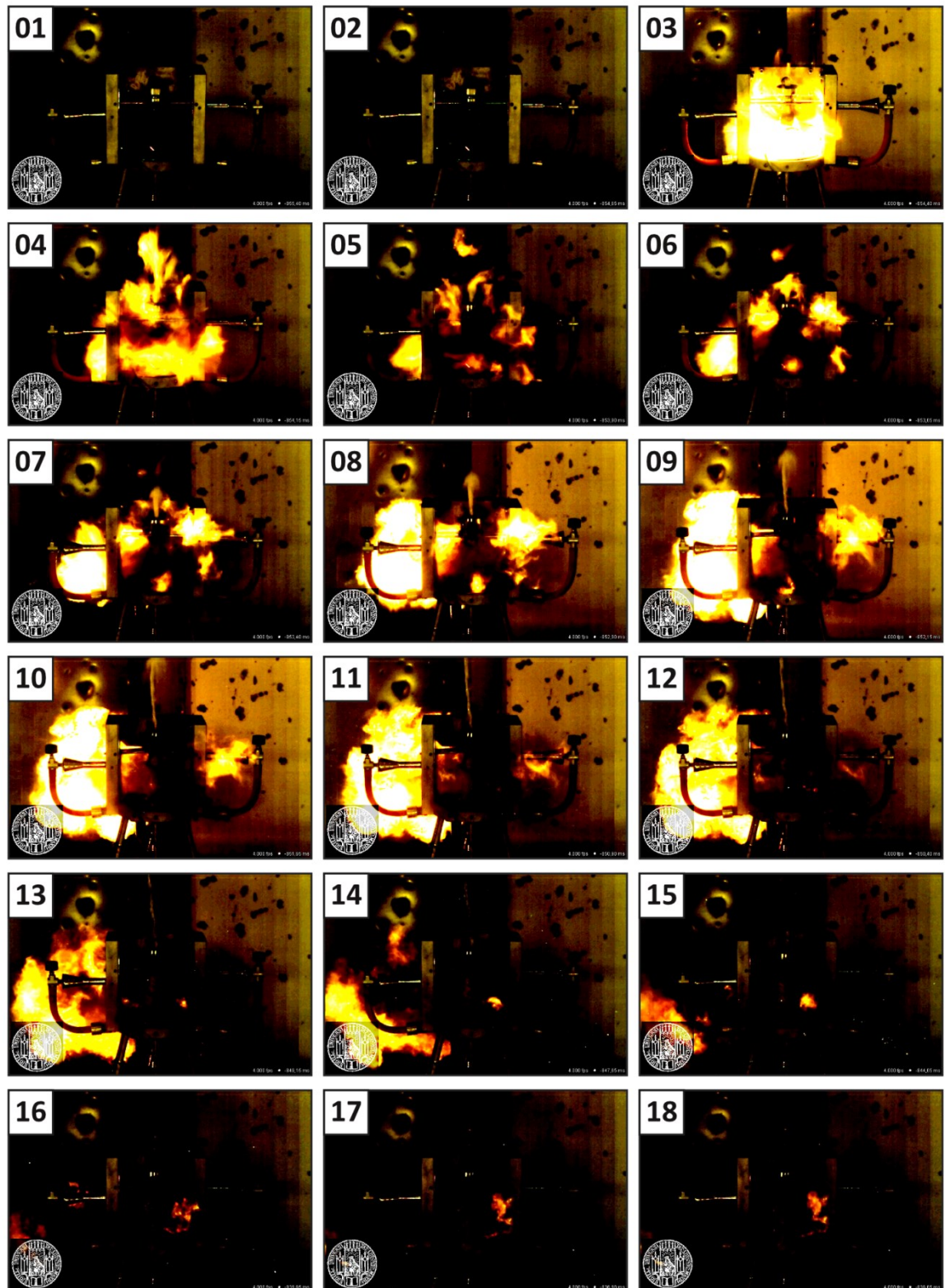


Figure 10. Highspeed pictures taken at 4000 fps showing the progress of the explosion starting at point 0ms with the explosion and ending 16.75 ms later.

The Koenen or steel sleeves test is used to test on the one side standardized the slow cook off properties of energetic material on the other side it is possible evaluate roughly the performance. 34 grams of BTNMM-oxamide were confined in steel sleeve and heated up with four Bunsen burners from two from the sides, one from bottom and one from behind. Figure 6 shows the explosion to the bottom on picture three to six followed by a jet stream out of the 10 mm hole on the top. This means the denser material was found in the bottom part of the sleeve whereas the top powdery material was pushed out by the pressure of the explosion.



Figure 11. Koenen test: first row (before), second row (after), third row no explosion only combustion due to less density but only minimal residue.

Influence from the filling of the steel sleeves on the behavior of the tests: first test setup with 36 g BTNMMoxamide led to four fragments and second test setup with 29.7 g BTNMMoxamide no fragmentation at all burning nearly residue less.

3 Conclusions

The calculated and experimental data for N,N'-bis-(tris-(nitratomethyl)-methyl)-oxamide shows strong similarity with PETN. But the directional aspect of the impact sensitivity of PETN is not found in the oxamide derivative. This makes N,N'-bis-(tris-(nitratomethyl)-methyl)-oxamide a good alternative to PETN. In particular, powder

samples of N,N'-bis-(tris-(nitratomethyl)-methyl)-oxamide show low sensitivity to impact and friction which is important for handling and processing.

4 Experimental

4.1 Crystal structures

The molecular structure of **I** was determined by single crystal X-ray diffraction. The X-ray crystallographic data were collected using an Oxford Xcalibur diffractometer with a CCD area detector and graphite-monochromated Mo K α radiation ($\lambda = 0.71073$ Å). The structure was solved with SIR97^[15] and refined with using SHELXL-97^[16]. Ortep^[17] plots (Figs. 2 + 3) showing thermal ellipsoids with 50% probability for the non-hydrogen atoms in **I** is illustrated in Figs. 2+3.

4.2 Properties

Decomposition points, enthalpies, melting points and dehydration points were determined using a Linseis DSC PT10. Additionally, the melting point and dehydration points were also determined using Büchi B-540 melting point apparatus. The friction and impact sensitivity data were obtained using the BAM drophammer and friction tests, in accordance with the BAM methods ^[17].

4.3 Spectroscopic data and elemental analysis

IR spectra were obtained using a Perkin Elmer Spectrum BX FT-IR System and a Raman spectra were measured using Perkin Elmer Spectrum 2000 FT- Raman spectrometer fitted with a Nd-YAG-laser ($\lambda = 1064$ nm) as solids at room temperature (resolution = 4 cm⁻¹)

NMR spectra were obtained with a Jeol Eclipse 400 spectrometer operating at 400.2 MHz for ¹H, 100.6 MHz for ¹³C and 28.9 MHz for ¹⁴N. Chemical shifts (in ppm) are given with respect to TMS (¹H/¹³C), MeNO₂ (¹⁴N) as internal standard.

4.4 Preparation

N,N'-Bis-(tris-(nitroxymethyl)-methyl)-oxamide (BTHMMoxamide). 7 mL (51.7 mmol) Ethyloxalate was added to a solution of 10 g (82.6 mmol) tris(hydroxymethyl)aminomethane (THMAM / TRIS) in 150 mL ethanol. As catalyst 0.4 mL of conc. hydrochloric acid was added and the reaction mixture was refluxed for two hours. At the boiling point the solution becomes clear and immediately a precipitate was formed. The yield is 8.92 g (30.1 mmol, 58.4%).

Properties: $M = 296.23$ g mol⁻¹. **NMR:** ¹H NMR (400 MHz, DMSO-d₆, ppm): 4.94 (s, 12H, CH₂), 9.21 (s, 2H, NH₂). ¹³C- NMR (100 MHz, DMSO-d₆, ppm): 159.8 (CO), 69.7 (CH₂), 56.0 (C). **IR (KBr)($\tilde{\nu}$ /cm⁻¹):** 3413(s), 3339(s), 3262(br), 2956(s), 2091(w), 1668(s), 1516(s), 1120(s), 687(s), 530(s).

N,N'-Bis-(tris-(nitroxymethyl)-methyl)-oxamide (BTNMMoxamide). To ice-cooled HNO₃ (98%, 3 mL) 200 mg (0.68 mmol) N,N'-bis-(tris-(hydroxymethyl)-methyl)-oxamide were added under stirring followed by 2 mL acetic anhydride which were added carefully drop-wise. After leaving the reaction mixture stirring for three hours, the mixture was poured on ice. The precipitate formed was filtered off and washed with 200 mL water, whereby 363 mg (0.64 mmol) pure N,N'-bis-(tris-(nitratomethyl)-methyl)-oxamide was obtained in 94% yield.

Properties: DSC (2°C / min): mp.155 °C; T_{dec.} 161°C; ΔH_m +19.9 kJ mol⁻¹; ΔH_{dec} -1200 kJ mol⁻¹. **NMR** ¹H NMR (d⁶-DMSO, 400 MHz, ppm): δ 4.94 (s, 12H, CH₂), 9.21 (s, 2H, NH₂); ¹³C NMR (d⁶-DMSO, ppm): δ 159.8 (CO), 69.7 (CH₂), 56.0 (C); ¹⁴N NMR: -42 (ONO₂). **IR** (KBr-disc, ν̄ = cm⁻¹): 751(m), 846(m), 871(m)(O-N), 1008(m), 1033(s)(C-O), 1284(m), 1509(m), 1634(s) (N-O₂), 1658(s)(C=O), 2922 (w)(C-H), 3338 (m,br)(N-H). **Raman** (1085 nm, 100 mW, ν̄ = cm⁻¹): 3318(15), 3031 (25), 2974(58), 1638(23), 1552(18), 1464(33), 1419(34), 1391(18), 1289(100), 1264(37), 1159(17), 1032(23), 880(91), 842(34), 627(64), 608(32), 560(21), 265(38). **Elemental analysis** (calc. % / found %): N 19.8 / 19.1, C 21.2 / 21.8, H 2.49 / 2.36.

Sensitivity data:

Calc Lead Block value 146 (TNT=100)^[8]

Calc Ballistic Mortar Block value 133 (TNT=100)^[8]

Impact sensitivity: > 30 J (powder) , 2 J (crystal)

Friction sensitivity: >360 N (powder) , >360 N (crystal)

RADEX: stable at 117°C / 24h

5 References

- [1] Dick J. J., Mulford R. N., Spencer W. J., Pettit D. R., Garcia E., Shaw D. C., *J. Appl. Phys.* **1991**, 70 (7), 3572.
- [2] Hiskey M. A., Hatch M. J., Oxley J. C., *Propellants, Explos. Pyrotech.* **1991**, 16, 40.
- [3] Rice B. M., Hare J. J., *J. Phys. Chem. A* **2002**, 106, 1770.
- [4] Rice B. M., Byrd E. F. C., *J. Mater. Res.* **2006**, 21 (10), 2444.
- [5] J. Trotter, *Acta Crystallographica* **1963**, 16, 698 (PERYTN10).
- [6] Gruzdkov Y. A., Gupta Y. M., *J. Phys. Chem. A* **2000**, 104, 11169.
- [7] Chambers D. M., Brackett C. L., Sparkman D.O., *Perspectives on PETN Decomposition*, URCL-ID-148956, **2002**, Lawrence Livermore National Laboratory.
- [8] Fankel M. B., Park M., *US 3,228,929*, **Jan.1966** & *US 3,278,578*, **Oct 1966**.
- [9] Ross J. N., Low J. N., Fernandes C., Wardell J.L., Glidewell C., *Acta Crystallographica, Section C*, **2001**, 57 (8), 949.
- [10] U.S. National Institute of Standards and Technology, Chemistry Webbook, <http://webbook.nist.gov/chemistry/>.

- [11] *EXPLO5.V2*, Computer program for calculation of detonation parameters, P. M. Suceska, /Proc. of 32nd Int. Annual Conference of ICT/, July 3-6, Karlsruhe, German, **2001**, pp. 110/1 a software for determining detonation parameter, *2006*.
- [12] Pospisil M.; Vavra P.; *Proceedings of the VII. Seminar: New Trends in Research of Energetic Materials* **2004**, 613.
- [13] *Gaussian 03, Revision C.02*, Frisch, M. J.; Trucks, G. W.; Schlegel, H. B.; Scuseria, G. E.; Robb, M. A.; Cheeseman, J. R.; Montgomery, Jr., J. A.; Vreven, T.; Kudin, K. N.; Burant, J. C.; Millam, J. M.; Iyengar, S. S.; Tomasi, J.; Barone, V.; Mennucci, B.; Cossi, M.; Scalmani, G.; Rega, N.; Petersson, G. A.; Nakatsuji, H.; Hada, M.; Ehara, M.; Toyota, K.; Fukuda, R.; Hasegawa, J.; Ishida, M.; Nakajima, T.; Honda, Y.; Kitao, O.; Nakai, H.; Klene, M.; Li, X.; Knox, J. E.; Hratchian, H. P.; Cross, J. B.; Bakken, V.; Adamo, C.; Jaramillo, J.; Gomperts, R.; Stratmann, R. E.; Yazyev, O.; Austin, A. J.; Cammi, R.; Pomelli, C.; Ochterski, J. W.; Ayala, P. Y.; Morokuma, K.; Voth, G. A.; Salvador, P.; Dannenberg, J. J.; Zakrzewski, V. G.; Dapprich, S.; Daniels, A. D.; Strain, M. C.; Farkas, O.; Malick, D. K.; Rabuck, A. D.; Raghavachari, K.; Foresman, J. B.; Ortiz, J. V.; Cui, Q.; Baboul, A. G.; Clifford, S.; Cioslowski, J.; Stefanov, B. B.; Liu, G.; Liashenko, A.; Piskorz, P.; Komaromi, I.; Martin, R. L.; Fox, D. J.; Keith, T.; Al-Laham, M. A.; Peng, C. Y.; Nanayakkara, A.; Challacombe, M.; Gill, P. M. W.; Johnson, B.; Chen, W.; Wong, M. W.; Gonzalez, C.; and Pople, J. A.; Gaussian, Inc., Wallingford CT, **2004**.
- [14] a) J. A. Montgomery Jr., M. J. Frisch, J. W. Ochterski, and G. A. Petersson, "A complete basis set model chemistry. VII. Use of the minimum population localization method," *J. Chem. Phys.*, **2000**, *112*, 6532-42. !!!!! second on CBS-4M. b) J. A. Montgomery Jr., M. J. Frisch, J. W. Ochterski, and G. A. Petersson, "A complete basis set model chemistry. VI. Use of density functional geometries and frequencies," *J. Chem. Phys.*, **1999**, *110*, 2822-27. c) J. A. Montgomery Jr., J. W. Ochterski, and G. A. Petersson, "A complete basis set model chemistry. IV. An improved atomic pair natural orbital method," *J. Chem. Phys.* **1994**, *101* 5900-09. d) J. W. Ochterski, G. A. Petersson, and J. A. Montgomery Jr., "A complete basis set model chemistry. V. Extensions to six or more heavy atoms," *J. Chem. Phys.* **1996**, *104*, 2598-619. e) G. A. Petersson and M. A. Al-Laham, "A complete basis set model chemistry. II. Open-shell systems and the total energies of the first-row atoms," *J. Chem. Phys.* **1991**, *94*, 6081-90. f) G. A. Petersson, T. G. Tensfeldt, and J. A. Montgomery Jr., "A complete basis set model chemistry. III. The complete basis set-quadratic configuration interaction family of methods," *J. Chem. Phys.* **1991**, *94*, 6091-101. g) M. R. Nyden and G. A. Petersson, "Complete basis set correlation energies. I. The asymptotic convergence of pair natural orbital expansions," *J. Chem. Phys.* **1981**, *75*, 1843-62. h) G. A. Petersson, A. Bennett, T. G. Tensfeldt, M. A. Al-Laham, W. A. Shirley, and J. Mantzaris, "A complete basis set model chemistry. I. The total energies of closed-shell atoms and hydrides of the first-row atoms," *J. Chem. Phys.* **1988**, *89*, 2193-218.
- [15] a) Joback K.G., Reid R.C., "Estimation of Pure-Component Properties from Group-Contributions", *Chem. Eng. Commun.* **1987**, *57*, 233-243; b) Lydersen A.L., "Estimation of Critical Properties of Organic Compounds", University of Wisconsin College Engineering, *Eng. Exp. Stn. Rep. 3*, Madison, Wisconsin, **1955**; c)

- Constantinou L., Gani R., "New Group Contribution Method for Estimating Properties of Pure Compounds", *AIChE J.* **1994**, *40*(10), 1697-1710; d) Nannoolal Y., Rarey J., Ramjugernath J., "Estimation of pure component properties Part 2. Estimation of critical property data by group contribution", *Fluid Phase Equilib.* **2007**, *252*(1-2), 1-27; e) Stein S.E., Brown R.L., "Estimation of Normal Boiling Points from Group Contributions", *J. Chem. Inf. Comput. Sci.* **1994**, *34*, 581-587.
- [16] a) Giacobazzo C. (**1997**) SIR-97 Program for Crystal Structure Solution, Inst. di Ric. per lo Sviluppo di Metodologie Cristallografiche, CNR, Univ. of Bari, Italy; b) Altomare, A.; Burla, M. C.; Camalli, M.; Cascarano, G. L.; Giacobazzo, C.; Guagliardi, A.; Moliterni, A. G. G.; Polidori, G.; Spagna, R. *J. Appl. Cryst.* **1999**, *32*, 115-119.
- [17] Sheldrick, G. (**1997**) SHELXL-97 Program for Crystal Structure Refinement, Institut für Anorganische Chemie der Universität, Tammanstrasse 4, D-3400 Gottingen, Germany
- [18] Johnson, C.K. (**1976**) ORTEP-II. A Fortran Thermal-Ellipsoid Program, Report ORNL-5138. Oak Ridge National Laboratory, Oak Ridge Tennessee.
- [19] a) Reichel & Partner GmbH, <http://reichel-partner.de/> b) Test methods according to the UN Recommendations on the Transport of Dangerous Goods, Manual of Test and Criteria, fourth revised edition, United Nations Publication, New York and Geneva, **2003**, ISBN 92-1-139087-7, Sales No. E.03.VIII.2; 13.4.2 Test 3(a)(ii) BAM Fallhammer.

Chapter II

ENERGETIC CYANURIC ACID DERIVATIVES

Abstract:

The explosive properties of N,N',N'' -tris(nitratomethyl)-isocyanuric acid and N,N',N'' -tris(nitratoethyl)-isocyanuric acid are investigated with respect to sensitivity and performance. Therefore these compounds were synthesized and a comprehensive study of the crystal structure, the thermodynamical and chemical properties as well as vibrational and magnetic resonance data was carried out. The calculation of the electrostatic surface potential (ESP) and the comparison of the N,N',N'' -tris(nitratomethyl)-isocyanuric acid and N,N',N'' -tris(nitratoethyl)-isocyanuric acid with common explosives explain the performance and sensitivity increase between these compounds. N,N',N'' -tris(nitratomethyl)-isocyanuric acid proves to be a low sensitive explosive with explosive performance data slightly below PETN but better than TNT.

Keywords: PETN, N,N',N'' -tris(nitratomethyl)-isocyanuric acid, N,N',N'' -tris(nitratoethyl)-isocyanuric acid, sensitivity, crystal structure, ESP, thermodynamic data, DFT, B3LYP, CBS-4M, Joback method, enthalpy of formation, energetic data.

1 Introduction

Explosives are need for the very most in civil application like building tunnels and blowing old buildings up in cities. Therefore requirements of performance, stability for handling, safety at work and health protection are always increasing. The decomposition products of explosives should be waste neutral, which means not effecting environment or persist for a long term. Thus explosives should decompose mostly to carbon dioxide, nitrogen and water. That means they have to show a good oxygen balance. Also the residue of the explosive material should be biodegradable. So that ground water or soil is not polluted. For those so called green explosives it is necessary to avoid heavy metal ions and halogens.

For application halogens should be avoided, too, as they create mostly corrosion by aggressive gases e.g. hydrochloride, chlorine dioxide or mineral acids.

By the use of explosives and propellants both in the training of civil security staff and of soldiers there happened to be middle and long term problems like endangerment of the environment and health. This has been pointed out in health study of FBI agents during the term of U.S. president W.J. Clinton. It has been proved that intensive use of weapons leads to a tenth higher dosage of lead in the body of the agents.^[1] Explosives like RDX and HMX were also found in the ground water of drill grounds and in war zones.^[2-4] In the last years some biologists worked on the decomposition of RDX in the human body or by some microbes. Here the most frequently steps in the decomposition is the cleavage of a nitro group and the scission of nitro derivatives (fig. 1).^[5]

To minimize these decomposition products there are two routes possible. One option is to craft molecules that can be metabolized easily by some bacteria. Within this class of molecules are all kinds of nitrates like nitroglycerin and PETN. Another alternative is to gain few steps of decomposition and products that are preferably natural

intermediates. This could be some kind of ureas or biurets like RDX-oxide or mono- and dinitrobiurets.^[6]

With respect to the environmental aspects the explosive and propellant properties may not be neglected. This should be guaranteed by high nitrogen content and a good oxygen balance.

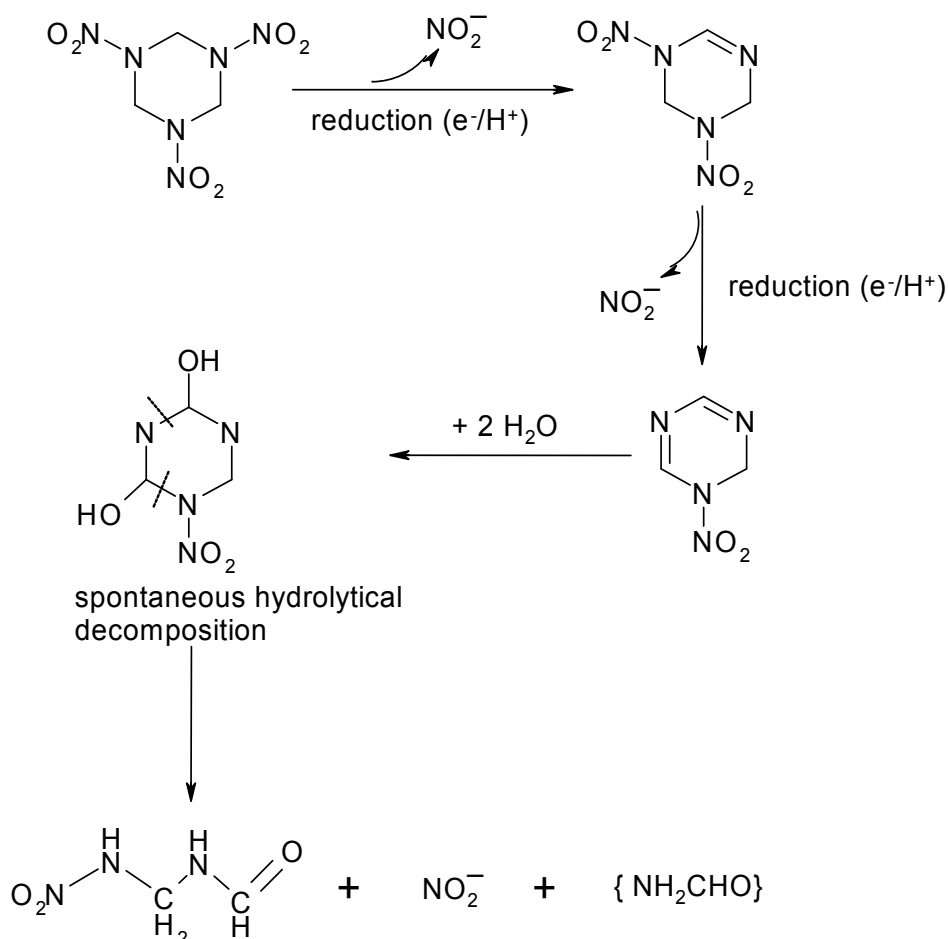


Figure 1. Decomposition scheme of RDX by bacteria *Rhodococcus* sp. Strain DN225.

Therefore the objective of the latest research has been restricted by the following corner stone pollution control, safety and efficiency of high energetic materials. This means to cover a wide field of relevant molecular compounds for explosives and propellants and to investigate promising new molecule classes.

1.1.1 Nitro urea compounds

The synthesis of keto-RDX was a material to further investigation and research in the field of nitrourea, which was brought forward by the synthesis of mono- and dinitrobiuret by the working group of T.M. Klapoetke *et al.*^[7] For engrossing of this research topic further urea derivatives like urazole and isocyanuric acid have now been focused on, to gain further knowledge of structure-property-relationship by nitration of cyclic ureas and some derivatives.

Some interesting molecules might also be the following derivatives of cyanuric acid. The N,N',N'' -tris(4-mononitrophenyl)-cyanuric acid^[8] and the N,N',N'' -tris(2-mononitrophenyl)-isocyanuric acid^[9] are known from literature. Some examples of energetic isocyanuric derivatives are shown in figure 2.

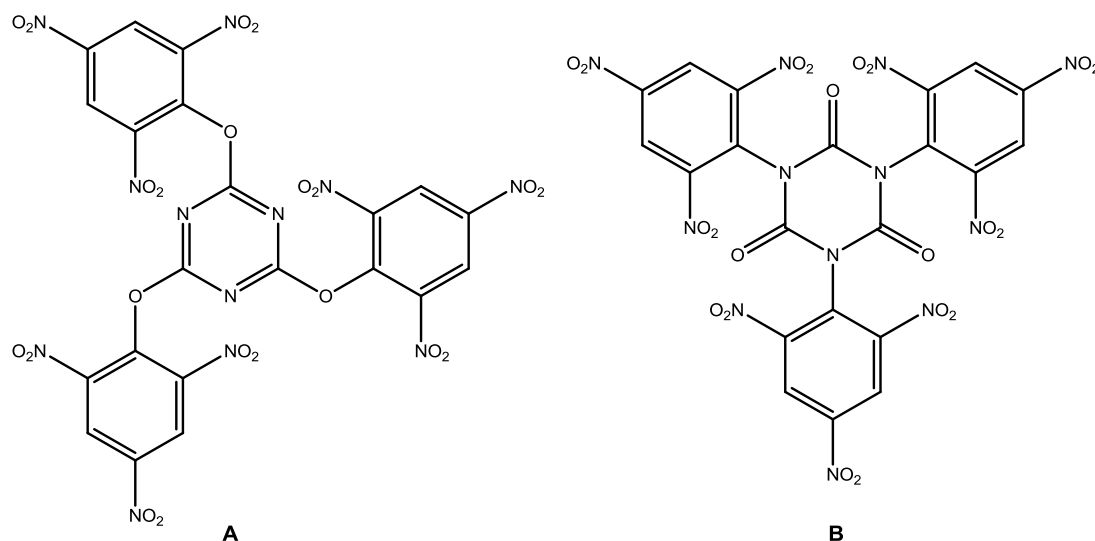


Figure 2. Tris (2,4,6-trinitrophenyloxy) triazine (A)^[10], N,N',N'' -Tris(2,4,6-trinitrophenyl) isocyanuric acid (B).

Green explosives from urea derivatives seem to be a good choice between high energy and insensibility. The characterization data of isocyanuric acid and oxamide derivatives (like BTNMMoxamide, Chapter I) show that the performance of these explosives is little better than TNT but rather less than RDX. The crystal structures result in a high theoretical density around 1.8 g cm^{-3} which is a common density for an explosive. The decomposition of both are exothermic and the temperature of explosion is very low.

New urea based explosives are investigated due to the fact that performance and stability as well as sensitivity are in a good correspondence.

Therefore a comprehensive fully characterization of the the N,N',N'' -tris(nitroxymethyl)-isocyanuric acid (TNM-CA, **3**) and N,N',N'' -tris(2-nitroxyeth-1-yl)-isocyanuric acid (TNE-CA, **4**) was carried out in the following Chapter.

2 Discussion

2.1 Synthesis

The synthesis of the N,N',N''-tris(nitroxymethyl)-isocyanuric acid (TNM-CA, **3**) and N,N',N''-tris(2-nitroxyeth-1-yl)-isocyanuric acid (TNE-CA, **4**) was done according to standard nitration procedures.^[11,12] The starting material N,N',N''-tris(2-hydroxyeth-1-yl)-isocyanuric acid (THE-CA, **2**) was purchased by Sigma-Aldrich and used as delivered and the N,N',N''-tris(hydroxymethyl)-isocyanuric acid (TME-CA, **1**) was prepared according to the literature from isocyanuric acid and 20 % formaldehyde solution.^[13]

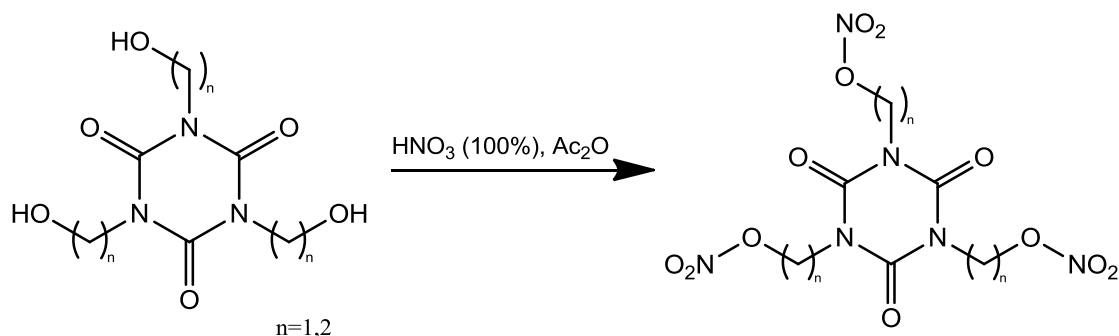


Figure 3. Nitration of the THM-CA (n=1)(**1**) and THE-CA(n=2)(**2**) resulting in TNM-CA(n=1)(**3**) and TNE-CA (n=2)(**4**)

In the following the analytical data of the starting material and nitrate compounds are discussed due to their characteristics and compared to each other.

2.2 Vibrational spectroscopy

2.2.1 N,N',N''-Tris-(nitroxymethyl)-isocyanuric acid (**3**)

The infrared spectrum of the TNM-CA(**3**) shows the expected values for the functional groups at the respective wave number. Noticable for are the high values in comparison of the carbonyl group at about 1700 cm^{-1} , the nitrate group at about 1350 cm^{-1} and very low but included the methylene absorption at about 3000 cm^{-1} . The comparison of the absorption pattern of the theoretical calculated and the experimental data are in recognizable good accordance.

The theoretical values have been calculated with the DFT method B3LYP at 6-31G level of theory including higher orbital (2d,p) contribution for better reliability. These values have been corrected by standard factor to fit those to the experimental determined values and estimate properly which bond and functional group was affected by the observed absorption (Table 1).

Table 1. IR-vibrations calculated with gaussian03 B3LYP/ 6-31g (2d,p) of TNM-CA(3). Stretching modes are just assigned with the affected bondings, other modes are described.

Wave number (cm ⁻¹)	Intensity D(10 ⁻⁴⁰ esu ² cm ³)	Corrected (0.925)	Measured (IR- KBr)	Assigned to FG
510	93.00762	471.75	508	Ring-torsion
590	110.00863	545.75	605	Ring-torsion
760	73.32217	703	766	torsion
840	658.22838	777	843	O-NO ₂
950	66.81863	878.75	943	N-CH ₂
1000	312.5913	925	970	CH ₂ -O
1060	57.36807	980.5	1050	N-CH ₂
1330	454.62095	1230.25	1280	N-O, N=O
1420	213.23803	1313.5	1420	CH ₂ -torsion
1480	403.69174	1369	1452	CH ₂ -wagging
1780	675.51143	1646.5	1647	N-O, N=O
1820	806.1758	1683.5	1747	C=O
3135	6.2867050	2899.9	2927	C-H ₂
3210	9.760061	2969.25	3066	C-H ₂

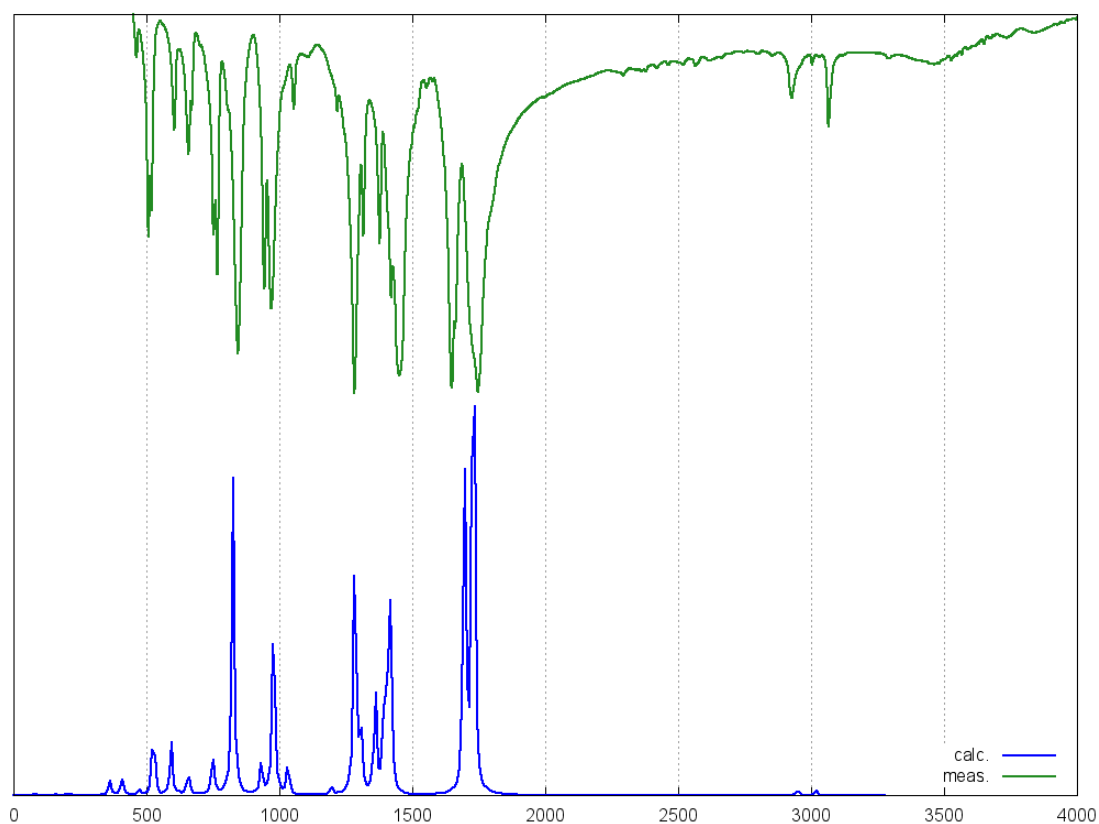


Figure 4. Calculated IR-spectrum, gaussian03 B3LYP/ 6-31g (2d,p) (corrected), compared to the experimental IR spectrum of TNM-CA(3).

2.3 Thermostability

2.3.1 N,N',N''-Tris-(nitroxymethyl)-isocyanuric acid (3)

The thermostability of the compounds was investigated with differential scanning calorimetry (DSC). The graph is presented in figure 5 and shows a sharp melting point at 151°C with a following decomposition at 180°.

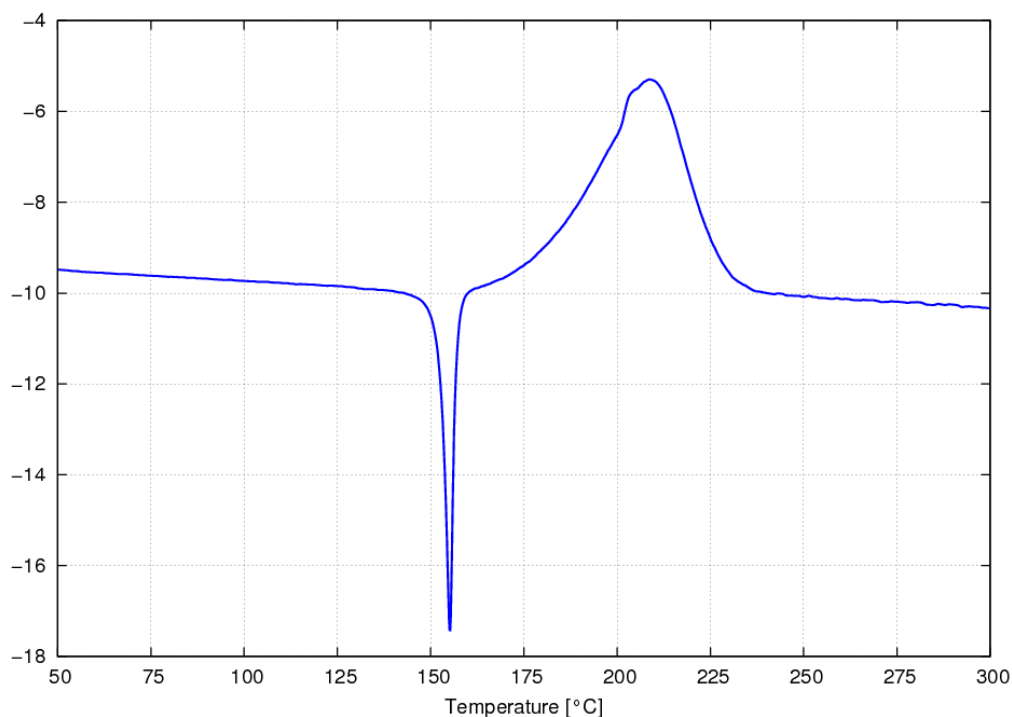


Figure 5. Differential Scanning Calorimetry graph of TNM-CA(3). (Exothermic peaks up), heating 5°C/min. Temperature measurement according to IUPAC rules Onset point of the graph.

Although the definition of the formal description of the decomposition point leads to a high decomposition the graph shows only a small difference between decomposition and melting. That leads to the conclusion that the decomposition is triggered by the melting as the liquid is obviously more reactive as the solid state of compound 3. The decomposition is not occurring during melting means that it can be melt casted without difficulties whilst the temperature does not rise to the decomposition zone.

2.4 Crystal structure

2.4.1 *N,N',N''*-Tris-(nitroxymethyl)-isocyanuric acid (3)

TNM-CA(3) crystallizes in the monoclinic space group $P2_1/c$ with 4 molecules in the unit cell.

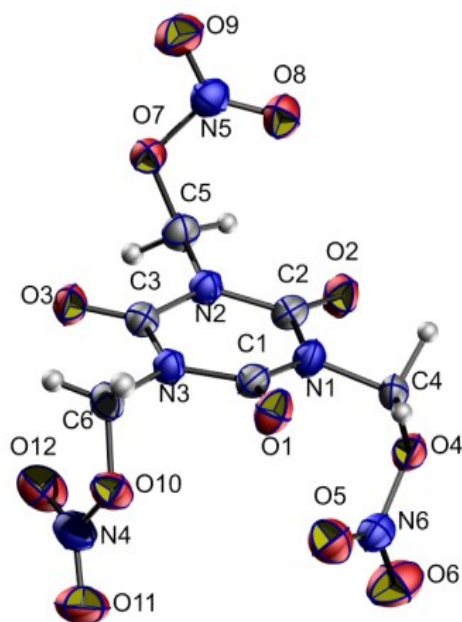


Figure 6. Molecular structure of TNM-CA(3), ellipsoids plotted at 50% probability level.

The molecular structure is two side chains up and one down. This configuration of the molecule leads to the best stacking of the molecules and the densest ordered crystals.

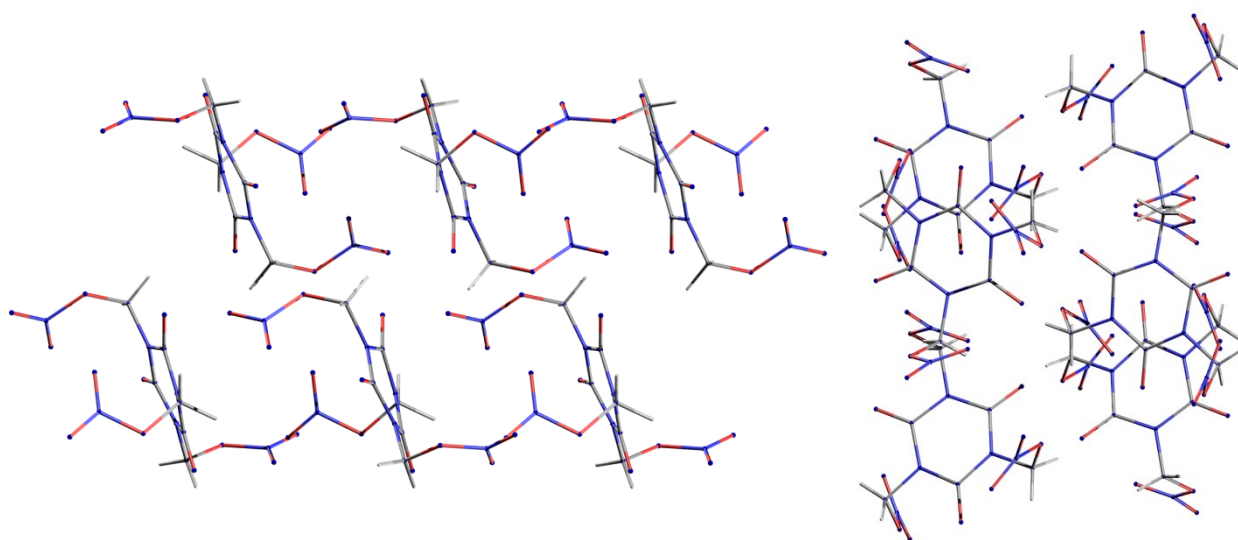


Figure 7. View along b-axis(left) – view along c-axis(right) of TNM-CA(3).

Although there is distortion in the crystals as described in the following the configuration will not change. This remarkable observation was used in calculation of the electrostatic potential later on and unexpectedly found the most stable form regarding sensitivity to external forces.

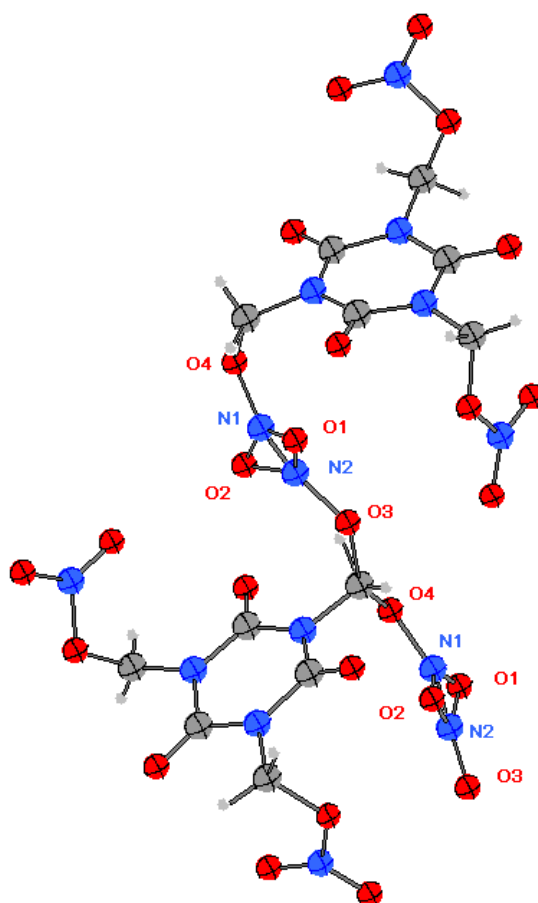


Figure 8. Two molecular units of TNM-CA showing disordered nitro group, plotted as ball and sticks.

The atoms N(2) and O(3) build a nitro-group with O(1) and O(2) with an occurrence of 77% and the atoms N(1) and O(4) with a percentage of 23%. This disordering happens during crystallization as the crystals are aging while the crystal grows. Although there were used different solvents and temperatures to grow the crystals, they always had some kind of disordering when they are big enough to measure them.

There is a possibility of distortion of the crystal that may lead to the bad W_R2 and R_i values after solution of the crystal structure.

Table 2. Selected bond lengths and angles of TNM-CA(3) (*Blue isocyanuric acid moiety, red nitrate moiety*).

Atoms 1,2	d 1,2 [Å]	Atoms 1,2	d 1,2 [Å]
O4—N6	1.409(4)	C2—O2	1.201(3)
O4—C4	1.448(6)	C2—N1	1.391(3)
N6—O5	1.198(4)	C2—N2	1.399(3)
N6—O6	1.199(4)	C3—O3	1.198(3)
C4—N1	1.459(5)	C3—N3	1.392(3)
N6A—O5	1.11(2))	C3—N2	1.399(3)
N6A—O4Aⁱ	1.36(2)	C6—O10	1.432(3)
N6A—O6	1.43(2)	C6—N3	1.454(3)
O4A—N6Aⁱⁱ	1.36(2)	N4—O11	1.198(3)
O4A—C4A	1.44(4)	N4—O12	1.198(3)
C4A—N1	1.62(3)	N4—O10	1.413(3)
C1—O1	1.204(3)	N5—O8	1.193(3)
C1—N1	1.385(3)	N5—O9	1.202(3)
C1—N3	1.398(3)	N5—O7	1.414(3)
C5—O7	1.433(3)	C5—N2	1.454(3)

Atoms 1,2,3	Angle 1,2,3 [°]	Atoms 1,2,3	Angle 1,2,3 [°]
N6—O4—C4	114.1(3)	C1—N1—C2	125.2(2)
O5—N6—O6	128.0(3)	C1—N1—C4	118.0(3)
O5—N6—O4	117.9(3)	C2—N1—C4	116.5(3)
O6—N6—O4	114.0(3)	C1—N1—C4A	122.0(12)
O4—C4—N1	111.8(3)	C2—N1—C4A	110.8(11)
O5—N6A—O4Aⁱ	112.7(16)	C4—N1—C4A	21.5(9)
O5—N6A—O6	116.0(14)	C2—N2—C3	124.2(2)
O4Aⁱ—N6A—O6	130.8(14)	C2—N2—C5	119.0(2)
N6Aⁱⁱ—O4A—C4A	110.6(16)	C3—N2—C5	116.4(2)
O4A—C4A—N1	110.(2)	C3—N3—C1	124.6(2)
O1—C1—N1	123.6(2)	C3—N3—C6	118.6(2)
O1—C1—N3	121.9(2)	C1—N3—C6	116.7(2)
N1—C1—N3	114.5(2)	O11—N4—O12	129.1(3)
O2—C2—N1	122.7(2)	O11—N4—O10	112.2(3)
O2—C2—N2	122.8(2)	O12—N4—O10	118.7(2)
N3—C3—N2	114.7(2)	O8—N5—O9	129.8(3)
O7—C5—N2	110.1(2)	O8—N5—O7	118.6(2)
O10—C6—N3	110.8(2)	O9—N5—O7	111.6(2)
N6—O6—N6A	52.2(7)	N6A—O5—N6	61.1(10)
N1—C2—N2	114.5(2)	N5—O7—C5	114.4(2)
O3—C3—N3	123.7(2)	N4—O10—C6	114.6(2)
O3—C3—N2	121.6(2)		

(i) x, 0.5−y, 0.5+z; (ii) x, 0.5−y, −0.5+z.

2.4.2 1,3,5-Tris(hydroxyethyl)cyanuric acid(2)

The THE-CA crystallizes in the monoclinic space group $P2_1/n$ with 4 molecules in the unit cell.

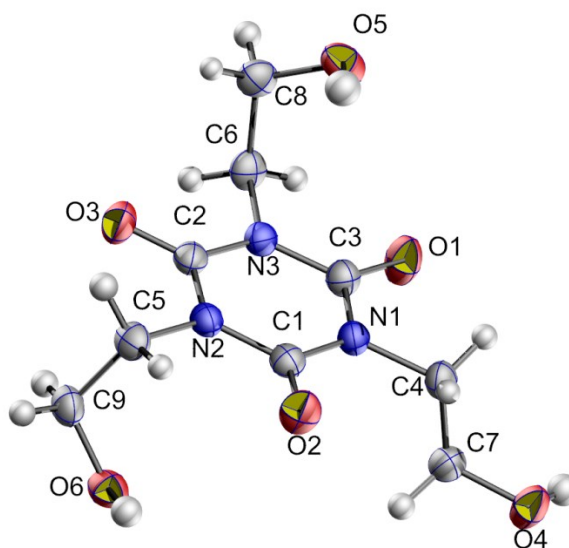


Figure 9. Molecular structure of THE-CA(2) plotted at 50% probability level.

The results are in good accordance with those described in literature by M. Tremayne *et al.* [14]

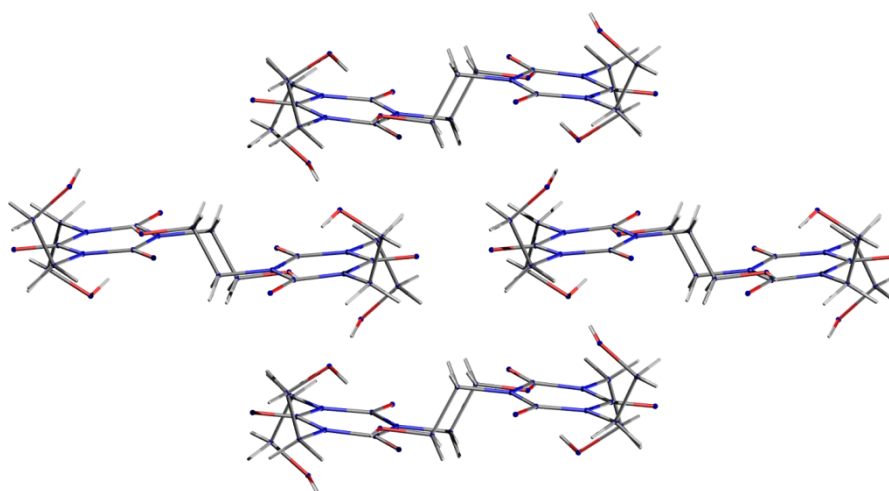


Figure 10. View along a-axis of THE-CA(2).

2.4.3 1,3,5-Tris(nitratoethyl)-cyanuric acid (4)

1,3,5-Tris(nitratoethyl) cyanuric acid (TNE-CA, **4**) crystallizes in the monoclinic space group $P2_1/c$ with 4 molecules in the unit cell.

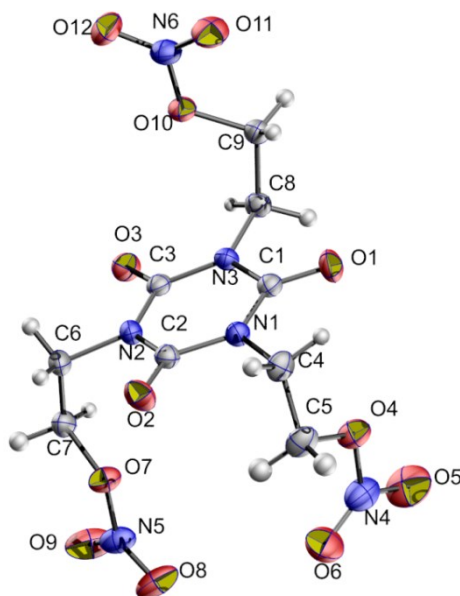


Figure 11. Molecular structure TNE-CA(**4**) plotted at 50% probability level.

Again the motif with two down and one up side chain is found to form stacked pillars that are lying packed side by side as shown in figure 12 when looking along a-axis. The view from the top along c-axis displays the stacked rings (figure 12).

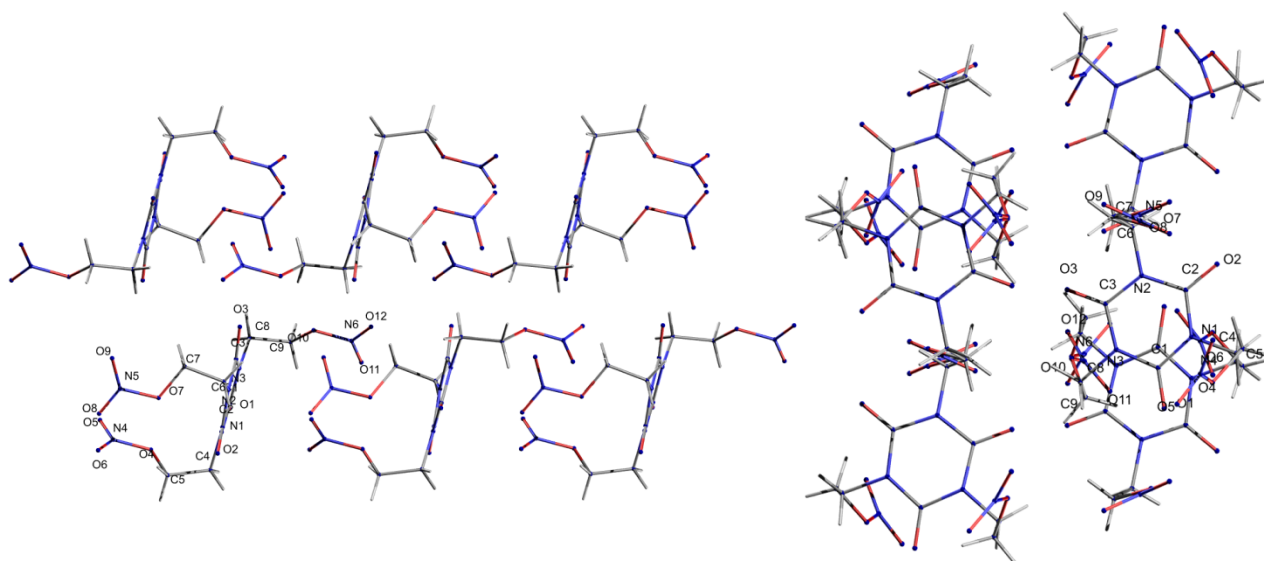


Figure 12. View along b-axis (left) and view along c-axis (right) of TNE-CA(**4**).

Table 3. Selected bond lengths and angles of TNE-CA(4) (*Blue isocyanuric acid moiety, red nitrate moiety*).

Atoms 1,2	d 1,2 [Å]	Atoms 1,2	d 1,2 [Å]
C1—O1	1.209(2)	C7—O7	1.456(2)
C1—N1	1.381(2)	C8—N3	1.471(2)
C1—N3	1.387(2)	C8—C9	1.510(2)
C2—O2	1.208(2)	C9—O10	1.459(2)
C2—N1	1.387(2)	N4—O6	1.189(2)
C2—N2	1.389(2)	N4—O5	1.211(2)
C3—O3	1.213(2)	N4—O4	1.392(2)
C3—N3	1.385(2)	N5—O8	1.201(2)
C3—N2	1.385(2)	N5—O9	1.202(2)
C4—N1	1.473(2)	N5—O7	1.394(2)
C4—C5	1.514(3)	N6—O11	1.207(2)
C5—O4	1.456(2)	N6—O12	1.208(2)
C6—N2	1.474(2)	N6—O10	1.384(2)
C6—C7	1.507(2)		

Atoms 1,2,3	Angle 1,2,3 [°]	Atoms 1,2,3	Angle 1,2,3 [°]
O1—C1—N1	123.1(2)	O6—N4—O5	128.7(2)
O1—C1—N3	121.4(2)	O6—N4—O4	119.4(2)
N1—C1—N3	115.5(2)	O5—N4—O4	112.0(2)
O2—C2—N1	121.9(2)	O8—N5—O9	128.8(2)
O2—C2—N2	122.8(2)	O8—N5—O7	112.8(2)
N1—C2—N2	115.3(1)	O9—N5—O7	118.4(2)
O3—C3—N3	122.8(2)	O11—N6—O12	128.4(2)
O3—C3—N2	122.1(2)	O11—N6—O10	118.8(2)
N3—C3—N2	115.2(2)	O12—N6—O10	112.8(2)
N1—C4—C5	110.2(2)	N5—O7—C7	114.1(1)
N4—O4—C5	114.5(2)	N6—O10—C9	114.4(1)
O4—C5—C4	105.2(2)	C1—N1—C2	124.3(2)
N2—C6—C7	111.6(2)	C1—N1—C4	118.9(2)
O7—C7—C6	105.5(2)	C2—N1—C4	116.7(2)
N3—C8—C9	111.3(2)	C3—N2—C2	124.5(2)
O10—C9—C8	105.2(2)		

2.5 Calculation of thermodynamic data and surface potential

The calculation of the electrostatic surface potential (ESP) will help to understand how stability in crystalline systems is connected to the internal separation of charge in molecules. Also there are a lot of different models that describe stability to impact and friction this method has been shown to be very accurate and helpful discussing this topic.^[15-20]

2.5.1 Electrostatic surface potential of N,N',N''-Tris-(nitroxymethyl)-isocyanuric acid(3)

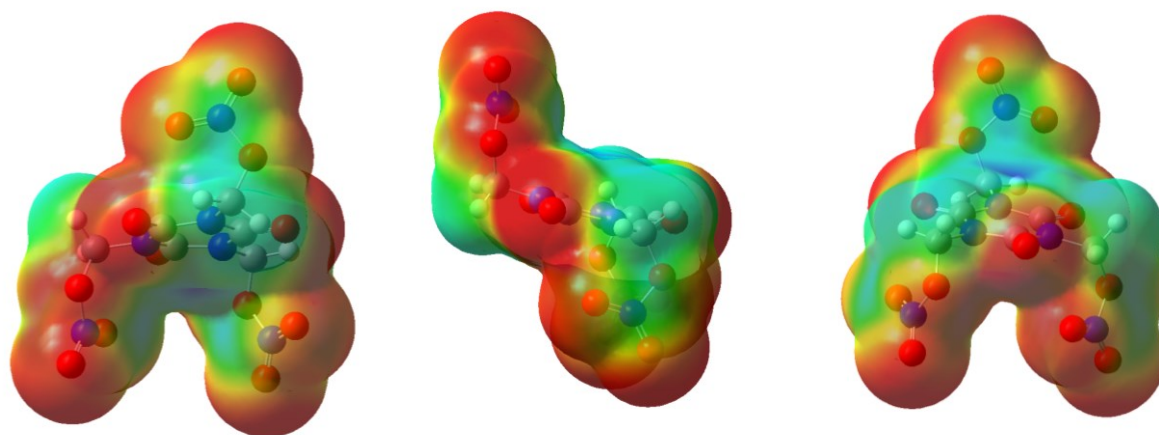


Figure 13. Electrostatic Surface Potential of TNM-CA (3)(calculation Gaussian03 B3LYP/ 6-31g (2d,p)), plot was outlined with 0.001 e bohr⁻³ in GaussView^[21]), rendering from -0.020 (red) till 0.080 (blue).

The electrostatic surface potential was calculated with Gaussian03 at B3LYP/ 6-31g (2d,p) level of theory.

The remarkable ESP of the molecule is the nearly symmetrical distribution of the negative potential on the surface. This belt like potential may lead to an increased stability to impact, shock and friction. Also the big positive potentials between the negative regions may stabilize the molecule.

These electrostatic surface potentials show that the negative potentials are located at the outer rim, and wind themselves like a negative band around the molecule, whereas the positive areas are situated in the middle of the ring and near the methylene moiety.

This separation of positive and negative electrostatic potential implies a high sensitivity towards friction and impact. As the slightest external force to bring the potential out of its natural state will result in a collapse of the whole molecule and the decomposition of the molecule will start as shown in chapter I by the split off of a nitrogen dioxide molecule and in a chain reaction the whole molecule will be ripped apart. The evolution of gaseous products will result in carbon monoxide, carbon dioxide, water and nitrogen or nitrogen oxides.

2.5.2 Electrostatic surface potential of N,N',N''-Tris-(nitroxyethyl)-isocyanuric acid (4)

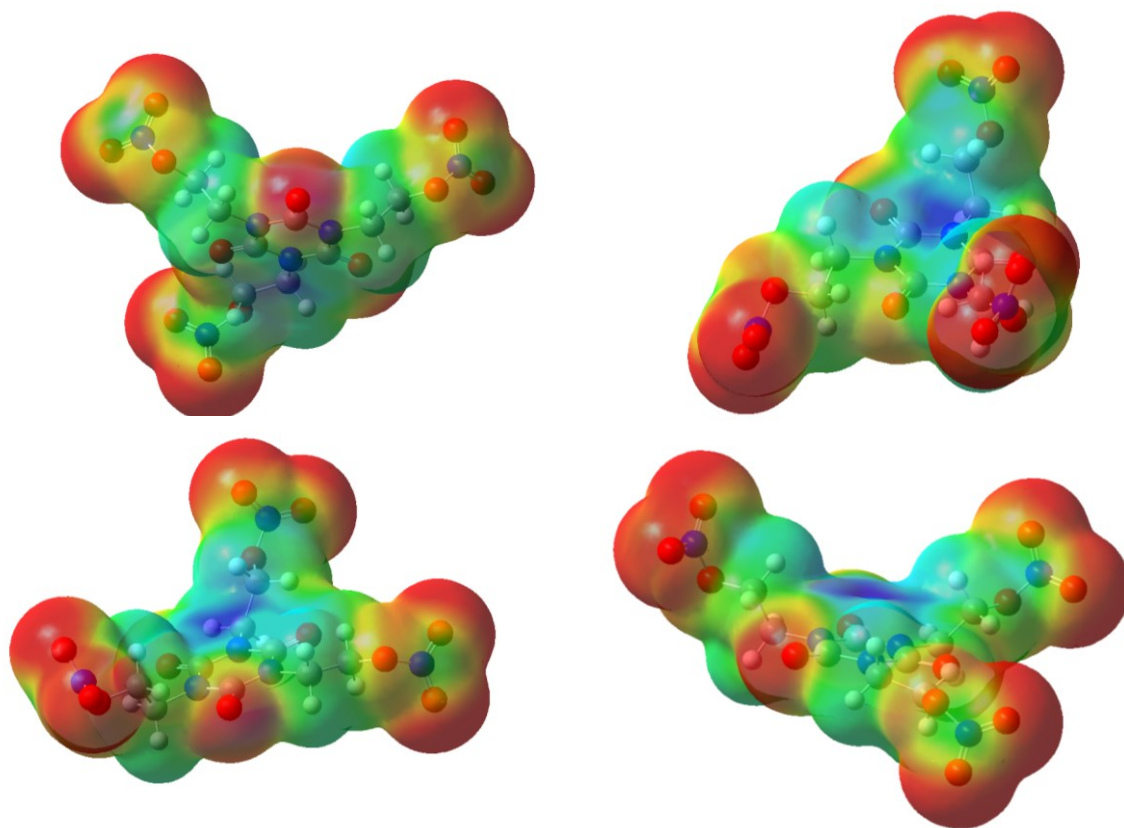


Figure 14. Electrostatic Surface Potential of TNE-CA(4)(calculation Gaussian03 B3LYP/ 6-31g (2d,p)), plot was outlined with $0.001 e \text{ bohr}^{-3}$ in GaussView^[21], rendering from -0.020 (red) till 0.080 (blue).

The electrostatic surface potential (ESP) of **4** shows that the highest negativity is found around the nitro groups and the oxygen atoms of the ring motif. Looking at this separate distribution charge density distribution the stability of the molecule will be higher due to the fact that none of the negative regions influence each other and a minor shift in the distribution might affect only a small part of the molecule. This is not as drastic as in the TNM-CA (**3**) where even a small shift is leading to a whole distortion of the molecules charge density distribution.

So TNE-CA(**4**) is more stable to friction and impact than TNM-CA(**3**).

2.5.3 Calculation of the enthalpy of formation

CBS4-M CALCULATIONS

The heats of formation were computed theoretically using the Gaussian G09 program package.^[22] To obtain very accurate energies the enthalpies (H) and free energies (G) were calculated by using the complete basis set (CBS) method of Petersson and coworkers. The CBS models use the known asymptotic convergence of pair natural

orbital expressions to extrapolate using a finite basis set to the estimated complete basis set limit. The CBS-4 first starts with a HF/3-21G(d) geometry optimization; the zero point energy is computed at the same level. Then a large basis set SCF calculation as a base energy, and a MP2/6-31+G calculation with a CBS extrapolation to correct the energy through second order is used. A MP4(SDQ)/6-31+(d,p) calculation was used to approximate higher order contributions. The modified CBS-4M method (M referring to the use of minimal population localization), which is a reparametrized version of the original CBS-4 method and includes some additional empirical corrections is used in these studies.^[23] The enthalpies of the gas phase species M were computed according to the atomization energy method [Equation (1)]^[24] described in the literature.^[25]

$$\Delta_f H^\circ_{(g,M,298)} = H_{(molecule,298)} - \Sigma H^\circ_{(atoms,298)} + \Sigma \Delta_f H^\circ_{(atoms,298)} \quad (1)$$

Using calculated heats of sublimation by Trouton's Rule^[26]

$$\text{sub}H^\circ(s) = T_{\text{sub}} \times 88 \text{ J/mol K} \quad (2)$$

and lattice enthalpies for the ionic compounds, the gas phase enthalpies of formation were converted into the solid state (standard conditions) enthalpy of formation $\Delta_f H_m^\circ$ (Table 3). Lattice energies (U_L) and lattice enthalpies (ΔH_L) were calculated from the corresponding molecular volumes according to Jenkin's equations.^[27] Lastly, the molar standard enthalpies of formation (ΔH_m) were used to calculate the molar solid state energies of formation (ΔU_m) according to Equation (2).

$$\Delta U_m = \Delta H_m - \Delta n RT \quad (3)$$

where Δn is the change of mol of gaseous components.

Table 4. CBS4-M calculated enthalpies of formation in gas phase

Compound	$\Delta_f H^\circ(g) / \text{kcal mol}^{-1}$	$T_{\text{dec}} / \text{K}$	$\Delta_{\text{sub}} H^\circ / \text{kcal mol}^{-1}$	$\Delta_f H^\circ(s) / \text{kcal mol}^{-1}$	N	$\Delta_f U^\circ(s) / \text{kJ kg}^{-1}$
TNE-CA	-210.3	427.2	19.2	-229.5	-15	-2329,08
TNM-CA	-188.0	418.2	18.8	-206.8	-12	-2358.56

JOBACK-ESTIMATION

The Joback method for estimating the heat of formation uses fragments of a carbon, hydrogen, nitrogen and oxygen containing backbone and assigns to those specific values for heat of formation and heat of fusion. The following equation show how the fragment values are summed up.^[28]

Heat of Formation (Ideal Gas, 298 K)

$$\Delta H_{\text{formation}} = 68.29 + \Sigma H_i \quad (4)$$

Heat of Fusion

$$\Delta H_{\text{fusion}} = -0.88 + \Sigma G_i \quad (5)$$

Table 5. Functional groups are assigned with values for heat of formation and heat of fusion given in kcal mol⁻¹

Functional group	Heat of formation	Heat of fusion
-CH ₂ -	-20.640	2.590
-O- (nonring)	-132.220	1.188
-NO ₂	-66.570	9.679
-N= (ring)	93.700	3.649
>C=O (Ring)	-164.500	4.189

Table 6. The values of table 3 are used with the stated equations to result in the following heat of formation of TNM-CA(3) and TME-CA(4) in solid state.

	ΔH_f^0 (gas)	-802.400	kJ mol ⁻¹	-191.778	kcal mol ⁻¹
	ΔH_{fusion}	52.058	kJ mol ⁻¹	12.442	kcal mol ⁻¹
TNM-CA(3)	ΔH_f^0(solid)	estimated		-179.336	kcal mol⁻¹
	ΔH_f^0 (gas)	-864.320	kJ mol ⁻¹	-206.775	kcal mol ⁻¹
	ΔH_{fusion}	59.828	kJ mol ⁻¹	14.299	kcal mol ⁻¹
TNE-CA(4)	ΔH_f^0(solid)	estimated		-192.476	kcal mol⁻¹

The rough estimation by this fragmental method is compared to the CBS4-M calculated value (TNM-CA: -188 kcal mol⁻¹, TNE-CA: -210 kcal mol⁻¹) very close (TNM-CA: -192 kcal mol⁻¹, TNE-CA: -192 kcal mol⁻¹).

Therefore it is found to be in good accordance with all the other methods applied to determine or calculate the enthalpy of formation. To have fast results and get an exceptional good estimation this method is used in further investigations as a first shot or a substitute for calculations which cannot be carried out by the other used methods properly.

2.1 Energetic Properties

2.1.1 Detonation Parameters

With the use of the program EXPLO5 V5.02 the detonation parameters were calculated.^[29] Based on the steady-state model of equilibrium detonation the program also uses the Becker–Kistiakowsky–Wilson’s equation of state (BKW E.O.S) for gaseous detonation products and Cowan–Fickett E.O.S. for solid carbon. The equilibrium composition of the detonation products is calculated by applying modified White, Johnson, and Dantzig’s free energy minimization technique. The program is designed to enable the calculation of detonation parameters at the CJ point. The BKW equation in the following form was used with the

BKWN set of parameters ($\alpha, \beta, \kappa, \theta$) where X_i is the mol fraction of the i^{th} gaseous product and k_i is the molar covolume of the i^{th} gaseous product:

$$pV/RT = 1 + xe^{\beta x} \quad (6)$$

$$x = (\kappa \sum X_i k_i) / [V(T + \theta)]^\alpha \quad (7)$$

$$\alpha = 0.5, \beta = 0.96, \kappa = 17.56, \theta = 4950 \quad (8)$$

The calculations were performed using the maximum densities according to the crystal structures.

The most important criteria of high explosives are the detonation velocity V_{Det} , the detonation pressure p_{CJ} and the energy of explosion $\Delta_{\text{Ex}}U^\circ$. Commonly used explosives like TNT, HNS or RDX, were also calculated with the EXPLO5.04 code. (V_{Det} : TNT: 7253, HNS: 7436, RDX: 8747 ms^{-1} ; p_{CJ} : TNT: 216, HNS: 242, RDX: 348 kbar; $\Delta_{\text{Ex}}U^\circ$: TNT: -5227, HNS: -5476, RDX: -6125 kJ kg^{-1})

In terms of detonation velocity, compounds **3** and **4** reached the level of commonly used secondary explosives such as TNT. A reason for the comparably high detonation velocity and detonation pressure is the low negative oxygen balance of -14% of **3** and the high density (Table 5).

Table 7. Calculation based on EXPLO5 (Version 5.02, 2006) BKWG type of constants in BKW E.O.S is used in calculation (Alpha=0,5; Beta=0,096; Kappa=17,56; Theta=4950)

comp	TMD / g cm^{-3}	U°_f / kJ kg^{-1}	Ox. bal.	Q_v / kJ kg^{-1}	V_0 / L kg^{-1}	T_{ex} / K	P / kbar	D / ms^{-1}	imp / J(Nm)	fric./ N	mp / $^\circ\text{C}$	T_{dec} / $^\circ\text{C}$
TNT exptl	1.64 1.64	-184.9	-74	-5089	622	3741	202 210	7150 6950	15	>353	81	300
RDX exptl	1.80 1.80	+417	-21	-6034	769	4334	340 347	8882 8750	7.4	120	204	213
PETN [12] (EXPLO 5)	1.77	-1594	-10	-5975	769	4140 4398	331 318	8350 8599	3		141	163
TNE-CA	1.695	-2329	-49	-4155	675	3062	221	7368	>30	>360	154	154
TNM-CA	1.828	-2359	-14	-4532	652	3595	279	7808	>10	>180N	145	145

3 Conclusions

Although the N,N',N''-tris(nitroxyethyl) isocyanuric acid (**4**) and N,N',N''-tris(nitroxymethyl) isocyanuric acid (**3**) do not reach the explosive properties of RDX. Their explosive properties exceed those of TNT. The comparison between those two compounds displayed clearly the influence of the electrostatic surface potential and crystal structure on stability, performance and sensitivity.

4 Experimental

4.1 Crystal structures

The molecular structures were determined by single crystal X-ray diffraction. The X-ray crystallographic data were collected using an Oxford Xcalibur diffractometer with a CCD area detector and graphite-monochromated Mo-K α radiation ($\lambda = 0.71073 \text{ \AA}$). The structure was solved with SIR97^[30] and refined with using SHELXL-97^[31], Ortep^[32] and Diamond^[33] plots showing thermal ellipsoids with 50% probability for the non-hydrogen atoms.

4.2 Properties

Decomposition points, enthalpies, melting points and dehydration points were determined using a Linseis DSC PT10. Additionally, the melting point and dehydration points were also determined using Büchi B-540 melting point apparatus. The friction and impact sensitivity data were obtained using the BAM drophammer and friction tests, in accordance with the BAM methods^[34].

4.3 Spectroscopic data and elemental analysis

IR spectra were obtained using a Perkin Elmer Spectrum BX FT-IR System and a Raman spectra were measured using Perkin Elmer Spectrum 2000 FT- Raman spectrometer fitted with a Nd-YAG-laser ($\lambda = 1064 \text{ nm}$) as solids at room temperature (resolution = 4 cm^{-1})

NMR spectra were obtained with a Jeol Eclipse 400 spectrometer operating at 400.2 MHz for ^1H , 100.6 MHz for ^{13}C and 28.9 MHz for ^{14}N . Chemical shifts (in ppm) are given with respect to TMS ($^1\text{H}/^{13}\text{C}$), MeNO_2 (^{14}N) as internal standard.

4.4 Preparation

1,3,5-TRIS(HYDROXYMETHYL)-ISOCYANURIC ACID (1)

1.35 g (10.5 mmol) Isocyanuric acid was solved in 3.3 g (41 mmol) pyridine. To the mixture 5 g (1.85 g formaldehyde, 61.6 mmol) formalin (>37 %)-solution was added, that had been brought to pH 9 by sodium carbonate. After stirring the reaction mixture at room temperature for 12 hours the pyridine and water was evaporated. The reduced suspension was mixed with acetone and filtered. The precipitate was washed once with acetone. The white plate-like solid was removed instantly from the filter and stored under dry inert gas, because the product is very hygroscopic. *Yield: 30%* (because product was not fast enough removed from filter)

$^{13}\text{C}\{^1\text{H}\}$ NMR(101 MHz, DMSO, ppm): 65.4, 151.7. ^1H NMR(400MHz, DMSO, ppm): 5.12 (s, 6H), 6.0 (ws, 3H).

1,3,5-TRIS(NITROXYMETHYL)-ISOCYANURIC ACID (3)

1.0 g (4.56 mmol) N,N',N''-Tris(hydroxymethyl)isocyanuric acid was cooled to -20°C . 2 mL nitric acid(fuming) was added under stirring. 2 mL acetic anhydride was added dropwise and the mixture was allowed to raise temperature to room temperature.

After 10 hours a white solid precipitated and the reaction was stopped by pouring the mixture on ice. The solid was filtered off and dried. The solid was recrystallized from acetone. *Yield: 1.34 g (0.83%, 3.78 mmol).*

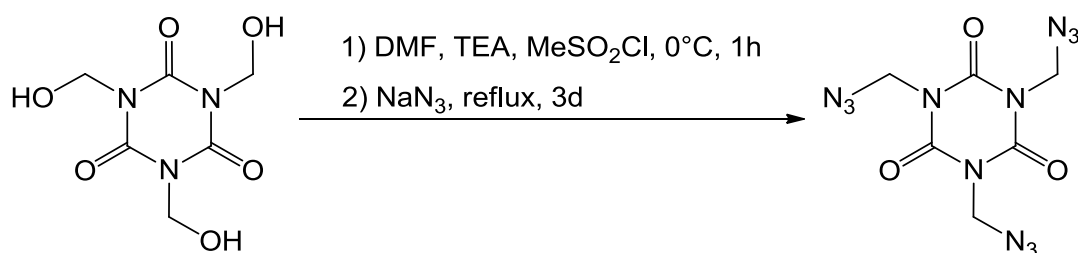
e.a. (calc./meas.%): N 23.73 / 23.25, C 20.35 / 20.63, H 1.71 / 1.73. **¹H NMR** (400 MHz, DMSO-d₆, ppm): 6.21 (s, 6H, CH₂); **¹³C {¹H} NMR** (101 MHz, DMSO-d₆, ppm): 147.1 (CO), 71.5 (CH₂); **¹⁴N NMR** (63 MHz, DMSO-d₆, ppm): -42.0 (ONO₂). **DSC (2°C/min):** ΔH_m -35.1 kJ mol⁻¹, **mp.:** 150°C, **T_{dec.}:** 181°C. **IR (KBr; $\tilde{\nu}/\text{cm}^{-1}$)** 766(NO₂), 843 (NO₂), 943(CH₂), 969 (CH₂), 1282(CH₂), 1377(CH₂), 1451(CH₂), 1647(NO₂), 1747 (CO). **Impact:** insensitive(>30 J); **Friction:** insensitive (>360 N); **Oxygen bal.:** -13.55%; **Energies (calc.):** $\Delta U_f^0 = -2681 \text{ kJ kg}^{-1}$, $\Delta H_f^0 = -2743.99 \text{ kJ kg}^{-1}$.

1,3,5-TRIS-(NITROXYETHYL)-CYANURIC ACID (4)

200 mg (0.766 mmol) 1,3,5-tris-(2-hydroxyethyl)-cyanuric acid was stirred under ice-cooling, solved in 2 mL (47.6 mmol) 98% HNO₃ and carefully 3 mL (283.6 mmol) acetic anhydride added. After 2.5 hours of stirring the clear mixture was poured onto ice. The precipitate was filtered and washed neutral with a solution of sodium carbonate. The white solid was dried and crystallized from acetone. *Yield: 291 mg (0.712 mmol, 96%).*

m.p.: 153.4-154°C. **elemt. anal.** (calc./meas.): 21.21(N), 27.28(C), 3.05(H)/21.57(N), 27.30(C), 3.23(H); **MS (DEI+):** m/z 349. **Raman [$\tilde{\nu}/\text{cm}^{-1}$]:** 572, 1002, 1036, 1281, 1424, 1603, 1756, 2906, 2976, 3058. **IR [$\tilde{\nu}/\text{cm}^{-1}$]:** 522, 535, 570, 707, 759, 886, 906, 1000, 1040, 1081, 1186, 1284, 1323, 1360, 1384, 1456, 1625, 1699, 2543, 2637, 2888, 2981, 3049, 3390, 3456. **¹³C NMR** (101 MHz, DMSO, ppm): 36.6, 70.26, 148.9. **¹H NMR** (400 MHz, DMSO, ppm): 4.14 (t, ³J=4.3, 6H), 4.67 (t, ³J=4.4, 6H). **¹⁴N NMR** (63 MHz, DMSO, ppm): -37.6. not sensitive to impact and friction.

N,N',N''-TRIS-(AZIDOMETHYL)-ISOCYANURIC ACID (5)



1.0 g (4.56 mmol) N,N',N''-tris(hydroxymethyl)isocyanuric acid was solved in 100 mL dimethylformamide and 2.76 mL triethylamine. 1.33 mL (17.28 mmol) mesylchloride was added dropwise under ice-cooling. After one hour of stirring 1.61 g (24.8 mmol) sodium azide was added and refluxed for three days. The solution was quenched with saturated sodium bicarbonate solution and extracted three times with 50 mL diethylether. The united organic phases were dried over NaSO₄ and the solvent was evaporated. The product was a brownish honey like oil. After a short flash column chromatography (silica-gel) with 2:1 ethylacetate:n-hexane the product was obtained as yellow oil. *Yield 173 mg (0.59 mmol, 13%).*

¹H NMR (DMSO-d₆, 400 MHz, ppm): 5.22 (s, CH₂); ¹³C NMR (DMSO-d₆, 100.6 MHz, ppm): 148.3 (s, CO); 57.5 (s, CH₂) ¹⁴N NMR (DMSO-d₆, 28.9 MHz, ppm): -131 (β-N); -158 (g-N); -294 (α-N).

Deflagration in flame.

5 References

- [1] Barsan M.E., Miller A., Lead Health Hazard Evaluation. *HETA Report* **1996**, Nat. Inst. for Occupational Safety and Health, Cincinnati, No. 91-0346-2572.
- [2] 58. Federal Register 190, **1993**, 580.
- [3] Keith L.H., Telliard W.A., Priority pollutants: a perspective view, *Environ. Sci. Technol.* **1979**, 13, 416.
- [4] Lachance B., Robidoux P.Y., Hawari J., Ampleman G., Thiboutot S., Sunahara G.I., Cytotoxic and genotoxic effects of energetic compounds on bacterial and mammalian cells in vitro, *Mutat. Res.* **1999**, 444, 25.
- [5] Robidoux P.Y., Hawari J., Thiboutot S., Ampleman G., Sunahara G.I., Chronic toxicity of HMX in soil determined using the earthworm (*Eisenia andrei*) reproduction test, *Environ. Pollut.* **2001**, 111, 283.
- [6] Fournier D., Halsz A., Spain J., Fiurasek P., Halwari J., Determination of Key Metabolites during Biodegradation of RDX with *Rhodococcus* sp. Strain DN22, *Appl Environ. Microbiol.* **2002**, 68, 166.
- [7] Geith J., Holl G., Klapötke T.M., Weigand J.J., Pyrolysis experiments and thermochemistry of MNB, DNB, *Combustion and Flame* **2004**, 139, 358.
- [8] Broda, W.; Dehmlow, E. V.; Schulz, H. J., Applications of phase-transfer catalysis. Part 28. Onium salt-catalyzed preparations of isocyanurates, *Israel Journal of Chemistry* **1985**, 26(3), 222-4.
- [9] Kogon, I. C.E. I. du Pont de Nemours & Co., Wilmington, DE, New reactions of phenyl isocyanate and ethyl alcohol, *J. Am. Chem. Soc.* **1956**, 78, 4911-14.
- [10] Vyas, S.M., Krishnamurthy, V.N., Kusurkar, R.S., *Proc. of IASPEP* **2001**, 48-54.
- [11] a) Goncharov, T. K.; Dubikhin, V. V.; Nazin, G. M.; Fedorov, B. S.; Shastin, A. V., *Russian Journal of General Chemistry* **2005**, 75(6), 901-904. b) Ermakov, A. S.; Bulatov, P. V.; Vinogradov, D. B.; Tartakovskii, V. A., *Russian Journal of Organic Chemistry* **2005**, 41(2), 255-256. c) Manelis, G. B.; Nazin, G. M.; Prokudin, V. G., *Russian Chemical Bulletin* **2011**, 60(7), 1440-1447.
- [12] Xu, Ruoqian; Ji, Yueping; Ding, Feng; Yang, Wei; Liu, Weixiao, *Huozhayao Xuebao* **2009**, 32(4), 38-40, 44.
- [13] a) Richard, Brigitte; Richard, Michel; Lenzi, Michel, Comptes Rendus de l'Académie des Sciences, Serie II: Mécanique, Physique, Chimie, *Sciences de la Terre et de l'Univers* **1989**, 309(18), 1749-52. b) Richard, B.; Richard, M.; Lenzi, M., *Bulletin de la Société Chimique de France* **1990**, (May-June), 461-7.

- [14] Chong S. Y., Seaton C. C., Kariukia B. M., Tremayne M., *Acta Cryst.* **2006**, B62, 864–874. Molecular versus crystal symmetry in tri-substituted triazine, benzene and isocyanurate derivatives.
- [15] Dick J. J., Mulford R. N., Spencer W. J., Pettit D. R., Garcia E., Shaw D. C., *J. Appl. Phys.* **1991**, 70 (7), 3572.
- [16] Hiskey M. A., Hatch M. J., Oxley J. C., *Propellants, Explos. Pyrotech.* **1991**, 16, 40.
- [17] Rice B. M., Hare J. J., *J. Phys. Chem. A* **2002**, 106, 1770.
- [18] Rice B. M., Byrd E. F. C., *J. Mater. Res.* **2006**, 21 (10), 2444.
- [19] Gruzdkov Y. A., Gupta Y. M., *J. Phys. Chem. A* **2000**, 104, 11169.
- [20] Ross J. N., Low J. N., Fernandes C., Wardell J. L., Glidewell C., *Acta Crystallographica, Section C*, **2001**, 57 (8), 949.
- [21] GaussView, Version 5, Dennington, R.; Keith, T.; Millam, J. *Semichem Inc.*, Shawnee Mission KS, **2009**.
- [22] *Gaussian 03, Revision C.02*, Frisch, M. J.; Trucks, G. W.; Schlegel, H. B.; Scuseria, G. E.; Robb, M. A.; Cheeseman, J. R.; Montgomery, Jr., J. A.; Vreven, T.; Kudin, K. N.; Burant, J. C.; Millam, J. M.; Iyengar, S. S.; Tomasi, J.; Barone, V.; Mennucci, B.; Cossi, M.; Scalmani, G.; Rega, N.; Petersson, G. A.; Nakatsuji, H.; Hada, M.; Ehara, M.; Toyota, K.; Fukuda, R.; Hasegawa, J.; Ishida, M.; Nakajima, T.; Honda, Y.; Kitao, O.; Nakai, H.; Klene, M.; Li, X.; Knox, J. E.; Hratchian, H. P.; Cross, J. B.; Bakken, V.; Adamo, C.; Jaramillo, J.; Gomperts, R.; Stratmann, R. E.; Yazyev, O.; Austin, A. J.; Cammi, R.; Pomelli, C.; Ochterski, J. W.; Ayala, P. Y.; Morokuma, K.; Voth, G. A.; Salvador, P.; Dannenberg, J. J.; Zakrzewski, V. G.; Dapprich, S.; Daniels, A. D.; Strain, M. C.; Farkas, O.; Malick, D. K.; Rabuck, A. D.; Raghavachari, K.; Foresman, J. B.; Ortiz, J. V.; Cui, Q.; Baboul, A. G.; Clifford, S.; Cioslowski, J.; Stefanov, B. B.; Liu, G.; Liashenko, A.; Piskorz, P.; Komaromi, I.; Martin, R. L.; Fox, D. J.; Keith, T.; Al-Laham, M. A.; Peng, C. Y.; Nanayakkara, A.; Challacombe, M.; Gill, P. M. W.; Johnson, B.; Chen, W.; Wong, M. W.; Gonzalez, C.; and Pople, J. A.; Gaussian, Inc., Wallingford CT, 2004.
- [23] a) Ochterski J. W., Petersson G. A., Montgomery Jr. J. A., *J. Chem. Phys.* **1996**, 104, 2598; b) Montgomery Jr. J. A., Frisch M. J., Ochterski J. W., Petersson G. A., *J. Chem. Phys.* **2000**, 112, 6532.
- [24] a) Curtiss L. A., Raghavachari K., Redfern P. C., Pople J. A., *J. Chem. Phys.* **1997**, 106, 1063; b) Byrd E. F. C., Rice B. M., *J. Phys. Chem. A* **2006**, 110, 1005–1013; c) Rice B. M., Pai S. V., Hare J., *Combust. Flame* **1999**, 118, 445–458.
- [25] Altenburg T., Klapötke T. M., Penger A., Stierstorfer J., *Z. Anorg. Allg. Chem.* **2010**, 636, 463–471.
- [26] a) Westwell M. S., Searle M. S., Wales D. J., Williams D. H., *J. Am. Chem. Soc.* **1995**, 117, 5013–5015; b) Trouton F., *Philos. Magn.* **1884**, 18, 54–57.
- [27] a) Jenkins H. D. B., Roobottom H. K., Passmore J., Glasser L., *Inorg. Chem.* **1999**, 38, 3609–3620; b) Jenkins H. D. B., Tudela D., Glasser L., *Inorg. Chem.* **2002**, 41, 2364–2367.

- [28] a) Joback K.G., Reid R.C., "Estimation of Pure-Component Properties from Group-Contributions", *Chem.Eng.Commun.* **1987**, 57, 233-243; b) Lydersen A.L., "Estimation of Critical Properties of Organic Compounds", University of Wisconsin College Engineering, *Eng. Exp. Stn. Rep. 3*, Madison, Wisconsin, **1955**; c) Constantinou L., Gani R., "New Group Contribution Method for Estimating Properties of Pure Compounds", *AIChE J.* **1994**, 40(10), 1697-1710; d) Nannoolal Y., Rarey J., Ramjugernath J., "Estimation of pure component properties Part 2. Estimation of critical property data by group contribution", *Fluid Phase Equilib.* **2007**, 252(1-2), 1-27;; e) Stein S.E., Brown R.L., "Estimation of Normal Boiling Points from Group Contributions", *J. Chem. Inf. Comput. Sci.* **1994**, 34, 581-587.
- [29] a) *EXPLO5.V2*, Computer program for calculation of detonation parameters, P, M. Suczeska, /*Proc. of 32nd Int. Annual Conference of ICT*/, July 3-6, Karlsruhe, German, **2001**, pp. 110/1 a software for determining detonation parameter, *2006*. b) Pospisil M.; Vavra P.; *Proceedings of the VII. Seminar: New Trends in Research of Energetic Materials* **2004**, 613.
- [30] a) Giacobazzo C. (**1997**) SIR-97 Program for Crystal Structure Solution, Inst. di Ric. per lo Sviluppo di Metodologie Cristallografiche, CNR, Univ. of Bari, Italy; b) Altomare, A.; Burla, M. C.; Camalli, M.; Cascarano, G. L.; Giacobazzo, C.; Guagliardi, A.; Moliterni, A. G. G.; Polidori, G.; Spagna, R. *J. Appl. Cryst.* **1999**, 32, 115-119.
- [31] Sheldrick, G. (**1997**) SHELXL-97 Program for Crystal Structure Refinement, Institut für Anorganische Chemie der Universität, Tammanstrasse 4, D-3400 Gottingen, Germany
- [32] Johnson, C.K. (**1976**) ORTEP-II. A Fortran Thermal-Ellipsoid Program, Report ORNL-5138. Oak Ridge National Laboratory, Oak Ridge Tennessee.
- [33] Brandenburg, K.; Putz, H., Berndt, M. (**2011**) *DIAMOND 3.2g*, Crystal Impact GbR, Bonn, Germany.
- [34] a) Reichel & Partner GmbH, <http://reichel-partner.de/> b) Test methods according to the UN Recommendations on the Transport of Dangerous Goods, Manual of Test and Criteria, fourth revised edition, United Nations Publication, New York and Geneva, **2003**, ISBN 92-1-139087-7, Sales No. E.03.VIII.2; 13.4.2 Test 3(a)(ii) BAM Fallhammer.

Chapter III

***N²,N⁴,N⁶-TRIS(TRIS(NITRATOMETHYL)METHYL)-1,3,5-
TRIAZINO-2,4,6-TRICARBOXAMIDE (NOX-1)***

-

BIG AND BANG

Abstract:

The explosive properties of N^2,N^4,N^6 -Tris(tris(nitratomethyl)methyl)-1,3,5-triazino-2,4,6-tricarboxamide (NOX-1) and the sensitivity is explained by consideration of the crystal structures. The calculated and experimental data for N^2,N^4,N^6 -Tris(tris(nitratomethyl)methyl)-1,3,5-triazino-2,4,6-tricarboxamide (NOX-1) shows strong similarity with PETN. This makes N^2,N^4,N^6 -Tris(tris(nitratomethyl)methyl)-1,3,5-triazino-2,4,6-tricarboxamide (NOX-1) good alternative to PETN. In particular, powder samples of N^2,N^4,N^6 -Tris(tris(nitratomethyl)methyl)-1,3,5-triazino-2,4,6-tricarboxamide (NOX-1) show low sensitivity to impact and friction which is important for handling and processing.

Keywords: PETN, Tris-(hydroxymethyl)-aminomethane (TRIS), triazine, triethyl-triazine-tricarboxylate, N^2,N^4,N^6 -Tris(tris(nitratomethyl)methyl)-1,3,5-triazino-2,4,6-tricarboxamide (NOX-1), sensitivity, crystal structure, thermodynamic data, DFT, B3LYP, CBS-4M, enthalpy of formation, energetic data.

1 Introduction

The search for insensitive explosives and propellants has found its beginning as always in a catastrophe. An ammunition ship exploded in the harbor and not only a big amount of people lost their lives but also the quay and the buildings were destroyed. To avoid another disaster there was established a new way of thinking on explosives and propellants. There should be only one way to bring an explosive to detonation and that is by the respective ignition chain. Same thing was proposed for ammunition as this is often transported in battleships and flight carriers as well as over land in convoys. Also they are stored in warehouses on military bases in foreign territory. During an attack there should be no explosion but a fire which can easily extinguished and does not harm people by flying projectiles.^[1]

“Though preventing accidents with explosive ordnance may not always be possible, their disastrous effects can certainly be diminished. There are overwhelming data that support the conclusion that the use of Insensitive Munitions technology can reduce the number of lives lost and limit material damage in accidents. In 1995, the Joint Requirements Oversight Council, JROC, supported the concept and as a result, an IM policy statement was included in the revised DOD Acquisition document, DODI 5000.2.”^[2]

Finding new insensitive explosives and propellants, which have an appropriate performance has led to investigate the following molecule N^2,N^4,N^6 -Tris(tris(nitratomethyl)methyl)-1,3,5-triazino-2,4,6-tricarboxamide.

2 Discussion

2.1 Structure of triazine derivatives

The first reports on the conversion of cyanides to triazines date to the early times of chemical research at the beginning of the 19th century.^[3] The correct constitutional formula and classification into the group of triazines was established by M.Neck in 1876. Around by the same time the cyclization reaction of other nitriles and cyanides to triazines was found.^[4,5]

The reaction mechanism and various enhancements in that field of research was performed by Grundmann, Weisse and Seide in 1957.^[6] One of the starting materials investigated was the methyl cyano formate ester which undergoes the same reactions as the ethyl cyano formate ester later described in this publication. Figure 1 shows the suggested mechanism for this reaction, a hydrochloride catalyzed trimerization.

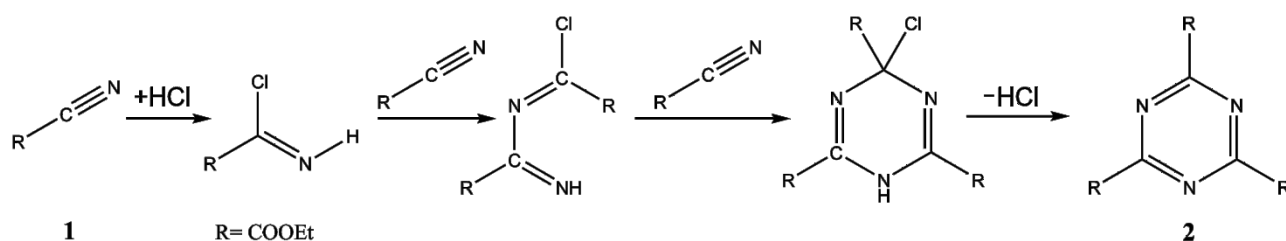


Figure 1. Mechanism for the hydrochloride catalyzed ring closure reaction from nitrile **1** to triazine **2**.^[6]

The described mechanism may be the reason why there is a disorder implicated in the crystal structure of this molecule. The triethyl-1,3,5-triazine-2,4,6-tricarboxylate starts to crystallize directly out of the ethyl cyano formate after 12 hours following the intake of gaseous hydrogen chloride and forms columns of hexagonal habitus.

This habitus implicates a hexagonal structure which has been found in single crystal x-ray structure and described by Tremayne *et al.*^[7] In contrary to the measurement at room temperature, as detailed in the mentioned publication, the dataset in here was collected at 100 K. This temperature has proven to be a good compromise for crystals containing only light elements like carbon, oxygen and nitrogen. But in this case it was not the right choice as a temperature depending phase transition can be found at 265 K and was first observed with low temperature DSC measurements (fig. 3) and proven by low temperature powder diffraction x-ray measurement (fig. 2). The hexagonal structure changes to a lower symmetry and twinning is observed.

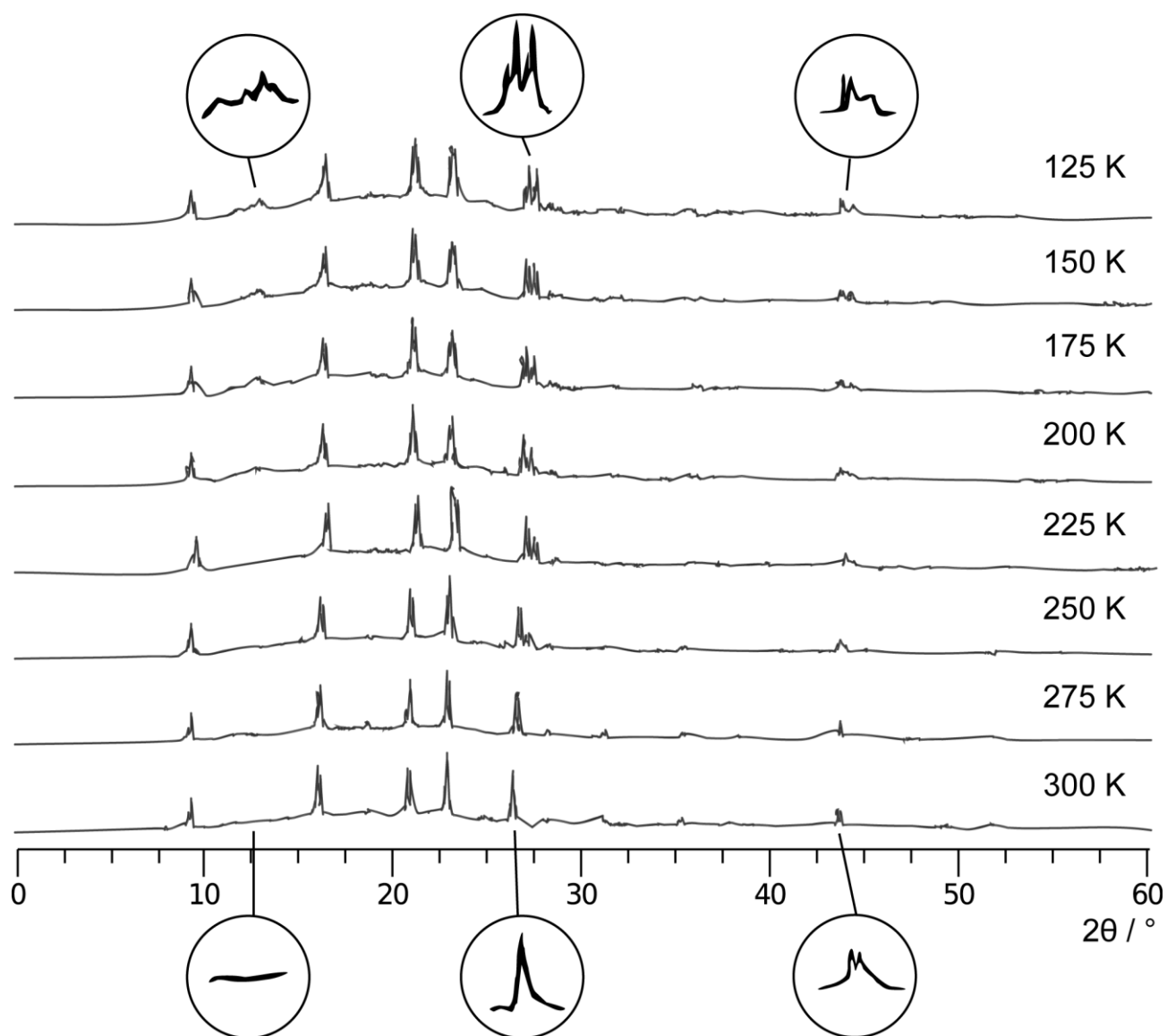


Figure 2. Powder x-ray measurements at cooling sample with 10 K min^{-1} ; the phase transition can be noticed at the appearing of the peak at 12.5° and the double peak at 27° and 27.3° or 44.1° and 44.6° which correspond to new formed lattices. Simulation of reflections in the powder diffraction using the literature value for the hexagonal phase and the here shown monoclinic phase support this observations.

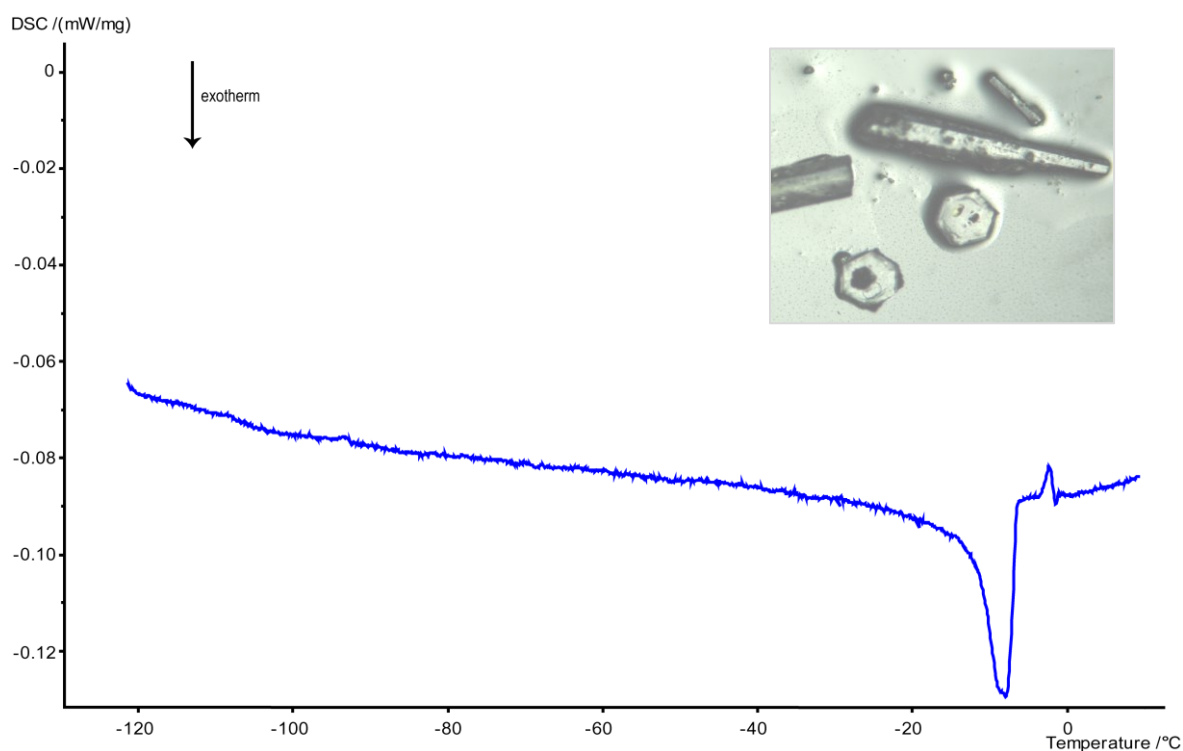


Figure 3. Phase transition at 265 K, Differential Scanning Calorimetry measurement at a cooling rate of 10 K min⁻¹; exothermic peak downwards.

The solved twinned system is presented below and the resulting molecule structure and difference to the hexagonal structure will be also described in the following.

2.1.1 Description of the molecule structure and the monoclinic crystal structure in comparison to the reported hexagonal structure

The structural differences in the two structures compared thereafter are mainly given by their different space groups. Therefore the hexagonal structure **2**–298 K can be described by an asymmetric unit which is only the third of the molecular structure (fig. 4). But in the monoclinic structure of **2**–100 K the whole molecule is one asymmetric unit (fig. 5).



Figure 4. An ORTEP^{III}^[8] view of triazine **2**, showing the atom-labeling scheme. Displacement ellipsoids are drawn at the 50 % probability level and H atoms are shown as small spheres of arbitrary radii. Measurement at 298 K.[6] (left) Measurement at 100 K (right).

Looking at the molecular structure of the **2**–298K the C₃-symmetry leads to a whole molecule that is planar, and the exocyclic groups are ordered in the same plane as the ring (fig.4). Also there are big thermal ellipsoids at the oxygen which is not uncommon for room temperature measurements. Comparing the molecular structure of the **2**–100K with the **2**–298K structure, it may be recognized that the exocyclic groups show little torsion shift (fig.5). That means the O3 and O5 atoms as well as the C9 and C12 are not in ring plane but turned out. This fixed, non-symmetric behavior is typical for the phase change as the molecules are not able to vibrate around the ground state at lower temperatures as much as at room temperature and the distortion of symmetry leads to a lower energy molecular structure. By rotation around the CH₂–CH₃ or the O–CH₂ bond all degrees of freedom are considered that could minimize the molecular and crystal symmetry.

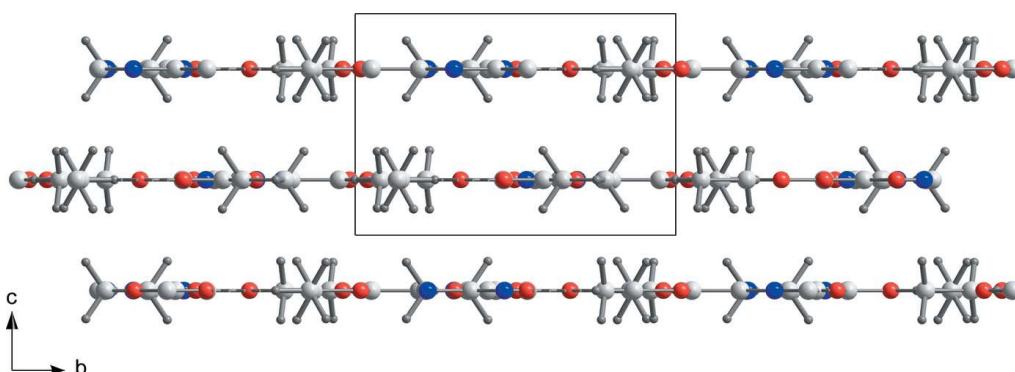


Figure 5. A view of **2** at 298 K showing the stacking of layers in the [001] direction.^[5]

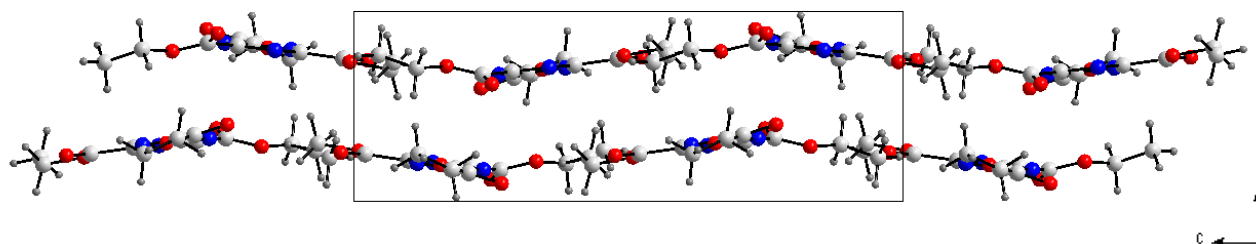


Figure 6. A view of **2** at 100 K showing the stacking of layers in the [100] direction.

Comparing the crystal structures there can be seen in the **2**-298 K structure - looking in the [001] direction (fig.6) - that the molecules are even stacked, which is another effect of the planar molecular structure. Else in the **2**-100 K structure, there you find a wave-like packing looking in the [100] direction. The cell dimension is nearly doubled up as you can assume from the figures 6 and 7 or looking up the crystal data. The length of the c-axis of **2**-100 K is 21.77 Å and in **2**-298 K the corresponding b-axis is 10.98 Å.^[7]

Hydrogen bonding in both of those molecules are not possible through classical concepts with nitrogen or oxygen as donor groups, but in this case the rare carbon hydrogen bonds takes the role as hydrogen donor. In the **2**-298 K crystal structure the intermolecular bonding are covered by the connection C—H O=C of the C5 at (x, y, z) via H5A to O2 at (2y, x y, z) as does the O2 (x, y, z) act as acceptor of the H5A (2x + y, 2x, z). As there is a C3 symmetry in the molecular structure this bonding can be found three times each molecule, which makes a surrounding of six different molecules in the plane (001) for one molecule (fig. 8). This behavior can be found in a similar way in the plane (010) of the **2**-100 K structure, where the you can see connections between the C11 and C12 at (x,y,z) via H12B and H11B to the acceptor bifurcated O1 at (-1+x, 0.5-y, -0.5+z) as does the O1 (x,y, z) to the C11 and C12 at (1+x, 0.5-y, 0.5+z). There is another connection from the C9 (x, y, z) via H9B to the acceptor O5 at (1+x, y, z) and the O5 (x, y, z) binds at the C9 at (-1+x, y, z). The last bonding to mention is the interaction between the donor C6 at (x, y, z) via H6B to the O3 (x, 0.5-y, 0.5+z), which can be found at O3 at (x, y, z) connection to C6 at (x, 0.5-y, -0.5+z).

These hydrogen bonds form a network, where one molecule interacts with six other molecules as it does in the **2**-298 K structure. The lengths of all bonds are shown in table 1.

Table 1. Intermolecular hydrogen-bond parameters (d [Å]; \angle [°]) of **2**–298 K and **2**–100 K.

D—H...A	H...A	D...A	\angle D—H...A
Compound 2-298K			
C5—H5A...O2 ⁱ	2.580(2)	3.286(4)	130.6(3)
Compound 2-100K			
C12—H12B...O1 ⁱⁱ	2.558(1)	3.232(2)	125.96(8)
C11—H11B...O1 ⁱⁱ	2.661(1)	3.094(1)	106.74(4)
C6—H6B...O3 ⁱⁱⁱ	2.706(1)	3.385(1)	126.67(5)
C9—H9B...O5 ^{iv}	2.652(1)	3.331(1)	126.60(6)

Symmetry codes: (i) $2y, xy, z$; (ii) $-1+x, 0.5-y, -0.5+z$; (iii) $x, 0.5-y, 0.5+z$; (iv) $1+x, y, z$

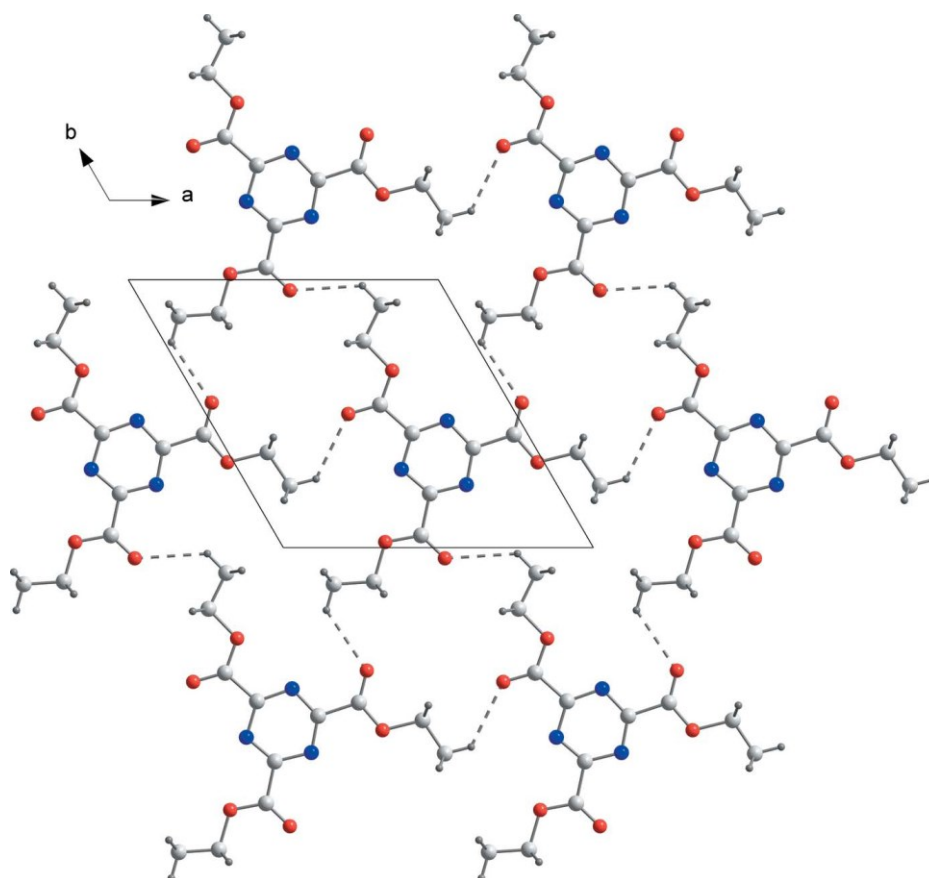


Figure 7. Part of the crystal structure of **2**–298 K, showing a hydrogen-bonded sheet in the (001) plane. Hydrogen bonds are shown as dashed lines^[5].

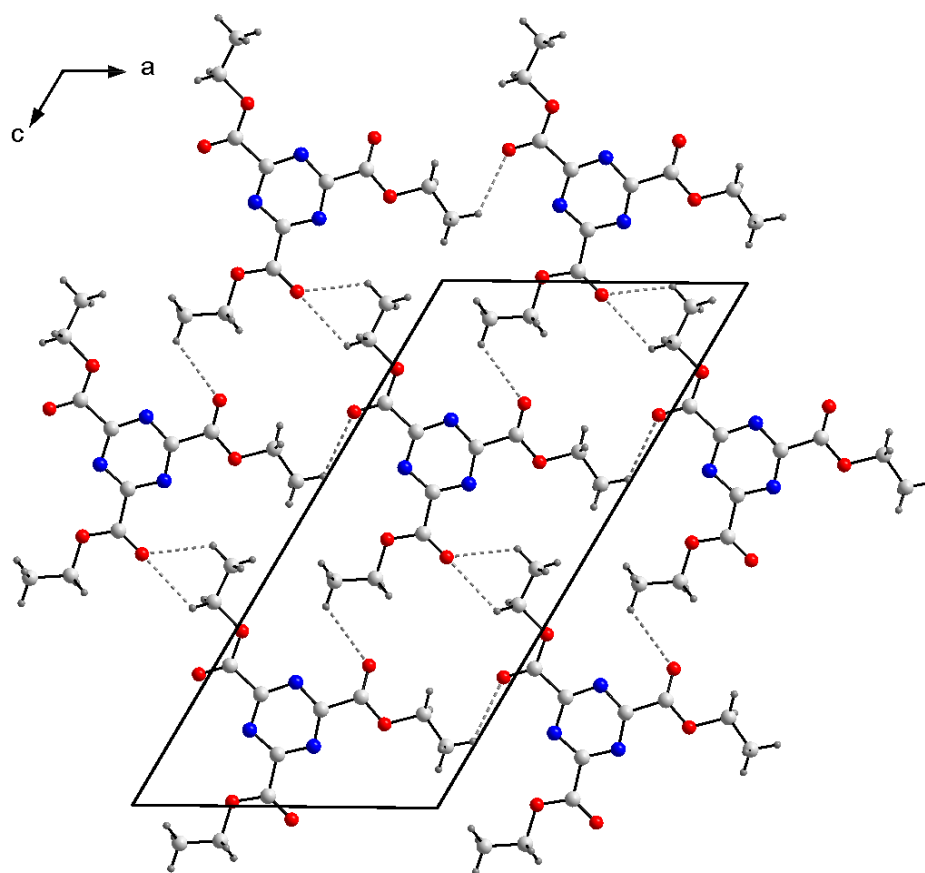


Figure 8. Part of the crystal structure of **2**–100 K, showing a hydrogen-bonded sheet in the (010) plane. Hydrogen bonds are shown as dashed lines.

2.2 Synthesis

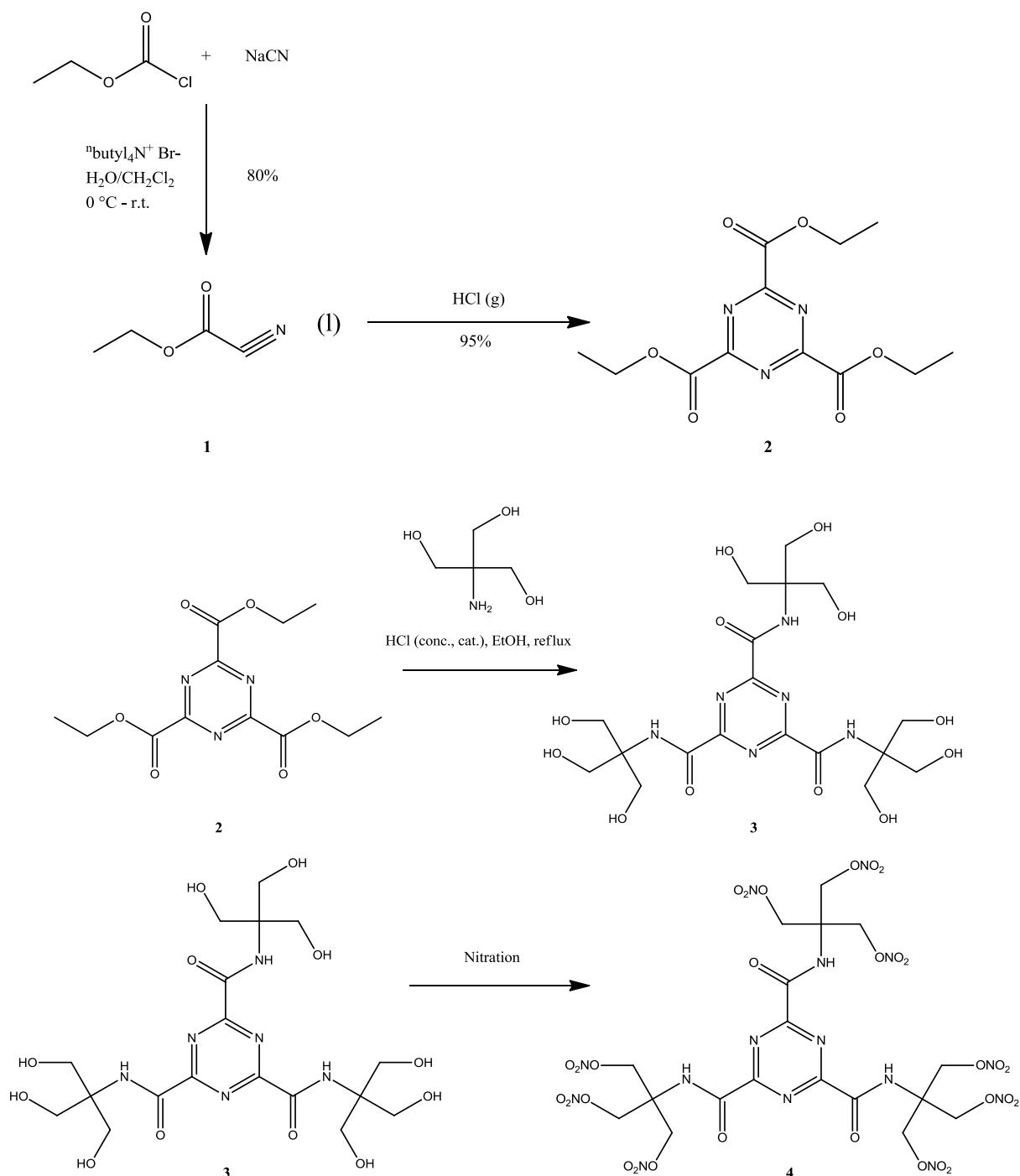


Figure 9. Synthesis of NOX (Nitration with acetic anhydride/ nitric acid).

The synthesis starts with the cheap common bulk materials sodium cyanide and ethyl chloro formate. The sodium cyanide is solved in water and the ethyl chloro formate in dichloromethane. The solutions are stirred together rapidly under cooling and the addition of the phase transfer catalyst tetrabutylammonium bromide. The product could be easily separated from the organic phase by removing the solvent and subsequently distillation to remove residues of ethyl chloro formate. The yield was over 80 %. The formed ethyl cyano formate (**1**) was undergoes cyclization by adding

gaseous hydrogen chloride for half an hour. It was found that the product has not to be hundred percent free of chloroformate for this reaction. So for mass production the distillation could possibly be omitted. The reaction yields in over 90 % pure crystalline product tri-ethyl-1,3,5-triazine-2,4,6-tri-carboxylate(**2, TECT**). The TECT and TRIS were added to an ethanol containing flask. To the mixture little concentrated hydrogen chloride solution was added and afterwards refluxed for four hours. The product (**3, TTHMM-TCA**) was filtered at a temperature of 40°C and washed with cold ethanol. The product was recrystallized from water. The yield was 65 %. Nitration was done in acetic anhydride with 100% nitric acid under ice-cooling. The yield was about 84.5 % of **4 (NOX)**. Crystals were obtained by recrystallization from acetone.

2.3 Thermodynamical and Spectroscopic Characterization

The thermodynamical data were gained by bomb calorimetry and by calculations also the Gaussian program code used to be the most accurate calculation due to the fact that the molecule has a lot of degrees of freedom to rotate bondings the B3LYP and the CBS4-M calculation were fruitless and ended always with timeouts, memory problems or in an infinite loop. So the Joback estimation method which was already described in Chapter I and II and had proven to be mostly very close to the experimental value as to the other calculated methods, was applied here to confirm the range of the experimental value.

Table 2. Thermodynamical data of NOX: calculation and experiment.

ΔH_f° (experimental)	-329.3 kcal mol ⁻¹
ΔH_f° (calculated by Gaussian03 ^[9] B3LYP/6-31G(2d,p))	Not available
ΔH_f° (calculated by Gaussian03 ^[9] CBS-4M)	Not available
ΔH_f° (Joback estimation method) ^[10]	-314.7 kcal mol ⁻¹

JOBACK – METHOD – ESTIMATION

The Joback method for estimating the heat of formation uses fragments of a carbon, hydrogen, nitrogen and oxygen containing backbone and assigns to those specific values for heat of formation and heat of fusion. The following equation show how the fragment values are summed up. ^[10]

Heat of Formation (Ideal Gas, 298 K)

$$\Delta H_{formation} = 68.29 + \sum H_i$$

Heat of Fusion

$$\Delta H_{fusion} = -0.88 + \sum G_i$$

Table 3. Functional groups are assigned with values for heat of formation and heat of fusion given in kcal mol⁻¹.

Functional group	Heat of formation	Heat of fusion
-CH ₂ -	-20.640	2.590
>C<	82.230	-1.460
>C=O (nonring)	-133.220	4.189
-O-(nonring)	-132.220	1.188
-COO- (ester)	-337.920	6.959
>NH (non-ring)	53.470	5.099
-NO ₂	-66.570	9.679
-N= (ring)	22.394	0.8721
=C< (ring)	11.097	0.5722

Table 4. The values of table 3 are used with the stated equations to result in the following heat of formation of in solid state.

ΔH_f^0 (gas)	-1478.750	kJ mol ⁻¹	-353.421	kcal mol ⁻¹
ΔH_{fusion}	161.846	kJ mol ⁻¹	38.681	kcal mol ⁻¹
ΔH_f^0 (solid)	estimated		-314.740	kcal mol ⁻¹

The rough estimation by this fragmental method is compared to the experimental value -329.3 kcal mol⁻¹ very close with a value of -314,740 kcal mol⁻¹.

2.4 Crystal structure data

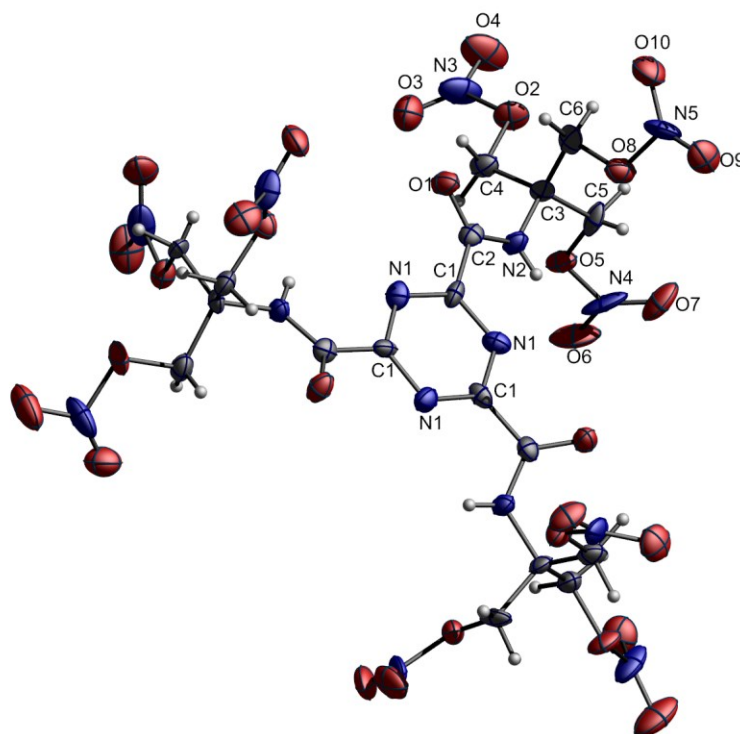


Figure 10. Molecular structure of NOX (ellipsoids plotted at 50% probability level), symmetry operations: $C1'(-y, -1+x-y, z)$ and $C1''(1-x+y, -x, z)$.

NOX crystallizes in the trigonal space group $R\bar{3}$ with 6 molecules in one unit cell. There is also one disordered water molecule included at the 3-folded symmetric centers which makes it very difficult to refine the water according to its real orientation in space.

Looking into the coordination of the NOX molecules in the unit cell we find a stacking of the triazine rings with a rotation of 60 degrees in each layer that results in helix like structure (fig.10 and 11). This triazine rings do not have any contact but the nitrate groups are having contact to each other which leads to the observed regular structural motif and stabilizes the crystal structure. The aforementioned water molecule is found on the edges and in-between the layered structures the disordered water resolves only the oxygen atom with a fixed but not well refinable ellipsoid while the surrounding hydrogen atoms are not refinable at all due to the little molecular mass which is in a normal x-ray diffraction analysis hard to find if the surrounding atoms are heavily involved in the diffraction. There might be an obscure guess according to the orientation of the surrounding moiety which may be the most likely positions but this has no fundamental prove and is therefore left out.

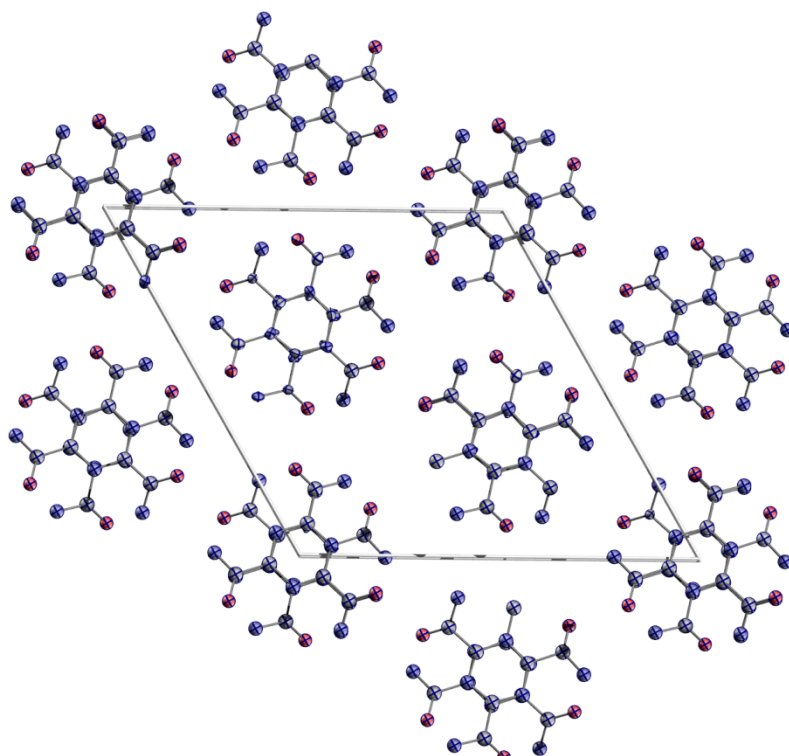


Figure 11. View along c-axis, model ball and sticks, nitrated TRIS moiety hidden for better view.

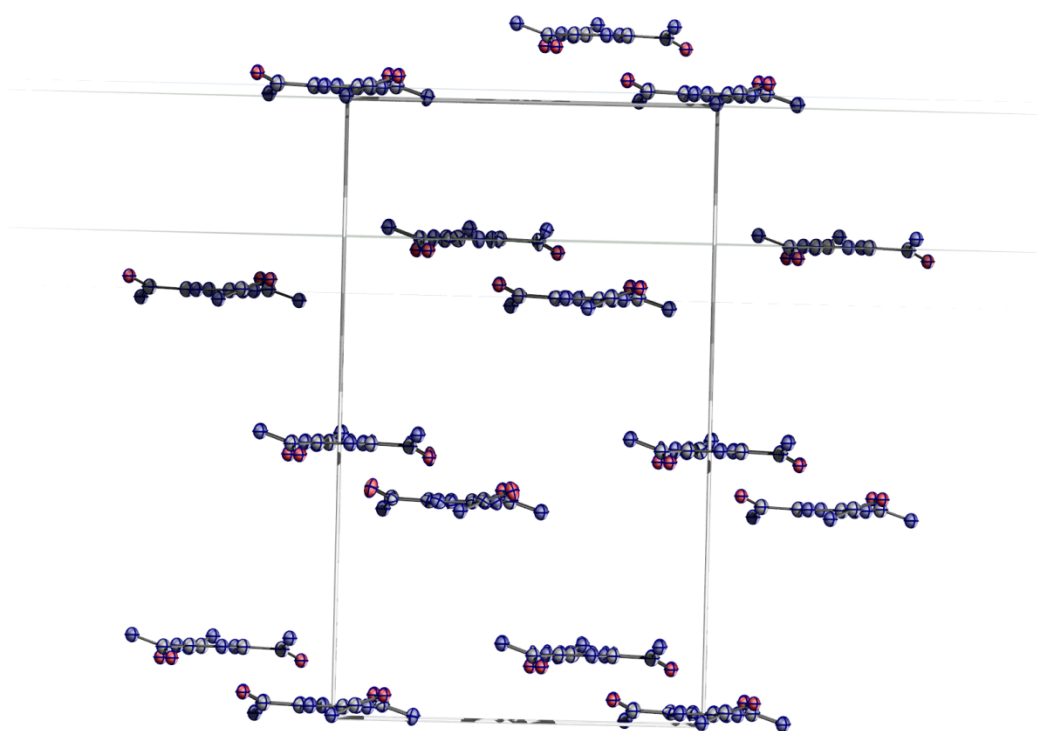


Figure 12. View along b-axis, model ball and sticks, nitrated TRIS moiety hidden for better view, parallel layers pointed out by lines.

2.5 Energetic data

The molecular structure of NOX shows that the nitrato groups are oriented on an outer rim which would result in an electrostatic surface potential that has negative areas at the outside and positive in the inside assuming from the ESP pictured in Chapter I figure 6. Discussing sensitivity that will influence on the impact, friction and ESD as evaluated in literature spherical particles are known to be less sensitive cRDX/ IS-RDX but looking on to molecular scale the spherical distribution of charge seems to be without any effect. Although there has been found a reduced sensitivity to friction and discharge the impact sensitivity is slightly less than PETN and more sensitive compared to RDX.

Table 5. Calculation based on EXPLO5.02^[11].

compound	TMD / g cm ⁻³	U ^o _f / kJ kg ⁻¹	Ox. bal.	Q _v / kJ kg ⁻¹	V ₀ / L kg ⁻¹	T _{ex} / K	P / kbar	D / ms ⁻¹	imp / J(Nm)	fric ./ N	mp / °C	T _{dec} / °C
TNT exptl	1.64 1.64	-184.9	-74	-5089	622	3741	202 210	7150 6950	15	>353	81	300
RDX exptl	1.80 1.80	+417	-21	-6034	769	4334	340 347	8882 8750	7.4	120	204	213
PETN [12] (EXPLO 5)	1.77	-1594	-10	-5975	769	4140 4398	331 318	8350 8599	3	-	141	163
NOX	1.61 1.80	-1501	-24	-5121 -5173	667 642	3822 3812	230 281	7423 8208	5	>360	-	151
TNM-CA	1.828	-2359	-14	-4532	652	3595	279	7808	>30	>360	145	145
BTNMMoxamide (powder, crystal)	- 1.81	-2488	-20	-4729	730	3670	282	8181	>30 2	>360 (>360)	155 -	160 157

The theoretical density of 1.8 gcm⁻³ as loading density can be estimated from the crystal structure which includes a water molecule that lowers the whole density. The values of the heat of explosion, volume of explosive gases and pressure as well as temperature of explosion are slightly above those of TNT, while the oxygen balance is next to RDX.

3 Conclusions

NOX is one of the biggest single molecules known to be explosive. Although the performance of NOX lies between the performance of PETN and TNT, it combines the good parts of TNT like the low temperature of explosion with the higher oxygen balance therefore calculation of the isobaric combustion shows very interesting data for a propellant, which will be the more suitable application for this molecule.

4 Experimental part

4.1 Instrumental setups

PD-XRAY

Low temperature powder x-ray measurements were taken at the HUBER G670 powder diffractometer. The sample temperature was maintained between 10 K and 300 K with a cryo cooling system (Cooling head, CTI-Cyrogenics, Modell 22 CP). For the control of the exact temperature a silicium diode probe (LakeShore, Modell 331) was applied which allows preciseness of 0.1 K. The sample was prepared by crushing in an agate mortar to a fine powder that was placed at the sample holder by fixing it between to polyacetate foils.

IR samples were measured with a *Perkin Elmer Spectrum BX-FTIR* equipped with a *Smith Dura Sample IRII-ATR-module*.

NMR-samples were measured with *Jeol Eclipse 400* at 25 °C. The obtained chemical shift are referenced with the internal standard: tetramethylsilane (^{13}C , 100.6 MHz; ^1H , 399.8 MHz)

RAMAN samples were measured with a *Perkin Elmer Spectrum 2000 NIR FT Raman* device including a *Perkin Elmer Diode Pumped Nd: YAG-Laser*-light source.

DSC Measurements were obtained a *Linseis DSC-PT 10 device*. Low temperature DSC data were measured by a *Netsch DSC Phönix* device equipped with separate cooling unit and autosampler μDSC .

SC-XRAY data were gathered with an *Oxford Xcalibur 3* diffractometer including a CCD-detector. The radiation source is a $\text{Mo K}\alpha$ -beam of wave length 0.71073 Å. The structure was solved with SIR97^[13] and refined with using SHELXL-97^[14], Ortep^[8] and Diamond^[15] plots showing thermal ellipsoids with 50% probability for the non-hydrogen atoms.

NCS-Elemental analysis was performed with a *Netsch Simultaneous Thermal Analyser STA 429*.

Mass Spectrometry was performed on a *Jeol MStation JMS 700*.

Friction and impact sensitivity data were obtained using the BAM drophammer and friction tests, in accordance with the BAM methods ^[16].

4.2 Preparation

4.2.1 [1,3,5]Triazine-2,4,6-tricarboxylic acid triethyl ester (2)

[1,3,5]Triazine-2,4,6-tricarboxylic acid triethyl ester was prepared according to Grundmann *et al.*^[6] by treating 5.03 g ethylcyanoformiate with gaseous HCl for 30 min. The solution turned yellow. After 24 h crystals started to grow and after another 48 h the crystallization was almost complete. After filtration, the product *yield*

was 2.85 g (56.7%). Impurities were removed and good crystals were obtained by recrystallization from ethanol. The melting point is at 172.8 °C.

¹H NMR (400 MHz, DMSO-d₆, ppm): 4.48 (q, ³J=7.2, 6H), 1.37 (t, ³J=7.2, 9H). **¹³C NMR (101 MHz, DMSO-d₆, ppm):** 166.2 (C=O), 161.8 (C=N), 63.6 (CH₂), 14.5 (CH₃). **IR (KBr, $\tilde{\nu}$ /cm⁻¹):** 3463 (s), 3000(s), 2973 (s), 2950(s), 2905(w), 2884(w), 1745(s), 1629(w), 1533(s), 1470(s), 1402(s), 1380(s), 1352(s), 1242(s), 1118(w), 1015(s), 938 (s), 861(s), 743(s), 697(s). **Raman:** 467(20), 535(6), 674(12), 828(7), 856(9), 1099(100), 1301(7), 1346(21), 1403(5), 1512(31), 1533(18), 1709(7), 2832(3), 3041(11), 3146(6), 3337(9). **e.a. (found/calc):** C 48.52/48.49; N 14.20/14.14 ; H 5.29/5.09. **DEI+ m/z:** 298(2), 282(6), 253(37), 225(100), 197(34), 168(3), 125(21), 98(10), 81(8), 56(16), 29(71). **m.p.** 172.8°C.

4.2.2 N²,N⁴,N⁶-Tris(tris(hydroxymethyl)methyl)-1,3,5-triazino-2,4,6-tricarboxamide (TTHMM-TCA, 3)

The TECT (2 g, 6.73 mmol) and TRIS (2.45 g, 20.24 mmol) were added into 200 mL ethanol and 0.2 ml concentrated hydrochloric acid solution. The mixture was refluxed for four hours, although after 30 minutes a clouding was observed which indicates the precipitation of the product. After cooling the product was filtered and washed with cold ethanol. The reaction yields 2.34 g (65%).

¹H NMR (400 MHz, DMSO-d₆, ppm): 4.82 (s, 12 H, OH, NH) and 3.64(s, 18 H, CH₂). **¹³C NMR (101 MHz, DMSP-d₆, ppm):** 166.5 (C=O), 159.2 (C=N), 61.8 (CH₂), 59.3 (C_q). **IR (KBr, $\tilde{\nu}$ /cm⁻¹):** 3396(b) (ν OH), 2950(w) (ν CH), 2890(w), 1688(s) (ν C=O), 1530(s) (ν C=N), 1465 (m), 1367(m), 1257(m), 1045(s), 1015(s), 850(w), 746(m). **m.p.** (Büchi): 216.5-220.8 °C.

4.2.3 N²,N⁴,N⁶-Tris(tris(nitratomethyl)methyl)-1,3,5-triazino-2,4,6-tricarboxamide (TTNMM-TCA, NOX, 4)

The TTHMM-TCA (1.07 g, 2 mmol) was added to a ice-cooled mixture of nitric acid (100%, 3.4 mL, 80 mmol) and acetic anhydride (100 %, 6.7 mL, 80 mmol). The solution was stirred for 2 hours under ice-cooling and another hour at room temperature. The reaction mixture was added to ice-water. The precipitate was filtered and washed with cool water four times. The product was recrystallized from acetone. *Yield 84.5%* (1.57g, 1.69mmol)

IR(KBr, $\tilde{\nu}$ /cm⁻¹): 3358(m), 3250(m), 3031(m), 2908(m), 1695(m), 1637(s), 1522(s), 1463(w), 1429(w), 1371(w), 1275(s), 1005(w), 847(m). **¹³C NMR (101 MHz, DMSO-d₆, ppm):** 56.3, 69.7, 161.2, 166.3; **¹H NMR (400 MHz, DMSO-d₆, ppm):** 5.23 (s, 18 H, CH₂), 10.01 (s, 3 H, NH). **¹⁴N NMR (63 MHz, DMSO-d₆, ppm):** 43.0. **¹H NMR (400 MHz, acetone-d₆, ppm):** 5.26 (s, 18H, CH₂), **¹³C NMR (100 MHz, acetone-d₆, ppm):** 167.9(C=O), 163.1 (C=N), 71.3 (CH₂), 59.2(^qC), **¹⁴ N NMR (29 MHz, acetone-d₆, ppm):** 43.0 (ONO₂). **elemental analysis: found(calc.)** N 20.98 (23.31), C 23.17 (22.65), H 2.78 (2.28). **Ω**=-28.5 %. **IS:** 5J [5kg-10cm, 3x] crystals. **FS:** none. **ESD:** not det. **DSC :** T_{dec} 148°C (onset, 5°C/min) ΔH_{dec} 1309.8 kJ/mol. **MS (FAB+)** 927.06 (100%), 928.06 (27.0%), 929.06 (9.5 %), 930.06 (1.9 %) (measured). 927.06 (100.0%), 928.06 (20.9%), 928.05 (5.5%), 929.06 (9.1%), 930.07 (1.4%) (theoretical) fragmentation 882.9, 838.2 split off of NO₂. **MS(DEI+)** 46 (100%) 44 (21%) 43 (18%) = NO₂.

5 References

- [1] a) SEA-64E Memo to SEA-06 Via Sea-06I, Ser. 64E/150, dated 13 August **1984**; Subject: *Summaries of Explosive Incidents* (ammunition ship SS BADGER STATE); b) U.S.S. ORISKANY, Press release of 10 March **1953**, *U.S. Naval Institute files*, Naval Academy, Annapolis, MD; c) U.S.S. FORRESTRAL - "Forrestal Disaster – Inferno at Sea", *Life Magazine* **1967**, August 11.
- [2] "The History of Insensitive Munitions", Raymond L Beauregard", **2004-2011**, <http://www.insensitivemunitions.org>.
- [3] a) J. v. Liebig, *Annalen der Pharmacie* **1834**, 10, 1-47. b) Sérullas A., *Ann. Chim. Phys.* **1828**, 38 (2), 390.
- [4] Nencki M., *Ber. dtsch. Chem. Ges.* **1876**, 9,244-250.
- [5] a) Cloëz S., *Annalen der Chemie und Pharmacie* **1860**, 115, 23-29. b) Engler C., *Annalen der Chemie und Pharmacie* **1860**, 133 (2), 137-154.
- [6] a) Grundmann Ch., Weisse G., Seide S., *Justus Liebigs Annalen der Chemie* **1952**, 577, 77-96.
b) Grundmann Ch., Kober E., *J.Org.Chem.* 1956, 1392-1394
- [7] Chong S. Y., Seaton C. C., Kariukia B. M., Tremayne M., *Acta Cryst.* **2006**, B62, 864–874.
Molecular versus crystal symmetry in tri-substituted triazine, benzene and isocyanurate derivatives
- [8] Burnett, M. N. & Johnson, C. K., *ORTEP III* **1996**, Report ORNL-6895. Oak Ridge National Laboratory, Tennessee, USA.
- [9] *Gaussian 03, Revision C.02*, Frisch, M. J.; Trucks, G. W.; Schlegel, H. B.; Scuseria, G. E.; Robb, M. A.; Cheeseman, J. R.; Montgomery, Jr., J. A.; Vreven, T.; Kudin, K. N.; Burant, J. C.; Millam, J. M.; Iyengar, S. S.; Tomasi, J.; Barone, V.; Mennucci, B.; Cossi, M.; Scalmani, G.; Rega, N.; Petersson, G. A.; Nakatsuji, H.; Hada, M.; Ehara, M.; Toyota, K.; Fukuda, R.; Hasegawa, J.; Ishida, M.; Nakajima, T.; Honda, Y.; Kitao, O.; Nakai, H.; Klene, M.; Li, X.; Knox, J. E.; Hratchian, H. P.; Cross, J. B.; Bakken, V.; Adamo, C.; Jaramillo, J.; Gomperts, R.; Stratmann, R. E.; Yazyev, O.; Austin, A. J.; Cammi, R.; Pomelli, C.; Ochterski, J. W.; Ayala, P. Y.; Morokuma, K.; Voth, G. A.; Salvador, P.; Dannenberg, J. J.; Zakrzewski, V. G.; Dapprich, S.; Daniels, A. D.; Strain, M. C.; Farkas, O.; Malick, D. K.; Rabuck, A. D.; Raghavachari, K.; Foresman, J. B.; Ortiz, J. V.; Cui, Q.; Baboul, A. G.; Clifford, S.; Cioslowski, J.; Stefanov, B. B.; Liu, G.; Liashenko, A.; Piskorz, P.; Komaromi, I.; Martin, R. L.; Fox, D. J.; Keith, T.; Al-Laham, M. A.; Peng, C. Y.; Nanayakkara, A.; Challacombe, M.; Gill, P. M. W.; Johnson, B.; Chen, W.; Wong, M. W.; Gonzalez, C.; and Pople, J. A.; Gaussian, Inc., Wallingford CT, 2004.
- [10] a) Joback K.G., Reid R.C., "Estimation of Pure-Component Properties from Group-Contributions", *Chem.Eng.Commun.* **1987**, 57, 233-243; b) Lydersen A.L., "Estimation of Critical Properties of Organic Compounds", University of Wisconsin College Engineering, *Eng. Exp. Stn. Rep. 3*, Madison, Wisconsin, **1955**; c) Constantinou L., Gani R., "New Group Contribution Method for Estimating Properties of Pure Compounds", *AIChE J.* **1994**, 40(10), 1697-1710; d) Nannoolal Y.,

- Rarey J., Ramjugernath J., "Estimation of pure component properties Part 2. Estimation of critical property data by group contribution", *Fluid Phase Equilib.* **2007**, 252(1-2), 1-27;; e) Stein S.E., Brown R.L., "Estimation of Normal Boiling Points from Group Contributions", *J. Chem. Inf. Comput. Sci.* **1994**, 34, 581-587.
- [11] *EXPLO5.V2*, Computer program for calculation of detonation parameters, P. M. Suceska, /Proc. of 32nd Int. Annual Conference of ICT/, July 3-6, Karlsruhe, German, **2001**, pp. 110/1 a software for determining detonation parameter, *2006*.
- [12] Pospisil M.; Vavra P.; *Proceedings of the VII. Seminar: New Trends in Research of Energetic Materials* **2004**, 613
- [13] a) Giacobazzo C. (**1997**) SIR-97 Program for Crystal Structure Solution, Inst. di Ric. per lo Sviluppo di Metodologie Cristallografiche, CNR, Univ. of Bari, Italy; b) Altomare, A.; Burla, M. C.; Camalli, M.; Cascarano, G. L.; Giacobazzo, C.; Guagliardi, A.; Moliterni, A. G. G.; Polidori, G.; Spagna, R. *J. Appl. Cryst.* **1999**, 32, 115-119.
- [14] Sheldrick, G. (**1997**) SHELXL-97 Program for Crystal Structure Refinement, Institut für Anorganische Chemie der Universität, Tammanstrasse 4, D-3400 Göttingen, Germany
- [15] Brandenburg, K.; Putz, H., Berndt, M. (**2011**) *DIAMOND 3.2g*, Crystal Impact GbR, Bonn, Germany.
- [16] a) Reichel & Partner GmbH, <http://reichel-partner.de/> b) Test methods according to the UN Recommendations on the Transport of Dangerous Goods, Manual of Test and Criteria, fourth revised edition, United Nations Publication, New York and Geneva, **2003**, ISBN 92-1-139087-7, Sales No. E.03.VIII.2; 13.4.2 Test 3(a)(ii) BAM Fallhammer.

Part III

ENERGETIC MATERIALS BASED ON 1,2,4-OXADIAZOLE DERIVATIVES

Chapter IV

3,3'-BIS-(1,2,4-OXADIAZOL-5-ONE) AND DERIVATIVES

–

A COMPREHENSIVE STUDY

1 Comparison of 3,3'-Bis-1,2,4-oxadiazol-5-one and 5,5'-Bis-1H-Tetrazole

Abstract:

3-substituted-1,2,4-oxadiazol-5-one derivatives may replace or complement tetrazole derivatives as pyrotechnics and propellants. As oxadiazolones have better oxygen balances (-47 % compared to 57% for tetrazole), both generate the same amount of gaseous products per molecule. Comparison of 3,3'-Bis-1,2,4-oxadiazol-5-one (H_2OD) with 5,5'-Bis-1H-tetrazole (H_2BT) shows some similarities and some differences which are discussed. The H_2OD decomposes at 376 °C and has a density obtained from x-ray diffraction of 1.90 g cm^{-3} . H_2BT already decomposes at 254°C and has a density of only 1.74 g cm^{-3} .

Keywords: 3-substituted-1,2,4-oxadiazol-5-one, H_2OD , 5,5'-Bis-1H-tetrazole, H_2BT , crystal structure, density, decomposition.

1.1 Introduction

The challenges in energetic materials' development include the search for higher performance, better safety and better environmentally compatibility. In order to meet these goals the gas output, oxygen balance, density, heat of formation and sensitivity to impact and friction are necessary properties to investigate and compare to those of standard explosives like RDX, HMX, TNT and gas generating molecules such as azide salts. In the recent years nitrogen-rich compounds such as tetrazole derivatives have successfully fulfilled many of these requirements. Although research in this area is ongoing, new energetic materials with similar or improved properties and simpler syntheses for appropriate large scale synthesis are needed. The derivatives of 3-substituted-1,2,4-oxadiazol-5-ones, which have not been investigated as energetic materials but as pharmaceuticals^[1], seem to be excellent candidates for pyrotechnics and propellants with similar properties to tetrazole based compounds.

1.2 Discussion

Recent research on tetrazoles shows that stable compounds with nearly the same oxygen balance or better would be rather preferable for application in propellants. The 3,3'-bis-1,2,4-oxadiazol-5-one (**1**, referred to as H_2OD) and the 5,5'-bis-1H-tetrazole (**2**, referred to as H_2BT) and are discussed below.

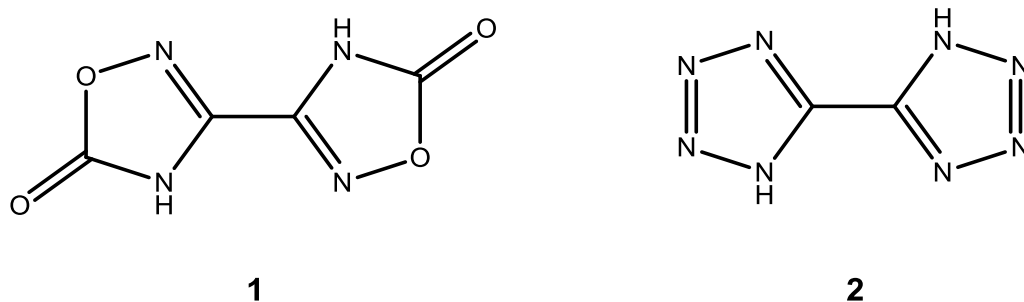
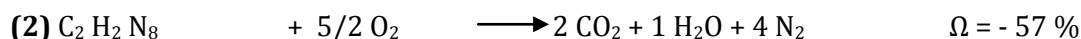
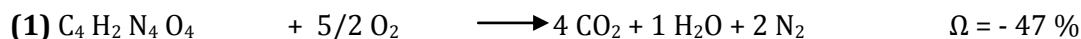


Figure 1. 3,3'-bis-1,2,4-oxadiazol-5-one (1) and 5,5'-bis-1H-tetrazole (2).

There are general synthetic routes to compound **(1)** which is a good ligand for transition metal ions. As described in a publication by Mubarak et al. the H₂OD was combined with Mn, Zn, Pd, Ni, Cd and Co ions to form stable complexes that have been investigated by IR spectroscopy and elemental analysis [2,3]. However further investigations yet not been carried out on this molecule. The obvious similarity of H₂BT to H₂OD, makes H₂OD a potential substitute for or alternative to H₂BT. Since the oxygen balance of H₂OD is less negative than that of H₂BT and the gas output and oxygen input shall be identical. H₂OD derivatives have different densities but do not differ much structurally as shown by by their crystal structures..

Oxygen balance and gas evolution



Compound **(2)** is well described in the literature. Steel et al. describe the crystal and molecular structure.^[4] A Japanese patent lists the friction and impact sensibility of the H₂BT and some amino salts of BT²⁻ (Tab 1).^[5a] Hiskey et al. describe the use of metal BT²⁻ salts for low-smoke pyrotechnic compositions in a patent.^[5b]

Table 1. Impact and friction sensitivity (JIS K 4810).

Compound	H ₂ OD	H ₂ BT
Friction sensitivity	>180 N	JIS Class 2 (> 1 kg =10N) ^[4a]
Impact sensitivity	none	JIS Class 4 (15-20 cm) ^[4a]
Decomposition temperature	375 °C	254 °C ^[4b]

The molecule structure determined by x-ray-diffraction is nearly identical to that which was determined by theoretical methods. The bond lengths correspond best to the literature values for the C1-O1 double bond (121.1 pm) and the N2-O2 single bond (142.4 pm) . The C1-O2 single bond (136.6 pm) is shorter than a normal C-O bond (143 pm). The C2-C2(i) bond (145.5 pm) is elongated as it is shorter than an sp³-sp³ carbon bond (154 pm) and longer than a sp²-sp² (133 pm) carbon bond, which indicates π -conjugation.^[6] Compared to other compounds measured by x-ray diffraction all bond lengths are in good agreement with the bond lengths of imidazole (C1-N1, C2-N1) and isooxazole (C2-N2, N2-O2, C1-O2).^[7]

Each molecule hydrogen bonds up to 4 other molecules over H1 and H1(i) and over O1 and O1(i) leading to a strong and stable network (Fig.3).

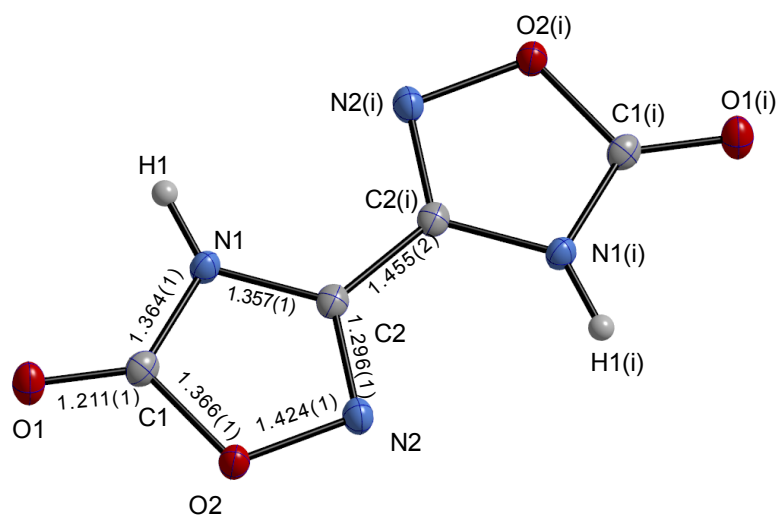


Figure 2. The molecular structure of 3,3'-bis-1,2,4-oxadiazol-5-one (50% probability ellipsoids, bond lengths in Å).

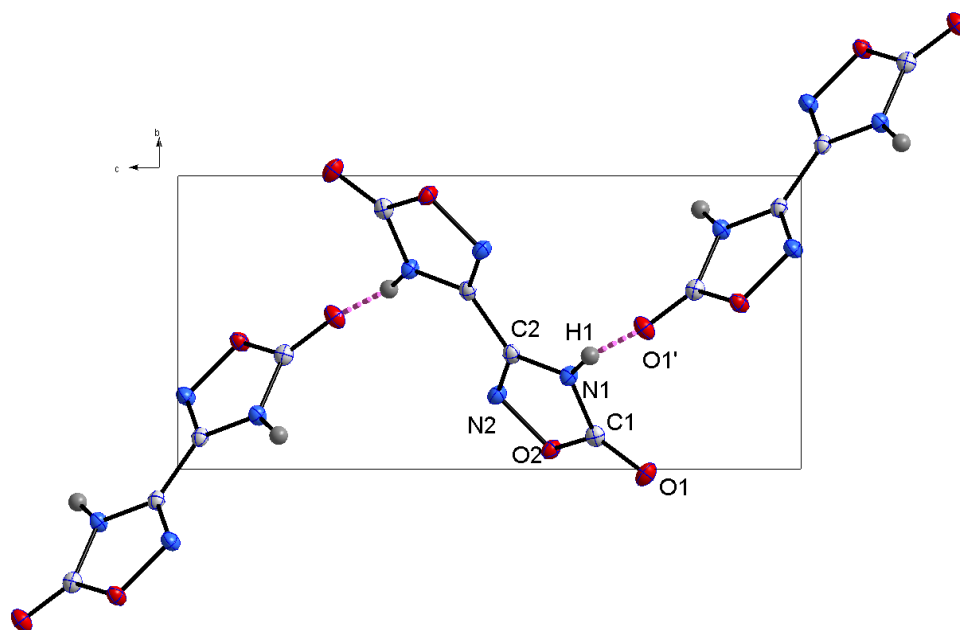


Figure 3. View along a-axis the showing hydrogen bond between N1 and O1' over H1.

Table 2. Crystallographic Data for H₂OD and H₂BT

Compound	H ₂ OD	H ₂ BT
Formula	C ₄ H ₂ N ₄ O ₄	C ₂ H ₂ N ₈
Formula weight / g mol ⁻¹	170.1	138.1
Color/shape	colorless/block	colorless/block
Crystal system	monoclinic	monoclinic
Space group	P 2 ₁ /n (14)	P 2 ₁ /n (14)
a / Å	4.7437(3)	4.945(1)
b / Å	5.4028(3)	6.367(1)
c / Å	11.6654(7)	8.491(1)
α / °	90	90
β / °	95.84(1)	99.233(7)
γ / °	90	90
Cell volume / Å ³	297.4(2)	263.87
Z	2	2
D _{calc} / g cm ⁻³	1.899	1.738
T / K	100	130
GooF	1.087	1.09
R (All)	0.043	0.034

Table 3. Selected bond lengths, angles, torsion angles and hydrogen bondings from x-ray diffraction and *d_{calc}* calculated bond lengths with Gaussian03 (B3lyp/cc-pVDZ)^[8].

Bond lengths					
Atoms 1,2	d 1,2 [Å]	d _{calc}	Atoms 1,2	d 1,2 [Å]	d _{calc}
O2—C1	1.366(1)	1.390	N1—H1	0.89(2)	1.013
O2—N2	1.424(1)	1.402	O1—C1	1.211(1)	1.196
N1—C2	1.357(1)	1.367	N2—C2	1.296(1)	1.299
N1—C1	1.364(1)	1.391	C2—C2i	1.455(2)	1.452

Angles			
Atoms 1,2,3	Angle 1,2,3 [°]	Atoms 1,2,3	Angle 1,2,3 [°]
C1—O2—N2	109.30(7)	N2—C2—C2i	121.9(1)
C2—N1—C1	106.62(9)	N1—C2—C2i	124.2(1)
C2—N1—H1	130.5(9)	O1—C1—N1	131.1(1)
C1—N1—H1	122.8(9)	O1—C1—O2	122.42(9)
C2—N2—O2	103.65(8)	N1—C1—O2	106.49(9)
N2—C2—N1	113.93(9)		

Torsion angles				
Atoms 1,2,3,4	Tors. an. 1,2,3,4 [°]	Atoms 1,2,3,4	Tors. an. 1,2,3,4 [°]	
C1—O2—N2—C2	0.72(10)	C2—N1—C1—O1	-179.54(10)	
O2—N2—C2—N1	0.1(1)	C2—N1—C1—O2	1.3(1)	
O2—N2—C2—C2i	179.3(1)	N2—O2—C1—O1	179.49(9)	
C1—N1—C2—N2	-0.9(1)	N2—O2—C1—N1	-1.3(1)	
C1—N1—C2—C2i	179.9(1)			
(i) -x, 1-y, 1-z.				
Selected hydrogen bonds				
Atoms D,H,A	Dist. D,H [Å]	Dist. H,A [Å]	Dist. D,A [Å]	Angle D,H,A [°]
N1—H1—O1 ⁱ	0.89(2)	1.86(2)	2.749(1)	170 (1)
(i) -0.5-x, -0.5+y, 1.5-z.				

1.3 Synthesis

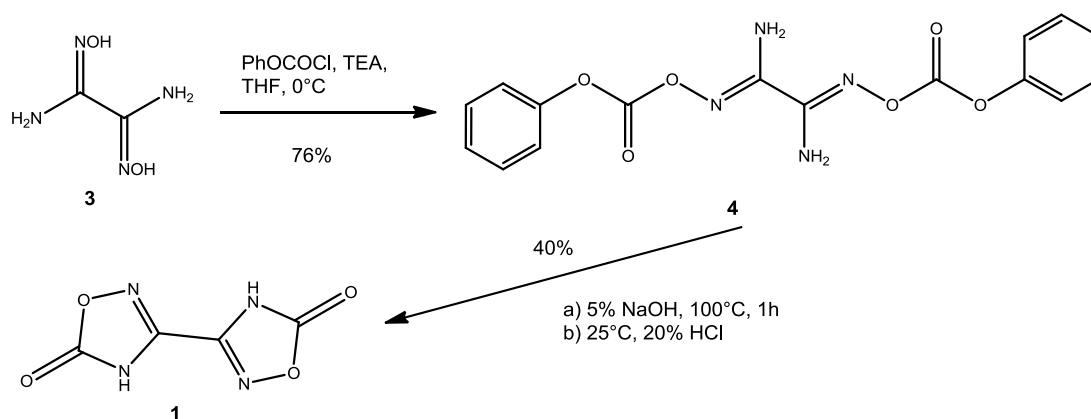


Figure 4. Synthetic route starting from oxamidedioxime to H₂OD.

The synthesis of the H₂OD proceeds from an inexpensive starting material oxamidedioxime (**3**) which is easily prepared by the method of Trudell et al.^[9] Through further treatment with phenyl chloroformate the carbonyl function is introduced and the ring closing reaction takes place via attack of the amino group and subsequent cleavage of phenol. This simple reaction scheme was adopted from literature known path used by Rehse et al. and combined with the route of Khalili et al.^[2,3]. The yields and synthesis may be optimized for industrial production.^[10]

1.4 Conclusions

Oxadiazolone derivatives may replace or complement tetrazole derivatives since the oxadiazolones have better oxygen balances and generate equal amounts of gas on combustion. The obvious bonding in H₂OD is weaker as there is no aromatic stabilization in oxadiazolones but this is no hindrance to its application since H₂OD is stable at temperatures up to 373 °C. All in all this makes the class of H₂OD and its derivatives promising candidates for pyrotechnics and propellants.

1.5 Experimental

1.5.1 Crystal structures

The molecular structure of **I** was determined by single crystal X-ray diffraction. The X-ray crystallographic data were collected using an Oxford Xcalibur diffractometer with a CCD area detector and graphite-monochromated Mo K α radiation ($\lambda = 0.71073$ Å). The structure was solved with SHELXS-97^[11] and refined with using SHELXL-97^[12]. Ortep^[13] plots (Figs. 2 + 3) showing thermal ellipsoids with 50% probability for the non-hydrogen atoms in **I** is depicted in Figs. 2+3.

1.5.2 Properties

Decomposition points, enthalpies, melting points and dehydration points were determined using a Linseis DSC PT10. Additionally, the melting point and dehydration points were also determined using Büchi B-540 melting point apparatus. The friction and impact sensitivity data were obtained using the BAM drophammer and friction tests, in accordance with the BAM methods ^[14].

1.5.3 Spectroscopic Data and elemental analysis

IR spectra were obtained using a Perkin Elmer Spectrum BX FT-IR System and a Raman spectra were measured using Perkin Elmer Spectrum 2000 FT- Raman spectrometer fitted with a Nd-YAG-laser ($\lambda = 1064$ nm) as solids at room temperature (resolution = 4 cm⁻¹)

NMR spectra were obtained with a Jeol Eclipse 400 spectrometer operating at 400.2 MHz for ¹H, 100.6 MHz for ¹³C and 28.9 MHz for ¹⁴N. Chemical shifts (in ppm) are given with respect to TMS (¹H/¹³C), MeNO₂ (¹⁴N) as internal standard.

1.5.4 Preparation

O,O'-DI-(PHENOXYCARBONYL)-OXAMIDODIOXIME (**4**)

To a ice-cooled solution of 1 g (8.5 mmol) oxamidedioxime (**3**) in 30 mL THF was added 2.5 mL (3.1 g, 20 mmol) phenyl chloroformate and 3.2 mL (2.3 g, 22.9 mmol) triethylamine dropwise. After one hour of stirring 50 mL water and 20 mL diethylether were added a white precipitate was formed. The solid was filtered, washed with 10 mL diethylether and dried.

Yield: 2.33 g (6.5 mmol); 76 %.¹H NMR ([D₆]DMSO): δ = 7.04 (s, 4H; NH₂), 7.28 (d, 4 H; ArH₂, ArH₆; ²J = 8.5 Hz, ³J = 1.2 Hz, ³J = 0.9 Hz), 7.31 (t, 2H; ArH₄; ²J = 7.5 Hz, ³J = 1.0 Hz),

7.46 (t, 4H; ArH3, ArH5; $^2J = 7.5$ Hz, $^2J=8.1$ Hz) ppm. **$^{13}\text{C}\{^1\text{H}\}$ NMR** ([D6]DMSO): $\delta = 121.3$ (4C; ArC2,ArC6), 126.4 (4C; 2C,ArC4), 129.8 (4C; ArC3, ArC5), 150.7 (2C; ArC1), 151.0 (2C; Carbonate), 151.8 (2C; oxime-C) ppm. **IR:** $\tilde{\nu}(\text{cm}^{-1}) = 3627$ s, 3502 s, 3448 s, 3336 s, 3073 m, 3043 s, 1772 vs, 1613 vs, 1589 s, 1493 s, 1483 s, 1457 m, 1326 m, 1296 m, 1222 w, 1205 s, 1162 m, 1038 s, 1070 s, 1042 s, 1020 s, 955 vs, 832 m, 793 m, 753 vs, 738 vs, 687 s. **elemental analysis: found(calc.)** C 54.01 (53.63), H 3.89 (3.94), N 15.64 (15.64).

3,3'-BIS-1,2,4-OXADIAZOL-5-ONE (1)

1.00 g (2.8 mmol) O,O'-Di-(phenoxy carbonyl)-oxamidedioxime(4) was suspended in 10 mL 5 % solution of sodium hydroxide and heated for one hour at 100 °C, until the mixture has become a slightly brown clear solution. The solution allowed to cool to room temperature and afterwards acidified with 10 mL 20 % hydrochloric acid until no further precipitate was formed. The white solid was filtered and washed with diluted hydrochloric acid and water and then dried.

Yield: 0.19 g (1.1 mmol) 40 %, **^1H NMR** ([D6]DMSO): $\delta = 12.27$ (2H, br) ppm. **$^{13}\text{C}\{^1\text{H}\}$ NMR** ([D6]DMSO): $\delta = 142.9$ (2C, C2), 154.5 (2C, C1) ppm. **Elemental analysis: found (calc.)** C 32.82 (32.94), H 1.35 (1.19), N 28.23 (28.25). **IR:** $\tilde{\nu}(\text{cm}^{-1}) = 3524$ s, 3114 m, 2748 m, 2578 vs, 2505 vs, 1766 w, 1537 s, 1435 s, 1252 vs, 1171 vs, 984 vs, 935 vs, 887 s, 750s, 616s. **DSC:** no melting; decomposition between 3; decomposition enthalpy 330.39 J/g (62.5 kJ/mol); max. peak: 172.6 C / -2.4 mJ/s.

1.6 References

- [1] F. ELOY, *Fortschr. Chem. Forsch.* **1965**, 4, 807-876.
- [2] K. A. AL-SOU'OD, F. I. KHALILI, M. MUBARAK, *J. Saud. Chem. Soc.* **2000**, 4(2), 143-151.
- [3] N. AL-SAYYED AHMAD, F. KHALILI, *Synth. React. Inorg. Met.-Org. Chem.* **1990**, 20(4), 425-436.
- [4] P. J. STEEL, *J. Chem. Cryst.* **1996**, 26 (6), 399-402.
- [5] (a) O. ATSUHIRO, T. HIROAKI, *JP6166678*, **1992**; (b) M.A. Hiskey, D.E. Chaves, D.L. Naud., *US6214139*, **2001**.
- [6] A. F. HOLLEMAN,, E. WIBERG,, *Lehrbuch der Anorganischen Chemie*, 101. Edition by N. WIBERG,, Walter de Gruyter, Berlin, **1995**, 1842.
- [7] F. H. ALLEN, O. KENNARD, D. G. WATSON, L. BRAMMER, A. G. ORPEN, R. TAYLOR, *J. Chem. Soc. Perkin Trans 2*, **1987**, 12, S1-S19.
- [8] *Gaussian 03, Revision C.02*, FRISCH, M. J.; TRUCKS, G. W.; SCHLEGEL, H. B.; SCUSERIA, G. E.; ROBB, M. A.; CHEESEMAN, J. R.; MONTGOMERY, Jr., J. A.; VREVEN, T.; KUDIN, K. N.; BURANT, J. C.; MILLAM, J. M.; IYENGAR, S. S.; TOMASI, J.; BARONE, V.; MENNUCCI, B.; COSSI, M.; SCALMANI, G.; REGA, N.; PETERSSON, G. A.; NAKATSUJI, H.; Hada, M.; EHARA, M.; TOYOTA, K.; FUKUDA, R.; HASEGAWA, J.; ISHIDA, M.; Nakajima, T.; HONDA, Y.; KITAO, O.; NAKAI, H.; KLENE, M.; LI, X.; KNOX, J. E.; HRATCHIAN, H. P.; CROSS, J. B.; BAKKEN, V.; ADAMO, C.; JARAMILLO, J.; GOMPERTS, R.; STRATMANN, R. E.; YAZYEV, O.; AUSTIN, A. J.; CAMMI, R.; POMELLI, C.; Ochterski, J. W.; AYALA, P. Y.; MOROKUMA, K.; VOTH, G. A.

- SALVADOR, P.; DANNENBERG, J. J.; ZAKRZEWSKI, V. G.; DAPPRICH, S.; DANIELS, A. D.; STRAIN, M. C.; FARKAS, O.; MALICK, D. K.; RABUCK, A. D.; RAGHAVACHARI, K.; FORESMAN, J. B.; ORTIZ, J. V.; CUI, Q.; BABOUL, A. G.; CLIFFORD, S.; CIOŚLOWSKI, J.; STEFANOV, B. B.; LIU, G.; LIASHENKO, A.; PISKORZ, P.; KOMAROMI, I.; MARTIN, R. L.; FOX, D. J.; KEITH, T.; AL-LAHAM, M. A.; PENG, C. Y.; NANAYAKKARA, A.; CHALLACOMBE, M.; GILL, P. M. W.; JOHNSON, B.; CHEN, W.; WONG, M. W.; GONZALEZ, C.; and POPLER, J. A.; Gaussian, Inc., Wallingford CT, 2004.
- [9] M.L. TRUDELL, *J.Heterocyclic Chem.* **1997**, 34,1057-1060.
- [10] RHESE, K.; BADE, S.; HARS DORF, A.; CLEMENT, B.; *Arch. Pharm. Pharm. Med. Chem.* **1997**, 330, 392-398.
- [11] SHELDRICK, G. (**1997**) SHELXS-97 Program for Crystal Structure Solution, Institut für Anorganische Chemie der Universität, Tammanstrasse 4, D-3400 Gottingen, Germany.
- [12] SHELDRICK, G. (**1997**) SHELXL-97 Program for Crystal Structure Refinement, Institut für Anorganische Chemie der Universität, Tammanstrasse 4, D-3400 Gottingen, Germany.
- [13] JOHNSON, C.K. (**1976**) ORTEP-II. A Fortran Thermal-Ellipsoid Program, Report ORNL-5138. Oak Ridge National Laboratory, Oak Ridge Tennessee.
- [14] a) REICHEL & PARTNER GmbH, <http://reichel-partner.de/> b) Test methods according to the UN Recommendations on the Transport of Dangerous Goods, Manual of Test and Criteria, fourth revised edition, United Nations Publication, New York and Geneva, **2003**, ISBN 92-1-139087-7, Sales No. E.03.VIII.2; 13.4.2 Test 3(a)(ii) BAM Fallhammer.

2 Insensitive Explosives and Propellants based 1,2,4-oxadiazol derivatives

Abstract

The aims of research for new explosives are a better or equal performance to RDX, safety in handling, a high temperature and longterm stability and also a low toxicity. These necessary properties are accomplished by the class of oxadiazol derivatives. The most common compound for explosives are the 1,2,5-oxadiazol derivatives (furazanes) which have high performance but often a lack of stability. The 1,2,4-oxadiazol derivatives are combined with a selection of energetic synthons. The nitrogen rich bis-1,2,4-oxadiazol-5-one salts show interesting properties as propellants.

Keywords: Propellant, Explosive, Energetic Salt, Nitrogen Rich, Oxadiazole, Guanidine

2.1 Introduction

The challenges in energetic materials' development include the search for higher performance, better safety and better environmentally compatibility. In order to meet these goals the gas output, oxygen balance, density, heat of formation and sensitivity to impact and friction are necessary properties to investigate and compare to those of standard explosives like RDX, HMX, TNT and gas generating molecules such as azide salts. In the recent years nitrogen-rich compounds such as tetrazole derivatives have successfully fulfilled many of these requirements. Although research in this area is ongoing, new energetic materials with similar or improved properties and simpler syntheses for appropriate large scale synthesis are needed.

The lately introduced system of 1,2,4-oxadiazol-5-one as building block is not an uncommon step. The similarity to tetrazole derivatives was earlier shown by Klapötke et al.^[1] Also 1,2,5-oxadiazole(furazane) compounds have been examined for over thirty years as building blocks in energetic materials.^[2]

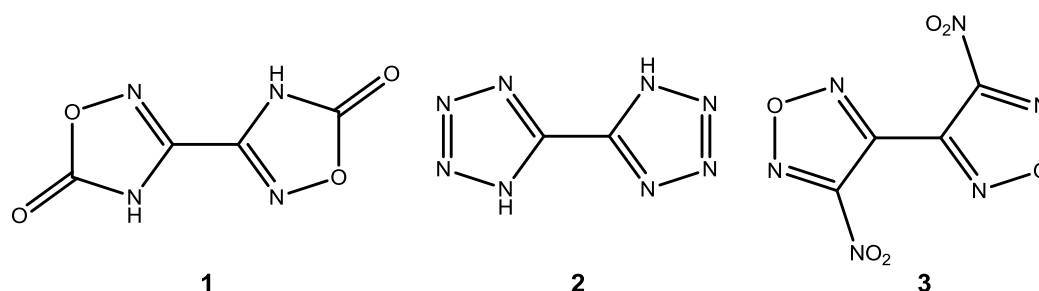


Figure 1. 3,3'-Bis(1,2,4-Oxadiazol-5-one) (H₂OD, **1**)^[3], 5,5' bis-1H-tetrazole (H₂BT, **2**)^[4], 4,4' dinitro-3,3' bisfurazanes (**3**).^[2]

To increase the heat of formation and to apply more nitrogen content to the 3,3'-bis-(1,2,4-oxadiazol-5-one) (**1**), this acidic heterocycle was combined with a bunch of

nitrogen rich cations. Besides the ammonium and the hydrazinium cation, the guanidine derivatives were chosen.

The obtained compounds are compared in their thermodynamic and energetic data. The crystal structures of some of those compounds are discussed with respect to their thermostability and sensitivity. All those compounds have been synthesized and fully characterized.

2.2 Syntheses

The strategies to obtain nitrogen rich salts of **1** can be divided in three main ideas. The first is to directly use the acidic properties of **1** and combine it with strong bases in adequate solvent. This was used to obtain the ammonium and the hydrazinium salts. The second idea was to use a nitrogen rich salts which could be in combination with **1** only result in a pure product. This is possible by using the hydrogen carbonate salt, which only evolves carbon dioxide while stirred with **1**. The third route takes to steps. The first of those is to obtain a silver or barium salt of **1**, which could be easily done by the combination with barium nitrate or silver nitrate while adding alkaline solution. Those salts are not good soluble in water which results in a high yield. The barium and the silver salts can be used to perform a metathesis reaction with the appropriate guanidinium sulfate or chloride to precipitate a very bad soluble barium sulfate or silver chloride.

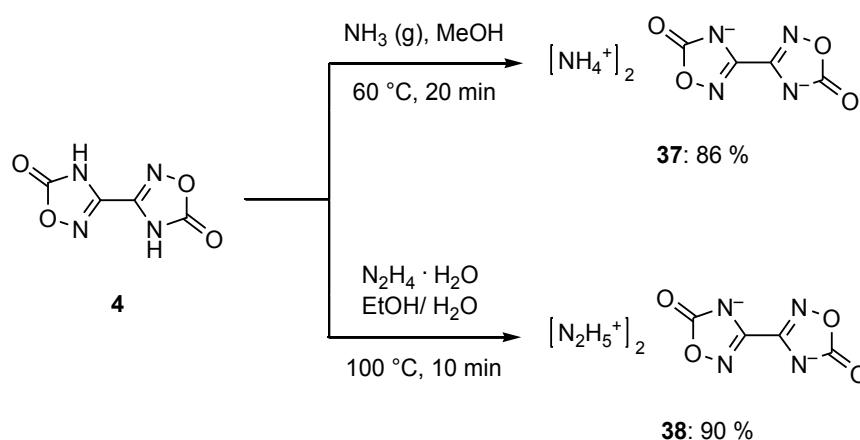


Figure 2. Synthesis of $(\text{NH}_4)_2\text{OD}$ (**4**) and $(\text{N}_2\text{H}_5)_2\text{OD}$ (**5**).

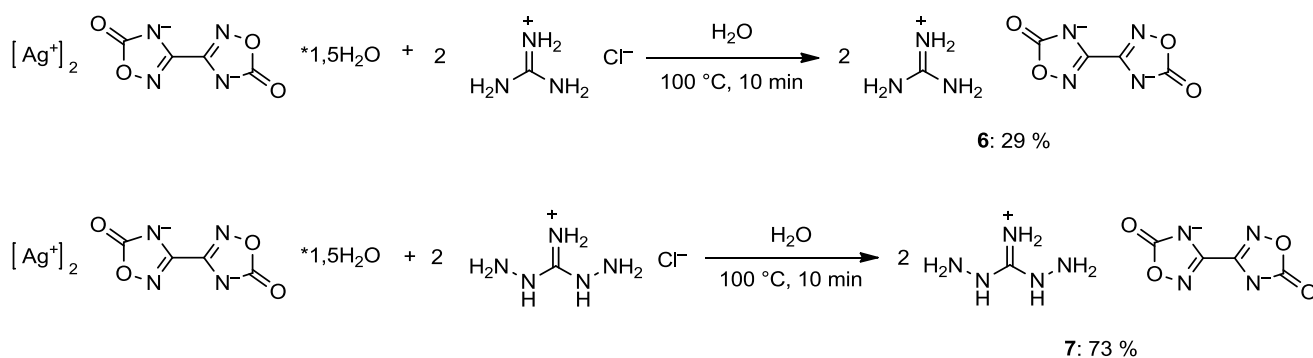
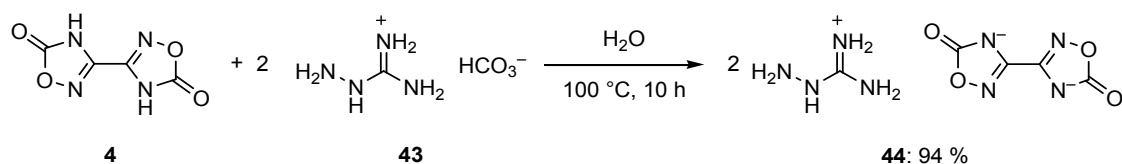
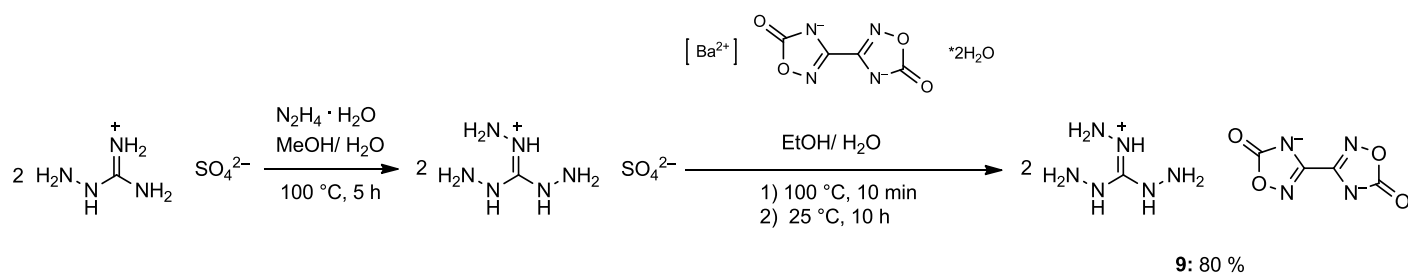


Figure 3. Synthesis of G₂OD (6) and DAG₂OD (7).

Figure 4. Synthesis of AG₂OD (8).

Figure 5. Synthesis of TAG₂OD (9).

2.3 Crystal structures

The crystal structures of (NH₄)₂OD (4) and (N₂H₅)₂OD (5) are discussed with respect to similarities and differences.

2.3.1 Diammonium bis-(1,2,4-oxadiazol-5-onate)

Figure 5 shows the molecular structure of the ammonium-3,3'-bis(1,2,4-oxadiazol-5-onate) (4). The compound crystallizes in the monoclinic space group *P*2₁/*c* with four formula units per unit cell.

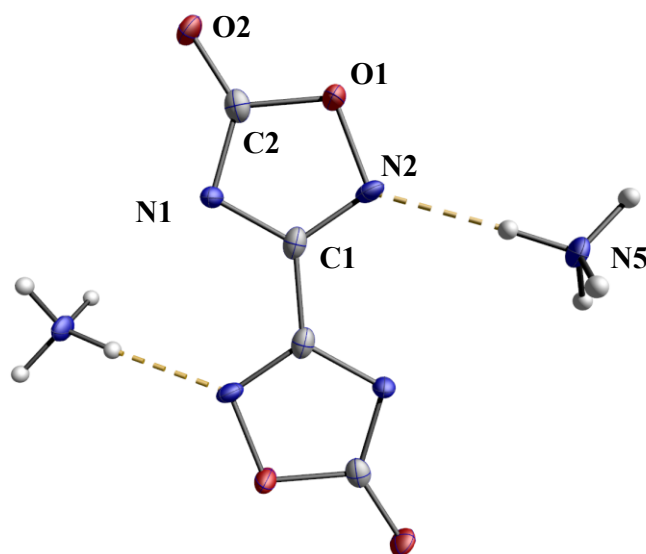


Figure 6. Molecular structure of $(\text{NH}_4)_2\text{OD}$ (**4**) (50% probability ellipsoids). Selected bond lengths(Å) and angles (°): O1—C2 1.383(3), O1—N2 1.420(2), O2—C2 1.247(3), N2—C1 1.304(3), N1—C2 1.335(3), N1—C1 1.362(3), C1—C1i 1.458(5); C2—O1—N2 106.7(2), C1—N2—O1 102.7(2), C2—N1—C1 102.5(2), N2—C1—N1 117.0(2), N2—C1—C1i 119.6(3), N1—C1—C1i 123.4(3), O2—C2—N1 131.0(2), O2—C2—O1 117.9(2), N1—C2—O1 111.1(2); O1—N2—C1—C1i 179.7(3), C2—N1—C1—C1i-179.3(3), C1—N1—C2—O2 179.0(3), N2—O1—C2—O2 - 179.0(2); (i) 2-x, -y, 1-z.

The bond lengths and angles are listed in table 1. All those bonds are in good agreement with the neutral compound **1**, which has been discussed in detail in the latter mentioned publication of Klapötke *et al.* .

In comparison with the neutral compound **1** the oxadiazolonate anion reveals an extension of the C2-O2 double bond and an of the C2-O1 single bond. This effect is observed in a special manner in the structure of $(\text{NH}_4)_2\text{OD}$ (**4**). The C2-O2 double bond is elongated from 1.211 in the H_2OD (**1**) to 1.247 angstrom and the C2-O1 bond length is expanded from 1.366 to 1.388 angstrom. The conventional double bond length is 1.21 angstrom and the C-O single bond 1.43 angstrom.^[5] As there is no coordination observed in this structure the ester is more delocalized. The increased double bonding character of the bond N1-C2 the lengths is shortened from 1.364 angstrom in **1** to 1.336 angstrom in $(\text{NH}_4)_2\text{OD}$ (**4**).

Table 1. Selected hydrogen bonds of $(\text{NH}_4)_2\text{OD}$ (**4**).

Atoms D,H,A	Dist. D,H [Å]	Dist. H,A [Å]	Dist. D,A [Å]	Angle D,H,A [°]
N5—H1—N2 ⁱ	0.94(3)	1.99(3)	2.932(3)	176.(2)
N5—H3—N1	1.03(3)	2.04(3)	3.021(4)	158.(2)
N5—H2—O2 ⁱⁱ	0.99(3)	1.86(3)	2.845(4)	172.(2)
N5—H2—O1 ⁱⁱ	0.99(3)	2.61(3)	3.158(3)	115.(2)
N5—H4—O2 ⁱⁱⁱ	0.96(3)	1.89(3)	2.846(3)	175.(2)

(i) 1-x, -y, 1-z; (ii) x, -1+y, z; (iii) 1-x, -0.5+y, 0.5-z.

One single ammonium cation is connected to four different oxadiazolonate anions by five hydrogen bonds. Looking along the a-axis the assembly of the anion itself can be described as a perpendicular band structure in one dimension which shows one band along the c-axis and one along the b-axis (fig. 7). Figure 8 shows that this bands are raked and also that the layers are only connected by the hydrogen bonds of the ammonium cation.

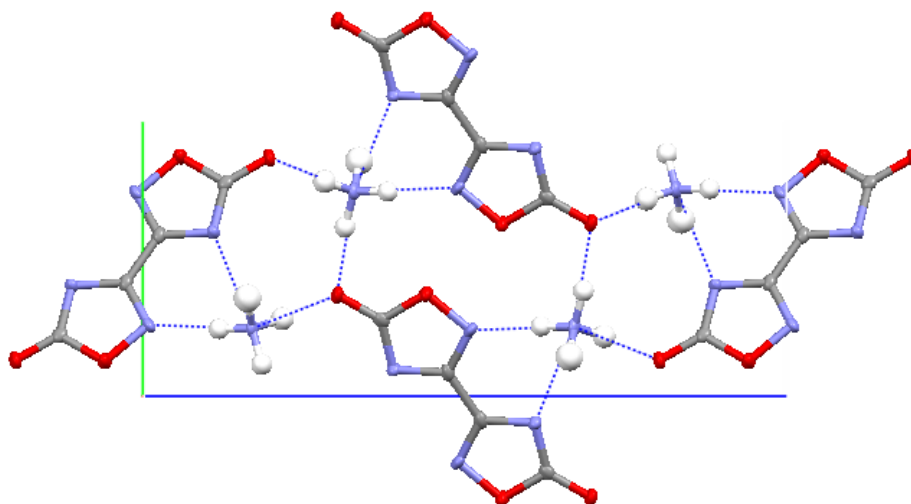
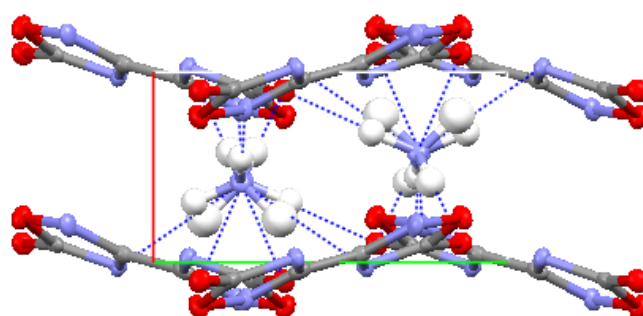


Figure 7. View along a-axis von $(\text{NH}_4)_2\text{OD}$ (**4**).

Between the single layers of the oxadiazolonate anion the ammonium cation is situated and connects the layers by hydrogen bonds (Fig. 8). This very compact and through many hydrogen bonds stabilized assembly is responsible for the high melting of 259 to 266 °C.



View along c-axis of $(\text{NH}_4)_2\text{OD}$ (**4**).

2.3.2 Dihydrazinium bis-(1,2,4-oxadiazol-5-onate)

The molecular structure of $(\text{N}_2\text{H}_5)_2\text{OD}$ (**5**) is shown in Fig. 9. The compound crystallizes in the triclinic space group *P*-1 with one formula unit per unit cell. The bond lengths and angles of the oxadiazolonate anion is in good agreement with the previously discussed ammonium salt.

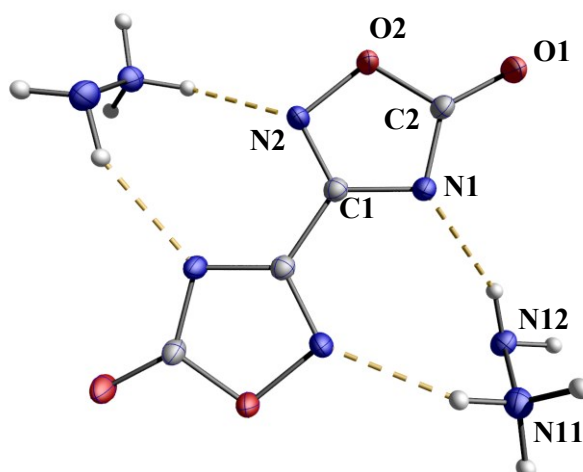


Figure 8. Molecular structure of $(\text{N}_2\text{H}_5)_2\text{OD}$ (**5**) (50% probability ellipsoids). Selected bond lengths(Å) and angles (°): C1—N2 1.313(1), C1—N1 1.357(1), C1—C1i 1.470(2), C2—O1 1.237(1), C2—N1 1.340(1), C2—O2 1.386(1), N2—O2, 1.420(1), N11—N12 1.452(1); N2—C1—N1 116.8(1), N2—C1—C1i 119.8(1), N1—C1—C1i 123.4(1), O1—C2—N1 130.9(1), O1—C2—O2 118.4(1), N1—C2—O2 110.7(1), C2—N1—C1 102.99(9), C1—N2—O2 102.66(8), C2—O2—N2 106.85(8); O1—C2—N1—C1-178.2(1), C1—C1—N1—C2 178.6(1), C1—C1—N2—O2 -179.4(1), O1—C2—O2—N2 178.27(9); (i) 1-x, 2-y, -z.

For compound $(\text{N}_2\text{H}_5)_2\text{OD}$ (**5**) the bond lengths in the oxadiazolone anion are very similar to that of $(\text{NH}_4)_2\text{OD}$ (**4**). The N11-N12 single bond (1.452 angstrom) of the hydrazinium cation lies in the typical range for N-N single bonds (1.46 angstrom).^[1,5] The hydrazinium cation is connected over hydrogen bonds to the oxadiazolone anion so that a two-dimensional network in the b-c-plane is formed (fig.10). The two hydrogen bonds N12-H12-N1 and N11-H15-N2 to the nitrogen atoms of the anion and one hydrogen bond N11-H16-O1 to the carbonyl oxygen atom of a neighbor oxadiazolone anion (table 2).

Table 2. Hydrogen bonds $(\text{N}_2\text{H}_5)_2\text{OD}$ (**5**).

Atoms D,H,A	Dist. D,H [Å]	Dist. H,A [Å]	Dist. D,A [Å]	Angle D,H,A [°]
N12—H12—N1 ⁱ	0.91(2)	2.15(2)	2.995(2)	154.(1)
N11—H14—N12 ⁱⁱ	0.95(2)	1.98(2)	2.924(2)	176.(1)
N11—H15—N2 ⁱⁱⁱ	0.92(2)	2.10(2)	2.919(2)	147.(1)
N11—H16—O1	0.97(2)	1.84(2)	2.780(1)	165.(1)

(i) x, -1+y, z; (ii) -1+x, y, z; (iii) 1-x, 1-y, -z.

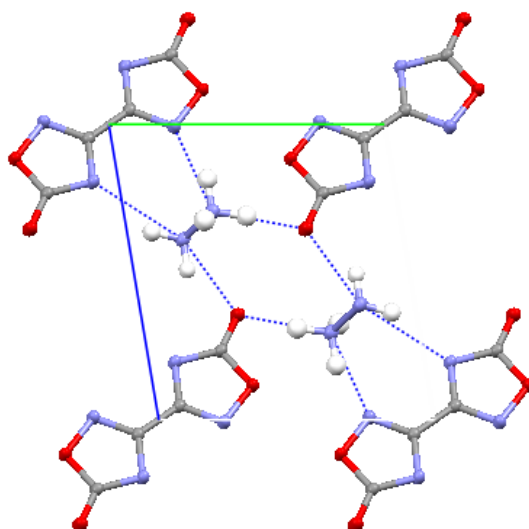


Figure 9. View along a-axis $(\text{N}_2\text{H}_5)_2\text{OD}$ (**5**).

In the structure of $(\text{N}_2\text{H}_5)_2\text{OD}$ (**5**) the oxadiazolonate anions are also packed in layers. The single layers are connected with hydrogen bonds only between the NH_2 and NH_3 group of hydrazinium cations Fig.11. This results in a congruent stacking of the layers so that the exact same order of molecules appears in each direction. In figure 10 the band structure of oxadiazolonate anion can be recognized.

Instead of the strong three-dimensional network of hydrogen bonds in the $(\text{NH}_4)_2\text{OD}$ (**4**) crystal, the connection between the layer structure of the $(\text{N}_2\text{H}_5)_2\text{OD}$ (**5**) only by the N11-H-N12 hydrogen bond lacks stability. This can be observed by the comparison of the melting points which is 264°C for the $(\text{NH}_4)_2\text{OD}$ (**4**) and 213 to 223°C for $(\text{N}_2\text{H}_5)_2\text{OD}$ (**5**) which is significantly lower.

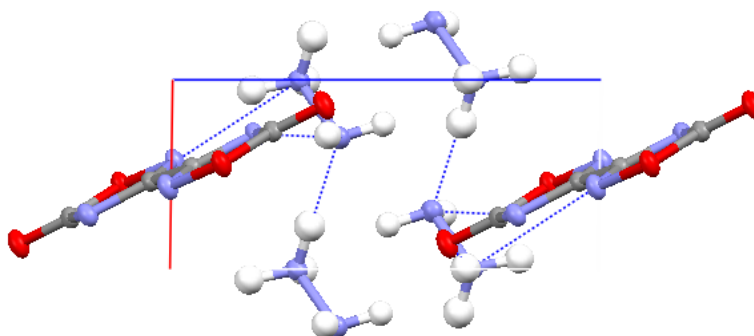


Figure 10. View along b-axis $(\text{N}_2\text{H}_5)_2\text{OD}$ (**5**).

2.3.3 Diguanidinium bis-(1,2,4-oxadiazol-5-onate) (G_2OD , **6**)

The molecular structure of G_2OD is shown in figure 12. . The compound crystallizes in the triclinic space group $P2_1/n$ with four formula units per unit cell. The bond lengths and angles of the oxadiazolonate anion are in good agreement with the previously discussed ammonium salt.

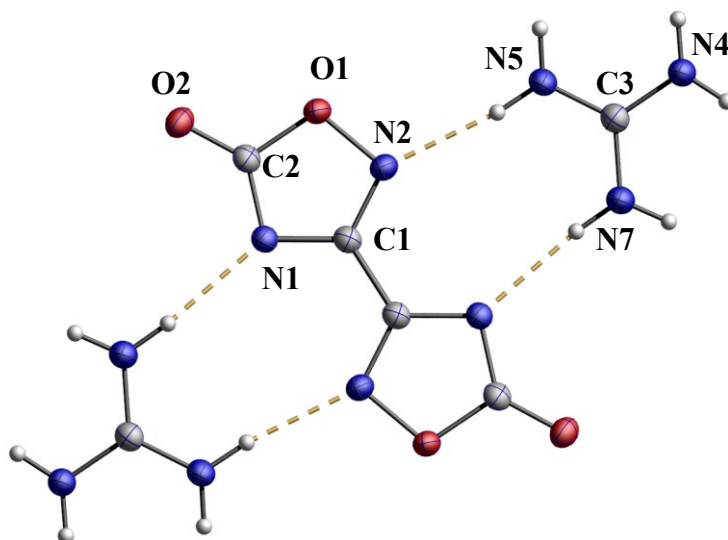


Figure 11. Molecular structure of G₂OD (50% probability ellipsoids). Selected bond lengths(Å) and angles (°): O1—C2 1.382(2), N5—C3 1.319(2), O1—N2 1.420(2), O2—C2 1.242(2), N1—C2 1.330(2), N2—C1 1.304(2), N1—C1 1.357(2), N7—C3 1.323(2), N4—C3 1.328(2), C1—C1ⁱ 1.463(3); C2—O1—N2 106.9(1), C2—N1—C1 103.2(1), O2—C2—N1 130.8(1), O2—C2—O1 118.6(1), N1—C2—O1 110.6(1), N5—C3—N7 120.0(1), N5—C3—N4 120.5(1), N7—C3—N4 119.5(2), N2—C1—N1 116.8(1), C1—N2—O1 102.5(1), N2—C1—C1ⁱ 119.7(2), N1—C1—C1ⁱ 123.5(2); C1—N1—C2—O2 -179.4(2), O1—N2—C1—C1ⁱ 179.5(2), N2—O1—C2—O2 179.1(1), C2—N1—C1—C1ⁱ -179.8(2); (i) 2-x, -y, 1-z.

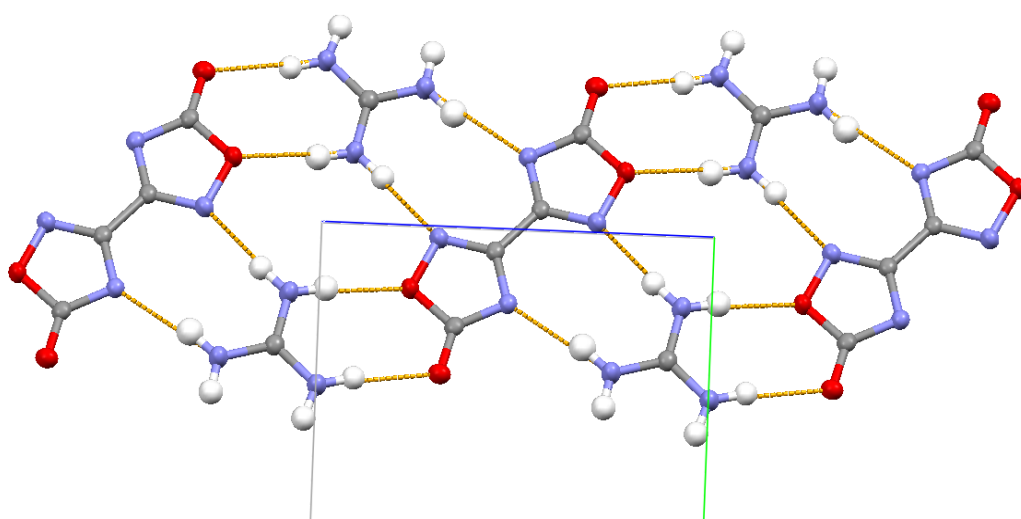


Figure 12. View along a-axis of G₂OD, hydrogen bonds(orange)

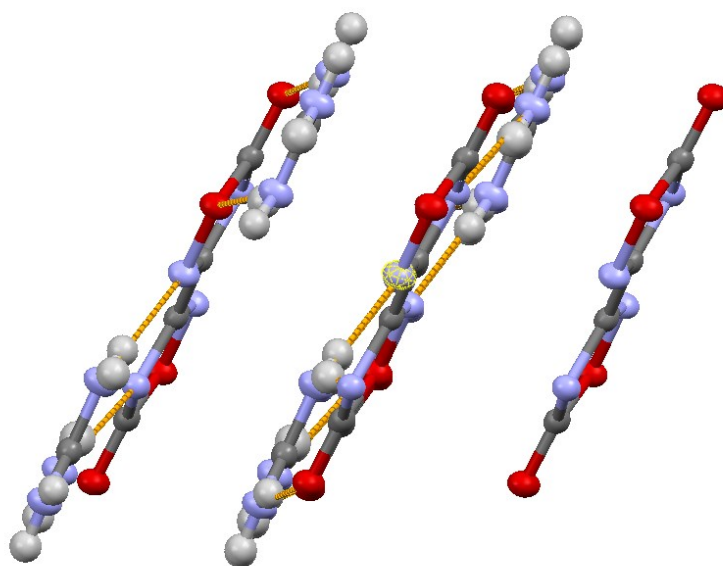


Figure 13. View along c-axis of G₂OD: no interactions between layers, no hydrogen bonds

Table 3. Selected hydrogen bonds of G₂OD (6)

Atoms D,H,A	Dist. D,H [Å]	Dist. H,A [Å]	Dist. D,A [Å]	Angle D,H,A [°]
N5—H4—N2 ⁱ	0.890(19)	2.06(2)	2.941(2)	171.8(16)
N7—H6—O2 ⁱⁱ	0.87(2)	2.17(2)	2.960(2)	151.9(16)
N4—H2—O2	0.870(19)	2.11(2)	2.970(2)	168.4(16)
N5—H3—O1	0.88(2)	2.13(2)	3.001(2)	169.0(17)
N7—H5—N1 ⁱⁱⁱ	0.89(2)	2.10(2)	2.972(2)	167.0(17)
N4—H1—O2 ⁱⁱ	0.87(2)	2.12(2)	2.938(2)	156.4(16)

(i) 2-x, -y, 2-z; (ii) -0.5+x, 0.5-y, 0.5+z; (iii) x, y, 1+z.

The G₂OD (6) shows the highest decomposition temperature of all investigated guanidinium salts. The cause for this maybe the two-dimensional layer structure of the guanidinium cation and the oxadiazolonate anion which is comparable to the structure of guanidinium nitroformate.^[6] This network is built by intermolecular hydrogen bonds which are only situated in the layer. The single layers are held together by π - π -stacking between the oxadiazolonate anions. Through those interactions, a very dense packing is possible, which can be correlated with the high decomposition temperature. Because of the lack of symmetry the cations of AG₂OD (7) and DAG₂OD (8) are expected to have lower decomposition temperature and form crystals with lower density. In the structure of TAG₂OD (9) the relatively voluminous cation would be a hindrance for the formation of a high-density material so a decomposition temperature for TAG₂OD (9) is observed at 197°C.

2.3.4 Bis-aminoguanidinium 3,3'-bis-(1,2,4-oxadiazol-5-onate) (AG₂OD, 7)

The molecular structure of AG₂OD is shown in figure 15. The compound crystallizes in the triclinic space group *P*-1 with 2 formula units per unit cell. The bond lengths and angles of the oxadiazolonate anion are in good agreement with the previously discussed ammonium salt.

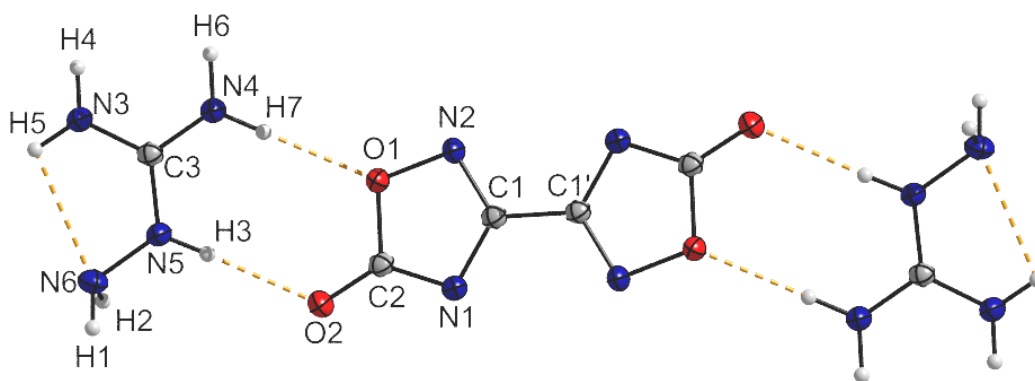


Figure 14. Molecular structure of AG₂OD, **7** (50% probability ellipsoids).

Selected bond lengths(Å) and angles (°): O1—C2 1.3919(18), O1—N2 1.4178(15), N1—C1 1.3595(18), O2—C2 1.2373(18), N2—C1 1.3081(19), N3—C3 1.3200(19), C2—N1 1.3383(18), N3—N6ⁱⁱ 3.5706(31), N4—C3 1.3289(19), N1—N6ⁱⁱⁱ 3.5193(22) O2—N6ⁱⁱⁱ 3.2306(24), N5—C3 1.3363(19), N5—N6 1.4095(18); C2—O1—N2 107.32(10), C2—N1—C1 103.41(11), C1—N2—O1 102.56(10), O2—C2—N1 131.37(12), O2—C2—O1 118.71(12), N1—C2—O1 109.92(12), N2—C1—N1 116.79(12), N2—C1—C1ⁱ 119.62(15), N1—C1—C1ⁱ 123.59(15), N3—C3—N4 120.48(13), C3—N5—N6 119.34(12), N3—C3—N5 120.75(14), N4—C3—N5 118.74(13); N2—O1—C2—O2 179.70(11), O1—N2—C1—C1ⁱ 179.43(14), N2—O1—C2—N1 -0.83(13), C2—N1—C1—N2 0.07(15), O2—C2—N1—C1 179.86(14), C2—N1—C1—C1ⁱ -179.91(15), O1—C2—N1—C1 0.48(13), N6—N5—C3—N3 2.8(2), C2—O1—N2—C1 0.81(13), N6—N5—C3—N4 -179.17(11), O1—N2—C1—N1 -0.56(14); (i) 1-x, -y, 2-z; (ii) -x, 1-y, 1-z; (iii) -x, -y, 1-z.

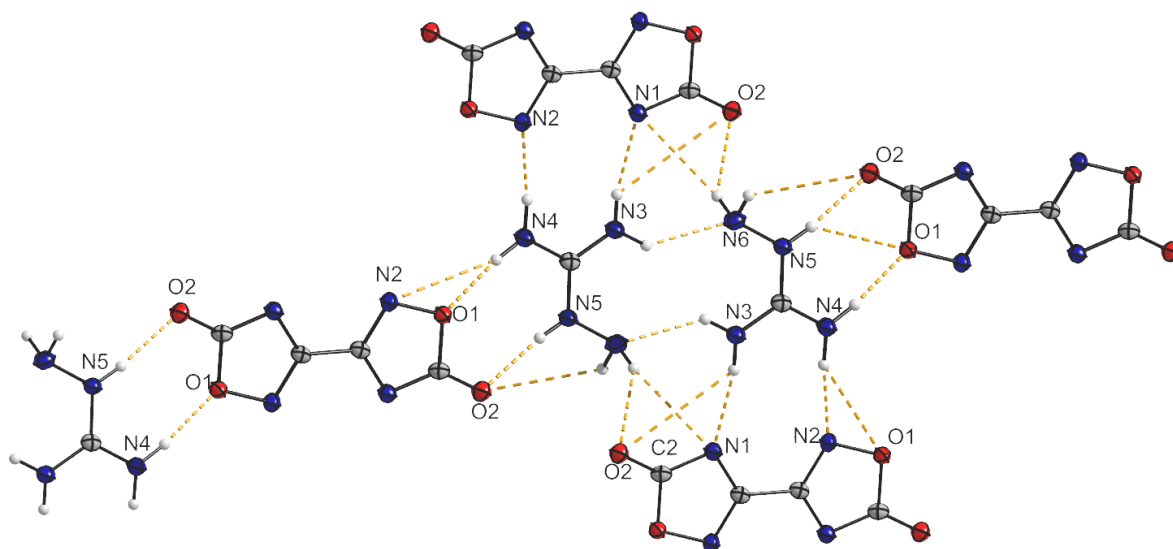


Figure 15. Hydrogen bridged bonds in the AG₂OD, view along a-axis.

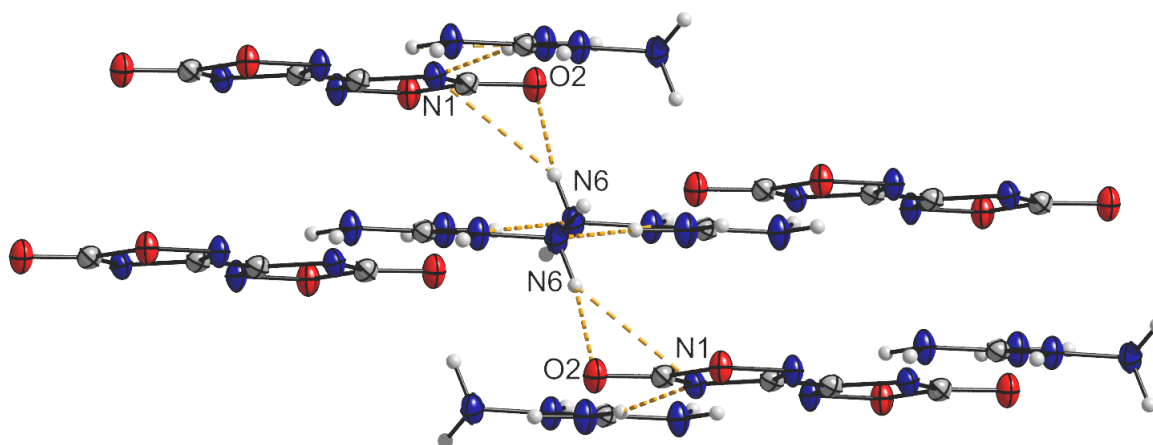


Figure 16. Hydrogen bridged bonds in AG₂OD, view along b-axis.

Table 4. Selected hydrogen bonds

Atoms D,H,A	Dist. D,H [Å]	Dist. H,A [Å]	Dist. D,A [Å]	Angle D,H,A [°]
N4—H6—N2 ⁱ	0.93(2)	2.01(2)	2.933(2)	171.0(17)
N3—H4—N1 ⁱⁱ	0.86(2)	2.11(2)	2.964(2)	168.9(18)
N6—H1—O2 ⁱⁱⁱ	0.92(2)	2.23(2)	3.031(2)	144.4(16)
N5—H3—O2	0.86(2)	2.06(2)	2.918(2)	171.5(17)
N4—H7—O1	0.90(2)	2.09(2)	2.977(2)	169.3(17)
N6—H2—O2 ^{iv}	0.90(2)	2.46(2)	3.231(2)	144.1(16)
N3—H5—N6 ^v	0.92(2)	2.34(2)	3.117(2)	142.1(16)

(i) 1-x, 1-y, 2-z; (ii) x, 1+y, z; (iii) -1-x, -y, 1-z; (iv) -x, -y, 1-z;

(v) -1-x, 1-y, 1-z.

2.3.5 Di-triaminoguanidinium 3,3'-bis-(1,2,4-oxadiazol-5-onate) (TAG₂OD, 9)

The molecular structure of TAG₂OD is shown in figure 18. The compound crystallizes in the triclinic space group *P*-1 with four formula units per unit cell. The bond lengths and angles of the oxadiazolonate anion are in good agreement with the previously discussed ammonium salt.

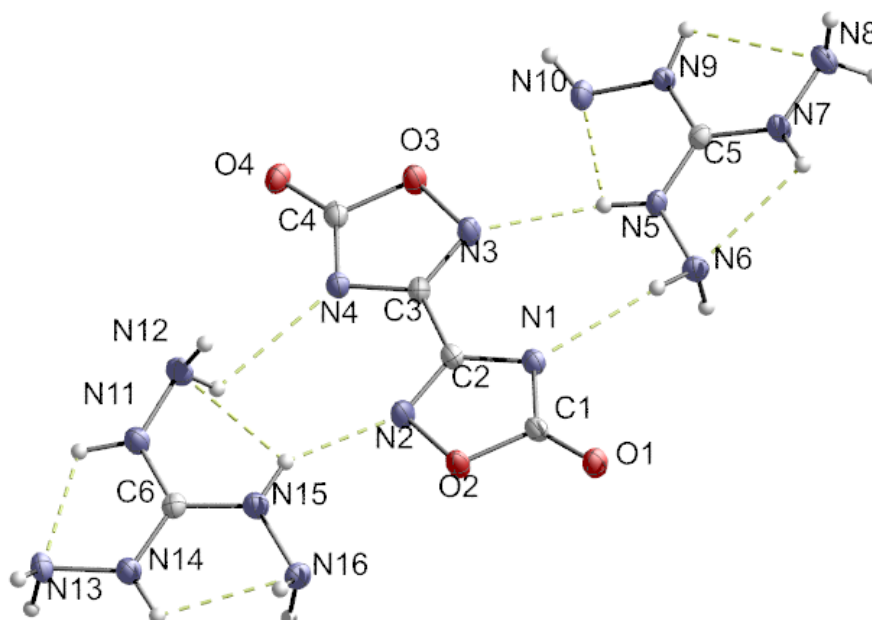


Figure 17. Molecular structure of TAG₂OD (50% probability ellipsoids). Selected bond lengths(Å) and angles (°): C2—N2 1.304(2), C2—N1 1.358(2), C2—C3 1.465(2), C3—N3 1.306(2), C3—N4 1.3599(19), C5—N9 1.322(2), C5—N7 1.325(2), C5—N5 1.333(2), C6—N11 1.327(2), C6—N14 1.330(2), C6—N15 1.332(2), C1—O1 1.2389(19), C1—N1 1.336(2), C1—O2 1.3859(19), C4—O4 1.2408(19), C4—N4 1.338(2), C4—O3 1.387(2), N9—N10 1.417(2), N15—N16 1.403(2), N13—N14 1.418(2), N3—O3 1.4196(17), N2—O2 1.4181(17), N11—N12 1.411(2), N7—N8 1.412(2), N5—N6 1.4097(19); N2—C2—N1 116.74(15), N2—C2—C3 120.68(14), N1—C2—C3 122.57(14), C5—N7—N8 118.27(15), N3—C3—N4 117.26(15), N3—C3—C2 119.37(14), N4—C3—C2 123.36(14), C5—N5—N6 120.45(14), N9—C5—N7 120.40(15), N9—C5—N5 119.31(15), N7—C5—N5 120.29(15), C1—N1—C2 103.25(13), N11—C6—N14 119.73(15), N11—C6—N15 120.69(15), N14—C6—N15 119.57(15), O1—C1—N1 131.48(15), C3—N3—O3 102.28(12), O1—C1—O2 118.24(14), C6—N15—N16 122.03(15), N1—C1—O2 110.27(13), O4—C4—N4 131.59(16), O4—C4—O3 118.06(14), N4—C4—O3 110.35(14), C5—N9—N10 117.84(14), C2—N2—O2 102.68(12), C4—N4—C3 102.84(13), C1—O2—N2 107.06(11), C6—N11—N12 124.29(14), C4—O3—N3 107.25(11); O1—C1—N1—C2 179.30(17); N2—C2—C3—N4 2.0(2); O2—C1—N1—C2 0.21(17).

Table 5. Selected hydrogen bonds TAG₂OD (9)

Atoms D,H,A	Dist. D,H [Å]	Dist. H,A [Å]	Dist. D,A [Å]	Angle D,H,A [°]
N14—H13—O4 ⁱ	0.93(2)	2.03(2)	2.894(2)	154.1(16)
N6—H2—N1	0.876(18)	2.476(18)	3.203(2)	140.8(14)
N6—H3—N1 ⁱⁱ	0.886(17)	2.381(18)	3.204(2)	154.8(14)
N9—H7—O1 ⁱⁱⁱ	0.886(19)	2.05(2)	2.912(2)	163.3(17)
N7—H4—N12 ^{iv}	0.869(18)	2.153(18)	2.962(2)	154.9(15)
N13—H15—N10 ^v	0.897(18)	2.455(19)	3.312(3)	159.9(15)
N11—H10—N13	0.95(2)	2.11(2)	2.640(2)	114.1(15)
N11—H10—N6 ^{iv}	0.95(2)	2.23(2)	3.031(2)	141.5(17)
N10—H9—N16 ^{vi}	0.87(2)	2.42(2)	3.092(3)	134.6(16)
N10—H9—O2 ⁱⁱⁱ	0.87(2)	2.55(2)	3.090(2)	121.0(16)
N10—H8—N8 ⁱⁱⁱ	0.86(2)	2.41(2)	3.259(3)	170.9(19)
N5—H1—N3 ⁱⁱ	0.868(18)	2.248(18)	3.054(2)	154.6(16)
N15—H16—N2 ^{vii}	0.936(19)	2.066(19)	2.879(2)	144.4(16)
N16—H18—O4 ^{iv}	0.885(18)	2.215(18)	2.982(3)	144.8(15)
N8—H5—O4 ^{viii}	0.88(2)	2.23(2)	2.972(2)	142.5(18)
N16—H17—N16 ^{vi}	0.87(2)	2.59(2)	3.010(4)	110.9(16)
N12—H12—N3 ⁱⁱ	0.88(2)	2.44(2)	3.320(3)	178.1(19)
N12—H11—N4 ^{vii}	0.886(19)	2.612(19)	3.109(2)	116.4(14)
N8—H6—O1 ^v	0.91(2)	2.32(2)	3.173(3)	156.0(16)
N13—H14—O1 ⁱⁱⁱ	0.90(2)	2.37(2)	3.160(3)	146.8(17)
N13—H14—O1 ^v	0.90(2)	2.47(2)	2.923(2)	111.1(15)

(i) 1+x, 1+y, -1+z; (ii) -x, 1-y, -z; (iii) 1-x, 1-y, -1-z; (iv) 1-x, 1-y, -z;
 (v) 1+x, y, z; (vi) 1-x, 2-y, -1-z; (vii) x, 1+y, z; (viii) 1-x, -y, -z.

2.4 Energetic properties

The energetic properties for the guanidium, diaminoguanidium salts are not calculated due to the fact that the enthalpy of formation may be wrong. This has to be verified by further bomb calorimetric measurements. In addition, it is possible to claim other products except N_2 , CO_2 and H_2O , to happen in the calorimeter bomb like NO and NO_2 , which are endothermic products and would consume a remarkable sum of energy so that the calculated value from the measurement could be wrong.

Table 6. Energetic properties of guanidinium salts.

Compound	H_2OD	$(NH_4)_2OD$	$(N_2H_5)_2OD$	G_2OD	AG_2OD	DAG_2OD	TAG_2OD	RDX
Sum formula	$C_4H_2N_4O_4$	$C_4H_8N_6O_4$	$C_4H_{12}N_8O_4$	$C_6H_{12}N_{10}O_4$	$C_6H_{14}N_{12}O_4$	$C_6H_{16}N_{14}O_4$	$C_6H_{18}N_{16}O_4$	$C_3H_5N_6O_6$
M [g mol ⁻¹]	170.08	204.2	234.2	288.23	318.26	348.29	378.31	222.12
T _{dec} [°C]	375	270	215	328	253	188	197	234
ΔfH [kJ · mol ⁻¹]	-364.7 [#]	-591.2 [#]	-236.1 [#]	-496.1 [#]	-297.1 [#]	-95.4	+107.5 [#]	+79.1 [#]
	-334.6 ⁺	-635.9	-275.5	-629.4 ⁺	-334.9 ⁺	-604.5 ⁺	-436.7 ⁺	
ΔfU [kJ kg ⁻¹]	-2071,41	-2786,7	-873,69	-1609,6	-816,7	-152,81	+408,68	
ρ [g cm ⁻³]	1.899	1.739	1.733	1.675	1.847	1.74*	1.724	1.80
Ω [%]	-47.0	-62.7	-61.5	-77.8	-75.5	-73.6	-71.9	-21
Q _v [kJ · kg ⁻¹]	-2727	-1924	-3354	-1928	-2470	-2926	-3309	-6034
Tex [K]	2569	1815	2556	1744	1975	2203	2387	4334
P [kbar]	201	148	225	157	238	232	248	340
D [m s ⁻¹]	7038	6444	7707	6726	7883	7852	8091	8882
V ₀ [L kg ⁻¹]	604	768	810	752	775	795	812	769
Impact sen. [J]	>100	>100	>100	>100	>100	>100	>100	>7.5
Friction sen.[N]	>180	>288	>144	>324	-	>168	>218	>120

Detonation parameters calculated with EXLPO V 5.02, * estimated from density measurements with a Pycnometer ($1.50 \text{ g} \cdot \text{cm}^{-3}$) and crystal density of ammonium, hydrazinium and guanidinium salts ($1.73 \text{ g} \cdot \text{cm}^{-3}$), # calculated (Gaussian 03 (MP2/6-31+G und MP4(SDQ)/6-31+(d,p))^[7], + measured by bomb calorimetry

The oxygen balances of $(NH_4)_2OD$ (**4**) and $(N_2H_5)_2OD$ (**5**) are not as good as the one of H_2OD (**1**). Due to the fact that oxygen is consumed by the formation of water and nitrogen at the combustion of the nitrogen rich cation, for the hydrazinium salt, the oxygen balance is slightly better because the gain of molecular weight is little higher compared to the additional consumed oxygen (table 4).

The enthalpy of formation for $(NH_4)_2OD$ (**4**) is $-275,5 \text{ kJ/mol}$ and for $(N_2H_5)_2OD$ (**5**) it is -635.9 kJ/mol determined by bomb calorimetric measurements.

This leads to better explosive performance data for $(NH_4)_2OD$ (**4**) than for $(N_2H_5)_2OD$ (**5**) because they bare similar crystal density and similar oxygen balance but the enthalpy of formation of **4** is nearly half of that of **5**.

Table 7. Oxygen balances of H_2OD , $(NH_4)_2OD$, $(N_2H_5)_2OD$

(1) $C_4H_2N_4O_4$	+ 5/2 O_2	→	4 CO_2 + H_2O + 2 N_2	N = 33 %	Ω = -47 %
(2) $C_4H_8N_6O_4$	+ 4 O_2	→	4 CO_2 + 4 H_2O + 3 N_2	N = 41 %	Ω = -63 %
(3) $C_4H_{10}N_8O_4$	+ 9/2 O_2	→	4 CO_2 + 5 H_2O + 4 N_2	N = 48 %	Ω = -61 %

The equations in table 5 show the oxygen balances of the guanidinium salts. As expected the oxygen balance decreases from G₂OD (6) with -78% to TAG₂OD (9) with -72 % due to the fact that the relative molar mass of the compounds increases more than the consumed oxygen. At the same time the nitrogen content increases about 10% from 49% of G₂OD (6) to the TAG₂OD (9) with 59%. With every amino group, which is introduced in the system, the sum of gaseous products while decomposing rises? This evolution of a high gas volume during the decomposition of the guanidinium salts makes them most suitable for the use as gun propellants. The released gas volume of TAG₂OD (9) (848 L/kg) outnumber even the value for common RDX (769 L/kg). This makes TAG₂OD (9) most likely for application.

Table 8. Oxygen balances of the guanidinium compounds 6-9

(1) C ₄ H ₂ N ₄ O ₄	+ 5/2 O ₂	→	4 CO ₂ + H ₂ O + 2 N ₂	N = 33 %	Ω = -47 %
(6) C ₆ H ₁₂ N ₁₀ O ₄	+ 7 O ₂	→	6 CO ₂ + 6 H ₂ O + 5 N ₂	N = 49 %	Ω = -78 %
(7) C ₆ H ₁₄ N ₁₂ O ₄	+ 15/2 O ₂	→	6 CO ₂ + 7 H ₂ O + 6 N ₂	N = 53 %	Ω = -75 %
(8) C ₆ H ₁₆ N ₁₄ O ₄	+ 8 O ₂	→	6 CO ₂ + 8 H ₂ O + 7 N ₂	N = 56 %	Ω = -74 %
(9) C ₆ H ₁₈ N ₁₆ O ₄	+ 17/2 O ₂	→	6 CO ₂ + 9 H ₂ O + 8 N ₂	N = 59 %	Ω = -72 %

The enthalpy of formation becomes more positive with every introduced amino group in the series of G₂OD(6) to TAG₂OD. This fact leads to increased explosive performance but also to decreased friction sensitivity.

The values for detonation pressure *P* and detonation velocity *D* of the guanidinium salts are lower than those of RDX so that an application as secondary explosive is not favorable.

2.5 Conclusions

Obviously, the 1,2,4-oxadiazole derivatives can be used as energetic materials. Although they do not reach the performance of RDX they show a lot of interesting properties. The nitrogen rich bistriaminoguanidinium-1,2,4-oxadiazol-5-onate salts show high gas volume and low temperatures of explosion, which are important for low erosive gun propellants.

2.6 Experimental

2.6.1 Crystal structures

The molecular structure of **1** was determined by single crystal X-ray diffraction. The X-ray crystallographic data were collected using an Oxford Xcalibur diffractometer with a CCD area detector and graphite-monochromated Mo K α radiation ($\lambda = 0.71073$ Å). The structure was solved with SHELXS-97^[8] and refined with using SHELXL-97^[9]. Ortep^[10] plots.

2.6.2 Properties

Decomposition points, enthalpies, melting points and dehydration points were determined using a Linseis DSC PT10. Additionally, the melting point and dehydration points were also determined using Büchi B-540 melting point apparatus. The friction and impact sensitivity data were obtained using the BAM drophammer and friction tests, in accordance with the BAM methods ^[11].

2.6.3 Spectroscopic Data and elemental analysis

IR spectra were obtained using a Perkin Elmer Spectrum BX FT-IR System and a Raman spectra were measured using Perkin Elmer Spectrum 2000 FT- Raman spectrometer fitted with a Nd-YAG-laser ($\lambda = 1064$ nm) as solids at room temperature (resolution = 4 cm⁻¹). NMR spectra were obtained with a Jeol Eclipse 400 spectrometer operating at 400.2 MHz for ¹H, 100.6 MHz for ¹³C and 28.9 MHz for ¹⁴N. Chemical shifts (in ppm) are given with respect to TMS (¹H/¹³C), MeNO₂ (¹⁴N) as internal standard.

2.6.4 Preparation

AMMONIUM-3,3'-BIS(1,2,4-OXADIAZOL-5-ONATE) (4)

Preparation: Gaseous ammonia was bubbled through a warm solution of 0.85 g (5.00 mmol) **4** in 100 mL methanol for 20 min. The resulting crystals were collected and dried in vacuo. **Yield:** 0.88 g (4.31 mmol); 86 %.

IR (ATR): $\tilde{\nu}$ (cm⁻¹) = 3159 m, 3015 vs, 2866 s, 1628 vs, 1589 m, 1474 m, 1425 vs, 1267 m, 1227 s, 954 m, 901 m, 781 m, 767 m. **Raman** (200 mW): $\tilde{\nu}$ (cm⁻¹) = 1582 (100), 1517 (19), 1233 (19), 961 (35), 941 (42), 789 (21), 744 (12), 616 (13), 409 (11), 345 (11), 250 (13). **MS** (FAB⁺, Xenon, 6 keV, *m*-NBA Matrix): m/z = 18.3 [M]⁺. **MS** (FAB⁻, Xenon, 6 keV, *m*-NBA Matrix): m/z = 169.0 [M+H]. **Elemental analysis:** found (calc.) C 23.56 (23.53), H 3.92 (3.95), N 41.01 (41.17). **DSC:** melting point between 259.8 and 266.6 °C; melting enthalpy -80.10 J/g (-16.4 kJ/mol); max.: 264.5 °C / -5.8 mJ/s; decomposition between 266.6 and 280.7 °C; decomposition enthalpy 220.88 J/g (45.1 kJ/mol); max.: 270.1 °C / 1.4 mJ/s. **Impact sensitivity:** >100 J; **Friction sensitivity:** > 288 N.

HYDRAZINIUM-3,3'-BIS(1,2,4-OXADIAZOL-5-ONATE) (5)

Preparation: 2.04 g (12.0 mmol) **1** was dissolved in a mixture of 120 mL water and 60 mL ethanol while heating and 1.20 g (24.0 mmol, 1.17 mL) hydrazine monohydrate was added. The solution was stored for crystallization at room temperature over night.

The colorless crystals were collected and dried in vacuo. Evaporation of the solvent from the filtrate resulted in further product **5**. **Yield**: 2.52 g (10.8 mmol); 90 %.

IR (ATR): $\tilde{\nu}$ (cm⁻¹) = 3269 m, 3045 m, 2939 m, 2845 m, 2721 m, 2654 m, 1681 vs, 1624 s, 1564 m, 1513 m, 1458 vs, 1275 vs, 1224 s, 1142 m, 1101 vs, 970 s, 943 m, 886 m, 778 m, 578 m. **Raman** (200 mW): $\tilde{\nu}$ (cm⁻¹) = 1573 (100), 1517 (9), 1504 (9), 1226 (27), 1113 (7), 1076 (6), 974 (25), 949 (44), 923 (28), 783 (24), 747 (10), 617 (11), 414 (25), 346 (14), 249 (14), 213 (14). **MS** (FAB⁺, Xenon, 6 keV, *m*-NBA Matrix): m/z = 33.2 [M]⁺. **MS** (FAB⁻, Xenon, 6 keV, *m*-NBA Matrix): m/z = 169.0 [M+H]. **Elemental analysis**: found (calc.) C 20.21 (20.52), H 3.85 (4.30), N 47.75 (47.85). **DSC**: no melting point; decomposition between 213.7 and 223.5 °C; decomposition enthalpy 493.24 J/g (115.5 kJ/mol); Max.: 216.7°C / 7.4 mJ/s. **Impact sensitivity**: >100 J; **Friction sensitivity**: > 144 N.

GUANIDINIUM-3,3'-BIS(1,2,4-OXADIAZOL-5-ONATE) (6)

Preparation: To hot slurry of 3.84 g (10.0 mmol) silver bis-(1,2,4-oxadiazol-5-onate) in 80 mL water a hot solution of w1.91 g (20.0 mmol) guanidine hydrochloride in 20 mL water was added and stirred at 100 °C for 10 min. The silver chloride precipitates as colorless solid. The hot mixture was filtered and the solid was washed with water. To crystallize the product **6** the filtrate was allowed to cool down slowly. The obtained colorless crystals were collected and dried in vacuo. **Yield**: 0.84 g (2.92 mmol); 29 %.

IR (ATR): $\tilde{\nu}$ (cm⁻¹) = 3466 m, 3417 m, 3340 m, 3261 m, 3211 m, 1744 m, 1715 s, 1698 s, 1657 vs, 1606 m, 1485 s, 1284 vs, 1243 m, 1229 w, 980 w, 960 m, 884 w, 766 m. **Raman** (200 mW): $\tilde{\nu}$ (cm⁻¹) = 3204 (12), 1582 (85), 1509 (17), 1486 (14), 1224 (29), 1081 (11), 1014 (100), 947 (4), 915 (31), 784 (36), 745 (14), 605 (13), 544 (35), 413 (30), 340 (19), 253 (25). **MS** (FAB⁺, Xenon, 6 keV, *m*-NBA Matrix): m/z = 60.1 [M]⁺. **MS** (FAB⁻, Xenon, 6 keV, *m*-NBA Matrix): m/z = 169.0 [M+H]. **Elemental analysis**: gef. (ber.) C 24.42 (25.00), H 3.97 (4.20), N 48.11 (48.60). **DSC**: Melting point between 324.8 and 327.8 °C; melting enthalpy -53.72 J/g (-15.5 kJ/mol); max.: 326.8 °C / -4.5 mJ/s; decomposition between 327.8 and 332.3 °C; decomposition enthalpy 98.27 J/g (28.3 kJ/mol); max.: 329.1 °C / 3.0 mJ/s. **Impact sensitivity**: >100 J; **Friction sensitivity**: > 324 N.

AMINOGUANIDINIUM-3,3'-BIS(1,2,4-OXADIAZOL-5-ONATE) (7)

Preparation: 1.36 g (10.0 mmol) Aminoguanidinium bicarbonate and 0.85 g (5.00 mmol) **1** was suspended in 30 mL methanol and 5 mL water. The slurry was refluxed for 10 h until no further gas evolution was observed. After cooling to room temperature the light yellow solid **7** was filtered and dried in vacuo. **Yield**: 1.50 g (4.72 mmol); 94 %.

IR (ATR): $\tilde{\nu}$ (cm⁻¹) = 3418 m, 3404 s, 3326 m, 3147 s, 3071 m, 3009 m, 2891 m, 1648 vs, 1598 m, 1570 m, 1473 s, 1458 m, 1277 m, 1212 m, 1105 w, 1015 m, 943 m, 878 m, 776 m, 764 w. **Raman** (200 mW): $\tilde{\nu}$ (cm⁻¹) = 3264 (6), 1714 (16), 1686 (17), 1661 (18), 1580 (100), 1508 (27), 1217 (42), 1079 (25), 969 (86), 947 (43), 911 (52), 782 (65), 743 (34), 627 (36), 606 (35), 519 (49), 412 (51), 341 (46), 243 (43). **MS** (FAB⁺, Xenon,

6 keV, *m*-NBA Matrix): $m/z = 75.1$ [M]⁺. **MS** (FAB⁺, Xenon, 6 keV, *m*-NBA Matrix): $m/z = 169.0$ [M+H]. **Elemental analysis**: found (calc.) C 22.39 (22.64), H 4.31 (4.43), N 52.74 (52.81). **DSC**: no melting point; decomposition between 250.5 and 257.3 °C; decomposition enthalpy 426.01 J/g (161.2 kJ/mol); max.: 253.1°C / 6.0 mJ/s. **Impact sensitivity**: >100 J; **Friction sensitivity**: not measured.

DIAMINO GUANIDINIUM-3,3'-BIS(1,2,4-OXADIAZOL-5-ONATE) (8)

Preparation: To hot slurry of 2.10 g (5.50 mmol) silver bis-(1,2,4-oxadiazol-5-onate in 15 mL water a hot solution of 1.38 g (11.0 mmol) diaminoguanidine hydrochloride in 10 mL water was added and heated for 5 min at 100 °C. The silver chloride precipitated as colorless solid. The hot reaction mixture was filtered and the solid was washed with hot water. The solution was allowed to cool down slowly to room temperature and stored in the fridge over night for crystallization. The colorless crystals were collected and dried in vacuo. Reduction of the filtrate to dryness resulted in getting further product **8**. **Yield**: 1.39 g (3.99 mmol); 73 %.

IR (ATR): $\tilde{\nu}$ (cm⁻¹) = 3437 m, 3311 s, 3218 s, 2966 m, 2657 m, 1665 vs, 1552 m, 1457 m, 1428 m, 1290 m, 1230 m, 1025 m, 959 m, 951 m, 939 m, 867 w, 775 w. **Raman** (200 mW): $\tilde{\nu}$ (cm⁻¹) = 3312 (18), 3246 (22), 1655 (15), 1562 (100), 1510 (21), 1232 (4), 1180 (20), 1084 (14), 968 (75), 900 (27), 777 (53), 740 (13), 604 (13), 528 (56), 412 (39), 366 (20), 336 (28), 273 (18), 232 (20). **MS** (FAB⁺, Xenon, 6 keV, *m*-NBA Matrix): $m/z = 90.1$ [M]⁺. **MS** (FAB⁺, Xenon, 6 keV, *m*-NBA Matrix): $m/z = 169.0$ [M+H]. **Elemental analysis**: found (calc.) C 19.51 (20.69), H 4.35 (4.63), N 54.00 (56.3). **DSC**: no melting point; decomposition between 184.7 and 204.7 °C; decomposition enthalpy 517.42 J/g (180.2 kJ/mol); Max.: 190.4°C / 3.6 mJ/s. **Impact sensitivity**: >100 J; **Friction sensitivity**: > 168 N.

BIS-TRIAMINO GUANIDINIUM-3,3'-BIS(1,2,4-OXADIAZOL-5-ONATE) (9)

TRIAMINO GUANIDINIUM SULFATE

Preparation: To slurry of 30.0 g (121.8 mmol) Aminoguanidinium sulfate in 200 mL methanol and 50 mL water, 41.1 g (822 mmol, 40.0 mL) hydrazine monohydrate was added. The reaction mixture was refluxed for five hours until no further gas evolution was observed. After cooling to room temperature the light pink product precipitated. The product was filtered, washed with ethanol and methanol, and dried in vacuo. **Yield**: 28.12 g (91.80 mmol); 75 %.

IR (ATR): $\tilde{\nu}$ (cm⁻¹) = 3309 s, 3277 s, 3171 s, 3082 m, 2971 m, 2876 w, 1686 s, 1631 w, 1206 w, 1059 vs, 972 m, 607 m.

Triaminoguanidinium-3,3'-bis(1,2,4-oxadiazol-5-onate) (9)

Preparation: 2.45 g (7.00 mmol) barium 1,2,4-oxadiazol-5-onate heptahemihydrate was suspended in 80 mL of a water : ethanol mixture (3:1) while boiling and a solution of 2.14 g (7.00 mmol) triaminoguanidinium sulfate in 20 mL water was added. The mixture was heated for 30 min at 100 °C and stirred for further 3 h at room temperature. After one hour of reaction time the pH-value was checked and little sulfuric acid was added to obtain pH 5. The barium sulfate precipitates and was filtered

and washed with water. The solvent of the filtrate was evaporated and the colorless product **9** was gained. **Yield:** 2.11 g (5.58 mmol); 80 %.

IR (ATR): $\tilde{\nu}$ (cm⁻¹) = 3427 vs, 3404 s, 3326 m, 3155 vs, 3087 m, 1702 s, 1663 vs, 1474 m, 1280 m, 1212 m, 1099 s, 1083 s, 1019 w, 943 w, 880 w, 776 w, 610 w. **Raman** (200 mW): $\tilde{\nu}$ (cm⁻¹) = 3279 (27), 1684 (19), 1577 (68), 1561 (54), 1508 (24), 1216 (31), 1077 (17), 975 (100), 945 (41), 910 (32), 779 (42), 740 (16), 605 (19), 552 (17), 525 (28), 411 (40), 338 (28), 271 (18), 242 (21), 146 (13). **MS** (FAB⁺, Xenon, 6 keV, *m*-NBA Matrix): *m/z* = 105.1 [M]⁺. **MS** (FAB⁻, Xenon, 6 keV, *m*-NBA Matrix): *m/z* = 169.0 [M+H]. **Elemental analysis:** found (calc.) C 17.44 (17.16), H 4.65 (4.95), N 51.78 (58.53). **DSC:** no melting point; decomposition between 182.9 and 212.2 °C; Decompositions enthalpy 261.04 J/g (98.8 kJ/mol); max.: 192.6°C / 3.8 mJ/s. **Impact sensitivity:** >100 J; **Friction sensitivity:** not measured.

2.7 References

- [1] T.M. Klapötke, A.J. Maier, N. T. Mayr, *New Trends in Research of Energetic Materials, Proceedings of the Seminar, 11th*, Pardubice, Czech Republic, Apr. 09-11, **2008** (2008), (Pt. 2), 653.
- [2] M.D. Coburn, *J. Heterocycl. Chem.*, **1968**, 5(1), 83.
- [3] F. Eloy, *Fortschr. Chem. Forsch.* **1965**, 4, 807-876.
- [4] (a) O. Atsuhiro, T. Hiroaki, *JP6166678*, **1992**; (b) M.A. Hiskey, D.E. Chaves, D.L. Naud., *US6214139*, **2001**.
- [5] A. F. Holleman, E. Wiberg, *Lehrbuch der Anorganischen Chemie*, 101. Edition by N. Wiberg, Walter de Gruyter, Berlin, **1995**, 1842.
- [6] M. Göbel, T.M. Klapötke, *Anorg. Allg. Chem.* **2007**, 633, 1006
- [7] *Gaussian 03, Revision C.02*, Frisch, M. J.; Trucks, G. W.; Schlegel, H. B.; Scuseria, G. E.; Robb, M. A.; Cheeseman, J. R.; Montgomery, Jr., J. A.; Vreven, T.; Kudin, K. N.; Burant, J. C.; Millam, J. M.; Iyengar, S. S.; Tomasi, J.; Barone, V.; Mennucci, B.; Cossi, M.; Scalmani, G.; Rega, N.; Petersson, G. A.; Nakatsuji, H.; Hada, M.; Ehara, M.; Toyota, K.; Fukuda, R.; Hasegawa, J.; Ishida, M.; Nakajima, T.; Honda, Y.; Kitao, O.; Nakai, H.; Klene, M.; Li, X.; Knox, J. E.; Hratchian, H. P.; Cross, J. B.; Bakken, V.; Adamo, C.; Jaramillo, J.; Gomperts, R.; Stratmann, R. E.; Yazyev, O.; Austin, A. J.; Cammi, R.; Pomelli, C.; Ochterski, J. W.; Ayala, P. Y.; Morokuma, K.; Voth, G. A.; Salvador, P.; Dannenberg, J. J.; Zakrzewski, V. G.; Dapprich, S.; Daniels, A. D.; Strain, M. C.; Farkas, O.; Malick, D. K.; Rabuck, A. D.; Raghavachari, K.; Foresman, J. B.; Ortiz, J. V.; Cui, Q.; Baboul, A. G.; Clifford, S.; Cioslowski, J.; Stefanov, B. B.; Liu, G.; Liashenko, A.; Piskorz, P.; Komaromi, I.; Martin, R. L.; Fox, D. J.; Keith, T.; Al-Laham, M. A.; Peng, C. Y.; Nanayakkara, A.; Challacombe, M.; Gill, P. M. W.; Johnson, B.; Chen, W.; Wong, M. W.; Gonzalez, C.; and Pople, J. A.; Gaussian, Inc., Wallingford CT, 2004.
- [8] Sheldrick, G. (1997) SHELXS-97 Program for Crystal Structure Solution, Institut für Anorganische Chemie der Universität, Tammanstrasse 4, D-3400 Gottingen, Germany.

- [9] SHELDRICK, G. (**1997**) SHELXL-97 Program for Crystal Structure Refinement, Institut für Anorganische Chemie der Universität, Tammanstrasse 4, D-3400 Gottingen, Germany.
- [10] JOHNSON, C.K. (**1976**) ORTEP-II. A Fortran Thermal-Ellipsoid Program, Report ORNL-5138. Oak Ridge National Laboratory, Oak Ridge Tennessee.
- [11] a) REICHEL & PARTNER GmbH, <http://www.reichelt-partner.de> b) Test methods according to the UN Recommendations on the Transport of Dangerous Goods, Manual of Test and Criteria, fourth revised edition, United Nations Publication, New York and Geneva, **2003**, ISBN 92-1-139087-7, Sales No. E.03.VIII.2; 13.4.2 Test 3(a)(ii) BAM Fallhammer.

3 Smokeless Pyrotechnical Colorants Based on 3,3'-Bis-(1,2,4-Oxadiazol-5-one Salts

Abstract:

Pyrotechnical compositions are created from polymeric binders, oxidizers and colorants. For bright and illuminating fireworks this colorants need to be of high color purity and bare smokeless combustion. Especially in commercial fireworks as in theme parks or during holiday celebrations used there should be also low toxicity. The class of colorful bis-1,2,4- oxadiazol-5-onate salts fulfills these requirements in a very good way. The copper salts show a saturated green color and the lithium and strontium salts a very shiny red color. The toxicity was reduced through the exchange of the commonly used perchlorate anion.

Keywords: *Pyrotechnics, Colorant, Energetic Salt, Strontium, Copper, Oxadiazol, Crystal Structure*

3.1 Introduction

The research in the past years focused on the nitrogen rich compounds as triazoles and tetrazoles according to its high endothermic reaction energy and gas generation. These properties are especially important to achieve high explosion pressures and detonation velocity. For a high explosion temperature also good oxygen balances are useful. But in pyrotechnical compounds gas generation is not argued. The main achievements that are supposed to be important are brilliant color without smoke at low explosion temperature. Because most of the colorants used in pyrotechnical compositions are well oxygen balanced for example the nitrate salts of barium and strontium. The exchange colorants for the highly toxic barium namely copper as nitrate and elemental boron are used. Both do well jobs as green colorant. But copper nitrate is highly hygroscopic and not very useful for long storage and boron colorants are not that brilliant. So the most promising candidate would be a non-hygroscopic, high temperature stable copper complex as green colorant and strontium or lithium salts as red colorant. In fireworks the toxic perchlorates, which are often used as additional oxidizer in the pyrotechnical compositions, have to be substituted in for environmentally reasons, too. The challenge has only encountered by nitrogen rich energetic compounds which are originally used for propellants or high explosives as mentioned before. As anions or ligands they do a good job but show often high sensitivities and bad oxygen balances. [1,2]

Therefore the 3,3'-bis-1,2,4-oxadiazol-5-one (**1**, H_2OD) has been proved to be a good ligand and anion. The structural and electronic similarity with the 5,5'-bis-1H-tetrazole promise good explosion values for pyrotechnical application. The high thermostability of the 3,3'-bis-1,2,4-oxadiazol-5-one (**1**) stabilizes the complexes and salts. [3]

The metal salts presented in the following are especially chosen from the alkaline metals, the alkaline earth metals and the transition metals by the aspect of color

creation. Beyond this there have been investigated 3,3'-bis-(1,2,4-oxadiazol-5-on)-ate (**OD**) transition metal salts before.^[4,5]

As red colorant $\text{SrOD} \cdot 3.5 \text{ H}_2\text{O}$ (**2**) and $\text{Li}_2\text{OD} \cdot 4 \text{ H}_2\text{O}$ (**5**) have been made. As green colorant the $[\text{Cu}(\text{H}_2\text{O})_4] \text{OD}$ (**6**) and $[\text{Cu}(\text{NH}_3)_2] \text{OD}$ (**7**) were formed. All burned with bright color and show smokeless deflagration in the flame. As comparison also the orange color substituent $\text{CaOD} \cdot 4 \text{ H}_2\text{O}$ (**4**) and $\text{BaOD} \cdot 2 \text{ H}_2\text{O}$ (**3**), which burnt with a pale green color, have been also made.

3.2 Discussion

3.2.1 Syntheses

The different synthetic steps are shown in the figures 1-4. These simple one step reactions are metathesis reactions (fig.1 and fig.3), neutralization reactions (fig.1 and fig.2) or exchange of a ligand (fig.4). All those syntheses show high yields and short reaction times upto three hours maximum.

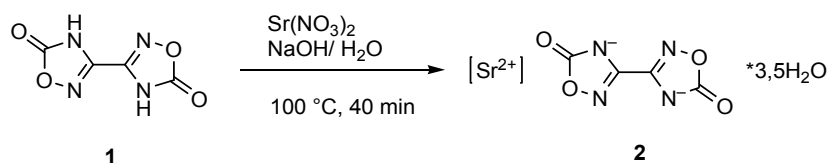


Figure 1. Synthesis of SrOD (**2**).

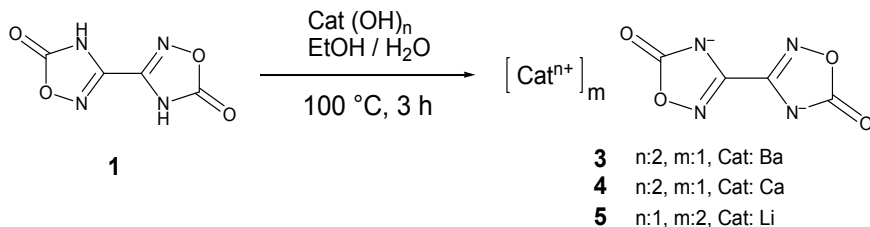


Figure 2. Synthesis of BaOD (**3**), CaOD (**4**) and Li_2OD (**5**).

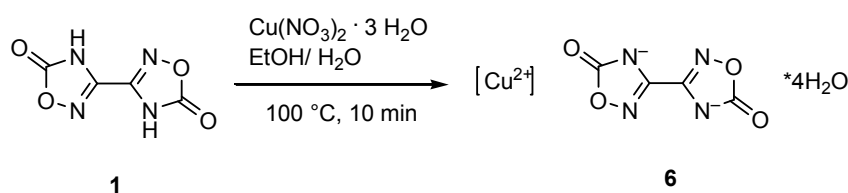


Figure 3. Synthesis of CuOD (**6**).

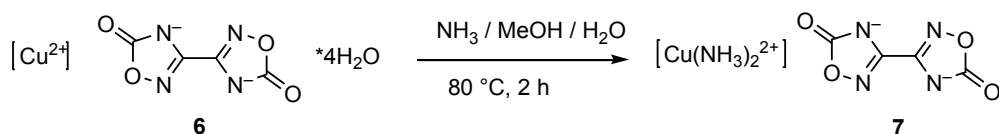


Figure 4. Synthesis of $\text{Cu}(\text{NH}_3)_2\text{OD}$ (**7**).

3.2.2 Crystal structures

TETRAAQUA-3,3'-BIS(1,2,4-OXADIAZOL-5-ON)-ATO CALCIUM (4, CAOD)

The CaOD (**4**) crystallizes in the triclinic space group $P-1$ with two formula units per unit cell. The bond lengths and angles of the 3,3'-bis-(1,2,4-oxadiazol-5-on)-ate anion are in good agreement with the previously reported.^[3] The molecular structure of **4** is shown in Fig. 5 as one of two nearly identical clusters as the comparison shows in table 1. The dihedral $N1-C1-C2-N4$ is 180° so the oxadiazolonate anion is planar and builds a plane with the Ca2 ($Ca2^i$) over O1 ($O1^i$), N1 ($N1^i$) N3 ($N3^i$). This plane is perpendicular to $O22-Ca2-O22^i-Ca2^i$ plane. The O21 and O24 respectively $O21^i$ and $O24^i$ show a zigzag line related to second mentioned plane (fig. 6). The O23 shows no pattern at all. The distance between the Ca2 and $Ca2^i$ is slightly wider with 4.1 Å than the combination of the van-der-Waals-radii of Ca (2.0 Å).^[6] The oxygen atoms and nitrogen atoms overlap with the calcium vdW-radii, because the distances between oxygen and calcium are around 2.5 Å and between calcium and nitrogen around 2.6 Å (table 1). The vdW-radii are for nitrogen 1.55 Å and for oxygen 1.52 Å.^[6]

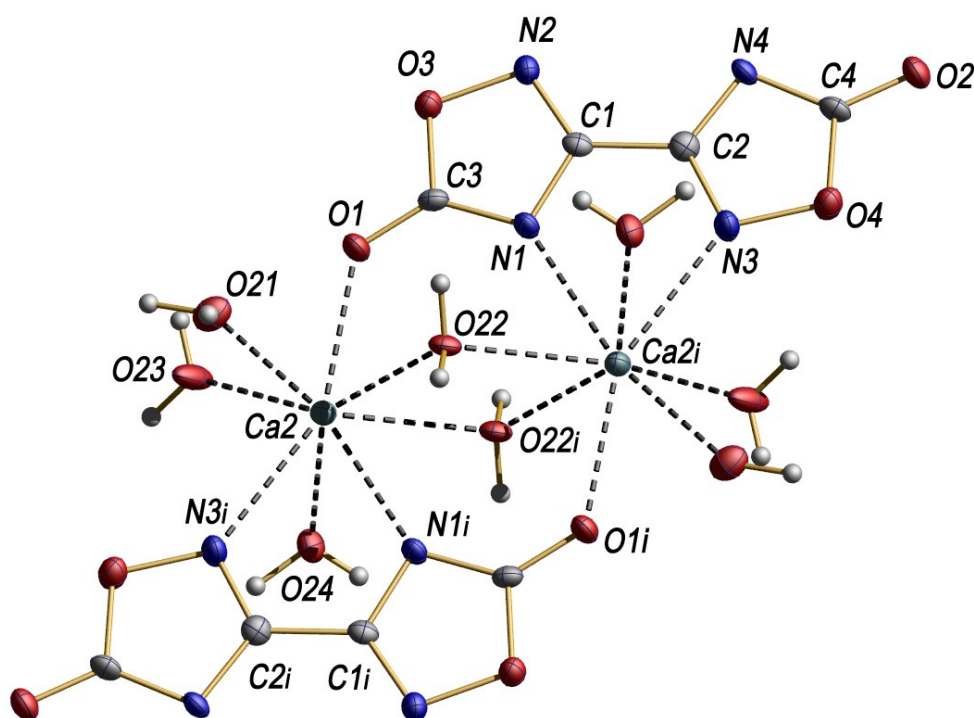


Figure 5. Molecular structure of CaOD (**4**) (50% probability ellipsoids) showing Cluster 1; symmetry parameter: (i) $-x, 1-y, 1-z$.

Table 9. Selected bond lengths(Å) and angles (°):

Cluster 1		Cluster2	
Atoms 1,2	d 1,2 [Å]	Atoms 1,2	d 1,2 [Å]
C1—N2	1.301(4)	C5—N5	1.307(4)
C1—N1	1.357(4)	C5—N6	1.356(4)
C1—C2	1.459(5)	C5—C6	1.459(4)
C2—N3	1.302(4)	C6—N7	1.304(4)
C2—N4	1.357(4)	C6—N8	1.348(4)
C3—O1	1.239(4)	C7—O5	1.248(4)
C3—N1	1.339(4)	C7—N6	1.321(4)
C3—O3	1.373(4)	C7—O8	1.376(4)
C4—O2	1.231(4)	C8—O6	1.243(4)
C4—N4	1.349(4)	C8—N8	1.337(4)
C4—O4	1.385(4)	C8—O7	1.366(4)
C1—N2	1.301(4)	N5—O8	1.421(4)
N2—O3	1.421(4)	N7—O7	1.426(3)
N3—O4	1.418(4)	N5—O8	1.421(4)
N1—Ca2 ⁱ	2.607(3)	N8—Ca1 ⁱⁱ	2.565(3)
O1—Ca2	2.421(2)	O6—Ca1	2.371(2)
N3—Ca2 ⁱ	2.672(3)	N5—Ca1 ⁱⁱ	2.690(3)
O21—Ca2	2.426(3)	O10—Ca1	2.429(3)
O22—Ca2	2.520(3)	O13—Ca1	2.545(3)
O22—Ca2 ⁱ	2.560(3)	O13—Ca1 ⁱⁱ	2.598(3)
O23—Ca2	2.359(3)	O12—Ca1	2.395(3)
O24—Ca2	2.452(3)	O11—Ca1	2.476(3)
Ca2—O22 ⁱ	2.560(3)	Ca1—O13 ⁱⁱ	2.598(3)
Ca2—N1 ⁱ	2.607(3)	Ca1—N8 ⁱⁱ	2.565(3)
Ca2—N3 ⁱ	2.672(3)	Ca1—N5 ⁱⁱ	2.690(3)
Ca2—Ca2 ⁱ	4.122(2)	Ca1—Ca1 ⁱⁱ	4.096(2)
(i) -x, 1-y, 1-z;		(ii) -1-x, 2-y, -z.	

Atoms 1,2,3	Angle 1,2,3 [°]	Atoms 1,2,3	Angle 1,2,3 [°]
Ca2—O22—Ca2 ⁱ	108.5(1)	Ca1—O13—Ca1 ⁱⁱ	105.58(9)
N1 ⁱ —Ca2—N3 ⁱ	62.27(9)	N8 ⁱⁱ —Ca1—N5 ⁱⁱ	62.47(9)
O22—Ca2—O22 ⁱ	71.6(1)	O13—Ca1—O13 ⁱⁱ	74.42(9)
O21—Ca2—O22 ⁱ	146.96(9)	O12—Ca1—O13	143.33(9)
O23—Ca2—O22 ⁱ	118.3(1)	O10—Ca1—O13	123.3(1)
O21—Ca2—O22	81.2(1)	O11—Ca1—O13	72.30(9)
O24—Ca2—O22 ⁱ	74.48(9)	O12—Ca1—O13 ⁱⁱ	73.6(1)
O24—Ca2—O22	139.2(1)	O10—Ca1—O13 ⁱⁱ	142.3(1)
O23—Ca2—O22	146.2(1)	O11—Ca1—O13 ⁱⁱ	142.89(9)
O22—Ca2—N3 ⁱ	109.34(9)	O13 ⁱⁱ —Ca1—N5 ⁱⁱ	109.65(9)
O22 ⁱ —Ca2—N3 ⁱ	127.70(9)	O13—Ca1—N5 ⁱⁱ	128.22(9)
O22—Ca2—N1 ⁱ	67.65(9)	N8 ⁱⁱ —Ca1—O13 ⁱⁱ	67.20(9)
O22 ⁱ —Ca2—N1 ⁱ	71.60(9)	O13—Ca1—N8 ⁱⁱ	73.82(9)
O1—Ca2—N1 ⁱ	137.88(9)	O6—Ca1—N8 ⁱⁱ	137.48(9)
O1—Ca2—N3 ⁱ	153.85(9)	O6—Ca1—N5 ⁱⁱ	153.84(9)
O1—Ca2—O22	75.27(9)	O6—Ca1—O13 ⁱⁱ	75.05(8)
O1—Ca2—O22 ⁱ	78.43(9)	O6—Ca1—O13	77.93(9)

Atoms 1,2,3,4	Tors. an. 1,2,3,4 [°]	Atoms 1,2,3,4	Tors. an. 1,2,3,4 [°]
N4—C2—N3—Ca2 ⁱ	168.9(2)	N6—C5—N5—Ca1 ⁱⁱ	170.6(2)
O3—C3—N1—Ca2 ⁱ	163.7(2)	O7—C8—N8—Ca1 ⁱⁱ	167.9(2)
O3—C3—O1—Ca2	-179.2(2)	O7—C8—O6—Ca1	174.4(2)
C3—O1—Ca2—N1 ⁱ	15.1(3)	C8—O6—Ca1—N8 ⁱⁱ	21.6(3)
C3—O1—Ca2—N3 ⁱ	147.8(3)	C8—O6—Ca1—N5 ⁱⁱ	153.6(3)
Ca2—O22—Ca2—O22 ⁱ	0.000	Ca1—O13—Ca1—O13 ⁱⁱ	0.000
Ca2—O22—Ca2—O21	-161.1(1)	Ca1—O13—Ca1—O11	-163.3(1)
Ca2—O22—Ca2—O24	35.2(2)	Ca1—O13—Ca1—O12	30.1(2)
Ca2—O22—Ca2—O23	-113.5(2)	Ca1—O13—Ca1—O10	143.12(11)

(i) -x, 1-y, 1-z; (ii) -1-x, 2-y, -z.

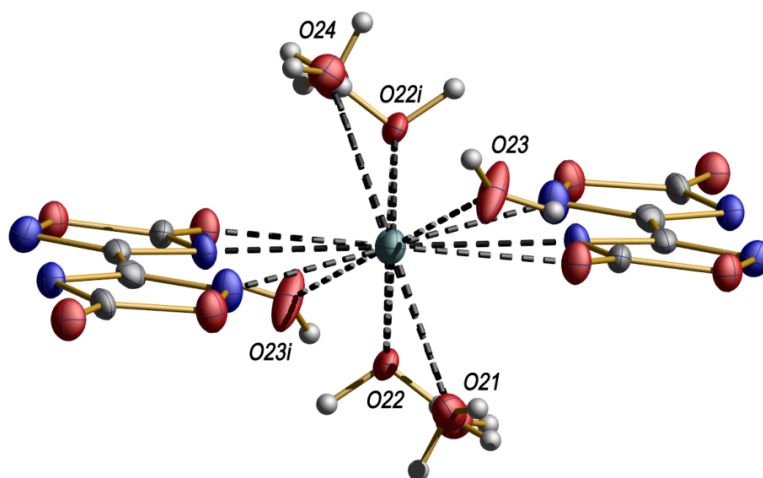


Figure 6. Zigzag O24 and O21 coordination; view along O22i-Ca2-O22 plane.

TETRAAQUA-3,3'-BIS(1,2,4-OXADIAZOL-5-ON)-ATO COPPER(II) (6)

The complex structure of the tetraaqua-3,3'-bis(1,2,4-oxadiazol-5-on)-ato copper(II) (6) is displays in figure 7. The compound crystallizes in the monoclinic space group $C2/c$ with 8 formula units per unit cell. The bond lengths and angles of the oxadiazolonate anion are in good accordance with the previously reported.^[3]

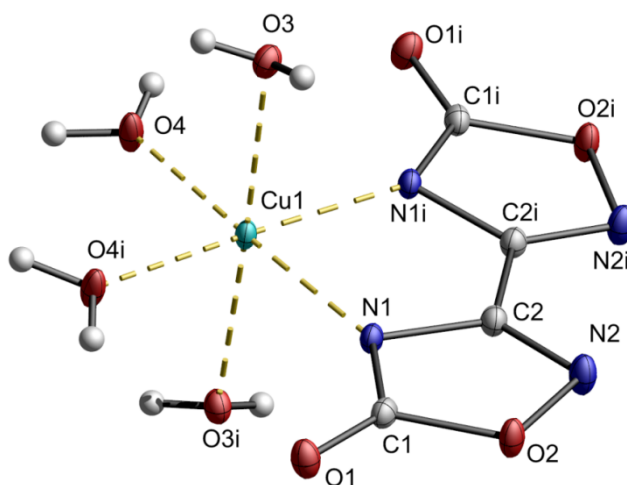


Figure 7. Molecular structure of $[\text{Cu} (\text{H}_2\text{O})_4] \text{OD}$ (6) (50% probability ellipsoids). Symmetry operator: (i) $1-x, y, 0.5-z$.

Table 10. Selected bond length and angles of the $[\text{Cu}(\text{H}_2\text{O})_4]\text{OD}$ (6).

Atoms 1,2	d 1,2 [Å]	Atoms 1,2,3	Angle 1,2,3 [°]
Cu1—O4	1.9708(9)	O4—Cu1—O4 ⁱ	86.94(5)
Cu1—O4 ⁱ	1.9708(9)	O4 ⁱ —Cu1—N1	95.43(4)
Cu1—N1	2.0508(9)	O4—Cu1—N1 ⁱ	95.43(4)
Cu1—N1 ⁱ	2.0508(9)	N1—Cu1—N1 ⁱ	82.20(5)
Cu1—O3	2.3522(9)	O4—Cu1—O3	89.85(4)
Cu1—O3 ⁱ	2.3522(9)	O4 ⁱ —Cu1—O3	88.81(4)
O2—C1	1.383(1)	N1—Cu1—O3	90.11(4)
O2—N2	1.422(1)	N1 ⁱ —Cu1—O3	91.29(3)
N2—C2	1.298(1)	O4—Cu1—O3 ⁱ	88.81(4)
N1—C2	1.357(1)	O4 ⁱ —Cu1—O3 ⁱ	89.85(4)
N1—C1	1.353(1)	N1—Cu1—O3 ⁱ	91.29(3)
O1—C1	1.225(1)	N1 ⁱ —Cu1—O3 ⁱ	90.11(4)
C2—C2 ⁱ	1.460(2)	O3—Cu1—O3 ⁱ	178.14(5)

(i) 1-x, y, 0.5-z.

Table 11. Selected hydrogen bonds

Atoms D,H,A	Dist. D,H [Å]	Dist. H,A [Å]	Dist. D,A [Å]	Angle D,H,A [°]
O3—H1—O1 ⁱ	0.72(2)	2.00(2)	2.6948(13)	163.(2)
O3—H3—O1 ⁱⁱ	0.74(2)	2.06(2)	2.7838(12)	167.(2)
O4—H5—O3 ⁱⁱⁱ	0.69(2)	1.99(2)	2.6732(13)	169.(2)
O4—H6—N2 ^{iv}	0.81(2)	2.05(2)	2.8341(13)	163.6(19)

(i) x, 1-y, 0.5+z; (ii) 0.5-x, 0.5-y, -z; (iii) 1-x, 1-y, 1-z; (iv) 1-x, 1+y, 0.5-z.

Through the coordination of the 3,3'-bis(1,2,4-oxadiazol-5-one) (1) to the copper complex center the bond length and angles have little changed. The C1-O1 double bond and also the C1-O2 single bond are weakened and elongated whereas the C1-N1 is a little shortened. This is explained by the delocalization of the electron in the anion. The axial copper Cu1-O3 with 2.35 Å is longer than the equatorial Cu1-O4 bond length. This is typical for Jahn-Teller-effect which leads to tetragonal distortion in the copper crystal field.

The carbonyl oxygen is bridge by two hydrogen bonds (O3-H1-O1 and O3-H3-O1) to the water ligands of the neighbor molecules (table 3). Additional the hydrogen bonds O4-H6-N2 and O4-H5-O5 between the water ligands are observed.

The oxadiazolonate anion are directly packed on each other, which could be explained by π -stacking of the anion (fig.8).

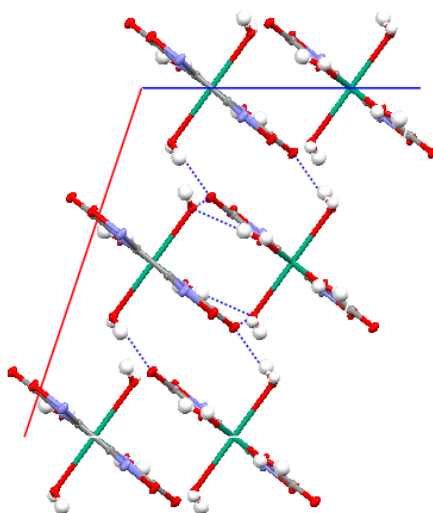


Figure 8. View along the b-axis of $[\text{Cu}(\text{H}_2\text{O})_4] \text{OD}$ (**6**).

BIS-POTASSIUM AND BIS-CESIUM 3,3'-BIS(1,2,4-OXADIAZOL-ON)ATE

The potassium and cesium salt of 3,3'-bis(1,2,4-oxadiazol-one) were crystallized from water/ethanol to gain suitable crystals for the determination of the crystal structure.

The potassium salt crystallizes in the space group $P 2_1/c$ with 2 formula units in the unit cell. The unit cell has the range of $a = 6.8207(14) \text{ \AA}$, $b = 9.0164(18) \text{ \AA}$, $c = 6.5895(13) \text{ \AA}$, and the angles of $\alpha = 90^\circ$, $\beta = 102.25(3)^\circ$, $\gamma = 90^\circ$. The total cell volume is $396.02(14) \text{ \AA}^3$ and the density is 2.065 g cm^{-3} at a measurement temperature of -100°C . Figure 32 shows the molecular unit of the potassium salt and in table 3 the respective bond lengths and angles are listed. The moiety of the OD-anion is similar to the neutral molecule only half refined because the symmetry center lies directly on the bond C3-C3' which leads to a reduced subset of bond lengths and angles.

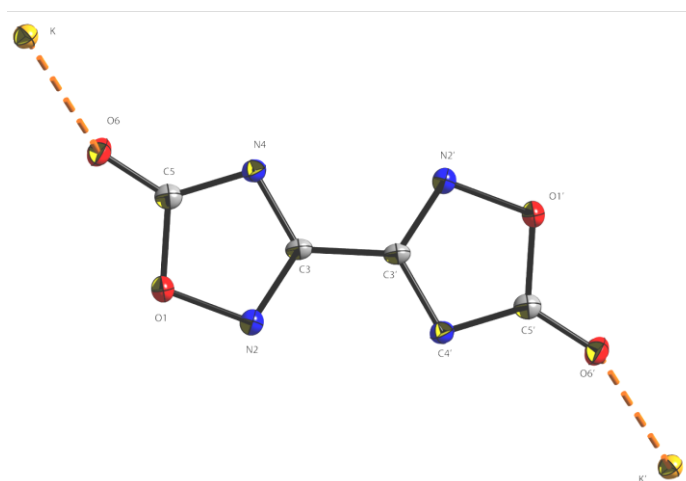
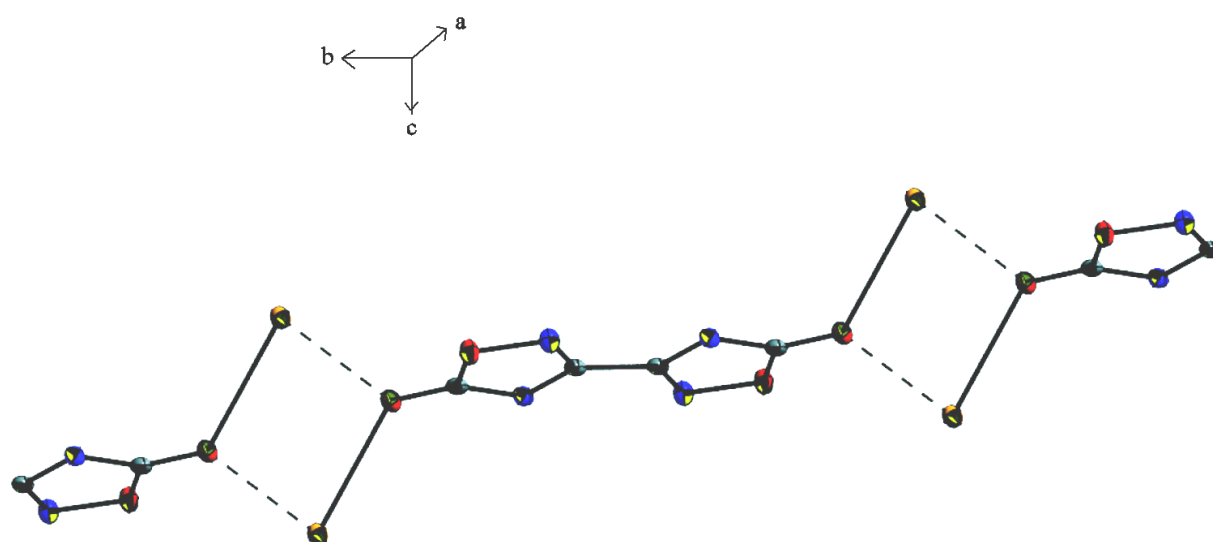
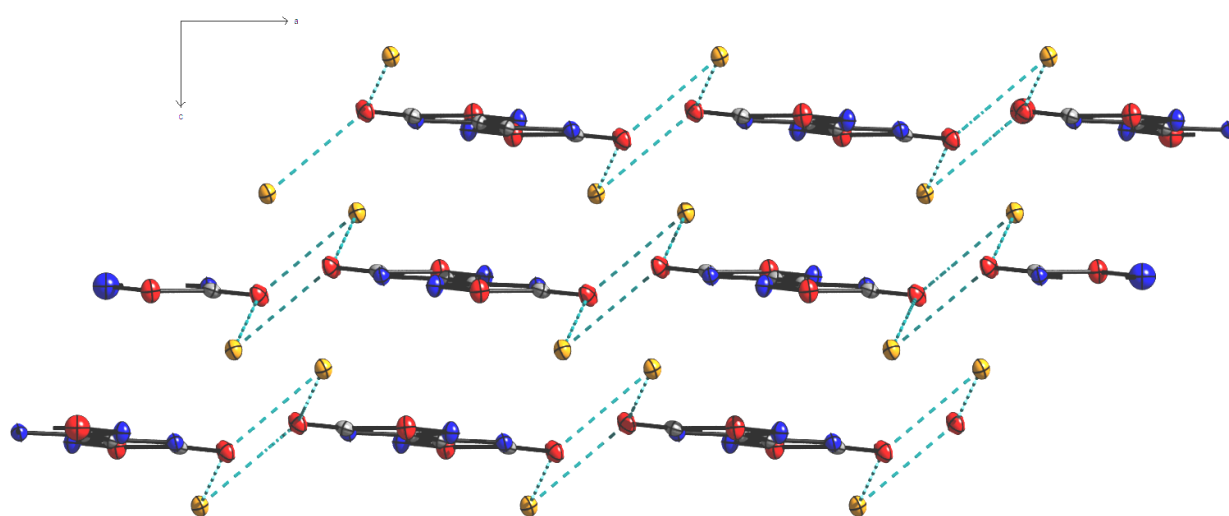


Figure 9. Molecular unit of Bis potassium-3,3'-bis-(1,2,4-oxadiazol-5-on)-ate

Table 12. Selected bond lengths and angles

Bond lengths [Å]		Angles [°]	
O1-N2	1.424(2)	O1-N2-C3	102.35(10)
N2-C3	1.306(2)	N2-C3-N4	117.29(13)
C3-N4	1.357(2)	C3-N4-C5	102.91(12)
N4-C5	1.339(2)	N4-C5-O1	110.50(12)
C5-O6	1.236(1)	C5-O1-N2	106.95(9)
C5-O1	1.388(1)	N4-C5-O6	130.26(14)
C3-C3'	1.470(2)	O1-C5-O6	119.22(12)
		N2-C3-C3'	119.60(53)
		N4-C3-C3'	122.54(56)

**Figure 10.** Linear connected anion biforkated coordination of potassium.**Figure 11.** View along b-axis to show the layer structure with the potassium coordination

Looking into figure 10 and 11 there the OD-anion is completely planar and composes with the potassium a linear chain. The OD-anion is stacked in layers on top of each other. Compared to already known structures of the OD-anion with different cation like the ammonium and hydrazinium there is a total agreement of the bond lengths and angles in these asymmetric units up to the second decimal place.^[7]

In figure 10 the OD-anion shows a coordinative connection to two potassium cations by the O6 and O6' atom of the OD-anion. This parallelogram of the two potassium cations and the respective oxygen atoms of the OD-anion display angles of $77.934(31)^\circ$ and $102.066(34)^\circ$ with identical bond lengths of opposite situated bonds (dashed line 2.738 Å, non-dashed line = 2.713 Å). The figure 11 displays the layer structure along the b-axis. The distance between the layers of the OD-anion is 4.5 Å. The potassium cation has four nitrogen and five oxygen atom in its coordination sphere (fig. 12).

The number after the atom symbol in figure 12 is describing the atom in the asymmetrical unit (see figure 10) and the number in the bracket names a new anion. For better overview there were chosen three modes of transparency.

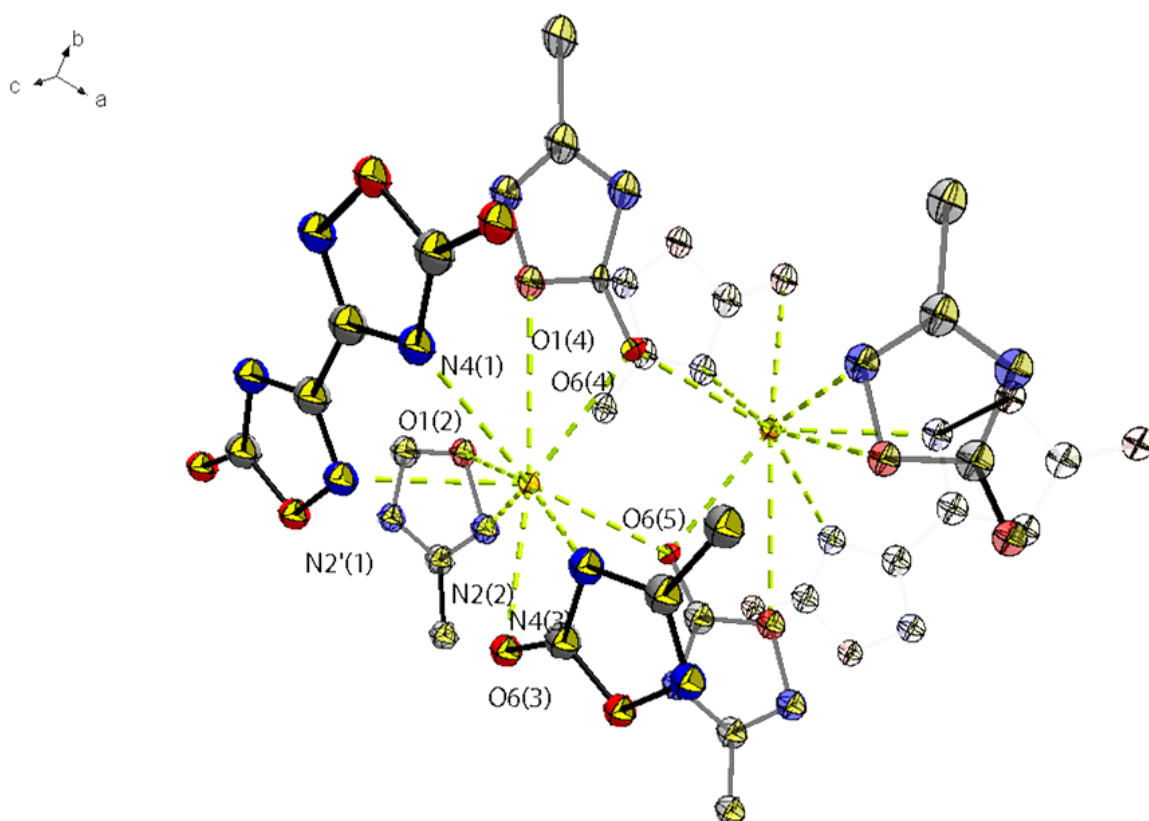


Figure 12. Coordination of potassium at diagonal view to show the interconnection between layers each layer highlighted by different transparency (3 layers: bold, translucent and bw).

The anions 1 and 3 are positioned along the c-axis in front of potassium cation and the anions 2, 4 and 5 behind. The completely transparent drawn anions are behind this middle layer and show the same assembly as the layer in the front. Every potassium cation is coordinated to two layers. From the layer behind the potassium cation in c-direction an O-atom (O1 (4)) of the ring is coordinating to the potassium cation. Along the b-axes the OD-ring is attracting the potassium cation by the nitrogen (N2(2)) and oxygen (O1(2)). In the same layer the oxygen of the carbonyl functions (O6(4),O6(5)) are bifurcatedly coordinating as well to before mentioned potassium cation as to the potassium cation in the next structural layer which results in a bicedentate coordination complex, which is bridged by those oxygens atoms. The layer in front of the potassium cation two OD-anions are involved in the coordination one with N2'(1) and N4(1) the other with N4(3) and O6(3). As the structure is water free there is no stabilization by hydrogen bonding.

The cesium salt is also water free and was isolated as thin colorless needles. It crystallizes in the monoclinic space group P21/n with two formula unit per unit cell. The unit cell is defined by edges of $a = 4.4772(4) \text{ \AA}$, $b = 13.5033(11) \text{ \AA}$, $c = 7.6400(7) \text{ \AA}$ and angles $\alpha = 90^\circ$, $\beta = 106.179(10)^\circ$ and $\gamma = 90^\circ$. The total cell volume is $443.60(7) \text{ \AA}^3$ and the calculated density is 3.248 g/cm^3 at a measuring temperature of -73°C . Figure 13 shows the molecular unit with an inversion centre between C3 and C3' the asymmetric unit would only include one half of the complex.

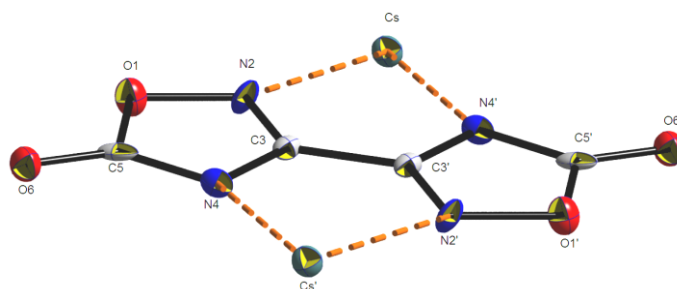


Figure 13. Molecular unit of Bis-cesium-3,3'-bis(1,2,4-oxadiazol-5-on)-ate

The bond lengths and angles in the cation are very similar to those of the potassium salt. They are listed in table 4.

Table 13. Selected bond lengths and angles

Bond length [\AA]		Angle [$^\circ$]	
O1-N2	1.426(8)	O1-N2-C3	101.44(47)
N2-C3	1.306(9)	N2-C3-N4	117.87(56)
C3-N4	1.354(8)	C3-N4-C5	103.81(52)
N4-C5	1.338(9)	N4-C5-O1	108.92(57)
C5-O6	1.225(1)	C5-O1-N2	107.96(45)
C5-O1	1.388(8)	N4-C5-O6	131.69(64)
C3-C3'	1.488(9)	O1-C5-O6	119.40(58)
		N2-C3-C3'	120.11(26)
		N4-C3-C3'	122.60(12)

In contrast to the K_2OD the cesium cation is coordinated to eleven atoms. Therefore a coordination distance of 3.655 Å for Cs-N und 3.755 Å for Cs-O as maximum sphere of interaction was preassumed.

The cesium cation is coordinated by two different layers of three levels. The coordination is very similar to the potassium salt. But there are differences in the direction of the OD-anion. The OD-anions in the cesium salt show a zig zag chain. Therefore two nearly identical layers are positioned perpendicular. In each crossing of the layers there is a cesium cation that is coordinated with six OD-anions. The anion 5 and 6 are in the same direction of a layer and coordinate with two oxygen atoms of the carbonyl function (O6) and one nitrogen (N4) to the cesium.

The coordination from the other layer is carried out by two levels. From the upper level there are the ring atoms (O1(1), N2(1), N2(2), O1(2)). From the lower level of the same layer the cesium is coordinated by the nitrogen atoms (N2'(3), N4(3)). This coordination is similar to the potassium salt. The second ring of OD-anion (no. 4) is coordinated only over two oxygen atoms (O6(4) and O1(4)). This bilayer system is shown in figure 15. This is compared with the potassium salt a little wider which is due to the fact that the cesium cation is a little bigger.

If directly looked at the differences of the cesium salt and the potassium salt, the decomposition point at 385°C of the cesium may directly refer to the binding in the crystal structure. In contrast the decomposition point of potassium salt is over 400°C. While the cesium has more covalent bond character the small potassium cation leads to a more ionic character. The stronger ionic interactions may influence the thermodynamic stability of the potassium salt in that way. No phase transition and decomposition was observed in the DSC-analysis, which shows a range of 50-400°C. As both salts are incredibly stable towards decomposition in the following comparison of the thermostability these two salts are left out for that reason.

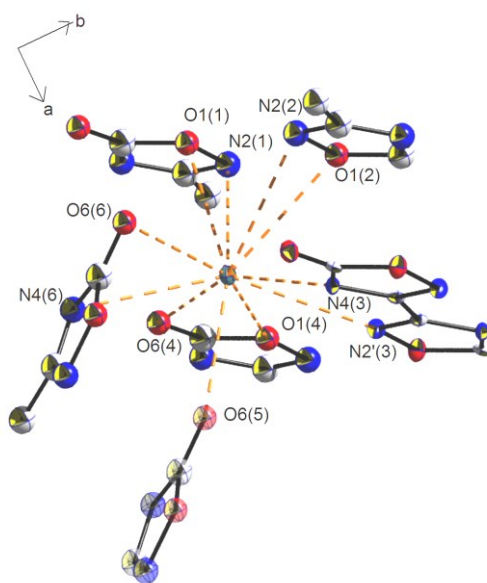


Figure 14. View along c-axis to show the coordination of cesium.

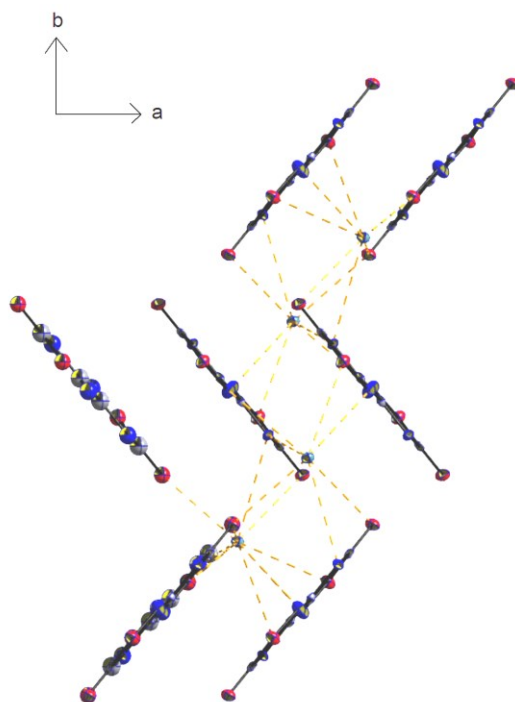


Figure 15. Zig-zag-chain like structure of the 3,3'-bis(1,2,4-oxadiazol-5-on)ate fixed by the cesium coordination.

3.2.3 Thermostability

The OD salts are all very stable especially the alkaline and alkaline earth salts. Most of them show cleavage of water between 140°C and 180°C and have a decomposition point over 350°C (fig. 16).

The barium salt (**3**) shows only one dehydration point at 184°C and later a two-stage decomposition at 398°C, which is the highest dec. point in this series. The lithium (**5**) and strontium OD (**2**) salts display two single points for their loss of water. For the strontium salt (**2**) it is 149°C and 164°C and for the lithium (**5**) salt it is 180°C and 221°C. The calcium OD salt (**4**) even shows three dehydration points at 157°C, 196°C and 250°C, which could be explained by the order of the water in the molecule. The discussed crystal structure of CaOD (**4**) has revealed different kinds of water molecules, those interconnected between the calcium atoms are the once supposed to be last to leave. The other three water molecules could leave in a defined way depending on the hydrogen bonding. The decomposition points for the alkaline earth metal salts are determined over 360°C whereas the lithium salt decomposes at 350°C.

The transition metal complexes namely the two copper complexes show much lower decomposition points with a maximum at 270°C.

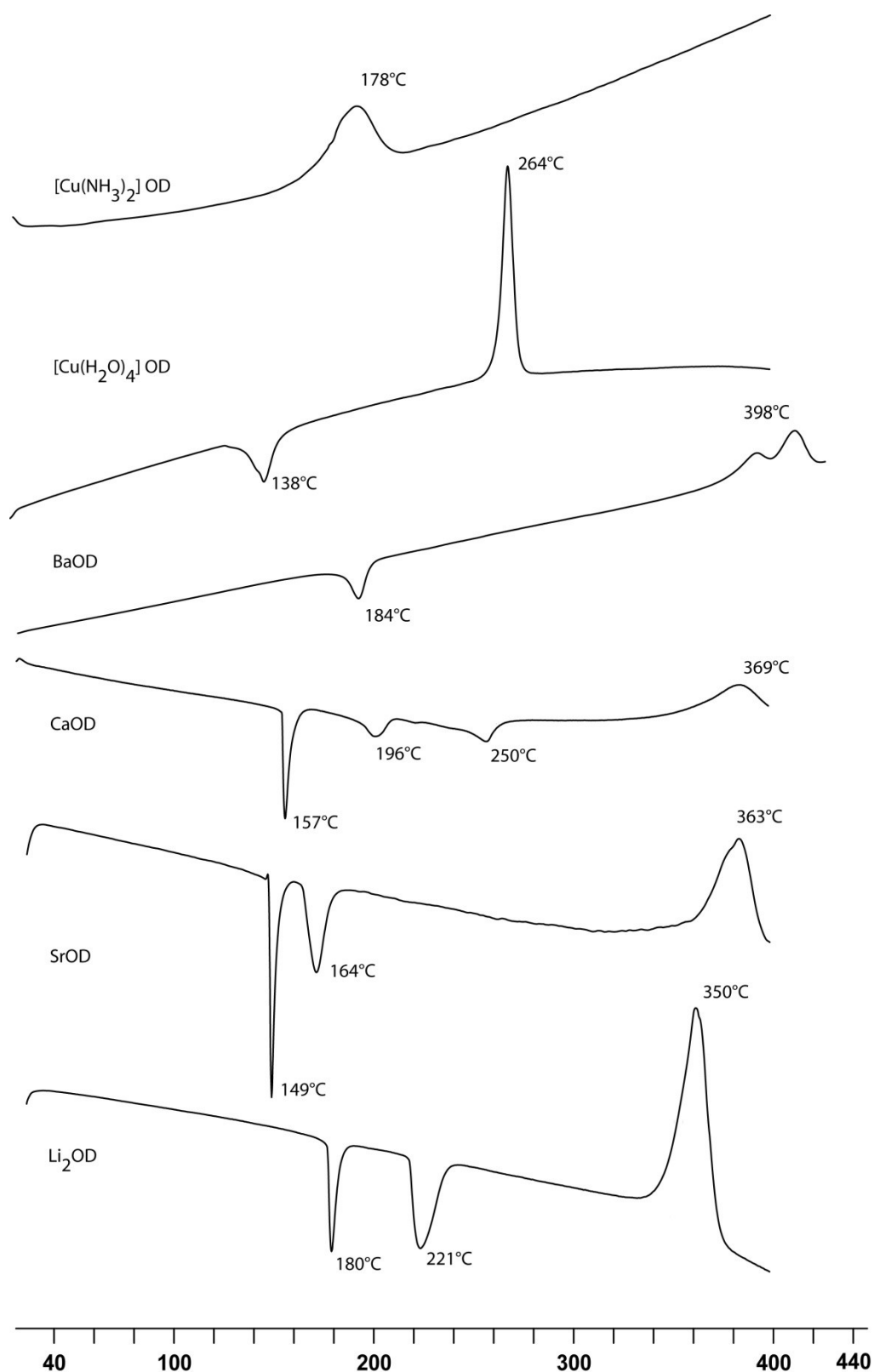


Figure 16. Differential Scanning Calorimetry graphs (exo up) were collected at a heating rate of 5°C min⁻¹ and the decomposition and dehydration temperatures were measured as onset points.

The decomposition point for the copper aqua complex (**6**), which is first dehydrated at a temperature of 138°C, is at 264°C. There is also a copper complex with $[\text{Cu}(\text{NH}_3)_2]\text{OD}$ (**7**), which is not soluble in any common solvent, even in liquid ammonia. But regardless to that the properties as colorant with a decomposition temperature of 178°C should be really good, especially as DSC measurements show no abstraction of the ammonia from the complex. The complex is stable until decomposition.

All of those 3,3'-bis(1,2,4-oxadiazol-5-on)ate salts were tested with BAM standard test to friction and impact.^[7] And they do not bare any sensitivity. This property is especially interesting for save handling. The salts are also not hygroscopic, which is good for long-term stable and working pyrotechnical compositions.

3.3 Conclusion

It has been shown that the alkaline earth, alkaline and transition metal 3,3'-bis-(1,2,4-oxadiazol-5-on)-ate salts are promising as colorants for pyrotechnic compositions. They show good thermal stabilities, rather low sensitivities and long term stabilities. The earth alkaline salts are not very good soluble in water, which lowers the rate of ground water intake. Further the toxicity was reduced through the exchange of the commonly used perchlorate anion. All in all this will give these compounds a good chance of application as green and red pyrotechnic colorants in commercial fireworks.

3.4 Experimental

3.4.1 Crystal structures

The molecular structure of **4** and **6** was determined by single crystal X-ray diffraction. The X-ray crystallographic data were collected using an Oxford Xcalibur diffractometer with a CCD area detector and graphite-monochromated Mo K α radiation ($\lambda = 0.71073 \text{ \AA}$). The structure was solved with SHELXS-97^[8] and refined with using SHELXL-97^[9]. The crystal figures are rendered Ortep^[10] plots.

3.4.2 Properties

Decomposition points, enthalpies, melting points and dehydration points were determined using a Linseis DSC PT10. Additionally, the melting point and dehydration points were also determined using Büchi B-540 melting point apparatus. The friction and impact sensitivity data were obtained using the BAM drophammer and friction tests, in accordance with the BAM methods.^[7]

3.4.3 Spectroscopic Data and elemental analysis

IR spectra were obtained using a Perkin Elmer Spectrum BX FT-IR System and a Raman spectra were measured using Perkin Elmer Spectrum 2000 FT- Raman spectrometer fitted with a Nd-YAG-laser ($\lambda = 1064 \text{ nm}$) as solids at room temperature (resolution = 4 cm^{-1}). NMR spectra were obtained with a Jeol Eclipse 400 spectrometer operating at 400.2 MHz for ^1H , 100.6 MHz for ^{13}C and 28.9 MHz for ^{14}N . Chemical shifts (in ppm) are given with respect to TMS ($^1\text{H}/^{13}\text{C}$), MeNO_2 (^{14}N) as internal standard.

3.4.4 Preparation

STRONTIUM(II)-3,3'-BIS(1,2,4-OXADIAZOL-5-ONATE) HEPTAHEMIHYDRATE (2)

Preparation: To a suspension of 0.50 g (2.94 mmol) **4** in 10 mL water 1.8 mL 2M sodium hydroxide solution was added to obtain pH-value of 4 and get a solution of the mono sodium salt of acid **4**. To the solution 0.62 g (2.94 mmol) strontium nitrate in 10 mL water was added and the reaction mixture was refluxed for 20 minutes. With 1.2 mL 2M sodium hydroxide solution the mixture was neutralized and for further 20 min refluxed. The volume of the solution was reduced to 10 mL and crystallized overnight in the fridge. The colorless crystals were collected, washed with little water and dried in vacuo. Yield: 0.59 g (1.80 mmol); 61 %.

IR (ATR): $\tilde{\nu}$ (cm⁻¹) = 3502 m, 3345 m, 3241 m, 3143 m, 1676 vs, 1634 vs, 1556 m, 1474 m, 1435 vs, 1278 m, 1234 m, 1226 m, 959 w, 901 w, 775 w. **Raman** (200 mW): $\tilde{\nu}$ (cm⁻¹) = 1581 (100), 1435 (10), 1241 (16), 1224 (9), 963 (50), 940 (11), 794 (18), 771 (9), 745 (6), 419 (10), 368 (12), 196 (9). **Elemental analysis:** found (calc.) C 15.11 (15.07), H 2.12 (2.21), N 17.65 (17.58). **DSC:** dehydration at 149°C and 164°C; decomposition between 363 and 395°C. **Impact sensitivity:** >100 J; **Friction sensitivity:** > 360 N.

BARIUM(II)-3,3'-BIS(1,2,4-OXADIAZOL-5-ON)-ATE DIHYDRATE (3)

Preparation: 4.08 g (24.0 mmol) **4** was dissolved in 100 mL ethanol at 78 °C. To the solution a suspension of 7.57 g (24.0 mmol) barium hydroxide-octahydrate in 80 mL water was added and refluxed for 3 h. After one hour of reaction time the pH-value was checked and further amounts of barium hydroxide-octahydrate was added if necessary. The colorless product **33** was filtered, washed with ethanol and dried in vacuo. **Yield:** 8.07 g (23.63 mmol); 98 %.

IR (ATR): $\tilde{\nu}$ (cm⁻¹) = 3382 m, 2940 m, 1638 vs, 1470 vs, 1457 vs, 1294 s, 1278 s, 1241 m, 1229 vs, 959 w, 950 m, 897 m, 775 m, 763 m, 653 w. **Raman** (200 mW): $\tilde{\nu}$ (cm⁻¹) = 1577 (100), 1523 (15), 1234 (12), 978 (32), 955 (34), 935 (23), 793 (22), 743 (10), 423 (15), 350 (10), 258 (10). **Elemental analysis:** found (calc.) C 13.63 (14.08), H 1.17 (1.17), N 16.03 (16.42). **DSC:** dehydration between 184 and 198 °C; decomposition between 398 and 421 °C. **Impact sensitivity:** > 100 J; **friction sensitivity:** > 360 N.

CALCIUM (II)-3,3'-BIS(1,2,4-OXADIAZOL-5-ON)-ATE TETRAHYDRATE (4)

Preparation: 2.55 g (15 mmol) **1** was dissolved in 100 mL hot methanol. A solution of 1.11g (15 mmol) calcium hydroxide in 20 mL water was added to the methanol solution. After the three hours of stirring at room temperature the white precipitate was filtered and washed with little water. **Yield:** 3.53 g (82%, 12.25 mmol).

IR (ATR): $\tilde{\nu}$ (cm⁻¹) = 3236 w, 2196 w, 1632 m, 1477 s, 1290 s, 1242 m, 1228 m, 961 m, 953m, 938 m, 899 m, 776 s. **Raman** (300 mW): $\tilde{\nu}$ (cm⁻¹) = 1595 (100), 1532(8), 1473(4), 1242(10), 1088 (5), 965(34), 938(14), 795(16), 477(5), 616(4), 423(9), 360(6). **DSC:** dehydration at 157°C, 196°C and 250°C; decomposition between 369 and 402°C. **Impact sensitivity:** >100 J; **Friction sensitivity:** > 360 N.

LITHIUM (I)-3,3'-BIS(1,2,4-OXADIAZOL-5-ON)-ATE TETRAHYDRATE (5)

Preparation: According to the procedure for barium OD (3) and calcium OD (4).

IR (ATR): $\tilde{\nu}$ (cm⁻¹) = 3335 s, 3201 s, 1694 s, 1485 s, 1278 s, 1244 s, 973 m, 921 s, 791 m, 745 m, 667 m. **DSC**: dehydration at 180°C and 221°C; decomposition at 350°C;. **Impact sensitivity**: >100 J; **Friction sensitivity**: > 360 N.

TETRAAQUA-3,3'-BIS(1,2,4-OXADIAZOL-5-ON)-ATO COPPER(II) (6)

Preparation: 0.85 g (5.00 mmol) 4 was dissolved in 9 mL Millipore water and 2 mL ethanol at 80 °C. While heating and stirring a hot solution of 1.21 g (5.00 mmol) copper nitrate trihydrate in 5 mL Millipore water was added. The deep green solution was stored in the fridge overnight. The gained turquoise crystals were filtered and washed with little ethanol and dried in vacuo. **Yield**: 0.86 g (2.84 mmol); 57 %.

IR (ATR): $\tilde{\nu}$ (cm⁻¹) = 3335 vs, 1723 m, 1697 vs, 1666 vs, 1589 m, 1454 s, 1448 vs, 1304 s, 1241 w, 1223 m, 971 w, 901 w, 767 m. **Elemental analysis**: found (calc.) C 15.82 (15.82), H 2.44 (2.66), N 18.45 (18.45). **DSC**: dehydration between 141 and 156 °C, decomposition between 263 and 274 °C. **Impact sensitivity**: >100 J; **Friction sensitivity**: > 240 N.

DIAMMINE- 3,3'-BIS(1,2,4-OXADIAZOL-5-ON)-ATO COPPER(II) (7)

Preparation: 1,2 g (7.00 mmol) 1 was dissolved in methanol at 70 °C. While heating and stirring a hot solution of 1,7 g (7.00 mmol) copper nitrate trihydrate in 5 mL methanol and 2.1 mL ammonia solution was added. The deep green solution was refluxed for two hours and the pH value was adjusted to pH 8 with sodium hydroxide solution. The mixture was stored in the fridge for two hours. The gained purple powder was filtered and washed with little cold methanol and dried in vacuo. **Yield**: 1.54 g (5.81 mmol); 83 %.

IR (ATR): $\tilde{\nu}$ (cm⁻¹) = 3550 s, 3377s, 3307m, 3251s 3214 m, 3173m, 1702 vs, 1617 vs, 1501 vs, 1417 vs, 1303 s, 1282 s, 1221 s, 957 s, 878s, 773s. **Raman** (200 mW): $\tilde{\nu}$ (cm⁻¹) = 3271 (12), 2546 (3), 1705 (8), 1606 (100), 1538 (12), 1296 (8), 1215 (10), 1078 (4), 957 (28), 914 (20), 778 (40), 730 (5). **Elemental analysis**: found (calc.) C 17.7 (18.1), H 2.3 (2.3), N 30.5, (31.6). **DSC**: decomposition between 178°C and 203 °C. **Impact sensitivity**: >100 J; **Friction sensitivity**: > 360 N.

3.5 References

- [1] T.M. Klapötke, G. Steinhauser, *Angw. Chem. Int. Ed.* **2008**, 47 (18), 3330.
- [2] M.A. Hiskey, D.E. Chaves, D.L. Naude, *US6214139*, **2001**.
- [3] T.M. Klapötke, A.J. Maier, N. T. Mayr, *New Trends in Research of Energetic Materials, Proceedings of the Seminar, 11th*, Pardubice, Czech Republic, Apr. 25-27, **2008** (2008), (Pt. 2), 653.
- [4] K.A. Al-Sou'od, F. I. Khalili, M. Mubarak, *J. Saud. Chem. Soc.* **2000**, 4(2), 143-151.

- [5] N. AL-SAYYED AHMAD, F. KHALILI, *Synth. React.Inorg.Met.-Org. Chem.* **1990**, 20(4), 425-436.
- [6] A. F. HOLLEMAN,, E. WIBERG,, *Lehrbuch der Anorganischen Chemie*,101. Edition by N. WIBERG,, Walter de Gruyter, Berlin,**1995**, 1842.
- [7] a) REICHEL & PARTNER GmbH, <http://www.reichelt-partner.de> b) Test methods according to the UN Recommendations on the Transport of Dangerous Goods, Manual of Test and Criteria, fourth revised edition, United Nations Publication, New York and Geneva, **2003**, ISBN 92-1-139087-7, Sales No. E.03.VIII.2; 13.4.2 Test 3(a)(ii) BAM Fallhammer.
- [8] SHELDRICK, G. (**1997**) SHELXS-97 Program for Crystal Structure Solution, Institut für Anorganische Chemie der Universität, Tammanstrasse 4, D-3400 Gottingen, Germany.
- [9] SHELDRICK, G. (**1997**) SHELXL-97 Program for Crystal Structure Refinement, Institut für Anorganische Chemie der Universität, Tammanstrasse 4, D-3400 Gottingen, Germany.
- [10] JOHNSON, C.K. (**1976**) ORTEP-II. A Fortran Thermal-Ellipsoid Program, Report ORNL-5138. Oak Ridge National Laboratory, Oak Ridge Tennessee.

Chapter V

3,5-DIAMINO-1,2,4-OXADIAZOLE –

A SUBSTITUTE FOR GUANYLUREA

IN ENERGETIC MATERIALS

Abstract:

3,5-Diamino-1,2,4-oxadiazole derivatives may replace or complement the standard explosives and propellants like RDX and TNT in some cases. The dinitramide salt of 3,5-Diamino-1,2,4 oxadiazole exceeds the properties of FOX-12, which is used as modifier for explosives and propellants. The formation of energetic salts from 3,5-amino-1,2,4-oxadiazole was investigated as well as the behavior to nitration and oxidation agents. A comprehensive study of the crystal structure of 3,5-diamino-1,2,4-oxadiazole as well as some derivatives is revealed and thoroughly discussed.

Keywords: 3,5-diamino-1,2,4-oxadiazole, DAOd, picrate, perchlorate, FOX-12, GUDN, crystal structure, density, decomposition.

1 Introduction

As the concept of explosive materials includes the nitro group as one of the most valuable supplier for energetic behavior, the invention of the dinitramide anion has provided a wide range of synthetic approaches.^[1] Therefore some salts of this compound have been formed by the inventors and published as energetic materials. The most promising out of those has been to date the FOX-12.^[2] Also in the working group of T.M. Klapoetke a lot of energetic anions like some tetrazolates^[3] which do not provide oxygen for the chemical explosion but form high amounts of nitrogen are investigated. A series of these anions with the guanylyurea which is the cation in the FOX-12 or guanylylurionium dinitramide (GUDN), were investigated by Klapoetke *et al.*^[4]

Having in mind that the oxidized and ring closed derivative of guanylyurea compound would be the 3,5-diamino-1,2,4-oxadiazole as shown in figure 1.

Therefore the aim of this chapter is the description and characterization of new energetic materials based on 3,5-diamino-1,2,4-oxadiazole derivative.

Therefore the characterization of 3,5-diamino-1,2,4-oxadiazole(**1**, **DAOd**) including synthesis and crystal structure is depicted. Afterwards the treatment of **1** with different oxidizing agents to oxidize one or both amino groups to nitro groups as well as diazotation and direct nitration is described.

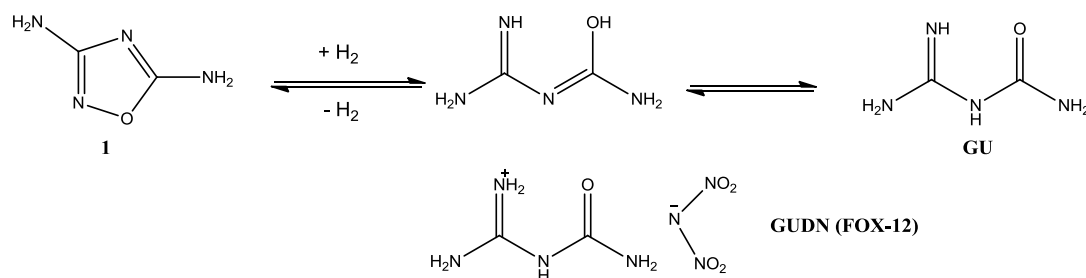


Figure 1. Ring opening and closing reaction from guanylyurea to **1**.

Furthermore, ionic compounds are to be synthesized, as they generally offer some attractive advantages. First, they can be made quite easily by acid-base reactions and the anions can be usually replaced without much effort by metathesis reaction. Second, the advantage is the generally low to non-existent amount of by-products. As in the synthesis of TNT or RDX there are significant amounts of by-products that must be removed at great expense. Also through the easy exchange of the ions important parameters such as density, education, energy or oxygen balance are easily adapted to specific problems. Another advantage is the tendency to significantly lower vapor pressures which drastically reduces the risk of poisoning via inhalation. 1,2,4-oxadiazole-3,5-diamine (**1**) will now be on one hand reacted with different acids, some of which will serve as a starting material for the preparation of compounds with energetic anions, such as dinitramide, 5-aminotetrazolate or 5-nitrotetrazolate. Likewise, should also be tried to synthesize an aprotic cation by selective methylation, which could be combined with weak acid anions such as azide.

2 Results and Discussion

2.1 Synthesis and Characterization of 3,5-diamino-1,2,4-oxadiazole (DAOd, **1**)

This section points out the synthesis and characterization of the starting compound 3,5-diamino-1,2,4-oxadiazole (**1**, DAOd). It is a literature known compound but only one patent describes the synthesis without further investigation. The application in energetic materials is unknown so far. In the following *chapter 1* and derivatives thereof are fully characterized and combined with quantum chemical calculations. The derivatives result from different reaction, with acids, oxidizing and nitrating agents.

2.1.1 3,5-diamino- 1,2,4-Oxadiazole (**1**, DAOd)

SYNTHESIS

The synthesis of **1** was carried out according to the methods of Roemer *et al.*^[5] but with prolonged reaction time (Figure 2).

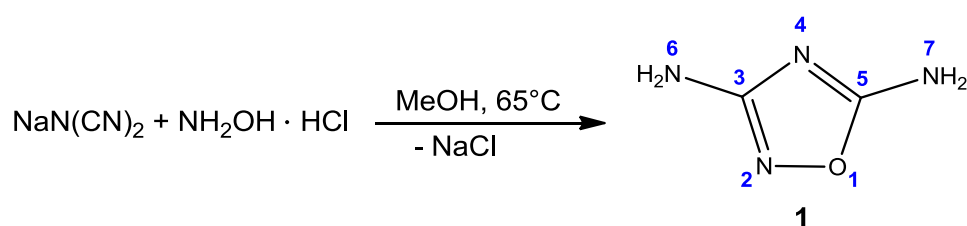


Figure 2. Synthesis of **1**.

During crystallization from water mostly colorless, limpid needles were obtained, which tarnish while drying. If the solvent is moved rapidly by vacuum distillation the product precipitates as fine powder.

Sodium dicyanamide reacts with hydroxylammonium chloride in different solvents not to **1a** but to **1**. To synthesize **1** according to the procedure of Boemer, Stamford und Kaiser^[5] a suspension of sodium dicyanamide and hydroxylammonium chloride in

methanol was heated to reflux. After separation of the solid sodium chloride the solvent was removed by vacuum distillation and the remaining product recrystallized from a mixture of ethanol/water and a second time from pure water. **1** was obtained in 56% yield as pale yellow crystalline solid.

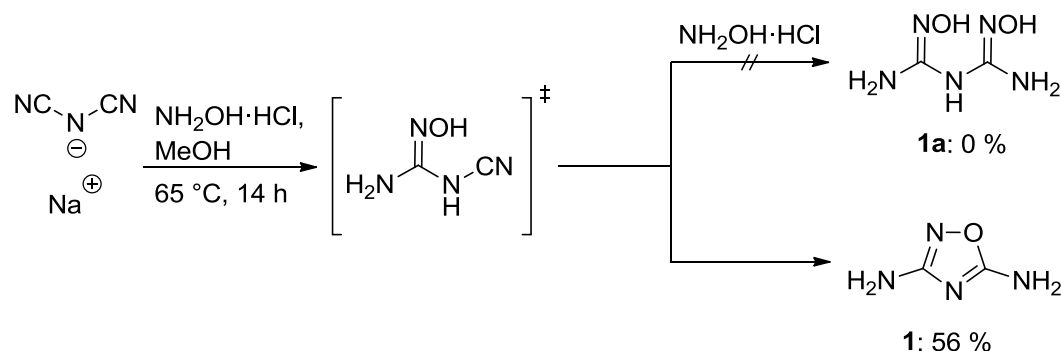


Figure 3. Synthesis von 3,5-Diamino-1,2,4-oxadiazole (**1**) first route.

The IR spectrum of the product shows characteristic signals at 3326 cm^{-1} (N-H-valence vibration), 1657 cm^{-1} (C=N-valence vibration), 1560 cm^{-1} (NH_2 -torsion vibration) and 1274 cm^{-1} (N-O-valence vibration). There are no signals at about 3570 cm^{-1} (O-H-V valence vibration) and $\approx 2250\text{ cm}^{-1}$ (CN- valence vibration) that means the product does not contain any impurities or side product **1a**. The ^1H NMR spectrum shows two sharp peaks at 5.57 and 7.27 ppm and in the ^{13}C NMR spectrum can be observed to signals at 168.6 and 170.2 ppm. The mass spectrum displays the expected molecule peak ($m/z = 100.2$) and the elemental analysis confirms a pure product. Only the melting point of $153\text{ }^{\circ}\text{C}$ is lower than the literature reference of $167\text{ }^{\circ}\text{C}$.

The synthesis of **1** was carried out under other reaction conditions and leads to lower yield but even purer product. Therefore sodium dicyanide was added to a solution of hydroxylammonium chloride in a mixture of water and ethanol. Then carefully sodium hydroxide solution was dropped in and after stirring for a while the mixture was neutralized by hydrochloric acid. The solvents were removed by vacuum distillation and the resulting solid was recrystallized first from ethanol and afterwards from water. **1** yields 34 % of yellow-brownish crystalline solid. The NMR and mass spectra are in good accordance with the aforementioned synthesis and the melting point of $164\text{ }^{\circ}\text{C}$ is very close to the literature reference of $167\text{ }^{\circ}\text{C}$. The DSC thermogram of **1** shows a decomposition point of 178°C (onset). Pure **1** is not applicable due to low decomposition temperature, therefore salts of **1** were made to raise the melting point and put more energy into the composition.

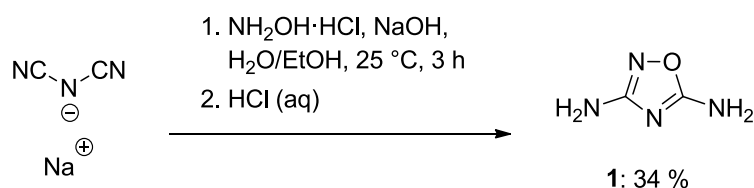


Figure 4. Synthesis of 3,5-Diamino-1,2,4-oxadiazole (**1**) second route.

In the second synthetic route **1** was obtained as crystalline needles by the recrystallization from water. The crystals have been measured by x-ray diffraction analysis. The crystal structure was solved by *SIR97*^[6], refined by *SHELXL-97*^[7] and the visualization was created by *Diamond 3*^[8]. Figure 5 displays the molecular structure of 3,5-diamino-1,2,4-oxadiazole(**1**). The compound crystallizes in the monoclinic space group $P2_1/c$ with 4 formula units per unit cell. Further information on the crystal is listed under Part XII (Crystal structure data). Figure 6 shows the planar structure of **1**. The atoms are all arranged in one plane except the four hydrogen atoms. Both of the hydrogen atoms at N3 are stick out of plane of the ring contrariwise to the both at N4. The bond lengths and angles are listed in table 1.

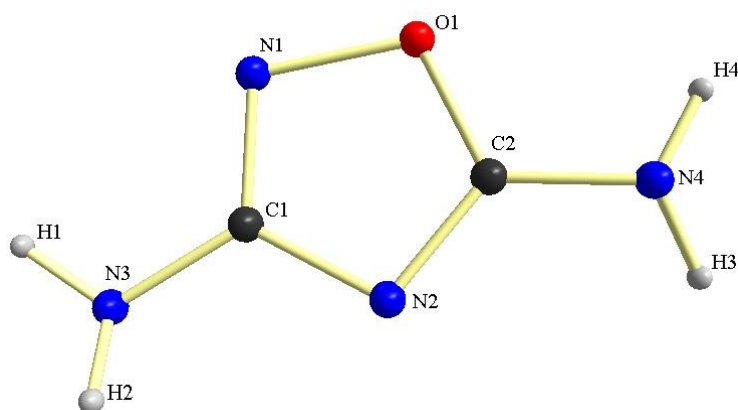


Figure 5. Molecular structure of DAOd (**1**).

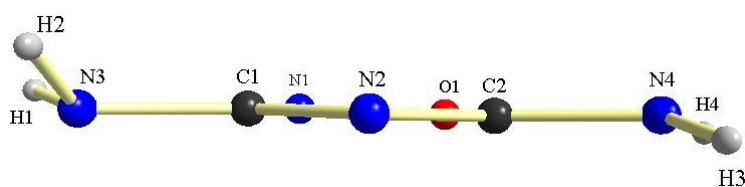
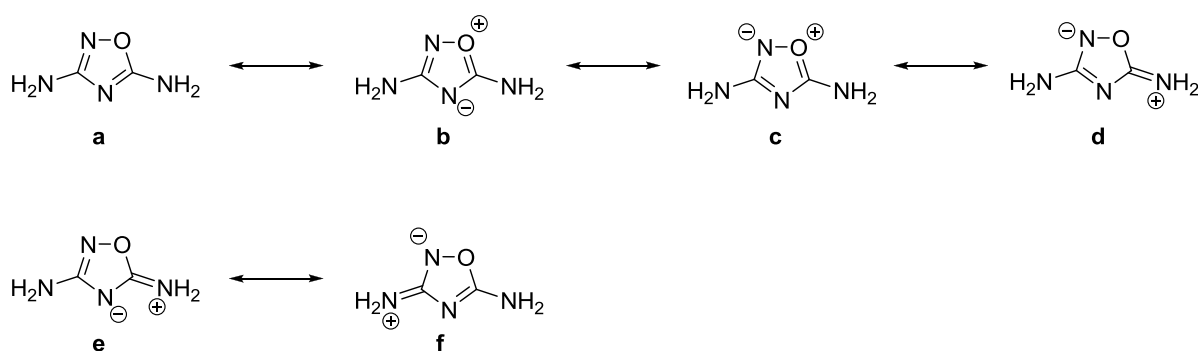


Figure 6. Visualization of the planar 5-membered ring of DAOd (**1**).

Table 1. Selected bond lengths and angles of DAOd (1).

Bond lengths [Å]		Angles [°]	
O1-N1	1.448(1)	O1-C2-N4	118.5(1)
O1-C2	1.340(2)	O1-C2-N2	113.8(1)
N1-C1	1.312(2)	N4-C2-N2	127.4(1)
N2-C1	1.363(2)	N3-C1-N2	121.6(1)
N2-C2	1.318(2)	N1-C1-N3	122.3(1)
N3-C1	1.371(2)	N1-C1-N2	115.9(1)
N3-H1	0.92(2)	H4-N4-H3	122(1)
N3-H2	0.86(2)	H2-N3-H1	117(1)
N4-C2	1.32(2)	C2-N4-H4	116(1)
N4-H3	0.87(2)	C2-O1-N1	105.50(8)
N4-H4	0.90(2)	C2-N2-C1	102.23(9)
		C2-N4-H3	116(1)
		C1-N1-O1	102.40(9)
		C1-N3-H2	111(1)
		C1-N3-H1	114(1)

The bond lengths of O1-N1-single bond (1.448 Å) are in good accordance with the literature known value of O-N-single bonds (1.43–1.47 Å). The O1-C2-bond (1.340 Å) is shorter than a common O-C single bond (1.43–1.46 Å). The bond lengths of the N1-C1 and N2-C2 double bonds (1.312 and 1.318 Å) are in the range of a normal N-C double bond (1.28 Å), the other N2-C1, N3-C1 and N4-C2-single bond (1.363, 1.371 and 1.32 Å) are shorter than a typical N-C-single bond (1.47 Å)^[9,10]. The deviant bond lengths are described best by the resonance structure in figure 7. As a result of the long bond (range of a single bond) there is no evidence for an aromaticity in the 5-membered ring system according to the 6-electron (Hueckel rule). Aromaticity is implied by an overlap of the pi-electrons which would cause a shortening of the bond distance.

**Figure 7.** Resonance structure of DAOd(1).

Hydrogen bridged bonding are displayed in fig. 8. As shown there the molecule is involved in eight hydrogen bonds from atom O1, N1, N2, N3 over H1, H2, H3 and H4 so a stable three-dimensional network is formed. The molecule of one layer are interconnected by two hydrogen bond ($2 \times \text{N3-H1-N1}$ and $2 \times \text{N4-H3-N2}$), while the layers are stuck together by one hydrogen bridge on each molecule (N3-H2-O1 and

N4-H4-N3). Overall one molecule is connected to six neighbors (with two in the same layer and two each in the layer above and beneath) by hydrogen bonds.

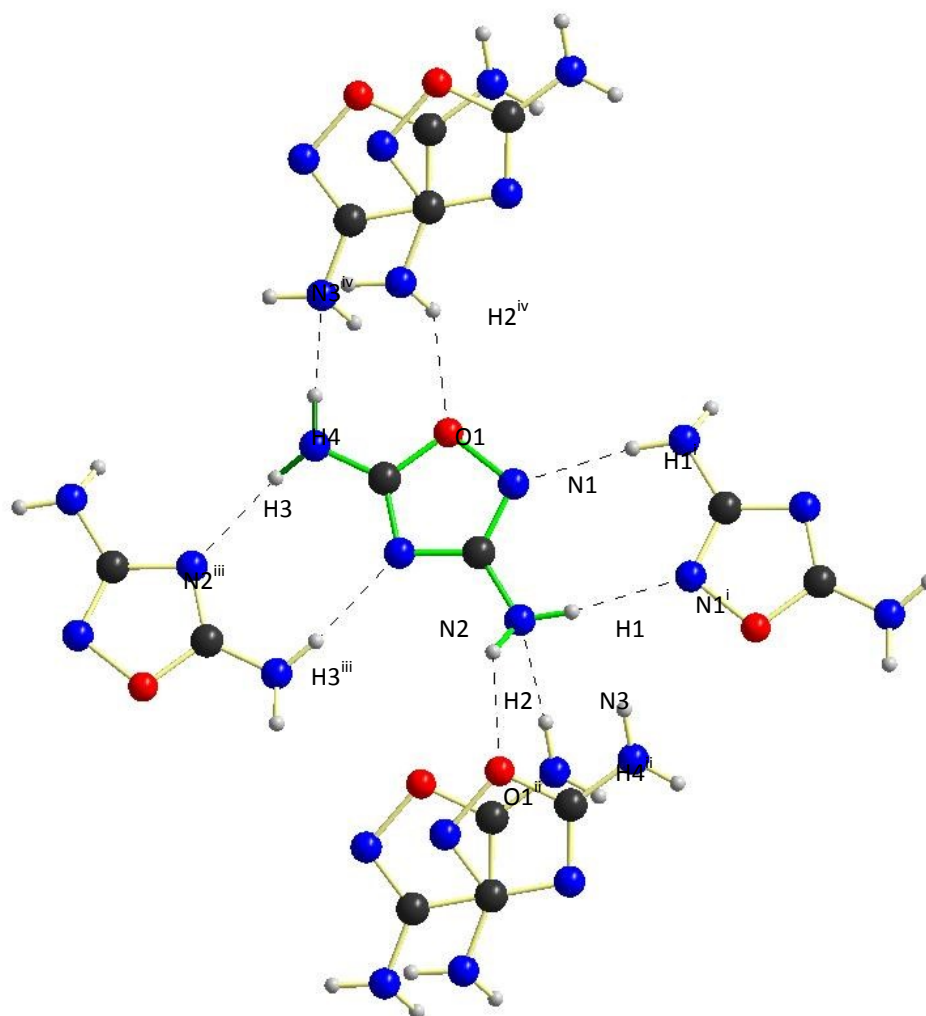


Figure 8. Visualization of the hydrogen bonds in DAOd (**1**).

Table 2. Hydrogen bonds of DAOd (**1**).

Atoms D, H, A	Bond lengths D, H [Å]	Bond lengths H, A [Å]	Bond lengths D, A [Å]	Angles D, H, A [°]
N3-H1-N1 ⁱ	0.92(2)	2.13(2)	3.048(2)	170.(1)
N3-H2-O1 ⁱⁱ	0.86(2)	2.37(2)	3.118(2)	143(1)
N4-H3-N2 ⁱⁱⁱ	0.87(2)	2.08(2)	2.951(2)	172(1)
N4-H4-N3 ^{iv}	0.90(2)	2.21(2)	3.085(2)	160(1)
(i) 2-x, -y, -z; (ii) 2-x, -0.5+y, 0.5-z; (iii) 1-x, -y, 1-z; (iv) 1-x, 0.5+y, 0.5-z.				

Figure 9 shows the orientation of the DA0d molecule along the a-axis. The molecules are stacked along the a-axis in the crystal that means they lay directly above each other. In figure 10 the layers of the DA0d molecule in the crystal are displayed.

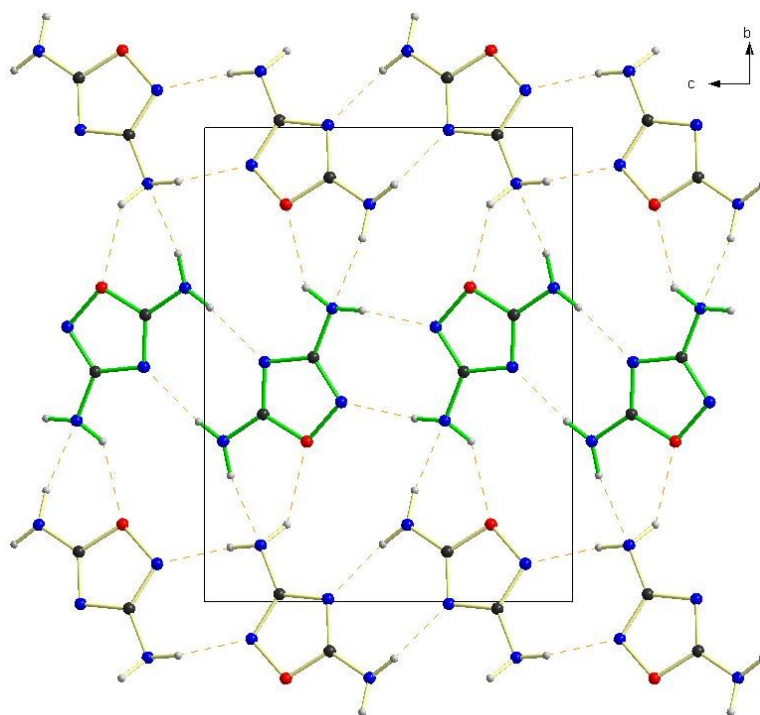


Figure 9. View along a-axis of DA0d (1).

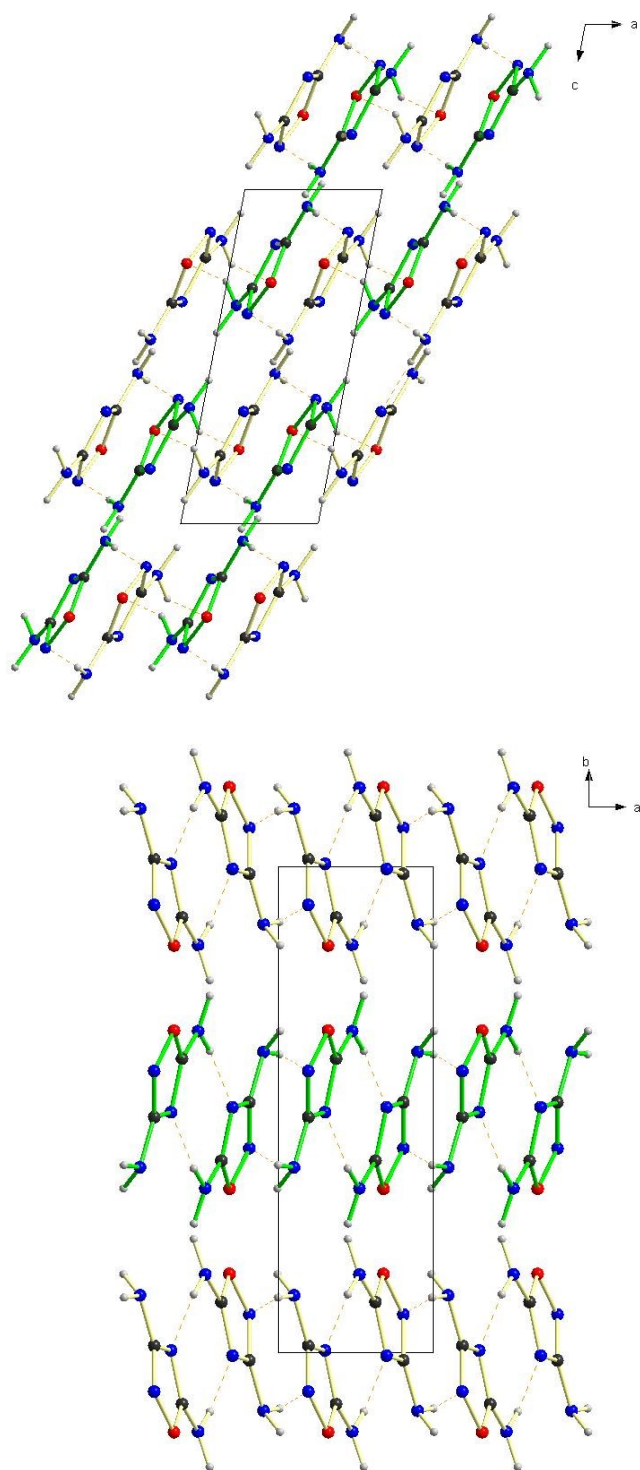


Figure 10. View along b-axis (left) and c-axis (right) of DA0d.

Furthermore figure 9 shows all hydrogen bonds, in spite of figure 10 which shows inter layer hydrogen bridges (left) and displays intra-layer hydrogen bonds (right).

CHARACTERIZATION

Compound **1** was fully characterized. In the IR-spectrum there are at 3395, 3314, 3173 and 3096 cm^{-1} the symmetrical and asymmetrical N-H valence vibrations of the amino groups. At 1690 cm^{-1} the C5_N7 bond as sharp peak, at 1642, 1577 and 1455 cm^{-1} as ring valence vibrations and with high intensity at 799 cm^{-1} an *out-of-plane* deformation vibration of C3 and C5 are found. In the ^1H NMR-spectrum hydrogen of the N6 and N7 amino group are observed at 5.56 and 7.26 ppm. Although the hydrogen atoms of both groups should be diastereotop they appear as two strong singlets. In the ^{13}C NMR-spectrum the expected peaks for C3 and C5 are observed at 168.7 and 170.3 ppm. In the DEI^+ -mass spectrum the molecule peak is found at $m/z=100.07$.

THEORETICAL CALCULATIONS

To assign the IR-absorption more easily and to identify the carbon signals in the ^{13}C NMR-spectrum, the optimized structure, the vibration and resonance frequencies of **1** were calculated at the MPW1PW91 level of theory with a augmented coupled cluster double zeta basis set: aug-cc-pVDZ.

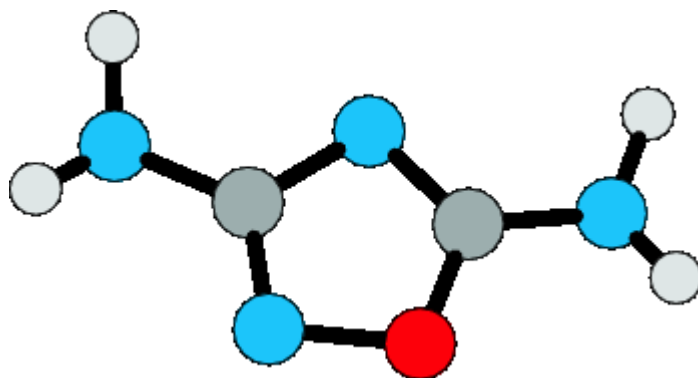


Figure 11. Calculated molecular structure **1**.

1 shows a completely planar ring structure, the hydrogen atoms at the amino groups stick out of the plane ring in the direction. The point group is C_1 .

Table 3. Calculation Results: Structural optimization of **1**.

Bond lengths / Å		Angles / °	
d(O1-N2)	1.419	$\angle(\text{O1}, \text{N2}, \text{C3})$	102.2
d(N2-C3)	1.314	$\angle(\text{N2}, \text{C3}, \text{N4})$	116.0
d(C3-N4)	1.372	$\angle(\text{C3}, \text{N4}, \text{C5})$	100.9
d(N4-C5)	1.306	$\angle(\text{N4}, \text{C5}, \text{O1})$	109.3
d(C5-O1)	1.329	$\angle(\text{C5}, \text{O1}, \text{N2})$	114.8
d(C3-N6)	1.368	$\angle(\text{N2}, \text{C3}, \text{N6})$	122.9
d(C5-N7)	1.354	$\angle(\text{O1}, \text{C5}, \text{N7})$	117.8

The O1-N2 bond is the longest bond with 1.419 Å and in the range of a common N-O single bond according to the covalence radii as listed in the text book of Holleman and Wiberg.^[11] The two shortest bonds are found between N2-C3 and N4-C5 with a bond length of 1.314 and 1.306 Å which represents a double bond with single bond character. Mesomeric boundary structures like drawn in figure 7 are possible but not

found in the calculated structure which is concluded from the nearly exact bond length of single bonds that would be expected to be slightly shortened in a resonance state. Also the boundary structures are only possible if charge separation occurs which leads to increased energy values. So an aromatic system according to Hückel's rules (six π -electrons, conjugated planar system) which could be possible here is not found represented by the bond value of the O1-N2 whether in calculation nor in the crystal structure, while the N-C bonds are completely delocalized as they are all between a C-N single bond 1.47 Å and a C-N double bond 1.22 Å.

In table 4 the calculated characteristic IR vibration values of **1** are listed with the direct assignment of the respective vibrational mode. The calculated wavenumbers were adjusted by the factor 0.985 so that the best agreement with experimental values was achieved.

Table 4. Calculated and experimental characteristic IR absorptions of **1**.

$\tilde{\nu}_{\text{calc.}}^{\text{a)}} / \text{cm}^{-1}$	Intensity / %	$\tilde{\nu}_{\text{exp.}} / \text{cm}^{-1}$	Intensity	Assignment
3704	19	3395	s	$\nu_{\text{as}}(\text{N}^7\text{H}_2)$
3680	13	3314	s	$\nu_{\text{as}}(\text{N}^6\text{H}_2)$
3578	21	3173	s	$\nu_{\text{s}}(\text{N}^7\text{H}_2)$
3562	11	3096	s	$\nu_{\text{s}}(\text{N}^6\text{H}_2)$
1692	100	1690	vs	$\nu(\text{C}^5\text{-N}^7)$
1655	86	1642	s	$\nu(\text{N}^2\text{-C}^3)$
1592	33	1577	m	$\nu(\text{Ring})$
1481	86	1455	vs	$\nu(\text{C}^3\text{-N}^4)$
a) scaling factor 0.985				

The NMR shifts δ were calculated for ^{13}C NMR with 168.6 (C3) and 169.5 (5) ppm and 3.35 (N6H₂), 3.56 (N6H₂), 4.09 (N7H₂) and 4.27 (N7H₂) ppm for ^1H NMR. The theoretical signals of the carbon atoms are in good accordance with the experimental values while the theoretic signals of the hydrogen atoms are shifted to higher field and diastereotopic.

2.2 Syntheses of 3,5-diamino-1,2,4(4H)-oxadiazolium salts

2.2.1 The 3,5-diamino-1,2,4(4H)-oxadiazolium cation

The objective of this part was to synthesize ionic energetic compounds of **1**. Because of the easy and fast preparation **1** was combined with different acids to form products which were subsequently used for other metathesis reactions. The combinations are limited by the acidity of the protonated **1** (cation) to overcome this limitation it was tried to methylate **1** to form a aprotic cation (xi). This cation should be able to serve as basis for more compounds with a nearly unlimited range of energetic anions. As all synthesized compounds have the same cation (DAOdH⁺) it was calculated by quantumchemical methods to identify it in the IR-spectrum.

THEORETICAL CALCULATIONS

The optimized molecular structure and as well the vibration and resonance frequencies of the 3,5-diamino-1,2,4-oxadiazolium cation (DAOdH⁺) are calculated at MPW1PW91 level of theory with complex basis set (aug-cc-pVDZ) .

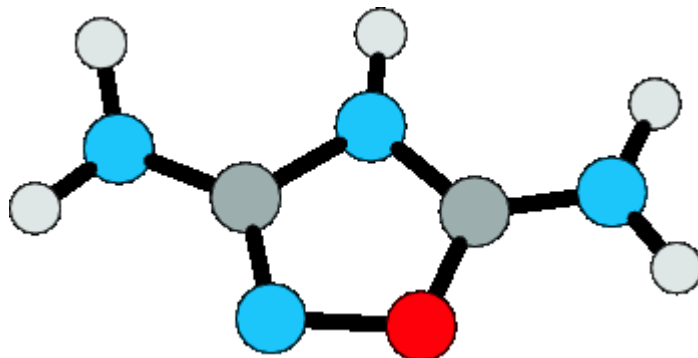


Figure 12. Calculated molecule DAOdH⁺, numbers assigned as in **1**.

The cation displays a nearly plane structure. N6 is not completely sp²-hybridized, one hydrogen sticks out of the plane. The calculation shows that the positive charge appears to be mostly on the N7 which leads to the correct name 3-amino-1,2,4-oxadiazol-5(4H)-iminium. The point group is C₁.

Table 5. Results of the calculation of DAOdH⁺.

Bond length / Å		Angles / °	
d(O1-N2)	1.426	∠ (O1N2C3)	104.143
d(N2-C3)	1.303	∠ (N2C3N4)	111.086
d(C3-N4)	1.394	∠ (C3N4C5)	105.833
d(N4-C5)	1.340	∠ (N4C5O1)	109.325
d(C5-O1)	1.302	∠ (C5O1N2)	109.587
d(C3-N6)	1.344	∠ (N2C3N6)	125.986
d(C5-N7)	1.317	∠ (O1C5N7)	121.556

As in **1** again the bond length of O1-N1 with 1.426 Å is the longest bond and corresponds to N-O single bond, compared to **1** (1.419 Å) is it slightly longer. The C3-N4 bond is prolonged with 1.394 Å in spite of 1.373 Å, due to the change of the double bond compared to **1** (1.306 Å) the N4-C5 bond is very much longer with 1.340 Å, but all in all it lies between a C-N single and double bond. Especially the C5-N7 bond has shortened from 1.354 Å to 1.317 Å so the double bond character of the bonding rises. Due to the enhanced mesomeric stabilization the C5-O1 bond is also shortened from 1.329 Å to 1.302 Å. The formulation of further reasonable resonance structures in comparison to **1** is limited to the atoms N4, C5, O1 and N7. Because of the two single bonds between O1-N2 and C3-N4 the ring is suspected not to show aromaticity although the Hueckel rules are fulfilled, likewise already found in **1**.

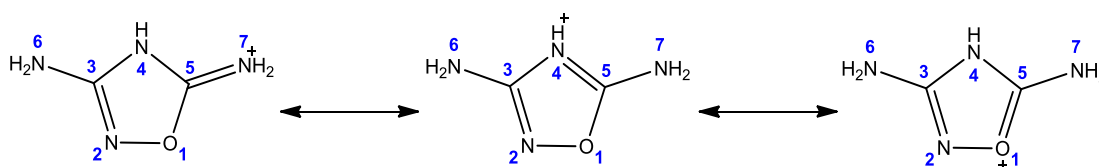


Figure 13. Mesomeric Lewis structures of DAOdH⁺, numbers assigned.

The NMR shift δ was calculated with 155.4 (C3) and 162.5 ppm (C5) in the ¹³C NMR and 3.93 (N6-H2), 4.91 (N6-H2), 5.63 (N7-H1), 6.17 (N7-H2) and 7.36 ppm (N4-H) in the ¹H NMR spectrum. In table 6 the calculated characteristic IR vibrations of DAOdH⁺ are listed and assigned according to the vibration mode. The wave numbers have not been scaled.

Table 6. Calculated IR vibrations of DAOdH⁺ (unscaled).

$\tilde{\nu}/\text{cm}^{-1}$	intensity / %	mode
3729	31	ν_{as} (N7-H2)
3712	20	ν_{as} (N6-H2)
3650	26	ν (N4H)
3600	28	ν_{s} (N7-H1)
3595	56	ν_{s} (N6-H1)
1779	100	ν (C5-N7)
1746	98	ν (N2-C3)
1633	13	δ (N6-H2)
1576	19	ν (C3-N4)

Schematic overview of the synthesis of the following compounds is presented in figure 14. While **2** to **4** were synthesized directly by the reaction of **1** with the corresponding acid. The reaction for **5** and **6** followed a metathesis route. Therefore first was the sulfate salt of **1** prepared and reacted with barium aminotetrazolate. For the dinitramide salt the energetic perchlorate salt of **1** was mixed with the potassium dinitramide which yielded potassium perchlorate and the corresponding dinitramide salt of **1**.

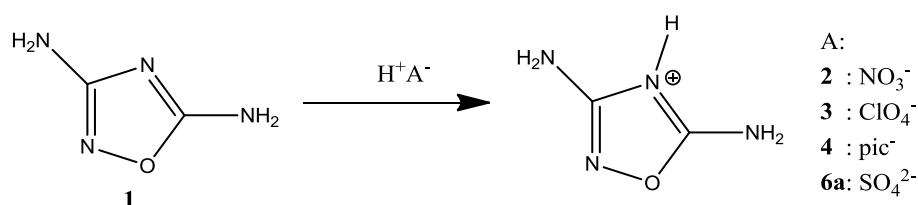


Figure 14. Synthesis of the compounds **1** to **4** and **6a**.

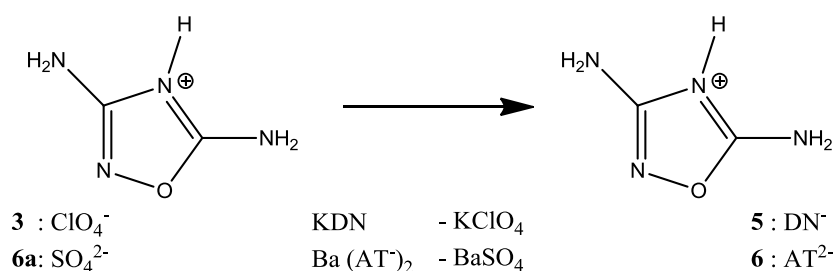


Figure 15. Metathesis reaction of **3** and **6a** to **5** and **6**.

2.2.2 3,5-Diamino-1,2,4-oxadiazolium nitrate (**2**)

SYNTHESIS

For synthesizing 3,5-Diamino-4*H*-1,2,4-oxadiazolium nitrate (DAOdH nitrate) (**2**) **1** was dissolved in water and nitric acid (2 M) was added carefully while ice-cooling. The yellow precipitate was filtered and dried in vacuo. **2** yielded 92 % of a yellow microcrystalline solid.

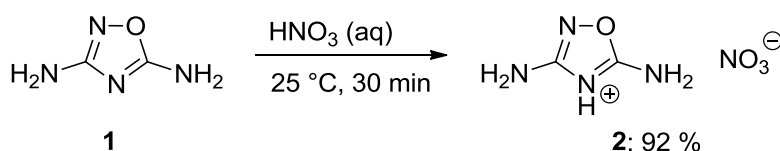


Figure 16. Synthesis of DAOdH nitrate (**1**).

The product was a colorless powder which is soluble in DMSO but only little in water.

CHARACTERIZATION

The IR spectrum displays valence vibrations of the amino groups at wave number 3319 (N-H-valence vibration), 3172 and 3096 cm^{-1} and the C5-N7 and N2-C3 at 1719 and 1660 cm^{-1} as sharp absorptions (C=N valence vibration). Also an absorption at 1581 cm^{-1} (NH_2 -torsion vibration) was recognized. The absorptions at 2442, 1386, 1314 (N-O-valence vibration) and 1045 can be assigned to the nitrate.^[12,13] In the ^1H NMR spectrum the hydrogen atoms of the amino groups are found as one broad signal at 6.68 ppm, the hydrogen attached to the ring appears at 7.62 ppm also as broad signal. In the ^{13}C NMR two signals are detected at 167.5 and 169.5 ppm. The nitrate anion is observed in the ^{14}N NMR at 5 ppm. The mass spectrum displays in FAB⁺ a peak for DAOdH⁺ at $m/z = 101.0$ and in the FAB⁻ a peak for the nitrate at $m/z = 62.1$.

ENERGETIC PROPERTIES

The impact sensitivity of **2** is >40 J, the friction sensitivity >288 N and the sensitivity towards electrostatic discharge >0.24 J. So far **2** is a secondary explosive with little sensitivity to friction and impact. The DSC showed a sharp decomposition point at 110°C and a melting of the residues at 269°-276°C. The calculated value (CBS-4M level of theory) of the enthalpy of formation is -855.50 kJ kg^{-1} and the experimental

determined density is 1.67 g cm^{-3} . The detonation parameters are listed in table 7 and were calculated by EXPL05.2.^[14]

Table 7. Calculated detonation parameters of **2**.

$\Delta_f U^\circ / \text{kJ kg}^{-1}$	$\Omega / \%$	$\rho / \text{g cm}^{-3}$	$Q_v / \text{kJ kg}^{-1}$	T_{ex} / K	p / kbar	D / ms^{-1}	$V_0 / \text{L kg}^{-1}$
-855.50	-24.5	1.67	-4418	3449	240	7878	819

The performance data of **2** exceeds those of TNT but do not reach those of RDX. The compound shows a good oxygen balance of -24.5% , high detonation velocity and little sensitivity but with a low decomposition point of 110°C it is not suitable for application.

2.2.3 3,5-Diamino-1,2,4-oxadiazolium perchlorate (**3**)

SYNTHESIS

As displayed in figure 17, the synthesis of 3,5-Diamino-4*H*-1,2,4-oxadiazolium perchlorate (DAOdH PC) (**3**) was done by carefully dropping perchloric acid (2 M) to a solution of **1** in little water. After stirring at room temperature the solid the solvent was removed under reduced pressure. A crystalline yellow solid was obtained and dried in vacuo. The product yield was 88 %. The yellow crystalline solid is soluble in polar solvents like DMSO but little in water.

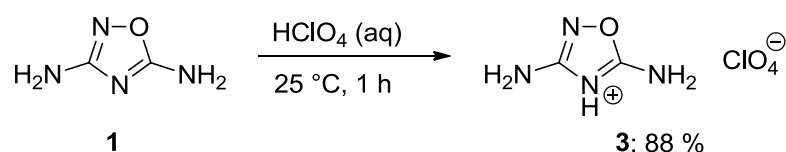


Figure 17. Synthesis of DAOdH perchlorate (**3**).

CHARACTERIZATION

The vibrations of the amino groups in the IR spectrum are observed in the common range with the strongest vibration 3321 cm^{-1} (N-H-valence vibration). The vibrations at 1714 and 1665 cm^{-1} (C=N-valence vibration) can be assigned to C5-N7 and N2-C3 bonds. Typical absorptions were observed at 1566 cm^{-1} (NH_2 -torsion vibration) and 1233 cm^{-1} (N-O-valence vibration). The broad absorptions at 1099 and 1064 cm^{-1} derive from the perchlorate anion.^[15,16] Like for compound **2** in the ^1H NMR the signal of the hydrogen atoms of the amino group are found as broad signal at 6.35 ppm and the hydrogen attached to the ring at 7.92 ppm. In the ^{13}C NMR spectrum their signals are observed at 166.7 and 169.2 ppm. The FAB⁺ mass spectrum displays the DAOdH⁺ peak at $m/z = 101.01$ and the FAB⁻ shows a peak at $m/z = 99.0$ for perchlorate. Furthermore DSC measurements show two decomposition points at 125.2°C and 355°C . The impact sensitivity is 8 J and the friction sensitivity is higher than 168 J.

CRYSTAL STRUCTURE

It was possible to grow single crystals of **3** and measure them by single crystal x-ray diffraction analysis. The crystal structure was solved with *SHELXS-97*^[17], refined with *SHELXL-97*^[17] and the pictures created with *Diamond 3*^[18]. Figure 18 displays the molecular structure of **3**. The compound crystallizes in the orthorhombic space group

$Pna2_1$ with 4 molecular units in the unit cell. Figure 19 shows the planar structure of the cation in **3**. Again like in molecule **1** the four hydrogen atoms on the nitrogen N3 and N4 are not located in the plane but stick out in opposite directions. The bond lengths and angles are listed in table 8.

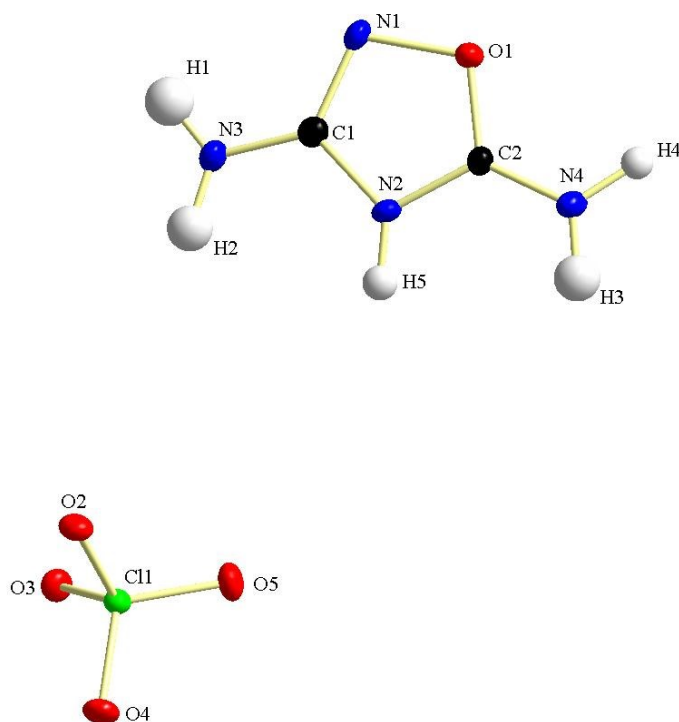


Figure 18. Molecular structure of DAOdH-Perchlorate (**3**).

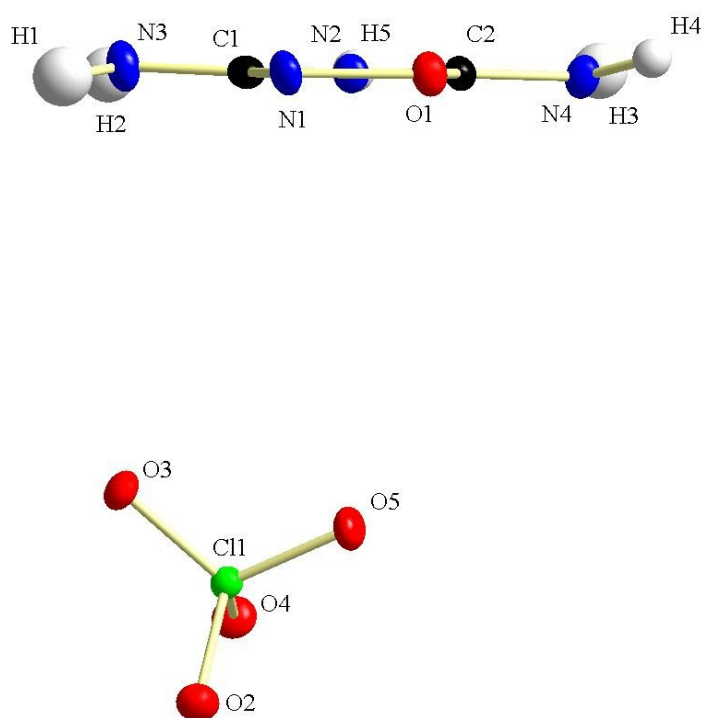
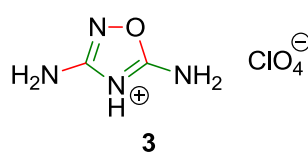


Figure 19. Visualization of the planar 5-ring of HDAOd-PC (**3**).**Table 8.** Bond lengths and angles of DAOdH-PC (**3**).

Bond lengths [Å]		Angles [°]	
O1-N1	1.466(3)	O1-C2-N4	122.1(3)
O1-C2	1.313(3)	O1-C2-N2	109.9(2)
N1-C1	1.307(3)	N4-C2-N2	127.8(3)
N2-C1	1.379(4)	N3-C1-N2	121.9(3)
N2-C2	1.332(4)	N1-C1-N3	126.6(3)
N2-H5	0.88(3)	N1-C1-N2	111.4(2)
N3-C1	1.321(4)	H4-N4-H3	118(3)
N3-H1	0.86(4)	H2-N3-H1	123(3)
N3-H2	0.93(4)	C2-N2-H5	121(2)
N4-C2	1.313(4)	C2-N4-H4	119(2)
N4-H3	0.91(4)	C2-O1-N1	107.7(2)
N4-H4	0.95(3)	C2-N2-C1	106.9(2)
		C2-N4-H3	119(2)
		C1-N2-H5	131(2)
		C1-N1-O1	103.8(2)
		C1-N3-H2	117(2)
		C1-N3-H1	116(2)

The bond lengths of **3** have changed little in comparison to **1**. The O1-N1 single bond became longer from 1.448 Å to 1.466 Å and the O1-C2 single bond became shorter from 1.340 Å to 1.313 Å. The N3-C1 single bond was shortened severely from 1.371 Å to 1.321 Å. The N1-C1 double bond was prolonged from 1.312 Å to 1.307 Å and also the N2-C2 double bond from 1.318 Å auf 1.332 Å. The N2-C1 single bond became longer from 1.363 Å auf 1.379 Å and the N4-C2 became slightly shorter from 1.32 Å to 1.313 Å. Figure 20 displays an overview of the prolonged and shortened bonds.

**Figure 20.** In comparison to **1** shortened (red) and prolonged (green) bonds of DAOdH-PC (**3**).

The resonance structures (fig. 21) explain the changed bonding conditions. A delocalization of the positive charge (resonance structure b) through the whole molecule but with maximum localization on the oxygen explains a weakened N1-O1 single bond as well as a strengthening of the O1-C2 bond to a double bond. Also on the other side the N1-C1 bond is now in the range of double bond and the C1-N2 is more likely a single bond. The outer ring nitrogen carbon bond C2-N4 and C1-N3 are in between double and single bond and show resonance behavior like in the guanidinium or the uronium cation.

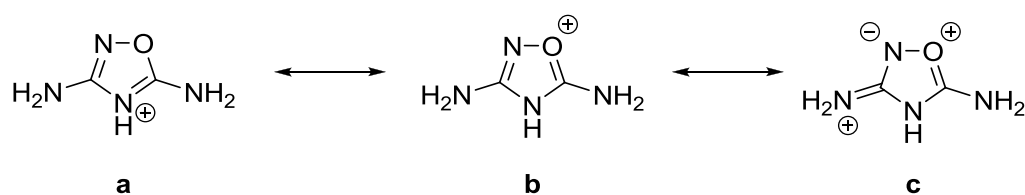


Figure 21. Resonance structure of the 3,5-Diamino-4*H*-1,2,4-oxadiazolium cation.

The hydrogen bonds of DA0dH-PC (3) are displayed in figure 22. One 3,5-diamino-4*H*-1,2,4-oxadiazolium-cation (DA0dH⁺) is connected to O1, N1 and N2 over H2, H3 and H5 of other DA0dH⁺ cations by 6 hydrogen bonds. The H2 and H3 are further bind to perchlorate anions whereas H1 and H4 only bind to perchlorate ions. Therefore a stable three dimensional network is formed where one DA0dH⁺ ion forms hydrogen bonds to 9 other ions (4 DA0dH⁺ cations and 5 perchlorate anions).

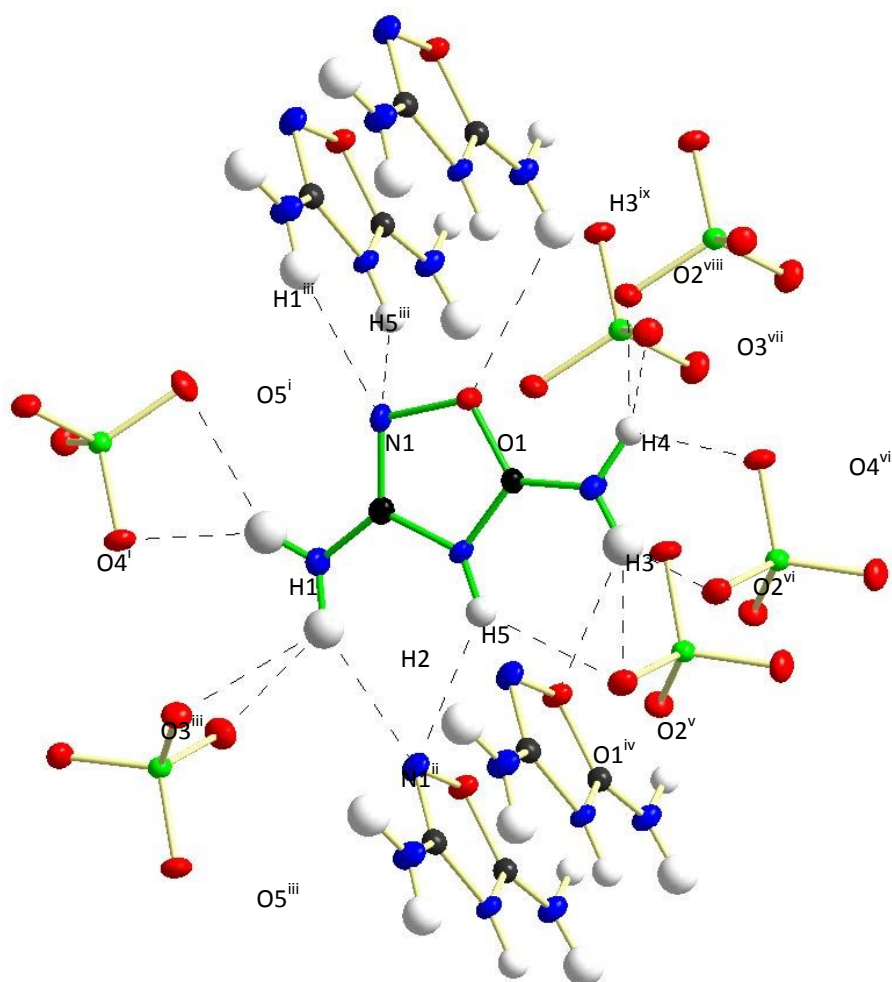


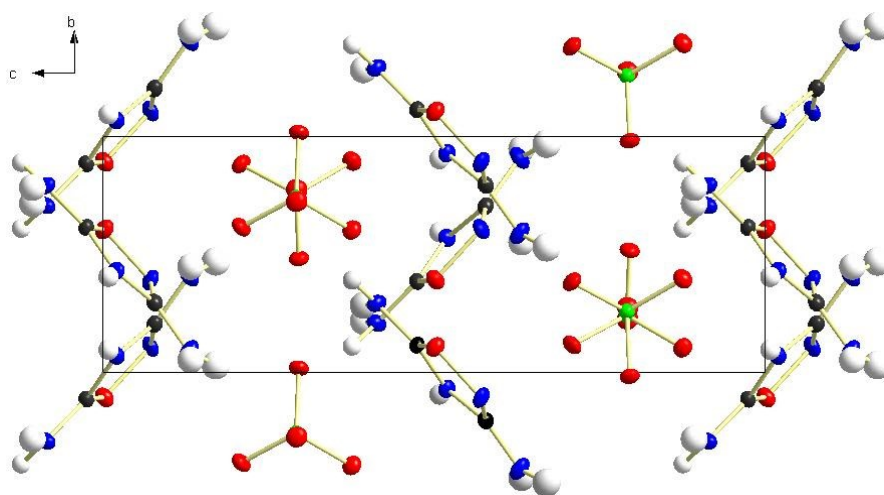
Figure 22. Visualization of the hydrogen bonds of DA0dH-PC (3).

Table 9. Hydrogen bonds of DAOdH-PC (3).

Atoms D, H, A	Bond lengths D, H [Å]	Bond lengths H, A [Å]	Bond lengths D, A [Å]	Angles D, H, A [°]
N3-H1-O4 ⁱ	0.86(4)	2.19(4)	2.971(4)	148(3)
N3-H1-O5 ⁱ	0.86(4)	2.56(4)	3.339(3)	149(3)
N3-H2-N1 ⁱⁱ	0.93(4)	2.37(4)	3.221(3)	150(3)
N3-H2-O3 ⁱⁱⁱ	0.93(4)	2.50(4)	3.023(4)	114(3)
N3-H2-O5 ⁱⁱⁱ	0.93(4)	2.57(4)	3.147(3)	119(3)
N4-H3-O1 ^{iv}	0.91(4)	2.70(4)	3.312(3)	124(3)
N4-H3-O2 ^v	0.91(4)	2.48(3)	3.147(3)	130(3)
N4-H3-O2 ^{vi}	0.91(4)	2.21(4)	2.983(3)	141(3)
N4-H4-O2 ^{viii}	0.95(3)	2.00(3)	2.847(3)	146(3)
N4-H4-O3 ^{vii}	0.95(3)	2.83(3)	3.245(3)	107(2)
N4-H4-O4 ^{vi}	0.95(3)	2.50(3)	3.000(3)	112(2)
N2-H5-N1 ⁱⁱ	0.88(3)	2.47(3)	3.164(3)	135(2)
N2-H5-O2 ^v	0.88(3)	2.25(4)	2.936(3)	134(3)

(i) $1+x, -1+y, z$; (ii) $-0.5+x, -0.5-y, z$; (iii) $0.5+x, -0.5-y, z$; (iv) $-0.5+x, 0.5-y, z$; (v) $0.5-x, -0.5+y, 0.5+z$; (vi) $0.5-x, 0.5+y, 0.5+z$; (vii) $1-x, -y, 0.5+z$; (viii) $1-x, 1-y, 0.5+z$; (ix) $0.5+x, 0.5-y, z$.

Figures 23 and 24 show the orientation of the ions in the crystal along a-, b- and c-axis. In figure 19 (left) the DAOdH⁺ ions are stacked and cations as well as the anions form bands along the a-axis which are looking opposite directions. In figure 24 the band along the b-axis are wave like and contrariwise while the perchlorate intercalate.

**Figure 23.** View along a-axis of DAOdH-PC (3).

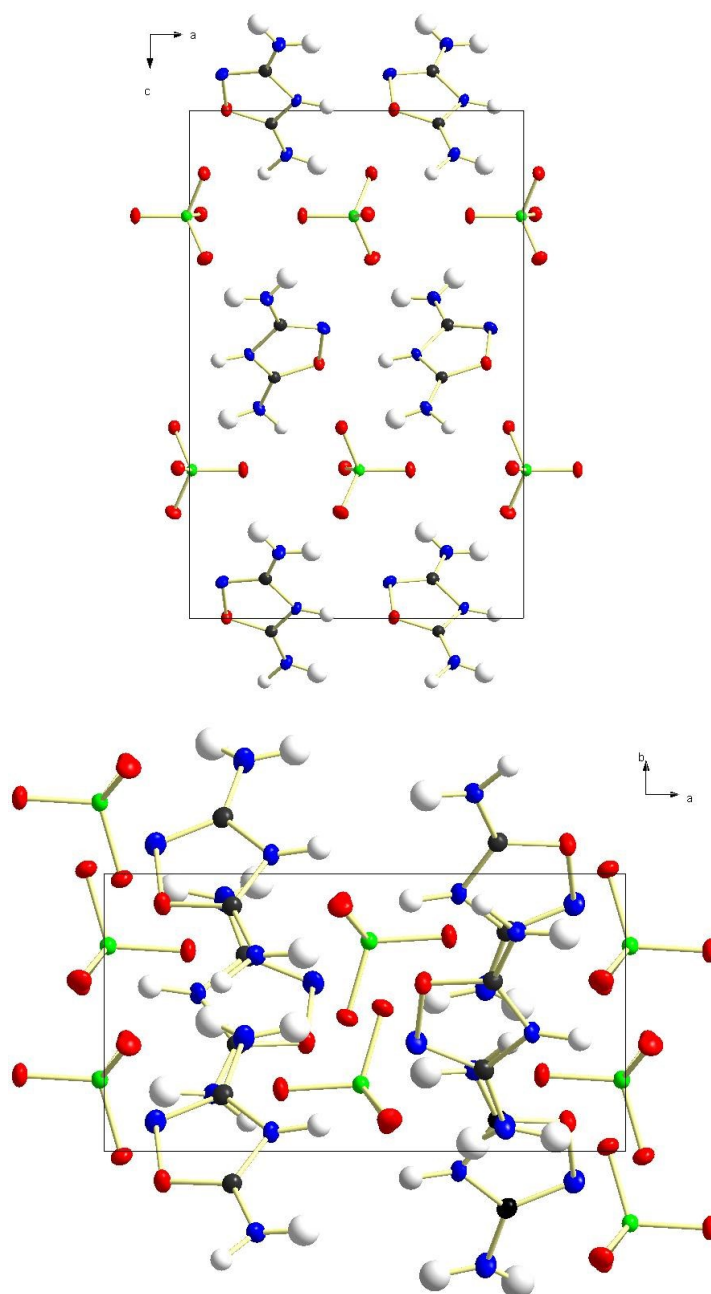


Figure 24. View along b-axis (left) and along c-axis (right) of **3**.

ENERGETIC PROPERTIES

The impact sensitivity of compound **3** is determined with 8 J, the friction sensitivity with >168 N. The value for electrostatic discharge was not determined. The investigation by DSC displays two decomposition points one at 125°C and another 355°C.

The calculated value (at CBS-4M level of theory) of the enthalpy of formation is -392 kJ kg^{-1} and the theoretical maximum density of the crystal structure with 1.991 g cm^{-3} . Calculation of the detonation parameters was not possible as the used software EXPL05 v5.02^[14,18] cannot cope with chlorine containing compounds. The performance data can be estimated to be similar to compound **4** which has nearly the same enthalpy of formation and a very high density.

2.2.4 3,5-Diamino-1,2,4-oxadiazolium picrate (4)

The synthesis of compound **4** was carried out by reacting picric acid in methanol. The formed product was a yellow powder which is soluble in polar solvents like acetone and DMSO. Crystals suitable for SC-XRD were obtained from acetone.

In the IR-spectrum the vibrations of the amino group of DAODH⁺ are recognized and the absorptions of the C5-N7 and the N2-C3 bonds appear at 1710 and 1673 cm⁻¹. At 1533 cm⁻¹ the symmetrical vibration and at 1263 cm⁻¹ the asymmetrical vibrations of the nitro group of the picrate are observed as intense absorptions. The structural vibrations of the aryl moiety are found at 739 and 704 cm⁻¹. In the ¹H NMR-spectrum the DAODH⁺ signals are found according to compound **2** and **3** at 6.33 ppm (amino groups) and 7.46 ppm (protonated ring). Additional at 8.59 ppm the two hydrogen atoms of the picrate is observed, which matches perfectly the literature value with a shift of 8.62 ppm for potassium picrate in DMSO-d₆.^[19] In the ¹³C NMR-spectrum the signal for the DAODH⁺ are found again at 168.0 and 168.8 ppm. The signals for the picrate are observed at 124.1, 125.2, 141.8 and 160.7 ppm are very suitable, compared to the literature values of 124.3, 125.1 141.9 and 160.9 ppm for potassium picrate in DMSO-d₆.^[19] The broad and weak signal at -7 ppm in the ¹⁴N NMR is assigned to the nitro groups of the picrate. The FAB⁺ mass spectrum displays a DAODH⁺ peak at bei m/z = 101.01 and in the FAB⁻ at m/z = 228.0 a peak shows up for the picrate anion.

CRYSTAL STRUCTURE

Single crystals were obtained from water. The compound crystallizes in the orthorhombic space group *Pbca* with eight formula units in the unit cell.

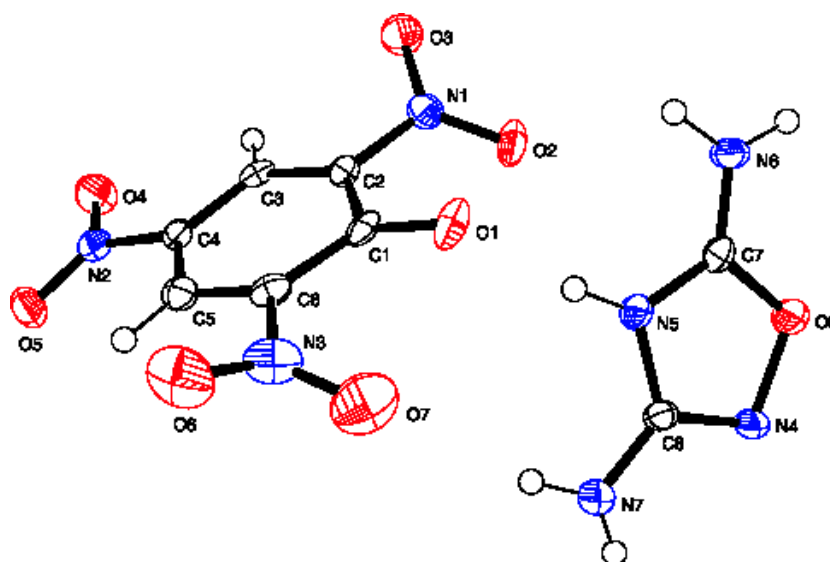


Figure 25. Asymmetric unit of **4**.

The ring planes of both ions are inclined with an angle of 68°, which is displayed in figure 26. The structural parameters of picrate are in the expected range.^[20] The two nitro group in ortho-position are twisted out of plane clockwise and counterclockwise inversely by the same angle. The structural data of DAODH⁺ is listed in table 10. Those

are in good agreement with theoretical calculated values (table 5) as well as for the discussed perchlorate salt.

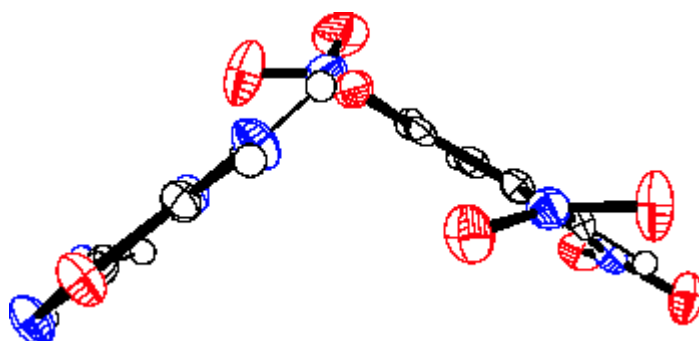


Figure 26. Side view of the two ring planes of the asymmetric unit of **4**.

Table 10. Bond lengths and angles of DAOdH^+ in **4**.

	Bond lengths / Å		Angles / °
d(O8-N4)	1.467	\angle (O8N4C8)	103.7
d(N4-C8)	1.295	\angle (N4C8N5)	112.5
d(C8-N5)	1.378	\angle (C8N5C7)	106.4
d(N5-C7)	1.334	\angle (N5C7O8)	109.8
d(C7-O8)	1.324	\angle (C7O8N4)	107.5
d(C8-N7)	1.340	\angle (N4C8N7)	125.4
d(C7-N6)	1.293	\angle (O8C5N6)	121.8

The shortest distance between both ions of the asymmetric unit is the hydrogen bonding from the hydroxyl group of the picrate to the protonated hydrogen on the ring of DAOdH^+ , which is 1.77(2) Å between oxygen and hydrogen. The found hydrogen bridged bonding are shown in figure 27 and listed in table 11.

Table 11. Hydrogen bonding of **4**.

D-H...A	D-H / Å	H...A / Å	D...A / Å	\angle D-H-A / °
N5-H...O1	0.89(2)	1.77(2)	2.657(2)	172.(2)
N6-H...N4 (i)	0.97(2)	2.02(2)	2.922(2)	154.(2)
N6-H...O1 (ii)	0.95(2)	1.82(2)	2.729(2)	159.(2)
N7-H...O4 (iii)	0.84(2)	2.38(2)	3.105(3)	145.(2)
N7-H...O2 (iv)	0.84(2)	2.49(2)	3.197(3)	143.(2)
(i) 0.5 +x, y, 0.5-z; (ii) 1-x, -0.5+y, 0.5-z; (iii) 1-x, -y, -z; (iv) 0.5-x, 0.5+y, z.				

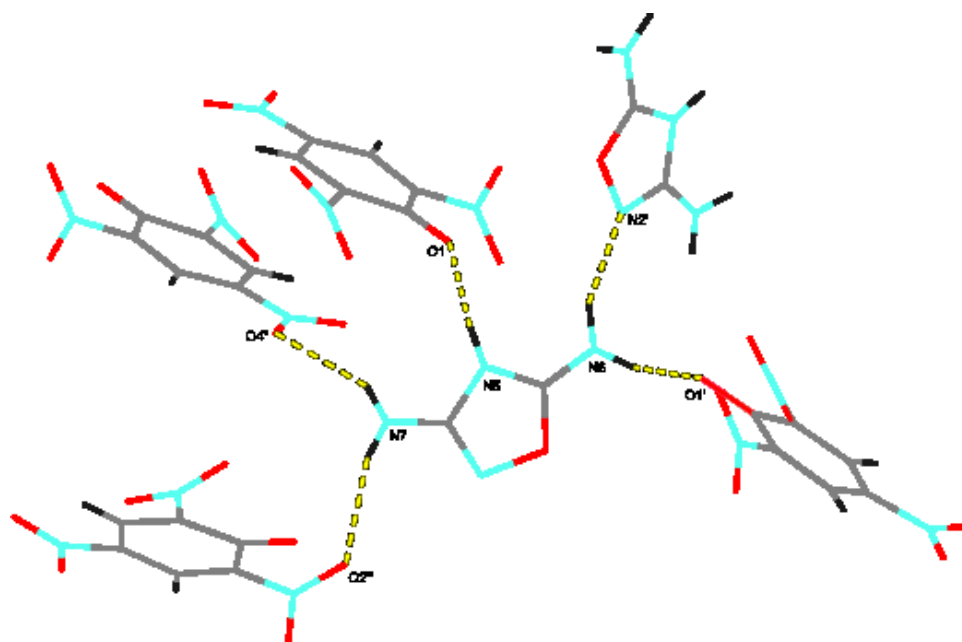


Figure 27. Hydrogen bonds of **4**. For better visualization the thermal ellipsoids were not plotted but a stick model is shown. Hydrogen atoms (black).

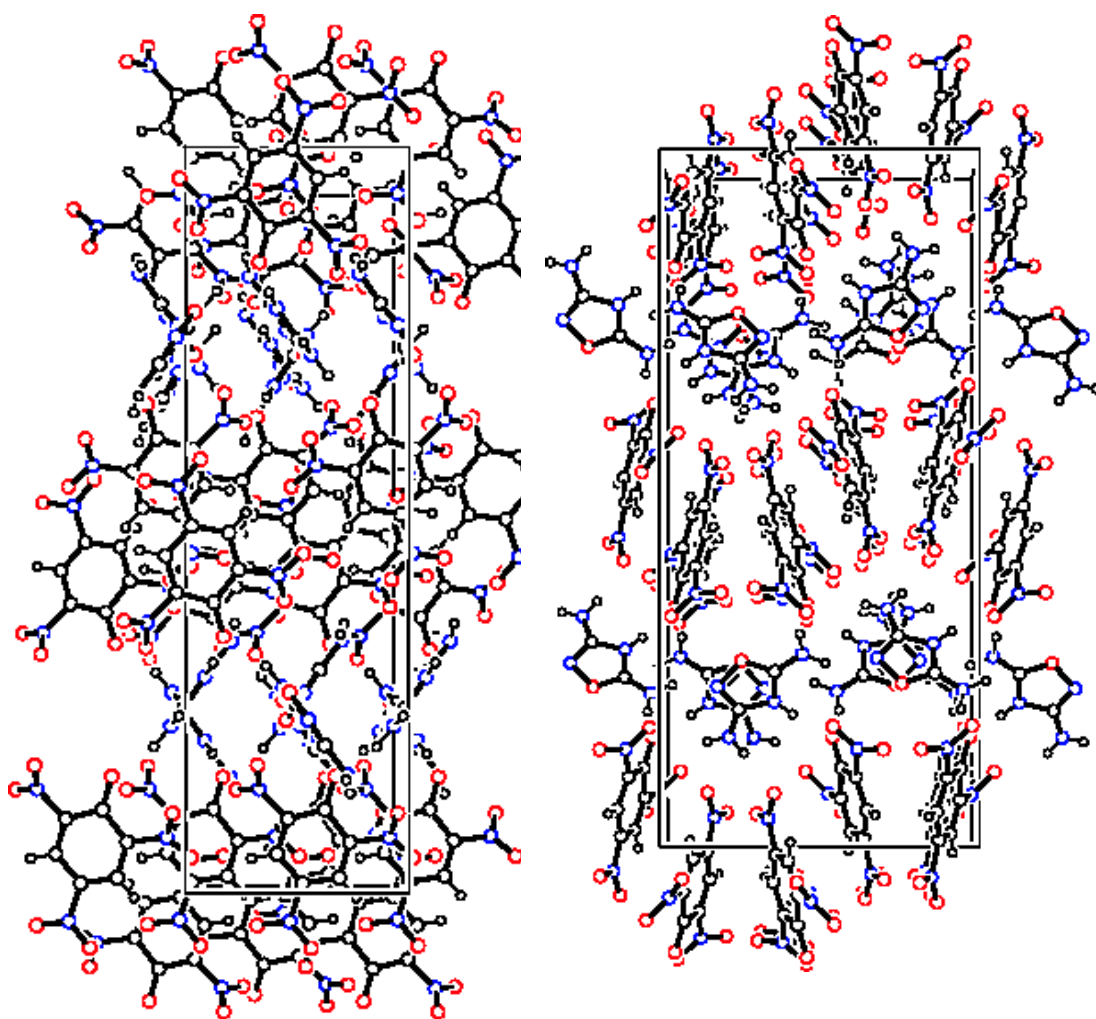


Figure 28. Crystal structure of **4**. View along $[100]$ (left), view along $[010]$. Atoms as balls.

ENERGETIC PROPERTIES

The impact sensitivity of **4** was determined with 20 J the friction sensitivity with >216 N and the sensitivity to electric discharge with >0.1 J. Therefore **4** is sensitive toward impact and friction. The DSC graph displays two decomposition points one at 177°C and the other at 246°C. A melting point was not observed. By bomb calorimetric measurements a mean value of -1495 kJ kg^{-1} for the energy of formation was obtained. Calculation on CBS-4M level of theory resulted in a value of $-301.1 \text{ kJ kg}^{-1}$. The crystal density is 1.787 g cm^{-3} . With these values the detonation parameters were calculated by EXPLO5.02 and listed in table 12.

Table 12. Calculated detonation parameters of **4** compared to 3,4,5-Triamino-1,2,4-triazolium picrate and guanylurionium picrate.

	$\Delta_f U^0 /$ kJ kg^{-1}	$\Omega /$ %	$\rho /$ g cm^{-3}	$Q_v /$ kJ kg^{-1}	$T_{\text{ex}} /$ K	$P /$ kbar	$D /$ ms^{-1}	$V_0 /$ L kg^{-1}
4	$-1495.00^{\text{a)}$	-55.9	1.787	-3593	2957	211	7261	650
4	$-301.10^{\text{b)}$	-55.9	1.787	-4689	3580	250	7751	663
Trz⁺ pic⁻	-1361.5	-62.9	1.746	-3147	2629	189	7017	680

a) experimental; b) calculated

The performance data pass those of TNT but not of RDX. Comparing **4** to similar explosives like the 3,4,5-triamino-1,2,4-triazolium picrate^[20] and the guanylurionium picrate it is slightly better. But the sensitivities are significantly lower than those of TNT and RDX. The high decomposition point of 177°C makes **4** suitable for application.

2.2.5 3,5-Diamino-1,2,4-oxadiazolium dinitramide (**5**)

The compound 3,5-diamino-1,2,4-oxadiazolium dinitramide (**5**) is interesting because of the neutral form of the cation 3,5-diamino-1,2,4-oxadiazole (**1**), which can be reduced at the N-O bond to yield *N*-guanyl urea (**GU**). The explosive formed from **GU** and the dinitraminic acid $\text{HN}(\text{NO}_2)_2$ is the well known FOX-12.^[3]

SYNTHESIS

Starting from **3** the dinitramide salt of **1** was made. First potassium dinitramide (**KDN**) was synthesized (figure 29). The ammonium dinitramide (**ADN**) and potassium hydroxide were solved each in little water and afterwards the solutions were mixed. The white precipitate was filtered and air dried. **KDN** yielded in 98 % colorless crystals. The Raman-spectrum shows the typical absorptions of the nitro functionality at 1514 and 1340 cm^{-1} .

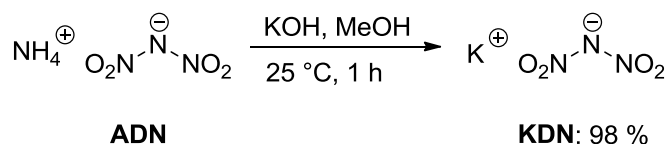


Figure 29. Synthesis of KDN.

The synthesis of 3,5-Diamino-4*H*-1,2,4-oxadiazolium dinitramide (DAOdH-DN, **5**) was performed according to the preparation of Klapötke, Stierstorfer *et. al.* [21, 22a] for 5-

aminotetrazolium dinitramide and also by Martin and Klapötke^[22b] for the 3,5-diamino-1,2,4-triazolium dinitramide where the respectively perchlorate salts were reacted with potassium dinitramide to form the product and poor soluble potassium perchlorate. After filtration of potassium perchlorate and solvent evaporation the obtained solid was recrystallized from ethanol. **5** was gained as yellow crystalline solid of 54 % yield (figure 30).

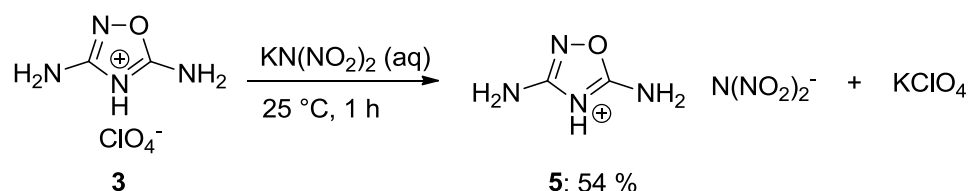


Figure 30. Synthesis of DA0dH-DN(**5**).

The resulting product was a colorless powder which solves easily in water, ethanol and DMSO.

CHARACTERIZATION

In the IR-spectrum the asymmetric in phase and symmetric out of phase nitro stretching vibrations as well as the asymmetric stretching vibration for the N3 unit of the dinitramide are found at 1520, 1175 and 1011 cm^{-1} as strong absorptions.^[23] The amine vibrations of the cation are in the common region and also the characteristic stretching vibration at (C5-N7) and 1666 cm^{-1} (N2-C3). In the FAB⁺ mass spectrum indicates the DA0dH⁺ peak at $m/z = 101.1$, but potassium at $m/z = 39.0$ was also found with a relative intensity of 10%. The FAB⁻ mass spectrum shows the dinitramide at $m/z = 106.0$ and left perchlorate at $m/z = 99.0$ with a relative intensity of 2 %.

In DSC measurements there were observed two decomposition points one at 100 °C and the other at 172 °C. The elemental analysis shows impurities potentially of potassium dinitramide or potassium perchlorate, which explain to decomposition points.

As the elemental analysis and the mass spectrum indicate compound **5** is still a mixture with a significantly higher amount of potassium than perchlorate, which is a hint for impure potassium dinitramide.

ENERGETIC PROPERTIES

Due to the impurities the standard enthalpy of formation was only calculated at CBS-4M level of theory to be 371.06 kJ kg^{-1} . The density of the unpurified substance was experimental determined to be 1.93 g cm^{-3} . As that value seems to be incredibly high and the impurity of potassium perchlorate and potassium dinitramide adulterate the results, for the calculation of the detonation parameters a density of 1.78 g cm^{-3} was estimated. This value was chosen because it is expected to be in the range of FOX-12 with a density of 1.7545 g cm^{-3} . The explosive properties are listed in the table below.

Table 13. Comparing the calculated detonation parameters of 5-aminotetrazolium dinitramide with **5** at density of 1.93 gcm⁻³ and a density of 1.78 gcm⁻³.

Compound	$\Delta_f U^0 /$ kJ kg ⁻¹	$\Omega / \%$	ρ / g cm ⁻³	$Q_v /$ kJ kg ⁻¹	$T_{\text{ex}} /$ K	$P /$ kbar	$D /$ ms ⁻¹	V_0 / L kg ⁻¹
5	371.06	-11.6	1.93	-5456	4122	390	9415	809
5	371.06	-11.6	1.78	-5363	4146	323	8824	822
HAT+DN⁻	1813	0	1.856	-6186	4657	384	9429	822

The performance at both densities is relatively good and comparable to those of similar energetic dinitramide compounds, like the mentioned 5-aminotetrazolium dinitramide. The calculated performance data of **5** outnumber FOX-12 ($p = 257$ kbar, $D = 8210$ ms⁻¹, calculated by Cheetah 2.0). This is a result of the additional ring formation energy of the cation in **5**.

Summing up the calculated properties of **5** it is very suitable for application although the synthesis has to be optimized to get rid of all impurities, which were in spite of repeatedly recrystallization still detectable. Therefore no single crystals suitable for x-ray diffraction measurement and bomb calorimetric measurement were obtained.

2.2.6 2.3.6 3,5-Diamino-1,2,4-oxadiazolium-5-aminotetrazolate (**6**)

SYNTHESIS

For the synthesis of **6** first 3,5-diamino-1,2,4-oxadiazolium sulfate (**a**) was made from a reaction of **1** with sulfuric acid and afterwards reacted with barium 5-aminotetrazolate (**b**), which was gained by the reaction of 5-aminotetrazole with barium hydroxide.

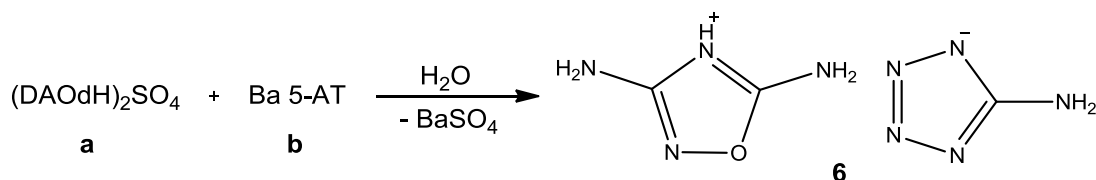


Figure 31. Synthesis of **6**.

Compound **a** is a yellow crystalline solid, which is soluble in polar solvents like DMSO, acetone and water, likewise **b** which is a colorless powder. Product **6** is also a colorless powder and very good soluble in polar solvents like acetone and DMSO.

STARTING MATERIALS

In the IR spectrum of **a** the N-H stretching vibrations are found at 3271 and 3087 cm⁻¹ as broad absorptions and the N2-C3 stretching vibrations at 1647 cm⁻¹ are strong and sharp absorptions. The absorption at 1081 cm⁻¹ is typical for the sulfate.^[19] In the ¹H NMR spectrum there is only one broad signal at 7.72 ppm. In the ¹³C NMR two signals are found at 167.4 and 169.5 ppm. In the FAB⁺ mass spectrum the DAOdH⁺ shows up at $m/z = 101.0$. In the FAB⁻ mass spectrum there is no sulfate but hydrogensulfate could be observed at $m/z = 97.0$. The elemental analysis confirmed a high purity of the compound. The IR vibrational absorptions of **b** are matching well the literature values.^[24]

PRODUCT

The IR-spectrum of **6** shows significantly the amine stretching vibration at 3396, 3326, 3193 and 3106 cm^{-1} , furthermore the characteristic stretching vibrations of DAOdH^+ appear at 1691 (C5-N7), 1636 (N2-C3) and 1457 cm^{-1} (C 3-N4). The stretching vibrations of cyclic C-N-bonds of the 5-aminotetrazolate is at 1587 cm^{-1} and the N-N-N azole vibrations are as sharp absorption at 1264 cm^{-1} . In the ^1H NMR two sharp singletts are observed at 5.57 and 7.24 ppm (DAOdH^+ amino function) and a further broad signal at 6.38 ppm for the amino group of the 5-aminotetrazolate. A signal of an acidic proton is not found. The ^{13}C NMR displays the DAOdH^+ - carbons at 168.6 and 170.2 ppm and the 5-aminotetrazolate carbon at 156.9 ppm. In the FAB^+ mass spectrum DAOdH^+ is found at $m/z = 101.0$ and in the FAB^- mass spectrum the 5-amino-tetrazolate at $m/z = 84.0$.

ENERGETIC PROPERTIES

The impact sensitivity of **6** was determined with >50 J, the friction sensitivity with >192 N and the sensitivity towards electric discharge with >0.3 J. So **6** is insensitive towards impact and sensitive towards friction. The melting point was observed in the DSC measurement at 130°C (onset) and a decomposition point at 170°C (onset). The energy of formation was calculated at CBS-4M level of theory to be about 4034 kJ kg^{-1} and the experimental density of 1.72 g cm^{-3} was measured by pycnometer. The EXPL05 calculated detonation parameters are listed in table 14.

Table 14. Calculated detonation parameters of **6**.

$\Delta_f U^0 / \text{kJ kg}^{-1}$	$\Omega / \%$	$\rho / \text{g cm}^{-3}$	$Q_v / \text{kJ kg}^{-1}$	T_{ex} / K	P / kbar	D / ms^{-1}	$V_0 / \text{L kg}^{-1}$
4033.99	-73.5	1.72	-5776	3719	348	9382	802

A literature known similarly insensitive compound ($E_d > 60$ J) is the hydrazinium 5-aminotetrazolate (HzAT).^[25] With a density of 1.55 g cm^{-3} and a $\Delta_f U^0$ of 3424 kJ kg^{-1} it shows a detonation velocity of $D = 8786\text{ ms}^{-1}$. As the detonation parameters in the publication were calculated by Cheetah 4.0^[26,27], the calculation was repeated with the EXPL05 code, which resulted in a heat of detonation of -4295 kJ kg^{-1} and a detonation velocity of 9516 ms^{-1} .^[28] Both compounds **6** and HzAT have in common that despite of a low oxygen balance they display good performance values, but also are due to there low sensitivities bad ignitable / detonable.

2.2.7 3,5-Diamino-1,2,4-oxadiazolium-5-nitrotetrazolat (**IX**)

The attempt to synthesize **IX** was prepared according to the synthesis of 5-amino-1,4-dimethyltetrazolium 5-nitrotetrazolate.^[29] The reaction of **1** with ammonium 5-nitrotetrazolate hemihydrates was carried out in methanol under slightly warming and nitrogen flux. The result after removing an unsolved component and the solvent was a colorless solid.

For the evaluation of the IR-spectrum a calculated spectrum at B3LY level of theory with increased basis set (aug-cc-pVDZ) and the experimental data of J. Welch were taken in account.^[30] The absorption at 1552 cm^{-1} is found to be the asymmetric stretching vibration of the nitro group, at 1447 cm^{-1} the asymmetric N1-C5-N4-

vibration, at 1417 cm^{-1} the combined symmetric *in phase* and at 1318 cm^{-1} the *out of phase* stretching vibration of the nitro and the N1-C5-N4-unit.

The absorptions are like in the literature sharp and strong, except the one at 1318 cm^{-1} which is only medium. Also an asymmetric tetrazole stretching vibration at 1182 cm^{-1} was identified as well as the combined symmetric *in phase* stretching vibration of the nitro and the tetrazole moiety at 1166 cm^{-1} . The last recognizable vibration at 834 cm^{-1} is the combined in phase deformation vibration of nitro- and N1-C5-N4 vibration. The vibrations of DAODH⁺ are only little observable.

Certainly identifiable were only the symmetric stretching vibrations of the N7 amino group which are at 3394 cm^{-1} very strong and sharp visible. The absorption at 3264 and 3318 cm^{-1} are also vibrations of the amino group, the one at 3264 cm^{-1} is most probably of ammonium (3255 cm^{-1} a very strong in ammonium dinitramide^[23]). The stretching vibrations of the C5-N7 moiety is observed as expected at 1691 cm^{-1} , the N2-C3 moiety at 1618 cm^{-1} . The vibrations of the C3-N4-unit at 1464 cm^{-1} are completely covered by the 5-nitrotetrazolate vibration of 1447 cm^{-1} . In the ^1H NMR spectrum two amino group of DAODH⁺ are found as sharp singlets at 5.57 and 7.24 ppm, the fifth hydrogen atom is not noticeable as well as in **6**. In the ^{13}C NMR spectrum only carbon signals of DAODH⁺ at 168.6 and 170.2 ppm are observed while the carbon of the 5-nitrotetrazolate at 169.5 ppm^[29] is not found. In the ^{14}N NMR spectrum a sharp signal at -354 ppm for ammonium and at -16 ppm for the nitro functionality and one broad signal at -54 ppm for the ring nitrogen of 5-nitrotetrazolate and strong broad signal at 29 ppm also ring nitrogen atoms. In the FAB⁺ mass spectrum the DAODH⁺ the $m/z = 101.0$ is observed and also 5-nitrotetrazolate at $m/z = 114.0$ in the FAB⁻ mass spectrum

The synthesis of the compound has worked so far but a lot of ammonium is still contaminating the product. As the acid strength of the ammonium is not strong enough to protonate **1**, another synthetic route according to **6** starting with **a** and barium nitrotetrazolate would be more effective and result in pure product.

2.2.8 3,5-Diamino-1,2,4-oxadiazolium-5,5'-azotetrazolate (**X**)

For the synthesis of **X** 3,5-diamino-1,2,4-oxadiazolium chloride (**c**) was made and reacted with the sodium 5,5'-azotetrazolate pentahydrate in methanol, to precipitate sodium chloride.

STARTING MATERIAL

The IR-spectrum of **c** shows strong absorptions in the area of the N-H vibrations, whereas the N6-H2 stretching vibration at 3062 cm^{-1} is the strongest. Also the stretching vibrations of C5-N7 and N2-C3 at 1710 and 1655 cm^{-1} are observed. In the ^1H NMR of **c** one broad signal shows up at 8.42 ppm and in the ^{13}C NMR there are two signals at 166.7 and 169.2 ppm. In the FAB⁺ mass spectrum the DAODH⁺ peak at $m/z = 101.0$ is observed as well as in the FAB⁻ mass spectrum the chloride at $m/z = 35.0$. The elemental analysis confirms a high purity of **c**.

CHARACTERIZATION

The vibrations of the amino group at 3397 and 3120 cm^{-1} , the stretching vibrations of the C5-N7, N2-C3 and C3-N4 moiety at 1694, 1620 and 1458 cm^{-1} and the ring stretching vibration at 1577 cm^{-1} of DA0dH⁺ are significantly observable. But there are not even traces of tetrazolate or 5,5'-azotetrazolate vibrations in the spectrum. In the mass spectral investigation only the $m/z=101.0$ of DA0dH⁺ in FAB⁺ and in FAB⁻ $m/z=35$ of chloride are found. There are little peaks of 8 to 15% at $m/z=99.1$, 109.0 and 188.1 which have no connection to the product.

DA0dH⁺ possibly is too acidic, so that the 5,5'-azotetrazolate is protonated and decomposes due to the great instability of the free acid – 5,5'-azotetrazole. Usually 5-azidotetrazole is formed but was not found in the mass spectrum also no other degradation products were observed. An alternative synthesis would start from the sulfate salt (**a**) and barium 5,5'-azotetrazolate, analogous to compound **6**.

2.2.9 3,5-Diamino-4-methyl-1,2,4-oxadiazolium iodide (XI)

The methylation of **1** to obtain an aprotic cation, which can be converted by exchange of the anion to any energetic salt without problems of the acidity of the cation, was done. The methylation reagent used was methyl iodide. The advantage of this methylation reagent is the high reactivity and the anion iodide can easily react with any energetic silver salt to form a highly stable silver iodide which can be separated easily from most solvents.

The attempt to synthesize **XI** was carried out according to the preparation of 5-amino-1,4-dimethyl-tetrazolium iodide.^[34] But the test of precipitate as well as the product on iodide with silver nitrate was negative. An IR-spectrum showed two strong vibrations at about 3200 cm^{-1} and on broad absorption around 1600 cm^{-1} and a slight absorption around 1350 cm^{-1} which all refer to water with little of **1**.

As the reaction went wrong, a possible alternative would be the synthesis in another solvent or with other amounts of **1** and methyl iodide or other reaction times.

2.3 Synthesis of complex bond 3,5-diamino-1,2,4-oxadiazole (7)

To furnish a copper complex **1** was solved in little water and some copper nitrate solution was added. The blue copper aqua complex disappeared, and a green solution was gained. After removing the solvent carefully until crystallization starts and a green solid was collected that refused to get analyzed by Raman spectroscopy ($P=300\text{ mW}$, nm) through decomposition. The IR spectrum shows characteristic absorptions at 3388 cm^{-1} (N-H valence vibrations), 1690 cm^{-1} (C=N valence vibrations) and 1634 cm^{-1} (NH₂-torsion vibrations). The absorption at 1250 cm^{-1} (N-O valence vibration) for a nitrate was not identified because of other strong absorption around this area. A single crystal could not be obtained.

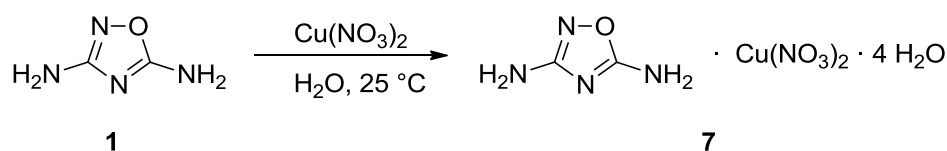


Figure 32. Synthesis of the copper complex of DAOd (7).

The elemental analysis shows that a monomer of the copper complex consists of one **DAOd** molecule, one copper ion, two nitrate ions and four water molecules. The copper(II)-ion has a d^9 -electron configuration and normally forms a Jahn-Teller distorted octahedral complex. As there are no single crystals available for analysis, the complex structure is unknown and some presumptions can be made relying on the actual data basis. A ligand coordinates with its most nucleophilic or best Lewis basic atom on the central metal cation. Crystal structure of **4** (shows that **DAOd** is protonated on N2 (or ring position 4), which makes it possible that N2 is the preferred atom to coordinate on the copper(II) ion. The presumption for the complex is that two nitrate ions in bottom and top position of an octahedral and the **1** over N2 and N3 of N4 and two water molecules as counter parts in the plane coordinate to Cu^{2+} center. Whereas the other two water molecules only form hydrogen bonds to connect the complex momomers.

2.4 Diazotation reaction of 1 by sodium nitrite (i)

It was tried to diazotize compound **1** with and equimolar amount of sodium nitrite in diluted hydrochloric acid. A yellow powder was obtained which only solved in DMSO, DMF and 2M sodium hydroxide solution. In concentrated sulfuric or nitric acid decomposition is observed by foaming and evolution of gas during addition.

2.4.1 Characterization

The IR-spectrum displays significantly the presence of amino functionality by transmission bands at 3457, 3393, 3315 and 3216 cm^{-1} . Also in the area of C-N and C-O valence vibrations some sharp and strong signals are observed. The ^1H NMR-spectrum shows four peaks with an integral ratio of 2:1:1:1 at 7.27, 7.54, 7.76 and 9.19 ppm. In the ^{13}C NMR four signals at 152.1, 154.5, 155.0 and 155.8 ppm are found. Due to the fact that the molecule consists of five hydrogen (NMR-integrals) and four carbon atoms (NMR-signals), a first structural estimation would be two unsymmetrical connected 1 over one amine group. The molecular mass of 183.13 g mol^{-1} does not exactly meet the observed mass $m/z=185.1$ in the mass spectrometry (DEI^+). But a ring opening of one ring at the N-O bond additional 2 hydrogens could be applied resulting in a mass of 185.14 ppm (see figure 33) In contrast to that in the elemental analysis 19.60 % carbon, 3.66 % hydrogen and 45.44 % nitrogen were found. The theoretical calculation of the ring opened molecule's composition results in 25.95% carbon, 3.81% hydrogen and 52.96% nitrogen. The calculation the other way round leads with a mass of 185 and considering the elemental analysis to a sum formula of $\text{C}_3\text{H}_7\text{N}_6\text{O}_4$ (19.60 % = 36.26 $\text{g mol}^{-1} \sim 3 \text{ C}$, 3.66 % = 6.7 $\text{g mol}^{-1} \sim 7 \text{ H}$, 45.44 % = 84.06 $\text{g mol}^{-1} \sim 6 \text{ N}$, $>58 \text{ g mol}^{-1} \sim 3.6 \text{ O}$) which does not match with the NMR spectroscopy anyway. Also

water which could have led to a discrepancy in the elemental analysis was not present regarding the ^1H NMR.

In the mind from the IR-spectrum having amino functionality in the molecule it was reacted with different strong acids in stoichiometrical amounts. The perchlorate and nitrate were obtained by adding **i** to the corresponding acid and removing the solvent. The dinitramide salt was obtained according to the metathesis reaction of **5**. In the ^1H NMR was the absence of the signal at 7.27 ppm observed and an acidic proton at 10.19 ppm in the perchlorate salt appeared neither the nitrate nor the dinitramide salt showed that peak. While in the nitrate salt the integral ratio of 1:1:1 of the remaining signals did not change, the other two salts showed a signal ratio of 4:4:3:1 at 7.60, 7.76, 9.33, 10.18 ppm. The lower or nearly absent intensity of the acidic proton leads to a high acidity of the proton and fast exchange processes. The ^{13}N NMR shows nearly unchanged signals comparing to the neutral species. In the ^{14}N NMR the signals of nitrate at -2 ppm and dinitramide (at -5 ppm) were observed according to the corresponding salts. The FAB⁺ mass spectrum showed the expected signals with low intensity at $m/z = 186.2$ (perchlorate) and 186.1 (nitrate). The three anions were observed significantly in the FAB⁻-mass spectrum.

It was tried to obtain single crystals of the neutral compound **i** which always happened to precipitate as powder and also of the salts which only formed very small, acicular and coadunate crystals which were not suitable for measurement. That is why the structural identification was not possible.

2.4.2 Energetic properties

Compound **i** has a high melting point of 192°C with subsequently decomposition.

For the perchlorate and dinitramide salts sensitivity data was determined with an impact sensitivity of >10 J and >15 J, a friction sensitivity of >360 N and >288 N and a sensitivity to electrostatic discharge of >0.15 J and >0.05 J.

2.4.3 Conclusion

In figure 33 two supposed structures are displayed. While the left structure would match the NMR results, the mass spectrometry and the acidic salts would corroborate the right structure. The elemental analysis does not correspond to either of them.

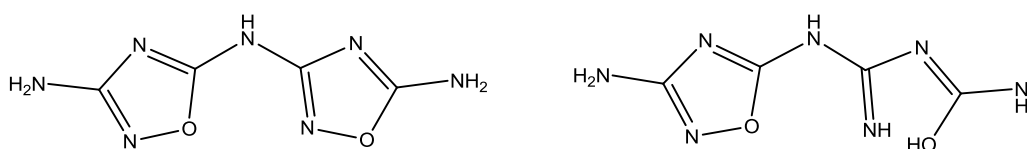


Figure 33. Possible structures of **i**.

2.5 Oxidation and Nitration of 3,5-diamino-1,2,4-oxadiazole (**1**)

The the oxidation of **1** with different oxidation agents was investigated. Foremost the oxidation agents were tested which were used successfully on 5-aminotetrazole (5-AT) and diamino furazane (DAF) to form nitro compounds. The mixtures include sodium

nitrite (ii-iv), sulfuric acid and hydrogenperoxide with ammonium peroxodisulfate (v) and potassium permanganate (vi). Furthermore standard oxidizers like ammonium dichromate (vii) and bromine (viii) were tried.

GENERAL

As mentioned before the goal was to oxidize the amino group to a nitro function. Figure 33 displays a short overview of the possible and desired products. Also the expected m/z -value is given. As there is a fragmentation possible due to used method (DEI⁺), the most probable leaving groups are nitrous acid (m/z 47.01), ammonia (m/z 17.03) and the nitronium cation or gaseous nitrogen dioxide (m/z 46.01). In table 2.3 the procentual composition of the oxidation product is listed.

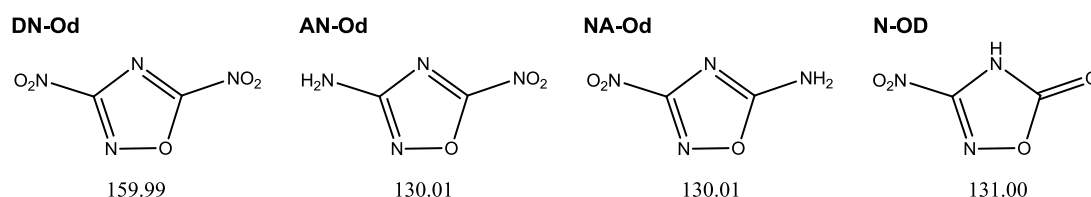


Figure 34. Supposed oxidation products of **1** including m/z -value.

Table 15. Constitution of different oxidation products of **1**.

	DN-Od	AN-Od	N-Od
carbon / %	15.01	18.47	18.33
hydrogen / %	—	1.55	0.77
nitrogen / %	35.01	43.08	32.06

Additionally NMR spectra (¹H, ¹³C and ¹⁴N) of the possible products (DN-Od, AN-Od and N-Od) were determined by quantum-chemical calculation at MPW1PW91 level of theory with a complex basis set (aug-cc-pVDZ) (table 16).

Table 16. Quantum chemical calculated NMR shifts of the supposed oxidation products of **1**.

	DN-OD	AN-OD	N-OD
nucleus	δ / ppm		
¹ H	--	3.99	7.65
	--	4.14	
¹³ C	167.0	167.9	154.5
	169.1	168.4	158.5
¹⁴ N	149	331	264
	27	156	34
	25	60	33
	22	22	

The oxidation of **1** was carried out under various conditions. An overview of the methods and conditions are given in figure 35 and table 17.

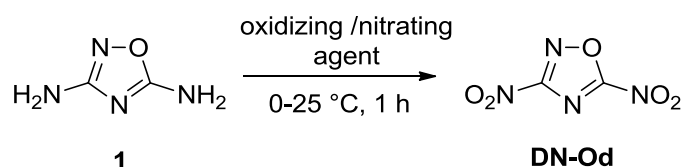


Figure 35. Oxidation or nitration of DAOD (**1**).

Table 17. Various conditions for the oxidation von DAOD (**1**).

Nr.	Oxidizing agent	Quantity (oxidizer)	m (DAOD)
2.2.1	HNO ₃ (100 %)	3 mL	200 mg
2.2.2	HNO ₃ (100 %) / H ₂ SO ₄ (konz.)	1.5 mL / 1.5 mL	200 mg
2.2.3	NaNO ₂ / HCl (aq)	2.78 g	2000mg
2.2.4	H ₂ SO ₄ (konz.) / H ₂ O ₂ (30 %) / (NH ₄) ₂ S ₂ O ₈	12.5 mL / 53.0 mL / 26.8 g	1000 mg
2.2.5	NaOH (15 %) / KMnO ₄ (aq)	4.00 mL / 1.00 g	1000 mg
2.2.6	(NH ₄) ₂ Cr ₂ O ₇	2.52 g	2000 mg
2.2.7	Br ₂ (aq)	1 mL	2000 mg
2.2.8	a) EtOCOCl, 1 ; b) HNO ₃ / Ac ₂ O		1000 mg

2.5.1 Oxidation or nitration with HNO₃ (100 %)

Nitric acid (100 %) was cooled with ice and **1** was added carefully. The reaction mixture was stirred for one hour and poured into ice water. The water mixture was extracted with dichloromethane. The combined organic layers were dried over sodium sulfate and the solvent was removed. A brown oil was obtained.

2.5.2 Oxidation or nitration with HNO₃ (100 %) and H₂SO₄ (conc.)

To nitric acid (100 %) was carefully added sulfuric acid under ice-cooling and stirring. **1** was added to the mixture in small amounts. The reaction was stirred for an hour and finally poured into ice-water. The procedure of a) was applied to obtain the product, a brown oil.

RESULTS

The products of the two reactions were analyzed. The result was that none of those reactions led to the desired product, but a bunch of unidentifiable decomposition products were formed.

2.5.3 Oxidation or nitration by sodium nitrite (ii-iv)

First **1** was tried to exchange the amino groups with sodium nitrite in hydrochloric acid to gain the 5-amino-3-nitro-1,2,4-oxadiazole or the 3,5-dinitro-1,2,4-oxadiazole.^[32] In the first try **1** was solved in hydrochloric acid and a sodium nitrite solution (two equiv.) was added. The NMR spectroscopy of the yellow solid only showed exact the same peaks as **i**.

The second try was carried out by solving **1** in hydrochloric acid an adding this solution carefully to an ice cooled sodium nitrite (two equiv.) solution. But it the reaction outcome resulted in **i** again.

To overcome the reaction to **1** there could be used a large excess of the sodium nitrite solution (10 equiv.) or a more diluted hydrochloric acid solution of **1**. Also the exchange of the acid to acidic acid or sulfuric acid could lead to other results.

The last tried method was analogous to the nitration of 5-amino tetrazole to the ammonium 5-nitro tetrazolate. This was done by sodium nitrite and copper sulfate in solution to which a sulfuric acid mixture of **1** was added. To avoid the cooking in strong bases like it was done in the original preparation to get rid of the copper. The procedure was changed to precipitate the copper by hydrogen sulfide. The resulting green solution was extracted with ethylacetate but no product was isolated thereof.

2.5.4 Oxidation with H₂SO₄ (conc.), H₂O₂ (30 %) and (NH₄)₂S₂O₈ (v)

Novikova *et al.* investigated the oxidation of aminofurazanes to nitrofurazanes by mixtures of hydrogen peroxide, sulfuric acid and different additional ingredients.^[33] As furazanes or better 1,2,5-oxadiazoles are similar to 1,2,4-oxadiazoles it was tried to apply the same methods on **1**. As there was no way to extract any product from the reaction mixture, the aqueous phase was neutralized by potassium hydroxide. Colorless crystals could be obtained.

CHARACTERIZATION

The observed absorptions in IR-spectrum two broad at 1262 and 1101 cm⁻¹, one sharp at 1058 cm⁻¹ and two weak at 688 and 614 cm⁻¹ point very clearly out the absence of any product. Also in NMR spectroscopy now signals showed up.

CONCLUSION

The obtained colorless product is only potassium sulfate.

2.5.5 Oxidation by potassium permanganate (vi)

5-Amino-1H-tetrazole can be coupled in alkaline potassium permanganate solution to sodium 5,5'-azotetrazolate. Possibly potassium permanganate is able to oxidize amino groups to nitro groups. But as **1** undergoes a ring opening reaction under strong alkaline conditions, the reaction was performed in hydrochloric acidic solution. As products yellow crystals were obtained, which were soluble in polar solvents.

CHARACTERIZATION

The product **vi** was characterized by IR, NMR-spectroscopy and mass spectrometry. The IR-spectrum shows the presence of an amino group e.g. the valence vibration of N7-H and N6-H bonds of **1** at 3393 and 3313 cm⁻¹. The observed vibration signal at 1692 cm⁻¹ refers to the C5-N5 valence vibration. The characteristic N-O valence bonds of a nitro group, which appear at 1570–1530 cm⁻¹ (ν_{as}) and 1400–1360 cm⁻¹ (ν_{sym}) are not found in the spectrum. A NMR investigation was not possible, as there were no signals observed in the ¹H-, ¹³C- and ¹⁴N NMR not even those of the solvent (DMSO-d₆). The reason for this may be the inclusion of manganese(II) chloride in the product. The analytic team explained the fault by the presence of a ⁵⁵Mn nucleus which is an NMR active nucleus with a nuclear spin of 5/2. although in the mass spectra (DEI⁺) fragment

at 55 was found. The elemental analysis resulted in 6.50 % carbon, 14.46 % nitrogen and 3.26 % which is out of the expected range of any desired product (see table 15).

CONCLUSION

The infrared spectrum shows that either there is starting material left or the oxidation has not really changed much of **1**. Due to the uncommon resistance to NMR spectroscopy and the non-existence of suitable crystals for x-ray measurement the identification of the product was not possible. Finally there has no desired product formed.

2.5.6 Oxidation by ammonium dichromate (vii)

It was investigated if **1** is oxidized by the strong oxidation agent. All obtained products were colorless powders which could not be solved in most and little in some solvents. In concentrated potassium hydroxide solution vii decomposed with evolution of gas.

CHARACTERIZATION

In the IR-spectrum a sharp and strong absorption at 3398 cm^{-1} and a broad absorption at 3178 cm^{-1} indicate the presence of amino functionality. The C=N, C=O region is dominated by some sharp and strong absorption bands. At 1690 cm^{-1} the C5-N7 unit is observed. There were no characteristic absorptions found for nitro groups which normally occur at $1570\text{--}1530$ and $1400\text{--}1360\text{ cm}^{-1}$. The ^1H NMR-spectrum shows four signals at 2.63, 7.06 (broad), 8.36 and 9.61 ppm with an integral ratio of 3:1:2:1. In the ^{13}C NMR-spectrum there are signals at 13.9, 154.2, 154.6, 157.9, 162.0 and 171.9. The 2D-HMQC NMR spectrum shows that the hydrogen signal at 2.63 ppm is related to the carbon signal at 13.9 ppm of a methyl group. The elemental analysis leads to a sum formula of $\text{C}_5\text{H}_7\text{N}_5\text{O}_2$, which is the minimal unit that could be built of the values for carbon 31.06 %, hydrogen 3.70 % and nitrogen 48.36 %. This sum formula corresponds to the NMR results, although one signal is not assignable. In the DEI^+ mass spectrum no signals or fragments of any desired product is observed. In the NMR-spectra impurities of ethanol, diethylether or acetone were definitely excluded.

Further investigation on the functional groups with ninhydrine for primary amines and 2,4-dinitrophenylhydrazine for carbonyl groups were negative, which could be a result of the bad solubility of vii. As these tests are working in traces, the observation of little positive should have been occurred, but that did not.

CONCLUSION

Again an oxidation product was formed which could not be identified. Some hints are given in IR and NMR spectroscopy by the discussed data that the ring system of **1** has been opened and the fragments condensate to different products.

2.5.7 Oxidation by bromine (viii)

The last oxidizing agent was tested the quite uncommon mild bromine in aqueous solution. A yellow powder was obtained.

CHARACTERIZATION

The IR-spectrum displays a broad signal at 3300 cm^{-1} and a sharp absorption at 3179 cm^{-1} . These can be assigned to the N-H valence vibration. The signals in region from 1700 to 1400 cm^{-1} show similarity to those of **1**. But according to NMR-spectroscopy the starting material is not there anymore. The strong signal at 1401 cm^{-1} may be an absorption of a N-O valence vibration of a nitro group. In the ^1H NMR only one signal at 8.37 ppm and in the ^{13}C NMR two signals at 172.2 and 175.2 ppm were observed. In the ^{14}N NMR no signal for a nitro functionality showed up. In the mass spectrum neither mass peak nor fragments of any desired product was found.

CONCLUSION

Summarizing the results of **viii** indicate at least one amino group, no nitro group. The oxadiazole ring seems to be preserved according to the ^{13}C NMR. The little left product did not last for further investigation and were not done since there is no prove for any desired product.

2.5.8 Nitration with HNO_3 (100%) and Ac_2O

In the first step of the nitration **1** was protected with ethyl chloroformate to obtain the diethyl-1,2,4-oxadiazole-3,5-diylldicarbamate (**8**) (figure 36) and subsequently followed by the nitration of **8** in a mixture of HNO_3 and Ac_2O (figure 37). For the nitration 4 mL nitric acid was cooled to 0°C and carefully acetic anhydrate was added. Afterwards 200 mg of **8** were added and stirred for one hour at room temperature. Finally the reaction mixture was poured to ice water, which was extracted by dichloromethane and dried with sodium sulfate. The organic solvent was removed to gain brown oil, which only matched the melting point of **8**.

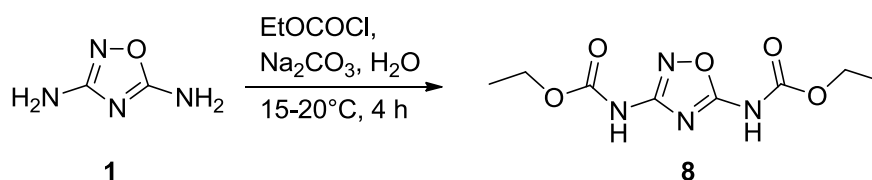


Figure 36. Synthesis of diethyl-1,2,4-oxadiazole-3,5-diylldicarbamate (**8**).

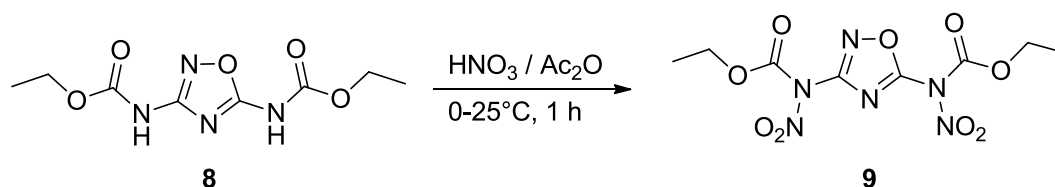


Figure 37. Nitration to the diethyl-1,2,4-oxadiazole-3,5-diylbis(nitrocarbamate) (**8**).

2.6 Energetic Data

The energetic values of all compounds formed in this chapter are summarized in table 18 to give a short overview (figure 38) of the values in comparison.

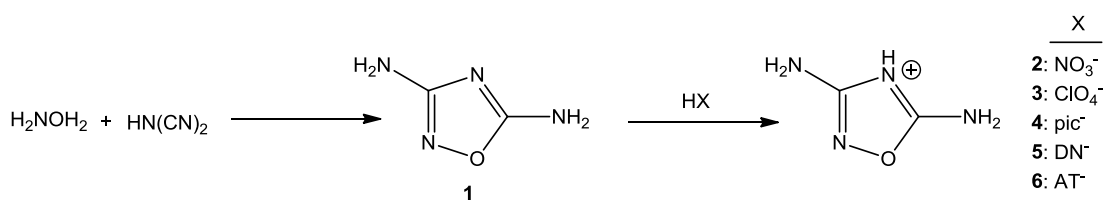


Figure 38. Overview of Synthesized energetic compounds from 3,5-diamino-1,2,4-oxadiazole (1).

Table 18. Calculated detonation parameters by EXPLO5 code and sensitivities of all synthesized compounds.

	2 a)	3 a)	4 b)	4 a)	5 a)	5 a)	6 a)
$T_{\text{dec}} / ^\circ\text{C}$	110	125	177			108	170
$\Delta_f U^0 / \text{kJ kg}^{-1}$	-856	-393	-1495	-301	371.	371	4034
$\Omega / \%$	-24.5	-8.0	-55.9	-55.9	-11.6	-11.6	-73.5
$\rho / \text{g cm}^{-3}$	1.67	1.991	1.787	1.787	1.93	1.78 c)	1.72
$Q_V / \text{kJ kg}^{-1}$	-4418	—	-3593	-4689	-5456	-5363	-5776
T_{ex} / K	3449	—	2957	3580	4122	4146	3719
p / kbar	240	—	211	250	390	323	348
D / ms^{-1}	7878	—	7261	7751	9415	8824	9382
$V_0 / \text{L kg}^{-1}$	819	—	650	663	809	822	802
E_{dr} / J	>40	8	20	20	—	—	>50
F_R / N	>288	≥ 168	≥ 216	≥ 216	—	—	≥ 192
E_{el} / J	>0.24	—	>0.1	>0.1	—	—	>0.3

a) $\Delta_f U^0$ calculated; b) $\Delta_f U^0$ experimental; c) reasonable estimated value

Also the most of the compound show high sensitivities to impact the energetic data of compound 5 and 6 are comparable to RDX regarding detonation velocity. While 2 shows less detonation velocity the same high output of gas volume with over 800 L kg⁻¹ is achieved. For application the decomposition temperatures are very important therefore only 4 and 6 would be in a suitable range. As 5 shows two decomposition points the lower was chosen.

3 Summary and Conclusions

3.1 Summary

The aim of this chapter was the preparation and characterization of new energetic materials and their starting compounds based on 1,2,4-oxadiazole-3,5- diamine (1). Therefore, initially the parent compound itself was presented. The structure has been calculated quantum-chemically at MPW1PW91 level of theory with increased basis set (aug-cc-pVDZ) as well as the vibration and resonance frequencies.

It was possible to synthesize pure 1 (DAOd) and get crystals for x-ray structure analysis. The planar molecule shows only slightly twisted hydrogen atoms out of the molecular plane. The molecules are very stable connected by hydrogen bondings and stacked along the a-axis eclipsedly.

3.1.1 Energetic salts of DAOd

The first topic was the synthesis of energetic ionic compounds of **1**. The attempt of the synthesis of an aprotic cation by methylation with methyl iodide (**xi**) did not work. It was therefore reacted due to its simple and fast reaction with different acids. The cation of these salts, 3,5-diamino-1, 2,4-oxadiazolium (DAOdH⁺), was quantum chemically calculated at MPW1PW91 level of theory and compared with the neutral compound **1**. Overall, in this way, the chloride (**c**), sulfate (**a**), nitrate (**2**), perchlorate (**3**) and picrate salts (**4**) are obtained. Compound **3** was reacted with the potassium dinitramide Dinitramid salt (**5**), with a barium-5-aminotetrazolate to 5-aminotetrazolate salt (**6**). By direct reaction of **1** with ammonium-5-nitrotetrazolate should be made the 5-nitrotetrazolat salt (**ix**). In the resulting colorless, crystalline solid, however, is too much ammonium. From **c** and sodium 5,5'-azotetrazolate was tried to synthesize the 5,5'-azotetrazolate salt(**x**). The resulting orange-colored powder could not be identified beyond doubt, but it can be assumed that the 5,5'-azotetrazolate anion was destroyed during the reaction.

It was possible to analyze by single crystal x-ray defraction measurement the molecular structure of **3** and **4**. The molecule geometry of DAOdH⁺ fits very well with the calculated values and those of perchlorate and picrate are exactly those known from literature.

For their suitability as explosives the compounds with nitrate (**2**), perchlorate (**3**), picrate (**4**), dinitramide (**5**) and 5-aminotetrazolate (**6**) were examined. The standard energies of formation were calculated for this purpose at CBS-4M level. For **4** due to the high purity was also an experimental determination carried out by bomb calorimetry. The calculated EXPL05 detonation parameters are summarized in table 18, just as by the BAM standards determined sensitivities compounds **2**, **3**, **4** and **6**.

The reaction with copper(II) nitrate resulted in a green copper complex (**7**) with a copper cation coordinated in distorted octaeder by one DAOd (**1**), two nitrate and three water molecules. During the Raman spectroscopy at 300 mW the complex decomposes.

3.1.2 Oxidation, Nitration and Diazotation of DAOd.

The diazotation of **1** resulted reproducible in an unindifiable compound (**i**)

The first issue of this chapter was to study the oxidizability of **1** with sodium nitrite (**ii-iv**), sulfuric acid acidified hydrogen peroxide with ammonium peroxodisulphate (**v**), potassium permanganate (**vi**), ammonium dichromate (**vii**) and bromine (**viii**). In the reaction with sodium nitrite in two cases (**ii-iii**) compound **i** can be obtained. In combination with copper sulfate and sulfuric acid solution (**iv**) no product can be obtained. In the other experiments for the oxidation could either be received no product, or not be identified. However in most cases, the oxadiazole ring was probably destroyed.

All experiments to nitrate the DAOd by 100% HNO₃, HNO₃/H₂SO₄, HNO₃/Ac₂O or oxidize by mixtures of H₂SO₄/H₂O₂/(NH₄)₂S₂O₈, NaOH/KMnO₄ were unsuccessful.

3.2 Conclusion and Outlook

Regarding the oxidation of 1,2,4-oxadiazole-3,5-diamine is to say that this compound is very sensitive to strong oxidizing agents. This is likely in comparison to tetrazoles due to the lack of aromaticity of the compound and the easy attackable N-O bond. Only mild oxidants in neutral solution, such as bromine, appear to oxidize the substituents of the ring without destroying it.

The synthesis of protic salts of 1,2,4-oxadiazole-3,5-diamine is much easier and more efficient. The synthesized and investigated compounds have entirely good performance. The dinitramide salt **5** especially stands here out with a detonation velocity of 9000 ms⁻¹. The clean synthesis of the dinitramide salt could be the subject of future work.

Some ideas were omitted because of the high explosive nature of the required starting materials, but on the basis of the obtained results there could be developed even more promising compounds. To be mentioned among these are the salts with the high-energy 5-nitrotetrazolate anion and 5,5'-azotetrazolate whose synthesis by the reaction of a sulfate salt of 1,2,4-oxadiazole-3,5-diamine with the corresponding barium compounds should be quite promising. The synthesis of the methylated compound 3,5-diamino-4-methyl-1,2,4-oxadiazoliumiodid should also be of interest because its reaction with silver salts should be easy and clean-energy lead to salts with anions such as azide and dinitramide.

4 Experimental part

4.1 Common

Yield is given in percentage rounded to full numbers according to the compound with the lowest amount.

Starting compounds were purchased by commercial suppliers at a purity of 99% p.a. and used without further purification. Ammonium-5-nitrotetrazolat hemihydrate, potassium dinitramide, sodium-5,5'-azotetrazolate pentahydrate and picric acid were selfmade compounds and stored in the working group. All solvents are minimum technical grade 85% and were used as purchased.

Minimal pressures were about 10 mbar at the membran pump (MPV) and 1x10⁻² mbar at oil rotation pump (OPV) using glass vacuum apparatus with tubing.

4.2 Analytical apparatus

Infrared spectra of air insensitive samples were taken at a *PerkinElmer* BX FT-IR with a *Smiths DuraSamplIR II* Diamant-ATR-module. The range of the spectra 600–4000 cm⁻¹.

Raman spectroscopy was done on the working group's *Perkin Elmer Spectrum 2000 NIR-FT-Raman*-device with *Perkin Elmer Diode Pumped Nd: YAG-Laser*-light source

For the **nuclear resonance spectra** were used a *Jeol* Eclipse 270, *Jeol* Eclipse 400 and a *Jeol* ECX 400. The measurements were taken in glass NMR tubes (5 mm) and at a

standard temperature of 25°C. The external standards and frequencies of the cores are listed in table 19. As internal standard the literature values of the signals of the completely undeuterated solvents (^1H) as well as the completely deuterated solvents (^{13}C) [34] were used. ^{13}C NMR spectra were, as long as nothing else is mentioned, ^1H decoupled recorded. The evaluation of the data was done with MestReNova[34].

Table 19. NMR-Standards and –recording frequencies.

		Eclipse 270	Eclipse 400	ECX 400
Core	Standard	frequency / MHz		
1 H	Tetramethylsilane	270.17	400.18	399.78
13 C	Tetramethylsilane	67.93	100.63	100.53
14 N	Nitromethane	—	28.92	28.89

Mass spectra were recorded at a Jeol MStation JMS 700. As ionisation methods for normal resolution spectra *direct electron impact* (DEI) and *fast atom bombardment* (FAB) were used. The matrix for FAB-measurements was *para*- nitrobenzylic alcohol.

Elemental analysis was done in the micro analytical laboratory of the department. By combustion analysis with a *Elementar Vario EL* or a *Elementar Vario Micro* the elemental composition of a compound for C, H, N, S, Br, I, Cl was acquired. The results were given in percentages of the respective element.

The **melting point** of compound **1a,c** were determined with a *Büchi* Melting Point B-540 and are uncorrected.

Thermal analysis was recorded by *Linseis* DSC-PT10. A probe of 1-2 mg of the sample substance were confined in a small aluminum container with a 0.1 mm hole in the lid to exhaust vast gas. This probe was measured against a reference of a empty aluminum container with a heating rate of 5°C min⁻¹ and a temperature range of 25-400°C. The acquired temperature was the onset value according to IUPAC agreements.

Sensitivities towards impact, friction and electrostatic discharge were determined.[35] The sensitivity toward impact was recorded according to the STANAG 4489, [36] modified WIWEB 4-5.1.02[37] method by using a BAM drop hammer apparatus. The friction sensitivity was acquired according to the STANAG 4487, [38] modified WIWEB 4-5.1.03 procedure [39] by using a BAM friction apparatus. The compound was classified according to the UN *Recommendations on the Transport of Dangerous Goods*. [40] impact: insensitive > 40 J, low sensitive >35 J, sensitive >4 J, very sensitive <3 J. friction: insensitive > 360 N, low sensitive = 360 N, sensitive <360 N and >80 N, very sensitive < 80 N, extreme sensitive < 10 N. The determination of sensitivity to electrostatic discharge was done by an *OZM Research* ESD 2010 EN.

Density was determined - if a crystal structure of the compound was not available - by a *Quantachrome Instruments* Ultrapyc 1200e gas pycnometer with a sample amount of 50–100 mg.

Bomb calorimetric measurements were carried out by a *Parr* 1356 bomb calorimeter incl. a *Parr* 1755 printer for data output. 70-100 mg of compound were

grinded together with about 1 g of benzoic acid. The homogenous mixture pressed to small pallet and burned in a pure oxygen atmosphere at a pressure of 30 bars. The heat of burning is calculated from the arithmetic average of at least three measurements.

The determination of the **crystal structure** is accomplished by an *Oxford Diffraction Xcalibur 3* with a Sapphire CCD-detector, a four concentric circle kappa platform and Enhance™ Mo-K α -x-ray source with a wave length of $\lambda=71.073$ pm. The structures were solved with SIR92, SIR97^[41], SHELXS97^[7] and refined with SHELXL97^[6] by the method of smallest error square in full matrix referring to F^2 values. The illustrations were created in ORTEP-3^[42] and Diamond 3^[8].

4.3 Calculations

Quantum chemical calculations were executed by the GAUSSIAN^[43] program suite.

To determine the **IR and NMR frequencies** the optimized structures were calculated at MPW1PW91 level of theory with a double zeta basis set (aug-cc-pVDZ) and based on that the vibration and resonance frequencies. To get the standardized NMR-shift the respective standards were also calculated at MPW1PW91 level of theory with a double zeta basis set (aug-cc-pVDZ). The values for tetramethylsilane were in the proton spectrum 31.63 ppm and ^{13}C carbon spectrum 196.64 ppm and for nitromethane in the ^{14}N nitrogen spectrum -116.7 ppm. The respective values of the molecules had to be subtracted from the standard values to get a result that was compared to the experimental data.

To determine the standard energy of formation first the standard enthalpy of formation $H_f^0(M)$ of the molecule and $H^0(A)$ of the relevant atom at CBS-4M level of theory calculated. The standard enthalpy of formation $\Delta_f H^0(A)$ of the hydrogen, carbon, nitrogen, oxygen and chlorine atoms are gathered from literature.^[44] The values are listed in table 20.

Table 20. Literature values of $\Delta_f H^0$ and calculated CBS-4M values H^0 of the atoms (hydrogen, carbon, nitrogen, oxygen and chlorine)

	H	C	N	O	Cl
$\Delta_f H^0 / \text{kJ mol}^{-1}$	217.998	716.68	472.68	249.18	121.301
$-H^0 / \text{a. u.}$	0.500991	37.786156	54.522462	74.991202	459.674576

The standard enthalpy of formation of the molecule in the gas phase can be calculated by the method of the atomization energy.

$$\Delta_f H_g^0(M) = H^0(M) - \sum H^0(A) + \sum \Delta_f H^0(A). \quad (1)$$

To convert the standard enthalpy of formation $\Delta_f H_g^0(M)$ of the gas phase to the solid state in the case of an ionic compound the lattice enthalpy is needed. According to the method of Jenkins the lattice energy of a compound of the type $A_p B_q$ (with $p:q = 1:1, 1:2$ or $2:1$) can be calculated only from its molecular volumes V_M ^[45]. If a crystal structure

analysis of the compound was done the easiest way to get V_M is by dividing the Volume of the unit cell V_{UC} by the count of formular units Z in nm^3

$$V_M = \frac{V_{UC}}{Z}, \quad (2)$$

If a crystal structure of the respective compound is not available, the total molecular volume V_M can be estimated by the by the volume of cation and the anion according to the following equation [46]

$$V_M \approx pV(A^{q+}) + qV(B^{p-}) \quad (3)$$

The lattice energy ΔU_L is calculated by the equation

$$\Delta U_L = |z_+||z_-|v \left[\frac{\alpha}{\sqrt[3]{V_M}} + \beta \right] \quad (4)$$

In this equation $|z_+|$ and $|z_-|$ are the non-dimensional charges of the ions, v the total count of the ions in the compound α and β two constants in $kJ \text{ mol}^{-1}$, which refer to the constitution of the ionic compound. For type AB e.g. $\alpha=117.3 \text{ kJ mol}^{-1}$ and $\beta=51.9 \text{ kJ mol}^{-1}$. The lattice enthalpy is calculated according to equation 5 lattice energy.

$$\Delta H_L(\text{ApBq}) = \Delta U_L + \left[p \left(\frac{n_A}{2} - 2 \right) + q \left(\frac{n_B}{2} - 2 \right) \right] RT \quad (5)$$

Therefore $n_A, n_B = 6$ in the case of a polyatomic non-linear ion. The gas phase enthalpy of formation of the molecule $\Delta_f H_g^0(M)$ is now converted to a standard enthalpy of formation in the solid state $\Delta_f H_s^0(M)$

$$\Delta_f H_s^0(\text{ApBq}) = p\Delta_f H_g^0(Aq+) + q\Delta_f H_g^0(Bp-) - \Delta H_L(\text{ApBq}) \quad (6)$$

The energy of formation ΔU and the enthalpy of formation ΔH of a compound $C_aH_bN_cO_dCl_e$ is connected by the equation

$$\Delta H = \Delta U + \Delta n \cdot RT \quad (7)$$

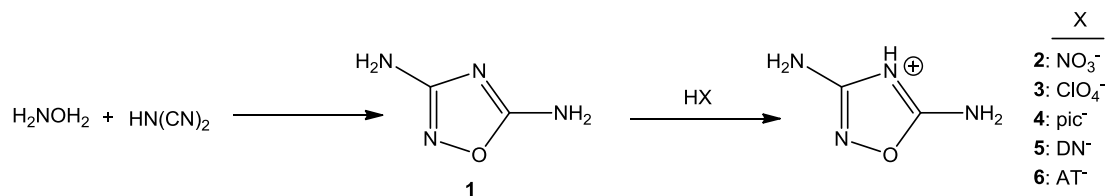
where Δn is the difference of the amount of gaseous components in the equation of formation of $C_aH_bN_cO_dCl_e$ from C, H_2 , N_2 , O_2 and Cl_2 .

The **oxygen balance** Ω of an explosive $C_aH_bN_cO_dCl_e$ with a molecular mass M is calculated under the assumption of a fully oxidation of the elements to CO_2 , H_2O and HCl and N_2 with the following equation.

$$\Omega = \frac{d - (2a) - \left(\frac{b-e}{2}\right)}{M} \times 1600. \quad (8)$$

Parameters of detonation (Q_v , T_{ex} , p and D) was calculated starting from the standard energy of formation $\Delta_f U^0$ and the density ρ of the compound with EXPL05 [14,18] by using BWK-EOS and the BKWN set of parameters.

4.4 Preparation of energetic DAOd (1) and salts thereof



3,5-DIAMINO-1,2,4-OXADIAZOLE (1)

A mixture of sodium dicyanamide (80.00 g, 898.6 mmol) and hydroxylamine hydrochloride (62.46 g, 898.8 mmol) in Methanol (500 mL) was stirred for 40 minutes at room temperature and refluxed for four hours. After cooling the white precipitate (NaCl) was filtered off and the solvent of the filtrate was removed. The product was recrystallized from water and a fluffy colorless solid was obtained (66.24 g, 661.9 mmol, 74 %).

IR: $\tilde{\nu}$ (cm^{-1}) = 3395 (s), 3314 (s), 3173 (s), 3096 (s), 2786 (m), 2724 (m), 2057 (w), 1690 (vs), 1642 (s), 1602 (m), 1577 (m), 1456 (vs), 1362 (m), 1150 (m), 1064 (m), 1000 (w), 887 (w), 799 (m), 760 (m), 688 (m) cm^{-1} . **^1H NMR** ($\text{DMSO}-d_6$): 5.56 (s, 2H, NH_2), 7.26 (s, 2H, NH_2) ppm. **^{13}C NMR** ($\text{DMSO}-d_6$): 168.7, 170.3 ppm. **MS** (DEI^+): m/z = 100.1 (100) [DAOd^+]. **Elemental analysis:** calculated ($\text{C}_2\text{H}_4\text{N}_4\text{O}$), found C 24.00, 23.98; H 4.03, 3.97; N 55.98, 48.47. **m.p.** 167 °C.

DIAMINO-1,2,4-OXADIAZOLIUM NITRATE (2)

1 (3.00 g, 30.0 mmol) was solved in nitric acid (2 M, 15 mL, 30 mmol). The water was removed and a colorless powder was obtained. (4.89 g, 30.0 mmol, 100 %).

IR: $\tilde{\nu}$ (cm^{-1}) = 3525 (m), 3473 (m), 3317 (s), 3171 (s), 3096 (s), 2842 (m), 2806 (m), 2672 (m), 2620 (m), 2545 (m), 2440 (m), 1716 (s), 1660 (vs), 1546 (m), 1419 (s), 1386 (s), 1314 (s), 1121 (m), 1080 (w), 1045 (m), 1007 (m), 864 (m), 818 (w), 780 (w), 744 (m), 674 (m), 654 (w), 616 (w) cm^{-1} . **^1H NMR** ($\text{DMSO}-d_6$): 6.68 (br, 4H, NH_2), 7.62 (br, 1H, NH^+) ppm. **^{13}C NMR** ($\text{DMSO}-d_6$): 167.5, 169.5 ppm. **^{14}N NMR** ($\text{DMSO}-d_6$): -5 (s, NO_3^-) ppm. **MS** (FAB^+): m/z = 101.0 [DAODH^+]. **MS** (FAB^-): m/z = 62.1 [NO_3^-]. **Elemental analysis:** calculated ($\text{C}_2\text{H}_5\text{N}_5\text{O}_4$), found: C 14.73, 14.12; H 3.09, 3.58; N 42.94, 40.82. **DSC:** T_{dec} = 110 °C, T_m = 269 °C. **Sensitivities:** E_{dr} > 40 J, F_r > 288 N, E_{el} > 0.24 J..

3,5-DIAMINO-1,2,4-OXADIAZOLIUM PERCHLORATE (3)

1 (2.50 g, 25.0 mmol) was solved in perchloric acid (1 m, 25 mL, 25 mmol). The water was removed and a slightly yellow crystalline product was obtained (4.73 g, 23.6 mmol, 94 %).

IR: $\tilde{\nu}$ (cm^{-1}) = 3415 (s), 3321 (vs), 3267 (vs), 3168 (s), 2889 (m), 2716 (m), 1714 (s), 1665 (vs), 1566 (m), 1541 (s), 1469 (m), 1396 (w), 1367 (w), 1099 (s), 1064 (s), 1013 (s), 926

(m), 868 (w), 774 (w), 743 (w), 625 (w) cm^{-1} . **Raman** $\tilde{\nu}(\text{cm}^{-1})$, 300mW): 1724 (4), 1617 (6), 1569 (9), 1547 (10), 1400 (23), 1107 (13), 1065 (21), 953 (19), 924 (100), 869 (10), 776 (18), 660 (35), 630 (29), 498 (14), 456 (41), 342 (14). **M.S.**(FAB⁺, m/z): 101.0; (FAB⁻, m/z): 99.0/101.0 (3:1). **¹H NMR** (DMSO-D₆): 6.35 (br, 4H, NH₂), 7.92 (br, 1H, NH⁺) ppm. **¹³C NMR** (DMSO-D₆): 166.7, 169.2 ppm. **Elemental analysis**: calculated (C₂H₅ClN₄O₅), found: C 11.98, 20.02; H 2.51, 2.57; N 27.94, 28.00. **DSC**: $T_{\text{dec}} = 125\text{ }^{\circ}\text{C}$, $T_{\text{dec}} = 355\text{ }^{\circ}\text{C}$. **TMD**: 1.991 g cm⁻³. **Sensitivities**: $E_{\text{dr}} = 8\text{ J}$, $F_{\text{r}} = 168\text{ N}$.

3,5-DIAMINO-1,2,4-OXADIAZOLIUM PICRATE (4)

A suspension of **1** (0.10 g, 1.0 mmol) in methanol (6 mL) was added carefully at 0 °C to a solution of picric acid (0.23 g, 1.0 mmol) in methanol (6 mL). The solvent was removed under reduced pressure at 44 °C and the product dried. A yellow powder was obtained (0.28 g, 0.85 mmol, 85 %).

IR: $\tilde{\nu}(\text{cm}^{-1}) = 3453\text{ (s)}$, 3326 (s), 3164 (s), 3085 (s), 2964 (m), 1710 (s), 1674 (s), 1634 (s), 1620 (s), 1564 (s), 1533 (vs), 1497 (s), 1424 (m), 1362 (m), 1337 (s), 1314 (vs), 1262 (vs), 1160 (s), 1076 (m), 1051 (m), 1009 (m), 938 (w), 925 (w), 914 (m), 873 (w), 788 (m), 739 (m), 704 (m), 660 (w) cm^{-1} . **¹H NMR** (DMSO-D₆): 6.33 (br, 4H, NH₂), 7.46 (br, 1H, NH⁺), 8.59 (s, 2H, Ar-H) ppm. **¹³C NMR** (DMSO-D₆): 124.1, 125.2, 141.8, 160.7, 168.0, 169.8 ppm. **¹⁴N NMR** (DMSO-D₆): -7 (br, NO₂) ppm. **MS** (FAB⁺): m/z = 101.1 [DAODH⁺]. **MS** (FAB⁻): m/z = 228.0 [Pic⁻]. **Elemental analysis**: calculated (C₈H₇N₇O₈), found: C 29.19, 28.94; H 2.14, 2.20; N 29.78, 29.65. **DSC**: $T_{\text{dec}} = 177\text{ }^{\circ}\text{C}$, $T_{\text{dec}} = 246\text{ }^{\circ}\text{C}$. **Sensitivities**: $E_{\text{dr}} = 20\text{ J}$, $F_{\text{r}} = 216\text{ N}$, $E_{\text{el}} > 0.1\text{ J}$.

3,5-DIAMINO-1,2,4-OXADIAZOLIUM DINITRAMIDE (5)

To a solution of **3** (1.84 g, 9.18 mmol) in water (5 mL) was added potassium dinitramid (1.33 g, 9.16 mmol) in water (5 mL) and stirred for 30 min. at room temperature. Ethanol (2.5 mL) was added and stirred for ten minutes more. The mixture was filtered and the solvent of the filtrate was removed under reduced pressure. A colorless powder was obtained (1.66 g, 8.02 mmol, 87 %).

IR: $\tilde{\nu}(\text{cm}^{-1}) = 3426\text{ (s)}$, 3328 (s), 3225 (vs), 3161 (vs), 1713 (s), 1666 (s), 1589 (m), 1520 (vs), 1408 (m), 1326 (m), 1175 (s), 1047 (w), 1011 (m), 866 (w), 820 (w), 773 (w), 758 (w), 742 (w), 727 (w) cm^{-1} . **¹H NMR** (DMSO-D₆): $\delta = 5.44$ (br, 5H), 7.83 (br, 1H, NH⁺) ppm. **¹³C NMR** (DMSO-D₆): 167.1, 169.4 ppm. **¹⁴N NMR** (DMSO-D₆): $\delta = -5$ (s, NO₂) ppm. **MS** (FAB⁺): m/z = 101.1 [DAODH⁺], 39.0 [K⁺]. **MS** (FAB⁻): m/z = 106.0 [N(NO₂)⁻], 99.0 [ClO₄⁻]. **Elemental analysis**: calculated (C₂H₅N₇O₅), found: C 11.60, 11.67; H 2.43, 3.01; N 47.34, 43.27.

3,5-DIAMINO-1,2,4-OXADIAZOLIUM SULFATE (A)

To a suspension of **1** (2.00 g, 20.0 mmol) in water (50 mL) was add carefully at 0 °C sulphuric acid (1 m, 10 mL, 10 mmol). The solvent was removed under reduced pressure and yellow crystals precipitated (1.21 g, 4.06 mmol, 41 %).

IR: $\tilde{\nu}(\text{cm}^{-1}) = 3271\text{ (s)}$, 3087 (s), 1713 (m), 1647 (vs), 1557 (s), 1512 (s), 1339 (m), 1132 (m), 1081 (s), 1042 (s), 970 (m), 812 (w), 757 (m), 683 (w), 665 (w) cm^{-1} . **¹H NMR** (DMSO-D₆) $\delta = 7.72$ (br) ppm. **¹³C NMR** (DMSO-D₆): $\delta = 167.4$, 169.5 ppm. **MS** (FAB⁺): m/z = 101.0 [DAODH⁺]. **MS** (FAB⁻): m/z = 97.0 [HSO₄²⁻]. **Elemental analysis**:

calculated ($C_4H_{10}N_8O_6S$), found: C 16.11, 15.72; H 3.38, 3.45; N 37.57, 36.08; S 10.75, 10.78. **m.p.**: 131 °C.

BARIUM-5-AMINOTETRAZOLATE-TETRAHYDRATE (B)

To a solution of bariumhydroxide-octahydrate (6.31 g, 20 mmol) in water (20 mL) was added a solution of 5-amino-1*H*-tetrazol-monohydrate (4.12 g, 40 mmol) in water (60 mL). The mixture was refluxed for five hours and hot filtered. The solvent of the filtrate was removed and the crude product was washed with ethanol and diethylether. After drying a colorless solid was obtained (5.96 g, 15.8 mmol, 79 %).

IR: $\tilde{\nu}$ (cm^{-1}) = 3395 (vs), 3326 (vs), 3213 (vs), 2362 (w), 1626 (s), 1522 (vs), 1470 (m), 1443 (m), 1376 (w), 1340 (w), 1226 (w), 1157 (w), 1128 (w), 1042 (w), 1013 (w), 877 (w), 852 (w), 794 (w), 751 (w), 683 (w). **Elemental analysis:** calculated ($C_2H_{12}BaN_{10}O_4$), found: C 6.36, 6.72; H 3.20, 3.11; N 37.10, 35.83.

3,5-DIAMINO-1,2,4-OXADIAZOLIUM-5-AMINOTETRAZOLATE (6)

To a suspension of **a** (0.50 g, 1.7 mmol) in water (20 mL) was added **b** (0.63 g, 1.7 mmol) and stirred for 3 hours at r.t. undissolved precipitate was filtered and the solvent was removed. A colorless powder was obtained (0.51 g, 15.8 mmol) Yield: 79 %.

IR: $\tilde{\nu}$ (cm^{-1}) = 3396 (vs), 326 (vs), 3193 (vs), 3106 (vs), 2786 (m), 1691 (s), 1636 (vs), 1587 (vs), 1557 (vs), 1359 (m), 1264 (m), 1143 (m), 1066 (m), 1046 (m), 1000 (m), 887 (w), 796 (m), 762 (m), 735 (m), 678 (m). **¹H NMR** (DMSO- D_6): δ = 5.57 (s, 2H, NH₂), 6.38 (br, 2H, NH₂), 7.24 (s, 2H, NH₂) ppm. **¹³C NMR** (DMSO- D_6): δ = 156.6, 168.6, 170.2 ppm. **MS** (FAB⁺): m/z = 101.1 [DAODH⁺]. **MS** (FAB⁻): m/z = 84.0 [AT⁻]. **Elemental analysis:** calculated ($C_3H_7N_9O$), found: C 19.46, 18.35; H 3.81, 3.71; N 68.09, 64.81. **DSC:** T_m = 130 °C, T_{dec} = 170 °C. **Sensitivities:** E_{dr} > 50 J, F_r 192 N, E_{el} > 0.3 J.

3,5-DIAMINO-1,2,4-OXADIAZOLIUM-5-NITROTETRAZOLATE (IX)

1 (0.10 g, 1.0 mmol) was solved in methanol (30 mL) and ammonium 5-nitrotetrazolate hemihydrate (0.14 g, 0.99 mmol) added. Under nitrogen stream the mixture was stirred at 60 °C for two days. After cooling the insoluble rest was filtered and the solvent of the filtrate was removed to obtain a colorless solid (**ix**, 0.21 g).

IR: $\tilde{\nu}$ (cm^{-1}) = 3394 (vs), 3264 (s), 3118 (vs), 2846 (m), 1691 (s), 1618 (s), 1575 (s), 1552 (s), 1464 (s), 1447 (s), 1417 (s), 1318 (m), 1182 (w), 1166 (w), 1124 (w), 1064 (w), 1037 (w), 1006 (w), 834 (w), 774 (w), 646 (w). **¹H NMR** (DMSO- D_6): δ = 5.57 (s, 2H, NH₂), 7.24 (s, 2H, NH₂) ppm. **¹³C NMR** (DMSO- D_6): δ = 168.6, 170.2 ppm. **¹⁴N NMR** (DMSO- D_6): δ = 29 (br), -16 (s, NO₂), -54 (br), -353 (NH⁺ 4) ppm. **MS** (FAB⁺): m/z = 101.1 [DAODH⁺]. **MS** (FAB⁻): m/z = 114.0 [NT⁻]. **Elemental analysis:** calc. ($C_3H_5N_9O_3$), found: C 16.75, 21.90; H 2.34, 3.87; N 58.60, 56.11.

4.4.16 3,5-DIAMINO-1,2,4-OXADIAZOLIUM CHLORIDE (C)

Hydrochloric acid (2 M, 10 mL, 20 mmol) was added to a suspension of **1** (2.00 g, 20.0 mmol) in water (50 mL) at 0 °C. The solvent was removed and the solid was

washed with little cold ethanol and diethylether. Pale yellow crystals were obtained (1.83 g, 13.4 mmol, 67 %)

IR: $\tilde{\nu}$ (cm^{-1}) = 3452 (w), 3323 (m), 3204 (m), 3158 (s), 3062 (s), 2904 (m), 2806 (s), 2650 (s), 1710 (s), 1655 (vs), 1537 (s), 1388 (m), 1341 (m), 1109 (w), 1070 (w), 1047 (m), 1017 (m), 861 (m), 776 (w), 735 (w), 680 (w). **^1H NMR** (DMSO- D_6): δ = 8.42 (br) ppm. **^{13}C NMR** (DMSO- D_6): δ = 166.7, 169.2 ppm. **MS** (FAB^+): m/z = 101.0 [DAODH^+]. **MS** (FAB^-): m/z = 35.0 [Cl^-]. **Elemental analysis:** calc. ($\text{C}_2\text{H}_5\text{ClN}_4\text{O}$), found: C 17.59, 17.55; H 3.69, 3.68; Cl 25.96, 25.34; N 41.03, 40.83. **melting point:** 133 °C.

3,5-DIAMINO-1,2,4-OXADIAZOLIUM-5,5'-AZOTETRAZOLATE (X)

Sodium 5,5'-azotetrazolate pentahydrate (0.33 g, 1.0 mmol) was solved in ethanol (50 mL) and mixed with a solution of c (0.30 g, 2.0 mmol) in ethanol (50 mL). The mixture was stirred at room temperature till the half of the volume was evaporated. The precipitated yellow solid was removed and the solvent of the filtrate was evaporated and dried to obtain a orange powder (x, 0.13 g).

IR: $\tilde{\nu}$ (cm^{-1}) = 3397 (vs), 3337 (s), 3120 (vs), 2361 (w), 2341 (w), 2144 (m), 1694 (s), 1667 (m), 1620 (vs), 1577 (vs), 1522 (m), 1458 (vs), 1400 (s), 1335 (m), 1195 (w), 1162 (w), 1126 (w), 1051 (w), 890 (w), 774 (m), 722 (m), 654 (w). **MS** (FAB^+): m/z = 101.0 [DAODH^+]. **MS** (FAB^-): m/z = 99.1 (ca. 9 %), 109.0 (ca. 8 %), 188.1 (ca. 15 %). **Elemental analysis:** calc. ($\text{C}_6\text{H}_{10}\text{N}_{16}\text{O}_2$), found: C 21.31, 19.85; H 2.98, 3.27; N 66.25, 49.09.

3,5-DIAMINO-4-METHYL-1,2,4-OXADIAZOLIUM IODIDE (XI)

Iodo methane (12.5 mL, 200 mmol) was added to a suspension of 1 (5.00 g, 50.0 mmol) in acetonitrile (10 mL) and stirred at room temperature for 24 hours. The red brown solution was filtered and a pale brown precipitate was obtained (F1, 0.06 g). The filtrate was reduced and stored at 4°C for several hours. The further removal of the solvent led to a dark red oil. It was mixed with water and the excess methyl iodide removed by extraction with diethylether. After removal of the water a powder was obtained (F2, 0.21 g).

IR (F1): $\tilde{\nu}$ (cm^{-1}) = 3333 (vs), 3170 (vs), 2188 (w), 1690 (s), 1618 (vs), 1564 (vs), 1343 (vs), 1255 (m), 1115 (m), 982 (w), 799 (w), 773 (w).

IR (F2): $\tilde{\nu}$ (cm^{-1}) = 3318 (s), 3192 (s), 2186 (w), 1592 (vs), 1355 (s), 1109 (m), 766 (m).

4.5 Oxidation and Nitration products of DAOD(1)

DIAZOTIATION WITH SODIUM NITRITE(I)

At 0°C sodium nitrite (0.69 g, 10 mmol) was added carefully to a suspension of 1 (1.00 g, 10.0 mmol) in hydrochloric acid (1 M, 10 mL, 10 mmol). After 30 minutes of stirring at room temperature a yellow precipitate was filtered and washed with water, ethanol and diethylether. After drying a yellow powder (0.53 g) was obtained.

IR: $\tilde{\nu}$ (cm^{-1}) = 3457 (s), 3393 (s), 3315 (s), 3216 (s), 3018 (m), 2972 (m), 2916 (m), 2832 (m), 2362 (w), 2337 (w), 2186 (w), 1754 (s), 1715 (s), 1616 (s), 1586 (vs), 1403 (vs), 1333 (s), 1220 (m), 1125 (w), 1092 (w), 986 (w), 894 (w), 812 (w), 751 (m), 716 (m), 639 (w).

¹H NMR (DMSO-D₆): δ= 7.27 (s, 2H), 7.54 (s, 1H), 7.76 (s, 1H), 9.19 (s, 1H) ppm. **¹³C NMR** (DMSO-D₆): δ= 152.1, 154.5, 155.0, 155.8 ppm. **MS** (DEI⁺): *m/z* = 99.1 (100), 185.1 (8). **Elemental analysis**: found: C 19.60; H 3.66; N 45.44. **DSC**: T_m= 192 °C, T_{dec.}= 196 °C.

OXIDATION WITH SODIUM NITRITE (II–IV)

Route 1

To a suspension of **1** (2.00 g, 20.0 mmol) in hydrochloric acid(2 M, 10 mL) carefully sodium nitrite(2.78 g, 40.3 mmol) was added at 0°C. After 30 minutes stirring at room temperature a yellow solid precipitated. It was filtered and washed with water, ethanol and diethylether and after drying a yellow powder was obtained (ii).

¹H NMR (DMSO-D₆): δ= 7.27 (s, 2H), 7.54 (s, 1H), 7.77 (s, 1H), 9.14 (s, 1H) ppm. **NMR analysis shows similarity to i.**

Route 2

To a suspension of sodium nitrite (2.79 g, 40.4 mmol) in water(30 mL) at 0°C a suspension of **1** (2.02 g, 20.2 mmol) in hydrochloride acid(2 M, 10 mL) and water(20 mL) was added dropwise. After 30 minutes stirring at room temperature a yellow solid precipitated. It was filtered and washed with water, ethanol and diethylether and after drying a yellow powder was obtained (iii)

¹H NMR (DMSO-D₆): δ= 7.29 (s, 2H), 7.56 (s, 1H), 7.79 (s, 1H), 9.25 (s, 1H) ppm. **NMR analysis shows similarity with i and ii.**

Route 3

Copper sulfate pentahydrate (1.07 g, 4.29 mmol) and sodium nitrite (2.02 g, 29.3 mmol) was solved in water (8 mL) and cooled to 0°C. **1** (1.01 g, 10.1 mmol) was suspended in a mixture of water (15 mL) and sulfuric acid (96 %, 0.5 mL). This suspension was carefully added during 20 minutes to the dark green nitrite solution. The mixture was stirred for three hours at room temperature and the copper was removed by adding gaseous hydrogensulfide and precipitating copper sulfide. The black precipitate was filtered off. The pale green solution was extracted several times with ethyl acetate, which was dried over magnesium sulfate and removed under reduced pressure. No rest was obtained.

OXIDATION WITH HYDROGEN PEROXIDE AND AMMONIUM PEROXODISULFATE (V)

Hydrogen peroxide (50 %, 20.0 g) and sulfuric acid (96 %, 20.0 g) were mixed at 0°C and ammonium peroxodisulfate (20.0 g) was added. After stirring an hour **1** (2.00 g, 20.0 mmol) was added and the yellow solution was stirred for another hour. The changed green clear solution was poured on ice and neutralized with potassium hydroxide after 24 hours at 4°C. Colorless crystals (**v**) were obtained, filtered and dried.

IR: $\tilde{\nu}$ = 3235 (w), 1424 (w), 1262 (s), 1101 (s), 1058 (vs), 980 (m), 688 (m), 614 (m) cm^{-1} .

OXIDATION WITH POTASSIUM PERMANGANATE (VI)

To a solution of **1** (2.00 g, 20.0 mmol) in hydrochloric acid (2 M, 50 mL) was added potassium permanganate (3.16 g, 20.0 mmol) at 60 °C and water (50 mL). After one hour of stirring ethanol (10 mL) was added to reduce excess permanganate. After another five minutes the solution was filtered hot. The clear yellow solution was mixed with the same amount of ethanol and put in the refrigerator over night at 4°C. The still clear solution was evaporated and a crystalline yellow solid (4.49 g) was obtained. This was washed with hot methanol and the colorless solid was dumped while the combined methanol extracts were evaporated again. Yellow crystals were gained, yielding 1.64 g (**vi**).

IR: $\tilde{\nu}$ = 3393 (vs), 3313 (s), 3265 (s), 3194 (vs), 2362 (m), 2340 (m), 1692 (vs), 1603 (s), 1484 (s), 1411 (m), 1365 (m), 1330 (s), 1228 (m), 1218 (m), 1132 (m), 1111 (m), 937 (w), 770 (w), 754 (w), 722 (w), 667 (w), 625 (w) cm^{-1} . **MS** (DEI^+): m/z = 36.06 (28), 43.07 (100), 60.10 (73). **Elemental analysis:** found: C 6.50; H 3.26; N 14.46.

OXIDATION WITH AMMONIUM DICHROMATE (VII)

To a solution of **1** (2.00 g, 20.0 mmol) in hydrochloric acid (2 M, 50 mL) at 70 °C was added ammonium dichromate (2.52 g, 10.0 mmol) and stirred for an hour. After cooling the deep blue solution a colorless precipitate was filtered and washed with ethanol and diethylether, yielding 0.42 g (**vii**).

IR: $\tilde{\nu}$ = 3398 (vs), 3178 (s), 3085 (s), 3020 (s), 2977 (s), 1690 (vs), 1671 (vs), 1582 (vs), 1520 (vs), 1470 (vs), 1436 (s), 1412 (vs), 1351 (m), 1301 (s), 1209 (m), 1145 (m), 1086 (w), 1049 (w), 1021 (w), 1003 (w), 981 (m), 970 (m), 897 (w), 819 (w), 762 (m), 740 (m), 710 (m), 679 (w), 628 (w) cm^{-1} . **¹H NMR** ($\text{DMSO-}d_6$): δ = 2.63 (s, 3H), 7.06 (br, 1H), 8.36 (s, 2H),

9.61 (s, 1H) ppm. ^{13}C NMR (DMSO-D₆): δ = 13.9, 154.2, 154.6, 157.9, 162.0, 171.9 ppm. ^{14}N NMR (DMSO-D₆): δ = 1 ppm. MS (DEI⁺): m/z = 98.1 (20), 181.1 (100). **Elemental analysis**: found: C 31.06; H 3.70; N 48.36.

4.4.7 OXIDATION WITH BROMINE (VIII)

To a suspension of 1 (2.00 g, 20.0 mmol) in water (20 mL) was carefully added bromine (1.0 mL, 20 mmol) at 0°C. The vessel with reaction mixture was closed and stirred for one hour at 0°C and two hours at room temperature. Then the flask was opened and stirred over night at room temperature. The solvent was evaporated and the residue recrystallized from little water. The obtained precipitate was washed with ethanol and diethylether to yield 0.05g of a yellow powder (**viii**).

IR: $\tilde{\nu}$ = 3442 (m), 3256 (m), 3179 (s), 2176 (w), 1675 (vs), 1584 (m), 1513 (s), 1401 (s), 1344 (m), 1112 (w), 975 (w), 931 (w), 794 (w), 770 (w), 672 (w) cm^{-1} . ^1H NMR (DMSO-D₆): δ = 8.37 (s) ppm. ^{13}C NMR (DMSO-D₆): δ = 172.7, 175.2 ppm. MS (DEI⁺): m/z = 112.1 (54), 125.1 (92), 196.1 (24). **Elemental Analysis**: found: C 24.46; H 3.36; N 49.42.

5 References

- [1] N. Latypov, A. Langlet: *Method of producing dinitramide salts*. Försvarets Forskningsanstalt Sep, 16 **1999**: WO 1999/046202.
- [2] H. Östmark, U. Bemm, H. Bergman and A. Langlet, "N-Guanyllurea-Dinitramide: A New Energetic Material with Low Sensitivity for Propellants and Explosives Applications", *Termochimica Acta* **2002**, 384, 253-259.
- [3] A. Hammerl, G. Holl, M. Kaiser, T. M. Klapoetke, H. Piotrowski, "Nitrogen Rich Materials: Salts of N, N'-Bistetrazolatohydrazine", *Z Anorg. Allg. Chem.* **2003**, 629 (12-13), 2117-2121.
- [4] T. M. Klapoetke, C. Miró Sabaté, *Z. Anorg. Allg. Chem.* **2010**, 636 (1), 163-175.
- [5] J. J. Roemer, N. Stamford, D. W. Kaiser, U.S. Patent 2648669, **1953**, USA.
- [6] G. M. Sheldrick, *SHELXS-97*, Göttingen, Germany **1997**.
- [7] G. M. Sheldrick, *SHELXL-97*, Göttingen, Germany **1997**. K. Brandenburg, *Diamond 3.2c*, Crystal Impact GbR, Bonn, Deutschland, **2009**.
- [9] F. A. Carey, R. J. Sundberg, *Organische Chemie*, H. J. Schäfer, D. Hoppe, G. Erker (Hrsg.), VCH, Weinheim, New York **1995**, S. 13.
- [10] M. J. S. Dewar, W. Thiel, *J. Am. Chem. Soc.* **1977**, 99, 4907.
- [11] A. F. Holleman, E. Wiberg, N. Wiberg, *Lehrbuch der Anorganischen Chemie*, 102. Auflage, Walter de Gruyter, Berlin, New York, **2007**.
- [12] K. Williamson, P. Li, J. P. Devlin, *J. Chem. Phys.* **1968**, 48, 3891.
- [13] J. R. Fernandes, S. Ganguly, C. N. R. Rao, *Spectrochim. Acta, Part A*, **1979**, 35, 1013.
- [14] M. Sućeska, *EXPL05 5.02*, Zagreb, Hrvatska, **2008**.
- [15] O. Redlich, E. K. Holt, J. Bigeleisen, *J. Am. Chem. Soc.* **1944**, 55, 13.
- [16] H. Cohn, *J. Chem. Soc.* **1952**, 4282.

- [17] G. M. Sheldrick, *SHELXL-97*, Göttingen, Germany **1997**. M. Sućeska, *Propellants, Explos., Pyrotech.* **1991**, 16, 197.
- [19] Spectral Database for Organic Compounds,
http://riodb01.ibase.aist.go.jp/sdbs/cgi-bin/cre_index.cgi (13.09.2012).
- [20] C. Darwich, T. M. Klapötke, C. Miró Sabaté, *Propellants Explos., Pyrotech.* **2008**, 33, 336.
- [21] T. M. Klapoetke, J. Stierstorfer, *New Trends in Energetic Materials*, Czech Republic **2008**, 827.
- [22] T. M. Klapötke, J. Stierstorfer, *Dalton Transactions* **2009**, 643.
- [23] K. O. Christe, W. W. Wilson, M. A. Petrie, H. H. Michels, J. C. Bottaro, R. Gilardi, *Inorg. Chem.* **1996**, 35, 5068.
- [24] J. Stierstorfer, Dissertation, LMU München, **2009**.
- [25] G.-H. Tao, Y. Guo, Y.-H. Joo, B. Twamley, J. M. Shreeve, *J. Mater. Chem.* **2008**, 18, 5524.
- [26] L. E. Fried, K. R. Glaesemann, W. M. Howard, P. C. Souers, *CHEETAH 4.0 User's Manual*, Lawrence Livermore National Laboratory, **2004**.
- [27] J. P. Lu, *Evaluation of the Thermochemical Code-CHEETAH 2.0 for Modelling Explosives performance*, DSTOTR-1199, DSTO, Edinburgh, **2001**.
- [28] N. Fischer, T. M. Klapötke, S. Scheutzow, J. Stierstorfer, *Central Europ. J. of Energ. Mater.* **2008**, 5, 3.
- [29] J. M. Welch, Dissertation, LMU München, **2008**.
- [30] T. M. Klapoetke, P. Mayer, C. Miró Sabaté, J. M. Welch, N. Wiegand, *Inorg. Chem.* **2008**, 47, 6014.
- [31] H. E. Gottlieb, V. Kotlyar, A. Nudelman, *J. Org. Chem.* **1997**, 62, 7512.
- [32] A. A. Dippold, T. M. Klapoetke, F. A. Martin, S. Wiedbrauk, *Europ. J. Inorg. Chem.* **2012**, 2012, 14, 2429–2443.
- [33] T. S. Novikova, T. M. Mel'nikova, O. V. Kharitonova, V. O. Kulagina, N. S. Aleksandrova, A. B. Sheremetev, T. S. Pivina, L. I. Khmel'nitskii, S. S. Novikov, *Mendeleev Commun.* **1994**, 4, 138.
- [34] J. C. Cobas, S. Domínguez, N. Larin, I. Iglesias, C. Geada, F. Seoane, M. Sordo, P. Monje, S. Fraga, R. Cobas, *MestReNova 5.1.1-3092*, Mestrelab Research S.L., Santiago de Compostela, Spain, **2007**.
- [35] M. Sućeska, *Test Methods for Explosives*, Springer, New York, **1995**.
- [36] NATO Standardization Agreement 4489 (STANAG 4489), 17. September, **1999**.
- [37] WIWEB-Standardarbeitsanweisung 4-5.1.02, 08. November, **2002**.
- [38] NATO Standardization Agreement 4487 (STANAG 4487), 22. August, **2002**.
- [39] WIWEB-Standardarbeitsanweisung 4-5.1.03, 08. November, **2002**.

- [40] *Recommendations on the Transport of Dangerous Goods, Manual of Tests and Criteria*, 4th edition, United Nations, New York, Geneva, **1999**.
- [41] A. Altomare, G. Cascarano, C. Giacovazzo, A. Guagliardi, M. C. Burla, G. Polidori, M. Camalli, *J. Appl. Cryst.* **1994**, *27*, 435.
- [42] L. J. Farrugia, *ORTEP-3 2.02*, University of Glasgow, Scotland, **2008**.
- [43] M. J. Frisch, G. W. Trucks, H. B. Schlegel, G. E. Scuseria, M. A. Robb, J. R. Cheeseman, J. A. Montgomery, Jr., T. Vreven, K. N. Kudin, J. C. Burant, J. M. Millam, S. S. Iyengar, J. Tomasi, V. Barone, B. Mennucci, M. Cossi, G. Scalmani, N. Rega, G. A. Petersson, H. Nakatsuji, M. Hada, M. Ehara, K. Toyota, R. Fukuda, J. Hasegawa, M. Ishida, T. Nakajima, Y. Honda, O. Kitao, H. Nakai, M. Klene, X. Li, J. E. Knox, H. P. Hratchian, J. B. Cross, V. Bakken, C. Adamo, J. Jaramillo, R. Gomperts, R. E. Stratmann, O. Yazyev, A. J. Austin, R. Cammi, C. Pomelli, J. W. Ochterski, P. Y. Ayala, K. Morokuma, G. A. Voth, P. Salvador, J. J. Dannenberg, V. G. Zakrzewski, S. Dapprich, A. D. Daniels, M. C. Strain, O. Farkas, D. K. Malick, A. D. Rabuck, K. Raghavachari, J. B. Foresman, J. V. Ortiz, Q. Cui, A. G. Baboul, S. Clifford, J. Cioslowski, B. B. Stefanov, G. Liu, A. Liashenko, P. Piskorz, I. Komaromi, R. L. Martin, D. J. Fox, T. Keith, M. A. Al-Laham, C. Y. Peng, A. Nanayakkara, M. Challacombe, P. M. W. Gill, B. Johnson, W. Chen, M. W. Wong, C. Gonzalez, J. A. Pople, *Gaussian 03 Revision D.01*, Gaussian, Inc., Wallingford, CT, USA, **2004**.
- [44] P. J. Lindstrom, W. G. Mallard (Editors), NIST Standard Reference Database Number 69, <http://webbook.nist.gov/chemistry/>, (12.09.2009).
- [45] H. D. B. Jenkins, H. K. Roobottom, J. Passmore, L. Glasser, *Inorg. Chem.* **1999**, *38*, 3609.
- [46] H. D. B. Jenkins, J. F. Liebman, *Inorg. Chem.* **2005**, *44*, 6359.

Chapter VI

3-AMINO-1,2,4-OXADIAZOL-5-ONE –

THE INSENSITIVE 5-AMINO-TETRAZOLE ?

COMMONS AND DIFFERENCES

Abstract:

3-substituted-1,2,4-oxadiazol-5-one derivatives may replace or complement tetrazole derivatives as pyrotechnics and propellants. As oxadiazolones have better oxygen balances (-47 % compared to 57% for tetrazole), both generate the same amount of gaseous products per molecule. Comparison of 3-amino-1,2,4-oxadiazol-5-one (aOD) with 5-amino-1H-tetrazole (AT) shows some similarities and some differences which are discussed.

Keywords: 3-substituted-1,2,4-oxadiazol-5-one, aOD, 5-amino-1H-tetrazole, AT, crystal structure, density, decomposition.

1 Introduction

For years tetrazoles and their derivatives have been in use as building blocks for synthesis of various energetic materials.^[1] Although the performance of these compounds are very satisfying most of the lack stability regarding friction, impact or electrostatic discharge.^[2a] The oxadiazole moiety reveals also possible energetic properties as shown for furzanes (1,2,5-oxadiazole).^[3]

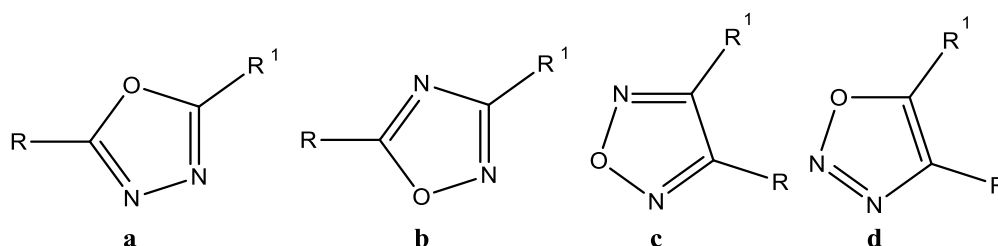


Figure 1. a) 1,3,4 oxadiazole; b) 1,2,4 oxadiazole; c) 1,2,5-oxadiazole (furazane); d) 1,2,3-oxadiazole.

Looking at figure 1 oxadiazole a and b are often found as this rings are fused from a hydroxyamino amide or from a hydrazino amide and an organic acid which is often used in pharmaceutical molecules.^[4] While the synthesis of d is rather complex and the molecule is only stable with the little substituents this moiety is only scarcely found.^[5]

The fundamental similarity of 1H-tetrazole-5-amine (**AT**) and 3-amino-1,2,4(4H)-oxadiazol-5-one (**aOD**, **1**) reveals itself in the consideration of possible decompositions of the two compounds (figure 2). As it is evident, 1H-tetrazole-5-amine is able to release nitrogen by breaking two N-N bonds and formation of a N-N triple bond. In 3-amino-1,2,4(4H)-oxadiazol-5-one by forming a double bond O-C instead it would result in carbon dioxide. This was the reason for the investigations on the suitability of the derivatives of 1,2,4-oxadiazole as possible high-energy materials.

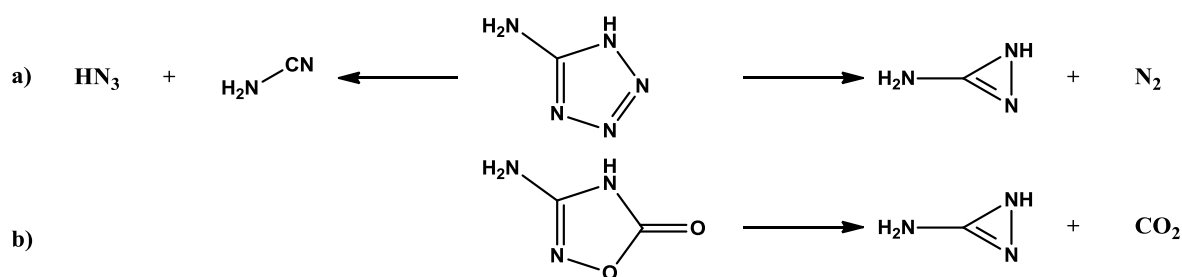


Figure 2. Decomposition of AT and aOD. a) Decomposition of 1*H*-tetrazole-5-amine to cyanamide and hydrazoic acid (left) or 1*H*-diaziren-3-amine and nitrogen (right). b) Decomposition of 3-amino-1,2,4-oxadiazol-5(4*H*)-one to 1*H*-diaziren-3-amine and carbondioxide.

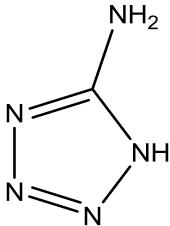
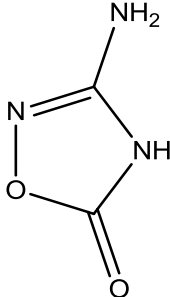
While the chemistry of tetrazole and its derivatives is well investigated with respect to their properties as explosives [2b], the chemistry of 1,2,4-oxadiazol-5(4*H*)-ones and its derivatives is largely unknown in this regard.

The investigation concentrated on finding a rather fast and good yielding synthesis for the 3-amino-1,2,4-oxadiazol-(4*H*)-5-one (**aOD**), which was synthesized before in a really long and very uncomfortable way. Because in two steps there is an evolution of methyl mercaptane which is unhealthy on the one hand and on the other hand it has an awful odor. The new synthesis shows good yields and less steps.

The aOD is interesting for research because of its similarity to the 5-amino-(1*H*)-tetrazole (**AT**). The investigation of the whole bunch of working syntheses for energetic materials, which has been done with AT before, should be rather easy applicable on the aOD.

The resulting compounds should be similar in energetic behavior but little different in sensitivity and thermostability and hopefully meet the demands of military and civil application of energetic materials.

Table 1. Comparision of AT and aOD.

5-amino-(1 <i>H</i>)-tetrazole (AT)	3-amino-1,2,4-oxadiazol-(4 <i>H</i>)-5-one (aOD)
	
$T_{\text{dec}} 205^\circ\text{C}$	$T_{\text{dec}} 207^\circ\text{C}$
$\Delta H_f^\circ = +49.7 \text{ kcal mol}^{-1}$	$\Delta H_f^\circ = -35 \text{ kcal mol}^{-1}$
$\rho_{\text{calc}} 1.72 \text{ g cm}^{-3}$	$\rho_{\text{calc}} 1.749 \text{ g cm}^{-3}$

2 Results and Discussion

2.1 Synthesis of aOD

The synthesis of 3-amino-1,2,4(4*H*)-oxadiazol-5-one (**aOD**, **1**) should be revised and improved. The main goal was to find a reaction path which starts from cheap reactants and leads to high yields.

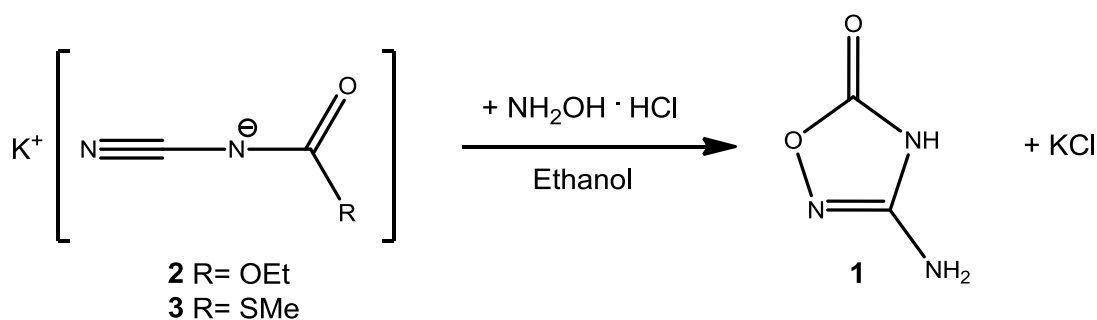


Figure 3. General ring closure by route A to 3-amino-1,2,4-oxadiazol-5-one.

The establishment of a new simple and cheap synthesis should be the basis for further investigation of aOD and to transfer the reaction of the well investigated to 5-amino-1*H*-tetrazole to the aOD.

Not only a new synthetic route was found but also this was simplified down to an easy accomplishable one-pot synthesis.

To learn about the chemistry of **1**, there were carried out some experiments on the solubility in the most common solvents in the laboratory.

A row of different salts of **1** have been made with aOD⁻ as anion and according to the reactivity of AT there has also been tried to protonate **1** to get aODH⁺. Both ways were examined carefully and supported by crystal structure analysis as well as calculations regarding energies and structures.

As example for reactivity compared to AT the well-known azo-coupling was transferred to **1**.

2.1.1 Overview

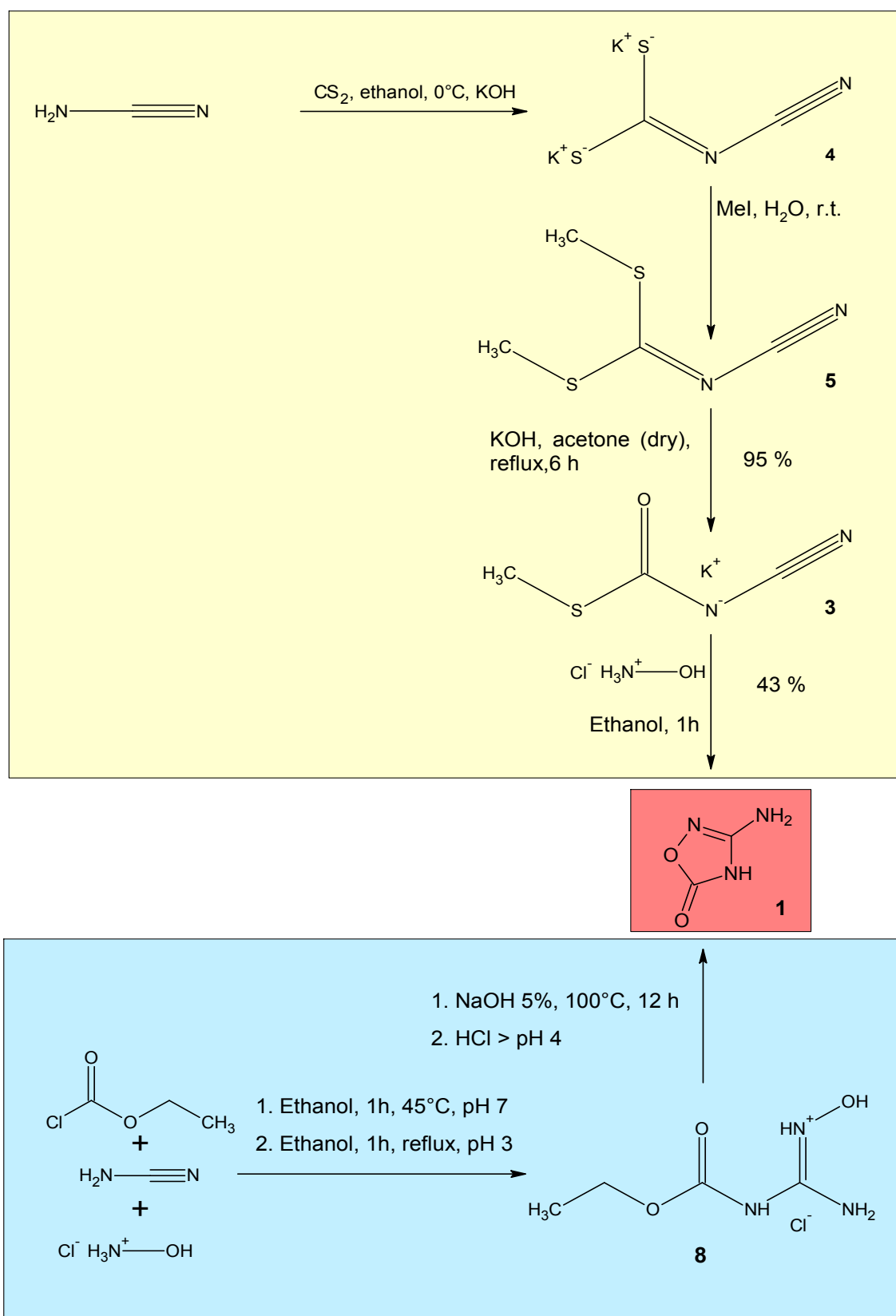


Figure 4. Scheme of Synthesis (Yellow box literature known route A, blue box new developed route B).

2.1.2 Synthetic Route A

REACTION PATHWAY ACCORDING TO LITERATURE

The first synthetic strategy was invented by Takayuki Suyama et al.^[6a] It starts from that potassium salt of ethyl-*N*-cyanocarbamate (**2**) or *S*-methyl-*N*-cyanocarbamate (**3**) and reacts with hydroxylamine-hydrochloride to form aOD (figure 3).

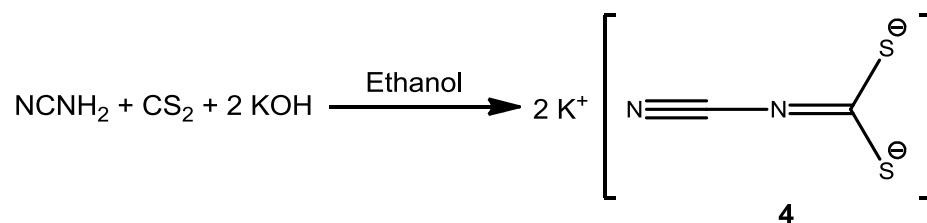


Figure 5. Synthesis of dipotassium cyanodithioimidocarbonate.

As starting material was chosen **3**, which was synthesized in three steps. First carbon disulfide, cyanamide and potassium hydroxide were mixed and furnished in dipotassium cyanodithioimidocarbonate (**4**) (figure 5).^[6 b,c]

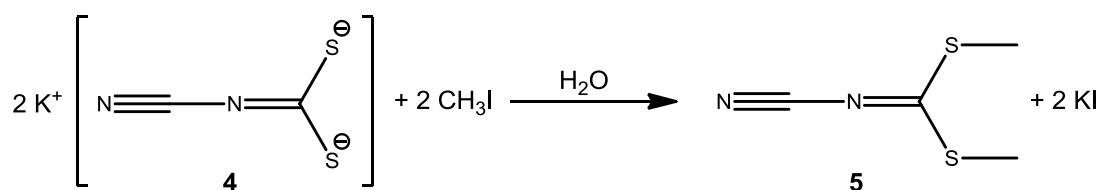


Figure 6. Synthesis of dimethylcyanodithioimidocarbonate.

4 was reacted with methyl iodide to give dimethylcyanodithioimidocarbonate (**5**) (figure 6).

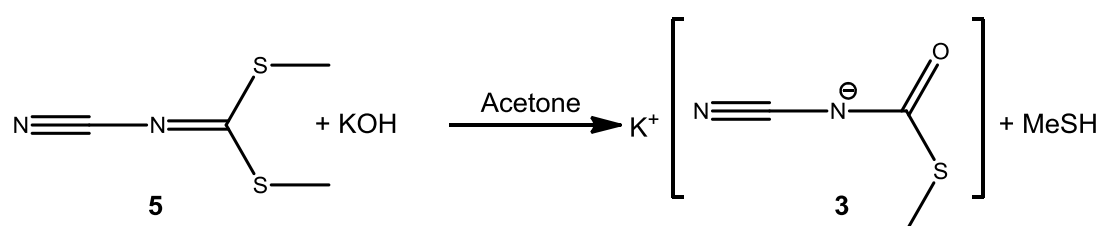


Figure 7. Synthesis of potassium *S*-methyl-*N*-cyanocarbamate.

To the obtained product **5** potassium hydroxide in acetone was added to form the potassium *S*-methyl-*N*-cyanocarbamate (**3**)^[7], which was the starting material for the ring closure reaction with hydroxylamine hydrochloride in route A (figure 7).

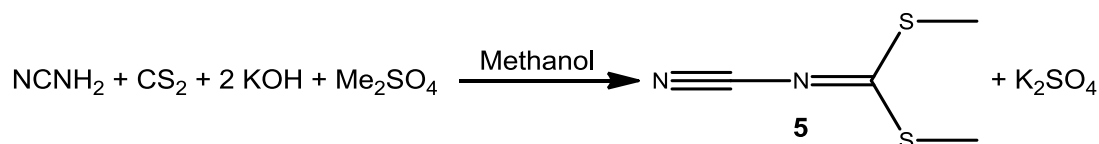


Figure 8. Alternative Synthesis of dimethylcyanodithioimidocarbonate.

Also it was tried to do the first two steps in a one pot reaction as reported in literature by Katsutoshi Shimada et al.^[8] (figure 8).

RESULTS OF SYNTHESIS

As shown in figure 8 the dimethyldithioimidocarbonate (**5**) is an intermediate product. To obtain that the compound the preparation was carried out according to Katsutoshi et al. versucht ^[8]. In the IR spectrum there can be observed a significant absorption of the NH₂-valence vibration of the cyanamide at 3385 cm⁻¹. At 2187 cm⁻¹ the signal of C-N valence vibration of the triple bond could be found that means the nitrile function is available but obviously the cyanamide was not reacted completely. A strong signal at 3000-2850 cm⁻¹ as expected for a methyl functionality is not observed. Also in the ¹H NMR and ¹³C NMR no methyl group was found. So the reaction as one pot synthesis failed. There are many different possibilities why the product was not obtained. First the carbon disulfide could have reacted with the potassium hydroxide to form carbon dioxide or carbonate. This competitive by-reaction is strongly influenced by concentration, solvent, reaction time and reaction temperature.

To obtain **5** the reaction was splitted into two reactions first to furnish **4** and subsequently reacting to **5**.

The preparation of **4** was carried out according to literature and ended up with a pure product in high yields.^[6a] In the IR-spectrum the broad N-H-valence vibration was gone, which was a hint on a fully reacted cyanamide. In the Raman spectrum the C-N-triple bond valence vibration was the strongest signal but also the C-N- double bond valence vibration at about 1587 cm⁻¹ was observed. In the ¹H NMR-spectrum only the solvent of D₂O at δ= 4.80 ppm was available. In the ¹³C NMR-spectrum the cyanamide moiety was found at δ= 121.5 ppm and the other C-atom at δ = 228.4 ppm.

The methylation of **4** was performed according to literature know synthesis.^[6b] But through slightly warming the solution to room temperature the reaction time was shortened from five days to 12 hours. Also the product was not dried in the air but in vacuo. The yield exceeded the literature values. The IR-spectrum shows the typical bond valence vibration at 1458 cm⁻¹ (literature: 1495 cm⁻¹) for C-N double bond and CN triple bond at 2179 cm⁻¹ (literature: 2190 cm⁻¹). The proton signal of the methyl group were observed in the ¹H NMR spectrum at δ = 2.59 (s, 6H) ppm (literature: δ = 2.64 ppm).

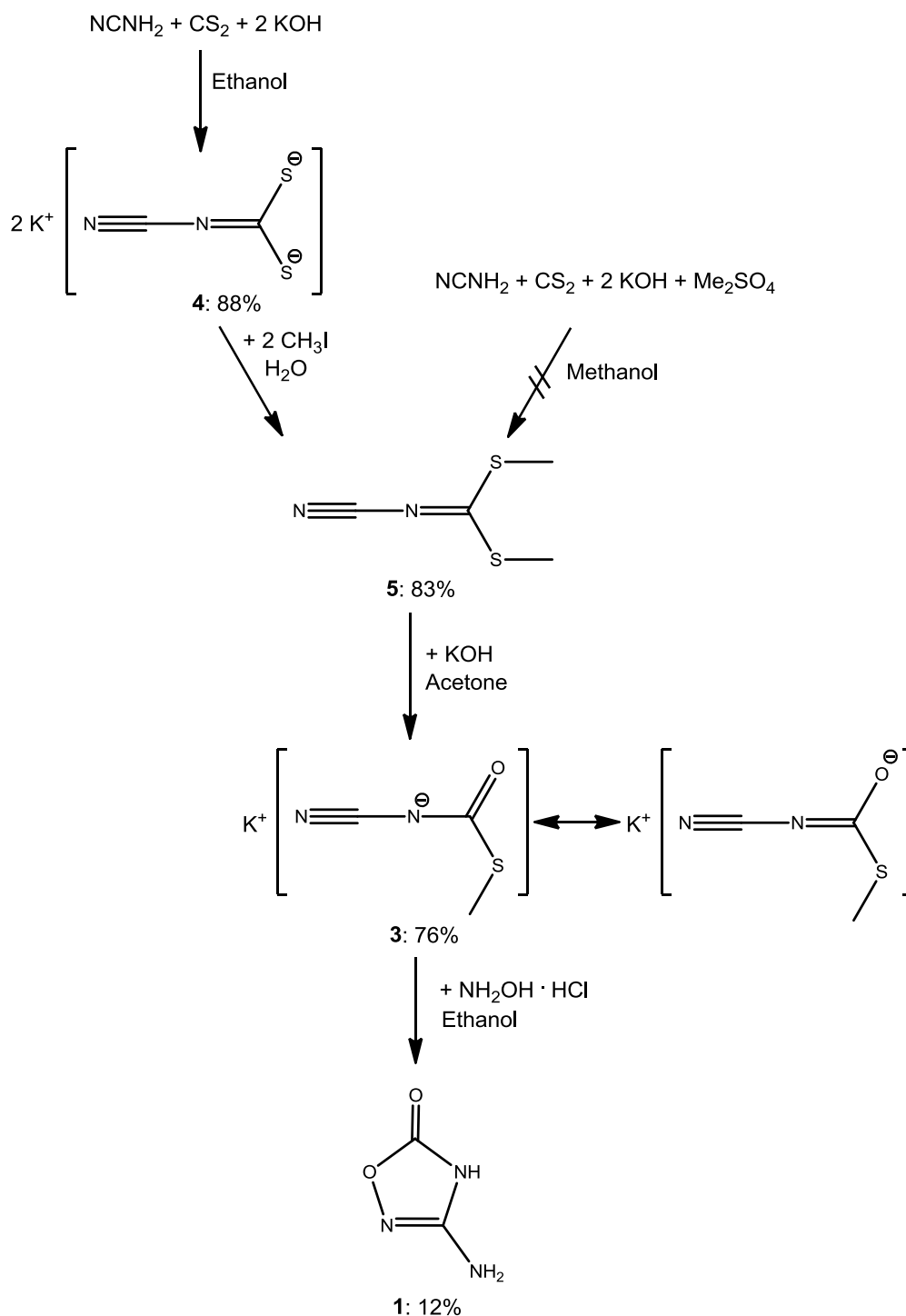


Figure 9. Total yield of synthetic route A only 7 %.

The synthesis of **3** was carried out according to the preparation described by T. Schafer et al.^[7]. Therefore compound **5** was refluxed in a solution of dry acetone and potassium hydroxide for six hours and stirred for 24 hours subsequently at room temperature. The product was dried in vacuo at 50°C. The literature yield was not obtained. Comparing the IR spectrum of **3** to **5** the C-N double bond valence vibration appears a higher wave numbers 1476 cm⁻¹. This maybe refers to the negative charge. No carbonyl valence vibration was observed. But in the ¹³C NMR the carbon atom shifted to deeper

field $\delta = 197.7$ ppm to that of **5** at $\delta = 193.9$ ppm, which gives a hint on the existence of **3**.

For the first step the synthesis was carried out according to Takayuki Sumaya *et al.* . Compound **3** was solved with hydroxylamine hydrochloride in ethanol and refluxed for two hours. The white precipitate was filtered, which was identified as potassium chloride. The solvent of the filtrate was removed and a white solid formed. In the IR spectrum there are observed N-H stretching vibrations at $3400\text{--}3200\text{ cm}^{-1}$, the C=O stretching vibrations at 1780 cm^{-1} and the C=N stretching vibrations at 1680 and 1540 cm^{-1} . The white solid product was solve by 5% sodium alkaline solution and filtered again to remove residues. After acidification with 2M hydrochloric acid, the solution was stored at 4°C for 72 hours and finally the solid was filtered again. The ^{13}C NMR spectrum shows to signals at 157.5 and 159.0 ppm. The ^1H NMR spectrum displays two signals at 6.21 ppm for the two protons of the amino function and at 11.41 ppm for the acidic ring proton.

While the yield in the steps one to three are in a good range the last step to form compound **1** had only a yield of 12%, which leads to an overall yield of 7% during **route A**. Additionally toxic and expensive methylation agents like dimethyl sulfate or iodomethane are used and also very toxic methyl mercaptane is evolved in nearly every step.

2.1.3 Synthesis route B

A synthetic strategy was inspired by the work of Norbert Götz and Bernd Zeeh [9]. The original method was carried out by adding sodium hydroxide to cyanamide and ethyl chloroformate and subsequently reacting with primary amines (figure 10).

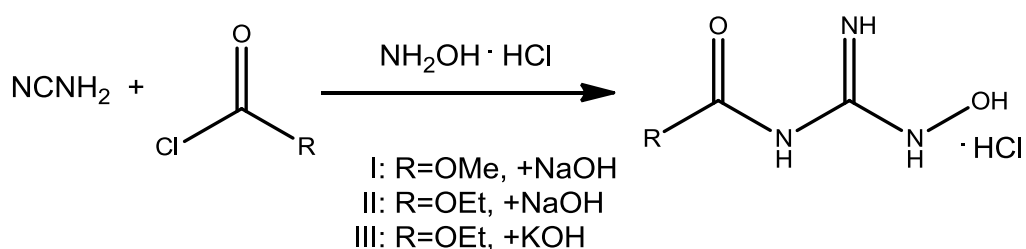


Figure 10. Synthesis by the open-chained intermediate of 3-Amino-1,2,4-oxadiazol-5-one (aOD).

To synthesize aOD a variation with ethyl chloroformate, sodium and potassium hydroxide and hydroxylamine hydrochloride as primary amine (II and III) was performed and another one using methyl chloroformate, sodium hydroxide and hydroxylamine hydrochloride (I).

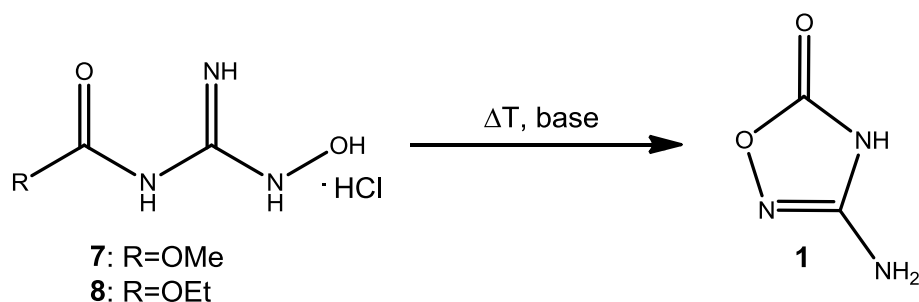


Figure 11. Ring closure to 3-Amino-1,2,4-oxadiazol-5-one (**1**).

By heating of the reaction mixture the open chain structure should form a ring system and the cleavage of ethanol or methanol residue was initiated by basic or acidic conditions (figure 11).

Furthermore there were synthesized some salts with aOD as anionic moiety and metal as well as nitrogen rich cations.

Synthesis route B is a good alternative to route A, as it has only a small number of steps and does not include any sulfur containing compounds which makes this way easier and more convenient.

The idea was to synthesis according to the preparation of Norbert Götz and Bernd Zeeh^[9] the open chained form of aOD (**1**) with the suitable primary amine and to close the ring by a subsequent reaction. This is generally visualized in figure 12.

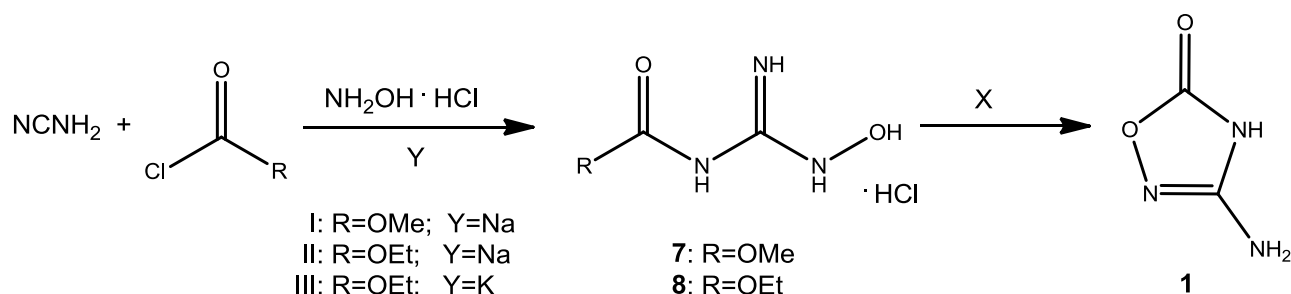


Figure 12. General procedure for synthesis route B. Work up X depends on the reaction I-III and is summed up in table 2.

In the first variation to a solution of cyanamide methyl chloro formate and sodium hydroxide were added dropwise and subsequently reacted with hydroxylamine hydrochloride. This reaction was carried out in water. In the ¹³C NMR spectrum the methoxy and carbonyl function are found at 52.3 ppm (CH₃) and 153.7 ppm (CO) respectively as well as the cyanid group of cyanamide at 155.0 ppm (CN). This result indicates no reaction. To start a reaction of the mixture it was boiled in concentrated hydrochloric acid for some hours, without result as the IR spectrum displays. Boiling the same mixture under alkaline (2M sodium hydroxide) conditions ends with no changes of the starting material.

In the second variation to the cyanamide was added solved sodium hydroxide in water and hydroxylamine hydrochloride. This time was used ethyl chloroformate and added afterwards. The ethoxy group was chosen because of its better ability as leaving group which should promote the ring closure reaction under the cleavage of ethanol. After the pH value was according to the preparation instruction adjusted to 3, the mixture was heated to 50°C for 2 hours and further five hours at 80°C to close the ring. Afterwards it was stirred for 72 hours at room temperature, the solid was filtered and the filtrate was acidified till pH value of 1 was reached. The filtrate was extracted with ethylacetate and the organic layer dried with potassium sulfate. After removing the solvent, yellow oil was obtained. The ^{13}C NMR spectrum of the solid and the oil are exactly the same while the ^1H NMR of the oil displays impurities. In the ^{13}C NMR a signal was found at 14.2 ppm (CH_3) and 61.1 ppm (CH_2) for the ethoxy group at 153.7 ppm (CO) of the carbonyl group and at 154.5 ppm (CN) of cyanamide. Again no reaction has occurred, the signals only show the starting material.

In the third variation again to cyanamide in water ethyl chloroformate and potassium hydroxide in ethanol were added and subsequently hydroxylamine hydrochloride was added. The potassium hydroxide solution and ethylchloroformate were added dropwise under ice-cooling and a pH value adjusted between 6 and 8. After this addition hydroxylamine hydrochloride was added and the mixture refluxed for 45 min., then slowly cooled and the white precipitate filtered off. After 12 hours of cooling to room temperature colorless crystal needles were obtained and investigated by x-ray diffraction, which turned out to be compound **8**.

An overview on the performed variations on **route B** is listed in table 2.

Table 2. Variations of synthetic route B with workup procedure.

Variation	R	Y	Intermediate	X (workup)	Result
I	OMe	Na	-	conz. HCl + heating	-
				2M NaOH + heating	-
II	OEt	Na	-	4.5 h bei 80 °C	-
III	OEt	K	8	Et_3N in DMF + heating	-
				a) Diphosgen + Et_3N bei 0 °C in THF b) 2M HCl + heating	-
				5% NaOH + heating → konz. HCl (pH 3-4)	1

CRYSTAL STRUCTURES

The results of the structure refinement are listed in table 3. The C4-N3, N1-C4 and C3-N1 single bonds are compared with the covalence radius of the atoms and the calculated bond lengths (1.47 Å) shorten by 0.09 to 0.16 Å. [11] The C4-N2 double bond is slightly longer than the calculated bond length of 1.22 Å. The C3-O2 double bond is

minimally expanded to 1.19 Å. The O1-C3 single bond is shorter than the calculated lengths (1.43 Å). The C2-O1 single bond is a little longer. The length of the C1-C2 single bond is slightly below the calculated value (1.54 Å). The C4-N2 double bond is with 1.305 Å only a bit longer than the calculated 1.22 Å. The N2-O3 single bond is shorter by 0.11 Å than the literature value of 1.45 Å.

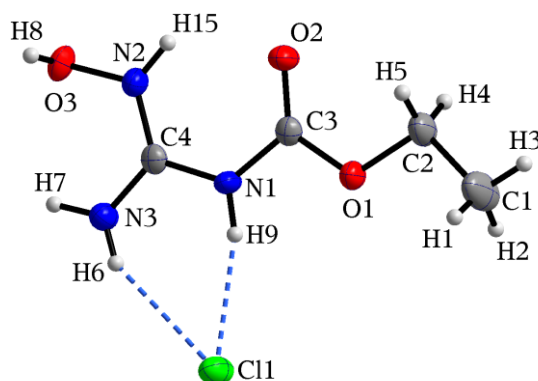


Figure 13. Molecular structure of **8**. Ellipsoids are plotted at 50% probability level.

Comparing the corresponding bond lengths with a hydroxyguanidinium cation^[12] there are some differences. While the bond N2-O2 in **8** approximately matches the distance between hydroxy oxygen atom and the nitrogen atom of about 1.396(4) Å, the carbon nitrogen bonds display a significant variance. The carbon-nitrogen bond next to the hydroxyl group of the hydroxyguanidinium cation is 1.337(5) Å and a little longer than the C4-N4 bond of **8**. The other carbon-nitrogen bonds are a little shorter than the corresponding bonds in **8**. The cause for that may be the missing carboxyl ester group in the hydroxyl guanidinium cation which tends to form mesomeric structures and like those of amides. Also the formal six membered ring formed by the intramolecular hydrogen bond on N2-H15...O2 can influence the whole bond lengths in the system.

Table 3. Selected bond lengths and angles of **8**.

Bond lengths [Å]		Angles [°]	
C1-C2	1.497(0)	C1-C2-O1	105.8(3)
C2-H5	0.940(6)	C2-O1-C3	115.3(0)
C2-O1	1.461(7)	O1-C3-O2	126.8(4)
O1-C3	1.325(0)	O1-C3-N1	108.6(5)
C3-O2	1.204(6)	O2-C3-N1	124.4(9)
C3-N1	1.379(1)	C3-N1-C4	125.7(5)
N1-C4	1.364(4)	H9-N1-C4	115.0(1)
C4-N2	1.304(5)	N1-C4-N2	120.9(8)
C4-N3	1.314(2)	N1-C4-N3	117.5(0)
N2-H15	0.869(0)	N2-C4-N3	121.5(1)
N2-O3	1.391(6)	C4-N2-H15	123.7(1)
O3-H8	0.834(1)	C4-N2-O3	117.3(3)
		H15-N2-O3	118.7(1)
		N2-O3-H8	101.7(2)

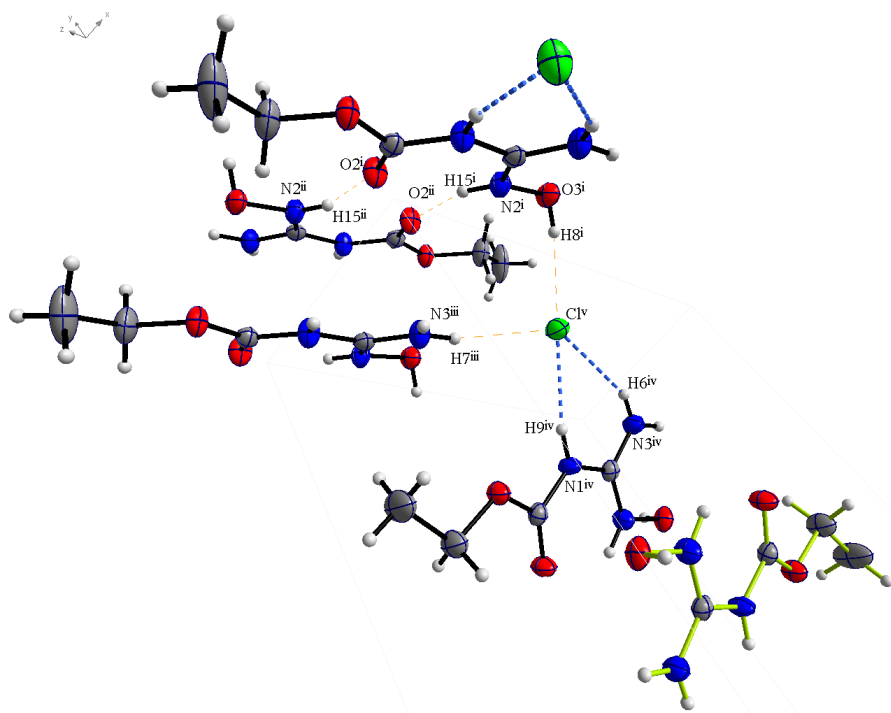


Figure 14. Hydrogen bonds (orange) in **8**. Thermal ellipsoids are plotted at 50% probability level.

Figure 14 displays all existing hydrogen bonds. For better visualisation only a representative cut through the unit cell was selected. While the hydrogen bridged bondings which coordinate to the chloride are repeated through the whole unit cell, the intermolecular hydrogen bonds $N2^{ii}-H15^{ii}-O2^i$ und $N2^i-H15^i-O2^{ii}$ only exist once per unit cell and are shown in figure 15.

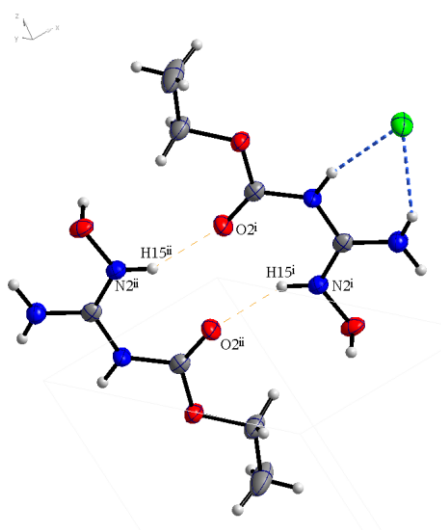


Figure 15. Intermolecular hydrogen bonds. Ellipsoids are plotted at 50% probability level.

The results for the hydrogen bonds are listed in table 4.

Table 4. Selected hydrogen bridged bondings of **8**.

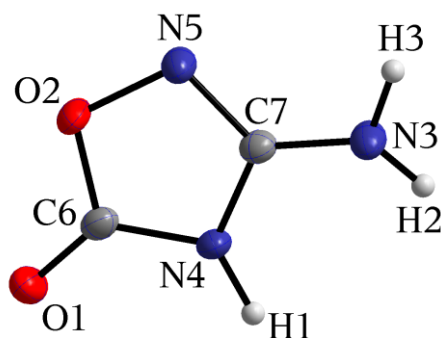
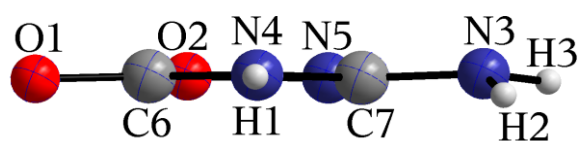
Atoms D-H...A	Bond lengths D-H [Å]	Bond lengths H...A [Å]	Distance D, A [Å]	Angle D-H...A [°]
N2 ⁱⁱ -H15 ⁱⁱ -O2 ⁱ	0.872	2.127	2.910	149.5
N2 ⁱ -H15 ⁱ -O2 ⁱⁱ	0.872	2.127	2.910	149.5
O3 ⁱ -H8 ⁱ -Cl ^v	0.843	2.168	2.997	172.5
N3 ⁱⁱⁱ -H7 ⁱⁱⁱ -Cl ^v	0.922	2.410	3.270	156.0
N1 ^{iv} -H9 ^{iv} -Cl ^v	0.862	2.264	3.103	164.1
N3 ^{iv} -H6 ^{iv} -Cl ^v	0.802	2.565	3.280	149.7

(i) 2-x, 0.5+y, 1.5-z; (ii) x, 1.5-y, 0.5+z; (iii) 1-x, 0.5+y, 1.5-z; (iv) 1-x, 1-y, 1-z;
(v) 2-x, 1-y, 1-z

As the crystal structure displays is **8** only the open chained form of **1**. To obtain the ring closed **1** without the protecting ethanol, there were three methods applied.

First was heating of **8** under basic conditions in DMF with triethylamine, which led to an orange, viscous oil that was not characterized further. Second was to add diphosgene and triethylamine in THF to **8** at 0°C and subsequently heating in 2M hydrochloric acid. The ¹³C NMR shows only signals which are very similar to those of **8**. So the ring closure failed again. Third method was to reflux **8** in 5% sodium hydroxide solution and following acidification of the solution to a pH-value of 3-4. The formed precipitate was analyzed and found to be the desired product **1**.

Crystals of **1** were shaped like a christmas tree and measured to obtain the molecular structure (figure 16).

**Figure 16.** Molecular structure of **1**. Thermal ellipsoids are plotted at 50% probability level.**Figure 17.** Side view of the molecular structure of **1**. Ellipsoids plotted at 50% probability level.

The results of the structure solution are listed in table 5. They show a nearly planar arrangement of the whole molecule. Merely the hydrogen atoms of the amine moiety are tilted from the plane which is spanned by the five-membered ring (figure 17).

Table 5. Selected bond lengths and angles of **1**.

Bond lengths [Å]		Bonding angles [°]	
N3–C7	1.336(4)	N3–C7–N5	124.7(1)
C7–N5	1.306(9)	N3–C7–N4	122.7(9)
N5–O2	1.456(9)	C7–N5–O2	103.5(6)
O2–C6	1.343(5)	N5–O2–C6	108.9(2)
C6–O1	1.220(5)	O2–C6–O1	122.9(8)
C6–N4	1.356(1)	O1–C6–N4	129.7(5)
N4–H1	0.941(4)	C6–N4–C7	107.8(5)
N4–C7	1.364(9)	C6–N4–H1	123.2(0)
		H1–N4–C7	128.8(6)

The variance of the bond lengths of the calculated bond lengths [11] are explained by the different resonance structures. The little elongation of the C6–O1 bond and the significant shortening of the C6–N4 and the O2–C6 bond are refer also to the resonance structures **a** and **b** in figure 18. The cause for the longer C7–N5 bond and the shorter N3–C7 and N4–C7 bond are the resonance structures **c** and **d** (figure 18).

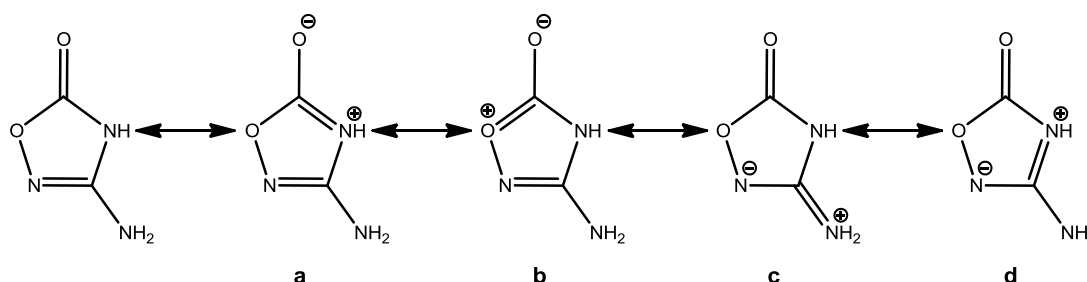


Figure 18. Resonance structures a-d to explain the bonding conditions in **1**.

The least variance to the calculated bond lengths is found in the N5–O2 bond. This is not amazing as there is only a single bond which is not involved in any resonance. Comparing it to the other bond lengths of the five-membered ring it is relatively long. There is no shortening or anything similar observed which would hint classical aromaticity in this ring system.

If the 3-amino-1,2,4(4H)-oxadiazole-5-one(**1**, **aOD**) is split virtually in a guanidine and a carbon dioxide molecule the bond lengths can also be discussed regarding according to those bond lengths. The C6–O1 and C6–O2 bonds are compared with carbon dioxide elongated.[11] The double bond character is lost in the ring system but C6–O1 bond is longer than C6–O2 which applies more double bond character to that bond. The bond length of the shortest bond in the guanidine is about 1.30 Å, which matches with the C7–N5 bond. The longer bonds in the guanidine (1.36 Å) are very similar to the N4–N7 bond and the N3–N4 bond is inbetween with 1.34 Å. [13] Considering this limitations the resonance structure **d** seems to be the least important.

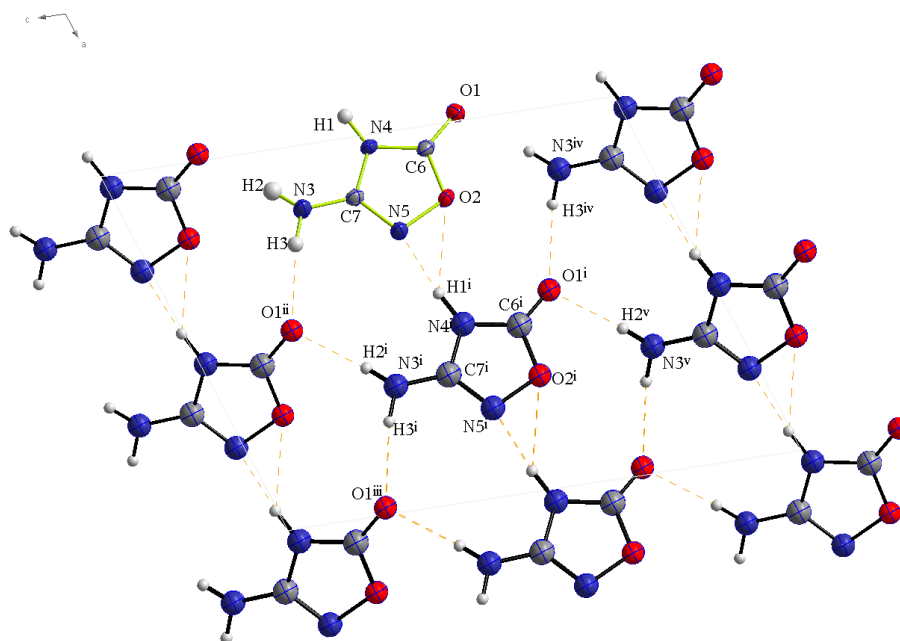


Figure 19. Hydrogen bridge bonding of **1**. View along b-axis. Thermal ellipsoids plotted at 50% probability level.

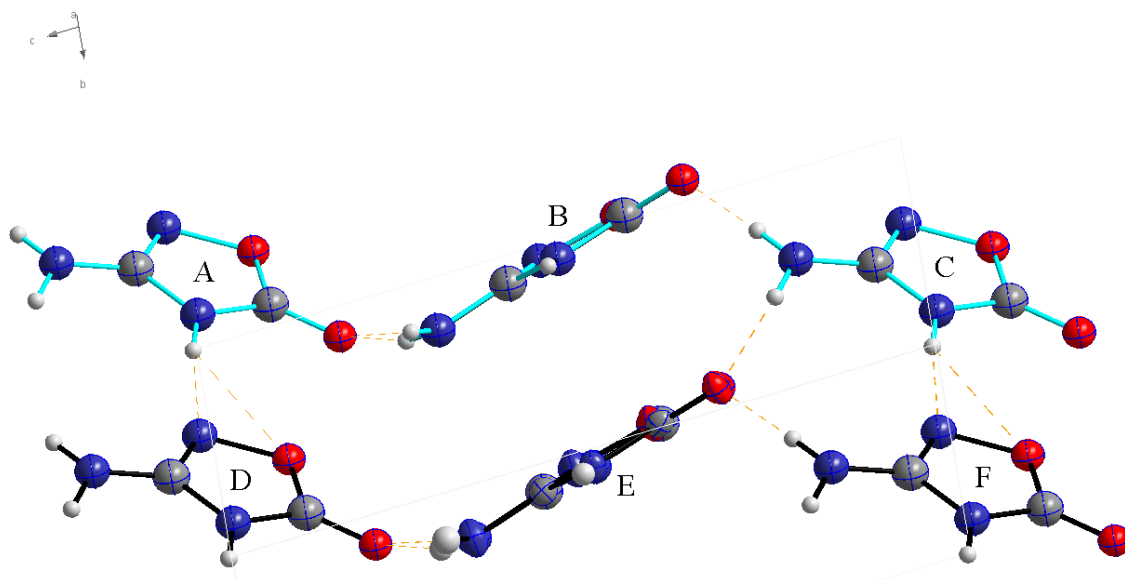
Figure 19 displays the hydrogen bond of **1** along the b-axis. In this visualization the molecules are stacked and the hydrogen bonds are shown best. There are bifurcated hydrogen bridged bonds, where one donor is connected to two accpetors (N4ⁱ-H1ⁱ-O2 and. N4ⁱ-H1ⁱ-N5) or two donors two one acceptor atom (N3-H3-O1ⁱⁱ and. N3ⁱ-H2ⁱ-O1ⁱⁱ). The properties of those bondings are listed in table 6.

Table 6. Hydrogen bridged bonding from the crystal structure of **1**.

Atoms D, H, A	Bond lengths D, H [Å]	Bond lengths H, A [Å]	Bond lengths D, A [Å]	Angles D, H, A [°]
N4 ⁱ –H ⁱ –N5	0.941	1.896	2.826	169.2
N4 ⁱ –H1 ⁱ –O2	0.941	2.616	3.373	137.8
N3 ⁱ –H2 ⁱ –O1 ⁱⁱ	0.870	2.083	2.952	176.3
N3 ⁱ –H3 ⁱ –O1 ⁱⁱⁱ	0.903	2.056	2.942	166.6
N3 ^{iv} –H3 ^{iv} –O1 ⁱ	0.903	2.056	2.942	166.6
N3 ^v –H2 ^v –O1 ⁱ	0.870	3.428	3.734	104.0

(i) 0.5+x, 0.5+y, z; (ii) 0.5+x, 0.5–y, 0.5+z; (iii) 1+x, 1–y, 0.5+z; (iv) x, 1–y, –0.5+z; (v) 0.5+x, 1.5–y, –0.5+z

The N4 donor hydrogen bridged bonding are exclusively connecting the neighbored layers while the N3-donor hydrogen bond shows as well intermolecular connections between molecules of one layer as connections between neighbored layers. This is displayed in figure 20. Also the change of the bonding in one layer and between the layers especially for the N3 donor is illustrated.

**Figure 20.** The layers (black and turquoise) in one unit cell of **1**. Thermal ellipsoids are plotted at 50% probability level.

The layers of turquoise molecules are parallel to layer of the black molecules below, so are molecule A and C. The parallelity is based on the identical distance between N4^A–N4^D, N4^B–N4^E and N4^C–N4^F which is 5.012 Å. Molecule B is turned by 180° compared to molecule A and C. The angle α (N5^A, O2^A, O2^B, N5^B) between the molecules A and B are like the angle β (N5^B, O2^B, O2^C, N5^C) between the molecules B and C 54.4°. The planar five-membered ring will be taken as plane (figure 21). Angle α and angle β are congruent which is based on the parallelity of the layers and are also found between molecule D and E as well as molecule E and F. As molecule A and C are obviously parallel the distance between can be measured at N4^A–N4^C with 11.655 Å. The distance between the virtual plane through molecule A and C (distance d_1) and molecule B and E (distance d_2) are 2.77 Å and 1.36 Å.

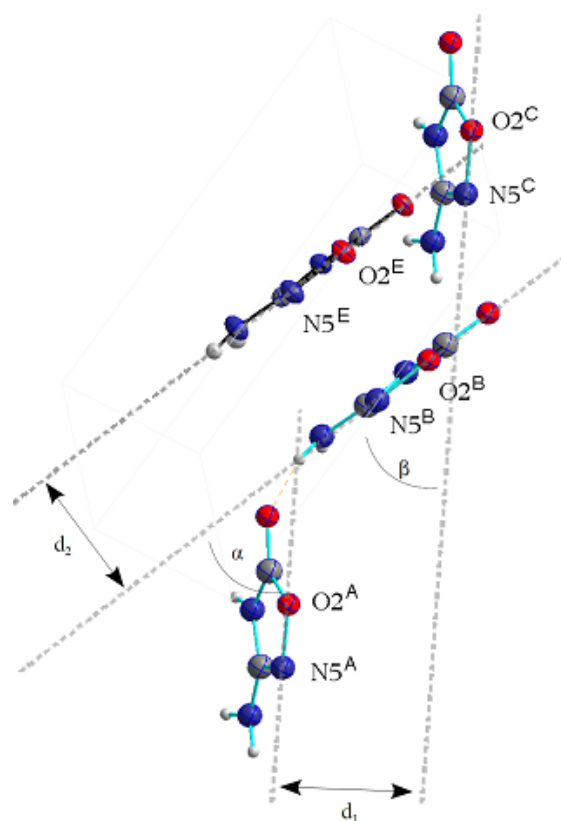


Figure 21. Visualization of molecules in the layers and planes. Thermal ellipsoids are plotted at 50% probability level.

The synthetic route B and the yields including all intermediates of the products are summarized in figure 22.

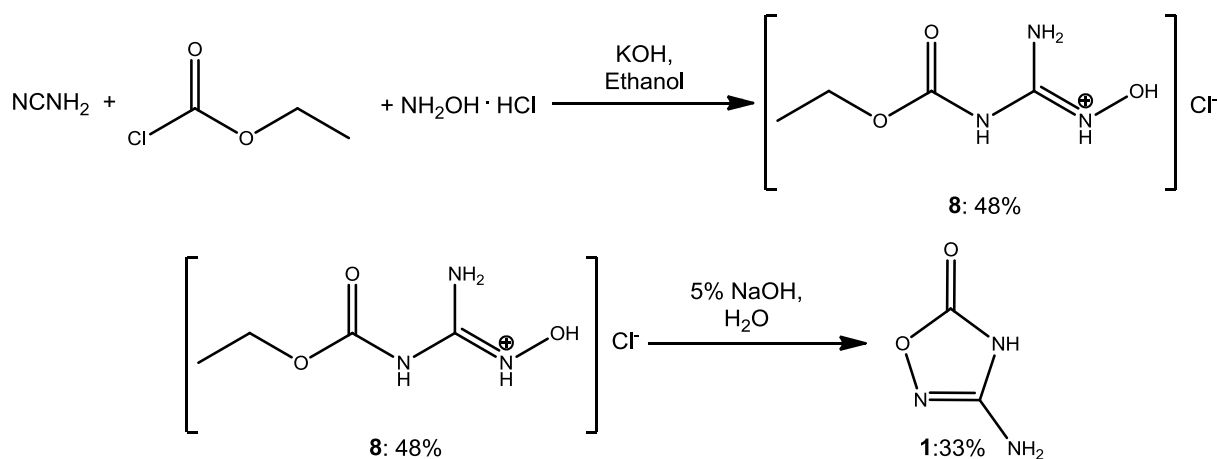


Figure 22. Overview of synthetic route B including all yields. Total yield about 16%.

Alternatively the ring closure reaction was tried with diphosgene as illustrated in figure 23.

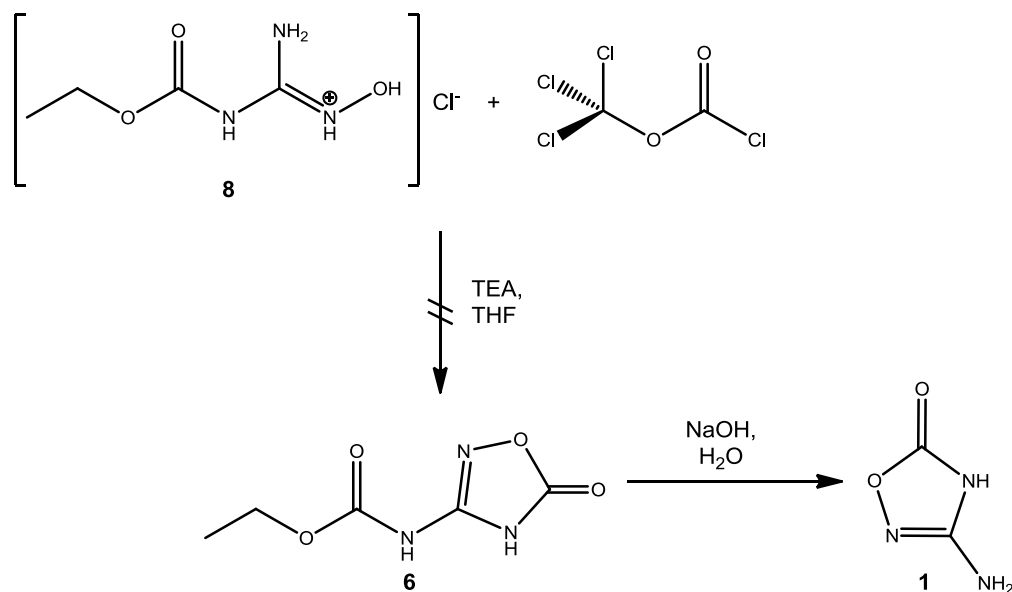


Figure 23. Alternative ring closure reaction starting from **8**.

Therefore **8** should be reacted with diphosgene and triethylamine to build the intermediate **6** which could be subsequently turned into **1**. But the intermediate **6** was not formed under the chosen conditions. So this alternative reaction was neglected.

2.1.4 One-Pot-Synthesis according to route B

To synthesize different compounds starting from aOD therefore aOD was made first. Therefore the synthetic route B was taken and optimized to one pot reaction.

20 g (476 mmol) Cyanamide was solved in 200 mL Ethanol and cooled with a ice/salt bath to 5 °C. Simultaneously a solution of 100 g(1786 mmol) potassium hydroxide and 100 mL was prepared. The hydroxide solution and 45 mL (476 mmol) ethyl chloroformate were added to the cyanamide solution carefully while the pH was maintained between pH 6-7 and the reaction temperature was kept below 30°C. After complete addition of ethyl chlor formate the ice bath was removed and the mixture was heated for one hour at 45°C. After cooling to R.T. the reaction mixture was filtered. An the solid (potassium chloride) dumped. To the filtrate 30 g (429 mmol) hydroxylamine hydrochloride and 1M hydrochloric acid was added till the pH was pH 3. Now the Reaktion mixture is heated under reflux condition for one hour. After cooling to R.T. the mixture was filtered again. So not reacted hydroxylamine and potassium chloride was removed. The solvent of the filtrate was removed and a yellow solid was obtained which was dissolved in 120 mL 1 to 2 % sodium hydroxide in water and boiled over night under reflux conditions. The cooled solution was again neutralized and acidified (pH1-3). The precipitate was filtered and is the first yield. The solvent was removed from the filtrate and the solid residue is recrystallized from little water to form more product. It was obtained a white powder of 3-amino-1,2,4-oxadiazol-5-one. The yield was 16.47 g (163 mmol, 34 %).

The low carbon and nitrogen values from the elemental analysis show that the product has still impurities of potassium or sodium chloride of 5-6%, which reduced the yield to 32% (15.92 g, 153 mmol aOD).

2.1.5 Summary

Synthesis B has proven to be a good choice and avoids toxic methyl mercaptane. The yield of the product is good and the synthesis is rather cheap so that a simple synthetic approach to the aOD is achieved. This makes it possible to do further chemistry based on the aOD.

Although the synthetic route B has a lot of steps and the intermediates are isolated, the whole synthesis can be done as one-pot-reaction. The isolation of the ethyl hydroxyaminoguanidine carbamate ester as intermediate is unnecessary as it is only followed by a ring closure reaction by heating in a slightly alkaline solution. As the product aOD is good soluble in ethanol and methanol it is very easy to get rid of the potassium and sodium chloride salts that form during the synthesis. The greatest challenge is to control during the addition of the reactants that the reaction of each step is completed, before applying other external conditions like heating, cooling or change of the pH value. Overall a yield of 32% was achieved in the one-pot synthesis.

2.2 Solubility of aOD

For further syntheses using the aOD solubility test were carried out with most of the common solvents, for example methanol, ethanol, isopropanol, acetonitrile, ethylacetate, dioxane, acetone, THF, methylene chloride, chloroform and toluene. Water was not considered as aOD has shown good solubility during the preparation of the salts.

For the solubility test 30 mg of aOD were combined with a solvent. The test was cancelled when the solvent volume exceeded 6 mL.

The solubility of the previous mentioned solvents goes down in the following order: Methanol > ethanol > acetone > isopropanol > ethyl acetate > acetonitrile \approx methylene chloride > chloroform \approx THF \approx dioxane > Toluene

Table 7. Overview of the solubility tests of **1** in different solvents..

Solvent	End volume[ml]	Completely solved?	Remarks
Methanol	2.5	yes	-
Ethanol	4.0	yes	-
Acetone	4.5	yes	-
Isopropanol	6.0	no	mostly solved
Ethyl acetate	6.0	no	little solid left
Acetonitrile	6.0	no	partly solved
Methylene chloride	6.0	no	partly solved
Chloroform	6.0	no	little solved
THF	6.0	no	little solved
Dioxane	6.0	no	little solved
Toluene	6.0	no	nothing solved

The aOD shows higher solubility in protic polar solvents, but acetone as aprotic polar solvent is the exception. As in the also aprotic polar solvent acetonitrile it displays only bad solubility. A possible explanation may be on the one hand a reaction of aOD with acetone on the other hand the building of hydrogen bridged bondings. Little till no solubility is found for aprotic unpolar solvents like toluene.

2.3 Azo-coupling of aOD

Finally an azo-coupling was performed according to the preparation of Johannes Thiele ^[13] (figure 9).

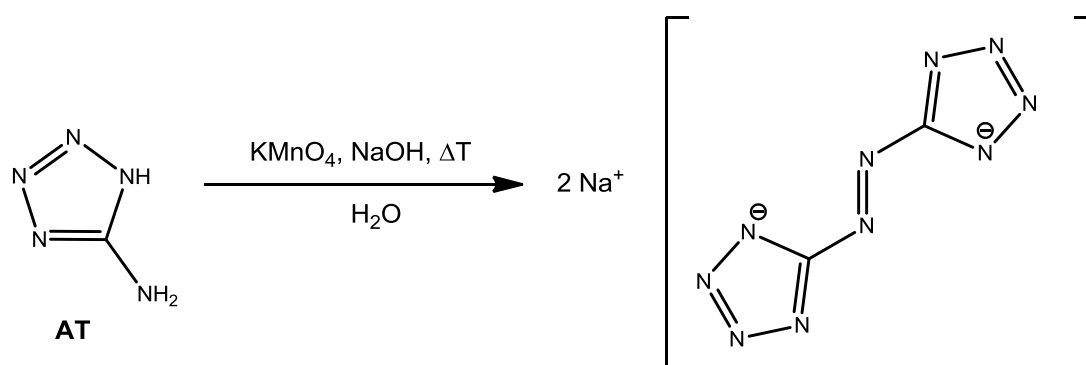


Figure 24. Azo-coupling of 5-amino-1*H*-tetrazole according to Thiele.

This preparation instruction refers to the coupling of two equivalents of amino tetrazole, but was applied in the same way to two equivalents of aOD. Both amino groups are oxidized by potassium permanganate (figure 24).

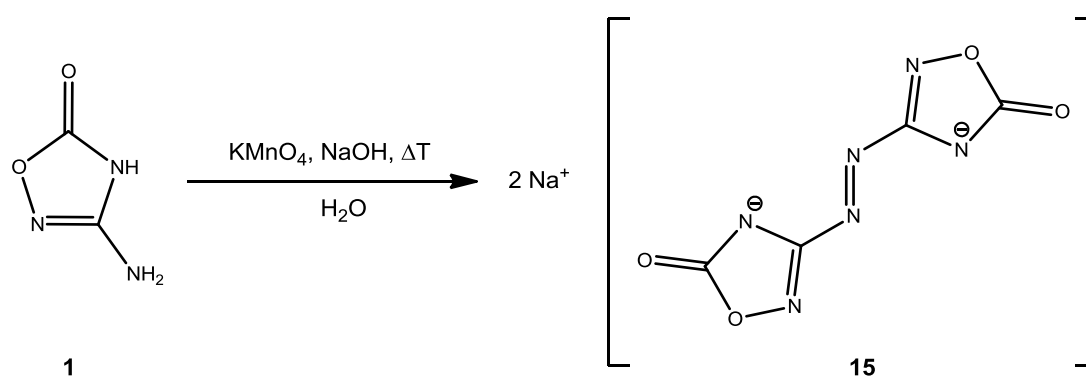


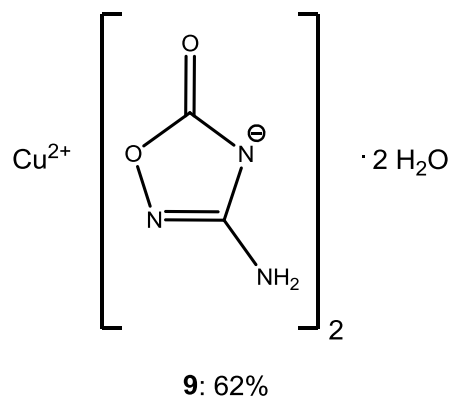
Figure 25. Azo-coupling of aOD analogous to AT.

The azo coupling of **1** was carried out according to the procedure for 5-amino-1*H*-tetrazole under alkaline conditions with potassium permanganate and heating. But the oxidation led to carbonate salt by decomposition of **1**.

This was the first hint that **1** is not stable in hot alkaline solutions and decomposes to carbonate or carbon dioxide and guanidine.

2.4 Salts of aOD

2.4.1 Copper aOD (9)



Two equivalents of aOD were solved in little methanol and reacted with slightly acidic (pH=5) copper nitrate solution. After filtration a blue-green solid was obtained. The IR spectrum shows amino vibrational absorptions and the N-H valence vibration at 3432 cm^{-1} and 3321 cm^{-1} . The characteristic dublett form of the amino vibration absorption is also observed here. The expected C-O valence vibration absorption at 1726 cm^{-1} and the C-N-valence vibration absorption at 1613 cm^{-1} are found. An elemental analysis was accomplished and besides of two aOD anions also two water molecules were observed. The complex geometry was not solved as there were no crystals obtained for analysis.

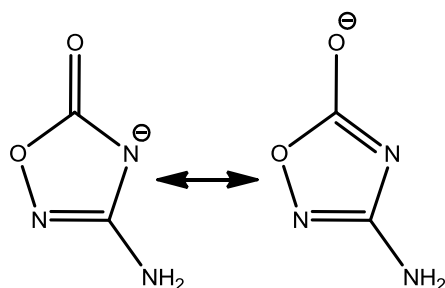


Figure 26. Mesomeric explanation of different coordination possibilities.

The Cu^{2+} cation as a d^9 -system normally forms Jahn-Teller distorted octahedral complexes^[14]. In such a case the aOD anion has the function of a bidental ligand that coordinates to the central cation to reach the coordination number of six. As shown in figure 26 due to the mesomeric form of the aOD anion to possible coordinations are possible on the one hand over N4 O1 and on the other hand by N4 and N3. As well the N-H valence vibration as the C-O valence vibration absorptions display a shift to higher wavenumbers in comparison to the neutral aOD (3340 cm^{-1} , 3251 cm^{-1} and 1659 cm^{-1}), so it is not possible to resolve the coordination in the end. Also the C-N valence vibration absorption is shifted to higher wave numbers with respect to the neutral aOD (1527 cm^{-1}). The temperature of decomposition is 194.4°C .

Both possible structural drafts of the copper complex are illustrated in figure 27.

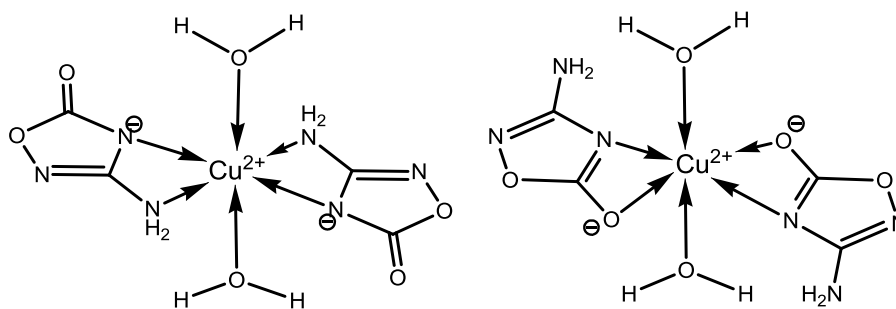
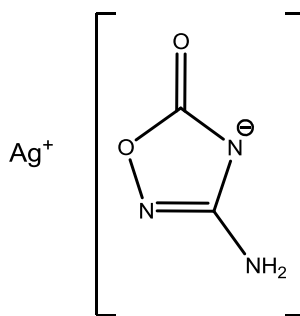


Figure 27. Coordination of the aOD anion according to a Jahn-Teller distorted copper complex.

2.4.2 Silver aOD (10)



10: 73%

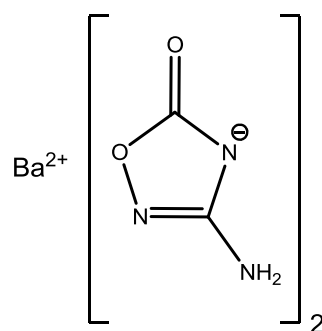
The silver salt was synthesized with light disclosure as it was not known from the beginning if the salt is light unstable. To a neutralized solution of **1** with sodium hydroxide in water a silver nitrate solution is added. A fine powdered white solid was obtained and characterized by IR spectroscopy and elemental analysis.

The IR spectrum displays compared to the neutral aOD little shifted absorption signals. So the N-H valence vibration absorption is observed at 3432 cm^{-1} (doublet shaped) slightly shifted to higher wave numbers but by the deprotonation of the N4 the intensity of the signal is going down. The C-O and the C-N valence vibration absorptions are in the region of 1704 cm^{-1} to 1633 cm^{-1} . Finally an amino torsion vibration is observed at 1580 cm^{-1} . The elemental analysis confirmed a composition of only Ag^+ cation and aOD^- anion.

2.4.3 Strontium aOD (11) trihemihydrate

The strontium salt is not precipitating as the solution of **1** and a solution of strontium hydroxide but when the solvent was slowly removed. The IR spectrum displays the amino group valence vibration (doublet shaped) at 3354 cm^{-1} , the C-O valence vibration absorption weak at 1765 cm^{-1} and C-N valence vibration absorption at 1658 cm^{-1} . The elemental analysis showed a composition of the salt as trihemihydrate ($1.5\text{ H}_2\text{O}$).

2.4.4 Barium aOD (12)

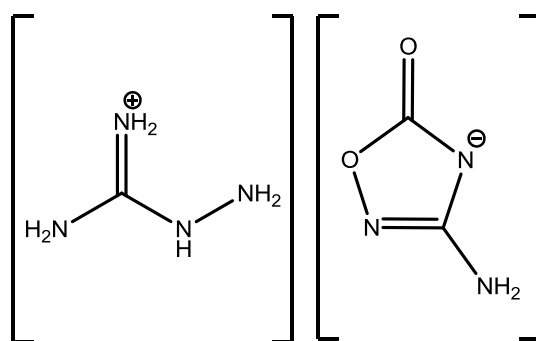


12: 44%

The barium salt was prepared according to the method for the strontium salt but with barium hydroxide octahydrate. The precipitate was obtained while removing the solvent.

The IR spectrum shows the amino valence vibration absorption at 3320 cm^{-1} , the C-O valence vibration absorption at 1684 cm^{-1} and the C-N valence vibration absorption in the region of 1670 to 1651 cm^{-1} . The elemental analysis showed an impurity which was neutral aOD. This is the case because of the barium hydroxide which reacts while standing as solid with carbon dioxide from the air to barium carbonate and so the stoichiometry of the supposed to be barium hydroxide does not fit to the amount of aOD.

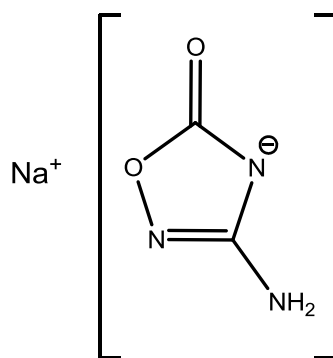
2.4.5 Aminoguanidinium aOD (13)



13

The aminoguanidine salt was synthesized from aminoguanidinium carbonate and **1**. It shows a viscous consistency. The assumption that the solvent was not fully removed was not confirmed by the elemental analysis. But the elemental analysis was not 100 percent accurate. The mass spectrometry confirmed the salt with FAB⁺ signal at $m/z=75.1$ which compares to the aminoguanidinium cation. The FAB⁻ signal at $m/z=100.1$ is found for the aOD anion. The ^{13}C NMR displays a shift to lower field of the carbon signals in the salt compared to the neutral aOD ($\delta = 166.4, 170.6\text{ ppm}$). But no solvent was observed. So the consistency could be related to an ionic liquid.

2.4.6 Sodium aOD (**14**) monohydrate



14: 48%

The sodium salt precipitates from a solution of sodium hydroxide and **1** after removing the solvent. In the ^{13}C NMR the carbon signal of the aOD-anion is shifted to lower field and the values are similar to those of the guanidinium at $\delta = 165.7$ ppm and 169.0 ppm. In the ^1H NMR the signal of the amino group is not observable. The IR spectrum shows the characteristic valence vibration absorptions for amino groups at 3450 cm^{-1} doublet shaped, the carbonyl group at 1722 cm^{-1} and the ring C-N bond at 1689 cm^{-1} .

The summarized values for the IR vibration absorptions of all described salts are listed in table 7

CRYSTAL STRUCTURE

Sodium aOD (**14**) crystallizes in the monoclinic space group $P2_1/c$ with 4 molecular units in the unit cell. The central sodium cation has the four aOD anions and two water molecules in its coordination sphere (fig. 28). The aOD anion coordinates over the nitrogen (N2, N3) and oxygen (O1, O5) to the sodium central ion.

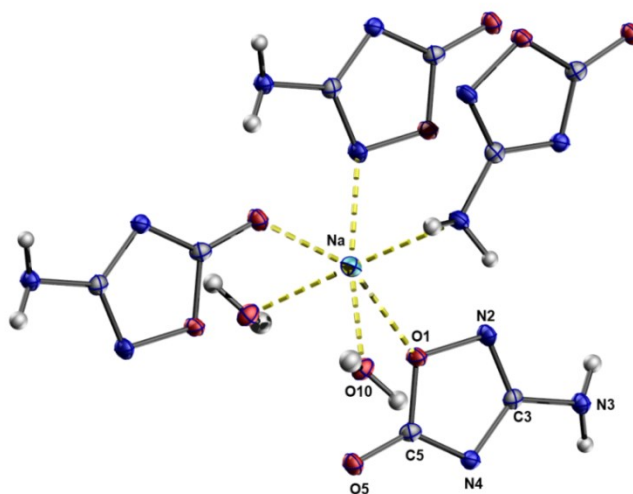


Figure 28. Coordination sphere of sodium in **14**.

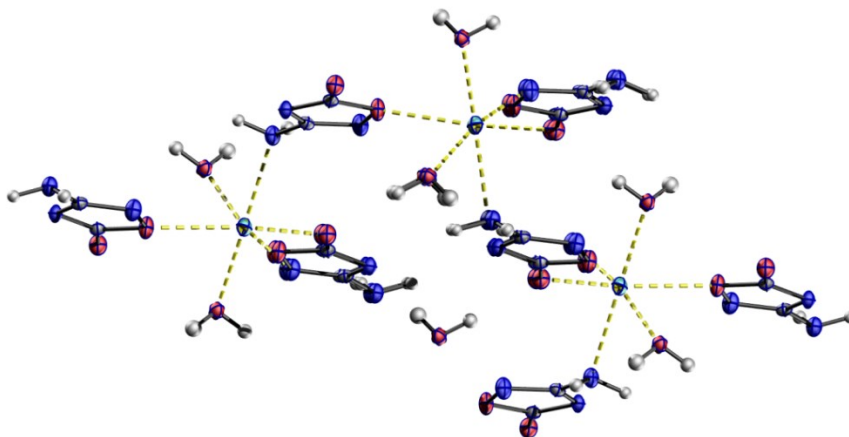


Figure 29. View along a-axis shows the coordinative connection to sodium between the layers in the structures.

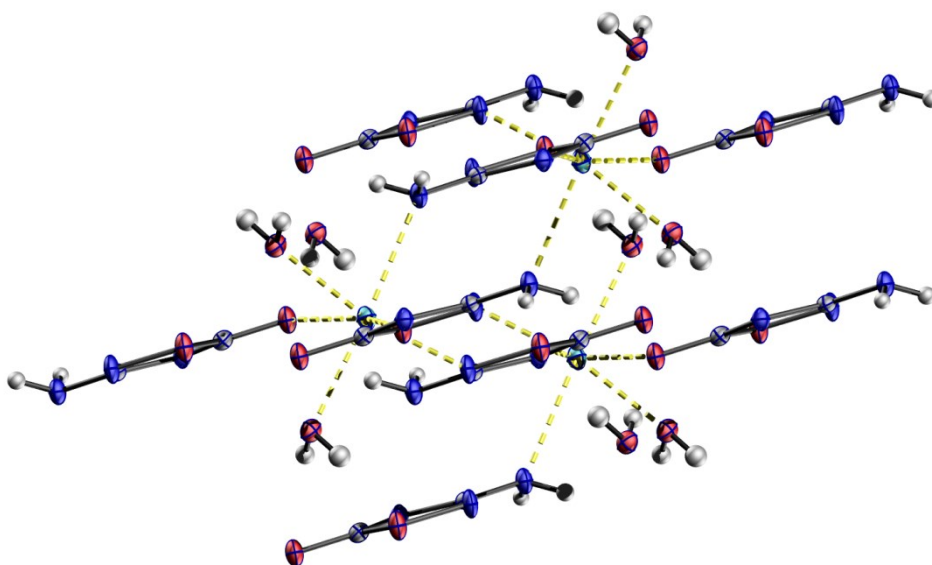


Figure 30. View along b-axis shows the coordinative connection to sodium between the layers in the structures.

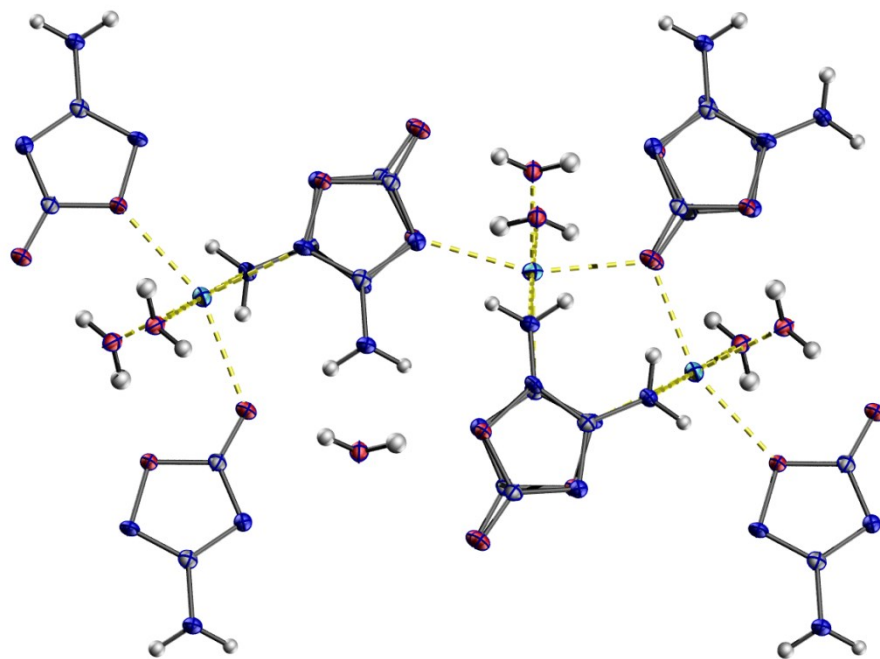


Figure 31. View along c-axis of the structure shows how the aOD anions are stacked along this direction.

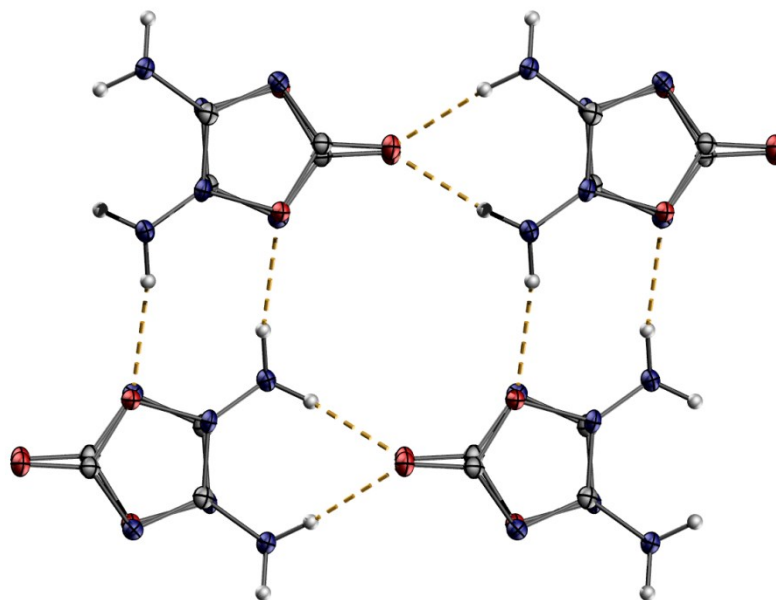


Figure 32. View along a-axis leaving out coordination of sodium only emphasising the hydrogen bonds between the aOD anions.

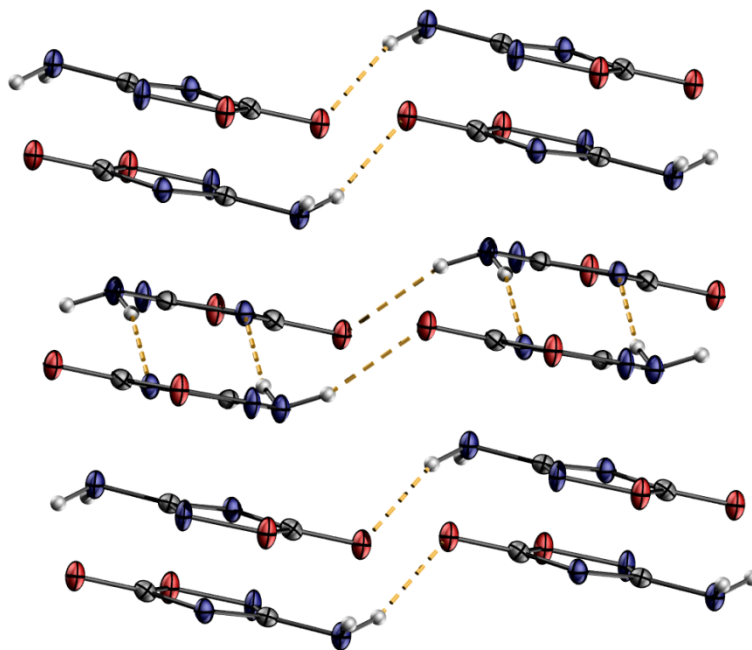


Figure 33. View along b-axis leaving out coordination of sodium only emphasising the hydrogen bonds between the layers of the aOD anions.

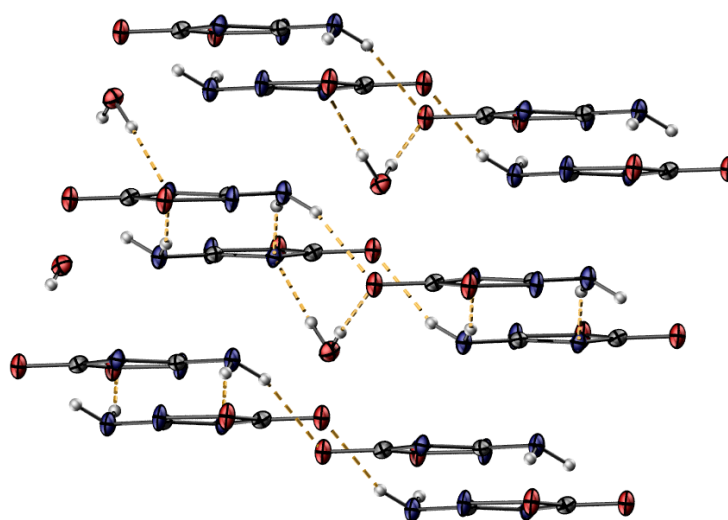


Figure 34. View along c-axis: leaving out coordination of sodium only emphasising hydrogen bonds between water and aOD anions.

Comparing the bond lengths and the angles of the aOD anion with the respective neutral compound all are in good accordance. Some bond length are a little longer C5-

O5 1.25 Å (1.22 Å), C3-N3 1.38 Å (1.34 Å) and C5-O1 1.37 Å (1.34 Å). The other bond lengths are little shorter.

The hydrogen bondings shown in figure 32-34, are stabilizing the crystal to a layer structure of aOD anions and the sodium cation is found in between as shown in figure 29-31.

Table 8. Selected bonds and angles of the sodium aOD (**14**): aOD moiety (purple)-water moiety (blue).

Atoms 1,2	d 1,2 [Å]	Atoms 1,2,3	Angle 1,2,3 [°]	Atoms 1,2,3	Angle 1,2,3 [°]
N4—C5	1.334(2)	C5—N4—C3	103.5(1)	C5—O1—Na1 ^{viii}	133.00(7)
N4—C3	1.362(2)	N2—C3—N4	116.5(1)	N2—O1—Na1 ^{viii}	118.21(7)
C3—N2	1.312(2)	N2—C3—N3	121.3(1)	C5—O5—Na1 ^{ix}	127.88(8)
C3—N3	1.379(2)	N4—C3—N3	122.1(1)	N2 ⁱⁱⁱ —Na1—O1 ^v	103.83(4)
C5—O5	1.249(2)	O5—C5—N4	123.0(1)	C3—N2—Na1 ^x	124.37(8)
C5—O1	1.370(2)	O5—C5—O1	119.0(1)	Na1 ⁱ —O10—Na1 ^{vii}	84.45(3)
O1—N2	1.446(1)	N4—C5—O1	111.0(1)	O10 ⁱ —Na1—O10 ⁱⁱ	95.55(3)
Na1—N2 ⁱⁱⁱ	2.418(1)	C5—O1—N2	106.97(9)	O10 ⁱ —Na1—N2 ⁱⁱⁱ	95.68(4)
Na1—O5 ^{iv}	2.425(1)	C3—N2—O1	101.96(9)	O10 ⁱⁱ —Na1—N2 ⁱⁱⁱ	168.71(4)
Na1—O1 ^v	2.476(1)	O5 ^{iv} —Na1—O1 ^v	158.06(3)	O10 ⁱ —Na1—O5 ^{iv}	84.06(3)
Na1—N3	2.516(1)	N2 ⁱⁱⁱ —Na1—N3	87.31(4)	O10 ⁱⁱ —Na1—O5 ^{iv}	86.34(3)
O1—Na1 ^{viii}	2.476(1)	O5 ^{iv} —Na1—N3	94.74(4)	O10 ⁱ —Na1—O1 ^v	81.12(3)
O5—Na1 ^{ix}	2.425(1)	O1 ^v —Na1—N3	99.19(4)	O10 ⁱⁱ —Na1—O1 ^v	79.12(3)
N2—Na1 ^x	2.418(1)	O1—N2—Na1 ^x	118.83(7)	O10 ⁱ —Na1—N3	176.83(4)
Na1—O10 ⁱ	2.364(1)	C3—N3—Na1	130.38(8)	O10 ⁱⁱ —Na1—N3	81.44(4)
Na1—O10 ⁱⁱ	2.384(1)	N2 ⁱⁱⁱ —Na1—O5 ^{iv}	93.64(4)		
O10—Na1 ⁱ	2.364(1)				
O10—Na1 ^{vii}	2.384(1)				

(i) 1-x, 1-y, -z; (ii) 1+x, y, z; (iii) x, 0.5-y, -0.5+z; (iv) 1+x, 0.5-y, -0.5+z;
(v) 1-x, 0.5+y, 0.5-z; (vi) 2-x, 1-y, -z; (vii) -1+x, y, z; (viii) 1-x, -0.5+y, 0.5-z;
(ix) -1+x, 0.5-y, 0.5+z; (x) x, 0.5-y, 0.5+z.

Table 9. Selected hydrogen bonds: aOD moiety (purple)-water moiety (blue).

Atoms D,H,A	Dist. D,H [Å]	Dist. H,A [Å]	Dist. D,A [Å]	Angle D,H,A [°]
N3—H3A—O5 ⁱ	0.87(2)	2.17(2)	3.005(2)	162(2)
O10—H10B—O5 ⁱⁱ	0.85(2)	2.03(2)	2.880(1)	174(2)
O10—H10A—N4	0.88(2)	2.00(2)	2.886(2)	177(2)
N3—H3B—N4 ⁱⁱⁱ	0.91(2)	2.20(2)	3.089(2)	167(2)

(i) 1+x, y, z; (ii) -x, 1-y, 1-z; (iii) 1-x, 1-y, 1-z.

2.4.7 Summary

The aOD salts with aOD as anion were synthesized and and characterized. Figure 35 shows as short overview. Most salts are found accompanied by water molecules like the sodium, copper, barium and strontium salt. The silver salt was water free. Although all salts were tried to crystallize only sodium aOD showed some measurable crystals. The copper and the silver salts could be isolated only as powders and the aminoguanidinium salt was a resin like substance as ionic liquid. The IR vibration wave numbers for the metal salts of aOD are listed in table 10.

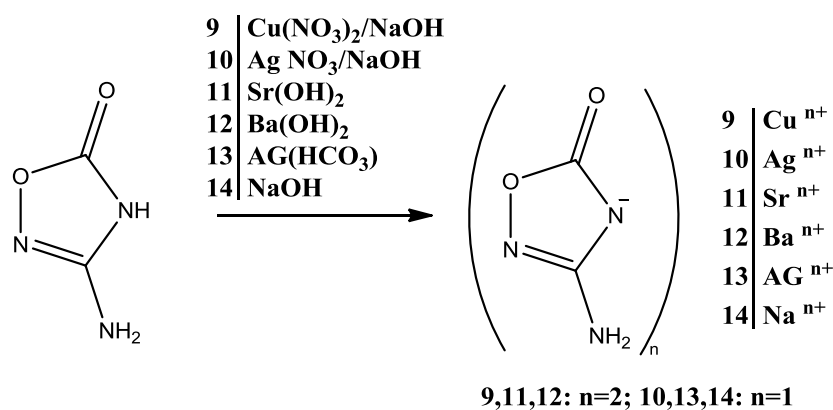


Figure 35. Synthesized salts of aOD.

Table 10. Summary of the described salts and for comparison neutral aOD.

compound	$\tilde{\nu}$ (N-H-/NH ₂ -vibration) [cm ⁻¹]	$\tilde{\nu}$ (C-O-vibration) [cm ⁻¹]	$\tilde{\nu}$ (C-N vibration) [cm ⁻¹]	yield [%]
aOD (1)	3340	1659	1527	12 (A) 16 (B) 32 (B-1)
Cu aOD ₂ x 2 H ₂ O (9)	3432	1726	1613	62
Ag aOD (10)	3432	1704	1633;1649	73
Sr aOD ₂ x 1.5 H ₂ O (11)	3354	1765	1658	36
Ba aOD ₂ x (12)	3320	1684	1670-1651	44
Na aOD (14)	3450	1722	1689	48

2.5 Methylation of 3-amino-1,2,4(4H)-oxadiazol-5-one

The methylation of the aOD may be possible in two positions. As methyl transfer reagent are used dimethyl sulfate (figure 36) and also methyl iodide (figure 37). Both result in the product 3-amino-4(*N*)-methyl-1,2,4-oxadiazol-5-one (N-Me-aOD, **16a**) and 3-amino-5-methoxy-1,2,4-oxadiazole (O-Me-aOD, **16b**).^[15]

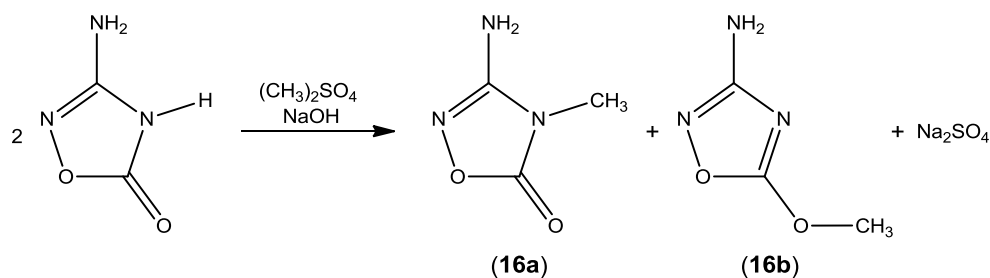


Figure 36. Methylation of aOD by dimethylsulfate.

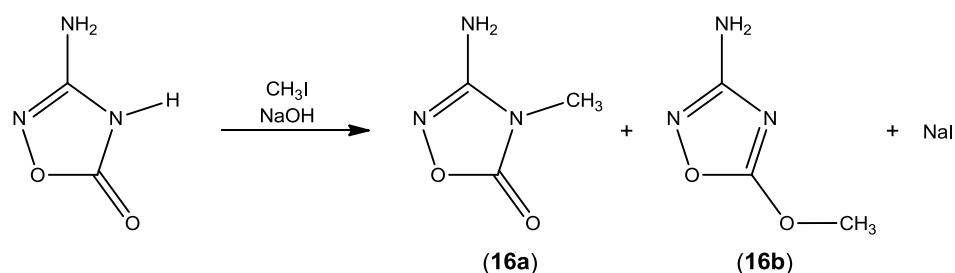


Figure 37. Methylation of aOD by methyl iodide.

2.6 Synthesis of salts with aODH⁺ as cation

The amino functionality and the literature known cation of 5-amino-1*H*-tetrazole [2b] was the starting point to investigate the possibility of forming also aODH⁺ cations.

The analytical data displays that no salts have been formed with the chosen strong acids, but the aOD was recrystallized in purest. The IR spectrum shows the typical valence vibration absorptions for the neutral aOD at 3346cm⁻¹ for the amino moiety and at 1653 cm⁻¹ for the ring carbon-nitrogen bond. In the elemental analysis the values for carbon 23%, nitrogen 41% and hydrogen 3% are found and fit perfectly to those of pure aOD.

There are two possibilities first aOD is not protonated or the acids used were not strong enough.

Therefore the acidity and basicity of the protons at the aOD molecule are investigated. The ring proton at the nitrogen (N4) is split of very easily, so the aOD is a very good Brønsted acid. In comparison the Brønsted basicity of the amino moiety (N3) is very weak, which means further protons are not added readily. In other case there would be a zwitter-ionic structure preferred which is not in consent with the discussed crystal structure.

The strength of the used acids in the respective solvents are important to discuss. Some strong acids are listed in table 11 according to their pK_a-values in water.

Table 11. *pK_a-value of the used strong acids*

Acid	pK _a (water)
Picric acid ^[10]	0.29
Nitric acid	-1.37
Perchloric acid	~ -10

Even the perchloric acid with a pK_a value of about -10 did not form the desired product. It is possible that super acidic systems like hydrogen fluoride with arsen or antimon pentafluoride will form such adduct.

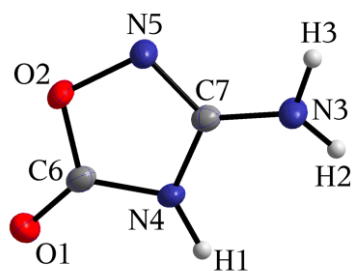


Figure 38. Molecular unit of aOD from crystal structure.

For discussion the numbering of the atoms was chosen according to the crystal structure of neutral aOD figure 38.

In the case of the protonation of the nitrogen at the amino group (N3) there is a positive charge at the N3 nitrogen. The N4 atom is neglected because of the high Brønsted acidity. The charge at the N3 can not be stabilized by mesomery, but a tautomeric form can be found with the charge at the N5 atom as illustrated in figure 39.

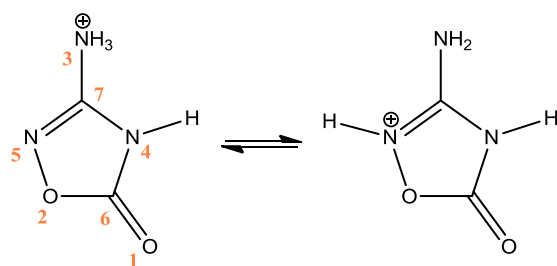


Figure 39. Tautomerism of the protonation: a) at the amino nitrogen, b) at the nitrogen in the ring.

Further structures with the additional proton at the carbonyl oxygen are possible for the neutral aOD, when a zwitter-ionic form is considered (fig.21).

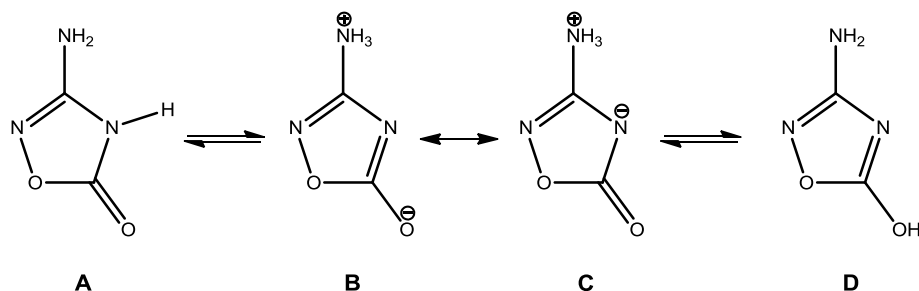


Figure 40. Zwitter-ionic and neutral structure of the aOD: **B** and **C** as mesomeric structures and tautomeric structure **A**, **B/C** and **D**.

Ab initio calculations which were carried out for the in figure 40 displayed structures of the aOD, show on a closer inspection of the *Hartree Fock* energies that the molecule geometry can be lined up in the following row.

$$\mathbf{A > D > B = C}$$

The calculation were performed by the Gaussian03^[16] program package at MP2 level of theory with a split-valence double-zeta basis set 6-31G(d) ^[15,17]. The combination of the tautomers and mesomeric structures of figure 40 with the energies of the species are illustrated in figure 41.

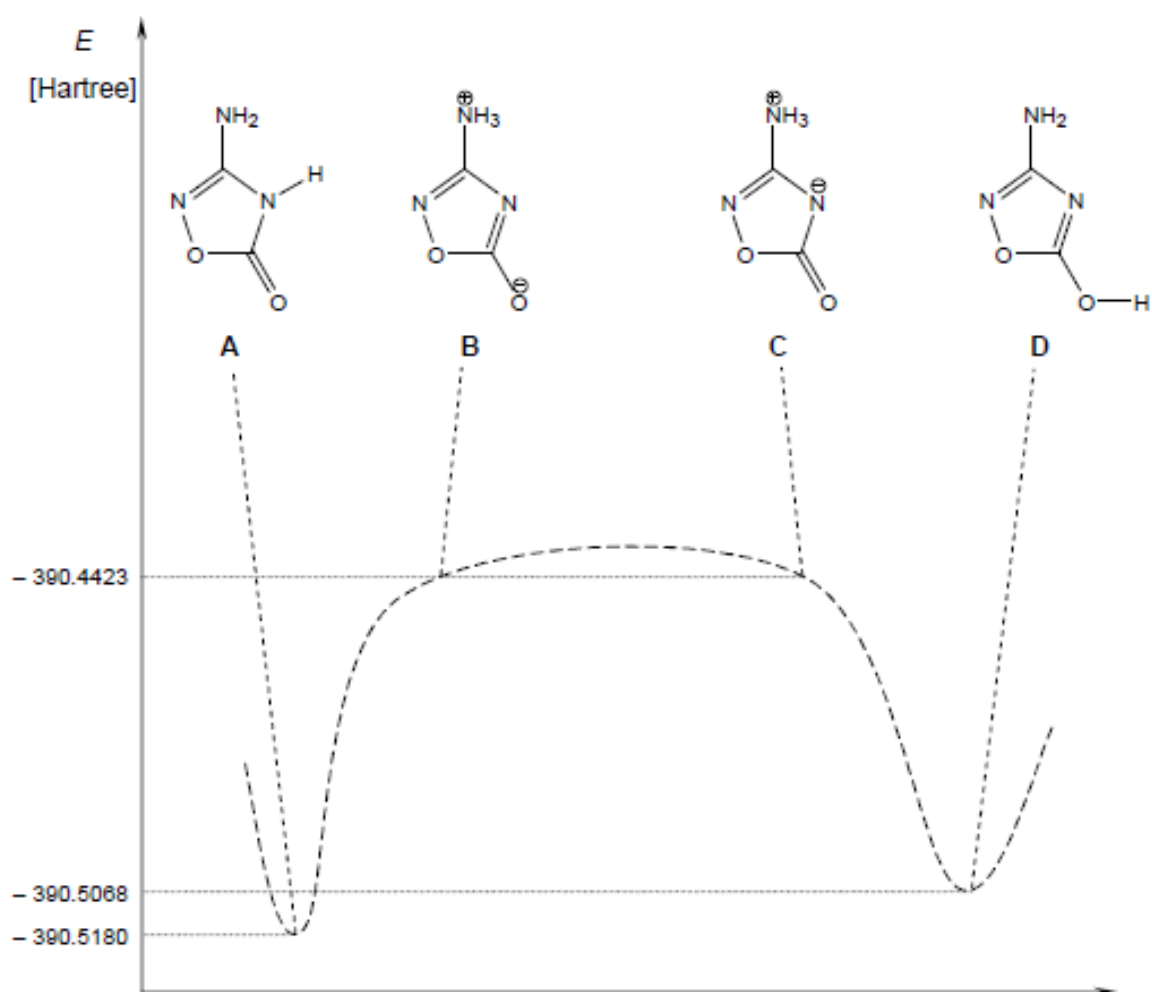


Figure 41. Hartree Fock-energies of the molecule forms **A** to **D** of aOD.

The structure that shows the lowest energy is structure **A** and matches with the one from the crystal structure analysis. The calculated energy of the tautomeric form **D** is the second important structure, which is especially important for the methylation reaction of aOD. This reaction was discussed before and explanation for the products **11a** and **11b** (fig. 36 and fig.37) is now underlined by the calculation.

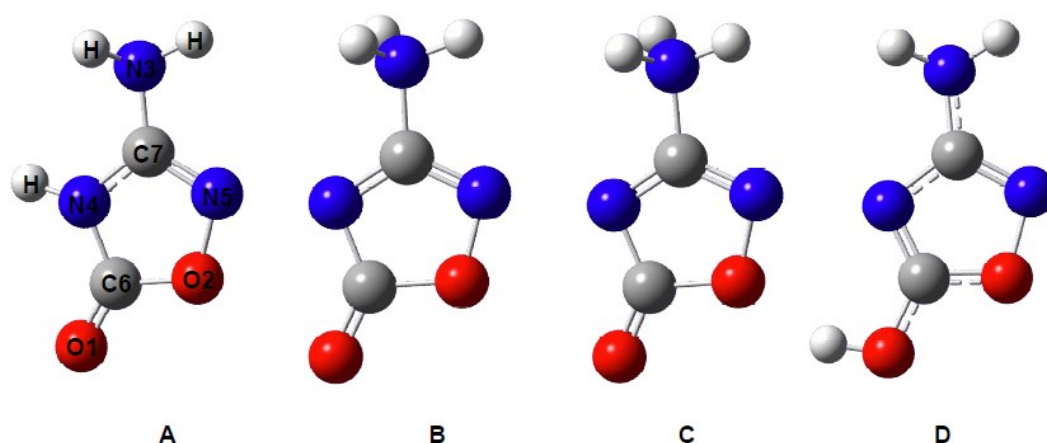


Figure 42. Visualization of the results from figure 33 by the ab-initio-calculation of aOD, illustrated by GaussView 5.0^[18] (drawn bonds do not correspond to real bonds but illustrate the calculated bond length with respect to the van-der-Waals radii)

Figure 42 displays the investigated structures A to D. In the picture are double and single bonds as well as bonds inbetween (dashed) are outlined. In table 12 the bond lengths for the different structures are listed. For structure A the gas phase calculation confirms the bond lengths in nearly all aspects of the crystal structure determination. In the mesomeric structures B and C the bond lengths of N3-C7 as well as C6-O2 are prolonged in comparison to the crystal structure. In the case of structure D the bond also C7-N3 is longer, while the bond C6-O2 and C7-N4 are slightly shorter, which is expected because of the hydrogen at O1. The shortened bond lengths especially in tautomer D are visualized by the dashed and double bonds, which may be an effect of a highly delocalized π -system.

The analogous procedure that was applied to aOD was used on the structures for the protonated aODH⁺ cation species **a** to **e** (fig. 43) by calculation with Gaussian03 at MP2level of theory and a split-valence double-zeta basis set 6-31G(d).

Table 12. Bond lengths, energies and point group for structure **A** to **D** (calculated by the Gaussian03 program package^[16], colored bonds differ from the literature value^[11]):

Structure	Point group	Bond	Bond lengths [Å]	Energy [Hartree]	Method and level of theory ^[9]
A	C₁	C7 – N5	1.304	– 390.5180	MP2/6-31G(d)
		C7 – N4	1.371		
		N4 – C6	1.389		
		C6 – O1	1.210		
		C6 – O2	1.378		
		O2 – N5	1.430		
		C7 – N3	1.385		
		C7 – N5	1.311		
		C7 – N4	1.321		
		N4 – C6	1.410		
B	C₁	C6 – O1	1.213	– 390.4423	MP2/6-31G(d)
		C6 – O2	1.445		
		O2 – N5	1.410		
		C7 – N3	1.475		
		C7 – N5	1.310		
		C7 – N4	1.321		
		N4 – C6	1.387		
		C6 – O1	1.213		
		C6 – O2	1.446		
		O2 – N5	1.410		
C	C₁	C7 – N3	1.475	– 390.4423	MP2/6-31G(d)
		C7 – N5	1.320		
		C7 – N4	1.381		
		N4 – C6	1.303		
		C6 – O1	1.334		
		C6 – O2	1.334		
		O2 – N5	1.425		
		C7 – N3	1.379		
		C7 – N5	1.320		
		C7 – N4	1.381		
D	C₁	C6 – O1	1.334	– 390.5068	MP2/6-31G(d)
		C6 – O2	1.334		
		O2 – N5	1.425		
		C7 – N3	1.379		
		C7 – N5	1.320		

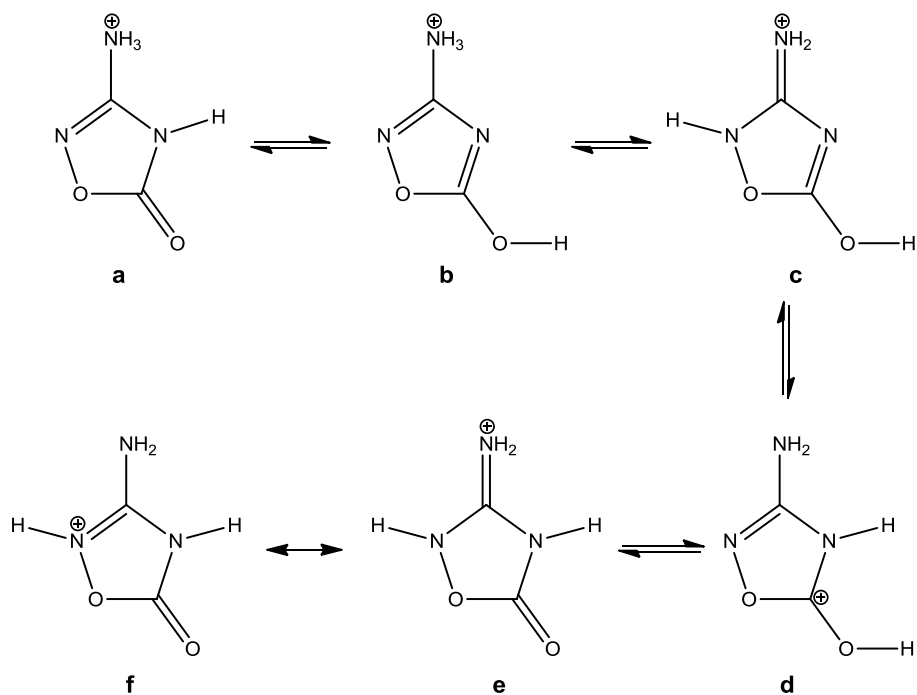


Figure 43. Tautomeric and mesomeric structures of aODH⁺ cation.

The molecule structures of the aODH⁺ cation can be lined up a row according to their *Hatree-Fock* energy.

$$\mathbf{c < e = f < d < b < a}$$

The positive charge is located mainly on the N3-atom. The illustration of the energies analogous to figure 41 is displayed in figure 44.

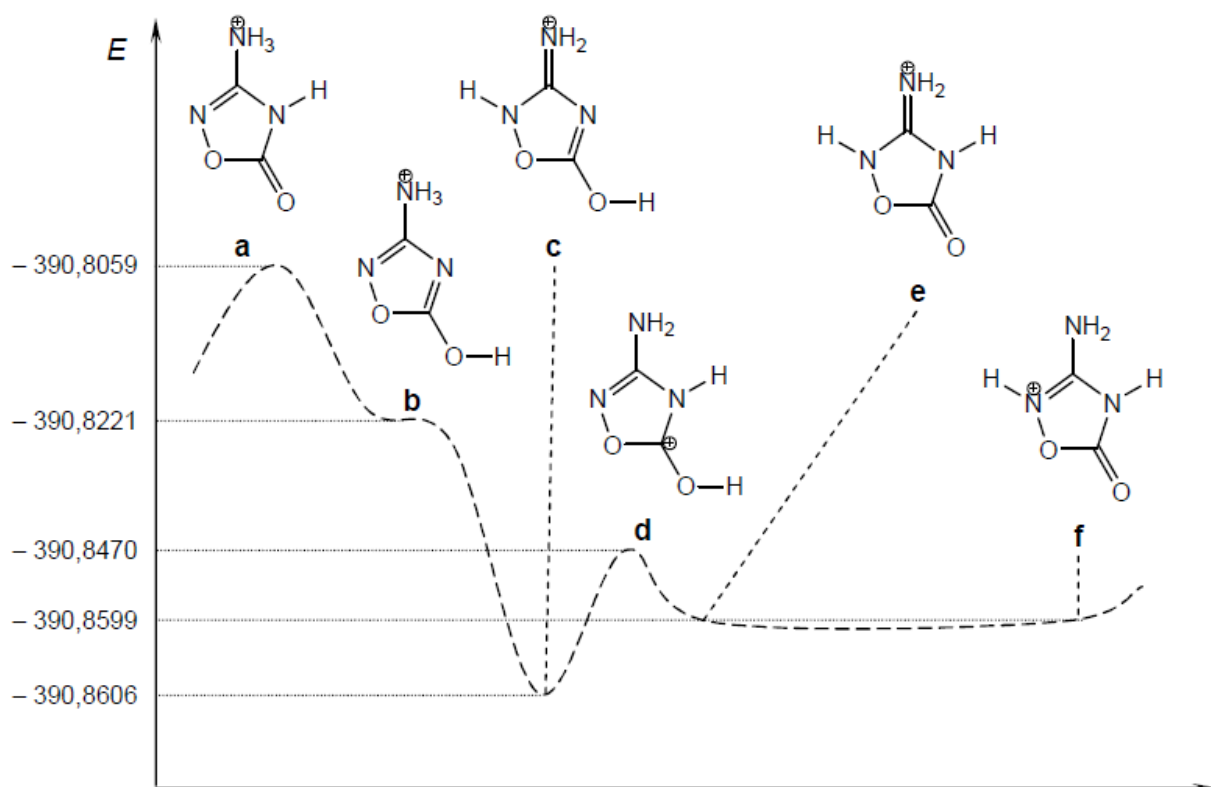


Figure 44. Hartree-Fock energies of the aODH⁺ cation **a** to **f**.

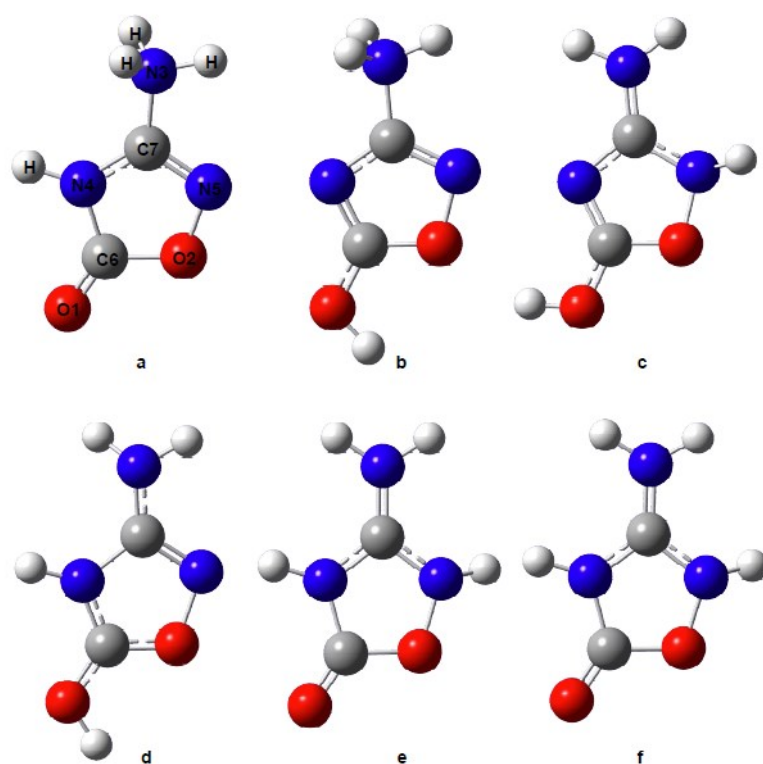


Figure 45. Visualization of the structures by ab initio calculations like in figure 25^[18] (bond lengths to not refer to real bonds but to their qualities).

Figure 44 shows in the calculated structural outline of the aODH⁺ cation structures **a** to **f**. Structure **c** displays a structure where delocalization is most widely spread, which results in the lowest energetic structure (fig. 45). The mesomeric structures **e** and **f** are second lowest in energy while the tautomeric structure **d** is higher in energy although the proton is only situated on the other side of the ring at the N4. Therefore delocalization happens at **e** and **f** only guandine like at the carbon C7 for the positive charge. The structure **d** has a single bond between N4 and N7 which implies a broken delocalization.

Looking at all calculated structures **a** to **f** it is obvious that the N5-O2 bond is not effected at all and always a single bond (see table 13). This bond is shortened in the aODH⁺ cation from 1.46 Å to a value around 1.41 to 1.39 Å.

Table 13. Bond lengths, energy and point group of the aODH⁺ cation (colored values differ from the literature [11]):

Structure	Point group	Bond	Bond length [Å]	Energy	Method ^[9]
a	C ₁	C7 – N5	1.297	– 390.8059	MP2 / 6-31G(d)
		C7 – N4	1.350		
		N4 – C6	1.418		
		C6 – O1	1.193		
		C6 – O2	1.406		
		O2 – N5	1.394		
		C7 – N3	1.456		
		C7 – N5	1.314		
b	C ₁	C7 – N4	1.345	– 390.8221	MP2 / 6-31G(d)
		N4 – C6	1.317		
		C6 – O1	1.307		
		C6 – O2	1.357		
		O2 – N5	1.399		
		C7 – N3	1.458		
		C7 – N5	1.363		
		C7 – N4	1.352		
c	C ₁	N4 – C6	1.314	– 390.8606	MP2 / 6-31G(d)
		C6 – O1	1.297		
		C6 – O2	1.346		
		O2 – N5	1.406		
		C7 – N3	1.319		
		C7 – N5	1.316		
		C7 – N4	1.398		
		N4 – C6	1.328		
d	C ₁	C6 – O1	1.298	– 390.8470	MP2 / 6-31G(d)
		C6 – O2	1.305		
		O2 – N5	1.438		
		C7 – N3	1.351		

e	C₁	C7 – N5	1.349	– 390.8599	MP2 / 6-31G(d)
		C7 – N4	1.340		
		N4 – C6	1.420		
		C6 – O1	1.190		
		C6 – O2	1.393		
		O2 – N5	1.410		
		C7 – N3	1.321		
		C7 – N5	1.349		
		C7 – N4	1.340		
		N4 – C6	1.420		
f	C₁	C6 – O1	1.190	– 390.8599	MP2 / 6-31G*
		C6 – O2	1.393		
		O2 – N5	1.410		
		C7 – N3	1.321		

The O2-N5 bond in structure **c** which has the lowest energy is 1.41 Å and C6-N4 is shortened to 1.31 Å compared to the neutral molecule structure **A**. Not only compared to the crystal structure but also to the literature values^[11], some statements can be made. In all structures **A** to **D** of the aOD and **a** to **f** of the aODH⁺ the one with most values differing to the literature is the one calculated with the lowest energy. While the C-N and C-O single bonds are in the range of 1.47 to 1.43 Å are noted as standard in nearly all structures they are found between 1.31 and 1.36 Å, which is significantly shorter but not at all a double bond which is noted standard with 1.22 Å for a C=O double bond and 1.29 Å for a C=N double bond.

In the energetically most preferred structure **c** of the aOD-cations the bond between O2 and N5 with 1.41 Å as well as the C6 to N4 bond with 1.31 Å are shorter than the molecular structure **A** of the neutral aOD. Not only the comparison of the bond lengths of the crystal structure analysis, but also according to literature values^[11] the following results can be approved.

As well the structures **A** to **D** of the neutral aOD molecule as the molecule geometry of **a** to **f** of the aOD cations show that those which are the most stable ones according to the gas phase ab-initio-calculation differ most from the literature values. While the C-N and C-O single bond lengths are known to be between 1.47 Å and 1.43 Å ^[11], in the structures **A** to **D** and **a** to **f** the C-N and C-O bond lengths are between 1.31 Å and 1.36 Å, which would only mean a delocalization of electrons which results in a contraction of the bond.

The C=O double bond length which is commonly about 1.22 Å is found in most of the calculated structures except **D** of the neutral aOD and **b** to **d** in the aODH⁺ which show a longer distance between C6 and O1 with 1.30 Å which is due to the additional hydrogen bond to the O1. That fact influences the charge density distribution in the oxadiazole ring. The structure which differs mostly from the literature value shows most delocalization and is energetically preferred.

If the N4-atom is deprotonated, the situation will change. The created negative charge is distributed through the whole ring system as delocalization. There is no need for tautomeric structures, intramolecular proton shifts and zwitter-ionic structures, which are unfavorable for the molecular state. Only the bond between the O2-oxygen and N5-nitrogen are not affected by the mesomeric stabilization and stay at single bond length (see table 13).

In figure 46 some mesomeric structures are drawn. If the free electrons of N3 take also part, separation of charges will occur, which are theoretically possible but practically avoided as this leads to a higher energetic state.

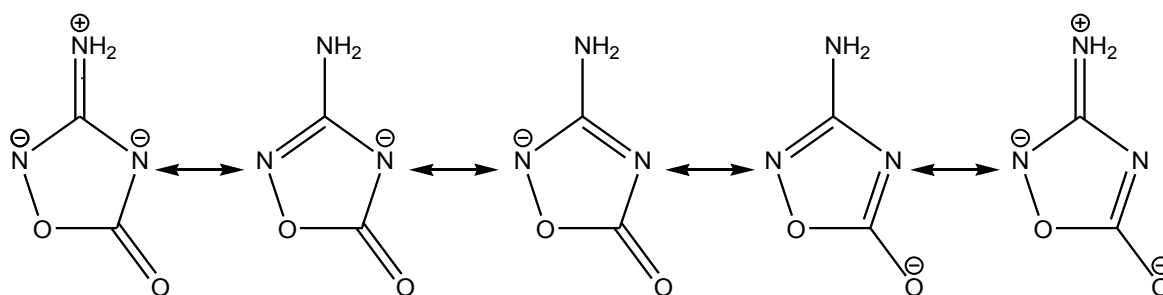


Figure 46. Mesomeric structures of aOD^- which show possible delocalization of the negative charge.

It is remarkable that the most preferred structure of aOD in the gas phase as shown by calculation is the same as in the solid state proved by crystal structure analysis. In the case of an aOD crystal the possible cause could be the hydrogen bridged bonds which stabilize the crystal structure. While the hydrogen bridged bonds are optimal formed with donor acceptor interactions with structure **A** of aOD, in the gas phase no hydrogen bonds are taken in account despite of that it is also the energetic most favorable structure.

In the case of the aODH^+ cation the structures in the gas phase with the best delocalization of the electrons are found to be the most occurring, like in structure **c**. The shift of the charge density is connected to the demands of the electronegativity principles. As the negative charge of the structure in compound **c** is found mainly located on oxygen while in structure **a** it is located on the nitrogen. Negative charge is transferred to the N5-atom and the lowered charge density at the O2-atom. The small separation of this charges as observed in the calculation leads to a better attraction and a slightly shortened O2-N5 bond in structure **a**.

Although the chemistry of aOD and 5-amino-1*H*-tetrazole is very similar and some analogia is observed the fact that the protonation of aOD was experimentally not possible has now been investigated theoretically and found to be plausible.

For comparison the amino-tetrazolium cation which is found in aminotetrazolium nitrate is shown in figure 47.

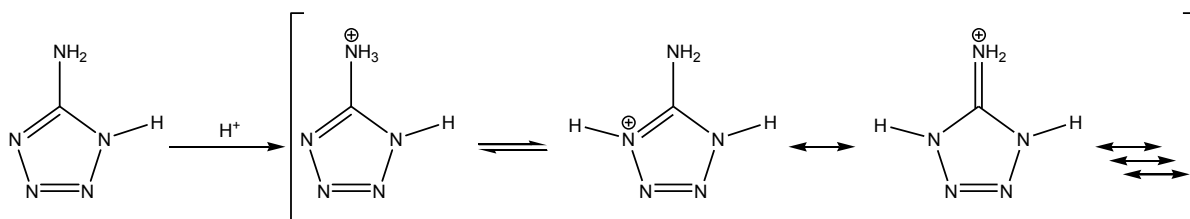


Figure 47. Mesomeric and tautomeric structure of the 5-amino-1,4 -dihydro-tetrazolium cation.

The positive charge can be delocalized through the whole tetrazole ring. The aromaticity of the system is only slightly influenced by the protonation and every nitrogen atom can work as acceptor for the proton which increases the possible mesomeric structures with minimum energetic state.

For the 5-amino-tetrazolium cation the salts with the anions nitrate, sulfate, chloride and perchlorate are known. The dinitramide salt of the aminotetrazole is nowadays a common explosive. [19, 20]

2.6.1 Summary

The synthesized aOD was tried to protonate by different strong mineral acids like hydrochloric acid, nitric acid, concentrated sulfuric acid and perchloric acid. The analytical result from IR-spectroscopy and elemental analysis of the precipitated product from the respective evaporating acid was pure aOD. Unlike 5-aminotetrazole which is similar to aOD regarding the chemical behavior and compounds including aminotetrazolium cations are known, aOD is not protonated in any way. For an explanation of this result besides the Bronsted acidity of the free amino group and the oxygen there was studied the mesomeric and tautomeric structures of aOD. The ab initio calculation of the respective mesomeric and tautomeric structure shows the most stable protonated form includes a hydrogen at the oxygen outside the ring and on the nitrogen next to the ring oxygen which is not obvious and surprising. As there is only one structure which is energetically preferred it is not likely to happen at crystallization to find this structure easily.

As all experiments have been performed in aqueous media a change to an aprotic polar solvent and a gaseous acid may possibly lead to a protonated form as the tautomeric structures are not likely to happen as proton exchange is less possible.

In contrast there are a lot of mesomeric structures found for the aOD⁻ anion which are optimized by ab initio calculation and found to end up in the same structure with delocalized electrons due to the measured shortened bond lengths in the calculated and observed structures.

2.7 Energetic data

The calculation of detonation values was carried out by the EXPLO 5 code.^[21, 22] Due to the fact that AT crystallizes always with one water molecule in its structure which can be removed by intense heating and explosion will take place then immediately, the results were compared at the same density of 1.75 g cm^{-3} , which is the measured density for crystalline aOD.

Table 14. Detonation values for AT and aOD calculated with EXPLO 5.04 code.

comp	TMD / g cm^{-3}	$U^\circ_f /$ kJ kg^{-1}	Ox. bal.	$Q_v /$ kJ kg^{-1}	$V_0 /$ L kg^{-1}	$T_{\text{ex}} /$ K	P / kbar	D / ms^{-1}	imp / J(Nm)	fric ./ N	mp /°C	T_{dec} /°C
TNT exptl	1.64 1.64	-184.9	-74	-5089	622	3741	202 210	7150 6950	15	>353	81	300
RDX exptl	1.80 1.80	+417	-21	-6034	769	4334	340 347	8882 8750	7.4	120	204	213
PETN [12] (EXPLO 5)	1.77	-1594	-10	-5975	769	4140 4398	331 318	8350 8599	3		141	163
aOD	1.75	-1531	-55	-2979	720	2454	206	7293	>40	>360	-	207
AT	1.75*	3035	-79	-3577	794	2517	284	8524	>40	>360		205

BKWG type of constants in BKW E.O.S is used in calculation (Alpha=0,5; Beta=0,096; Kappa=17,56; Theta=4950), *theoretical density as AT with one water is 1.54 g cm^{-3} and anhydrous AT 1.711 cm^{-3} .

Nonetheless the values are compared to standard explosives like TNT, RDX and PETN. So aOD does not competed with PETN or RDX in performance it outnumbers TNT easily. As there is completely no sensitivity towards any kind of external force found for aOD it can be seen as safe material. While AT shows even with water a slight brisance. The performance values are more comparable to those of PETN.

Looking in to the more specific behavior of both compounds aOD and AT regarding there properties when it comes to application as propellant there are some characteristic values to be discussed. To compare the values the calculation is done as isobaric combustion for rocket propellants and isochoric combustion for gun propellants.

One of the important values is the volume the gaseous products which is calculated directly from the mol number of gaseous products by multiplication with 24.8 L mol^{-1} .

Although the mass of gaseous products is higher at aOD which leaves little to no residues to a barrel the total mass of solid and gasous combustions products of aOD and AT are the same (table 15)

Table 15. Thermochemical parameters at the nozzle exit calculated with EXPLO 5.04 code:

	aOD	AT 175
Total enthalpy of products (He) (kJ/kg)	-2958.6	742.2
Total mol number of gaseous products (mol/kg expl.)	41.95	49.28
Temperature at nozzle exit (Te) (K)	534.6	761.0
Pressure at nozzle exit (pe) (bar)	1.00	1.00
Volume of gaseous products (at SATP) (L/kg expl.)	1039.99	1221.63
Mass of gaseous combustion products (g/kg expl.)	914.0	836.0
Mass of solid combustion products (g/kg expl.)	86.0	166.2
Total mass of combustion products (g/kg expl.)	1000	1002
Mean molecular mass of gaseous prod. (g)	21.786	16.965
Mean molecular mass of all products (g)	20.361	15.843
Specific gas constant (R) (J/kg K)	348.803	409.723
Specific heat ratio (Cp/Cv)	1.313	1.296

Combustion condition: Isobaric combustion ($p=\text{const.}$), Chamber pressure = 70,000 (bar); (Note: Combustion gases obey ideal gas equation of state).

The specific impuls is a characteristic property for a propellant used in a rocket motor. AT outnumbers aOD in this case also regarding the exhaust velocity by far. So aOD as pure compound will be not suitable for use as a rocket propellant.

Table 16. Characteristic parameters at the nozzle exit calculated with EXPLO 5.04 code:

	aOD	AT 175
Specific impulse (Is) (s)	166.21	212.
Exhaust (or nozzle exit) velocity (Ue) (m/s)	1630.5	2084.6
Characteristic exhaust velocity (c*) (m/s)	1031.4	1315.2
Thrust coefficient (CF)	1.581	1.585
Nozzle area expansion ratio (Ae/At)	7.37	7.59
Pressure ratio (pc/pe)	70.000	70.000
Sound velocity at nozzle exit (ae) (m/s)	494.77	635.63
Mach number at nozzle exit (Me)	3.295	3.280

Combustion condition: Isobaric combustion ($p=\text{const.}$), Chamber pressure = 70,000 (bar); (Note: Combustion gases obey ideal gas equation of state).

Comparing single, double and triple base gun propellants with AT and aOD there is also a lack of performance regarding pure aOD, while it is possible to use it as modifier. (see table 17).

Table 17. Computed (EXPL05) gun propellant for single, double and triple base propellants compared to NILE^[1], aOD and AT175 mixtures.

Propellant	$\rho /$ g cm^{-3}	Loading density	$f_E /$ kJ g^{-1}	$b_E /$ cm^3 g^{-1}	$T_{\text{comb}} /$ K	$P_{\text{max}} /$ bar	N_2/CO
NC(12.5)	1.66	0.2	1.05	1.08	3119	2674	0.26
NC:NG(50:50)	1.63	0.2	1.21	1.02	3987	3035	0.59
NC:NG:NQ(25:25:50)	1.70	0.2	1.13	1.06	3256	2875	1.25
TAGzT:NC(85:15)	1.63	0.2	1.09	1.22	2525	2875	6.07
aOD	1.75	0.2	0.62	1.04	1825	1572	1.53
aOD:NC(85:15)	1.74	0.2	0.67	1.07	1954	1727	1.11
aOD:NC(40:60)	1.69	0.2	0.87	1.12	2460	2240	0.52
aOD:NC(50:50)	1.70	0.2	0.82	1.11	2324	2122	0.60
aOD:NC(60:40)	1.71	0.2	0.78	1.11	2205	2005	0.71
aOD:NC:NG(20:40:40)	1.65	0.2	1.13	1.05	3537	2868	0.61
aOD:NC:NG(30:35:35)	1.66	0.2	1.08	1.06	3273	2750	0.62
AT175	1.75	0.2	0.95	1.15	2450	2458	No CO
AT175:NC(85:15)	1.74	0.2	0.94	1.17	2428	2461	5.70
AT175:NC(90:10)	1.74	0.2	0.94	1.16	2429	2454	8.85
AT175:NC(70:30)	1.72	0.2	0.95	1.18	2450	2488	2.60

NC (Nitrocellulose), NG (Nitroglycerine), NQ (Nitroguanidine), TAGzT (triaminoguanidinium azotetrate), AT175 (water free aminotetrazole with theoretical density of 1.75 g cm^{-3}), calculation under isochoric conditions/use of virial term for gas properties.

Overall pure aOD shows good performance as explosive but as propellant it is only suitable in combination. The best value for aOD is found in the triple base composition with NC (40%), NG(40%) and aOD (20%) as modifier. The pressure 2868 bar is similar to the triple based propellant NC:NG:NQ 2875 bar at a slightly increased combustion temperature of 3537 K and N_2/CO ratio which defines the corrosion ability of 0.61. This means the aOD is suitable as modifier but does not contribute to a good N_2/CO ratio. That is why nitrogen rich compounds like AT are more desired for gun and rocket propellants.

3 Conclusions

The comprehensive investigation of 3-amino-1,2,4(4*H*)-oxdiazol-5-one (**aOD**, **1**) shows a lot of similarities with the 5-amino-1*H*-tetrazole (**AT**) regarding stability and sensitivity. The literature known synthesis of aOD was improved by a factor 4 in yield and avoiding methylmercaptane by changing to a one-pot synthesis this synthesis can be called green and is easily upscaled (see 2.1). The detailed look into the behavior of the aOD regarding basic (see 2.4) and acidic conditions (see 2.6), examination of the solubility (see 2.2) and first application of the well studied reactions of AT to aOD have taken. (see 2.3, 2.5) Regarding energetic properties the AT proves to be the better choice also the aOD has energetic values comparable to TNT and performs rather well in propellant mixtures.

4 Outlook

The primary goal was to synthesis of 3-amino-1,2,4(4*H*)-oxadiazol-5-one (**aOD**, **1**) and examine its properties. Also some further reactions have been carried out. The azo-coupling according to the methods applied for AT was not successful as aOD is sensitive to strong base and strong oxidizers. Other mild oxidizing agents might be more successful like hypochlorite, hydrogen peroxide or oxone. Also changing condition to acidic medium may avoid the decomposition to carbonate.

Further investigations may follow the already described synthetic pathways like they were published in the PhD thesis of J. Stierstorfer on AT^[2b]. Now there is the possibility to start reactions like nitration, diazotation or as synthon with other energetic moieties to increase the brisance of aOD and tailor the sensitivities of other energetic molecules.

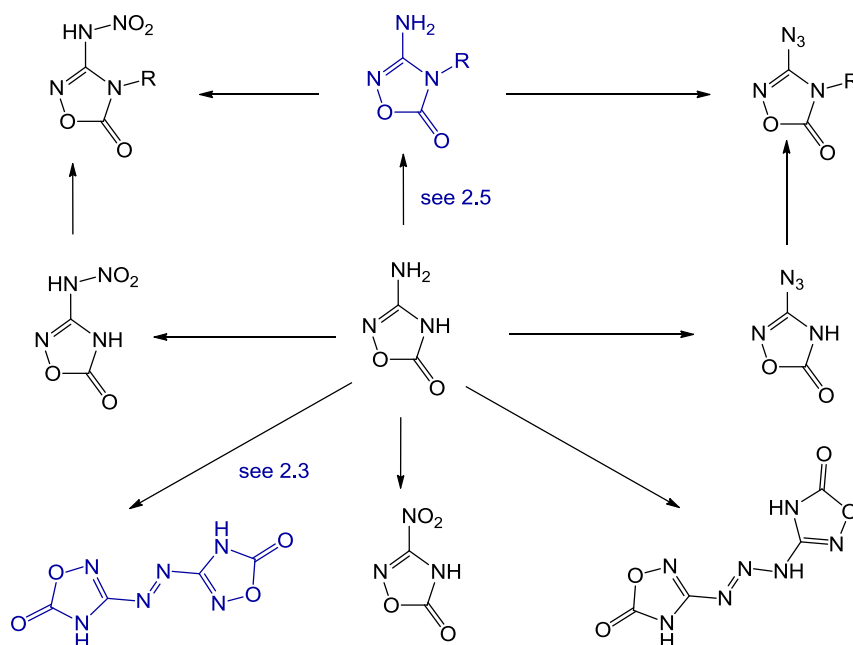


Figure 48. Suggested derivatives of aOD according to the investigated derivatives of AT.^[2b]

5 Experimental part

5.1 Chemicals and Methods

The chemicals used for the synthesis were taken from the local storage and used without further purification or drying, except the ethanol which was dried and stored over magnesium chips.

The NMR spectroscopy was done at the institutes *Jeol Eclipse 400 Spektrometer*, *Jeol EX 400* und *Jeol Eclipse 270* instruments. All ^{13}C and ^1H spectra were recorded at 25 °C. The chemical shift is indicated in ppm relative to the external standard tetramethylsilane (TMS).

Raman spectra were recorded at a *PerkinElmer Spektrum 2000 NIR-FT-Raman Spectrometer* ($\lambda=1064$ nm).

The Infrared spectra were recorded with a *PerkinElmer Spektrum BXII FT-IR System* equipped with a *Diamond-ATR DuraSampler*.

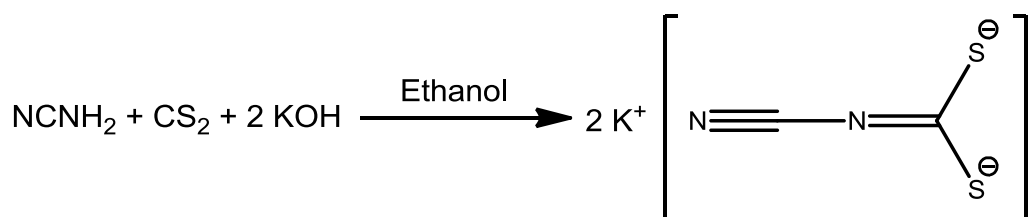
The mass specrometry (DEI+, FAB+/-) was done at a *Finnigan MAT 95*.

Elemental analysis for nitrogen, carbon and hydrogen content of the samples was determined with *Netzsch STA 429 Simultaneous Thermal Analyser*.

Differential Scanning Calorimetry to determine the melting and decomposition point of pure compounds was done by a *Linseis DSC-PT10*. The heating rate was 5 K per minute.

5.2 Preparation

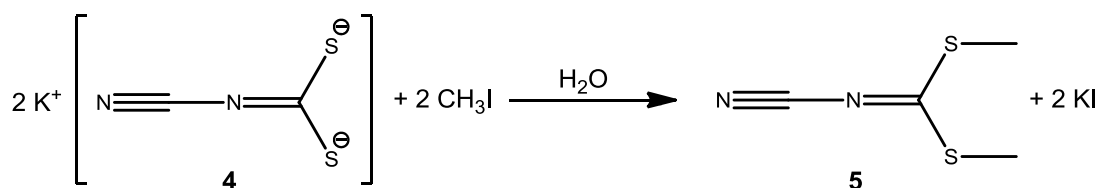
5.2.1 Dipotassium cyanodithioimidocarbonate (4)



5 g (120 mmol) cyanamide was solved in 10 mL ethanol and 8.05 ml (133 mmol) carbon disulfide was added. The solution was cooled to 0 °C and another solution consisting of 15.8 g (240 mmol) potassium hydroxide in 41 mL ethanol was added dropwise, while the temperature was maintained below 5 °C. Afterwards the solution was stirred at room temperature over night. The reaction solution was filtered and the precipitate was washed with little cold ethanol. The yield was 20.58 g (106 mmol, 88 %) white solid.

^1H NMR ($[\text{D}_2]\text{D}_2\text{O}$, 400 MHz): δ [ppm] = 4.80 (m, Lösemittel). **^{13}C NMR** ($[\text{D}_2]\text{D}_2\text{O}$, 68 MHz): δ [ppm] = 121.5 (1C, NC), 228.4 (1C, NCS_2). **Raman** (300 mW): $\tilde{\nu}$ [cm^{-1}] = 2138 (100), 1587 (14), 1324 (60), 965 (14), 685 (6), 524 (64), 398 (21), 212 (10). **IR** (ATR): $\tilde{\nu}$ [cm^{-1}] = 3531 (m), 3416 (w), 2362 (w), 2150 (vs), 1586 (m), 1486 (vw), 1337 (vs), 1148 (vw), 1035 (s), 970 (s), 682 (vw).

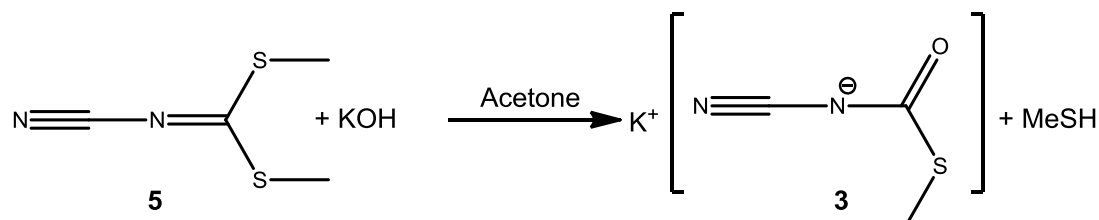
5.2.2 Dimethylcyanodithioimidocarbonat (5)



47.78 g (246 mmol) of **4** was dissolved in 300 mL water. The solution was cooled to 0°C and 30.6 mL (492 mmol) methyl iodide. The reaction solution was stirred for one hour at 0°C and afterwards at room temperature over night. The solution was cooled to 0°C again and filtered cold. The precipitate was washed with little cold water and dried. The yield was 29.98 g (205 mmol, 83 %) white solid.

¹H NMR ([D1]CDCl₃, 400 MHz): δ [ppm] = 2.59 (s, 6H, CH₃). **¹³C NMR** ([D1]CDCl₃, 100 MHz): δ [ppm] = 16.2 (2C, CH₃), 112.4 (1C, NC), 193.9 (1C, NCS₂). **Raman** (300 mW): $\tilde{\nu}$ [cm⁻¹] = 3011 (36), 2930 (90), 2182 (100), 1467 (75), 1420 (8), 1309 (5), 1020 (4), 717 (21), 506 (19), 377 (17), 353 (8), 254 (11). **IR** (ATR): $\tilde{\nu}$ [cm⁻¹] = 3011 (vw), 2930 (vw), 2505 (vw), 2362 (vw), 2179 (s), 1475 (s), 1415 (m), 1306 (m), 1134 (vw), 1078 (vw), 1035 (m), 1020 (m), 958 (w), 944 (m), 715 (vw). **MS** (DEI⁺): m/z (rel.int.) = 146.2 (54) [M⁺], 99.2 (100), 94.2 (1), 91.2 (4), 84.2 (4), 79.2 (5), 76.1 (3), 75.2 (2), 74.2 (38), 72.2 (10), 70.2 (2), 67.2 (3), 59.2 (4), 58.2 (5), 53.2 (1), 50.2 (1), 49.2 (1), 48.2 (12), 47.2 (19), 46.2 (11), 45.1 (24). **Elemental analysis**: found(calc.) C 32.49 (32.85), H 4.09 (4.14), N 18.99 (19.16), S 43.90 (43.86).

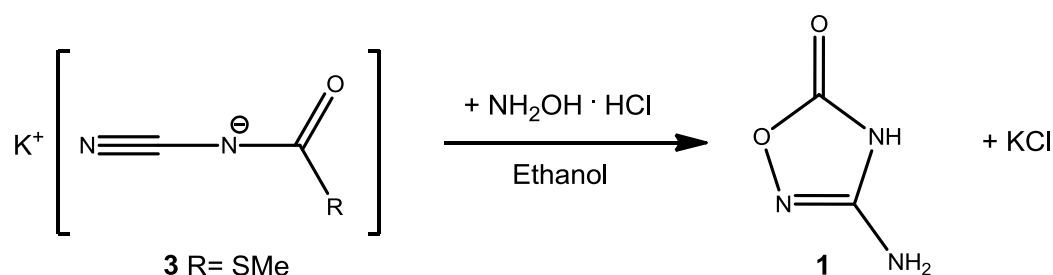
5.2.3 Potassium S-methyl-N-cyanocarbamate (3)



29.8 g (204 mmol) of **5** was solved with 11.43 g (204 mmol) potassium hydroxide in 100 mL dry acetone and heated for 6 hours under reflux condition. Afterwards the solution was cooled to room temperature and stirred for 24 hours. Then the mixture was cooled to 0°C and 300 mL n-heptane was added and stirred for 30 minutes. Now the solution was filtered and the precipitate was dried. The filtrate contained a brown oil that was treated with a mixture from dichloromethane and pentane. The prepipitate was filtered and recrystallized from heptane and dried. The yield was 24.02 g (156 mmol, 76 %) brownish solid.

¹H NMR ([D2]D₂O, 270 MHz): δ [ppm] = 2.29 (s, 3H, CH₃). **¹³C NMR** ([D2]D₂O, 68 MHz): δ [ppm] = 16.1 (1C, CH₃), 121.7 (1C, NC), 197.7 (1C, CO). **IR** (ATR): $\tilde{\nu}$ [cm⁻¹] = 3187 (vw), 2982 (vw), 2915 (vw), 2289 (vw), 2157 (vs), 1669 (vw), 1585 (m), 1476 (m), 1414 (s), 1357 (m), 1308 (m), 1274 (m), 1238 (w), 1213 (m), 1127 (w), 1055 (w), 1024 (w), 990 (w), 884 (w), 783 (vw), 724 (w), 680 (w).

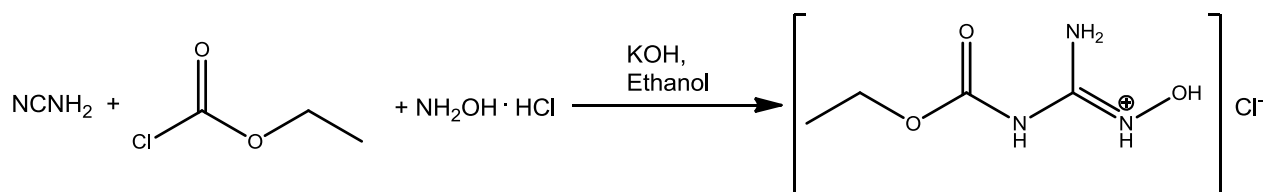
5.2.4 3-Amino-1,2,4(4H)-oxadiazol-5-one (A) (1)



17.50 g (114 mmol) of **3** was solved together with 7.85 g (114 mmol) hydroxylamine-hydrochlorid in 170 mL ethanol and heated for 2 h under reflux conditions. The solution was filtered hot, the filtrate was concentrated so that a white solid precipitated. This solid was filtered, and recrystallized from 5 % sodium hydroxide solution and stored at 0°C over night. The solution was filtered the and the solvent removed. The precipitated solid was solved in water and 2M hydrochloric acid was added. The solution was stored for 3 days at 4°C and the filtered solid was dried. The yield was 1.39 g (13.78 mmol, 12 %) brownish solid.

¹H NMR ([D₆]DMSO, 270 MHz): δ [ppm] = 6.21 (s, 2H, NH₂), 11.41 (s, 1H, NH). **¹³C NMR** ([D₆]DMSO, 68 MHz): δ [ppm] = 157.5 (1C, CNH₂), 159.0 (1C, CO). **Raman** (300 mW): $\tilde{\nu}$ [cm⁻¹] = 3477 (23), 3238 (24), 2940 (22), 1939 (22), 1777 (25), 1744 (33), 1630 (35), 1535 (28), 1261 (56), 1125 (26), 1069 (48), 988 (82), 906 (54), 769 (74), 667 (100), 584 (23), 423 (22), 370 (44). **IR** (ATR): $\tilde{\nu}$ [cm⁻¹] = 3340 (s), 3251 (m), 3199 (m), 3070 (m), 3016 (m), 2954 (m), 2871 (m), 2711 (s), 1790 (s), 1757 (s), 1687 (s), 1659 (s), 1618 (m), 1527 (vs), 1384 (m), 1261 (m), 1122 (w), 1069 (w), 986 (s), 905 (m), 786 (w), 735 (m), 684 (w), 657 (m). **MS** (DEI+): m/z (rel.int.) = 101.2 (53) [M⁺], 86.2 (1), 84.2 (2), 73.2 (1), 59.2 (41), 58.2 (37), 42.2 (38), 28.2 (23), 27.2 (5), 26.2 (1). **Elemental analysis**: found(calc.) C 22.88 (23.77), H 3.05 (2.99), N 39.92 (41.58).

5.2.5 (Z)-amino[(ethoxycarbonyl)amino]-N-hydroxymethaniminium chloride /N-(ethoxycarbonyl)-N'-hydroxy-guanidinium chloride (8)



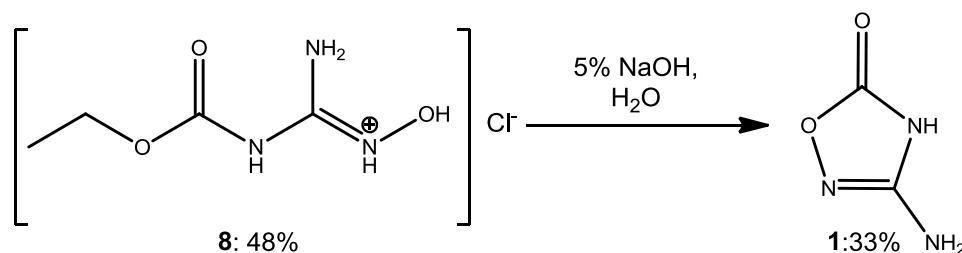
20 g (476 mmol) cyanamide was dissolved 200 mL ethanol and cooled to 5°C with a ice/salt bath. A solution of 50% potassium hydroxide (100 g KOH in 100 mL H₂O) and 45.11 mL (476 mmol) ethyl chloro formate were added carefully at the same time while the pH-value was maintained between 6 and 7 as well as the reaction temperature was not allowed to exceed 30°C. Afterwards the cooling bath was removed and the reaction mixture was heated for one hour at 45 °C. Afte cooling the reaction mixture down to 15°C the mixture was filtered.

29.79 g (429 mmol) hydroxylamine hydrochloride was added to the filtrate and the pH was adjusted with little conc. hydrochloric acid to pH 3. The reaction mixture was

heated under reflux condition for one hour. After cooling to room temperature the mixture was filtered and the filtrate was stored at 4°C over night. The white crystals were collected and the solvent of the filtrate was removed. The precipitate from the filtrate was recrystallized in little ethanol. The combined yield was 36.04 g (196 mmol, 46 %) white solid.

¹H NMR ([D₆]DMSO, 270 MHz): δ [ppm] = 1.23 (t, 3J = 7.0 Hz, 3H, CH₃), 4.19 (q, 3J = 7.3 Hz 2H, CH₂), 7.15 (d, 1H, HNOH), 8.64 (s, 1H, NH), 9.79 (s, 1H, OH), 11.27 (s, 2H, NH₂). **¹³C{¹H} NMR** ([D₆]DMSO, 68 MHz): δ [ppm] = 61.6 (1C, CH₃), 63.2 (1C, CH₂), 154.2 (1C, CNH₂), 155.0 (1C, OCO). **Raman** (500 mW): $\tilde{\nu}$ [cm⁻¹] = 2979 (79), 2938 (87), 2724 (16), 1740 (49), 1683 (14), 1621 (23), 1559 (26), 1461 (67), 1436 (28), 1276 (24), 1115 (46), 1062 (15), 980 (50), 955 (96), 453 (31), 429 (34), 359 (49). **IR** (ATR): $\tilde{\nu}$ [cm⁻¹] = 3275 (m), 3212 (m), 3164 (m), 3022 (m), 2988 (m), 2870 (s), 1730 (s), 1674 (vs), 1626 (s), 1581 (m), 1476 (w), 1454 (w), 1394 (vw), 1366 (vw), 1260 (m), 1145 (w), 1116 (vw), 1062 (vw), 1013 (w), 880 (vw), 760 (w), 742 (w), 668 (vw), 645 (vw). **MS** (DEI+): m/z (rel.int.) = 147.3 (2) [M⁺], 132.3 (18), 117.2 (4), 105.2 (100), 89.2 (16), 88.2 (20), 87.2 (16), 74.2 (11), 62.2 (51), 61.2 (10), 60.2 (15), 45.2 (35), 44.2 (82), 18.1 (47). **Elemental analysis**: found(calc.) C 25.66 (26.17), H 4.34 (5.49), N 19.61 (22.89). **T_{dec}** (DSC, 5°C / min, onset): 167 °C (m.p.) and 178 °C (dec.).

5.2.6 3-Amino-1,2,4(4H)-oxadiazol-5-one (B) (1)



12.17 g (66 mmol) of **8** was solved in 120 mL of 5% sodium hydroxide and heated over night under reflux conditions. After cooling the mixture to room temperature the pH value was adjusted to 4 with conc. hydrochloric acid. The white precipitated was filtered and the filtrate was treated with hydrochloric acid again until pH-value was 2. The precipitate was filtered again. From the remaining filtrate the solvent was evaporated. The collected solid was combined and recrystallized from little water. The yield was 2.17 g (21.5 mmol, 33 %) white solid.

¹H NMR ([D₆]DMSO, 270 MHz): δ [ppm] = 6.21 (s, 2H, NH₂), 11.39 (s, 1H, NH). **¹³C{¹H} NMR** ([D₆]DMSO, 68 MHz): δ [ppm] = 157.5 (1C, NCN), 159.1 (1C, OCO). **Raman** (500 mW): $\tilde{\nu}$ [cm⁻¹] = 3327 (17), 3322 (16), 3232 (16), 1743 (25), 1629 (22), 1526 (15), 1262 (58), 1070 (43), 997 (39), 987 (70), 905 (47), 769 (65), 686 (18), 667 (100), 369 (29). **IR** (ATR): $\tilde{\nu}$ [cm⁻¹] = 3340 (s), 3184 (m), 3018 (m), 2950 (m), 2870 (m), 2712 (s), 1791 (s), 1744 (m), 1682 (m), 1618 (m), 1527 (vs), 1383 (m), 1260 (m), 1122 (w), 1067 (w), 986 (s), 904 (m), 786 (vw), 733 (m), 684 (w), 656 (m). **MS** (DEI+): m/z (rel.int.) = 101.2 (13) [M⁺], 84.2 (2), 73.2 (1), 69.2 (1), 60.2 (1), 59.2 (51), 58.2 (10), 57.2 (1), 56.2 (1), 55.2 (1), 45.2 (2), 44.2 (100), 43.2 (70), 42.2 (45), 41.2 (8), 31.2 (3), 30.2 (2), 29.2 (4), 28.2 (14), 27.2 (5), 26.2 (2). **Elemental analysis**: found(calc.) C 23.61 (23.77), H 3.13 (2.99), N 41.67 (41.58). **T_{dec}** (DSC, 5°C / min, onset): 207.1 °C.

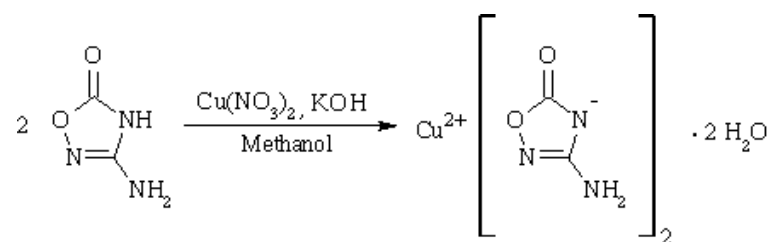
5.2.1 One-pot-synthesis of amino-1,2,4(4H)-oxadiazol-5-one (B) (1)

To synthesize different compounds starting from aOD therefore aOD was made first. Therefore the synthetic route B was taken and optimized to one pot reaction.

20 g (476 mmol) Cyanamide was solved in 200 mL Ethanol and cooled with a ice/salt bath to 5 °C. Simultaneously a solution of 100 g(1786 mmol) potassium hydroxide and 100 mL was prepared. The hydroxide solution and 45 mL (476 mmol) ethyl chloroformate were added to the cyanamide solution carefully while the pH was maintained between pH 6-7 and the reaction temperature was kept below 30°C. After complete addition of ethyl chlor formate the ice bath was removed and the mixture was heated for one hour at 45°C. After cooling to R.T. the reaction mixture was filtered. An the solid (potassium chloride) dumped. To the filtrate 30 g (429 mmol) hydroxylamine hydrochloride and 1M hydrochloric acid was added till the pH was pH 3. Now the Reaktion mixture is heated under reflux condition for one hour. After cooling to R.T. the mixture was filtered again. So not reacted hydroxylamine and potassium chloride was removed. The solvent of the filtrate was removed and a yellow solid was obtained which was dissolved in 120 mL 1 to 2 % sodium hydroxide in water and boiled over night under reflux conditions. The cooled solution was again neutralized and acidified (pH1-3). The precipitate was filtered and is the first yield. The solvent was removed from the filtrate and the solid residue is recrystallized from little water to form more product. It was obtained a white powder of 3-Amino-1,2,4-oxadiazol-5-one. The yield was 16.47 g (163 mmol, 34 %).

¹H NMR (D6-DMSO, 270 MHz): δ [ppm] = 6.22 (s, 2H, NH₂), 11.39 (s, 1H, NH). **¹³C NMR** (D6-DMSO, 68 MHz): δ [ppm] = 157.5 (1C, NCN), 159.0 (1C, OCO). **IR** (ATR): $\tilde{\nu}$ [cm⁻¹] = 3342 (w), 3178 (w), 3015 (w), 2952 (w), 2869 (w), 2711 (m), 1790 (m), 1738 (m), 1618 (s), 1524 (s), 1383 (w), 1260 (w), 1121 (w), 1068 (w), 986 (s), 904 (m), 786 (vw), 734 (m), 685 (w), 656 (m). **MS** (DEI+): m/z (rel. int.) = 101.0 [M⁺], 84.0 (1), 69.0 (4), 58.0 (73), 44.0 (66), 43.1 (27), 28.1 (24), 18.0 (4). **Elemental analysis:** found (calc.) C 22.40 (23.77), H 2.95 (2.99), N 39.44 (41.58).

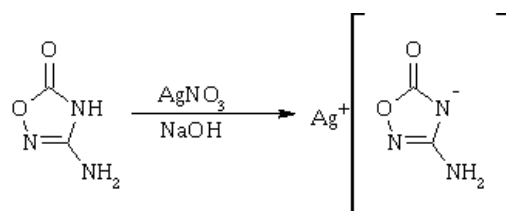
The low carbon and nitrogen values from the elemental analysis show that the product has still impurities of potassium or sodium chloride of 5-6%, which reduced the yield to 32% (15.92 g, 153 mmol aOD).

5.2.1 Copper aOD 2 H₂O (9)

400 mg (3.96 mmol) of **1** was dissolved together with 123.24 mg (1.98 mmol) potassium hydroxide in little methanol and 460.57 mg (1.98 mmol) copper nitrate, which also dissolved in little methanol, added. The solution was heated for half an hour under reflux conditions. The pH-value was slowly raised from 3 to 5 by addition of further potassium hydroxide. The green-blue solid was filtered, recrystallized from little water and dried. The yield was 376 mg (1.22 mmol, 62 %) of green-blue solid.

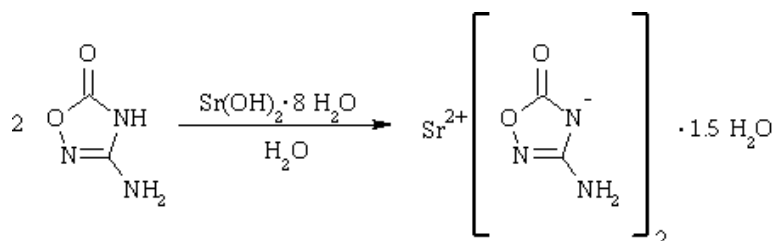
IR (ATR): $\tilde{\nu}$ [cm⁻¹] = 3432 (m), 3321 (m), 1726 (s), 1704 (m), 1613 (vs), 1541 (m), 1480 (vs), 1243 (w), 1125 (w), 1012 (w), 959 (vw), 799 (vw), 779 (w), 691 (w). **Elemental analysis:** found(calc.) C 16.01 (16.03), H 2.53 (2.67), N 27.83 (28.05). **DSC:** decomposition (Onset): 194.4 °C.

5.2.2 Silver aOD (10)



300 mg (2.18 mmol) of **1** was dissolved in little water and the pH was adjusted with 2M sodium hydroxide to pH-value of 7. Then 370.63 mg (2.18 mmol) silver nitrate in little water was added to the solution. The precipitated was filtered and dried. The yield was 330 mg (1.59 mmol, 73 %) white solid.

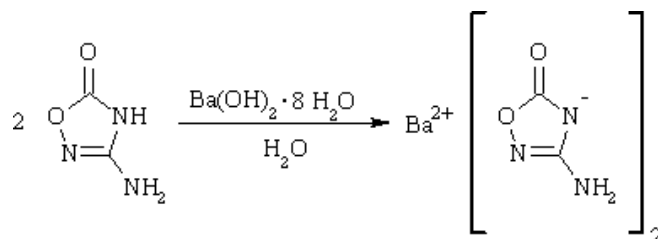
IR (ATR): $\tilde{\nu}$ [cm⁻¹] = 3432 (m), 3311 (w), 3281 (w), 3184 (w), 1704 (vs), 1649 (m), 1633 (m), 1580 (m), 1493 (s), 1250 (w), 1113 (w), 999 (w), 974 (vw), 951 (vw), 768 (m), 691 (w). **Elemental analysis:** found(calc.) C 11.71 (11.55), H 1.19 (0.97), N 19.93 (20.21).

5.2.3 Strontium aOD·x 1.5 H₂O (11)

500 mg (3.6 mmol) of **1** was dissolved in little water and mixed with a solution of 458.9 mg (1.8 mmol) strontiumhydroxide octahydrate in little water. The solvent was removed and the yield was 187.0 mg (0.6 mmol, 36 %) white solid

IR (ATR): $\tilde{\nu}$ [cm^{-1}] = 3354 (vs), 3306 (vs), 3200 (s), 2719 (w), 2359 (vw), 1765 (w), 1689 (m), 1658 (vs), 1628 (m), 1555 (m), 1454 (s), 1247 (w), 1231 (w), 1127 (w), 1092 (w), 981 (vw), 966 (w), 791 (w), 741 (vw). **Elemental analysis:** found(calc.) C 15.35 (15.35), H 3.16 (2.23), N 26.93 (26.75).

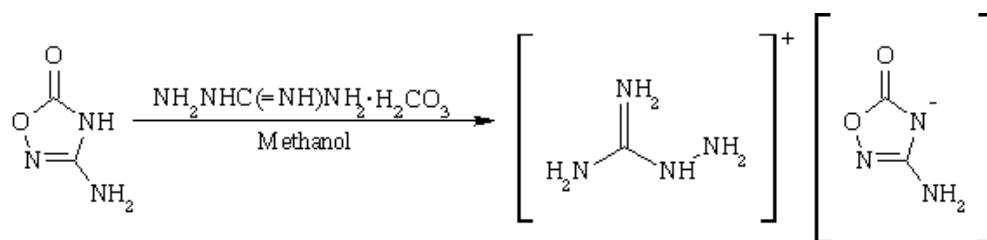
5.2.4 Barium aOD (12)



500 mg (4.95 mmol) of **1** dissolved in water. Also 781 mg (2.48 mmol) barium hydroxide octahydrate was solved in little water with slightly heating and combined with the solution of **1**. The solvent was removed and the yield was 357 mg (1.1 mmol, 44 %) white solid.

IR (ATR): $\tilde{\nu}$ [cm^{-1}] = 3320 (m), 3281 (m), 3139 (m), 2354 (w), 2329 (w), 2106 (vw), 1914 (vw), 1684 (s), 1670 (vs), 1651 (s), 1573 (m), 1543 (m), 1473 (vs), 1446 (s), 1242 (m), 1194 (m), 1090 (w), 971 (w), 903 (w), 854 (m), 779 (m), 703 (w), 668 (w). **Elemental analysis:** found(calc.) C 13.97 (14.24), H 1.37 (1.19), N 24.52 (24.91).

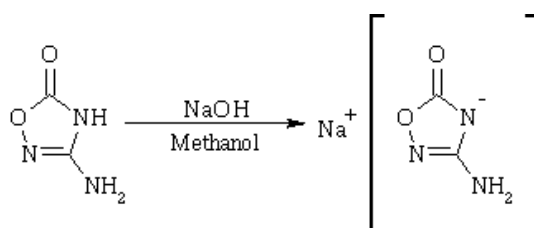
5.2.5 Aminoguanidinium aOD (13)



500 mg (4.95 mmol) of **1** were dissolved in little methanol. 337.6 g (2.48 mmol) of aminoguanidinium bicarbonate was suspended in 40 ml methanol and added to the solution of **1**. The mixture was heated to dissolve the salts and to evolve the carbon dioxide. After 2 hours the solvents was removed and the remainings dried. The yield was 818 mg (quantitive) orange resin like liquid (*ionic liquid*).

¹H NMR ([D6]DMSO, 400 MHz): δ [ppm] = 4.65 (s, 2H, NHNH₂), 5.08 (s, 4H, C(NH₂)₂), 7.63 (m, 3H, CNH₂, NH). **¹³C NMR** ([D6]DMSO, 100 MHz): δ [ppm] = 159.0 (1C, NC(NH₂)₂), 166.4 (1C, NCNH₂), 170.6 (1C, OCO). **Elemental analysis:** found(calc.) C 21.44 (20.57), H 5.39 (5.18), N 51.11 (55.98). **MS** [FAB⁺]: m/z = 75.1. **MS** [FAB⁻]: m/z = 100.1.

5.2.6 Sodium aOD (14)



300 mg (4.63 mmol) of **1** was dissolved in little and added to a solution of 87.2 mg (4.63 mmol) sodium hydroxide in little methanol. The solvent was evaporated and yield was 271.4 mg (2.21 mmol, 48 %) white solid.

¹H NMR ([D₆]DMSO, 270 MHz): δ [ppm] = 5.37 (s, 2H, NH₂). **¹³C NMR** ([D₆]DMSO, 68 MHz): δ [ppm] = 165.7 (1C, CNH₂), 169.0 (1C, OCO). **IR** (ATR): $\tilde{\nu}$ [cm⁻¹] = 3450 (m), 3332 (m), 2359 (vw), 1722 (s), 1689 (m), 1613 (m), 1564 (m), 1491 (m), 1243 (m), 1161 (vw), 1130 (vw), 1090 (w), 963 (w), 872 (w), 790 (m), 675 (w). **Elemental analysis:** found(calc.) C 19.97 (19.52), H 2.20 (1.64), N 34.66 (34.52). **DSC:** melting point (Onset): 112.1 °C. decomposition (Onset): 189.1 °C, 265.6 °C.

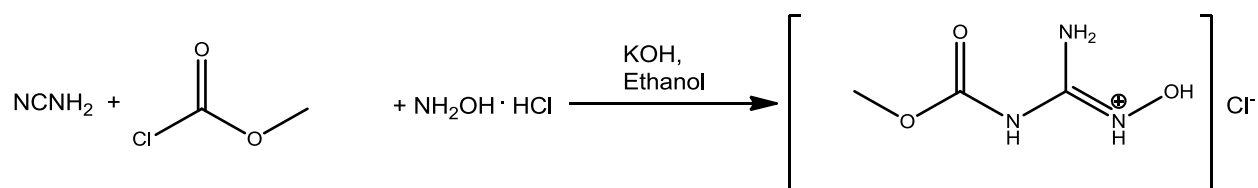
5.3 Solubility in different solvents

For the solubility test 30 mg **1** was dissolved, partly dissolved or not dissolved in these solvents: Methanol, ethanol, iso-propanol, acetonitrile, ethyl acetate, dioxane, actone, THF, dichloromethane, chloroform and toluene.

Therefore **1** was treated first with 0.5 mL of the respective solvent. If there is no dissolution observed neither in the ultrasonic bath nor by heating, the solvent amount was stepwise raised by 0.5 ml to a maximum of 6.0 mL.

5.4 Further investigated reactions

5.4.1 (Z)-amino[(methoxycarbonyl)amino] *N*-hydroxymethaniminium chloride (BI)



10 g (238 mmol) cyanamide were dissolved in 100 mL water and the mixture was cooled in an ice/salt bath to 5°C. A 50% sodium hydroxide solution and und 18.2 ml (238 mmol) methyl chloroformate were added carefully at the same time, while the pH value as maintained between 6 and 9 and also the temperature was not allowed to surpass 30 °C. After the addition the ice bath was removed and the reaction mixture heated for one hour at 50 °C. The mixture was filtered hot and after cooling to room temperature 13.76 g (198 mmol) hydroxylamine hydrochloride was added to the filtrate and with 2M hydrochloric acid the pH value was adjusted to 3. The reaction mixture was heated for 2.5 hours under reflux conditions. After cooling to room

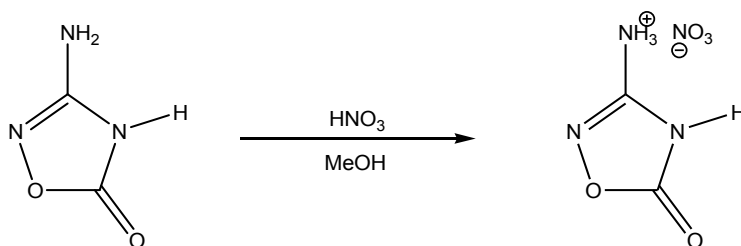
temperature the mixture was stirred over night. After filtration a solid precipitate was isolated the was identified to be the starting material.

5.4.2 Alternative ring closure reaction for aOD (1) with diphosgen (B III, 6)

To 3 g (16 mmol) **8** in 50 mL THF was added 1.62 g (8 mmol) diphosgene at 0 °C. .96 g (49 mmol) triethylamine was added dropwise to the reaction mixture. After addition the mixture was stirred for one hour at 0 °C and two hours at room temperature. The solution was filtered and solvent of the filtrate was removed under reduced pressure. The precipitate was extracted three times with ethyl acetate. The ethyl acetate was evaporated under reduced pressure and the precipitate was solved in little 2M hydrochloric acid and heated for two hours at 70 °C. The solution was allowed to cool overnight. The obtained precipitate was a crude mixture and could be not identified as product or by product.

5.5 Synthesis of aOD salts with aODH⁺ as cation:

5.5.1 Synthesis of aODH⁺ nitrate



2.0 g (20 mmol) **aOD** were solved in little methanol and 20mL 1M nitric acid was added carefully at 0 °C under stirring. The solution was stirred for another half an hour and the reaction mixture put into the refrigerator for two days at 4°C. After two days colorless crystals were observed and 80 mg (0.5 mmol, 2.5% yield) were isolated. The solvent was evaporated and resulted in 413 mg colorless solid.

IR (ATR): $\tilde{\nu}$ [cm⁻¹] = 3344 (vw), 3188 (vw), 2953 (vw), 2868 (vw), 2711 (vw), 1791 (w), 1741 (w), 1684 (w), 1620 (w), 1526 (m), 1382 (w), 1261 (w), 1121 (vw), 1068 (w), 986 (m), 904 (m), 787 (vw), 733 (m), 684 (w), 656 (m). **Elemental analysis:** fnd. (calc.) C 23.46 (14.63), H 2.99 (2.44), N 41.45 (34.15).

The experiment was repeated with half concentrated nitric acid instead of 1M nitric acid.

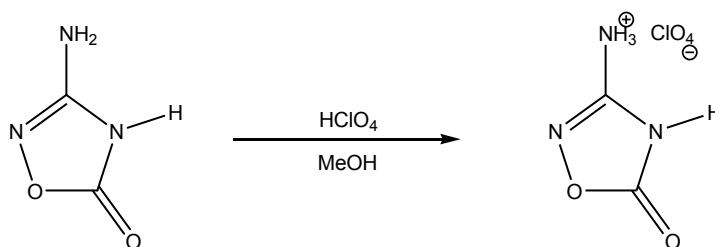
IR (ATR): $\tilde{\nu}$ [cm⁻¹] = 3346 (w), 3190 (w), 2868 (w), 2362 (vw), 1792 (m), 1653 (m), 1527 (s), 1384 (w), 1262 (w), 1120 (w), 1068 (w), 987 (s), 905 (m), 684 (w), 656 (m). **Elemental analysis:** fnd. (calc.) C 23.64 (14.46), H 3.05 (2.44), N 41.33 (34.15).

IR vibration of pure aOD:

IR (ATR): $\tilde{\nu}$ [cm⁻¹] = 3342 (w), 3178 (w), 3015 (w), 2952 (w), 2869(w), 2711 (m), 1790 (m), 1738 (m), 1618 (s), 1524 (s), 1383 (w), 1260 (w), 1121 (w), 1068 (w), 986 (s), 904 (m), 786 (vw), 734 (m), 685 (w), 656 (m).

The comparison of IR vibrations of the starting material with the obtained product display that there was no nitrate salt of aOD made but only starting material recrystallized. The elemental analysis backs this as the values are almost the values of the pure starting material.

5.5.2 Synthesis of aODH⁺ perchlorate



2.0 g (20 mmol) **aOD** were solved in little methanol and 20mL 1M perchloric acid was added carefully at 0 °C under stirring. The solution was stirred for 45 minutes and the reaction mixture put into the refrigerator for two days at 4°C. After two days colorless crystals were observed and 20 mg (0.09 mmol, 0.5% yield) were isolated. The solvent was evaporated and resulted in 242.4 mg colorless solid.

IR (ATR): $\tilde{\nu}$ [cm⁻¹] = 3548 (vw), 3471 (vw), 3346 (s), 3191 (s), 3069 (m), 3018 (m), 2953 (s), 2871 (m), 2714 (s), 2450 (w), 2244 (vw), 2034 (vw), 1975 (vw), 1832 (vw), 1792 (m), 1741 (m), 1680 (m), 1652 (m), 1526 (s), 1383 (w), 1261 (w), 1120 (w), 1067 (w), 987 (m), 904 (w), 787 (vw), 733 (w), 685 (vw), 656 (w). **MS** (FAB⁺): m/z (rel. int.) = 102.0 [M⁺], 89.0 (20), 77.0 (18), 65.1 (8), 39.0 (7), 31.1 (2). **Elemental analysis**: **found**. (calc.) C 22.91 (11.92), H 2.95 (2.00), N 40.63 (20.85).

The experiment was repeated only changing the 1M perchloric acid to conc. perchloric acid in excess.

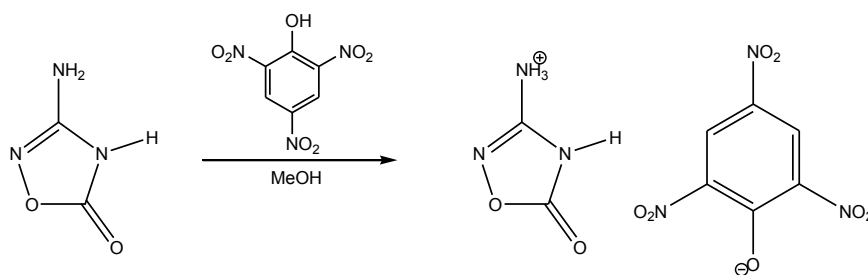
IR (ATR): $\tilde{\nu}$ [cm⁻¹] = 3528 (w), 3345 (w), 3168 (w), 2953 (w), 2870 (w), 2711 (w), 2051 (vw), 1827 (vw), 1790 (w), 1716 (w), 1619 (w), 1525 (w), 1381 (vw), 1260 (vw), 1088 (m), 1065 (m), 986 (m), 903 (w), 787 (vw), 732 (w), 656 (vw). **Elemental analysis**: **found**. (calc.) C 22.40 (11.92), H 2.95 (2.00), N 39.44 (20.85).

IR vibration of pure aOD:

IR (ATR): $\tilde{\nu}$ [cm⁻¹] = 3342 (w), 3178 (w), 3015 (w), 2952 (w), 2869 (w), 2711 (m), 1790 (m), 1738 (m), 1618 (s), 1524 (s), 1383 (w), 1260 (w), 1121 (w), 1068 (w), 986 (s), 904 (m), 786 (vw), 734 (m), 685 (w), 656 (m).

Like the experiment to build the nitrate salt the IR vibration of the product are in both terms those of pure aOD and the elemental analysis is backing this results.

5.5.3 Synthesis of aODH⁺ picrate



2.0 g (20 mmol) **aOD** were solved in little methanol. 7.0 g (20 mmol) 65 % solid picric acid were solved in little methanol. Both solutions was mixed carefully at 0 °C under stirring. The solution was stirred for 30-45 minutes and the reaction mixture put into the refrigerator for two days at 4°C. After two days pale yellow crystals were observed and 55 mg (0.09 mmol, 0.5% yield) were isolated. The solvent was evaporated to find further solids.

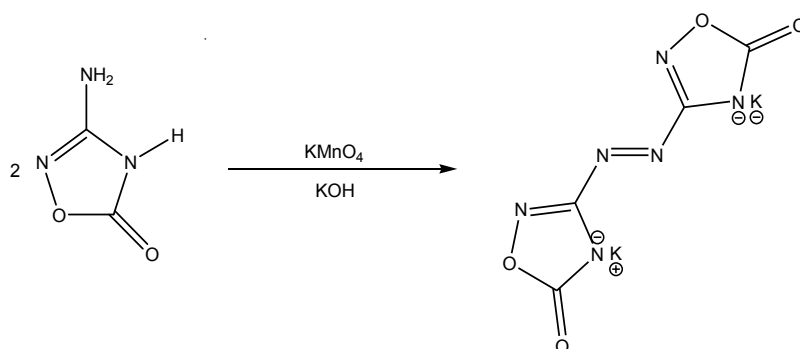
IR (ATR): $\tilde{\nu}$ [cm⁻¹] = 3346 (w), 3203 (w), 2956 (w), 2872 (w), 2715 (w), 1795 (w), 1748 (m), 1656 (m), 1526 (s), 1385 (w), 1342 (w), 1261 (w), 1122 (w), 1069 (w), 986 (m), 905 (m), 784 (vw), 736 (m), 685 (vw), 665 (w). **Elemental analysis:** fnd. (calc.) C 23.82 (29.09), H 2.84 (1.83), N 39.93 (25.46).

Although the experiment was repeated with raised concentration of picric acid the elemental analysis looks the same:

Elemental analysis: fnd. (calc.) C 24.37 (29.09), H 2.86 (1.83), N 37.71 (25.46)

Both experiments show as well in the IR spectrum as in the elemental analysis very clear that only the starting material was recrystallized. So a cocrystal of picric acid and aOD was obtained but no stoichiometric reaction took part. That is the reason for the elemental analysis, which displays neither pure aOD nor picric acid.

5.6 Azo-Coupling of aOD (15)



5.0 g (49 mmol) **aOD** was solved in 50 mL 10% sodium hydroxide. The solvent was heated for 45 minutes at 50°C while constantly adding 6.5 g (41 mmol) potassium permanganate in small potions. Afterwards the mixture was stirred 2 hours at 50°C. Then 250 mL ethanol was added and heated until boiling. The manganese oxide was

filtered hot through a glass filter the yellow liquid was left in the refrigerator at 4°C for one night.

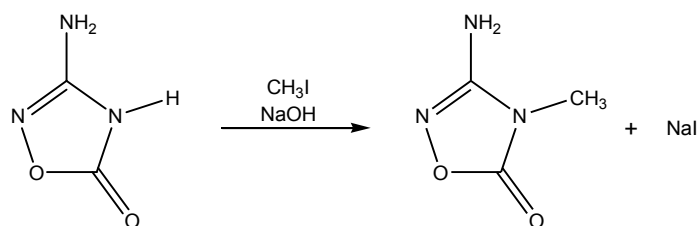
The obtained yellow to brown crystals were filtered and washed with ethanol and diethylether and dried. The mass was 42 mg.

IR (ATR): $\tilde{\nu}$ [cm⁻¹] = 2359 (vw), 2331 (vw), 2151 (vw), 1684 (m), 1500 (s), 1447 (s), 1402 (m), 1240 (w), 1212 (w), 1036 (vw), 963 (vw), 941 (w), 890 (w), 865 (w), 792 (s), 765 (vw), 725 (vw), 672 (w). **Elemental analysis:** fnd. (calc.) C 16.13 (24.25), H 0.45 (1.02), N 24.55 (42.42)

The solvent of the filtrate was removed but the yellow and brown residue was identified to be mainly decomposition products of aOD like potassium and sodium carbonate.

IR (ATR): $\tilde{\nu}$ [cm⁻¹] = 2956 (vw), 2508 (vw), 2262 (w), 2188 (vw), 2152 (vw), 1661 (vw), 1433 (s), 1306 (vw), 1243 (vw), 1216 (vw), 904 (vw), 880 (vw), 864 (vw), 792 (vw), 686 (vw).

5.7 Methylation of aOD (16a, 16b)



A solution 1.4 g (10 mmol) methyl iodide in 16 mL acetone was added to a solution of 1.0 g (10 mmol) **aOD** and 400 mg (10 mmol) sodium hydroxide in water. The mixture was heated for 3 hours under reflux conditions. Afterwards the solvent was removed. The colorless solid was washed five times with 50 mL toluene. The unsolved compound was recrystallized from hot water and put in the refrigerator for one night. The obtained crystals were filtered and analyzed (**16a**). The toluene solution was kept for further product (**16b**).

IR (ATR): $\tilde{\nu}$ [cm⁻¹] = 3370 (m), 3310 (m), 3158 (m), 2935 (vw), 2359 (vw), 2171 (vw), 2031 (vw), 1740 (m), 1626 (s), 1559 (m), 1511 (m), 1455 (w), 1413 (w), 1354 (w), 1248 (vw), 1215 (w), 1104 (w), 1007 (vw), 949 (vw), 926 (vw), 804 (vw), 780 (w), 760 (vw), 686 (vw), 626 (vw). **¹H NMR** (D6-DMSO, 400 MHz): δ [ppm] = 3.02 (s, 3H, CH₃), 6.59 (s, 2H, NH₂). **¹³C NMR** (D6-DMSO, 100 MHz): δ [ppm] = 27.3 (1C, CH₃), 163.6 (1C, NCN), 168.4 (1C, OCO).

6 References

- [1] T. M. Klapötke, *Chemie der hochenergetischen Materialien*, 1. Auflage, de Gruyter Verlag, Berlin, **2009**, ISBN 3110207451.
- [2] a) T. M. Klapötke, R. Alsfasser, C. Janiak, H.-J. Meyer, E. Riedel, *Moderne Anorganische Chemie*, 3. Auflage, de Gruyter Verlag, Berlin, **2007**, ISBN 978-3-11-019060-1;
b) J. Stierstorfer, *Advanced Energetic Material based on 5-Aminotetrazole – Synthesis, Characterization, Testing and Scale*, Dissertation, Muenchen **2009**.
- [3] M. D. Coburn, *J. Heterocycl. Chem.* **1968**, 5, 83-87.
- [4] K. Rehse, S. Bade, *Arch. Pharm. Pharm Med. Chem.* **1996**, 329, 535-540.
- [5] M. T. Nguyen, A. F. Hegarty, and J. Elguero, *Angew. Chem. Int. Ed. Engl.* **1985**, 24, 713-715.
- [6] a) T. Suyama, N. Ozawa and N. Suzuki, *Bull. Chem. Soc. Jpn.* **1994**, 67, 307-308;
b) L. S. Wittenbrook, G. L. Smith and J. Timmons, *J. Org. Chem.*, **1973**, 38 (3), 465-471;
c) J. J. D'Amico, K. Boustany, A. B. Sullivan and R. H. Campbell, *Int. J. Sulfur Chem.* **1972**, Part A, 2 (1), 37-41.
- [7] T. Schafer, L. A. Suba, P. G. Ruminski and J. J. D'Amico, *Phosphorus and Sulfur* **1986**, 29, 1-10.
- [8] K. Shimada et al., *Chem. Pharm. Bull.* **1984**, 32 (12), 4893-4906.
- [9] N. Götz, B. Zeeh, *Synthesis* **1976**, Heft 04, 268-270.
- [10] *CRC Handbook of Tables for Organic Compound Identification*, 3. Edition, CRC Press, Boca Raton, **1984**, ISBN 0-8493-0303-6.
- [11] A. F. Holleman, E. Wiberg und N. Wiberg, *Lehrbuch der Anorganischen Chemie*, 102. Auflage, de Gruyter Verlag, Berlin, **2007**, ISBN 3110177706.
- [12] R. Gilardi and R. J. Butcher, *Journal of Chemical Crystallography* **2002**, 32 (11), 477-484.
- [13] J. Thiele, *Just. Lieb. Ann. Chem.* **1898**, 303, 57-75.
- [14] a) Y. Takahiro et al., *Chemistry--A European Journal* **2009**, 15 (23), 5651-5655;
b) M. Goebel, T.M. Klapötke, *Chem. Commun.* **2007**, 43 (30), 3180-3182.
c) E. Riedel, *Anorganische Chemie*, 6. Auflage, de Gruyter Verlag, Berlin, **2004**, ISBN 3110181681.
- [15] D. Young Ra, N. Sook Cho, S. Kwon Kang, E. Suk Choi, *Bull. Korean Chem. Soc.* **1998**, 19 (8), 880 – 882.
- [16] *Gaussian 03*, M. J. Frisch, G. W. Trucks, H. B. Schlegel, G. E. Scuseria, M. A. Robb, J. R. Cheeseman, G. Scalmani, V. Barone, B. Mennucci, G. A. Petersson, H. Nakatsuji, M. Caricato, X. Li, H. P. Hratchian, A. F. Izmaylov, J. Bloino, G. Zheng, J. L. Sonnenberg, M. Hada, M. Ehara, K. Toyota, R. Fukuda, J. Hasegawa, M. Ishida, T. Nakajima, Y. Honda, O. Kitao, H. Nakai, T. Vreven, J. A. Montgomery, Jr., J. E.

- Peralta, F. Ogliaro, M. Bearpark, J. J. Heyd, E. Brothers, K. N. Kudin, V. N. Staroverov, R. Kobayashi, J. Normand, K. Raghavachari, A. Rendell, J. C. Burant, S. S. Iyengar, J. Tomasi, M. Cossi, N. Rega, J. M. Millam, M. Klene, J. E. Knox, J. B. Cross, V. Bakken, C. Adamo, J. Jaramillo, R. Gomperts, R. E. Stratmann, O. Yazyev, A. J. Austin, R. Cammi, C. Pomelli, J. W. Ochterski, R. L. Martin, K. Morokuma, V. G. Zakrzewski, G. A. Voth, P. Salvador, J. J. Dannenberg, S. Dapprich, A. D. Daniels, Ö. Farkas, J. B. Foresman, J. V. Ortiz, J. Cioslowski, and D. J. Fox, Gaussian, Inc., Wallingford CT, **2004**.
- [17] J. S. Binkley, J. A. Pople, W. J. Hehre, *J. Am. Chem. Soc.*, **1980**, 102, 939.
- [18] *GaussView, Version 5*, R. Dennington, T. Keith and J. Millam, *Semichem Inc.*, Shawnee Mission KS, **2009**.
- [19] J. Stierstorfer, T. M. Klapötke, *J. Chem. Soc., Dalton Trans*, **2008**, 643 – 653.
- [20] T. M. Klapötke, J. Stierstorfer, *Central Europ. J. of Energ. Mat.* **2008**, 5(1), 13.
- [21] M. Sućeska, *Test Methods for Explosives*, Springer, New York, **1995**.
- [22] M. Sućeska, *EXPLO5 5.02*, Zagreb, Hrvatska, **2008**.

Chapter VII

3-DINITROMETHYLENYL-1,2,4(4H)-OXADIAZOL-5-ONE AND DERIVATIVES – HIGH EXPLOSIVE, STABLE, INSENSITIVE

Abstract:

3-substituted-1,2,4-oxadiazol-5-one derivatives may replace or complement tetrazole derivatives as pyrotechnics and propellants. As oxadiazolones have better oxygen balances (-47 % compared to 57% for tetrazole), both generate the same amount of gaseous products per molecule. The 3-dinitromethyl-1,2,4(4H)-oxadiazol-5-one(DNM-OD) and its salts were investigated thoroughly and show remarkable properties as pyrotechnical, propellant and explosive ingredients.

Keywords: 3-substituted-1,2,4-oxadiazol-5-one, 3-dinitromethyl-1,2,4(4H)-oxadiazol-5-one, DNM-OD, FOX-7, crystal structure, density, decomposition.

1 Introduction

Having discussed the similarities and differences of the 3-amino-1,2,4(4H)-oxadiazol-5-one and 5-amino-1H-tetrazole. It was a logical step to apply the gained knowledge on the molecule class of 1,2,4-oxadiazol-5-ones on the 5-dinitromethylene-1H-tetrazole.^[1] This was comprehensively studied by F.-X. Steemann and T.M. Klapötke while the synthesis based on a publication of J.S. Kim and J.R. Cho^[2]. The overall good explosive performance values of these compounds combined with relatively low sensitivity of the salts was an interesting playground on which basis the following investigation were started. However a lot of other dinitromethylene and trinitromethyl derivatives were synthesized as energetic materials.^[3,4] The energetic moiety is similar to the known FOX-7,^[5,6] but in case of a tetrazole there is a nitrogen attached why not attach a carbon dioxide. That is what is done in the following.

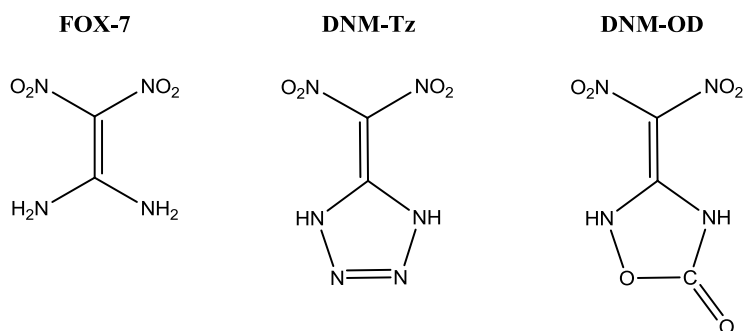


Figure 1. FOX-7, DNM-Tz and DNM-OD.

Those molecules are found to be less sensitive although energetic.

To compare similarities and differences in the molecular structure the dinitromethyl-oxadiazolone was investigated and characterized by various analytical methods. Also computational chemical methods were used to determine enthalpies and energies of formation and energetic properties

2 Synthesis

The synthetic approach of this molecule was that although the basic route should be followed exactly the same as in the procedure by Klapötke *et al.*^[1,2] The ring closure was not that simple as with the tetrazole.

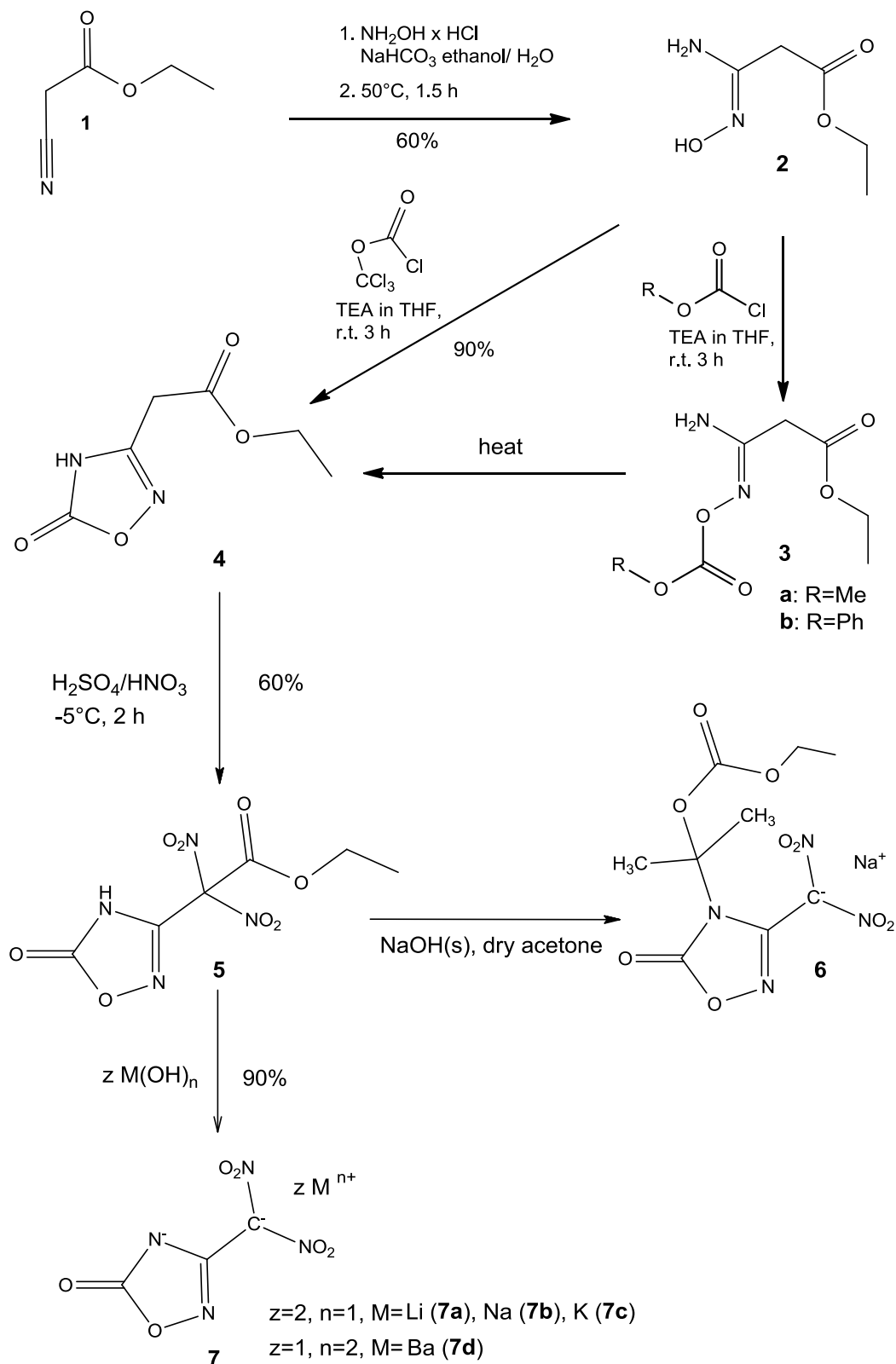


Figure 2. Synthesis of DNM-OD

Starting both of the 1-ethyl-2-cyano acetate the ring closure of the tetrazole was obtained by adding sodium azide under common conditions and getting a 5-substituted tetrazole.

However the 1,2,4-oxadiazole ring is - as shown in chapter 4 and 6 - subsequently formed by getting an oxime-amid group from nitriles reacting with hydroxylamine followed by a condensation reaction with a chloroformate derivative and a ring closure reaction under thermal conditions. This means that there are two additional steps to be applied with all the consequences of loss of yield and time of optimization of the reaction conditions.

Starting from the commercially available ethylcyano acetate (**1**) the synthesis to the hydroxy iminamido ethyl acetate (**2**) was done following the procedure by R. O. Bora et al.^[7] with little changes. The hydroxy iminamido acetate (**2**) was reacted by the methylchloroformate to form the ester (**3a**) at the hydroxyimino group^[8]. With this molecule **3a** it was tried to close the oxadiazol ring as described in a Japanese Patent^[9], but ended up with little product and a slurry oil.

As the synthesis of **3a** was not satisfactory, the synthesis of the 3-dinitromethylen-1,2,4-oxadiazolidin-5-one (**8**) was carried out differently. Therefore a reaction of ethylcyanoacetate (**1**) with hydroxylammonium chloride yielded 15% of ethyl-3-amino-3-(hydroxyimino)-propanoate (**2**). The further reaction of **2** with phenyloxy chloro formate ended in ethyl-3-amino-3-(phenoxycarbonyloxyimino) propanoate (**3b**) with 61 % yield. The ring closure of **3b** to ethyl-2-(5-oxo-4,5-dihydro-1,2,4-oxadiazol-3-yl)acetate (**4**) was done successfully but had a lot of phenyl impurities why this synthetic route was not followed any longer and switched to a more comprehensive route.

So another route was chosen which has proven to lead to the ring closed molecule under mild conditions. The hydroxy iminamido ethyl acetate (**2**) was reacted with diphosgene to yield the 1,2,4-oxadiazol-5-on-3-yl-ethylacetate (acidic acid ethyl ester) (**4**). The ester **5** was now nitrated according to the procedure by F.X. Steemann^[4] with white fuming nitric acid in concentrated sulfuric acid at -15°C to +5°C. (The product precipitated out of the solution at about 0°C and could be isolated by filtration.) While the critical point as in all nitrations was the temperature control, which makes the difference between 80-90% yield and nearly nothing. The isolation of the product (**4**) was a little tricky as it precipitates from conc. sulfuric acid and is filtered off and washed with water doing both at nearly zero degrees Celsius. The product the 2,2-dinitro-2-(1,2,4-oxadiazol-5-on-3-yl)-acetic acid ethyl ester (**5**) is stable as long as now water is added. It decomposes in strong acids. But could be washed with ice water and stored under dry conditions at room temperature for months.

2.1 By-product (6)

The splitting of the ester and decarboxylation was also tried in absolute acetone with sodium hydroxide (p.a). The resulting precipitate was identified as salt but not as double deprotonated species but as a rearranged product (**8**) with an insertion of

acetone in the molecule. The mechanism for formation can only be guessed from basic chemical principles.

2.2 Salts of DNM-OD (7,9)

Last step for getting energetic material is the splitting of the ester and subsequently decarboxylation. All metal salts have been synthesized starting from the ester (**5**). It could be easily transformed to the metal compounds by reacting it in methanol with the corresponding metal hydroxide. So lithium (**7a**), sodium (**7b**), potassium (**7c**) and, barium (**7d**) salts were obtained. The potassium salt contains no crystal water (e.a.) which makes it more sensitive compared to the others.

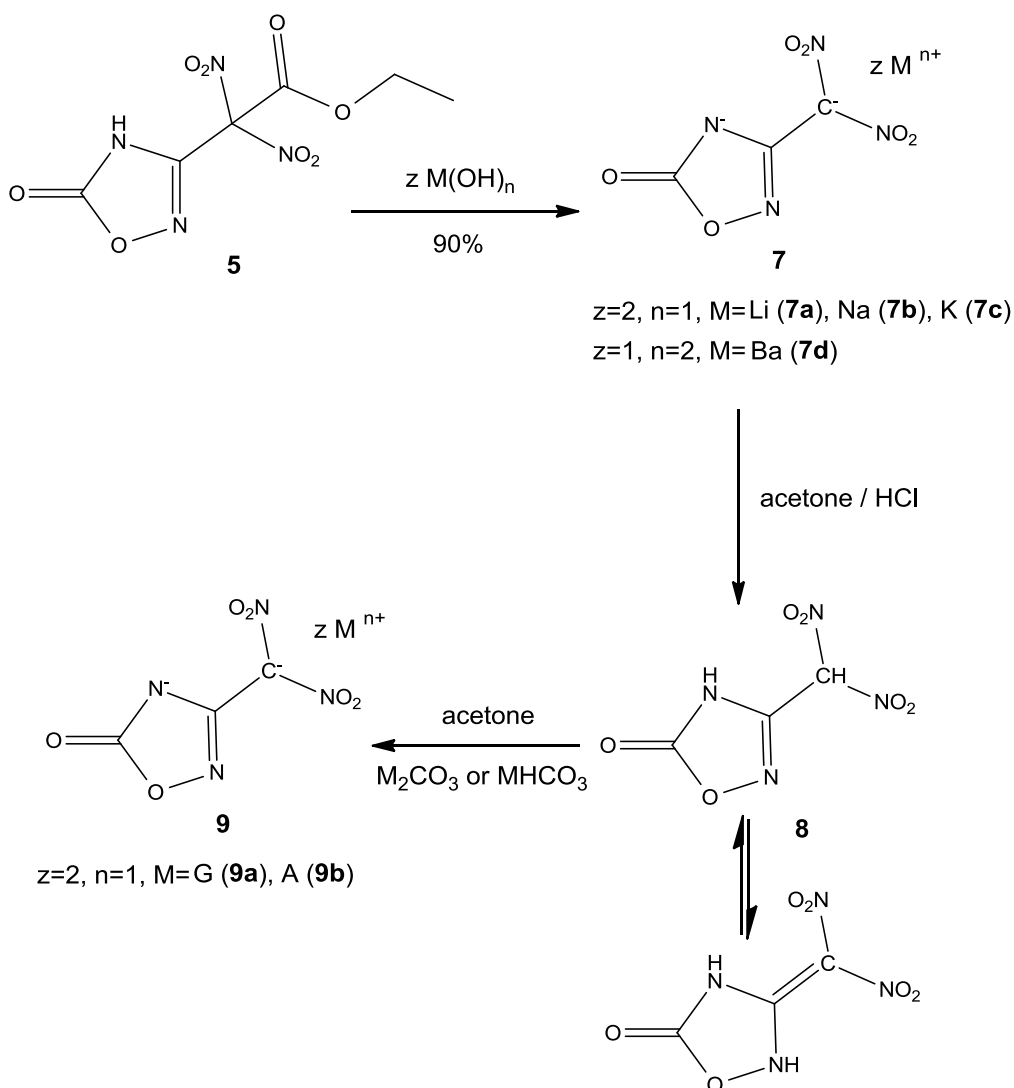


Figure 3. Synthesis of DNM-OD (**8**) and its salts.

The obtained salts were characterized and used to form the neutral DNM-OD (**8**) by adding to a sodium solution excess concentrated hydrochloric acid and extracting the neutral molecule. **8** could not be isolated but was utilized solved in ethyl acetate or dichloromethane for further reactions, which was treated with gaseous ammonia or reacted with guanidinium carbonate. Some nitrogen containing salts were synthesized that way e.g. the guanidinium (**9a**) and the ammonium salt (**9b**).

3 Discussion

In the following discussion the molecules which have been synthesized are described and characterized thoroughly regarding spectroscopy, crystal structure and energetic properties. As well as calculation are carried out to compare theoretical and practical values. Therefore the intermediates are described in short and the details for the desired DMN-OD and its derivatives are presented in extend.

3.1 Spectroscopic Properties

Vibrational and magnetic resonance spectroscopic investigations are done to trace the change in the molecules during the synthesis and describe the differences between the salts.

First the emphasis is put on the carbon of the hydroximinoamide group. For **2** the signal in the ^{13}C NMR is observed at 147.4 ppm which is shifted to 154.3 ppm in the oxadiazole **3**. After nitration at the carbon next to the oxadiazole-C3 the shift is 152.9 ppm and in the decarboxylated form **6** the carbon signal is at 151.5 ppm and in the deprotonated form **7** it is at 162.8 ppm.

This shifting of the carbon signal first to deep field and after nitration to lower field can be explained by the surrounding electronic configuration. While the open chained form is just a imin-imin mesomeric situation like in the carboxyl moiety the ring closure to the oxadiazole increases the electronic possibilities by adding a pulling carbonyl unit which also shows mesomeric and tautomeric forms like extensively described in chapter VI. Nonetheless looking at the situation after nitration the electronic environment has changed again an electron pulling system of the dinitromethylene moiety has been created, which is a counterbalance to the oxadiazole moiety. This means the shift at the carbon moves to the opposite direction. After the decarboxylation like in the by-product **6** the ring got an electron pushing systems which weakens the oxadiazole influence and a slight shift to the lower field is recognized. At last in the fully deprotonated molecule the 90 degrees twist of the dinitromethylene has a shielding effect to the carbon and at the same time the negative charge of the oxadiazole-5-onate is distributed in the ring moiety. This nearly spheric negative electronic surrounding are observed as deep field shift.

3.2 Crystal structures

3.2.1 2-Ethyl-3-amino-3-(hydroxyimin)-propanoate (**2**)

2 crystallizes in the orthorhombic space group $P2_12_12_1$ with eight molecules in the unit cell.

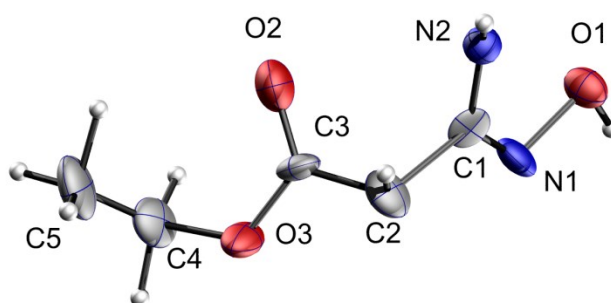


Figure 4. Molecular structure of **2**, Thermal ellipsoids plotted at 50% probability level.

3.2.1 Ethyl (3Z)-3-amino-3-[(methoxycarbonyl)oxy]imino}-propanoat (**3a**)

3a crystallizes in the monoclinic space group $P2_1/c$ with four molecules in the unit cell.

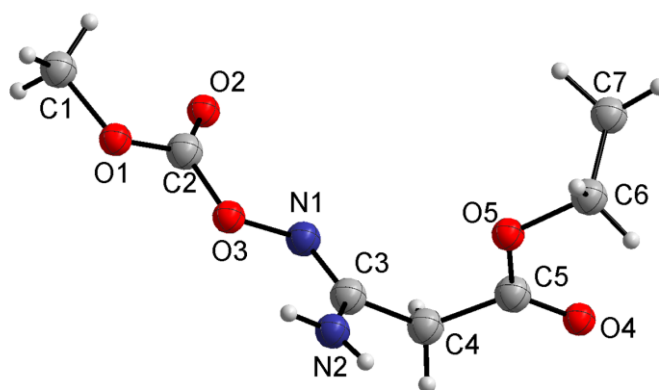


Figure 5. Molecular structure of **3a**, Thermal ellipsoids plotted at 50% probability level.

3.2.1 Dinitro-([1,2,4]oxadiazol-5-on-3-yl)-acetic acid ethyl ester (5)

5 crystallizes in the monoclinic space group $P2_1/c$ with four molecules in the unit cell. In the crystal structure of **5** the bond lengths and angles are in good accordance to literature^[10] and also with the discussed values for the 1,2,4-oxadiazol-5-one in chapter IV and VI. Remarkable is in this molecule the 90° twist from one nitro group respective to the other so that an oxygen contact to the nitrogen of the other nitro group is observe which has been described in many publication about di- and trinitromethyl derivatives. Also the nearly tetraedrical bond situation on C3 is recognized.

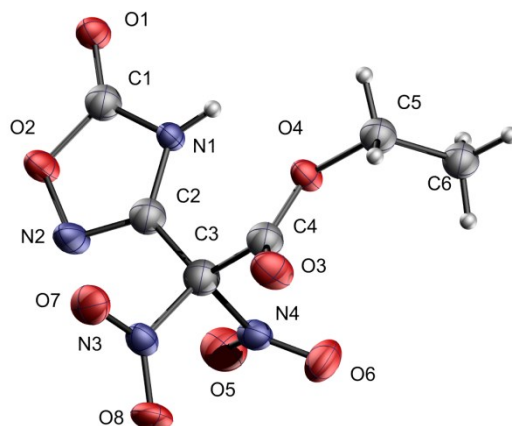


Figure 6. Molecular structure of **5**, Thermal ellipsoids plotted at 50% probability level. Selected bond lengths (Å) and angles (°): C1—O2 1.371(2), N2—O2 1.415(2), C3—C2 1.487(2), C3—N3 1.531(2); C3—C4 1.547(2), C2—N2 1.289(2), C2—N1 1.350(2), C1—O1 1.198(2), C1—N1 1.359(2), N4—O5 1.210(2), C4—O4 1.311(2), C4—O3 1.186(2); O3—C4—O4 129.8(1), C2—N1—C1 107.9(1), N3—C3—N4 105.6(1), C2—C3—C4 118.4(1), N3—C3—C4 106.6(1), O6—N4—O5 127.2(1), N4—C3—C4 107.1(1), O6—N4—C3 115.9(1), N2—C2—N1 112.9(1), O5—N4—C3 116.8(1), N2—C2—C3 120.5(1), C2—N2—O2 104.5(1), N1—C2—C3 26.6(1), O8—N3—O7 127.1(1), O1—C1—N1 131.5(1), O8—N3—C3 118.02(1), N1—C1—O2 105.5(1), C4—O4—C5 117.7(1), C1—O2—N2 109.2(1), N3—C3—N4—O5 87.6(1), N1—C2—N2—O2 -0.2(2), O3—C4—O4—C5 5.4(2), O2—C1—N1—C2 -2.4(1), O1—C1—O2—N2 -177.4(1), N1—C1—O2—N2 2.3(1), C2—N2—O2—C1 -1.3(1).

As expected only the H1 at N1 is contributing to the hydrogen bonding situation and connects intramolecular to the O4 and intermolecular to the O1, both stabilize the backbone in the crystal structure.

Table 18. Selected hydrogen bonds of **5**.

Atoms D,H,A	Dist. D,H [Å]	Dist. H,A [Å]	Dist. D,A [Å]	Angle D,H,A [°]
N1—H1A—O1 ⁱ	0.809(15)	2.029(16)	2.7935(14)	157.4(16)
N1—H1A—O4	0.809(15)	2.309(16)	2.7701(14)	116.8(15)
(i) 1-x, -y, -z.				

3.2.1 Sodium (4-{2-[(ethoxycarbonyl)oxy]propan-2-yl}-5-oxo-4,5-dihydro-1,2,4-oxadiazol-3-yl)(dinitro)methanide monohydrate (rearrangement product) (6)

6 crystallizes in the monoclinic space group $P2_1/n$ with four molecules in the unit cell.

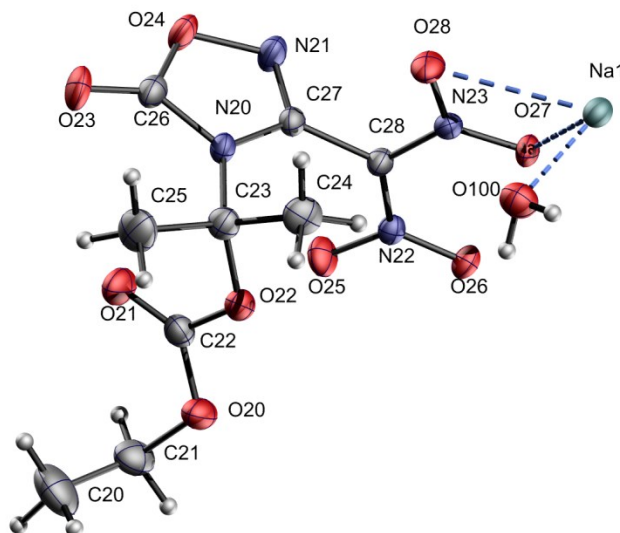


Figure 7. Molecular structure of **6**, Thermal ellipsoids plotted at 50% probability level.

Table 19. Selected bond lengths and angles of **6** (red oxadiazolone, green dinitomethyl, lightblue acetone moiety, darkblue/black ethylcarboxylate).

Atoms 1,2	d 1,2 [Å]	Atoms 1,2	d 1,2 [Å]	Atoms 1,2	d 1,2 [Å]
O26—Na1 ⁱⁱⁱ	2.387(1)	N21—O24	1.421(1)	C22—O21	1.198(2)
O26—Na2 ⁱⁱⁱ	2.511(1)	C26—O23	1.198(2)	C22—O20	1.325(2)
O27—Na1 ⁱⁱⁱ	2.310(1)	C26—O24	1.359(2)	C22—O22	1.343(2)
O27—Na1 ⁱⁱ	2.393(1)	C26—N20	1.378(2)	C21—O20	1.462(2)
O28—Na1 ⁱⁱ	2.870(1)	C27—N21	1.281(2)	C20—C21	1.485(2)
O16—Na1 ⁱ	2.421(1)	C27—N20	1.388(2)		
N23—Na1 ⁱⁱ	2.987(1)			C23—O22	1.452(2)
O13—Na1	2.329(1)	C28—N23	1.369(2)	C23—C24	1.509(2)
O100—Na1	2.324(1)	C28—N22	1.393(2)	C23—C25	1.515(2)
Na1—N23 ^{vi}	2.987(1)	N22—O25	1.242(1)		
Na1—O27 ^v	2.311(1)	N22—O26	1.243(1)	C27—C28	1.458(2)
Na1—O26 ^v	2.387(1)	N23—O27	1.248(1)	C23—N20	1.481(2)
Na1—O27 ^{vi}	2.393(1)	N23—O28	1.251(1)		
Na1—O16 ^{vii}	2.421(1)				
Na1—O28 ^{vi}	2.870(1)				

Atoms 1,2,3	Angle 1,2,3 [°]	Atoms 1,2,3	Angle 1,2,3 [°]
-------------	-----------------	-------------	-----------------

C26—O24—N21	109.9(9)	C28—N23—Na1 ⁱⁱ	160.0(8)
O23—C26—O24	122.2(1)	N22—O26—Na1 ⁱⁱⁱ	131.7(7)
O23—C26—N20	131.7(1)	N22—O26—Na2 ⁱⁱⁱ	124.5(7)
O24—C26—N20	106.0(1)	N23—O27—Na1 ⁱⁱⁱ	134.6(7)
N21—C27—N20	112.8(1)	N23—O27—Na1 ⁱⁱ	105.9(7)
C26—N20—C27	106.35(1)	Na1 ⁱⁱⁱ —O27—Na1 ⁱⁱ	101.9(4)
C26—N20—C23	127.1(1)	N23—O28—Na1 ⁱⁱ	82.9(7)
C27—N21—O24	104.9(1)	O27—N23—Na1 ⁱⁱ	50.3(6)
N20—C27—C28	127.6(1)	O27 ^v —Na1—O26 ^v	68.7(4)
C22—O22—C23	118.6(1)	O100—Na1—O26 ^v	89.0(4)
N23—C28—C27	117.8(1)	O27 ^v —Na1—O27 ^{vi}	78.1(4)
N22—C28—C27	118.1(1)	O100—Na1—O27 ^{vi}	101.5(4)
N21—C27—C28	119.7(1)	O26 ^v —Na1—O27 ^{vi}	143.7(4)
C27—N20—C23	126.6(1)	O27 ^v —Na1—O28 ^{vi}	120.8(4)
O25—N22—O26	121.5(1)	O100—Na1—O28 ^{vi}	86.4(4)
O25—N22—C28	115.7(1)	O28—N23—Na1 ⁱⁱ	72.4(7)
O26—N22—C28	122.8(1)	O26 ^v —Na1—O28 ^{vi}	168.6(3)
O27—N23—O28	119.9(1)	O27 ^{vi} —Na1—O28 ^{vi}	47.4(3)
O27—N23—C28	123.2(1)	O16 ^{vii} —Na1—O28 ^{vi}	111.1(4)
O28—N23—C28	116.8(1)	O27 ^v —Na1—N23 ^{vi}	97.3(4)
N23—C28—N22	123.8(1)	O100—Na1—N23 ^{vi}	90.3(4)
C22—O20—C21	115.5(1)	O26 ^v —Na1—N23 ^{vi}	166.0(3)
O20—C21—C20	111.3(1)	O27 ^{vi} —Na1—N23 ^{vi}	23.6(3)
O21—C22—O20	126.7(1)	O28 ^{vi} —Na1—N23 ^{vi}	24.5(2)
O21—C22—O22	125.9(1)		
O20—C22—O22	107.7(1)		
O22—C23—N20	108.3(1)	O22—C23—C25	110.6(1)
O22—C23—C24	104.5(1)	N20—C23—C25	112.3(1)
N20—C23—C24	110.45(1)	C24—C23—C25	110.4(1)

(i) 1.5−x, 0.5+y, 1.5−z; (ii) −0.5+x, 0.5−y, 0.5+z; (iii) 0.5−x, 0.5+y, 1.5−z;
(iv) −0.5+x, 0.5−y, −0.5+z; (v) 0.5−x, −0.5+y, 1.5−z; (vi) 0.5+x, 0.5−y, −0.5+z;
(vii) 1.5−x, −0.5+y, 1.5−z; (viii) 1−x, −y, 1−z; (ix) 0.5+x, 0.5−y, 0.5+z; (x) 1−x, −y, 2−z.

The listed bond lengths and angles are in good agreement with the before-mentioned 1,2,4-oxdiazol-5-one moiety. Also the dinitromethyl moiety is in good accordance with literature. The coordination sphere of sodium is eight. The surrounding includes one water and at least three further molecular units (Visualization see figure 8).

Table 20. Selected hydrogen bonds of **6**.

Atoms D,H,A	Dist. D,H [Å]	Dist. H,A [Å]	Dist. D,A [Å]	Angle D,H,A [°]
O100—H100—O21	0.77(2)	2.25(2)	2.992(2)	164.(2)
O100—H101—O15ⁱ	0.82(2)	2.11(2)	2.922(2)	171.(2)
O101—H102—O18ⁱⁱ	0.95(3)	2.31(3)	2.879(2)	118.(2)
O101—H102—O20	0.95(3)	2.64(3)	3.510(2)	152.(2)
O101—H103—O11ⁱ	0.93(2)	1.93(3)	2.798(2)	155.(2)

(i) −0.5+x, 0.5−y, −0.5+z; (ii) −1+x, y, z.

The hydrogen bonding in **6** includes the water molecules and interacts with oxygen of the nitro and carboxyl groups as well as the oxadiazole moiety. Remarkably interaction with nitrogen atom is not observed.

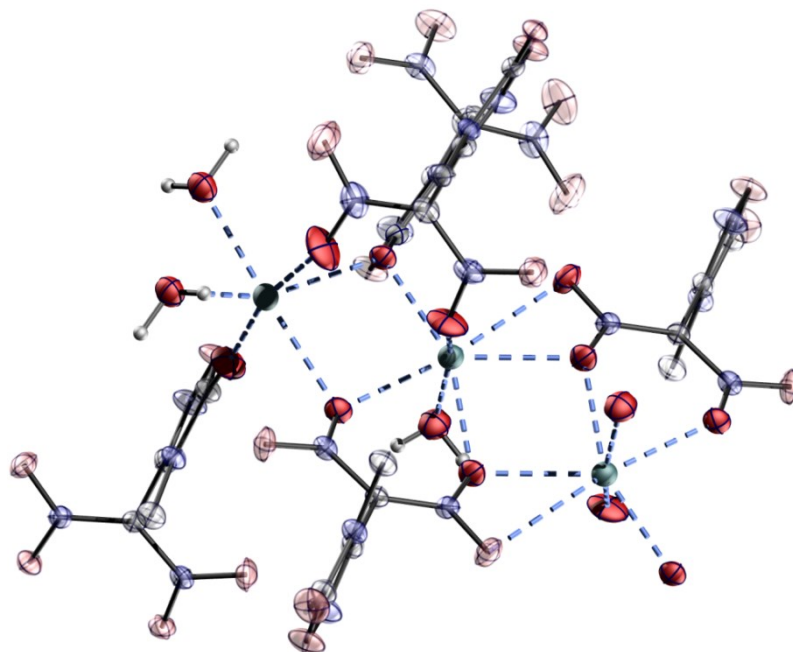


Figure 8. Coordination of sodium in the structure of **6**. Thermal ellipsoids plotted at 50% probability level.

3.2.2 Di-Sodium DNM-OD dihydrate (**7b**)

7b crystallizes in the monoclinic space group $P2_1/c$ with four molecules in the unit cell. As displayed in figure 9 **7b** nearly every oxygen and nitrogen atom coordinates to a sodium atom.

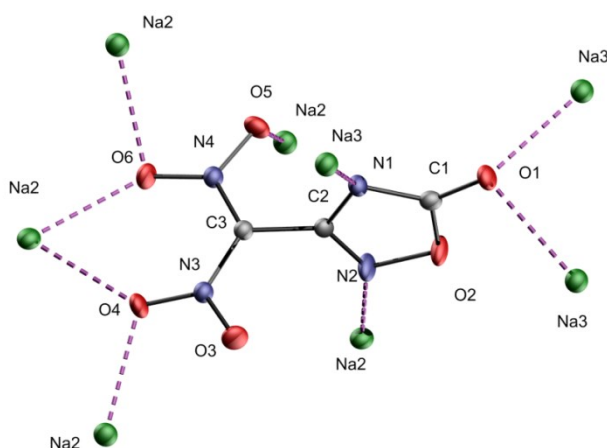


Figure 9. Molecular structure of **7b**, Thermal ellipsoids plotted at 50% probability level.

There are two different coordination schemes observed (see figure 10). One includes is a distorted octahedron that consists of three water molecules and two coordinating

oxygen (O5) and one nitrogen (N4) of the 1,2,4-oxadiazole-5-one moiety. The other coordination sphere is also a distorted octahedron but in one plane coordination of two dinitromethyl – oxygens from two different molecules and one oxygen coordination from another dinitromethyl oxygen of a third dinitromethyl moiety as well as a nitrogen (N4) coordination to an 1,2,4-oxadiazol-5-one moiety.

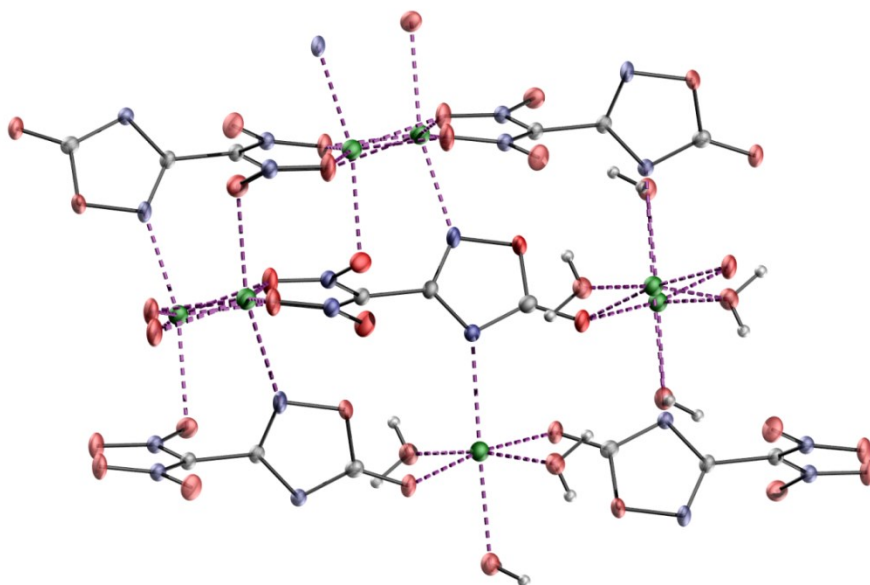


Figure 10. Coordination of the sodium in the structure of **7b**, Thermal ellipsoids plotted at 50% probability level.

3.2.3 Di-Ammonium DNM-OD (**9b**)

8b crystallizes in the monoclinic space group $P2_1/n$ with four molecules in the unit cell.

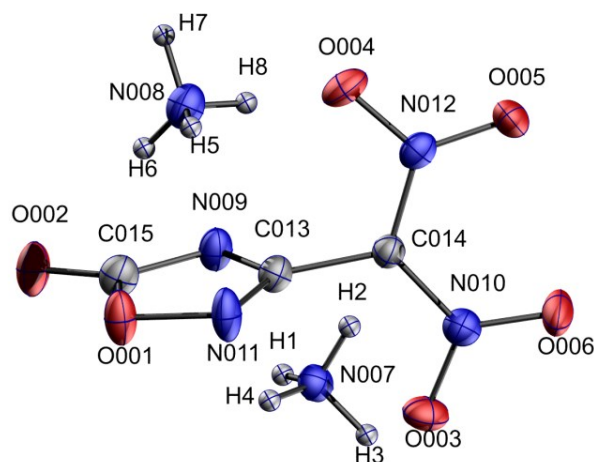


Figure 11. Molecular structure of **9b**. Thermal ellipsoids plotted at 50% probability level.

Table 21. Bond lengths and angles of **9b** (red oxadiazolone, green dinitomethyl).

Atoms 1,2	d 1,2 [Å]	Atoms 1,2	d 1,2 [Å]
O001—C015	1.381(2)	O006—N010	1.235(1)
O001—N011	1.422(1)	O005—N012	1.253(1)
O002—C015	1.242(2)	O004—N012	1.269(1)
N011—C013	1.307(2)	O003—N010	1.260(2)
N009—C013	1.353(2)	N012—C014	1.367(2)
N009—C015	1.339(2)	N010—C014	1.388(2)
		C013—C014	1.476(2)

Atoms 1,2,3	Angle 1,2,3 [°]	Atoms 1,2,3	Angle 1,2,3 [°]
C015—O001—N011	106.7(1)	O006—N010—C014	123.1(1)
C015—N009—C013	103.2(1)	O003—N010—C014	116.0(1)
O006—N010—O003	120.9(1)	O005—N012—O004	120.1(1)
C013—N011—O001	102.8(1)	O005—N012—C014	123.4(1)
N011—C013—N009	116.7(1)	O004—N012—C014	116.4(1)
O002—C015—N009	130.9(2)	N012—C014—N010	121.5(1)
O002—C015—O001	118.5(1)		
N009—C015—O001	110.6(1)		
N011—C013—C014	119.4(1)	N012—C014—C013	117.64(1)
N009—C013—C014	123.8(1)	N010—C014—C013	120.48(1)

Atoms 1,2,3,4	Tors. an. 1,2,3,4 [°]	Atoms 1,2,3,4	Tors. an. 1,2,3,4 [°]
O001—N011—C013—C014	176.0(1)	N011—C013—C014—N012	−98.0(2)
C015—N009—C013—C014	−175.3(1)	N009—C013—C014—N012	78.1(2)
C013—N009—C015—O002	178.8(2)	N011—C013—C014—N010	88.9(2)
N011—O001—C015—O002	−178.9(1)	N009—C013—C014—N010	−94.9(2)
O005—N012—C014—N010	2.3(2)		
O003—N010—C014—C013	1.0(2)		

In the table 21 the 1,2,4-oxadiazol-5-one moiety as well as the dinitromethyl moiety are in good accordance with the other discussed molecules (**6**, **7b**). Looking into the torsion angles the nitromethyl moiety is nearly complete planar as well as the 1,2,4-oxadiazol-5-one moiety which is slightly tilted at the C013-C014 axis as it is not exactly 90°.

Table 22. Selected hydrogen bonds of **9b**.

Atoms D,H,A	Dist. D,H [Å]	Dist. H,A [Å]	Dist. D,A [Å]	Angle D,H,A [°]
N007—H1—N011	0.86(2)	2.07(2)	2.900(2)	164.(2)
N007—H2—O005 ⁱ	0.88(2)	2.10(2)	2.921(2)	154.(2)
N007—H2—O003 ⁱⁱ	0.88(2)	2.39(2)	2.854(2)	113.(1)
N007—H3—O002 ⁱⁱⁱ	0.94(2)	1.94(2)	2.811(2)	153.(2)
N007—H4—O002 ^{iv}	0.92(2)	1.95(2)	2.854(2)	168.(2)
N008—H5—N009 ⁱⁱ	0.97(2)	1.89(2)	2.854(2)	171.(2)
N008—H8—O004	0.86(2)	2.28(2)	3.043(2)	149.(2)
N008—H8—O005 ⁱ	0.86(2)	2.34(2)	2.886(2)	122.(2)
N008—H7—O004 ^v	0.94(2)	1.95(2)	2.848(2)	158.(2)

(i) 1−x, 1−y, 2−z; (ii) x, 1+y, z; (iii) −0.5+x, 0.5−y, −0.5+z; (iv) 2−x, 1−y, 2−z;
(v) 1.5−x, 0.5+y, 2.5−z.

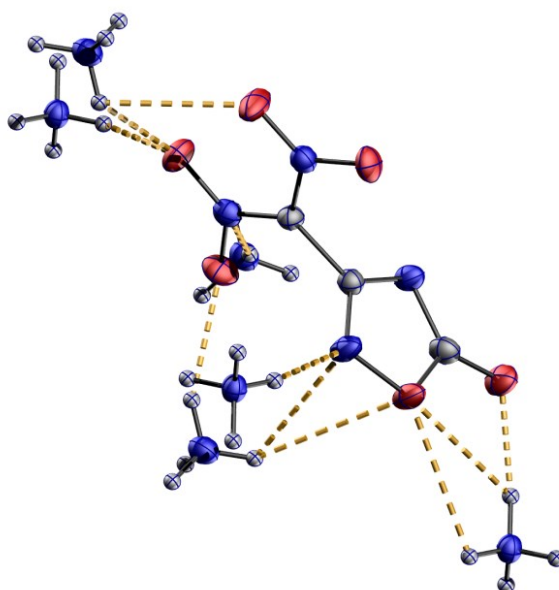


Figure 12. Hydrogen bonding of **8b**, Thermal ellipsoids plotted at 50% probability level.

The hydrogen bonding that stabilizes the crystal and leads to a high density. Bifurcated hydrogen bondings (H2 and H8) from one ammonium ion via one hydrogen either to two different oxygen atoms in two nitro groups (H8 and H2) or in the 1,2,4-oxadiazole-5-one to the N011, N009 and O002.

3.2.4 Bis-Guanidinium DNM-OD (**9a**)

9a crystallizes in the triclinic space group *P*-1 with four molecules in the unit cell.

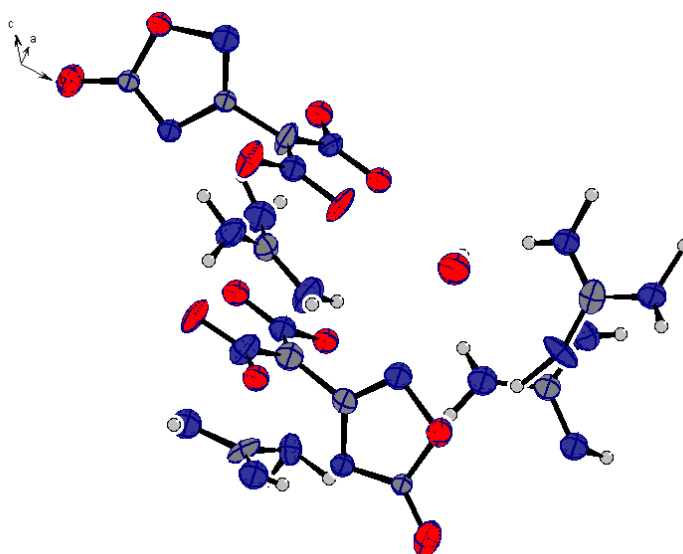


Figure 13. Molecular structure of **9a**, Thermal ellipsoids plotted at 50% probability level.

3.3 Calculations – thermodynamical properties

3.4 Structure Optimization of DNM-OD and DNM-OD²⁻

The structure of the DNM-OD could not be determined by NMR or crystal structure as it was only found in solution so there were carried out some calculations as well on the neutral DNM-OD as on the anion DNM-OD²⁻. Both were done by the Gaussian3 program package^[11] at HF level of theory and with a double zeta basis set including ionization potential 3-21G*.

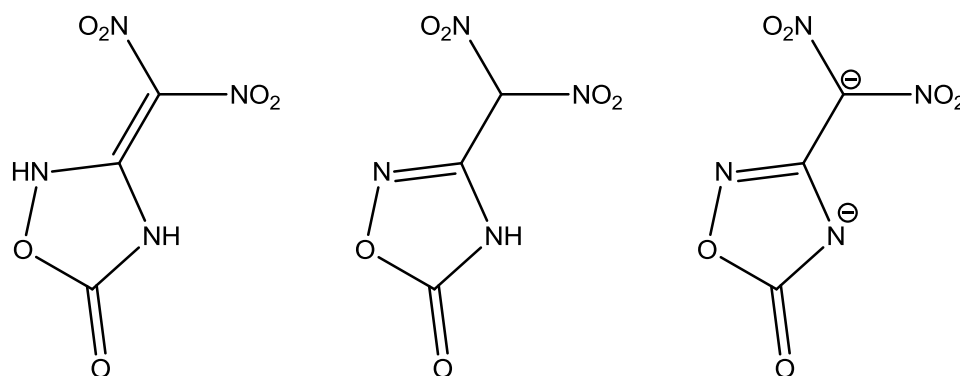


Figure 14. Protonated and deprotonated form of DNM-OD.

There are two possible structures for the DNM-OD and its anion imaginable. The planar fully mesomeric structure and the 45 to 90 degrees twisted form with partial or none mesomeric interchange of electrons.

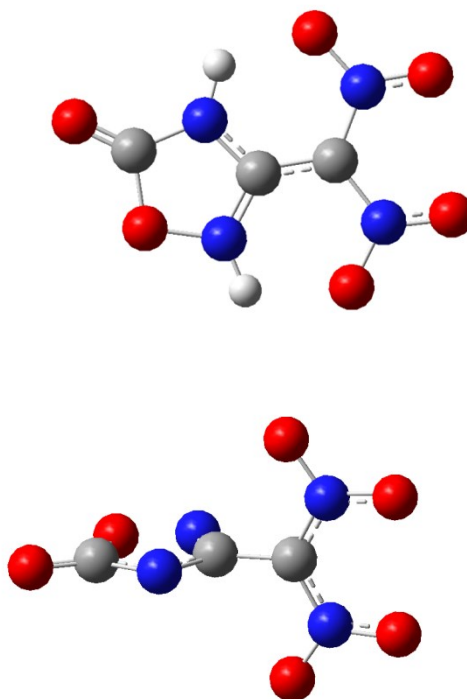


Figure 15. Results from Structure Optimization by Gaussian03 HF/3-21G*. Visualization by GaussView 5.0.^[12]

For DNM-OD a minimum at -776.9784111 a.u. was found which corresponds to a planar structure. While the DNM-OD²⁻ is twisted by 90 degrees to form two anionic moieties the oxadiazole-5-onate and the dinitromethylenidyl moiety. The bond lengths at the DNM-OD between C2 and C3 are little shorter to the anion. And the distance between the hydrogens at the ring and the oxygen of the nitro group are in the range of a normal hydrogen bonding.^[10] The push pull system is very similar to the FOX-7 system^[5,6].

The calculation of the DNM-OD²⁻ (**7**) is in good accordance with the crystal structures of the sodium and ammonium salt which both show an about 90 degree twist between the oxadiazole ring and the dinitromethyl moiety.

3.5 Energetic properties

The DNM-OD salts are capable of different energetic properties, while the alkaline and alkaline earth salts may be suitable for pyrotechnical compositions the high nitrogen containing salts might find some application as high explosives or modifiers in propellants for gun ammunition and rockets.

3.5.1 Pyrotechnical colorants

For pyrotechnical compositions it is essential that the ingredients do not affect the stability or sensitivity. This results in some requirements for the ingredients like high decomposition temperature, high color purity, low water content, non-hygroscopic and little sensitivity towards shock and electrostatic discharge.^[13]

Table 23. Alkaline and alkaline earth salts of DNM-OD.

	Li ₂ DNM-OD	Na ₂ DNM-OD	K ₂ DNM-OD	Ba DNM-OD
F.S. [N]	324	120	120	160
I.S. [J]	10	10	3	10
ESD [mJ]	100	100	100	100
Flame test	Burns red	Yellow fizzling	Pale violet explosion	Burns pale green
Grain size [μm]	1000	100-500	< 160	< 160
T _{dec.} [°C]	Not. Det.	211	219	165

Looking at the alkaline and alkaline earth metal salts of DNM-OD the most promising for application seems to be the sodium salt. Although the potassium salt and lithium salt show good colorant properties they lack either in sensitivity (potassium) or are hygroscopic (lithium). The barium salt displays a little too low decomposition temperature and could only be used in combination with chlorine containing ingredients to show full range of color.

3.5.2 High-Nitrogen containing cations

While the neutral DNM-OD is only existing in theory so far it can be estimated an average density 1.6 g cm⁻³ from the high nitrogen containing salts and the experience from the described molecules in chapter IV and VI. The energy of formation is calculated by Gaussian03^[11] at CBS-4M level of theory which includes a multiplicity step

refinement of the atomization energies. (see chapter III)^[14] and the energy of formation of the high nitrogen containing salts are calculated by the method by Jenkins et al. (see Chapter V).^[15] The calculations for the ammonium and guanidinium salts are based on experimental data regarding to the density. For comparison the other nitrogen containing salts like, triaminoguanidinium and hydrazinium as well as the standard explosive RDX are listed in the table below (table 24).

The performance of the nitrogen rich salts of DNM-OD are rather good as for all high gas volume of over 800 L kg⁻¹ is observed which outnumbers RDX, while the pressure at the same time is rather low as well as the released heat of explosion. Nonetheless A₂ DNM-OD, H₂ DNM-OD and TAG₂ DNM-OD show detonation velocities over 8000 m s⁻¹. Unfortunately **9b** is has a low decomposition point which does not make it suitable for applications. As hydrazinium and triaminoguanidinium salts were not obtained the values are only theoretical relevant and show the possible performance options of the DNM-OD.

Table 24. EXPLO5^[16] calculated values for the detonation parameters for DNM-OD and its salts.

	DNM-OD (8)	A ₂ DNM-OD (9b)	G ₂ DNM-OD (9a)	G ₂ DNM-OD	H ₂ DNM-OD	TAG ₂ DNM-OD	RDX ^[17]
T _{dec.} / °C	(120 ^b)	128	170	–	–	–	213
Δ _f U° / kJ kg ⁻¹	–428	–919	–1182	–1182	–383	+955	+417
Ω / %	–9	–29	–60	–60	–31	–52.	–21
ρ / g cm ⁻³	1.60 ^b	1.71	1.57 ^a	1.70 ^b	1.60 ^b	1.60 ^b	1.80
EXPLO5 values							
Q _V / kJ kg ⁻¹	–5797.2	–5019	–3034	–3042	–5042.8	–4770	–6034
T _{ex} / K	4692	3642	2439	2442	3513	3185	4334
p _{C-J} / kbar	246	273	163	204	254	253	340
D / m s ⁻¹	7648	8249	6846	7429	8040	8182	8882
V ₀ / L kg ⁻¹	653	828	805	803	836	846	769

a) measured values with crystal water; b) estimated c) EXPLO5 BKWN-Parameters: (Alpha=0.5; Beta=0.096; Kappa=17.56; Theta=4950); ρ = density, Ω = oxygen balance, Q_v = heat of detonation, T_{ex} = detonation temperature, P = detonation pressure, D = detonation velocity, V₀ = Volume of detonation gases;

4 Conclusions

The recent developments in the synthesis of the 3-dinitromethyl-1,2,4(4*H*)-oxadiazol-5-one show the wide capabilities of this class as energetic material. The alkaline and alkaline earth metals display good thermostabilities and except the potassium salt they are rather insensitive.

The DNM-OD and its derivatives perform as energetic materials very well but lack the thermal stability as well as provide high sensitivities to impact and friction. In comparison to the respective tetrazole derivatives they are more stable due to sensitivities, but do lack the performance. The synthesis of those two structural derivatives of FOX-7 with a ring moiety at the diamino side of the compound by the

group of T.M. Klapoetke shows that this is a promising way of tailoring the energetic properties and also the stability of well-known explosives by changing the ring moiety to imidazoles, triazoles and substituted six membered ring systems.

5 Outlook

Further investigations have to be carried out especially with the nitrogen rich cations like guanidine, triaminoguanidine, and the also copper complexes as are possible to make. Maybe some substitutions on the 4-N of the 1,2,4-oxadiazolone can stabilize the system to higher temperatures or enhance the possibilities of those structures.

6 Experimental

6.1 Common

Yield is given in percentage rounded to full numbers according to the compound with the lowest amount.

Starting compounds were purchased by commercial suppliers at a purity of 99% p.a. and used without further purification. Ammonium-5-nitrotetrazolat hemihydrate, potassium dinitramide, sodium-5,5'-azotetrazolate pentahydrate and picric acid were selfmade compounds and stored in the working group. All solvents are minimum technical grade 85% and were used as purchased.

Minimal pressures were about 10 mbar at the membran pump (MPV) and 1×10^{-2} mbar at oil rotation pump (OPV) using glass vacuum apparatus with tubing.

6.2 Analytical apparatus

Infrared spectra of air insensitive samples were taken at a *PerkinElmer* BX FT-IR with a *Smiths* DuraSamplIR II Diamant-ATR-module. The range of the spectra 600–4000 cm^{-1} .

Raman spectroscopy was done on the working group's *Perkin Elmer Spectrum 2000 NIR-FT-Raman*-device with *Perkin Elmer Diode Pumped Nd: YAG-Laser*-light source

For the **nuclear resonance spectra** were used a *Jeol* Eclipse 270, *Jeol* Eclipse 400 and a *Jeol* ECX 400. The measurements were taken in glass NMR tubes (5 mm) and at a standard temperature of 25°C. The external standards and frequencies of the cores are listed in table 19. As internal standard the literature values of the signals of the completely undeuterated solvents (^1H) as well as the completely deuterated solvents (^{13}C) [18] were used. ^{13}C NMR spectra were, as long as nothing else is mentioned, ^1H decoupled recorded. The evaluation of the data was done with MestReNova[19].

Table 25. NMR-Standards and –recording frequencies.

Core	Standard	Eclipse 270	Eclipse 400	ECX 400
		frequency / MHz		
1 H	Tetramethylsilane	270.17	400.18	399.78
13 C	Tetramethylsilane	67.93	100.63	100.53
14 N	Nitromethane	—	28.92	28.89

Mass spectra were recorded at a *Jeol* MStation JMS 700. As ionization methods for normal resolution spectra *direct electron impact* (DEI) and *fast atom bombardment* (FAB) were used. The matrix for FAB-measurements was *para*- nitrobenzylic alcohol.

Elemental analysis was done in the micro analytical laboratory of the department. By combustion analysis with a *Elementar* Vario EL or a *Elementar* Vario Micro the elemental composition of a compound for C, H, N, S, Br, I, Cl was acquired. The results were given in percentages of the respective element.

The **melting point** of compound 1,a,c were determined with a *Büchi* Melting Point B-540 and are uncorrected.

Thermal analysis was recorded by *Linseis* DSC-PT10. A probe of 1-2mg of the sample substance were confined in a small aluminum container with a 0.1 mm hole in the lid to exhaust vast gas. This probe was measured against a reference of an empty aluminum container with a heating rate of 5°C min⁻¹ and a temperature range of 25-400°C. The acquired temperature was the onset value according to IUPAC agreements.

Sensitivities towards impact, friction and electrostatic discharge were determined.^[20] The sensitivity toward impact was recorded according to the STANAG 4489, ^[21] modified WIWEB 4-5.1.02^[22] method by using a BAM drop hammer apparatus. The friction sensitivity was acquired according to the STANAG 4487, ^[23] modified WIWEB 4-5.1.03 procedure ^[24] by using a BAM friction apparatus. The compound was classified according to the *UN Recommendations on the Transport of Dangerous Goods*. ^[25] impact: insensitive > 40 J, low sensitive >35 J, sensitive >4 J, very sensitive <3 J. friction: insensitive > 360 N, low sensitive = 360 N, sensitive <360 N and >80 N, very sensitive < 80 N, extreme sensitive < 10 N. The determination of sensitivity to electrostatic discharge was done by an *OZM Research* ESD 2010 EN.

Density was determined - if a crystal structure of the compound was not available - by a *Quantachrome Instruments* Ultrapyc 1200e gas pycnometer with a sample amount of 50–100 mg.

Bomb calorimetric measurements were carried out by a *Parr* 1356 bomb calorimeter incl. a *Parr* 1755 printer for data output. 70-100 mg of compound were grinded together with about 1 g of benzoic acid. The homogenous mixture pressed to small pellet and burned in a pure oxygen atmosphere at a pressure of 30 bars. The heat of burning is calculated from the arithmetic average of at least three measurements.

The determination of the **crystal structure** is accomplished by an *Oxford Diffraction Xcalibur 3* with a Sapphire CCD-detector, a four concentric circle kappa platform and

Enhance™ Mo-K α -x-ray source with a wave length of $\lambda=71.073$ pm. The structures were solved with SIR92, SIR97^[26], SHELXS97^[27] and refined with SHELXL97^[28] by the method of smallest error square in full matrix referring to F^2 values. The illustrations were created in ORTEP-3^[29] and Diamond 3^[30].

6.3 Preparation

6.3.1 2-Ethyl-3-amino-3-(hydroxyimin)-propanoate (1)

To a solution of 28.2 mL (265 mmol) ethyl cyano acetate, 27.7 g (399 mmol) hydroxylamine hydrochloride and 33.6 g (400 mmol) sodium bicarbonate in 300 mL ethanol under vigorous stirring 150 mL water was added until solution is clear and pale yellow. The mixture was heated for one hour at 55°C and another hour at room temperature. The resulting precipitate was filtered and the filtrate was concentrated to about 150 mL in vacuo. The solution was extracted with three times 100 mL dichloromethane and the combined organic layers cleared with one time 100 mL brine. The organic layers were dried with sodium sulfate and the resulting yellow oil was covered with n-pentane. After short period the oil crystallizes to a pale brown solid, which was recrystallized from dichloromethane and n-pentane at room temperature. **Yield** 12.5 g (85.6 mmol, 32 %).

¹H NMR ([D₆]DMSO, 400 MHz): δ (ppm) = 1.19 (t, $^3J = 7.20$ Hz, 3H, H₅), 3.01 (s, 2H, H₆), 4.06 (q, $^3J = 6.80$ Hz, 2H, H₄), 5.47 (s, 2H, H₂), 9.02 (s, 1H, H₇). **¹³C{¹H} NMR** ([D₆]DMSO, 100 MHz): δ (ppm) = 14.1 (1C, C₅), 37.0 (1C, C₃), 60.3 (1C, C₄), 147.4 (1C, C₂), 169.1 (1C, C₁). **IR**: $\tilde{\nu}$ (cm⁻¹) = 3504 s, 3387 s, 3165 m, 3099 m, 2983m, 2941m, 2896 m, 2819m, 2391 vw, 2252 vw, 2119 vw, 1715 vs, 1662 vs, 1593 s, 1464 m, 1443 m, 1417 s, 1400 m, 1369 m, 1329 s, 1302 m, 1215 s, 1178 m, 1118 m, 1089 m, 1026 s, 979 s, 906 m, 852 m, 812 m, 755 m, 667 m, 588 w, 551 vw, 456 vw. **Raman** (300 mW): $\tilde{\nu}$ (cm⁻¹) = 2970 (52), 2984 (61), 2941 (100) 1714 (30) 1672 (69), 1593 (11) 1450 (27), 1420 (19), 1393 (20), 1329 (9) 1300 (8), 1179 (14), 1093 (13), 1025 (9), 926 (25), 851 (18), 815 (6), 670 (10), 585 (7), 548 (7), 453 (11), 403 (23), 354 (13), 334 (19), 313 (11).

Precipitated by-product

(not yet identified)

¹H NMR ([D₆]DMSO, 400 MHz): δ (ppm) = 2.17 (s, 2H, CH₂), 5.43 (s, 2H, NH₂), 8.97 (s, H₂, NH₂). **¹³C{¹H} NMR** ([D₆]DMS, 100 MHz): δ (ppm) = 37.0 (s, 1C, CH₂), 148.5 (s, 1C, CN), 165.1 (s, 1C, CO). **MS** (DEI⁺): m/z (rel.int.) = 42.2 (48.47), 73.2 (23.34), 101.2 (100.00), 133.2 (34.40). **Elemental analysis**: found C 26.65, H 4.03, N 27.99.

6.3.1 Ethyl-2-(1,2,4-oxadiazol-5-on-3-yl) acetate - two step reaction (10)

First step includes the reaction of **1** with methyl chloroformate and the second step the ring closure reaction.

6.3.2 Ethyl-(3Z)-3-amino-3-((methoxycarbonyl)oxy)imino}-propanoate (9)

To a solution of 5.00 g (32.2 mmol) ethyl-3-amino-3-(hydroxyimin)-propanoate in 100 mL THF and 2.71 mL (35.3 mmol) methyl chloro formate under stirring and ice-

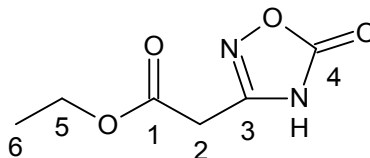
cooling 4.04 g (39.9 mmol) triethylamine in 10 mL THF was added dropwise during one hour. After the addition the solution was stirred for another hour at room temperature. The precipitate was filtered and the filtrate was extracted with dichloromethane and the combined organic solvents were cleared with brine and dried over sodium sulfate. The solvent was removed under reduced pressure and the precipitated recrystallized with ethyl acetate. The resulting colorless crystals were collected. **Yield** 3.05 g (14.9 mmol, 46 %).

¹H NMR ([D₆]DMSO, 400 MHz): δ (ppm) = 1.19 (q, 3J = 7.2 Hz, 3H, H₆), 3.13 (s, 2H, H₂), 3.71 (s, 3H, H₅), 4.09 (q, 3J = 7.20 Hz, 2H, H₆), 6.55 (s, 2H, NH₂). **¹³C{¹H} NMR** ([D₆]DMSO, 100 MHz): δ (ppm) = 14.0 (1C, C₆), 36.1 (1C, C₂), 54.5 (1C, C₅), 60.7 (1C, C₆), 153.3 (1C, C₃), 153.9 (1C, C₄), 168.2 (1C, C₁). **IR**: $\tilde{\nu}$ (cm⁻¹) = 3421 vs, 3332 vs, 3204 s, 2953 m, 2918 m, 2850 w, 1760 m, 1717 m, 1648 s, 1600 m, 1435 w, 1425 w, 1248 s, 1187 m. **Raman** (300 mW): $\tilde{\nu}$ (cm⁻¹) = 2974 (100), 2948 (89), 2872 (17), 1756 (24), 1714 (23), 1652 (45), 1613 (18), 1451 (31), 1411 (22), 1216 (19), 1120 (22), 973 (31), 955 (23), 855 (23), 756 (15), 296 (32).

Second step (cyclization)

The colorless crystals of ethyl (3Z)-3-amino-3-[(methoxycarbonyl)oxy]imino}propanoate were solved in 2.00 mL diethylene glycol dimethyl ether and heated under stirring for 5 hours at 130°C. A brown-black solid resulted, which was solved in water. The precipitated was collected. But proved not to be the wanted product. This step has to be investigated carefully.

6.3.3 3-Ethyl (5-oxo-4,5-dihydro-1,2,4-oxadiazol-3-yl)-acetate (2)



To a solution of 5.00 g (32.2 mmol) ethyl-3-amino-3-(hydroxyimin)-propanoate in 100 mL THF and 3.82 g (16.1 mmol) diphosgene under ice-cooling 6.52 g (64.4 mmol) triethylamine in 30 mL THF was added dropwise during one hour. After the addition the solution was stirred for another hour at room temperature. The precipitate was filtered and the filtrate was extracted with dichloromethane and the combined organic solvents were cleared with brine and dried over sodium sulfate. The solvent was removed under reduced pressure. The crude pale yellow oil was covered with n-pentane after short period the oil crystallized. The solid was filtered and dried in vacuo. **Yield** 3.47 g (20.2 mmol, 62 %).

¹H NMR ([D₆]DMSO, 400 MHz): δ (ppm) = 1.20 (q, 3J = 7.2 Hz, 3H, H₆), 3.79 (s, 2H, H₂), 4.47 (q, 3J = 7.2 Hz, 2H, H₅), 12.40 (s, 1H, NH). **¹³C{¹H} NMR** ([D₆]DMSO, 100 MHz): δ (ppm) = 13.9 (1C, C₆), 31.0 (1C, C₂), 61.5 (1C, C₅), 154.3 (1C, C₃), 159.5 (1C, C₄), 166.6 (1C, C₁). **IR**: $\tilde{\nu}$ (cm⁻¹) = 3206 br, 2971 m, 1775 vs, 1731 vs, 1656 s, 1604 s, 1486 s, 1374 m,

1347 m, 1190 s, 1022 m, 940 m, 878 w, 746 w, 673w. **MS (DEI+)**: m/z (rel.int.) = 29.2 (100), 56.2 (35), 68.2 (44), 9.2(37), 100.2(77), 126.2(31), 172.2 (51).

6.3.4 Dinitro-([1,2,4]oxadiazol-5-on-3-yl)-acetic acid ethyl ester (3)

To an ice-cooled solution of 2 mL nitric (100%) and conc. 3 mL sulphuric acid. 900 mg (5.2 mmol) ethyl 2-(1,2,4-oxadiazol-5-on-3-yl) acetate was added carefully and stirred for one hour at ice-cooling and one hour at room temperature. The solution becomes a suspension after short period of stirring the suspension is cooled to -32°C and also little ice is cooled to -32°C. The suspension and the ice are mixed at low temperature in an ice-salt bath. The suspension was filtered in a glass filter and washed once with little amount cooled water. The pure product showed a pale yellow color. **Yield** (600 mg, 2.3 mmol, 44 %)

¹H NMR ([D₆]DMSO, 400 MHz): δ (ppm) = 1.29 (q, ³J = 7.4 Hz, 3H, H₆), 4.54 (q, ³J = 7.5 Hz, 2H, H₆). **¹³C{¹H} NMR** ([D₆]DMSO, 100 MHz): δ (ppm) = 13.4 (1C, C₆), 67.1 (1C, C₅), 109.4 (1C, C₂), 152.9 (1C, C₃), 154.6 (1C, C₄), 163.6 (1C, C₁). **¹⁴N NMR** ([D₆]DMSO, 29 MHz): δ (ppm) = -21.4. **IR**: $\tilde{\nu}$ (cm⁻¹) = 3156 m, 3038 m, 2999 m, 1797 s, 1780 vs, 1601 vs, 1574 s, 1467 m, 1299 s, 1274 m, 1232 vs, 1092 s, 1035 m, 982 m, 963 m, 944 m, 903 s, 839 s, 812 m, 747 s. **Raman** (300 mW): $\tilde{\nu}$ (cm⁻¹) = 3040 (39), 2994 (90), 2948 (100), 1792 (63), 1598 (43), 1572 (57), 1457 (42), 1353 (42), 1269 (52), 1234 (39), 949 (63), 846 (36), 816 (35), 747 (28), 542 (32), 394 (69), 371 (47), 333 (85), 237 (33). **MS (DEI+)** m/z (rel.): 44 (100)[NO₂], 216 (60). **T_{dec}** (DSC, 5°C / min, onset) 91.3 °C and 195.6°C.

6.3.5 Sodium [4-{2-[(ethoxycarbonyl)oxy]propan-2-yl}-5-oxo-4,5-dihydro-1,2,4-oxadiazol-3-yl](dinitro)methanide monohydrate (rearrangement product) (5)

To 1.022 g (3.9 mmol) dinitro-([1,2,4]oxadiazol-5-on-3-yl)-acetic acid ethyl ester in acetone p.a. quality 312 mg (7.8 mmol) sodium hydroxide was added. After stirring for two hours the solution became turbid. The solvent was removed and the precipitate was slowly crystallized from ethyl acetate. That yielded not the desired product. But a rearrangement product was obtained.

¹H NMR ([D₆]DMSO, 400 MHz): δ (ppm) = 1.17 (t, ³J = 7.2 Hz, 3H), 1.81 (s, 6H), 4.03 (q, ³J = 7.2 Hz, 2H). **¹³C{¹H} NMR** ([D₆]DMSO, 100 MHz): δ (ppm) = 13.8 (1C, C₁), 25.1 (2C, C₅), 63.4 (1C, C₂), 68.5 (1C, C₄), 90.0 (1C, C₇), 121.4 (1C, C₈), 151.5 (1C, C₃), 156.1 (1C, C₆). **¹⁴N NMR** ([D₆]DMSO, 29 MHz): δ (ppm) = -19.4. **IR [KBr]**: $\tilde{\nu}$ (cm⁻¹) = 3607 m, 3515 s, 3269 w, 2989 m, 2964 m, 2549 w, 1793 s, 1747 s, 1698 w, 1646 m, 1624 w, 1586 m, 1493 s, 1423 m, 1401 m, 1374 m, 1258 s, 1153 s, 1127 m, 1094 w, 1075 w, 1061 w, 1017 m, 984 w, 909 m, 818 m, 784 m, 768 w, 749 w, 642 m, 611 m, 552 m. **MS (FAB⁻)** m/z (rel.): 44 (100)[NO₂], 216 (60).

6.4 Alkaline and alkaline earth metal salts of DNM-OD (7)

6.4.1 General procedure

508 mg (1.94 mmol) dinitro-([1,2,4]oxadiazol-5-on-3-yl)-acetic acid ethyl ester was reacted in 10 mL methanol with alkaline and alkaline earth hydroxides in an equivalent amount. The reaction was carried out under room temperature and vigorous stirring

while adding carefully the solved hydroxide. If the reaction product did not precipitate the solvent was removed under reduced pressure.

6.4.2 Lithium DNM-OD

83 mg (3.88 mmol) Lithium hydroxide was reacted. Due to its hygroscopic behaviour analysis was not carried out. As the water adduct is melting away at room temperature. But sensitivities of the dry product were obtained.

F.S. 324 N, **ESD** 100 mJ, **I.S.** 10 J, **grain size:** >1000 μm . **IR [KBr]:** $\tilde{\nu}$ (cm^{-1}) = 3438 br, 2188 w, 1666 s, 1580 w, 1533 m, 1487 s, 1420 m, 1384 s, 1352 w, 1308 w, 1250 s, 1138 s, 997 m, 953 m, 906 w, 824 m, 776 m, 753 m, 674 m.

6.4.3 Sodium DNM-OD x 2 H₂O

Yield: 168 mg (3.88 mmol).

MS (DCI⁺) m/z (rel.): 188. **MS (FAB⁺)** m/z (rel.): 23. **MS (DEI)** m/z (rel.): decomposition products 44 CO₂ and 84 OD / DNM group. **T_{dec}** (DSC, 5°C / min, onset): 211°C (dec.) **¹³C{¹H}** NMR ([D₆]DMSO, 100 MHz): δ (ppm) = 173.2 (1C, C1) 162.8 (1C, C2), 109.7 (1C, C3) 48.9 (1C, MeOH). **¹H NMR** ([D₆]DMSO, 400 MHz): δ (ppm) = 3.40 (s, 4H, H₂O), 3.16 (s, 3H, CH), 4.20 (s, 1H, OH) MeOH. **¹⁴N NMR** ([D₆]DMSO, 29 MHz): δ (ppm) = 0.0. **IR [ATR]:** $\tilde{\nu}$ (cm^{-1}) =: 3354 br, 3263 br, 2966 w, 2172 w, 1672 s, 1530 s, 1480 s, 1423 w, 1374 w, 1334 s, 1242 s, 1143 s, 1111 s, 1014 m, 996 m, 964 m, 922 m, 824 m, 781 m, 755 w. **F.S.** 120 N, **ESD** 100 mJ, **I.S.** 10 J, **grain size:** 100-500 μm .

6.4.4 Potassium DNM-OD

217 mg (3.88 mmol) potassium hydroxide precipitated 312 mg (0.81 mmol, 42%) yellow product.

T_{dec} (DSC, 5°C / min, onset): 219°C. **IR [ATR]:** $\tilde{\nu}$ (cm^{-1}) =: 1687 s, 1664 s, 1516 s, 1476 s, 1422 m, 1388 m, 1349 s, 1250 s, 1207 s, 1197 s, 1175 m, 1149 s, 1111 s, 985 m, 922 m, 875 m, 823 m, 795 m, 752 m. **F.S.** 120 N, **ESD** 100 mJ, **I.S.** 3 J, **grain size:** <160 μm .

6.4.5 Barium DNM-OD x 3.5 H₂O

612 mg (1.94 mmol) barium hydroxide octahydrate precipitated 635 mg (1.64 mmol, 84%) yellow product.

T_{dec} (DSC, 5°C / min, onset), 120°C (H₂O), 123°C (dec.), 165°C (dec.). **MS (FAB⁻)** m/z (rel.): 189. **MS (FAB⁺)** m/z (rel.): 137 + 5 x H₂O -> 229 (barium isotope pattern). **IR [ATR]:** $\tilde{\nu}$ (cm^{-1}) = 3606 s, 3529 m, 3468 m, 3350 m, 3261 m, 1663 s, 1629 s, 1602 m, 1526 s, 1509 s, 1458 s, 1388 s, 1317 s, 1296 s, 1240 m, 1148 s, 1127 s, 994 m, 958 w, 914 m, 830 m, 782 m, 764 m, 736 w. **F.S.** 160 N, **ESD** 100 mJ, **I.S.** 10 J, **grain size:** <160 μm .

6.5 Nitrogen rich salts of DNM-OD

Procedure A: Potassium DNM-OD was solved in 2 eq of 1 M HCl and extracted with ethyl acetate. The ethyl acetate phase was dried with sodium sulfate. After filtration the guanidine and aminoguanidine carbonate or bicarbonate in equivalent amounts was dissolved in little water and the ethylacetate phase was treated with that solution. The

water phase was separated and the water was evaporated to gain the product. The Product could be easily recrystallized by a water/ethanol mixture.

6.5.1 Bis-Guanidinium DNM-OD x H₂O (9a)

The salt was prepared by the procedure A and obtained in little yield only 6 mg.

The analytical data could not be found so far except temperature stability up to 170°C (DSC,onset).

6.5.1 Di-Ammonium DNM-OD x H₂O (9b)

The salt was prepared according to procedure A. There was ammonia bubbled for half an hour through the ethylacetate solution. The salt precipitated immediately.

The analytical data could not be found so far except temperature stability up to 128°C (DSC,onset).

7 References

- [1] F.-X. Steemann, *Dissertation*, LMU München, **2009**.
- [2] a) C. H. Lim, S. Hong, K.-H. Chung, J.S. Kim, and J. R. Cho, *Bull. Korean Chem. Soc.* **2008**, 29 (7), 1415; b) A. R Katritzky, G. L Sommen, A. V. Gromova, R. M. Witek, P. J. Steel, R. Damavarapu, *Chem. Heterocyclic Comp.* **2005**, 41(1), 111.
- [3] a) Z. Zeng,, H. Gao, B. Twamley, J. M Shreeve, *J. Mater. Chem.* **2007**, 17, 3819-3826; b) V.Thottempudi, J. M. Shreeve, *Synthesis*, **2012**, 44, 1253-1257.
- [4] a) A. A. Dippold,, T. M. Klapötke., *Z. anorg. allg. Chem.* **2011**, 637: 1453–1457; b) A. A Dippold, T. M. Klapötke, *Chem. Eur. J.* **2012**, 18: 16742–16753.
- [5] N.V. Latypov, J. Bemm, A. Langlet, U. Wellmar, U. Bemm, *Tetrahedron* **1998**, 54, 11525–11536.
- [6] a) T. M. Klapötke, *Chemie der hochenergetischen Materialien*, 1. Auflage, de Gruyter Verlag, Berlin, **2009**, ISBN 3110207451; b) J. M. Welch, *Dissertation*, LMU München, **2008**.
- [7] R. O. Bora, M. Farooqui, *J. Heterocyclic Chem.* **2007**, 44, 645-649.
- [8] R. O. Bora, M. Farooqui, *J. Heterocyclic Chem.* **2007**, 44, 645-649.
- [9] *Jap. Patent* **2001**.97964.
- [10] A. F. Holleman, E. Wiberg und N. Wiberg, *Lehrbuch der Anorganischen Chemie*, 102. Auflage, de Gruyter Verlag, Berlin, **2007**, ISBN 3110177706.
- [11] *Gaussian 03*, M. J. Frisch, G. W. Trucks, H. B. Schlegel, G. E. Scuseria, M. A. Robb, J. R. Cheeseman, G. Scalmani, V. Barone, B. Mennucci, G. A. Petersson, H. Nakatsuji, M. Caricato, X. Li, H. P. Hratchian, A. F. Izmaylov, J. Bloino, G. Zheng, J. L. Sonnenberg, M. Hada, M. Ehara, K. Toyota, R. Fukuda, J. Hasegawa, M. Ishida, T. Nakajima, Y. Honda, O. Kitao, H. Nakai, T. Vreven, J. A. Montgomery, Jr., J. E.

- Peralta, F. Ogliaro, M. Bearpark, J. J. Heyd, E. Brothers, K. N. Kudin, V. N. Staroverov, R. Kobayashi, J. Normand, K. Raghavachari, A. Rendell, J. C. Burant, S. S. Iyengar, J. Tomasi, M. Cossi, N. Rega, J. M. Millam, M. Klene, J. E. Knox, J. B. Cross, V. Bakken, C. Adamo, J. Jaramillo, R. Gomperts, R. E. Stratmann, O. Yazyev, A. J. Austin, R. Cammi, C. Pomelli, J. W. Ochterski, R. L. Martin, K. Morokuma, V. G. Zakrzewski, G. A. Voth, P. Salvador, J. J. Dannenberg, S. Dapprich, A. D. Daniels, Ö. Farkas, J. B. Foresman, J. V. Ortiz, J. Cioslowski, and D. J. Fox, Gaussian, Inc., Wallingford CT, **2004**.
- [12] *GaussView, Version 5*, R. Dennington, T. Keith and J. Millam, *Semichem Inc.*, Shawnee Mission KS, **2009**.
- [13] T. M. Klapötke, G. Steinhauser, *Angew. Chem.* **2008**, *120*, 3376.
- [14] J. W. Ochterski, G. A. Petersson, and J. A. Montgomery Jr., *J. Chem. Phys.* **1996**, *104*, 2598-619; b) J. A. Montgomery Jr., M. J. Frisch, J. W. Ochterski, and G. A. Petersson, *J. Chem. Phys.* **2000**, *112*, 6532-42.
- [15] a) H. D. B. Jenkins, H. K. Roobottom, J. Passmore, L. Glasser, *Inorg. Chem.* **1999**, *38*, 3609; b) H. D. B. Jenkins, J. F. Liebman, *Inorg. Chem.* **2005**, *44*, 6359.
- [16] M. Sućeska, *EXPL05 5.04*, Zagreb, Hrvatska, **2009**.
- [17] J. Köhler, R. Meyer, A. Homburg, *Explosivstoffe*, 10. Auflage, Wiley-VCH, Weinheim, **2008**.
- [18] a) *CRC Handbook of Tables for Organic Compound Identification*, 3. Edition, CRC Press, Boca Raton, **1984**, ISBN 0-8493-0303-6. b) T. S. Novikova, T. M. Mel'nikova, O. V. Kharitonova, V. O. Kulagina, N. S. Aleksandrova, A. B. Sheremetev, T. S. Pivina, L. I. Khmel'nitskii, S. S. Novikov, *Mendeleev Commun.* **1994**, *4*, 138.
- [19] J. C. Cobas, S. Domínguez, N. Larin, I. Iglesias, C. Geada, F. Seoane, M. Sordo, P. Monje, S. Fraga, R. Cobas, *MestReNova 5.1.1-3092*, Mestrelab Research S.L., Santiago de Compostela, Spain, **2007**.
- [20] M. Sućeska, *Test Methods for Explosives*, Springer, New York, **1995**.
- [21] NATO Standardization Agreement 4489 (STANAG 4489), 17. September, **1999**.
- [22] WIWEB-Standardarbeitsanweisung 4-5.1.02, 08. November, **2002**.
- [23] NATO Standardization Agreement 4487 (STANAG 4487), 22. August, **2002**.
- [24] WIWEB-Standardarbeitsanweisung 4-5.1.03, 08. November, **2002**.
- [25] *Recommendations on the Transport of Dangerous Goods, Manual of Tests and Criteria*, 4th edition, United Nations, New York, Geneva, **1999**.
- [26] A. Altomare, G. Cascarano, C. Giacovazzo, A. Guagliardi, M. C. Burla, G. Polidori, M. Camalli, *J. Appl. Cryst.* **1994**, *27*, 435.
- [27] G. M. Sheldrick, SHELXS-97, Göttingen, Germany **1997**.
- [28] G. M. Sheldrick, SHELXL-97, Göttingen, Germany **1997**.
- [29] L. J. Farrugia, ORTEP-3 2.02, University of Glasgow, Scotland, **2008**.

- [30] K. Brandenburg, Diamond 3.2c, Crystal Impact GbR, Bonn, Deutschland, 2009.

Part IV

CONCLUSIONS AND OUTLOOK

Doing a conclusion on different pieces of work this can only result in split part of conclusions and outlook. Therefore it is done according to the two big parts of research that very carefully investigated and finally set a basis for subsequent researcher in synthesizing and treating of the energetic compounds based on those introduced moieties.

1 Part II – Urea based derivatives

1.1 Conclusions

Although there might be a different opinion on what urea based means the moieties which were used in this work includes oxamide and isocyanuric acid. The found results in the comparison with other similar energetic explosives and the row of nitrate functionalized compounds in chapter I and II lead to a significant insight in the sensitivity and stability of those kinds of compounds. In chapter III the combination of the moiety of tris(nitratomethyl) methyl (TNMM) with the triazine backbone resulted in the energetic compound with the highest molecular weight besides any polymeric material. Although the performance is not comparable with RDX it proves to be a very stable compound with remarkable energetic properties as well.

1.2 Outlook

Studying further compounds based on those moieties may lead to very energetic performance and stable compounds. The triazine backbone offers a lot more synthetic possibilities by using unsymmetrical derivatives, adding N-oxides or having nitrogen rich ring systems attached to the TRIS moiety which may have really significant increase of power due to the positive enthalpy of formation.

2 Part III – 1,2,4- Oxadiazole and 1,2,4-oxdiazol-5-one based compounds

2.1 Conclusions

The chemistry performed in the work of former members of the working group of Prof. Dr. T. M. Klapoetke were the inspiration to find a chemical system which was on the one hand stable towards thermal and mechanical stress and on the other hand performs well as energetic material. As most former coworker have used the very energetic but also sensitive nitrogen rich tetrazole and triazole moiety, the chosen chemical environment in this thesis includes the oxadiazole moiety. The similarity of the 1,2,4-oxadiazole with the 1,2,4 triazole and the 1,2,4-oxadiazole-5-one with the respective tetrazole moiety was significant.

The stability of the oxadiazole to oxidation, nitration and other common functionalization methods used to be very astonishing. Therefore a lot of compounds which can be applied in different fields of energetic materials like pyrotechnics, explosives and propellants or modifiers of those have been investigated in this thesis. The most remarkable molecule class is the 3-dinitromethyl-1,2,4-oxadiazol-5-one derivatives

which stand in a row with the respective nitrogen rich derivatives and also refer to the common FOX-7 explosive.

2.2 Outlook

The work performed on the oxadiazole derivatives has already been leading to a follow up work of a master student and will if followed carefully result in a lot of stable energetic materials. Also some steps into the use of heterocyclic moieties other than nitrogen rich heterocycles have been accomplished. A lot of not yet characterized compounds is lying ahead to be investigated based on the foundational work performed in this thesis.

Part V

APPENDIX

Chapter VIII TABLES OF CRYSTAL STRUCTURES

1 Compounds- Chapter I

Compounds	BTNMMoxamide
Sum formula	C ₁₀ H ₁₄ N ₈ O ₂₀
Mol. mass [g mol⁻¹]	566.03
Crystal system	triclinic
Space group	<i>P</i> -1 (2)
habitus	colorless plates
<i>a</i> [Å]	6.911(5)
<i>b</i> [Å]	8.014(5)
<i>c</i> [Å]	10.163(5)
α [°]	79.262(5)
β [°]	74.543(5)
γ [°]	74.640(5)
<i>V</i> [Å³]	519.1(6)
<i>Z</i>	2
$\rho_{\text{calc.}}$ [g cm⁻³]	1.812
λ	Mo / K α
<i>T</i> [K]	200(2)
θ / °	4.16, 27.00
μ [mm⁻¹]	0.179
meas. reflexes	2224
indep. reflexes	2224
<i>R</i>_{int}	0.0404
<i>h</i>	-7, 8;
<i>k</i>	-9, 10
<i>l</i>	-7, 12
Parameter	200
<i>R</i>_I, <i>wR</i>₂ [<i>I</i> > 2σ (<i>I</i>)]	0.0360, 0.0717
GOOF (<i>F</i>²)	0.800

2 Compounds - Chapter II

Compound	Trihydroxyethyl isocyanuric acid	Trinitroethyl isocyanuric acid	Trinitromethyl isocyanuric acid
Sum formula	C ₉ H ₁₅ N ₃ O ₆	C ₉ H ₁₂ N ₆ O ₁₂	C ₆ H ₆ N ₆ O ₁₂
Mol. mass [g mol⁻¹]	261.24	396.25	354.17
Crystal system	monoclinic	monoclinic	monoclinic
Space group	P2(1)/n	P2(1)/c	P2(1)/c
Size [mm]	-	-	-
Habitus	Colorless block	Colorless needle	Colorless needles
a [Å]	8.6204(5)	13.6294(9)	12.426(1)
b [Å]	13.0819(7)	8.2368(5)	8.1921(6)
c [Å]	10.4023(5)	14.8193(11)	13.478(1)
α [°]	90.00	90.00	90.000(5)
β [°]	97.962(5)	111.027(7)	110.313(5)
γ [°]	90.00	90.00	90.000(5)
Cell volume [Å³]	1161.8(1)	1552.9(2)	1286.7(1)
Z	4	4	4
ρ_{calc} [g cm⁻³]	1.494	1.695	1.828
λ	Mo / K _α 0.71	Mo / K _α 0.71	Mo / K _α 0.71
T [K]	200(2)	100(2)	200(2)
θ / °	4.24-26.00	3.89-26.00	4.14-26.49
μ [mm⁻¹]	0.126	0.159	0.180
meas. reflexes	11595	15307	5325
indep. reflexes	2278	3037	3575
R_{int}	0.0265	0.0290	0.0769
h	-10...10	-16...16	-15...15;
k	-16...16	-10...10	-10...10
l	-12...12	-18...18	-16...16
Parameter	223	292	505
W_R	0.1099	0.0929	0.1194
R(F²)	0.0429	0.0439	0.0503
S(GooF)	1.133	1.146	0.997

3 Compounds - Chapter III

Compound	TECT	NOX-1
Sum formula	C ₁₂ H ₁₅ N ₃ O ₆	C ₁₈ H ₂₁ N ₁₅ O ₃₀
Mol. mass [g mol⁻¹]	297.27	927.50
Crystal system	Monoclinic	hexagonal
Space group	P2 ₁ /c	R-3
Size [mm]	0.30 x 0.25 x 0.02	-
Habitus	Yellow block	Colorless needle
a [Å]	10.8857(5)	16.6732(4)
b [Å]	6.5504(2)	16.6732(4)
c [Å]	21.7714(7)	24.1563(11)
α [°]	90.00	90.00
β [°]	120.00	90.00
γ [°]	90.00	120.00
Cell volume [Å³]	1344.44(9)	5815.7(3)
Z	4	6
ρ_{calc} [g cm⁻³]	1.469	1.589
λ	Mo / K _α 0.71	Mo / K _α 0.71
T [K]	100(2)	173(2)
θ / °	3.7-32.3	4.10-25.50
μ [mm⁻¹]	0.119	0.154
meas. reflexes	35477	9764
indep. reflexes	3078	2409
R_{int}	0.0637	0.0362
h	-14...14	-19...20
k	-8...8	-16...20
l	-18...280	-29...29
Parameter	195	292
W_R	0.1259	0.0766
R(F²)	0.0508	0.0337
S(GooF)	1.047	0.854

4 Compounds - Chapter IV

4.1 Metal salts

Compound	H ₂ OD	Cu OD x 4 H ₂ O	Ca OD x 4 H ₂ O	K ₂ OD	Cs ₂ OD
Sum formula	C ₄ H ₂ N ₄ O ₄	CuC ₄ N ₄ O ₄ · 4H ₂ O	CaC ₄ N ₄ O ₄ · 4H ₂ O	K ₂ C ₄ N ₄ O ₄	Cs ₂ C ₄ N ₄ O ₄
Mol. mass [g mol⁻¹]	170.1	303.67	560.45	246.28	433.90
Crystal system	Monoclinic	Monoclinic	Triclinic	Monoclinic	Monoclinic
Space group	<i>P</i> 2 ₁ / <i>n</i>	<i>C</i> 2/ <i>c</i>	<i>P</i> -1	<i>P</i> 2 ₁ / <i>c</i>	<i>P</i> 2 ₁ / <i>n</i>
<i>a</i> [Å]	4.7437(3)	12.94444(4)	6.539(5)	6.821(1)	4.4772(4)
<i>b</i> [Å]	5.4028(3)	8.0631(2)	8.580(5)	9.016(2)	13.503(1)
<i>c</i> [Å]	11.6654(7)	9.8345(3)	18.242(5)	6.589(1)	7.6400(7)
<i>α</i> [°]	90	90	85.487(5)	90.00	90.00
<i>β</i> [°]	95.84(1)	108.610(3)	86.477(5)	102.25(3)	106.18(1)
<i>γ</i> [°]	90	90	76.137(5)	90.00	90.00
<i>V</i> [Å³]	297.4(2)	972.78(5)	990.(1)	396.0(1)	443.60(7)
<i>Z</i>	2	8	2	2	2
<i>ρ</i>_{calc.} [g cm⁻³]	1.899	3.163	1.881	2.065	3.248
<i>λ</i>	Mo / K _α	Mo / K _α	Mo / K _α	Mo / K _α	Mo / K _α
<i>T</i> [K]	100	100	100	293	200
<i>θ</i> / °	4.16-32.20	4.03-32.36	3.83-32.65	4.51-26.00	4.78-26.00
<i>μ</i> [mm⁻¹]	0.172	4.47	0.679	1.189	8.212
meas. reflexes	1672	1676	9834	5637	3297
indep. reflexes	973	1485	3851	774	876
<i>R</i>_{int}	0.021	0.023	0.049	0.028	0.028
<i>h</i>	-4...6	-19...19	-8...8	-8...8	-5...5
<i>k</i>	-7...8	-11...11	-10...10	-11...11	-16...15
<i>l</i>	-16...17	-14...14	-22...22	-8...8	-9...8
Parameter	59	94	371	64	64
<i>w</i>_R²	0.087	0.06	0.08	0.048	0.030
<i>R</i>(F²)	0.031	0.02	0.04	0.019	0.072
<i>S</i>(GooF)	1.087	1.142	1.005	1.077	0.992

4.2 Nitrogen rich salts

Compound	(NH ₄) ₂ OD	(N ₂ H ₅) ₂ OD	G ₂ OD	AG ₂ OD	TAG ₂ OD
Sum formula	C ₄ H ₈ N ₆ O ₄	C ₄ H ₁₀ N ₈ O ₄	C ₆ H ₁₂ N ₁₀ O ₄	C ₆ H ₁₄ N ₁₂ O ₄	C ₆ H ₁₈ N ₁₆ O ₄
Mol. mass [g mol ⁻¹]	204.14	234.17	288.23	318.25	378.36
Crystal system	Monoclinic	Triclinic	Monoclinic	Triclinic	Triclinic
Space group	<i>P</i> 2 ₁ / <i>c</i>	<i>P</i> -1	<i>P</i> 2 ₁ / <i>n</i>	<i>P</i> -1	<i>P</i> -1
<i>a</i> [Å]	3.616(5)	3.6358(3)	3.612(5)	3.702(5)	7.635(5)
<i>b</i> [Å]	6.772(5)	7.7229(6)	17.920(5)	8.755(5)	10.220(5)
<i>c</i> [Å]	15.926 (5)	8.2499(7)	8.866(5)	10.666(5)	10.260(5)
α [°]	90.000(5)	80.381(7)	90.000(5)	113.741(5)	78.165(5)
β [°]	90.422(5)	89.020(7)	95.262(5)	91.300(5)	68.725(5)
γ [°]	90.000(5)	79.353(7)	90.000(5)	96.983(5)	82.393(5)
<i>V</i> [Å ³]	390.0(6)	224.44(3)	571.452	313.1(5)	728.7(7)
<i>Z</i>	4	1	4	2	2
ρ_{calc} [g cm ⁻³]	1.739	1.733	1.675	1.847	1.724
λ	Mo / K α 0.71	Mo / K α 0.71	Mo / K α 0.71	Mo / K α 0.71	Mo / K α 0.71
<i>T</i> [K]	100	100	200	100	100
θ / °	3.95-28.54	4.00-30.09	4.00-30.09	3.92-26.50	3.88-30.14
μ [mm ⁻¹]	0.15	0.15	0.15	0.15	0.14
meas. reflexes	865	1295	3701	2472	9962
indep. reflexes	387	920	1040	1299	4265
<i>R</i> _{int}	0.05	0.023	0.079	0.025	0.034
<i>h</i>	-4...4	-5...5	-4...4	-4...4	-10...10
<i>k</i>	-7...8	-10...10	-21...21	-10...10	-14...14
<i>l</i>	-19...20	-11...11	-10...10	-13...13	-14...14
Parameter	80	93	115	128	307
<i>W</i> _R	0.08	0.08	0.084	0.091	0.078
<i>R</i> (F ²)	0.11	0.05	0.080	0.034	0.038
<i>S</i> (GooF)	0.789	0.965	1.124	1.112	0.829

5 Compounds – Chapter V

Compound	3,5-Diamino-- 1,2,4-oxadizole	3,5-Diamino-4H- 1,2,4-oxadizolium perchlorate	3,5-Diamino-4H-1,2,4- oxadizolium picrate
Sum formula	C ₂ H ₄ N ₄ O	C ₂ H ₅ N ₄ O ₅ Cl	C ₈ H ₇ N ₇ O ₈
Mol. mass [g mol⁻¹]	100.09	200.54	329.21
Crystal system	Monoclinic	Orthorhombic	Orthorhombic
Space group	<i>P2₁/c</i>	<i>Pna2₁</i>	<i>Pcba</i>
Size [mm]	<i>0.3 x 0.15 x 0.1</i>	-	<i>0.32 X0.08 X0.02</i>
Habitus	<i>Colorless block</i>	-	<i>Yellow plates</i>
a [Å]	3.759(5)	9.4151(8)	11.9816(6)
b [Å]	11.733(5)	5.0130(4)	7.8271(4)
c [Å]	9.278(5)	14.173(1)	26.098(1)
α [°]	90	90	90
β [°]	100.912(5)	90	90
γ [°]	90	90	90
Cell volume [Å³]	401.8(6)	668.91	2447.5(2)
Z	4	4	8
ρ_{calc} [g cm⁻³]	1.655	1.991	1.787
λ	Mo / K _α 0.71	Mo / K _α 0.71	Mo / K _α 0.71
T [K]	100	100	173
θ / °	4.47-27.50	4.31-28.56	4.28-27.00
μ [mm⁻¹]	0.14	0.17	0.16
meas. reflexes	2203	1114	6202
indep. reflexes	911	937	2600
R_{int}	0.012	0.028	0.0439
h	-4...3	-12...12	-15...11
k	-15...12	-6...4	-5...9
l	-11...12	-11...18	-33...12
Parameter	80	129	236
W_R	0.079	0.069	0.054
R(F²)	0.031	0.035	0.034
S(GooF)	1.065	0.999	0.715

•

6 Compounds - Chapter VI

Compounds	N-(ethoxycarbonyl)- N'-hydroxy- guanidinium chloride (8)	3-Amino-1,2,4- oxadiazol-(4H)-5- one (aOD, 1)	Sodium 3-Amino- 1,2,4-oxadiazol-5- onate
Sum formula	C ₄ H ₁₀ N ₃ O ₃ Cl	C ₂ H ₃ N ₃ O ₂	C ₂ H ₄ N ₃ Na O ₃
Mol. mass [g mol⁻¹]	181.08	101.06	141.07
Crystal system	monoclinic	monoclinic	monoclinic
Space group	P 2 ₁ /c	C c	P 2 ₁ /c
size [mm]	0.3 x 0.15 x 0.1	0.8 x 0.2 x 0.1	0.2 x 0.15 x 0.1
habitus	Colorless needles	Colorles needles	Colorless block
a [Å]	5.063(5)	9.3690(11)	6.5739(2)
b [Å]	14.311(5)	3.5640(3)	10.6637(4)
c [Å]	11.443(5)	12.163(2)	7.2516(3)
α [°]	90	90	90
β [°]	98.587(5)	109.05(1)	91.416(3)
γ [°]	90	90	90
V [Å³]	819.827	383.89(7)	508.20(3)
Z	4	2	4
ρ_{calc.} [g cm⁻³]	1.467	1.749	1.844
λ	Mo / Kα	Mo / Kα	Mo / Kα
T [K]	100	100	173
θ / °	4.31- 25.99	4.60- 28.36	4.13-32.37
μ [mm⁻¹]	0.432	0.155	0.234
meas. reflexes	3075	677	4003
indep. reflexes	1566	517	1049
R_{int}	0.029	0.013	0.025
h	-5...5	-9...12	-8...8
k	-17...14	-4...4	-13...13
l	-10...14	-12...15	-9...9
Parameter	140	76	98
R₁, wR₂ [I > 2σ (I)]	0.032, 0.0552	0.0263, 0.0613	0.0247 / 0.0688
GOOF (F²)	0.870	1.066	1.097

7 Compounds - Chapter VII

Compound	Dinitro- ([1,2,4]oxadiazol- 5-on-3-yl)-acetic acid ethyl ester (4)	Sodium (4-{2-[(ethoxycar- bonyl)oxy]propan- 2-yl}-5-oxo-4,5- dihydro-1,2,4-oxa- diazol-3- yl)(dinitro)- methanide mono- hydrate (6)	2-[O-(methyl- oxycarbonyl)- oximeamido] ethyl acetate (3a)	A ₂ DNM-OD (9b)
Sum formula	C ₆ H ₆ N ₄ O ₈	C ₉ H ₁₁ N ₄ Na O ₁₀	C ₇ H ₁₂ N ₂ O ₅	C ₃ H ₈ N ₆ O ₆
Mol. mass [g mol⁻¹]	262.15	716.42	204.19	224.15
Crystal system	monoclinic	monoclinic	monoclinic	monoclinic
Space group	<i>P</i> 2 ₁ / <i>c</i>	<i>P</i> 2 ₁ / <i>n</i>	<i>P</i> 2 ₁ / <i>c</i>	<i>P</i> 2 ₁ / <i>n</i>
<i>a</i> [Å]	12.6727(7)	13.794(5)	7.5547(6)	10.5483(8)
<i>b</i> [Å]	7.8527(4)	15.592(5)	9.9731(7)	6.9081(5)
<i>c</i> [Å]	11.2767(6)	13.807(5)	13.2326(8)	12.614(1)
α [°]	90	90	90	90
β [°]	114.177(7)	91.805(5)	97.046(6)	108.459(8)
γ [°]	90	90	90	90
<i>V</i> [Å³]	1023.77(9)	2968.1(18)	989.5(1)	871.9(1)
<i>Z</i>	4	4	4	4
$\rho_{\text{calc.}}$ [g cm⁻³]	1.701	1.603	1.371	1.708
λ	Mo / K α	Mo / K α	Mo / K α	Mo / K α
<i>T</i> [K]	100	100	100	173
θ / °	4.17- 30.09	3.94- 30.14	3.86- 30	4.24-23.83
μ [mm⁻¹]	0.161	0.170	0.117	0.162
meas. reflexes	5805	8709	2893	3678
indep. reflexes	2967	5247	1396	1948
<i>R</i>_{int}	0.0282	0.0459	0.034	0.0261
<i>h</i>	-7...10	-19...19	-7...10	-8...14
<i>k</i>	-12...14	-21...22	-12...14	-8...9
<i>l</i>	-18...18	-19...19	-18...18	-16...16
Parameter	187	537	175	168
<i>w</i>_R²	0.059	0.068	0.082	0.058
<i>R</i>(F²)	0.035	0.033	0.037	0.032
<i>S</i>(GooF)	0.798	0.844	0.78	0.835

Chapter IX INDEX OF ABBREVIATIONS

In terms and equations the variables and abbreviations are mentioned in the text. SI-units and the prefixes are used according to DIN 1301, instead of Pascal (Pa) for pressure Bar (bar) is used. All percentage values are referring to weight percent. For atoms in molecular structures the colors were chosen dark-grey (carbon), light-grey (hydrogen), blue (nitrogen) and red (oxygen). Thermal ellipsoids are if not further mentioned drawn at 50% probability level.

Table 1. *Nomenclature of compounds*

RDX	Royal Demolition Explosive / Research Department Explosive
HMX	High Melting Explosive / His Majesty's Explosive
ONC	Octanitrocubane
CL-20	China Lake Explosive no. 20 – Hexanitro hexaaza wurtzitane
OD	1,2,4-Oxadiazol-5-one
Od	1,2,4-Oxadiazole
aOD	3-Amino-1,2,4-oxadiazol-5-one
BOD	3,3'-Bis-1,2,4(4 <i>H</i>)-oxadiazol-5-one
BOD²⁻	3,3'-Bis-1,2,4-oxadiazol-5-onate
TAG⁺	Triaminoguanidinium cation
DAG⁺	Diaminoguanidinium cation
AG⁺	Aminoguanidinium cation
G⁺	Guanidinium cation
Hz⁺	Hydrazinium cation
DN⁻	Dinitramide anion
DNM-OD	3-dinitromethyl-1,2,4(4 <i>H</i>)-oxadiazol-5-one
TRIS	Tris(hydroxymethyl)aminomethane
CS	Isocyanuric acid
TCA	1,3,5-triazine-2,4,6-carboxamide
TECT	2,4,6-Tris(ethylcarboxy)-1,3,5-triazine; triethyl 1,3,5-triazine-2,4,6-tricarboxylate
DMF	N,N-Dimethylformamide
DMSO	Dimethylsulfoxide
AT	5-amino-1 <i>H</i> -tetrazole
aOD	3-amino-1,2,4(<i>H</i>)-oxadiazol-5-one
OD	1,2,4(<i>H</i>)-oxadiazol-5-one
od	1,2,4-oxadiazole
daod	3,5-diamino-1,2,4-oxadiazole
daodH⁺	3,5-Diamino-1,2,4(4 <i>H</i>)-oxadiazolium cation
H₂OD	3,3'-bis-1,2,4(<i>H</i>)-oxadiazol-5-one
Et	ethyl
HEDM	engl. <i>high energy density materials</i>
HMX	Octogene, Tetramethylenetetranitramine High melting explosive
Me	Methyl
NTO	Nitrotriazolone
PETN	Pentaerythrite tetranitrate
RDX	Hexogen, Cyclotrimethylenetrinitramine
TNAZ	1,3,3-Trinitroazetidine
TNT	2,4,6-Trinitrotoluene

Table 2. Common used abbreviations in experimental section

°C	Degree Celsius
Å	Ångström (10^{-10} m)
BAM	Bundesanstalt für Materialprüfung
Calc.	calculated
Conc.	concentrated
D	Detonation velocity
DEI	direct electron impact
E_{dr}	Impact sensitivity
et al.	et alii (and others)
exp.	Experimental
F_R	Friction sensitivity
Fa.	Firma
FAB	fast atom bombardment
IR	Infrared spectroscopy
m	Molarity
M	Molecule peak (MS)
MPV	Membrane Pump Vacuum
MS	Mass spektrometry
m/z	Mass/ charge
NMR	nuclear magnetic resonance
$\tilde{\nu}$	Wave number
Ω	Oxygen balance
OPV	Oil Pump Vacuum
p	Detonation pressure
ppm	parts per million
Q_v	Heat of explosion
T_{dec}	Decomposition temperature
T_{ex}	Explosion Temperature
T_m	Melting Point
V₀	Exhaust volume
UC	Unit cell
FAB	<i>fast atom bombardment</i>
Fnd.	found
GOOF	<i>goodness of fit</i>
DEI	Direct electron ionsation
DSC	<i>differential scanning calorimetry</i>
ppm	<i>parts per million</i>
UN	United Nations
NATO	North Atlantic Treaty Organization
STANAG	Standardization Agreement of the NATO on procedures, processes, terms and technical equipment of military purpose

Table 3. *Spectroscopic abbreviations*

IR spectroscopy		NMR spectroscopy	
m	medium	d	dublett
s	strong	m	multiplett
vs	very strong	q	quartett
vw	very weak	s	singulett
w	weak	t	triplett

Chapter X ABSTRACT AND SUMMARY

Abstract

The synthesis and properties of explosive urea and triazine derivatives is investigated on behalf of the explosive parameters and the full characterization of the molecules. (Chapter I-III)

The class of oxadiazole derivatives is enhanced from the known explosive 1,2,5 oxadiazole (furazane) derivatives to the 1,2,4 oxadiazole derivatives. This molecule class is thoroughly investigated by all terms of chemical and explosive material matter and especially the 1,2,4-oxadiazol-5-one derivatives are compared to the corresponding tetrazole derivatives which were by far the most investigated molecule moiety of Prof. Dr. T.M. Klapoetke et al. for more than the last ten years.

The 1,2,4 oxadiazol-5-one derivatives do only value as comparable model molecule to the tetrazole but were found to be good explosives themselves. So the triaminoguanidinium 1,2,4-oxadiazol-5-onate is suitable as low temperature propellant, the potassium and cesium 1,2,4-oxadiazol-5-onate are found to be good additions for NIR-flares and last but not least the best performing molecule was found to be the 3,5-diamino-1,2,4-oxadiazolium 5-aminotetrazolate, which combines the stability of the oxadiazole moiety with the very exothermic properties of a tetrazole in its best way. (Chapter IV-V)

The 3-amino-1,2,4(4*H*)-oxadiazol-5-one is investigated thoroughly and detected to be a chemically and thermodynamically more stable system which can be functionalized according to methods known prior in the working group.

The 3-dinitromethyl-1,2,4(4*H*)-oxadiazol-5-one is found a promising explosive class which can be combined as anion with a wide range of cations to tailor the stability and performance.

The overall conclusion is that the 1,2,4-oxadiazole are chemical suitable as well as secondary explosives, propellants and pyrotechnics.

Chapter XI CURRICULUM VITAE



Dipl.-Chem. Norbert Thorsten Mayr

Geboren am 17. November 1978
in Dillingen (Donau)

BERUFLICHER WERDEGANG

04/2011 – heute **BIOTAGE AB, UPPSALA** – Mitarbeiter im Technischen Verkauf

AUSBILDUNG

03/2006 – 03/2011 Promotion **im Arbeitskreis Prof. Dr. T. M. Klapötke**
Thema „Energetic Materials based on Isocyanuric acid and 1,2,4-Oxadiazole Derivatives-Synthesis and Characterization“ **an der Ludwig-Maximilians-Universität, München**

03/2006 Abschluss mit Diplomzeugnis, Note 2.5

09/2000 – 02/2006 Studium im Studiengang Diplom-Chemie **an der Universität Ulm**
Diplomarbeit **im Arbeitskreis Prof. Dr. D. Volkmer**
Thema „Studien zur Kristallisation von Aragonit-Dünnschichten unter Monoschichten aus 5-(Octadecyloxy)isophthalsäure“

07/1998 – 06/2000 Ausbildung zum Reserveoffizier in der Bundeswehr im Bereich Fernmeldetechnik – Schwerpunkt Richtfunk

1998 Allgemeine Hochschulreife – Abschlussnote 2.1

1996 – 1998 Johann-Michael-Sailer-Gymnasium, Dillingen/Donau, BY

1994 – 1996 Herzog-Johann-Gymnasium, Simmern, RP

1990 – 1994 Johann-Michael-Sailer-Gymnasium, Dillingen/Donau, BY

1986 – 1990 Grundschule Nußberg in Iserlohn, NRW

EHRENAMTLICHE TÄTIGKEIT

02/2007 – heute Verbindungsoffizier im Kreisverbindungskommando München-Land, welches die Schnittstelle zwischen ziviler Verwaltung und Bundeswehr im Katastrophenfall darstellt.

09/2009 – 04/2011 Technische Betreuung für Vorträge des Ortsverbandes der GdCh an der Ludwig-Maximilians-Universität

MITGLIEDSCHAFT

06/2002 – heute GdCh – Gesellschaft deutscher Chemiker e.V.

01/2003 – heute BUND – Bund Naturschutz e.V.

PUBLICATIONS

"Silver nitrimminotetrazole - a promising primary explosive." Piercey, Davin G.; Klapoetke, Thomas M.; Mayr, Norbert T.; Scheutzow, Susanne; Stierstorfer, Joerg. *New Trends in Research of Energetic Materials*, Proceedings of the Seminar, 13th, Pardubice, Czech Republic, Apr. 21-23, 2010 (**2010**), (Pt. 2)624-629.

"Smokeless pyrotechnical colorants based on 3,3'-bis-(1,2,4-oxadiazol)-5-one salts." Klapoetke, Thomas M.; Mayr, Norbert T.; Seel, Stephanie. *New Trends in Research of Energetic Materials*, Proceedings of the Seminar, 12th, Pardubice, Czech Republic, Apr. 1-3, 2009 (**2009**), (Pt. 2), 596-607.

"Insensitive explosives and propellants based on 1,2,4-oxadiazol derivatives."Klapoetke, Thomas M.; Kunzmann, Martin H.; Mayr, Norbert T.; Seel, Stephanie. *New Trends in Research of Energetic Materials*, Proceedings of the Seminar, 12th, Pardubice, Czech Republic, Apr. 1-3, 2009 (**2009**), (Pt. 2), 581-595.

"Promising New High-explosives: Triaminoguanidinium (TAG) and Dinitramide (DN) Salts." Klapoetke, Thomas M.; Mayr, Norbert T.; Stierstorfer Joerg. *26th Army Science Conference 2008*, Orlando, Florida, USA, CP-11.

"Comparison of 3,3'-bis-1,2,4-oxadiazol-5-one and 5,5'-bis-1H-tetrazole." Klapoetke, Thomas M.; Maier, Andreas J.; Mayr, Norbert T., *New Trends in Research of Energetic Materials, Proceedings of the Seminar*, 11th, Pardubice, Czech Republic, Apr. 9-11, 2008 (**2008**), (Pt. 2) 653-660.

"New energetic materials for nitrocellulose based propellants." Heeb, Gerhard; Wilker, Stephan; Klapoetke, Thomas M.;Krumm, Burkhard; Mayr, N.; Sproll, Stefan; Steemann, F. Xaver. *WIWEB Ast Heimerzheim, Grosses Cent, Swisttal, Germany. International Annual Conference of ICT (2007)*, 38th 101/1-101/13.

"Comparison of explosive performance and sensitivity of N,N'-bis-(tris-(nitratomethyl)methyl)-oxamide with PETN." Klapoetke, Thomas M.; Mayr, Norbert T. *New Trends in Research of Energetic Materials*, Proceedings of the Seminar, 10th, Pardubice, Czech Republic, Apr. 25-27, 2007 (**2007**), (Pt. 2), 773-782.

"Crystal structure analysis of [Ca(O₃SC₁₈H₃₇)₂(DMSO)₂], a lamellar coordination polymer and its relevance for model studies in biomineralization. ", Volkmer, Dirk; Mayr, Norbert; Fricke, Marc. *Anorganische Chemie 2 (AC2), Materials and Catalysis, Universitaet Ulm, Ulm, Germany. Dalton Transactions (2006)*, (41), 4889.4895.

Part VI

INDEX

INDEX

1,2,4-oxadiazole	99	Cyanuric Acid	55
3,3'-Bis-(1,2,4-Oxadiazol-5-one).....	101	N,N'-	
3,5-Diamino-1,2,4oxadiazole	149	Bis(tris(nitratomethyl)methyl)oxamide	
3-Amino-1,2,4-oxadiazol-5-one.....	201	33
3-Dinitromethylen-1,2,4(4H)-oxadiazol-5-		N ² ,N ⁴ ,N ⁶ -Tris(trisnitratomethyl)methyl-	
one and Derivatives.....	261	1,3,5-triazino-2,4,6-carboxamide	79, 80
5-amino-tetrazole.....	201	Urea Derivatives	31
Crystal structures	293		

Chapter XII

FIGURES

FIGURE 1.	MOLECULAR STRUCTURE OF SECONDARY EXPLOSIVES.....	18
FIGURE 1.	STRUCTURES OF BTNMM-OXAMIDE(I) AND PETN (II).	35
FIGURE 2.	MOLECULAR STRUCTURE OF BTNMM-OXAMIDE IN CRYSTALLINE STATE DETERMINED BY SC-XRD WITH THERMAL ELLIPSOIDS AT 50% PROBABILITY LEVEL;SELECTED BOND LENGTH [Å] AND ANGLES [°] C1–C1* 1.531(4); C1–N1 1.337(2), C1–O1 1.222(2), N1–C2 1.461(2), C2–C3 1.529(3), C3–O2 1.444(2), O2–N2 1.404(2), N2–O3 1.205(2), N2–O4 1.194(2), C1*–C1–O1 121.9(2), C1*–C1–N1 112.1(2), O1–C1–N1 126.0(2), C1–N1–C2 125.2(2).	36
FIGURE 3.	A VIEW OF THE UNIT CELL OF BTNMM-OXAMIDE ALONG A-AXES; DETERMINED BY SC-XRD WITH THERMAL ELLIPSOIDS AT 50% PROBABILITY LEVEL; NO SHEAR PLANES AVAILABLE.	37
FIGURE 4.	A VIEW OF THE UNIT CELL OF BTNMM-OXAMIDE ALONG C-AXES; DETERMINED BY SC-XRD WITH THERMAL ELLIPSOIDS AT 50% PROBABILITY LEVEL; NO SHEAR PLANES AVAILABLE.	37
FIGURE 5.	EXPERIMENTAL RAMAN (RED) AND IR (BLACK) SPECTRUM OF BTNMM-OXAMIDE PLOTTED IN ONE DIAGRAM; SCALES ARE GIVEN IN WAVE NUMBERS (CM ⁻¹).....	40
FIGURE 6.	CALCULATED IR-SPECTRA, GAUSSIAN03 B3LYP/ 6-31G (2D,P) (BLUE) AND EXP. VALUES (BLACK) VIZUALISATION OF TABLE 2; SCALES GIVEN IN WAVE NUMBERS (CM ⁻¹).....	41
FIGURE 7.	ELECTROSTATIC SURFACE POTENTIAL; CALCULATION GAUSSIAN03 B3LYP/ 6-31G (2D,P) PLOT: GAUSSVIEW ^[13b] 0.001 E /BOHR ³ , RENDERING FROM –0.023 (RED) TILL 0.080 (BLUE).....	45
FIGURE 8.	ANALOGOUS SPLIT-OFF OF THE OXAMIDE FROM THE TO THE PROPAGATED MECHANISM OF CHAMBERS ET AL. FOR THE PETN MOLECULE AFTER LOOSING ONE NO ₂ ^[7]	46
FIGURE 9.	DSC MEASUREMENT OF BTNMM-OXAMIDE: ENDOTHERMIC DOWN AND EXOTHERMIC UP, ONSET POINT ACCORDING TO IUPAC STANDARDS.	47
FIGURE 10.	HIGHSPEED PICTURES TAKEN AT 4000 FPS SHOWING THE PROGRESS OF THE EXPLOSION STARTING AT POINT 0MS WITH THE EXPLOSION AND ENDING 16.75 MS LATER.....	49
FIGURE 11.	KOENEN TEST: FIRST ROW (BEFORE), SECOND ROW (AFTER), THIRD ROW NO EXPLOSION ONLY COMBUSTION DUE TO LESS DENSITY BUT ONLY MINIMAL RESIDUE.	50
FIGURE 1.	DECOMPOSITION SCHEME OF RDX BY BACTERIA RHODOCOCCUS SP. STRAIN DN225.	57
FIGURE 2.	TRIS (2,4,6-TRINITROPHENYLOXY) TRIAZINE (A) ^[10] , N,N',N''-TRIS(2,4,6-TRINITROPHENYL) ISOCYANURIC ACID (B).....	58
FIGURE 3.	NITRATION OF THE THM-CA (N=1)(1) AND THE-CA(N=2)(2) RESULTING IN TNM-CA(N=1)(3) AND TNE-CA (N=2)(4)	59
FIGURE 4.	CALCULATED IR-SPECTRUM, GAUSSIAN03 B3LYP/ 6-31G (2D,P) (CORRECTED), COMPARED TO THE EXPERIMENTAL IR SPECTRUM OF TNM-CA(3).	60
FIGURE 5.	DIFFERENTIAL SCANNING CALORIMETRY GRAPH OF TNM-CA(3). (EXOTHERMIC PEAKS UP), HEATING 5°C/MIN. TEMPERATURE MEASUREMENT ACCORDING TO IUPAC RULES ONSET POINT OF THE GRAPH.	61
FIGURE 6.	MOLECULAR STRUCTURE OF TNM-CA(3), ELLIPSOIDS PLOTTED AT 50% PROBABILITY LEVEL.	62
FIGURE 7.	VIEW ALONG B-AXIS(LEFT) – VIEW ALONG C-AXIS(RIGHT) OF TNM-CA(3).	62
FIGURE 8.	TWO MOLECULAR UNITS OF TNM-CA SHOWING DISORDERED NITRO GROUP, PLOTTED AS BALL AND STICKS. 63	
FIGURE 9.	MOLECULAR STRUCTURE OF THE-CA(2) PLOTTED AT 50% PROBABILITY LEVEL.	65
FIGURE 10.	VIEW ALONG A-AXIS OF THE-CA(2).	65
FIGURE 11.	MOLECULAR STRUCTURE TNE-CA(4) PLOTTED AT 50% PROBABILITY LEVEL.....	66
FIGURE 12.	VIEW ALONG B-AXIS (LEFT) AND VIEW ALONG C-AXIS (RIGHT) OF TNE-CA(4).	66
FIGURE 13.	ELECTROSTATIC SURFACE POTENTIAL OF TNM-CA (3)(CALCULATION GAUSSIAN03 B3LYP/ 6-31G (2D,P)), PLOT WAS OUTLINED WITH 0.001 E BOHR ⁻³ IN GAUSSVIEW ^[21]), RENDERING FROM –0.020 (RED) TILL 0.080 (BLUE).	68
FIGURE 14.	ELECTROSTATIC SURFACE POTENTIAL OF TNE-CA(4)(CALCULATION GAUSSIAN03 B3LYP/ 6-31G (2D,P)), PLOT WAS OUTLINED WITH 0.001 E BOHR ⁻³ IN GAUSSVIEW ^[21]), RENDERING FROM –0.020 (RED) TILL 0.080 (BLUE). 69	
FIGURE 1.	MECHANISM FOR THE HYDROCHLORIDE CATALYZED RING CLOSURE REACTION FROM NITRILE 1 TO TRIAZINE 2. ^[6] 81	

FIGURE 2.	POWDER X-RAY MEASUREMENTS AT COOLING SAMPLE WITH 10 K MIN^{-1} ; THE PHASE TRANSITION CAN BE NOTICED AT THE APPEARING OF THE PEAK AT 12.5° AND THE DOUBLE PEAK AT 27° AND 27.3° OR 44.1° AND 44.6° WHICH CORRESPOND TO NEW FORMED LATTICES. SIMULATION OF REFLECTIONS IN THE POWDER DIFFRACTION USING THE LITERATURE VALUE FOR THE HEXAGONAL PHASE AND THE HERE SHOWN MONOCLINIC PHASE SUPPORT THIS OBSERVATIONS.....	82
FIGURE 3.	PHASE TRANSITION AT 265 K, DIFFERENTIAL SCANNING CALORIMETRY MEASUREMENT AT A COOLING RATE OF 10 K MIN^{-1} ; EXOTHERMIC PEAK DOWNWARDS.	83
FIGURE 4.	AN ORTEPIII ^[8] VIEW OF TRIAZINE 2 , SHOWING THE ATOM-LABELING SCHEME. DISPLACEMENT ELLIPSOIDS ARE DRAWN AT THE 50 % PROBABILITY LEVEL AND H ATOMS ARE SHOWN AS SMALL SPHERES OF ARBITRARY RADII. MEASUREMENT AT 298 K.[6] (LEFT) MEASUREMENT AT 100 K (RIGHT).	84
FIGURE 5.	A VIEW OF 2 AT 298 K SHOWING THE STACKING OF LAYERS IN THE [001] DIRECTION. ^[5]	84
FIGURE 6.	A VIEW OF 2 AT 100 K SHOWING THE STACKING OF LAYERS IN THE [100] DIRECTION.....	85
FIGURE 7.	PART OF THE CRYSTAL STRUCTURE OF 2 –298 K, SHOWING A HYDROGEN-BONDED SHEET IN THE (001) PLANE. HYDROGEN BONDS ARE SHOWN AS DASHED LINES ^[5]	86
FIGURE 8.	PART OF THE CRYSTAL STRUCTURE OF 2 –100 K, SHOWING A HYDROGEN-BONDED SHEET IN THE (010) PLANE. HYDROGEN BONDS ARE SHOWN AS DASHED LINES.	87
FIGURE 9.	SYNTHESIS OF NOX (NITRATION WITH ACETIC ANHYDRIDE/ NITRIC ACID).....	88
FIGURE 10.	MOLECULAR STRUCTURE OF NOX (ELLIPSOIDS PLOTTED AT 50% PROBABILITY LEVEL), SYMMETRY OPERATIONS: $C1'(-Y, -1+X-Y, Z)$ AND $C1''(1-X+Y, -X, Z)$	91
FIGURE 11.	VIEW ALONG C-AXIS, MODEL BALL AND STICKS, NITRATED TRIS MOIETY HIDDEN FOR BETTER VIEW.	92
FIGURE 12.	VIEW ALONG B-AXIS, MODEL BALL AND STICKS, NITRATED TRIS MOIETY HIDDEN FOR BETTER VIEW, PARALLEL LAYERS POINTED OUT BY LINES.	92
FIGURE 1.	3,3'-BIS-1,2,4-OXADIAZOL-5-ONE (1) AND 5,5'-BIS-1H-TETRAZOLE (2).	103
FIGURE 2.	THE MOLECULAR STRUCTURE OF 3,3'-BIS-1,2,4-OXADIAZOL-5-ONE (50% PROBABILITY ELLIPSOIDS, BOND LENGTHS IN Å).....	104
FIGURE 3.	VIEW ALONG A-AXIS THE SHOWING HYDROGEN BOND BETWEEN N1 AND O1' OVER H1.	104
FIGURE 4.	SYNTHETIC ROUTE STARTING FROM OXAMIDEDIOXIME TO H_2OD	106
FIGURE 1.	3,3'-BIS(1,2,4-OXADIAZOL-5-ONE) (H_2OD , 1) ^[3] , 5,5' BIS-1H-TETRAZOLE (H_2BT , 2) ^[4] , 4,4' DINITRO-3,3' BISFURAZANES (3). ^[2]	110
FIGURE 2.	SYNTHESIS OF $(NH_4)_2OD$ (4) AND $(N_2H_5)_2OD$ (5).	111
FIGURE 3.	SYNTHESIS OF G_2OD (6) AND DAG_2OD (7).	112
FIGURE 4.	SYNTHESIS OF AG_2OD (8).	112
FIGURE 5.	SYNTHESIS OF TAG_2OD (9).	112
FIGURE 6.	MOLECULAR STRUCTURE OF $(NH_4)_2OD$ (4) (50% PROBABILITY ELLIPSOIDS). SELECTED BOND LENGTHS(Å) AND ANGLES (°): O1—C2 1.383(3), O1—N2 1.420(2), O2—C2 1.247(3), N2—C1 1.304(3), N1—C2 1.335(3), N1—C1 1.362(3), C1—C1i 1.458(5); C2—O1—N2 106.7(2), C1—N2—O1 102.7(2), C2—N1—C1 102.5(2), N2—C1—N1 117.0(2), N2—C1—C1i 119.6(3), N1—C1—C1i 123.4(3), O2—C2—N1 131.0(2), O2—C2—O1 117.9(2), N1—C2—O1 111.1(2); O1—N2—C1—C1i 179.7(3), C2—N1—C1—C1i-179.3(3), C1—N1—C2—O2 179.0(3), N2—O1—C2—O2 -179.0(2); (i) $2-x, -y, 1-z$	113
FIGURE 7.	VIEW ALONG A-AXIS VON $(NH_4)_2OD$ (4).	114
	VIEW ALONG C-AXIS OF $(NH_4)_2OD$ (4).	114
FIGURE 8.	MOLECULAR STRUCTURE OF $(N_2H_5)_2OD$ (5) (50% PROBABILITY ELLIPSOIDS). SELECTED BOND LENGTHS(Å) AND ANGLES (°):C1—N2 1.313(1), C1—N1 1.357(1), C1—C1i 1.470(2), C2—O1 1.237(1), C2—N1 1.340(1), C2—O2 1.386(1), N2—O2, 1.420(1), N11—N12 1.452(1); N2—C1—N1 116.8(1), N2—C1—C1i 119.8(1), N1—C1—C1i 123.4(1), O1—C2—N1 130.9(1), O1—C2—O2 118.4(1), N1—C2—O2 110.7(1), C2—N1—C1 102.99(9), C1—N2—O2 102.66(8), C2—O2—N2 106.85(8); O1—C2—N1—C1-178.2(1), C1—C1—N1—C2 178.6(1), C1—C1—N2—O2 -179.4(1), O1—C2—O2—N2 178.27(9); (i) $1-x, 2-y, -z$	115
FIGURE 9.	VIEW ALONG A-AXIS $(N_2H_5)_2OD$ (5).	116

FIGURE 10.	VIEW ALONG B-AXIS (N_2H_5) ₂ OD (5).	116
FIGURE 11.	MOLECULAR STRUCTURE OF G_2OD (50% PROBABILITY ELLIPSOIDS). SELECTED BOND LENGTHS(Å) AND ANGLES (°): O1—C2 1.382(2), N5—C3 1.319(2), O1—N2 1.420(2), O2—C2 1.242(2), N1—C2 1.330(2), N2—C1 1.304(2), N1—C1 1.357(2), N7—C3 1.323(2), N4—C3 1.328(2), C1—C1 ⁱ 1.463(3); C2—O1—N2 106.9(1), C2—N1—C1 103.2(1), O2—C2—N1 130.8(1), O2—C2—O1 118.6(1), N1—C2—O1 110.6(1), N5—C3—N7 120.0(1), N5—C3—N4 120.5(1), N7—C3—N4 119.5(2), N2—C1—N1 116.8(1), C1—N2—O1 102.5(1), N2—C1—C1 ⁱ 119.7(2), N1—C1—C1 ⁱ 123.5(2); C1—N1—C2—O2 -179.4(2), O1—N2—C1—C1 ⁱ 179.5(2), N2—O1—C2—O2 179.1(1), C2—N1—C1—C1 ⁱ -179.8(2); (i) 2-x, -y, 1-z.	117
FIGURE 12.	VIEW ALONG A-AXIS OF G_2OD , HYDROGEN BONDS(ORANGE)	117
FIGURE 13.	VIEW ALONG C-AXIS OF G_2OD : NO INTERACTIONS BETWEEN LAYERS, NO HYDROGEN BONDS	118
FIGURE 14.	MOLECULAR STRUCTURE OF AG_2OD , 7 (50% PROBABILITY ELLIPSOIDS). SELECTED BOND LENGTHS(Å) AND ANGLES (°): O1—C2 1.3919(18), O1—N2 1.4178(15), N1—C1 1.3595(18), O2—C2 1.2373(18), N2—C1 1.3081(19), N3—C3 1.3200(19), C2—N1 1.3383(18), N3—N6 ⁱⁱ 3.5706(31), N4—C3 1.3289(19), N1—N6 ⁱⁱⁱ 3.5193(22) O2—N6 ⁱⁱⁱ 3.2306(24), N5—C3 1.3363(19), N5—N6 1.4095(18); C2—O1—N2 107.32(10), C2—N1—C1 103.41(11), C1—N2—O1 102.56(10), O2—C2—N1 131.37(12), O2—C2—O1 118.71(12), N1—C2—O1 109.92(12), N2—C1—N1 116.79(12), N2—C1—C1 ⁱ 119.62(15), N1—C1—C1 ⁱ 123.59(15), N3—C3—N4 120.48(13), C3—N5—N6 119.34(12), N3—C3—N5 120.75(14), N4—C3—N5 118.74(13); N2—O1—C2—O2 179.70(11), O1—N2—C1—C1 ⁱ 179.43(14), N2—O1—C2—N1 -0.83(13), C2—N1—C1—N2 0.07(15), O2—C2—N1—C1 179.86(14), C2—N1—C1—C1 ⁱ -179.91(15), O1—C2—N1—C1 0.48(13), N6—N5—C3—N3 2.8(2), C2—O1—N2—C1 0.81(13), N6—N5—C3—N4 -179.17(11), O1—N2—C1—N1 -0.56(14); (i) 1-x, -y, 2-z; (ii) -x, 1-y, 1-z; (iii) -x, -y, 1-z.	119
FIGURE 15.	HYDROGEN BRIDGED BONDS IN THE AG_2OD , VIEW ALONG A-AXIS.	120
FIGURE 16.	HYDROGEN BRIDGED BONDS IN AG_2OD , VIEW ALONG B-AXIS.	120
FIGURE 17.	MOLECULAR STRUCTURE OF TAG_2OD (50% PROBABILITY ELLIPSOIDS). SELECTED BOND LENGTHS(Å) AND ANGLES (°): C2—N2 1.304(2), C2—N1 1.358(2), C2—C3 1.465(2), C3—N3 1.306(2) C3—N4 1.3599(19), C5—N9 1.322(2), C5—N7 1.325(2), C5—N5 1.333(2), C6—N11 1.327(2), C6—N14 1.330(2), C6—N15 1.332(2), C1—O1 1.2389(19), C1—N1 1.336(2), C1—O2 1.3859(19), C4—O4 1.2408(19), C4—N4 1.338(2), C4—O3 1.387(2), N9—N10 1.417(2), N15—N16 1.403(2), N13—N14 1.418(2), N3—O3 1.4196(17), N2—O2 1.4181(17), N11—N12 1.411(2), N7—N8 1.412(2), N5—N6 1.4097(19); N2—C2—N1 116.74(15), N2—C2—C3 120.68(14), N1—C2—C3 122.57(14), C5—N7—N8 118.27(15), N3—C3—N4 117.26(15), N3—C3—C2 119.37(14), N4—C3—C2 123.36(14) C5—N5—N6 120.45(14), N9—C5—N7 120.40(15), N9—C5—N5 119.31(15), N7—C5—N5 120.29(15), C1—N1—C2 103.25(13), N11—C6—N14 119.73(15), N11—C6—N15 120.69(15), N14—C6—N15 119.57(15), O1—C1—N1 131.48(15), C3—N3—O3 102.28(12), O1—C1—O2 118.24(14), C6—N15—N16 122.03(15), N1—C1—O2 110.27(13), O4—C4—N4 131.59(16), O4—C4—O3 118.06(14), N4—C4—O3 110.35(14), C5—N9—N10 117.84(14), C2—N2—O2 102.68(12) C4—N4—C3 102.84(13), C1—O2—N2 107.06(11), C6—N11—N12 124.29(14), C4—O3—N3 107.25(11); O1—C1—N1—C2 179.30(17); N2—C2—C3—N4 2.0(2); O2—C1—N1—C2 0.21(17).	121
FIGURE 1.	SYNTHESIS OF SROD (2).	131
FIGURE 2.	SYNTHESIS OF BAOD (3), CAOD (4) AND Li_2OD (5).	131
FIGURE 3.	SYNTHESIS OF CuOD (6).	131
FIGURE 4.	SYNTHESIS OF $\text{Cu}(\text{NH}_3)_2\text{OD}$ (7).	131
FIGURE 5.	MOLECULAR STRUCTURE OF CAOD (4) (50% PROBABILITY ELLIPSOIDS) SHOWING CLUSTER 1; SYMMETRY PARAMETER: (i) -x, 1-y, 1-z.	132
FIGURE 6.	ZIGZAG O24 AND O21 COORDINATION; VIEW ALONG O22i-CA2-O22 PLANE.	135
FIGURE 7.	MOLECULAR STRUCTURE OF $[\text{Cu}(\text{H}_2\text{O})_4]\text{OD}$ (6) (50% PROBABILITY ELLIPSOIDS). SYMMETRY OPERATOR: (i) 1-x, y, 0.5-z.	135
FIGURE 8.	VIEW ALONG THE B-AXIS OF $[\text{Cu}(\text{H}_2\text{O})_4]\text{OD}$ (6).	137

FIGURE 9.	MOLECULAR UNIT OF BIS POTASSIUM-3,3'-BIS-(1,2,4-OXADIAZOL-5-ON)-ATE.....	137
FIGURE 10.	LINEAR CONNECTED ANION BIFORKATED COORDINATION OF POTASSIUM.	138
FIGURE 11.	VIEW ALONG B-AXIS TO SHOW THE LAYER STRUCTURE WITH THE POTASSIUM COORDINATION	138
FIGURE 12.	COORDINATION OF POTASSIUM AT DIAGONAL VIEW TO SHOW THE INTERCONNECTION BETWEEN LAYERS EACH LAYER HIGHLIGHTED BY DIFFERENT TRANSPARENCY (3 LAYERS: BOLD, TRANSLUCENT AND BW).....	139
FIGURE 13.	MOLECULAR UNIT OF BIS-CESIUM-3,3'-BIS(1,2,4-OXADIAZOL-5-ON)-ATE.....	140
FIGURE 14.	VIEW ALONG C-AXIS TO SHOW THE COORDINATION OF CESIUM.	141
FIGURE 15.	ZIG-ZAG-CHAIN LIKE STRUCTURE OF THE 3,3'-BIS(1,2,4-OXADIAZOL-5-ON)ATE FIXED BY THE CESIUM COORDINATION.	142
FIGURE 16.	DIFFERENTIAL SCANNING CALORIMETRY GRAPHS (EXO UP) WERE COLLECTED AT A HEATING RATE OF 5°C MIN-1 AND THE DECOMPOSITION AND DEHYDRATION TEMPERATURES WERE MEASURED AS ONSET POINTS.	143
FIGURE 1.	RING OPENING AND CLOSING REACTION FROM GUANYLUREA TO 1	150
FIGURE 2.	SYNTHESIS OF 1	151
FIGURE 3.	SYNTHESIS VON 3,5-DIAMINO-1,2,4-OXADIAZOLE (1) FIRST ROUTE.....	152
FIGURE 4.	SYNTHESIS OF 3,5-DIAMINO-1,2,4-OXADIAZOLE (1) SECOND ROUTE.	152
FIGURE 5.	MOLECULAR STRUCTURE OF DAOd (1).	153
FIGURE 6.	VISUALIZATION OF THE PLANAR 5-MEMBERED RING OF DAOd (1).	153
FIGURE 7.	RESONANCE STRUCTURE OF DAOd(1).	154
FIGURE 8.	VISUALIZATION OF THE HYDROGEN BONDS IN DAOd (1).....	155
FIGURE 9.	VIEW ALONG A-AXIS OF DAOd (1).....	156
FIGURE 10.	VIEW ALONG B-AXIS (LEFT) AND C-AXIS (RIGHT) OF DAOd.	157
FIGURE 11.	CALCULATED MOLECULAR STRUCTURE 1	158
FIGURE 12.	CALCULATED MOLECULE DAOdH ⁺ , NUMBERS ASSIGNED AS IN 1	160
FIGURE 13.	MESOMERIC LEWIS STRUCTURES OF DAOdH ⁺ , NUMBERS ASSIGNED.	161
FIGURE 14.	SYNTHESIS OF THE COMPOUNDS 1 TO 4 AND 6A	161
FIGURE 15.	METATHESIS REACTION OF 3 AND 6A TO 5 AND 6	162
FIGURE 16.	SYNTHESIS OF DAOdH NITRATE (1).....	162
FIGURE 17.	SYNTHESIS OF DAOdH PERCHLORATE (3).	163
FIGURE 18.	MOLECULAR STRUCTURE OF DAOdH-PERCHLORATE (3).....	164
FIGURE 19.	VISUALIZATION OF THE PLANAR 5-RING OF HDAOd-PC (3).	165
FIGURE 20.	IN COMPARISON TO 1 SHORTENED (RED) AND PROLONGED (GREEN) BONDS OF DAOdH-PC (3).....	165
FIGURE 21.	RESONANCE STRUCTURE OF THE 3,5-DIAMINO-4H-1,2,4-OXADIAZOLIUM CATION.	166
FIGURE 22.	VISUALIZATION OF THE HYDROGEN BONDS OF DAOdH-PC (3).	166
FIGURE 23.	VIEW ALONG A-AXIS OF DAOdH-PC (3).	167
FIGURE 24.	VIEW ALONG B-AXIS (LEFT) AND ALONG C-AXIS (RIGHT) OF 3	168
FIGURE 25.	ASYMMETRIC UNIT OF 4	169
FIGURE 26.	SIDE VIEW OF THE TWO RING PLANES OF THE ASYMMETRIC UNIT OF 4	170
FIGURE 27.	HYDROGEN BONDS OF 4 . FOR BETTER VISUALIZATION THE THERMAL ELLIPSOIDS WERE NOT PLOTTED BUT A STICK MODEL IS SHOWN. HYDROGEN ATOMS (BLACK).	171
FIGURE 28.	CRYSTAL STRUCTURE OF 4 . VIEW ALONG [100] (LEFT), VIEW ALONG [010]. ATOMS AS BALLS.	171
FIGURE 29.	SYNTHESIS OF KDN.	172
FIGURE 30.	SYNTHESIS OF DAOdH-DN(5).	173
FIGURE 31.	SYNTHESIS OF 6	174
FIGURE 32.	SYNTHESIS OF THE COPPER COMPLEX OF DAOd (7).....	178
FIGURE 33.	POSSIBLE STRUCTURES OF I	179
FIGURE 34.	SUPPOSED OXIDATION PRODUCTS OF 1 INCLUDING M/Z-VALUE.	180
FIGURE 35.	OXIDATION OR NITRATION OF DAOd (1).	181
FIGURE 36.	SYNTHESIS OF DIETHYL-1,2,4-OXADIAZOLE-3,5-DIYLDICARBAMATE (8).	184
FIGURE 37.	NITRATION TO THE DIETHYL-1,2,4-OXADIAZOLE-3,5-DIYLBIS(NITROCARBAMATE) (8).....	184
FIGURE 38.	OVERVIEW OF SYNTHESIZED ENERGETIC COMPOUNDS FROM 3,5-DIAMINO-1,2,4-OXADIAZOLE (1). .	185

Figures

FIGURE 1.	A) 1,3,4 OXADIAZOLE; B) 1,2,4 OXADIAZOLE; C) 1,2,5-OXADIAZOLE (FURAZANE); D) 1,2,3-OXADIAZOLE. 202
FIGURE 2.	DECOMPOSITION OF AT AND AOD. A) DECOMPOSITION OF 1 <i>H</i> -TETRAZOLE-5-AMINE TO CYANAMIDE AND HYDRAZOIC ACID (LEFT) OR 1 <i>H</i> -DIAZIREN-3-AMINE AND NITROGEN (RIGHT). B) DECOMPOSITION OF 3-AMINO-1,2,4-OXADIAZOL-5(4 <i>H</i>)-ONE TO 1 <i>H</i> -DIAZIREN-3-AMINE AND CARBONDIOXIDE.203
FIGURE 3.	GENERAL RING CLOSURE BY ROUTE A TO 3-AMINO-1,2,4-XADIZOL-5-ONE.204
FIGURE 4.	SCHEME OF SYNTHESIS (YELLOW BOX LITERATURE KNOWN ROUTE A, BLUE BOX NEW DEVELOPED ROUTE B). 205
FIGURE 5.	SYNTHESIS OF DIPOTASSIUM CYANODITHIOIMIDOCARBONATE.206
FIGURE 6.	SYNTHESIS OF DIMETHYLCYANODITHIOIMIDOCARBONATE.206
FIGURE 7.	SYNTHESIS OF POTASSIUM S-METHYL-N-CYANOCARBAMATE.206
FIGURE 8.	ALTERNATIVE SYNTHESIS OF DIMETHYLCYANODITHIOIMIDOCARBONATE.207
FIGURE 9.	TOTAL YIELD OF SYNTHETIC ROUTE A ONLY 7 %.208
FIGURE 10.	SYNTHESIS BY THE OPEN-CHAINED INTERMEDIATE OF 3-AMINO-1,2,4-OXADIAZOL-5-ONE (AOD).209
FIGURE 11.	RING CLOSURE TO 3-AMINO-1,2,4-OXADIAZOL-5-ONE (1).210
FIGURE 12.	GENERAL PROCEDURE FOR SYNTHESIS ROUTE B. WORK UP X DEPENDS ON THE REACTION I-III AND IS SUMMED UP IN TABLE 2.210
FIGURE 13.	MOLECULAR STRUCTURE OF 8. ELLIPSOIDS ARE PLOTTED AT 50% PROBABILITY LEVEL.212
FIGURE 14.	HYDROGEN BONDS (ORANGE) IN 8. THERMAL ELLIPSOIDS ARE PLOTTED AT 50% PROBABILITY LEVEL.213
FIGURE 15.	INTERMOLECULAR HYDROGEN BONDS. ELLIPSOIDS ARE PLOTTED AT 50% PROBABILITY LEVEL.213
FIGURE 16.	MOLECULAR STRUCTURE OF 1. THERMAL ELLIPSOIDS ARE PLOTTED AT 50% PROBABILITY LEVEL.214
FIGURE 17.	SIDE VIEW OF THE MOLECULAR STRUCTURE OF 1. ELLIPSOIDS PLOTTED AT 50% PROBABILITY LEVEL.214
FIGURE 18.	RESONANCE STRUCTURES A-D TO EXPLAIN THE BONDING CONDITIONS IN 1.215
FIGURE 19.	HYDROGEN BRIDGE BONDING OF 1. VIEW ALONG B-AXIS. THERMAL ELLIPSOIDS PLOTTED AT 50% PROBABILITY LEVEL.216
FIGURE 20.	THE LAYERS (BLACK AND TURQUOISE) IN ONE UNIT CELL OF 1. THERMAL ELLIPSOIDS ARE PLOTTED AT 50% PROBABILITY LEVEL.217
FIGURE 21.	VISUALIZATION OF MOLECULES IN THE LAYERS AND PLANES. THERMAL ELLIPSOIDS ARE PLOTTED AT 50% PROBABILITY LEVEL.218
FIGURE 22.	OVERVIEW OF SYNTHETIC ROUTE B INCLUDING ALL YIELDS. TOTAL YIELD ABOUT 16%.218
FIGURE 23.	ALTERNATIVE RING CLOSURE REACTION STARTING FROM 8.219
FIGURE 24.	AZO-COUPLING OF 5-AMINO-1 <i>H</i> -TETRAZOLE ACCORDING TO THIELE.221
FIGURE 25.	AZO-COUPLING OF AOD ANALOGOUS TO AT.221
FIGURE 26.	MESOMERIC EXPLANATION OF DIFFERENT COORDINATION POSSIBILITIES.222
FIGURE 27.	COORDINATION OF THE AOD ANION ACCORDING TO A JAHN-TELLER DISTORTED COPPER COMPLEX.223
FIGURE 28.	COORDINATION SPHERE OF SODIUM IN 14.225
FIGURE 29.	VIEW ALONG A-AXIS SHOWS THE COORDINATIVE CONNECTION TO SODIUM BETWEEN THE LAYERS IN THE STRUCTURES.226
FIGURE 30.	VIEW ALONG B-AXIS SHOWS THE COORDINATIVE CONNECTION TO SODIUM BETWEEN THE LAYERS IN THE STRUCTURES.226
FIGURE 31.	VIEW ALONG C-AXIS OF THE STRUCTURE SHOWS HOW THE AOD ANIONS ARE STACKED ALONG THIS DIRECTION.227
FIGURE 32.	VIEW ALONG A-AXIS LEAVING OUT COORDINATION OF SODIUM ONLY EMPHASISING THE HYDROGEN BONDS BETWEEN THE AOD ANIONS.227
FIGURE 33.	VIEW ALONG B-AXIS LEAVING OUT COORDINATION OF SODIUM ONLY EMPHASISING THE HYDROGEN BONDS BETWEEN THE LAYERS OF THE AOD ANIONS.228
FIGURE 34.	VIEW ALONG C-AXIS: LEAVING OUT COORDINATION OF SODIUM ONLY EMPHASISING HYDROGEN BONDS BETWEEN WATER AND AOD ANIONS.228
FIGURE 35.	SYNTHESIZED SALTS OF AOD.230
FIGURE 36.	METHYLATION OF AOD BY DIMETHYLSULFATE.230
FIGURE 37.	METHYLATION OF AOD BY METHYL IODIDE.231

FIGURE 38.	MOLECULAR UNIT OF AOD FROM CRYSTAL STRUCTURE.	232
FIGURE 39.	TAUTOMERY OF THE PROTONATION: A) AT THE AMINO NITROGEN, B) AT THE NITROGEN IN THE RING.	232
FIGURE 40.	ZWITTER-IONIC AND NEUTRAL STRUCTURE OF THE AOD: B AND C AS MESOMERIC STRUCTURES AND TAUTOMERIC STRUCTURE A , B/C AND D	232
FIGURE 41.	HARTREE FOCK-ENERGIES OF THE MOLECULE FORMS A TO D OF AOD.	233
FIGURE 42.	VISUALIZATION OF THE RESULTS FROM FIGURE 33 BY THE AB-INITIO-CALCULATION OF AOD, ILLUSTRATED BY GAUSSVIEW 5.0 ^[18] (DRAWN BONDS DO NOT CORRESPOND TO REAL BONDS BUT ILLUSTRATE THE CALCULATED BOND LENGTH WITH RESPECT TO THE VAN-DER-WAALS RADII).	234
FIGURE 43.	TAUTOMERIC AND MESOMERIC STRUCTURES OF AODH ⁺ CATION.	236
FIGURE 44.	HARTREE-FOCK ENERGIES OF THE AODH ⁺ CATION A TO F	237
FIGURE 45.	VISUALIZATION OF THE STRUCTURES BY AB INITIO CALCULATIONS LIKE IN FIGURE 25 ^[18] (BOND LENGTHS TO NOT REFER TO REAL BONDS BUT TO THEIR QUALITIES).	237
FIGURE 46.	MESOMERIC STRUCTURES OF AOD ⁻ WHICH SHOW POSSIBLE DELOCALIZATION OF THE NEGATIVE CHARGE. 240	
FIGURE 47.	MESOMERIC AND TAUTOMERIC STRUCTURE OF THE 5-AMINO-1,4-DIHYDROTETRAZOLIUM CATION. .	241
FIGURE 48.	SUGGESTED DERIVATIVES OF AOD ACCORDING TO THE INVESTIGATED DERIVATIVES OF AT. ^[2a]	245
FIGURE 1.	FOX-7, DNM-Tz AND DNM-OD.	262
FIGURE 2.	SYNTHESIS OF DNM-OD.	263
FIGURE 3.	SYNTHESIS OF DNM-OD (8) AND ITS SALTS.	265
FIGURE 4.	MOLECULAR STRUCTURE OF 2 , THERMAL ELLIPSOIDS PLOTTED AT 50% PROBABILITY LEVEL.	267
FIGURE 5.	MOLECULAR STRUCTURE OF 3A , THERMAL ELLIPSOIDS PLOTTED AT 50% PROBABILITY LEVEL.	267
FIGURE 6.	MOLECULAR STRUCTURE OF 5 , THERMAL ELLIPSOIDS PLOTTED AT 50% PROBABILITY LEVEL. SELECTED BOND LENGTHS (Å) AND ANGLES (°): C1—O2 1.371(2), N2—O2 1.415(2), C3—C2 1.487(2), C3—N3 1.531(2); C3—C4 1.547(2), C2—N2 1.289(2), C2—N1 1.350(2), C1—O1 1.198(2), C1—N1 1.359(2) N4—O5 1.210(2) C4—O4 1.311(2), C4—O3 1.186(2); O3—C4—O4 129.8(1), C2—N1—C1 107.9(1), N3—C3—N4 105.6(1), C2—C3—C4 118.4(1), N3—C3—C4 106.6(1), O6—N4—O5 127.2(1), N4—C3—C4 107.1(1), O6—N4—C3 115.9(1), N2—C2—N1 112.9(1), O5—N4—C3 116.8(1), N2—C2—C3 120.5(1), C2—N2—O2 104.5(1), N1—C2—C3 26.6(1), O8—N3—O7 127.1(1), O1—C1—N1 131.5(1), O8—N3—C3 118.02(1), N1—C1—O2 105.5(1), C4—O4—C5 117.7(1), C1—O2—N2 109.2(1), N3—C3—N4—O5 87.6(1), N1—C2—N2—O2 -0.2(2), O3—C4— O4—C5 5.4(2), O2—C1—N1—C2 -2.4 (1) O1—C1—O2—N2 -177.4(1), N1—C1—O2—N2 2.3(1), C2—N2—O2—C1 -1.3(1).	268
FIGURE 7.	MOLECULAR STRUCTURE OF 6 , THERMAL ELLIPSOIDS PLOTTED AT 50% PROBABILITY LEVEL.	269
FIGURE 8.	COORDINATION OF SODIUM IN THE STRUCTURE OF 6 . THERMAL ELLIPSOIDS PLOTTED AT 50% PROBABILITY LEVEL.	271
FIGURE 9.	MOLECULAR STRUCTURE OF 7B , THERMAL ELLIPSOIDS PLOTTED AT 50% PROBABILITY LEVEL.	271
FIGURE 10.	COORDINATION OF THE SODIUM IN THE STRUCTURE OF 7B , THERMAL ELLIPSOIDS PLOTTED AT 50% PROBABILITY LEVEL.	272
FIGURE 11.	MOLECULAR STRUCTURE OF 9B . THERMAL ELLIPSOIDS PLOTTED AT 50% PROBABILITY LEVEL.	272
FIGURE 12.	HYDROGEN BONDING OF 8B , THERMAL ELLIPSOIDS PLOTTED AT 50% PROBABILITY LEVEL.	274
FIGURE 13.	MOLECULAR STRUCTURE OF 9A , THERMAL ELLIPSOIDS PLOTTED AT 50% PROBABILITY LEVEL.	274
FIGURE 14.	PROTONATED AND DEPROTONATED FORM OF DNM-OD.	275
FIGURE 15.	RESULTS FROM STRUCTURE OPTIMIZATION BY GAUSSIAN03 HF/3-21G*. VISUALIZATION BY GAUSSVIEW 5.0. ^[12]	275

Chapter XIII

TABLES

TABLE 1.	DETONATION PARAMETER OF TNT AND RDX. ^[2b]	17
TABLE 2.	VALUES FOR LOAD DENSITY ρ_0 AND THE BERTHELOT-ROTH PRODUCT B_R OF SOME SELECTED EXPLOSIVES. ^[2b]	23
TABLE 3.	CLASSIFICATIONS ACCORDING TO UN STANDARDS (NON-UN CONFORM ITALIC).	26
TABLE 4.	CRYSTALLOGRAPHIC DATA FOR THE PETN, BTHMM-OXAMIDE AND BTNMM-OXAMIDE.	39
TABLE 5.	IR-VIBRATIONS CALCULATED WITH GAUSSIAN03 B3LYP/ 6-31G (2D,P), THESE VIBRATIONS ARE CORRECTED BY AN FITTING FACTOR AND COMPARED TO THOSE OF THE EXPERIMENT.	40
TABLE 6.	THERMODYNAMICAL DATA OF BTNMM-OXAMIDE: CALCULATION AND EXPERIMENT.	42
TABLE 7.	ENTHALPY OF FORMATION CALCULATED VALUES BY GAUSSIAN03 (VALUES IN HATREE/PARTICLE); EXPERIMENTAL ENTHALPY OF FORMATION FOR THE ATOMS FROM THE DATABASE OF THE NATIONAL INSTITUTE OF STANDARDS AND TECHNOLOGY(US) CHEMISTRY WEBBOOK; (VALUES IN KCAL/MOL).	43
TABLE 8.	ENTHALPY OF FORMATION CALCULATED VALUES BY GAUSSIAN03 (VALUES IN HATREE/PARTICLE) ; EXPERIMENTAL ENTHALPY OF FORMATION FROM THE DATABASE OF THE NATIONAL INSTITUTE OF STANDARDS AND TECHNOLOGY (US) CHEMISTRY WEBBOOK; (VALUES IN KJ/MOL).....	43
TABLE 9.	FUNCTIONAL GROUPS ARE ASSIGNED WITH VALUES FOR HEAT OF FORMATION AND HEAT OF FUSION GIVEN IN KCAL MOL ⁻¹ .	44
TABLE 10.	THE VALUES OF TABLE 6 ARE USED WITH THE STATED EQUATIONS TO RESULT IN THE FOLLOWING HEAT OF FORMATION OF BTNMMOXAMIDE IN SOLID STATE.	45
TABLE 11.	COMPARISON OF THE THERMODYNAMICAL, SENSITIVITY AND EXPLOSION DATA (CALCULATED BY EXPLO 5 ^[11]) OF BTNMM-OXAMIDE (CRYSTAL A, POWDER) WITH TNT, RDX AND PETN.	48
TABLE 1.	IR-VIBRATIONS CALCULATED WITH GAUSSIAN03 B3LYP/ 6-31G (2D,P) OF TNM-CA(3). STRETCHING MODES ARE JUST ASSIGNED WITH THE AFFECTED BONDINGS, OTHER MODES ARE DESCRIBED.	60
TABLE 2.	SELECTED BOND LENGTHS AND ANGLES OF TNM-CA(3) (BLUE ISOCYANURIC ACID MOIETY, RED NITRATE MOIETY).	64
TABLE 3.	SELECTED BOND LENGTHS AND ANGLES OF TNE-CA(4) (BLUE ISOCYANURIC ACID MOIETY, RED NITRATE MOIETY).	67
TABLE 4.	CBS4-M CALCULATED ENTHALPIES OF FORMATION IN GAS PHASE	70
TABLE 5.	FUNCTIONAL GROUPS ARE ASSIGNED WITH VALUES FOR HEAT OF FORMATION AND HEAT OF FUSION GIVEN IN KCAL MOL ⁻¹	71
TABLE 6.	THE VALUES OF TABLE 3 ARE USED WITH THE STATED EQUATIONS TO RESULT IN THE FOLLOWING HEAT OF FORMATION OF TNM-CA(3) AND TME-CA(4) IN SOLID STATE.	71
TABLE 7.	CALCULATION BASED ON EXPLO5 (VERSION 5.02, 2006) BKWG TYPE OF CONSTANTS IN BKW E.O.S IS USED IN CALCULATION (ALPHA=0,5; BETA=0,096; KAPPA=17,56; THETA=4950).....	72
TABLE 1.	INTERMOLECULAR HYDROGEN-BOND PARAMETERS (D [Å]; < [°]) OF 2-298 K AND 2-100 K.	86
TABLE 2.	THERMODYNAMICAL DATA OF NOX: CALCULATION AND EXPERIMENT.	89
TABLE 3.	FUNCTIONAL GROUPS ARE ASSIGNED WITH VALUES FOR HEAT OF FORMATION AND HEAT OF FUSION GIVEN IN KCAL MOL ⁻¹ .	90
TABLE 4.	THE VALUES OF TABLE 3 ARE USED WITH THE STATED EQUATIONS TO RESULT IN THE FOLLOWING HEAT OF FORMATION OF IN SOLID STATE.	90
TABLE 5.	CALCULATION BASED ON EXPLO5.02 ^[11] .	93
TABLE 1.	IMPACT AND FRICTION SENSITIVITY (JIS K 4810).	103
TABLE 2.	CRYSTALLOGRAPHIC DATA FOR H ₂ OD AND H ₂ BT	105
TABLE 3.	SELECTED BOND LENGTHS, ANGLES, TORSION ANGLES AND HYDROGEN BONDINGS FROM X-RAY DIFFRACTION AND D _{CALC} CALCULATED BOND LENGTHS WITH GAUSSIAN03 (B3LYP/CC-PVDZ) ^[8] .	105
TABLE 1.	SELECTED HYDROGEN BONDS OF (NH ₄) ₂ OD (4).	113
TABLE 2.	HYDROGEN BONDS (N ₂ H ₅) ₂ OD (5).	115
TABLE 3.	SELECTED HYDROGEN BONDS OF G ₂ OD (6)	118
TABLE 4.	SELECTED HYDROGEN BONDS	120
TABLE 5.	SELECTED HYDROGEN BONDS TAG ₂ OD (9)	122

TABLE 6.	ENERGETIC PROPERTIES OF GUANIDINIUM SALTS.	123
TABLE 7.	OXYGEN BALANCES OF H_2OD , $(\text{NH}_4)_2\text{OD}$, $(\text{N}_2\text{H}_5)_2\text{OD}$	123
TABLE 8.	OXYGEN BALANCES OF THE GUANIDINIUM COMPOUNDS 6-9	124
TABLE 9.	SELECTED BOND LENGTHS(Å) AND ANGLES (°):	133
TABLE 10.	SELECTED BOND LENGTH AND ANGLES OF THE $[\text{Cu}(\text{H}_2\text{O})_4]$ OD (6).	136
TABLE 11.	SELECTED HYDROGEN BONDS	136
TABLE 12.	SELECTED BOND LENGTHS AND ANGLES	138
TABLE 13.	SELECTED BOND LENGTHS AND ANGLES	140
TABLE 1.	SELECTED BOND LENGTHS AND ANGLES OF DAOd (1).	154
TABLE 2.	HYDROGEN BONDS OF DAOd (1).	155
TABLE 3.	CALCULATION RESULTS: STRUCTURAL OPTIMIZATION OF 1	158
TABLE 4.	CALCULATED AND EXPERIMENTAL CHARACTERISTIC IR ABSORPTIONS OF 1	159
TABLE 5.	RESULTS OF THE CALCULATION OF DAOdH ⁺	160
TABLE 6.	CALCULATED IR VIBRATIONS OF DAOdH ⁺ (UNSCALED).	161
TABLE 7.	CALCULATED DETONATION PARAMETERS OF 2	163
TABLE 8.	BOND LENGTHS AND ANGLES OF DAOdH-PC (3).	165
TABLE 9.	HYDROGEN BONDS OF DAOdH-PC (3).	167
TABLE 10.	BOND LENGTHS AND ANGLES OF DAOdH ⁺ IN 4	170
TABLE 11.	HYDROGEN BONDING OF 4	170
TABLE 12.	CALCULATED DETONATION PARAMETERS OF 4 COMPARED TO 3,4,5-TRIAMINO-1,2,4- TRIAZOLIUM PICRATE AND GUANYLURONIUM PICRATE.	172
TABLE 13.	COMPARING THE CALCULATED DETONATION PARAMETERS OF 5-AMINOTETRAZOLIUM DINITRAMIDE WITH 5 AT DENSITY OF 1.93 g cm^{-3} AND A DENSITY OF 1.78 g cm^{-3}	174
TABLE 14.	CALCULATED DETONATION PARAMETERS OF 6	175
TABLE 15.	CONSTITUTION OF DIFFERENT OXIDATION PRODUCTS OF 1	180
TABLE 16.	QUANTUM CHEMICAL CALCULATED NMR SHIFTS OF THE SUPPOSED OXIDATION PRODUCTS OF 1	180
TABLE 17.	VARIOUS CONDITIONS FOR THE OXIDATION VON DAOd (1).	181
TABLE 18.	CALCULATED DETONATION PARAMETERS BY EXPLO5 CODE AND SENSITIVITIES OF ALL SYNTHESIZED COMPOUNDS.	185
TABLE 19.	NMR-STANDARDS AND –RECORDING FREQUENCIES.....	188
TABLE 20.	LITERATURE VALUES OF $\Delta_f H^0$ AND CALCULATED CBS-4M VALUES H^0 OF THE ATOMS (HYDROGEN, CARBON, NITROGEN, OXYGEN AND CHLORINE).....	189
TABLE 1.	COMPARISON OF AT AND AOD.	203
TABLE 2.	VARIATIONS OF SYNTHETIC ROUTE B WITH WORKUP PROCEDURE.....	211
TABLE 3.	SELECTED BOND LENGTHS AND ANGLES OF 8	212
TABLE 4.	SELECTED HYDROGEN BRIDGED BONDINGS OF 8	214
TABLE 5.	SELECTED BOND LENGTHS AND ANGLES OF 1	215
TABLE 6.	HYDROGEN BRIDGED BONDING FROM THE CRYSTAL STRUCTURE OF 1	217
TABLE 7.	OVERVIEW OF THE SOLUBILITY TESTS OF 1 IN DIFFERENT SOLVENTS..	220
TABLE 8.	SELECTED BONDS AND ANGLES OF THE SODIUM AOD (14): AOD MOIETY (PURPLE)-WATER MOIETY (BLUE). 229	
TABLE 9.	SELECTED HYDROGEN BONDS: AOD MOIETY (PURPLE)-WATER MOIETY (BLUE).....	229
TABLE 10.	SUMMARY OF THE DESCRIBED SALTS AND FOR COMPARISON NEUTRAL AOD.	230
TABLE 11.	PKA-VALUE OF THE USED STRONG ACIDS.....	231
TABLE 12.	BOND LENGTHS, ENERGIES AND POINT GROUP FOR STRUCTURE A TO D (CALCULATED BY THE GAUSSIAN03 PROGRAM PACKAGE ^[16] , COLORED BONDS DIFFER FROM THE LITERATURE VALUE ^[11]):	235
TABLE 13.	BOND LENGTHS, ENERGY AND POINT GROUP OF THE AODH+CATION (COLORED VALUES DIFFER FROM THE LITERATURE ^[11]):.....	238
TABLE 14.	DETONATION VALUES FOR AT AND AOD CALCULATED WITH EXPLO 5.04 CODE.....	242
TABLE 15.	THERMOCHEMICAL PARAMETERS AT THE NOZZLE EXIT CALCULATED WITH EXPLO 5.04 CODE:.....	243

Tables

TABLE 16.	CHARACTERISTIC PARAMETERS AT THE NOZZLE EXIT CALCULATED WITH EXPLO 5.04 CODE:	243
TABLE 17.	COMPUTED (EXPLO5) GUN PROPELLANT FOR SINGLE, DOUBLE AND TRIPLE BASE PROPELLANTS COMPARED TO NILE ^[1] , AOD AND AT175 MIXTURES.	244
TABLE 18.	SELECTED HYDROGEN BONDS OF 5	268
TABLE 19.	SELECTED BOND LENGTHS AND ANGLES OF 6 (RED OXADIAZOLONE, GREEN DINITOMETHYL, LIGHTBLUE ACETONE MOIETY, DARKBLUE/BLACK ETHYLCARBOXYLATE).	269
TABLE 20.	SELECTED HYDROGEN BONDS OF 6	270
TABLE 21.	BOND LENGTHS AND ANGLES OF 9B (RED OXADIAZOLONE, GREEN DINITOMETHYL).	273
TABLE 22.	SELECTED HYDROGEN BONDS OF 9B	273
TABLE 23.	ALKALINE AND ALKALINE EARTH SALTS OF DNM-OD.	276
TABLE 24.	EXPLO5 ^[16] CALCULATED VALUES FOR THE DETONATION PARAMETERS FOR DNM-OD AND ITS SALTS.	277
TABLE 25.	NMR-STANDARDS AND —RECORDING FREQUENCIES.	279
TABLE 1.	NOMENCLATURE OF COMPOUNDS	304
TABLE 2.	COMMON USED ABBREVIATIONS IN EXPERIMENTAL SECTION.	305
TABLE 3.	SPECTROSCOPIC ABBREVIATIONS.	306

“Science at its best provides us with better questions,
not absolute answers.”

Norman Cousins, 1976